frontiers | Research Topics

# The immune escape mechanism and novel immunotherapeutic strategies of leukemia

**Edited by**
Shenghui Zhang, Guoping Cai, Si Zhang and Kang Yu

**Published in**
Frontiers in Immunology

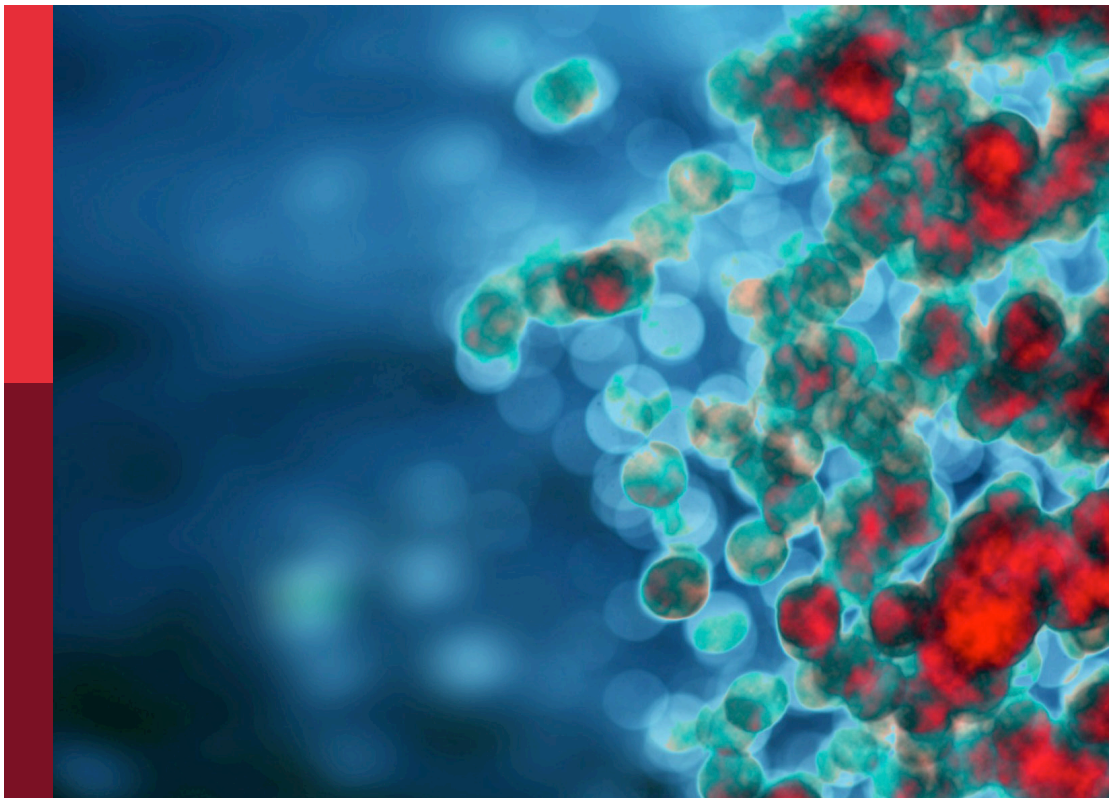

ISSN 1664-8714
ISBN 978-2-83252-201-1
DOI 10.3389/978-2-83252-201-1

## About Frontiers

Frontiers is more than just an open access publisher of scholarly articles: it is a pioneering approach to the world of academia, radically improving the way scholarly research is managed. The grand vision of Frontiers is a world where all people have an equal opportunity to seek, share and generate knowledge. Frontiers provides immediate and permanent online open access to all its publications, but this alone is not enough to realize our grand goals.

## Frontiers journal series

The Frontiers journal series is a multi-tier and interdisciplinary set of open-access, online journals, promising a paradigm shift from the current review, selection and dissemination processes in academic publishing. All Frontiers journals are driven by researchers for researchers; therefore, they constitute a service to the scholarly community. At the same time, the *Frontiers journal series* operates on a revolutionary invention, the tiered publishing system, initially addressing specific communities of scholars, and gradually climbing up to broader public understanding, thus serving the interests of the lay society, too.

## Dedication to quality

Each Frontiers article is a landmark of the highest quality, thanks to genuinely collaborative interactions between authors and review editors, who include some of the world's best academicians. Research must be certified by peers before entering a stream of knowledge that may eventually reach the public - and shape society; therefore, Frontiers only applies the most rigorous and unbiased reviews. Frontiers revolutionizes research publishing by freely delivering the most outstanding research, evaluated with no bias from both the academic and social point of view. By applying the most advanced information technologies, Frontiers is catapulting scholarly publishing into a new generation.

## What are Frontiers Research Topics?

Frontiers Research Topics are very popular trademarks of the *Frontiers journals series*: they are collections of at least ten articles, all centered on a particular subject. With their unique mix of varied contributions from Original Research to Review Articles, Frontiers Research Topics unify the most influential researchers, the latest key findings and historical advances in a hot research area.

Find out more on how to host your own Frontiers Research Topic or contribute to one as an author by contacting the Frontiers editorial office: frontiersin.org/about/contact

# The immune escape mechanism and novel immunotherapeutic strategies of leukemia

**Topic editors**

Shenghui Zhang — First Affiliated Hospital of Wenzhou Medical University, China
Guoping Cai — Yale University, United States
Si Zhang — Fudan University, China
Kang Yu — First Affiliated Hospital of Wenzhou Medical University, China

**Citation**

Zhang, S., Cai, G., Zhang, S., Yu, K., eds. (2023). *The immune escape mechanism and novel immunotherapeutic strategies of leukemia*. Lausanne: Frontiers Media SA. doi: 10.3389/978-2-83252-201-1

# Table of contents

05 Editorial: The immune escape mechanism and novel immunotherapeutic strategies of leukemia
Kang Yu, Jialing Zhang, Qianping Li and Shenghui Zhang

08 Association Analyses of *TP53* Mutation With Prognosis, Tumor Mutational Burden, and Immunological Features in Acute Myeloid Leukemia
Xiang-mei Wen, Zi-jun Xu, Ye Jin, Pei-hui Xia, Ji-chun Ma, Wei Qian, Jiang Lin and Jun Qian

21 Mechanisms of Immunosuppressive Tumor Evasion: Focus on Acute Lymphoblastic Leukemia
Silvia Jiménez-Morales, Ivan Sammir Aranda-Uribe, Carlos Jhovani Pérez-Amado, Julian Ramírez-Bello and Alfredo Hidalgo-Miranda

39 Tryptase Regulates the Epigenetic Modification of Core Histones in Mast Cell Leukemia Cells
Sultan Alanazi, Fabio Rabelo Melo and Gunnar Pejler

51 Chimeric Antigens Receptor T Cell Therapy Improve the Prognosis of Pediatric Acute Lymphoblastic Leukemia With Persistent/Recurrent Minimal Residual Disease in First Complete Remission
Guan-hua Hu, Yi-fei Cheng, Ying-xi Zuo, Ying-jun Chang, Pan Suo, Jun Wu, Yue-ping Jia, Ai-dong Lu, Ying-chun Li, Yu Wang, Shun-chang Jiao, Long-ji Zhang, Xiang-yu Zhao, Chen-hua Yan, Lan-ping Xu, Xiao-hui Zhang, Kai-yan Liu, Yu Wang, Le-ping Zhang and Xiao-jun Huang

61 A Specific CD44lo CD25lo Subpopulation of Regulatory T Cells Inhibits Anti-Leukemic Immune Response and Promotes the Progression in a Mouse Model of Chronic Lymphocytic Leukemia
Agnieszka Goral, Malgorzata Firczuk, Klaudyna Fidyt, Marta Sledz, Francesca Simoncello, Karolina Siudakowska, Giulia Pagano, Etienne Moussay, Jérôme Paggetti, Patrycja Nowakowska, Stefania Gobessi, Joanna Barankiewicz, Aleksander Salomon-Perzynski, Federica Benvenuti, Dimitar G. Efremov, Przemyslaw Juszczynski, Ewa Lech-Maranda and Angelika Muchowicz

76 Indoleamine 2, 3-Dioxygenase 1 Mediates Survival Signals in Chronic Lymphocytic Leukemia *via* Kynurenine/Aryl Hydrocarbon Receptor-Mediated MCL1 Modulation
Claudio Giacinto Atene, Stefania Fiorcari, Nicolò Mesini, Silvia Alboni, Silvia Martinelli, Monica Maccaferri, Giovanna Leonardi, Leonardo Potenza, Mario Luppi, Rossana Maffei and Roberto Marasca

88 Notch-Signaling Deregulation Induces Myeloid-Derived Suppressor Cells in T-Cell Acute Lymphoblastic Leukemia
Paola Grazioli, Andrea Orlando, Nike Giordano, Claudia Noce, Giovanna Peruzzi, Behnaz Abdollahzadeh, Isabella Screpanti and Antonio Francesco Campese

103 Impact of Consolidative Unrelated Cord Blood Transplantation on Clinical Outcomes of Patients With Relapsed/Refractory Acute B Lymphoblastic Leukemia Entering Remission Following CD19 Chimeric Antigen Receptor T Cells
Qianwen Xu, Lei Xue, Furun An, Hui Xu, Li Wang, Liangquan Geng, Xuhan Zhang, Kaidi Song, Wen Yao, Xiang Wan, Juan Tong, Huilan Liu, Xin Liu, Xiaoyu Zhu, Zhimin Zhai, Zimin Sun and Xingbing Wang

113 Increased serum level of alpha-2 macroglobulin and its production by B-lymphocytes in chronic lymphocytic leukemia
Regina Michelis, Lama Milhem, Evleen Galouk, Galia Stemer, Ariel Aviv, Tamar Tadmor, Mona Shehadeh, Lev Shvidel, Masad Barhoum and Andrei Braester

125 Decreased TCF1 and BCL11B expression predicts poor prognosis for patients with chronic lymphocytic leukemia
Taotao Liang, Xiaojiao Wang, Yanyan Liu, Hao Ai, Qian Wang, Xianwei Wang, Xudong Wei, Yongping Song and Qingsong Yin

139 Case Report: Successful engraftment of allogeneic hematopoietic stem cells using CAR-T cell therapy as the conditioning regimen in R/R $Ph^+$ B cell acute lymphoblastic leukemia
Lu Han, Ran Zhao, Jingyi Yang, Yingling Zu, Yanyan Liu, Jian Zhou, Linlin Li, Zhenghua Huang, Jishuai Zhang, Quanli Gao, Yongping Song and Keshu Zhou

146 Regulation of hematopoietic and leukemia stem cells by regulatory T cells
Carsten Riether

161 The Yin-Yang of myeloid cells in the leukemic microenvironment: Immunological role and clinical implications
Fábio Magalhães-Gama, Fabíola Silva Alves-Hanna, Nilberto Dias Araújo, Mateus Souza Barros, Flavio Souza Silva, Claudio Lucas Santos Catão, Júlia Santos Moraes, Izabela Cabral Freitas, Andréa Monteiro Tarragô, Adriana Malheiro, Andréa Teixeira-Carvalho and Allyson Guimarães Costa

frontiers | Frontiers in Immunology

TYPE Editorial
PUBLISHED 04 April 2023
DOI 10.3389/fimmu.2023.1188582



OPEN ACCESS

EDITED AND REVIEWED BY
Katy Rezvani,
University of Texas MD Anderson Cancer Center, United States

*CORRESPONDENCE
Shenghui Zhang
shenghuizhang1@126.com;
zhangshenghui@wmu.edu.cn

SPECIALTY SECTION
This article was submitted to Cancer Immunity and Immunotherapy, a section of the journal Frontiers in Immunology

RECEIVED 17 March 2023
ACCEPTED 27 March 2023
PUBLISHED 04 April 2023

CITATION
Yu K, Zhang J, Li Q and Zhang S (2023) Editorial: The immune escape mechanism and novel immunotherapeutic strategies of leukemia.
*Front. Immunol.* 14:1188582.
doi: 10.3389/fimmu.2023.1188582



# Editorial: The immune escape mechanism and novel immunotherapeutic strategies of leukemia

Kang Yu[1,2,3], Jialing Zhang[2], Qianping Li[2] and Shenghui Zhang[1,2,3,4]*

[1]Department of Hematology, The First Affiliated Hospital of Wenzhou Medical University, Wenzhou, Zhejiang, China, [2]Institute of Hematology, Wenzhou Medical University, Wenzhou, Zhejiang, China, [3]Wenzhou Key Laboratory of Hematology, Wenzhou, Zhejiang, China, [4]Laboratory Animal Center, The First Affiliated Hospital of Wenzhou Medical University, Wenzhou, Zhejiang, China

KEYWORDS

**leukemia, immune escape, immunotherapeutic strategies, regulatory T cells, chimeric antigen receptor T-cell therapy**

Editorial on the Research Topic
The immune escape mechanism and novel immunotherapeutic strategies of leukemia

Increasing evidence unravels that the immune cells within the bone marrow (BM) microenvironment play important roles in the occurrence and development of leukemia (DePasquale et al.; Wurzer et al.) (1). The clinical application of immune checkpoint inhibitors and chimeric antigen receptor (CAR) T-cell therapy has achieved considerable success in treating hematologic malignancies (Aru et al.; Guo et al.; Tomasik et al.; Yang et al.; Hu et al.), but limitations still remain. Therefore, clarifying the interaction of immune cells and leukemia cells and further understanding the mechanisms of immune escape of leukemia cells are the prerequisites for the development of novel immunotherapy strategies.

In this topic, Atene et al. found that chronic lymphocytic leukemia (CLL) cells expressed an active form of indoleamine 2, 3-dioxygenase 1 (IDO1) enzyme and interferon (IFN)-γ secreted from microenvironmental stimuli induced IDO1 expression *via* Jak/STAT1 pathway, and thereby promoting the conversion of tryptophan (Trp) into L-kynurenine (Kyn). Kyn upregulated the expression of myeloid leukemia cell differentiation protein (MCL1) by aryl hydrocarbon receptor (AHR) to promote CLL cell survival. In general, their data identified IDO1/Kyn/AHR signaling as a novel therapeutic target for CLL. Michelis et al. also found that serum alpha-2-macroglobulin (A2M) levels were significantly elevated in CLL patients, possibly due to A2M production by malignant B-lymphocytes. These excess A2M production could upregulate the IgG-hexamerization, resulting in chronic complement activation. Therefore, serum A2M levels were correlated with the disease severity and restraining its overproduction may improve complement activity and immunotherapy outcomes in CLL. TCF1 and its partner gene BCL11B are crucial for sustaining T cell commitment and proliferation, especially maintaining the stem-like properties of $CD8^+$ T cells. Liang et al. found that TCF1 and BCL11B were

downregulated in CLL patients, especially in $CD8^+$ T cells, and significantly correlated with poor time-to-first treatment and overall survival as well as short restricted survival time. More importantly, the combination of TCF1 and BCL11B assessed prognosis more accurately than either alone. In addition, reduced expression of TCF1 and BCL11B, which implied T cell immune dysfunction, was an independent risk factor for rapid disease progression, consistent with high-risk indicators including unmutated IGHV, TP53 changes, and advanced disease.

Grazioli et al. found that functional $CD11b^+Gr\text{-}1^+$ myeloid-derived suppressor cells (MDSCs) accumulated in the Notch3-transgenic murine model of T-ALL and aberrant $CD4^+CD8^+$ (DP) T cells from these mice could induce the expansion of MDSCs *in vitro*, as well as in NSG hosts. The MDSC induction was IL-6-dependent and induced MDSCs conversely sustained the expansion and proliferation of DP T-ALL cells. These results clarified a novel role of Notch-dergulated T cells in modifying MDSCs in the T-ALL environment. Jimenez-Morales et al. summarized recent findings on ALL studies and concluded that leukemic cells could avoid immune surveillance through a variety of immunosuppressive mechanisms, and the resulting immune evasioncan in turn boost their proliferation and invasion. How to resist the leukemic cell strategies to deactivate immune cells and favor an immunosuppressive tumor microenvironment (TME) to acquire apoptosis resistance has been applied broadly to develop personalized immunotherapy for ALL. For example, the infusion of co-stimulatory adapted CAR-T cells or neoepitope-specific ALL cells to increase cytotoxic T cell or MHC response is a current option for ALL treatment.

$CD4^+$ regulatory T cells (Tregs) are considerably enriched in the BM compared to other secondary lymphoid organs and are critically involved in the establishment of an immune privileged niche to maintain hematopoietic stem cell (HSC) quiescence and to protect HSC integrity. In leukemia, increased Tregs frequency has been recognized as a major immune-regulatory mechanism. Since the cure of leukemia means the elimination of leukemia stem cells (LSCs), it is particularly important to understand these immune-regulatory processes for the development of future treatments of leukemia (Riether). In CLL mouse models, a specific $CD44^{lo}CD25^{lo}$ Treg subpopulation was identified and characterized, which was activated to induce an immunosuppressive microenvironment for support of leukemia survival and proliferation. Tregs depletion could trigger the expansion of new anti-leukemic cytotoxic T cell clones to eradicate leukemia. And inhibition of Treg activation with an inhibitor of MALT1 also provided a therapeutic benefit (Goral et al.). Mast cells as immune cells synthesize and store a substantial number of proteases in their secretory granules, including tryptase. Alanazi et al. found that tryptase was also seen in the nuclear compartments of human mast cell line HMC-1. Treatment with cytotoxic agents led to histone 3 cleavage and reduced the levels of several epigentic histone marks, including H3 lysine-4-monomethyl (H3K4me1), H3K9me2, H3 serine-10 phosphorylation (H3S10p), and H2B lysine 16-acetylation (H2BK16ac), in HMC-1 cells. Tryptase inhibition reversed the effects of cytotoxic agents-induced cell death on these epigenetic markers, indicating that it has a profound influence on histone processing. TP53 gene mutations in AML are strongly enriched in complex karyotypes, and are associated with poor prognosis, high tumor mutation load and tumor-infiltrating immune cells, which can be used as biomarkers to predict the immune response to AML (Wen et al.). Myeloid cells as resident immune cells extensively infiltrate the leukemic microenvironment, mainly including populations of neutrophils, macrophages, and MDSCs. These infiltrating cells have been found to be associated with the clinical outcome of the AML patients, and can exert dichotomous functions based on the polarization status of each cell. N2 TANs, M2 TAM and MDSCs show strong immunosuppressive activities that contribute to leukemic progression, acting as a "Yin" role. N1 TANs and M1 TAM stimulate antitumor immune responses, acting as a "Yang" role. Unraveling characterization of the BM immune microenvironment can indicate relevant therapeutic targets and subsequent biomarkers for patients (Magalhaes-Gama et al.).

Although CAR-T cell therapy has revolutionized the treatment of hematological malignancies and achieved a remarkable remission rate, the high recurrence of leukemia after CAR-T cell therapy remains an obstacle to overcome. The value of consolidative transplantation following CAR-T cell-mediated remission is still controversial. Xu et al. conducted a retrospective study and found that patients with R/R B-ALL achieving remission following CD19 CAR-T therapy underwent consolidative unrelated cord blood transplantation (UCBT), conducing to abetter median event-free survival and relapse-free survival (RFS), but without a superior overall survival. And patients with the occurrence of acute graft-versus-host disease (aGVHD) after UCBT had a longer RFS.

The presence of minimal residual disease (MRD) is a well-recognized risk factor for poor prognosis in ALL patients. To investigate the role of CAR-T cell therapy in ALL patients with persistent/recurrent MRD, Hu et al. conducted a respective study and found that 90.7% of these patients achieved MRD negativity after CAR-T cell infusion. Patients who received CAR-T cell therapy had a higher 3-year RFS than those who received chemotherapy bridging to allogeneic HSC transplantation and those who received intensified chemotherapy, suggesting that CAR-T cell therapy can effectively and safely eliminate MRD and significantly improve survival in ALL patients with a suboptimal MRD response. Han et al. reported that a patient with relapsed/refractory $Ph^+$ B-ALL received allogeneic HSC infusion to support hematopoiesis after CAR-T cell therapy, and finally, HSC was successfully implanted, suggesting that CAR-T cell therapy can not only induce disease response, but also directly serve as a preconditioning regimen for HSC implantation.

In summary, although great advances have been made in the immune escape mechanism of leukemia in recent years, the roles of some immune cells in the TME have not yet been identified. Immunotherapy provides the possibility of long-term treatment with more specificity and less toxicity for leukemia (2, 3). Increased attention to new immunotherapy strategies and further clarification of the AML pathophysiology have resulted in a better

understanding of how TME plays pivotal roles in impeding therapeutic efficacy and exerting toxicity.

## Author contributions

KY, JZ, and QL drafted the manuscript. KY and SZ contributed to the concept, design, and critical revision of the manuscript.

## Acknowledgments

We would like to thank all authors and reviewers who contributed to the success of this research topic with their high-quality research or crucial comments.

## Conflict of interest

The authors declare that the research was conducted in the absence of any commercial or financial relationships that could be construed as a potential conflict of interest.

## Publisher's note



## References

1. Anand P, Guillaumet-Adkins A, Dimitrova V, Yun H, Drier Y, Sotudeh N, et al. Single-cell RNA-seq reveals developmental plasticity with coexisting oncogenic states and immune evasion programs in ETP-ALL. *Blood* (2021) 137:2463–80. doi: 10.1182/blood.2019004547

2. Tettamanti S, Pievani A, Biondi A, Dotti G, Serafini M. Catch me if you can: how AML and its niche escape immunotherapy. *Leukemia* (2022) 36:13–22. doi: 10.1038/s41375-021-01350-x

3. Jacoby E, Shahani SA, Shah NN. Updates on CAR T-cell therapy in b-cell malignancies. *Immunol Rev* (2019) 290:39–59. doi: 10.1111/imr.12774

frontiers in Immunology

ORIGINAL RESEARCH
published: 21 October 2021
doi: 10.3389/fimmu.2021.717527

# Association Analyses of *TP53* Mutation With Prognosis, Tumor Mutational Burden, and Immunological Features in Acute Myeloid Leukemia

*Xiang-mei Wen*[1,2,3†], *Zi-jun Xu*[1,2,3†], *Ye Jin*[2,4], *Pei-hui Xia*[2,4], *Ji-chun Ma*[1,2,3], *Wei Qian*[5*], *Jiang Lin*[1,2,3*] *and Jun Qian*[2,4*]

[1] *Laboratory Center, Affiliated People's Hospital of Jiangsu University, Zhenjiang, China,* [2] *Zhenjiang Clinical Research Center of Hematology, Affiliated People's Hospital of Jiangsu University, Zhenjiang, China,* [3] *The Key Lab of Precision Diagnosis and Treatment in Hematologic Malignancies of Zhenjiang City, Affiliated People's Hospital of Jiangsu University, Zhenjiang, China,* [4] *Department of Hematology, Affiliated People's Hospital of Jiangsu University, Zhenjiang, China,* [5] *Department of Otolaryngology-Head and Neck Surgery, Affiliated People's Hospital of Jiangsu University, Zhenjiang, China*

Acute myeloid leukemia (AML) is a heterogeneous disease related to a broad spectrum of molecular alterations. The successes of immunotherapies treating solid tumors and a deeper understanding of the immune systems of patients with hematologic malignancies have promoted the development of immunotherapies for the treatment of AML. And high tumor mutational burden (TMB) is an emerging predictive biomarker for response to immunotherapy. However, the association of gene mutation in AML with TMB and immunological features still has not been clearly elucidated. In our study, based on The Cancer Genome Atlas (TCGA) and BeatAML cohorts, 20 frequently mutated genes were found to be covered by both datasets in AML. And *TP53* mutation was associated with a poor prognosis, and its mutation displayed exclusiveness with other common mutated genes in both datasets. Moreover, *TP53* mutation correlated with TMB and the immune microenvironment. Gene Set Enrichment Analysis (GSEA) showed that *TP53* mutation upregulated signaling pathways involved in the immune system. In summary, *TP53* mutation is frequently mutated in AML, and its mutation is associated with dismal outcome, TMB, and immunological features, which may serve as a biomarker to predict immune response in AML.

**Keywords: mutation, *TP53*, prognosis, tumor mutational burden, tumor-infiltrating immune cells, acute myeloid leukemia**

OPEN ACCESS

***Edited by:***
*Loredana Ruggeri, University of Perugia, Italy*

***Reviewed by:***
*John Welch, Washington University in St. Louis, United States*
*Giridharan Ramsingh, University of Southern California, United States*

***Correspondence:**
*Jun Qian*
*qianjun0007@hotmail.com*
*Jiang Lin*
*2651329493@qq.com*
*Wei Qian*
*dwqian@yahoo.com*

[†]*These authors have contributed equally to this work*

***Specialty section:***
*This article was submitted to Cancer Immunity and Immunotherapy, a section of the journal Frontiers in Immunology*

***Received:*** *31 May 2021*
***Accepted:*** *27 September 2021*
***Published:*** *21 October 2021*

***Citation:***
*Wen X-m, Xu Z-j, Jin Y, Xia P-h, Ma J-c, Qian W, Lin J and Qian J (2021) Association Analyses of TP53 Mutation With Prognosis, Tumor Mutational Burden, and Immunological Features in Acute Myeloid Leukemia. Front. Immunol. 12:717527. doi: 10.3389/fimmu.2021.717527*

## INTRODUCTION

Immunotherapy of cancers has opened a new era in cancer treatment. A great quantity of immunomodulatory strategies has gradually been explored in the past decade such as engineered viruses and cells with enhanced functionalities, immune checkpoint inhibitors (ICIs), and so on (1). And ICIs are changing the treatment paradigms of many tumor types (2–4). The most well-depicted inhibitory immune checkpoint is the relationship of programmed death 1 (PD-1) receptor with PD-ligand 1 (PD-L1), where clinical activity was observed in multiple solid tumor types (5).

At present, several clinical trials using anti-PD-1 or PD-L1 antibodies treat patients with acute myeloid leukemia (AML) (6, 7). It is suggested that PD-1/PD-L1 blockade may be a revolutionary immunotherapeutic strategy for AML. However, clinical trials showed that the clinical response to PD-1/PD-L1 blockade varied in different AML patients (8, 9). It is thought that factors other than PD-1 and PD-L1 may aggravate their immunosuppression and affect their effects on immunotherapy of AML patients (8, 10). Additionally, ICIs can induce immune-related adverse events that can lead to fulminant and even fatal consequences and limit applications of ICIs in many patients (11). Therefore, identifying predictive biomarkers of both efficacy and toxicity connected with the use of ICIs would greatly help guide treatment decisions. Accurate identification of patients with tumors likely to respond to immunotherapy is crucial. High tumor mutational burden (TMB) is a sensitive biomarker for response to immunotherapy largely because tumor mutations provide more opportunities to generate immunogenic neoantigens, and neoantigens enable highly specific and effective anticancer immune responses that provide an exceptionally absorbing target for immunotherapy (12).

In AML, gene mutations devoted to disease features, survival, treatment response, and promising examples demonstrate that some of those mutations might be thought to be therapeutic targets (6, 13). A number of potential shared neoantigens have been recognized for hematologic malignancies, most of which originated from well-established mutations and fusions (14). The neoantigens derived from driver gene mutations are less likely to cause immune evasion since leukemic cells have to definitely express the critical driver mutated protein to maintain their malignant phenotype (14). *TP53* aberrations have been addressed to modulate both the immune and inflammatory responses in malignant tumors, involving the regulatory T cell (Treg) recruitment and T-cell differentiation (15–17). Mutations in the *TP53* gene are strongly enriched in complex karyotype AML and associated with adverse outcomes and treatment selection in AML (18, 19). It has been reported that *TP53* mutations are related to increased leukocyte infiltration across 30 diverse cancer types, and higher TMB and higher proportions of PD-L1–expressing CD8+ T cells correlate with beneficial responses to pembrolizumab immunotherapy in patients with *TP53*-mutated lung adenocarcinoma (20, 21). However, little research has been done on the association of *TP53* gene mutations with TMB and immune response in AML.

In our study, we first found somatic mutations in AML patients using The Cancer Genome Atlas (TCGA) dataset and BeatAML dataset and then identified the common mutant genes in the two cohorts. Furthermore, the association of these gene mutations with TMB and prognosis was investigated. Finally, we explored whether *TP53* mutation was related to immune response.

## MATERIALS AND METHODS

### Data Acquisition

Somatic gene mutations with clinical data were obtained from TCGA portal (https://cancergenome.nih.gov/) (n = 164). Meanwhile, BeatAML mutation, clinical, and sample annotation data were downloaded from source data (from **Table S3**) (22), and 558 cases were included in the analysis.

## BIOINFORMATICS ANALYSES

Circos plot was acquired by the use of Circos (http://circos.ca/). And somatic interactions, oncoplot, and Lollipop plot were performed by the "maftools" package. Somatic interaction function that performed pairwise Fisher's exact test was applied to survey mutually exclusive or co-occurring sets of genes. Lollipop plots were drawn for *TP53* mutation. Then, Mutation Annotation Format data files based on TCGA and BeatAML cohorts were functioned by "maftools" package to extract detailed mutational information. *TP53* mutation in AML was also evaluated by the cbioportal dataset (https://www.cbioportal.org/). Gene Set Enrichment Analysis (GSEA) (http://www.gsea-msigdb.org/gsea/index.jsp) was used based on analysis of Hallmark gene sets and curated gene sets.

### Assessment of Tumor Mutational Burden

TMB, defined as the number of somatic non-synonymous variations, which included nonsense mutation, deletion, missense mutation, splice site, and insertion. The corresponding TMB value was acquired by calculating the number of tumor mutations per Mb in each sample, and the relationship between gene mutations and TMB was visualized using the ggplot2 package.

### Tumor-Infiltrating Lymphocyte Cell Analysis

For TCGA and BeatAML datasets, the edgeR voom algorithm was used to convert the RNA sequencing data and the count data to values that were closer to the microarray results (23). CIBERSORT algorithm (24), a deconvolution approach that evaluates the proportions of 22 tumor-infiltrating lymphocyte cells (TILs) in a bulk tumor transcriptome, was used to examine the relative abundance of immune cell infiltration in different *TP53* mutation statuses. And the 22 cell types included B cells, T cells, natural killer (NK) cells, macrophages, dendritic cells, and myeloid subsets. Difference in immune cell abundance between wild group and mutation group was analyzed using a violin map.

TIDE, a novel computational method that can evaluate the potential of tumor immune escape, was used to calculate immune measures (http://tide.dfci.harvard.edu/).

## Statistical Analyses

Statistical analyses in this study were performed with R software version 4.0.4 (https://www.r-project.org/). The data were shown as either boxplots or violin plots using the ggplot2 package concerning comparison of two continuous variables, and the association between two categorical variables was evaluated by chi-square test and Fisher's exact test. Univariate Cox regression was used to test whether gene mutations had prognostic value in AML. The prognostic effects of gene mutations were verified through Kaplan–Meier survival analysis using a log-rank test. We employed the survival package to generate Kaplan–Meier survival curves. The correlation between mutant genes and TMB was examined by Wilcoxon rank sum test. The TMB value of each patient was calculated with the TMB function of the maftools package. The two-sided with a significance level of 0.05 in all comparisons was defined as statistically significant.

# RESULTS

## Somatic Genomic Mutations in Acute Myeloid Leukemia

Using TCGA and BeatAML cohorts, we revealed the key visualizations generated using maftools. We recognized 30 frequently mutated genes from TCGA cohort, and the 10 most frequently mutated genes were *FLT3* (27%), *DNMT3A* (25%), *NPM1* (17%), *IDH2* (10%), *IDH1* (9%), *TET2* (9%), *RUNX1* (8%), *TP53* (8%), *NRAS* (8%), and *CEBPA* (7%) (**Figure 1A**). At the same time, we also defined 30 frequently mutated genes from BeatAML cohort (**Figure 1B**), and the 10 most frequent mutations were *FLT3* (29%), *DNMT3A* (23%), *NPM1* (22%), *NRAS* (13%), *TET2* (12%), *RUNX1* (12%), *IDH2* (12%), *SRSF2* (12%), *WT1* (9%), and *TP53* (9%). Interestingly, there were 20 genes mutated in both TCGA and BeatAML cohorts of AML (**Figure S1**). Then, we analyzed these commonly mutated genes in the next study.

## Co-Occurrence of Genetic Alterations in Acute Myeloid Leukemia

As shown in **Figures 2A, B**, the length of the arc indicated the frequency of gene mutations, whereas the width of the connecting lines represented the frequency of co-occurrence between two genes. The frequency of co-mutation of *NMP1* with *DNMT3A* and *FLT3-ITD* was significantly higher. In addition, we identified potentially altered gene sets that showed co-occurrence or exclusiveness in their mutation pattern. Notably, the results indicated that only *TP53* and other common mutated genes were mutually exclusive in both TCGA and BeatAML cohorts (**Figures 2C, D**).

## Prognosis of *TP53* Mutations in Acute Myeloid Leukemia

Next, the prognostic effects of the commonly mutated genes were examined by Cox regression. As displayed in **Figure 3A**, patients with *U2AF1*, *TP53*, *TET2*, *STAG2*, *PHF6*, or *ASXL1* gene mutations had poor prognosis in BeatAML cohort and so do patients with *TP53*, *RUNX1*, *EZH2*, or *DNMT3A* mutations in TCGA cohort. Remarkably, we identified that *TP53* gene mutations were dramatically associated with worse overall survival (OS) in both TCGA and BeatAML cohorts [$p \leq 0.05$, hazard ratio (HR) >1] (**Figure 3A**). Furthermore, we performed Kaplan–Meier survival analysis to validate the relationship between mutated genes and the prognosis of patients with AML. We also observed the parallel results; as shown in **Figure 3B**, *TP53* mutation was associated with a poor prognosis ($p < 0.001$ and $p = 0$). Meanwhile, *DNMT3A* and *RUNX1* gene mutations predicted poor survival probability ($p = 0.001$, and $p = 0.042$) in TCGA cohort, and patients with *TET2* and *U2AF1* gene mutations had shorter survival time ($p = 0.006$ and $p = 0.001$, respectively) in the BeatAML cohort using Kaplan–Meier methods (**Figure S2**).

## *TP53* Mutations Are Associated With Tumor Mutational Burden

We compared TMB data from public databases (TCGA and BeatAML). Among commonly mutated genes, patients with mutation in *TET2*, *RUNX1*, *WT1*, *TP53*, *ASXL1*, *STAG2*, *U2AF1*, and *PHF6* displayed significantly higher TMB levels in TCGA cohort (**Figure 4A**). There were five types of *TP53* mutations such as frame shift deletion, missense mutation, splice site, frame shift insertion, and nonsense mutation. To address the different roles of *TP53* mutation subtypes in TMB, we then detected the association between different *TP53* mutation subtypes and TMB. No difference in TMB was observed between *TP53* mutation subtypes in both TCGA and BeatAML cohorts ($p = 0.682$ and $p = 0.369$, respectively) (**Figures 4B, C**). The TMB score of AML ranged from 0.00 to 0.68 mutation/per Mb with a median of 0.18 mutation/per Mb in TCGA cohort (**Figure S3A**), and the TMB score is ranging from 0.02 to 1.44 per Mb with a median of 0.17 per Mb in BeatAML cohort (**Figure S3B**). Also, patients with mutation in *TET2*, *RUNX1*, *IDH2*, *ASXL1*, *U2AF1*, *EZH2*, *PHF6*, and *RAD21* had higher TMB levels in BeatAML cohort (**Figure S3C**). We investigated the association of TMB with *NPM1* and *FLT3*, which were mutually exclusive genes of *TP53*, and found that *NPM1* mutation subtypes were significantly connected with TMB in BeatAML ($p < 0.001$) (**Figure S4**).

## *TP53* Mutations in Acute Myeloid Leukemia

The alteration frequencies of AML were 8.68% and 8.5% in BeatAML and TCGA cohort, respectively (**Figure 5A**). The patients of AML with myelodysplasia-related changes and therapy-related myeloid neoplasms had higher mutation rates (24.22% and 23.81%) (**Figure 5B**). Meanwhile, we compared *TP53* mutant subtypes and the *TP53* expression level, the results demonstrated that *TP53* mRNA expression was related to *TP53* mutant subtypes in TCGA ($p = 0.050$) (**Figure 5C**), while no differences were detected between each *TP53* group and the *TP53* expression level in BeatAML ($p = 0.201$) (**Figure S5**). **Figure 5D** exhibited Lollipop plot, generated by maftools, which showed

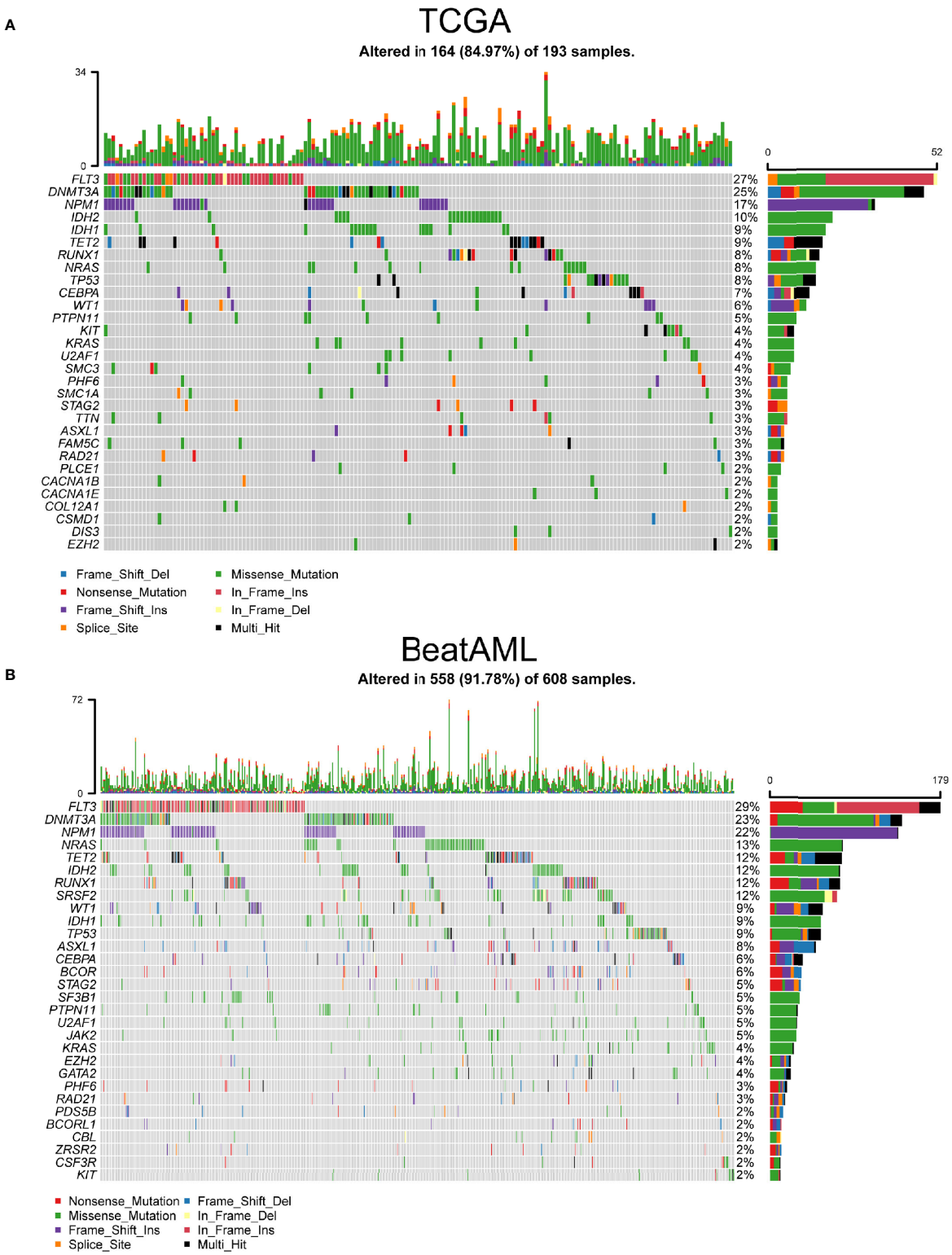


**FIGURE 1** | The most frequently mutated genes in acute myeloid leukemia (AML). **(A)** Waterfall plot of the frequently mutated genes in AML from The Cancer Genome Atlas (TCGA) cohort. **(B)** Oncoplot visualizing the frequently mutated genes in AML from BeatAML cohort. In the above two figures, top 30 mutated genes were ordered according to reducing mutation frequency from top to bottom. The upper panel presented mutation frequencies of genes. The bottom panel showed different gene mutation types.

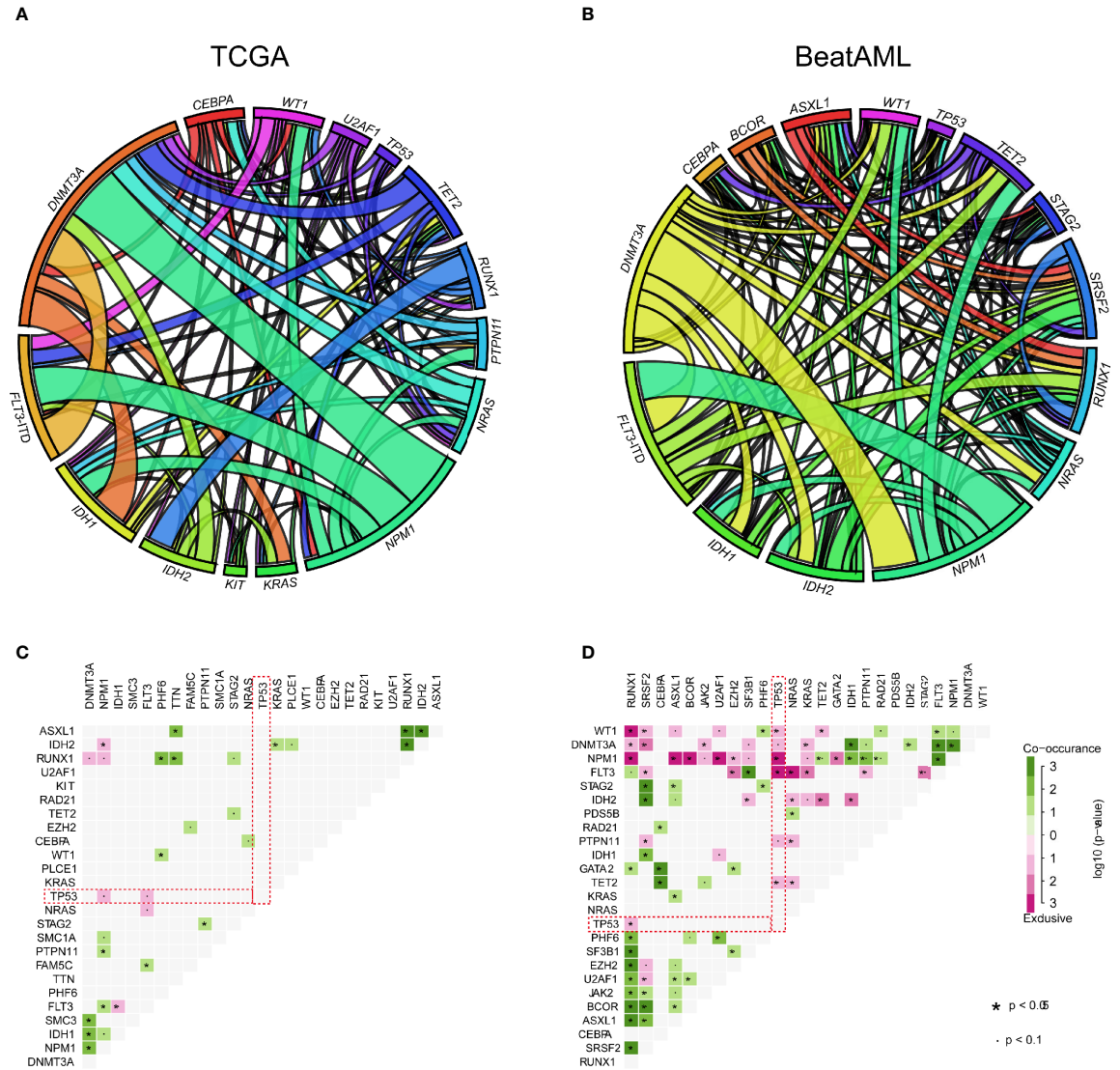


**FIGURE 2** | The relationship between common mutant genes in acute myeloid leukemia (AML). **(A, B)** Circos plot diagram showing the frequency of pairwise co-occurring gene mutations in AML from The Cancer Genome Atlas (TCGA) **(A)** and BeatAML **(B)** cohorts. The thickness of connecting lines between two genes denoted proportion of the number of such cases. **(C, D)** Gene pairs with co-occurrence or exclusiveness in their mutation pattern were illustrated as a triangular matrix in AML from TCGA **(C)** and BeatAML **(D)**. Green displayed tendency toward co-occurrence, whereas pink showed exclusiveness.

mutation distribution for *TP53* in AML. And *TP53* mutations mainly included missense mutation that exhibited a high proportion.

## *TP53* Mutations Are Associated With Tumor-Infiltrating Immune Cells

Tumor-infiltrating immune cells can illustrate either tumor-suppressive or tumor-promoting effects. We evaluated the relationship between *TP53* mutation and tumor-infiltrating immune cells in AML microenvironment using CIBERSORT algorithm. As shown in **Figure 6A**, we observed that resting memory CD4 T cells and resting NK cells were more enriched in *TP53* mutant type group from TCGA dataset ($p = 0.018$ and $p < 0.001$, respectively), while activated mast cells showed a tendency to be enriched in wild-type group ($p = 0.051$). Nevertheless, the *TP53* wild-type group had more naive CD4 T cells, activated mast cells, and eosinophils from BeatAML dataset ($p = 0.017$, $p = 0.022$, and $p = 0.033$, respectively) (**Figure 6B**). Besides, M2 macrophages had the tendency to be enriched in *TP53* wild-type group than *TP53* mutant group ($p = 0.05$), which would hamper the immune antitumor effect. Also, the *FLT3* mutant group had more M2 macrophages and eosinophils in both datasets (**Figure S6**). Likewise, eosinophils were more enriched in *NPM1* mutant group than *NPM1* wild-type group across two distinct datasets (**Figure S7**).

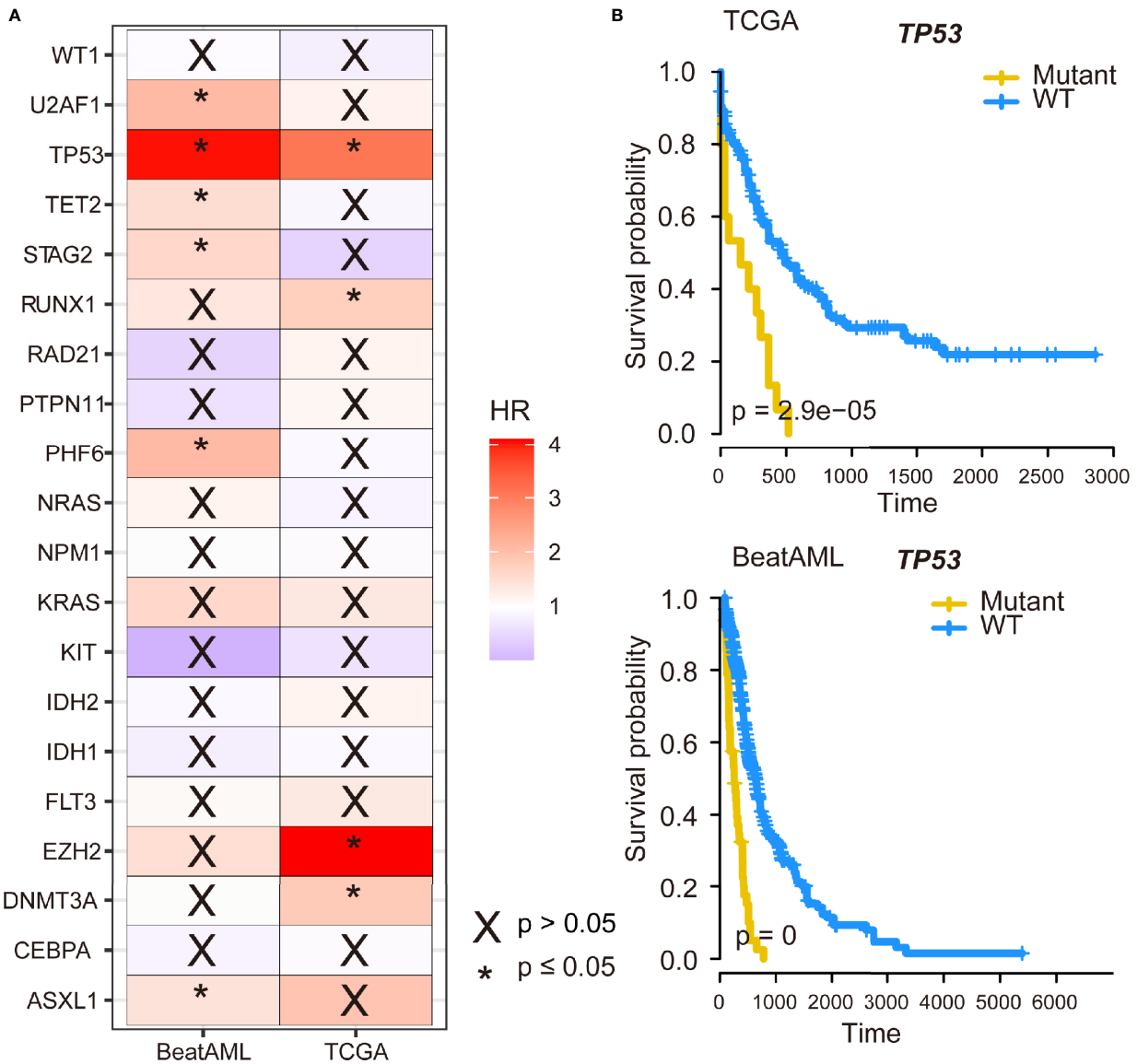


**FIGURE 3** | The impact of *TP53* mutation on survival of acute myeloid leukemia (AML) patients. **(A)** The 20 genes with the highest mutation frequency shared by The Cancer Genome Atlas (TCGA) and BeatAML datasets were subjected to Cox regression analysis. **(B)** Kaplan–Meier survival curves of *TP53* mutation on survival in AML.

Differences of CD8+ T cells between *TP53* mutated and wild-type were validated by multiple algorithms in pan-cancer, and CD8+ T cells were highly infiltrated in the *TP53* mutant group of TCGA AML dataset (**Figure 7A**). In immunotherapy prediction analysis with the online tool TIDE, *TP53* mutation was highly related to IFGN, Merck18, CD8, CD274, and dysfunction except for exclusion, which were widely used immunotherapy indicators (**Figures 7B–G**). *TET2*, *RUNX1*, *ASXL1*, *U2AF1*, and *PHF6* mutations presented increased TMB in both TCGA and BeatAML cohorts. We also evaluated the differences of CD8+ T cells of these gene mutated and wild–type groups; interestingly enough, no statistical difference was found in AML and other cancers (**Figure S8**).

## Enrichment Pathway Analysis of *TP53* Mutation

To further explore the difference between *TP53* mutant and wild-type groups, we performed GSEA based on RNA sequencing (RNA-seq) data from TCGA, which showed a prominent enrichment in *TP53* mutant group of signatures related to wnt beta catenin signaling, IL2 signal transducer and activator of transcription (stat)5 signaling, notch signaling, and inflammatory response (**Figure 8A**). These findings indicated that samples with *TP53* mutation upregulated signaling pathways involved in the immune system. Also, our results confirmed and extended the above findings (**Figure 8B**): 1) A set of genes that caused characteristic

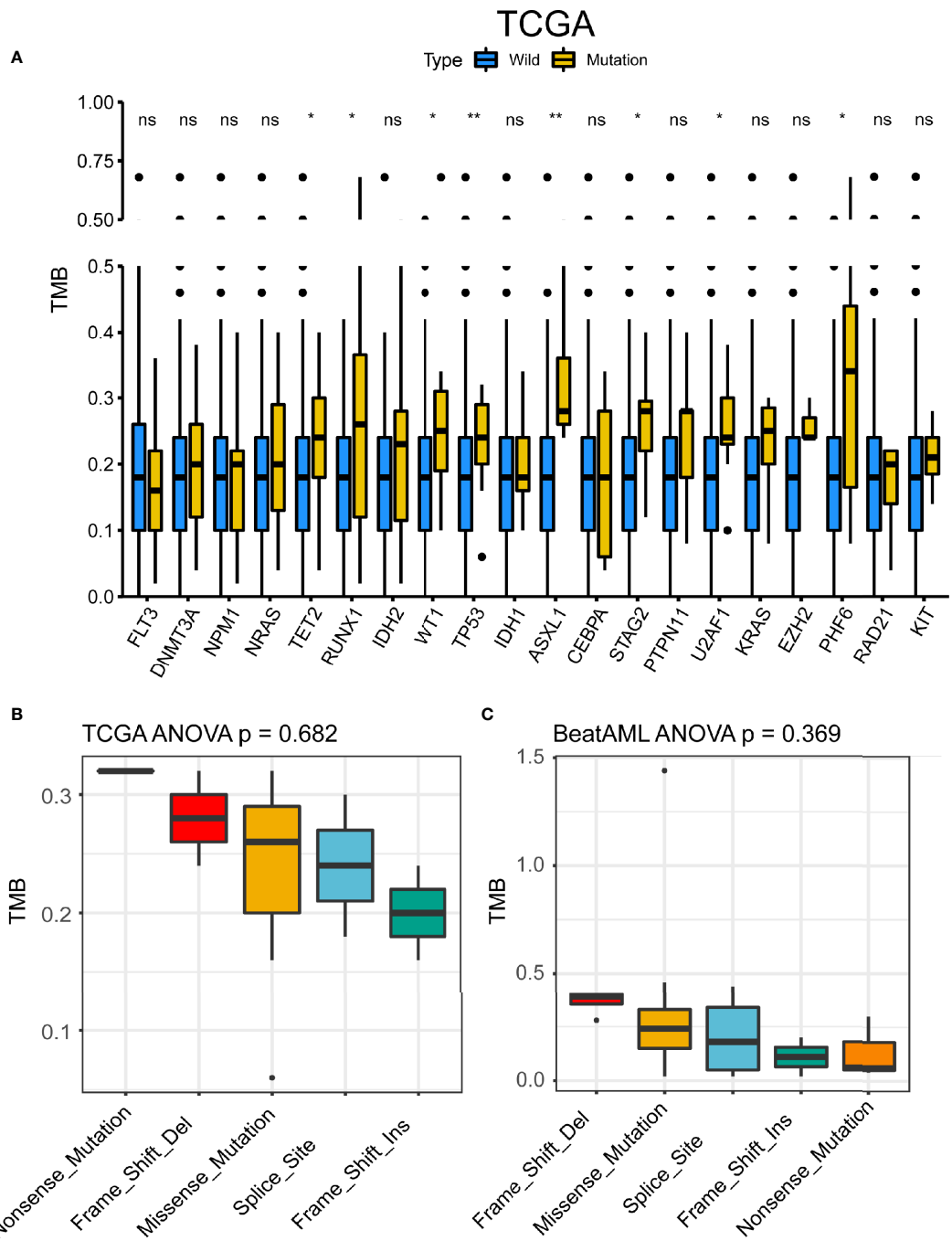


**FIGURE 4** | *TP53* mutation was associated with tumor mutational burden (TMB). **(A)** TMB differences between the mutant group and the wild-type group of the 20 genes with the highest mutation frequency shared by the two datasets in The Cancer Genome Atlas (TCGA). *p < 0.05, **p < 0.01, ns, not significant. **(B, C)** TMB differences of *TP53* mutant subtypes in TCGA **(B)** and BeatAML **(C)**.

downregulation after *KRAS* overexpression in the four epithelial cell lines was significantly enriched in the *TP53* mutant group. 2) *TP53* mutant group showed significant enrichment of genes downregulated in C57MG cells (mammary epithelium) by overexpression of *WNT1* gene. 3) *TP53* mutant group revealed enrichment of genes upregulated in HCT116 cells (colon carcinoma) upon knockdown of *PTEN* by RNAi. Together, these results further demonstrated that *TP53* mutation was associated with distinct molecular features in AML. For the C7 immunologic collection, the *TP53* mutated group had strong enrichment in genes downregulated in monocytes compared to macrophages treated with interleukin (IL)-4 (**Figure 8C**).

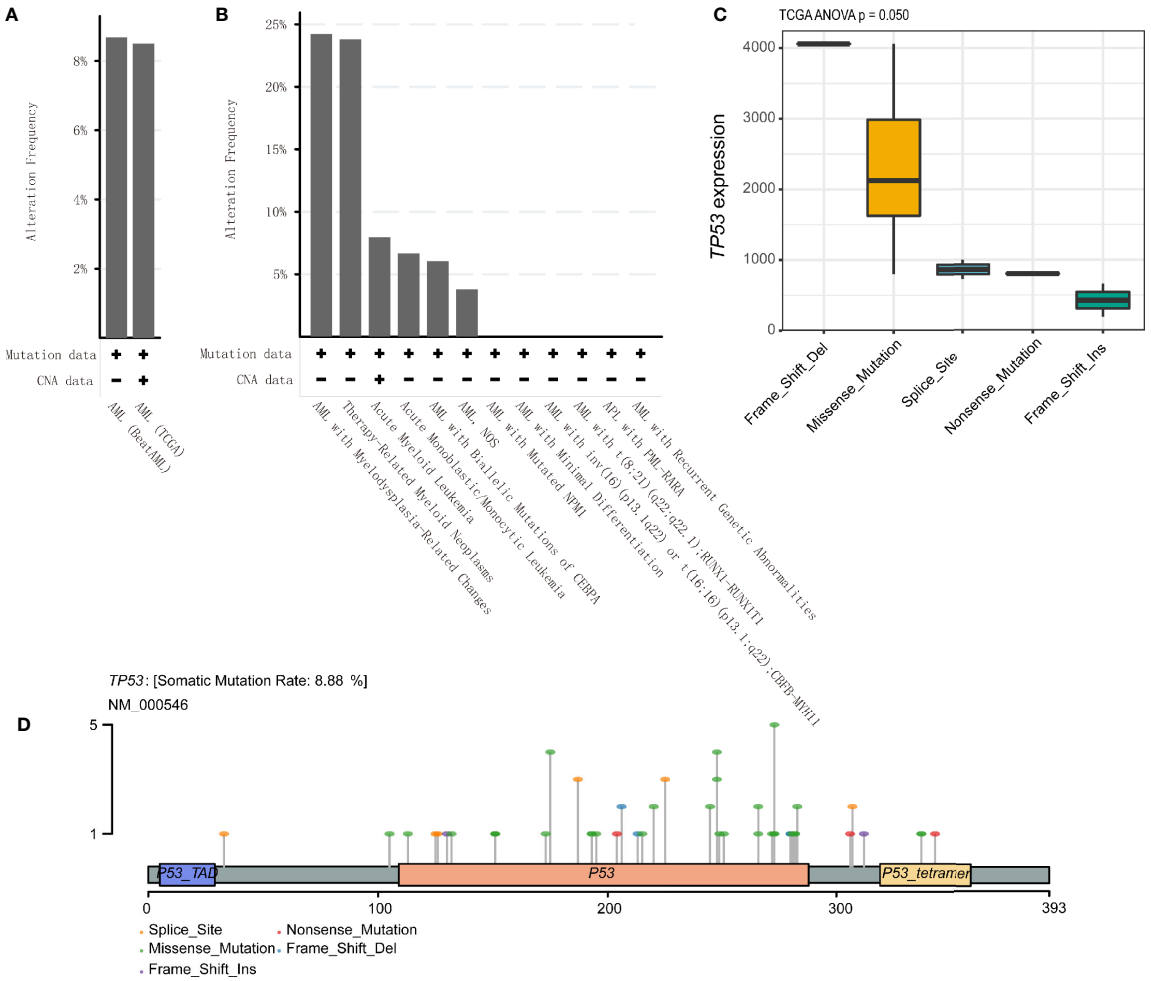


**FIGURE 5** | *TP53* alteration frequencies and location in acute myeloid leukemia (AML). **(A, B)** *TP53* alteration frequencies in AML were shown. **(C)** Correlation of *TP53* mutation status with *TP53* mRNA expression level in AML patients based on the analysis of The Cancer Genome Atlas (TCGA) database. **(D)** Lollipop plot indicating location and type of *TP53* mutation in AML. Circles representing individual mutations had distinct colored markings for different types of mutations.

## DISCUSSION

*TP53*, located on chromosome 17p13.1, encodes a 393-amino acid phosphoprotein and acts as a transcription factor with pivotal tumor suppressor functionality (25). *TP53* mutations are observed in about half of all cancers (26). However, compared with solid tumors, *TP53* mutations are rare and closely associated with AML with complex karyotype (13, 27, 28). Our findings underlined the poor prognostic impact of *TP53* mutation in AML patients. This observation was largely consistent with published data (18). AML patients with *TP53* mutations have dismal outcomes, with median OS of 5–9 months and complete remission (CR) rates of 20%–40% (18, 29–31). The mutation frequency of *TP53* is much higher in therapy-related AML (t-AML) than in *de novo* AML. The P53 protein contains three key regions: the N-terminal region, the central DNA-binding domain (DBD), and the C-terminal region (32). Meanwhile, most *TP53* mutations fall within the DBD (32).

High TMB has been proposed as a leading candidate biomarker for response to immunotherapy based on the underlying assumption that tumor mutations will generate antigenic peptides, allowing for enhanced immunogenicity (33, 34). Compared to highly mutated solid tumors, AML has low mutational burdens, with the exception of cases harboring mutations involving DNA mismatch repair genes (35). Nonetheless, profiling of AML patients relapsing after allogeneic hematopoietic stem cell transplantation displayed that T-cell exhaustion was a crucial contributor to failure of the leukemia relapse (36, 37), indicating that ICI can also be an appealing strategy for treatment of these patients. *TP53* mutations showed higher TMB levels in TCGA cohort of this study. We speculated that *TP53* mutation might participate in the immune response.

The biology of a tumor can only be understood by tumor-intrinsic alterations and the tumor microenvironment, especially the immune cells (38). Immune cells in the tumor immune microenvironment play a critical role in tumorigenesis, and

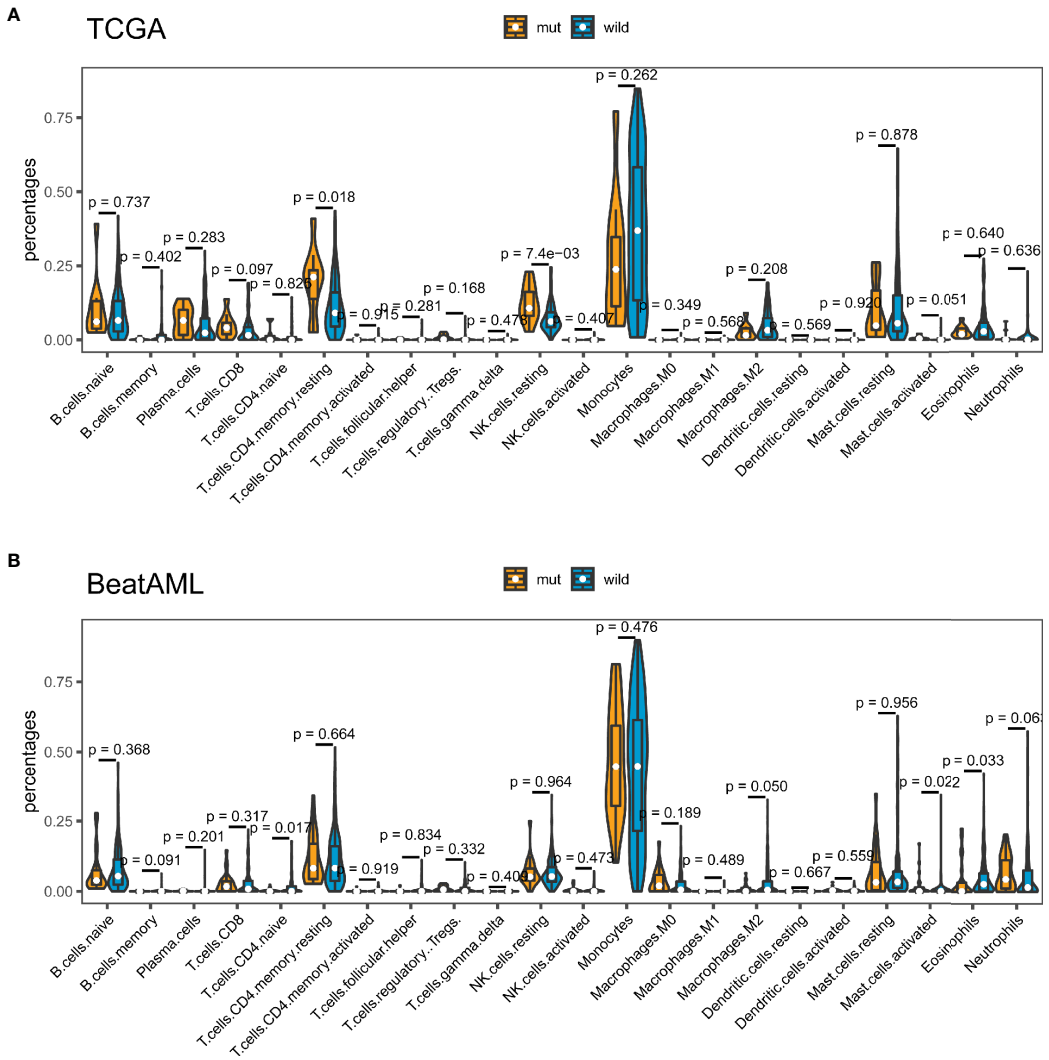


**FIGURE 6** | *TP53* mutation was related to tumor-infiltrating immune cells. Violin plots displayed the differences in the immune cell distribution between *TP53* mutant group and *TP53* wild-type group in The Cancer Genome Atlas (TCGA) cohort **(A)** and BeatAML cohort **(B)**.

tumor-related immune cells can act as antagonizing or promoting tumors. Apart from the recognition of the crucial role of the immune system in oncogenesis, tumor progression, and therapy response, more and more attention has been attracted by the potential predictive role of immune infiltration. For example, cytotoxic CD8+ T cells act as an indicator of favorable outcome in colorectal, ovarian, and esophageal cancer, whereas immunosuppressive cells such as Tregs and M2-polarized tumor-associated macrophages (TAMs) predict worse prognosis in several cancer types (39). Therefore, we need to investigate and understand the overall characteristics of the tumor immune microenvironment. In our study, *TP53* mutant group exhibited higher CD8+ T cell infiltration compared with *TP53* wild-type group in AML. However, no difference was found between *TET2*, *RUNX1*, *ASXL1*, *U2AF1*, and *PHF6* mutant and wild-type groups in AML and other cancers. And *TP53* mutation plays a key role in activating genes involved in immune responses and inflammation (40). Also, resting memory CD4 T cells and resting NK cells were found to be enriched in *TP53* mutant group, while naive CD4 T cells, activated mast cells, and eosinophils were more increased in *TP53* wild-type group. It is reported that resting memory CD4+ T cells are often related to prognosis of malignant tumor diseases, such as head and neck squamous cell carcinoma (41) and bladder cancer (42). Compared to naive T cells, memory CD4+ T cells show higher numbers, display distinct trafficking behaviors, and generally have faster effector function following reinfection (43). And NK cells were involved in tumor immune surveillance (44). Hsu et al. (45) proposed that blocking PD-1/PD-L1 may activate NK cells that were indispensable for the treatment effect of these therapies. Mast cells had higher proportions in *TP53* wild-type group than *TP53* mutant group in this study. It was reported that tumor-associated mast cells (TAMCs) were components of the microenvironment

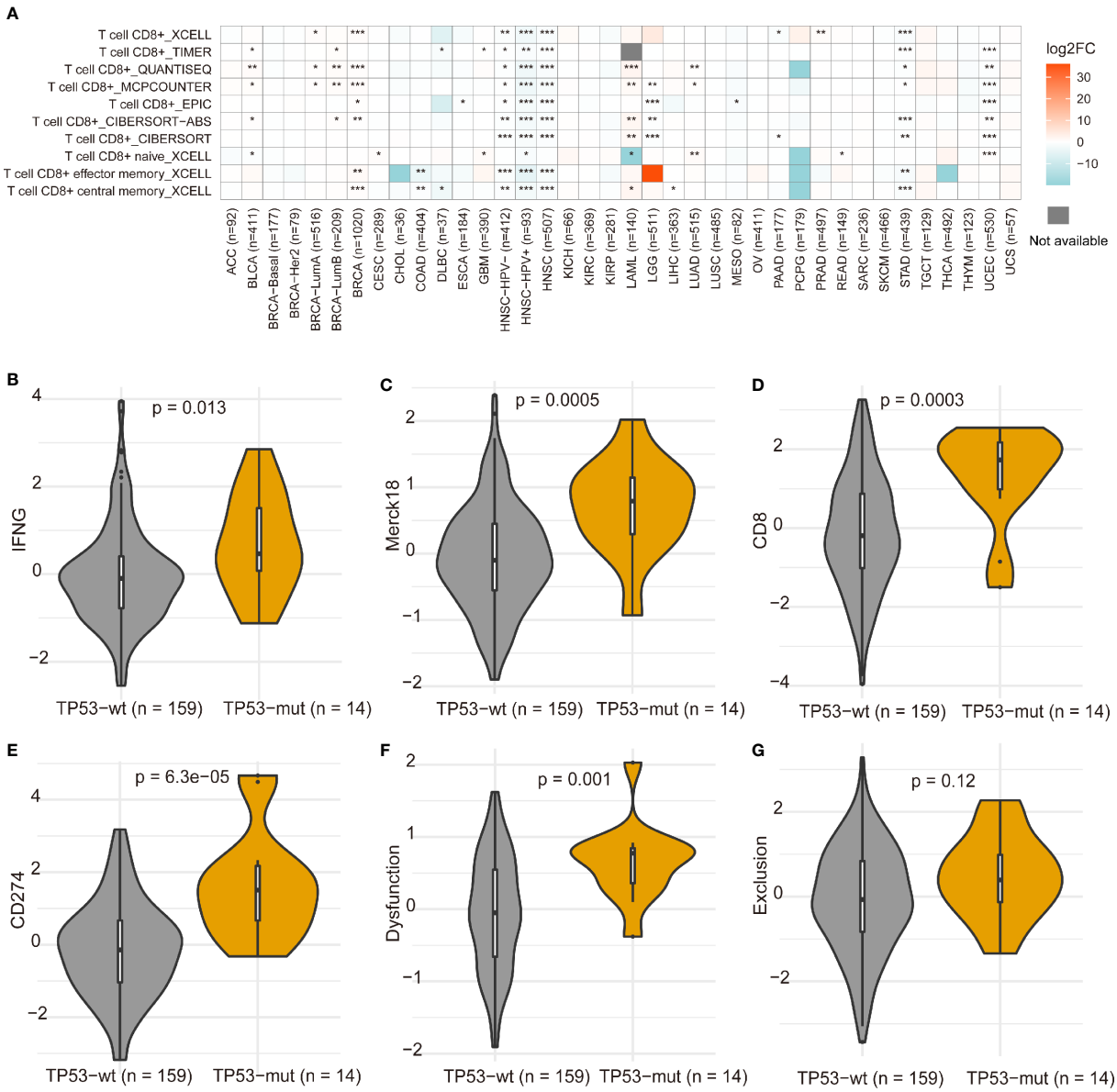


**FIGURE 7** | Differences of CD8+ T cells between *TP53* mutation and wild-type in pan-cancer **(A)**. *p < 0.05, **p < 0.01, ***p < 0.001. The differences of gene expression signatures calculated using TIDE between *TP53* mutant and non-mutant groups **(B–G)**. The immunotherapy clinical response prediction performance of TP53 mutant group and TP53 wild-type group was compared with those of the following biomarkers: IFGN, Merck18, CD8, CD274, dysfunction, and exclusion.

of hematologic human tumors (46). And mast cells owed both tumor-promoting and tumor-suppressive roles, which depend on local stromal conditions (47).

Our study revealed that IL-2 stat5 signaling was enriched in *TP53* mutant group. IL-2 was involved in Treg-mediated immunosuppressive mechanisms, and transforming growth factor (TGF)-β1 activates STAT5 binding to the promoter of Foxp3 to induce the differentiation of Tregs *via* IL-2 (48, 49). It indicated that *TP53* mutation may upregulate signaling pathways involved in the immune system. Further research is needed to study the underlying mechanism. *TP53* mutant groups showed significant enrichment of genes downregulated in C57MG cells (mammary epithelium) by overexpression of *WNT1* gene, and a prominent enrichment of signatures related to wnt beta catenin signaling in the present study. Deregulation of Wnt/β-catenin signaling is well-connected with AML initiation and progression and important to leukemia stem cell (LSC) self-renewal and survival (50, 51). Our results were further evidence that *TP53* mutation was associated with cancer hallmarks.

We analyzed the somatic mutation landscape of 164 AML samples from TCGA dataset and 558 AML patients from BeatAML dataset. We discovered that *TP53* was frequently

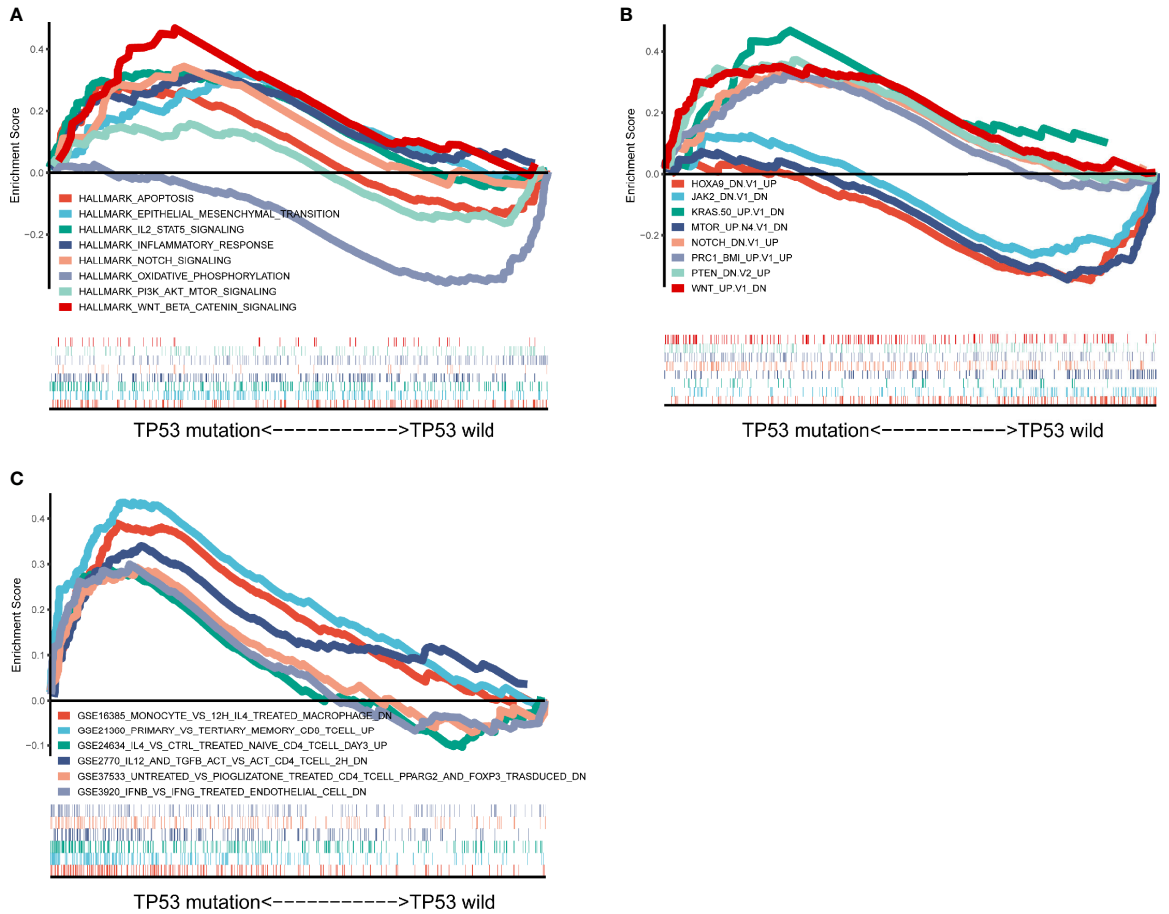


**FIGURE 8** | Significantly enriched pathways associated with *TP53* mutation. Gene set enrichment analyses were carried out with The Cancer Genome Atlas (TCGA) based on analysis of Hallmark gene sets **(A)**, curated gene sets **(B)**, and immunologic signature gene sets **(C)**.

mutated in both TCGA and BeatAML cohorts, and its mutation displayed exclusiveness with other common mutated genes and was associated with poor prognosis, TMB, and immune microenvironment. Further experiments are required to verify the relationship between *TP53* and TMB and immune infiltration in AML. Also, in view of the fact that CD8+ T cells showed high infiltration in the *TP53* mutant group of LAML, our findings therefore inspire further studies of T cell–targeting immunotherapeutic approaches in *TP53*-mutated AML. We consider co-cultivating T cells with *TP53* mutant and wild-type cells, then use flow cytometry, Cell Counting Kit-8 (CCK8), and other experiments to detect cytokines, cell proliferation and invasion, and so on in the following research to further validate these findings.

## DATA AVAILABILITY STATEMENT

The original contributions presented in the study are included in the article/**Supplementary Material**. Further inquiries can be directed to the corresponding authors.

## AUTHOR CONTRIBUTIONS

JQ conceived and designed the research. Z-JX and J-CM collected and analyzed data. X-MW, YJ, and P-HX prepared the figures and performed data analysis. X-MW and Z-JX drafted the article. JL and WQ participated in study supervision. All authors contributed to the article and approved the submitted version.

## FUNDING

This study was supported by the National Natural Science Foundation of China (81970118, 81900163), Medical Innovation Team of Jiangsu Province (CXTDB2017002), Zhenjiang Clinical Research Center of Hematology (SS2018009), Social Development Foundation of Zhenjiang (SH2019065, SH2019067), and Scientific Research Project of The Fifth 169 Project of Zhenjiang (21).

## SUPPLEMENTARY MATERIAL

The Supplementary Material for this article can be found online at: https://www.frontiersin.org/articles/10.3389/fimmu.2021.717527/full#supplementary-material

**Supplementary Figure 1 |** The most frequently mutated genes in AML. Venn diagram showing the overlap of frequently mutated genes covered by both TCGA and BeatAML cohorts.

**Supplementary Figure 2 |** Association of mutated genes with prognosis by Kaplan–Meier analysis. **(A)** *DNMT3A* mutation and *RUNX1* mutation were significantly correlated with poor outcome in TCGA cohort. **(B)** Kaplan-Meier survival analysis classified by *TET2* and *U2AF1* mutation status in BeatAML cohort.

**Supplementary Figure 3 |** Gene mutations were associated with TMB. **(A, B)** The range of TMB among mutated genes in TCGA **(A)** and BeatAML **(B)** cohorts. **(C)** Most gene mutations were associated with a higher TMB in BeatAML cohort. $^{*}p < 0.05$, $^{**}p < 0.01$, $^{***}p < 0.001$.

**Supplementary Figure 4 |** The association of *FLT3* and *NPM1* mutations with TMB in both TCGA and BeatAML cohorts.

**Supplementary Figure 5 |** Relationship between *TP53* mutation status and *TP53* mRNA expression level in BeatAML database.

**Supplementary Figure 6 |** Correlation of *FLT3* mutations with tumor-infiltrating immune cells in both TCGA and BeatAML cohorts.

**Supplementary Figure 7 |** The association of *NPM1* mutations with tumor-infiltrating immune cells in both TCGA and BeatAML cohorts.

**Supplementary Figure 8 |** Differences of CD8+ T cells between *TET2*, *RUNX1*, *ASXL1*, *U2AF1* and *PHF6* mutant and wild groups in pan-cancer calculated using TIDE.

**Supplementary Tables 1 and 2 |** Summary of the maf file, which displays number of variants in each gene of TCGA and BeatAML cohorts.

**Supplementary Tables 3 and 4 |** Original data with somatic genomic interactions from TCGA and BeatAML cohorts **(Figures 2C, D)**.

**Supplementary Tables 5 and 6 |** Original data used for Circos plot diagram **(Figures 2A, B)** from TCGA and BeatAML cohorts.

## REFERENCES


1. Finck A, Gill SI, June CH. Cancer Immunotherapy Comes of Age and Looks for Maturity. *Nat Commun* (2020) 11:3325. doi: 10.1038/s41467-020-17140-5
2. Wolchok J D, Chiarion-Sileni V, Gonzalez R, Rutkowski P, Grob JJ, Cowey CL, et al. Overall Survival With Combined Nivolumab and Ipilimumab in Advanced Melanoma. *N Engl J Med* (2017) 377:1345–56. doi: 10.1056/NEJMoa1709684
3. Overman M J, McDermott R, Leach JL, Lonardi S, Lenz HJ, Morse MA, et al. Nivolumab in Patients With Metastatic DNA Mismatch Repair-Deficient or Microsatellite Instability-High Colorectal Cancer (CheckMate 142): An Open-Label, Multicentre, Phase 2 Study. *Lancet Oncol* (2017) 18:1182–91. doi: 10.1016/S1470-2045(17)30422-9
4. Chung C H, Bonomi M, Steuer CE, Li J, Bhateja P, Johnson M, et al. Concurrent Cetuximab and Nivolumab as a Second-Line or Beyond Treatment of Patients With Recurrent and/or Metastatic Head and Neck Squamous Cell Carcinoma: Results of Phase I/II Study. *Cancers (Basel)* (2021) 13:1180. doi: 10.3390/cancers13051180
5. Topalian S L, Hodi FS, Brahmer JR, Gettinger SN, Smith DC, McDermott DF, et al. Safety, Activity, and Immune Correlates of Anti-PD-1 Antibody in Cancer. *N Engl J Med* (2012) 366:2443–54. doi: 10.1056/NEJMoa1200690
6. Metzeler K H, Herold T, Rothenberg-Thurley M, Amler S, Sauerland MC, Gorlich D, et al. Spectrum and Prognostic Relevance of Driver Gene Mutations in Acute Myeloid Leukemia. *Blood* (2016) 128:686–98. doi: 10.1182/blood-2016-01-693879
7. Hobo W, Hutten TJA, Schaap NPM, Dolstra H. Immune Checkpoint Molecules in Acute Myeloid Leukaemia: Managing the Double-Edged Sword. *Br J Haematol* (2018) 181:38–53. doi: 10.1111/bjh.15078
8. Stahl M, Goldberg AD. Immune Checkpoint Inhibitors in Acute Myeloid Leukemia: Novel Combinations and Therapeutic Targets. *Curr Oncol Rep* (2019) 21:37. doi: 10.1007/s11912-019-0781-7
9. Davids M S, Kim HT, Bachireddy P, Costello C, Liguori R, Savell A, et al. Ipilimumab for Patients With Relapse After Allogeneic Transplantation. *N Engl J Med* (2016) 375:143–53. doi: 10.1056/NEJMoa1601202
10. Chen C T, Wang PP, Mo WJ, Zhang YP, Zhou W, Deng TF, et al. Expression Profile Analysis of Prognostic Long non-Coding RNA in Adult Acute Myeloid Leukemia by Weighted Gene Co-Expression Network Analysis (WGCNA). *J Cancer* (2019) 10:4707–18. doi: 10.7150/jca.31234
11. Vitale M G, Pipitone S, Venturelli M, Baldessari C, Porta C, Iannuzzi F, et al. Correlation Between Immune-Related Adverse Event (IRAE) Occurrence and Clinical Outcome in Patients With Metastatic Renal Cell Carcinoma (mRCC) Treated With Nivolumab: IRAENE Trial, an Italian Multi-Institutional Retrospective Study. *Clin Genitourin Cancer* (2020) 18:477–88. doi: 10.1016/j.clgc.2020.05.010
12. Chalmers Z R, Connelly CF, Fabrizio D, Gay L, Ali SM, Ennis R, et al. Analysis of 100,000 Human Cancer Genomes Reveals the Landscape of Tumor Mutational Burden. *Genome Med* (2017) 9:34. doi: 10.1186/s13073-017-0424-2
13. Eisfeld A K, Mrozek K, Kohlschmidt J, Nicolet D, Orwick S, Walker CJ, et al. The Mutational Oncoprint of Recurrent Cytogenetic Abnormalities in Adult Patients With De Novo Acute Myeloid Leukemia. *Leukemia* (2017) 31:2211–8. doi: 10.1038/leu.2017.86
14. Biernacki M A, Bleakley M. Neoantigens in Hematologic Malignancies. *Front Immunol* (2020) 11:121. doi: 10.3389/fimmu.2020.00121
15. Frikeche J, Clavert A, Delaunay J, Brissot E, Gregoire M, Gaugler B, et al. Impact of the Hypomethylating Agent 5-Azacytidine on Dendritic Cells Function. *Exp Hematol* (2011) 39:1056–63. doi: 10.1016/j.exphem.2011.08.004
16. Kopp L M, Ray A, Denman CJ, Senyukov VS, Somanchi SS, Zhu S, et al. Decitabine has a Biphasic Effect on Natural Killer Cell Viability, Phenotype, and Function Under Proliferative Conditions. *Mol Immunol* (2013) 54:296–301. doi: 10.1016/j.molimm.2012.12.012
17. Gao X N, Lin J, Wang LL, Yu L. Demethylating Treatment Suppresses Natural Killer Cell Cytolytic Activity. *Mol Immunol* (2009) 46:2064–70. doi: 10.1016/j.molimm.2009.02.033
18. Rucker F G, Schlenk RF, Bullinger L, Kayser S, Teleanu V, Kett H, et al. TP53 Alterations in Acute Myeloid Leukemia With Complex Karyotype Correlate With Specific Copy Number Alterations, Monosomal Karyotype, and Dismal Outcome. *Blood* (2012) 119:2114–21. doi: 10.1182/blood-2011-08-375758
19. Kadia T M, Jain P, Ravandi F, Garcia-Manero G, Andreef M, Takahashi K, et al. TP53 Mutations in Newly Diagnosed Acute Myeloid Leukemia: Clinicomolecular Characteristics, Response to Therapy, and Outcomes. *Cancer* (2016) 122:3484–91. doi: 10.1002/cncr.30203
20. Dong Z Y, Zhong WZ, Zhang XC, Su J, Xie Z, Liu SY, et al. Potential Predictive Value of TP53 and KRAS Mutation Status for Response to PD-1 Blockade Immunotherapy in Lung Adenocarcinoma. *Clin Cancer Res* (2017) 23:3012–24. doi: 10.1158/1078-0432.Ccr-16-2554
21. Thorsson V, Gibbs DL, Brown SD, Wolf D, Bortone DS, Ou Yang TH, et al. The Immune Landscape of Cancer. *Immun* (2018) 48:812–30.e14. doi: 10.1016/j.immuni.2018.03.023
22. Tyner J W, Tognon CE, Bottomly D, Wilmot B, Kurtz SE, Savage SL, et al. Functional Genomic Landscape of Acute Myeloid Leukaemia. *Nature* (2018) 562:526–31. doi: 10.1038/s41586-018-0623-z
23. Law C W, Chen Y, Shi W, Smyth GK. Voom: Precision Weights Unlock Linear Model Analysis Tools for RNA-Seq Read Counts. *Genome Biol* (2014) 15:R29. doi: 10.1186/gb-2014-15-2-r29
24. Newman A M, Liu CL, Green MR, Gentles AJ, Feng W, Xu Y, et al. Robust Enumeration of Cell Subsets From Tissue Expression Profiles. *Nat Methods* (2015) 12:453–7. doi: 10.1038/nmeth.3337

25. Levine AJ. P53, the Cellular Gatekeeper for Growth and Division. *Cell* (1997) 88:323–31. doi: 10.1016/s0092-8674(00)81871-1
26. Vousden K H, Lu X. Live or Let Die: The Cell's Response to P53. *Nat Rev Cancer* (2002) 2:594–604. doi: 10.1038/nrc864
27. Ok C Y, Patel KP, Garcia-Manero G, Routbort MJ, Fu B, Tang G, et al. Mutational Profiling of Therapy-Related Myelodysplastic Syndromes and Acute Myeloid Leukemia by Next Generation Sequencing, a Comparison With De Novo Diseases. *Leuk Res* (2015) 39:348–54. doi: 10.1016/j.leukres.2014.12.006
28. Bowen D, Groves MJ, Burnett AK, Patel Y, Allen C, Green C, et al. TP53 Gene Mutation Is Frequent in Patients With Acute Myeloid Leukemia and Complex Karyotype, and Is Associated With Very Poor Prognosis. *Leukemia* (2009) 23:203–6. doi: 10.1038/leu.2008.173
29. Mrozek K, Eisfeld AK, Kohlschmidt J, Carroll AJ, Walker CJ, Nicolet D, et al. Complex Karyotype in De Novo Acute Myeloid Leukemia: Typical and Atypical Subtypes Differ Molecularly and Clinically. *Leukemia* (2019) 33:1620–34. doi: 10.1038/s41375-019-0390-3
30. Stengel A, Kern W, Haferlach T, Meggendorfer M, Fasan A, Haferlach C. The Impact of TP53 Mutations and TP53 Deletions on Survival Varies Between AML, ALL, MDS and CLL: An Analysis of 3307 Cases. *Leukemia* (2017) 31:705–11. doi: 10.1038/leu.2016.263
31. Mims A S, Kohlschmidt J, Eisfeld AK, Mromicronzek K, Blachly JS, Orwick S, et al. Comparison of Clinical and Molecular Characteristics of Patients With Acute Myeloid Leukemia and Either TP73 or TP53 Mutations. *Leukemia* (2021) 35:1188–92. doi: 10.1038/s41375-020-1007-6
32. Bode A M, Dong Z. Post-Translational Modification of P53 in Tumorigenesis. *Nat Rev Cancer* (2004) 4:793–805. doi: 10.1038/nrc1455
33. Chan T A, Yarchoan M, Jaffee E, Swanton C, Quezada SA, Stenzinger A, et al. Development of Tumor Mutation Burden as an Immunotherapy Biomarker: Utility for the Oncology Clinic. *Ann Oncol* (2019) 30:44–56. doi: 10.1093/annonc/mdy495
34. Cristescu R, Mogg R, Ayers M, Albright A, Murphy E, Yearley J, et al. Pan-Tumor Genomic Biomarkers for PD-1 Checkpoint Blockade-Based Immunotherapy. *Science* (2018) 362:eaar3593. doi: 10.1126/science.aar3593
35. Lawrence M S, Stojanov P, Polak P, Kryukov GV, Cibulskis K, Sivachenko A, et al. Mutational Heterogeneity in Cancer and the Search for New Cancer-Associated Genes. *Nature* (2013) 499:214–8. doi: 10.1038/nature12213
36. Noviello M, Manfredi F, Ruggiero E, Perini T, Oliveira G, Cortesi F, et al. Bone Marrow Central Memory and Memory Stem T-Cell Exhaustion in AML Patients Relapsing After HSCT. *Nat Commun* (2019) 10:1065. doi: 10.1038/s41467-019-08871-1
37. Toffalori C, Zito L, Gambacorta V, Riba M, Oliveira G, Bucci G, et al. Immune Signature Drives Leukemia Escape and Relapse After Hematopoietic Cell Transplantation. *Nat Med* (2019) 25:603–11. doi: 10.1038/s41591-019-0400-z
38. Hanahan D. Weinberg R A. Hallmarks of Cancer: The Next Generation. *Cell* (2011) 144:646–74. doi: 10.1016/j.cell.2011.02.013
39. Senovilla L, Vacchelli E, Galon J, Adjemian S, Eggermont A, Fridman WH, et al. Trial Watch: Prognostic and Predictive Value of the Immune Infiltrate in Cancer. *Oncoimmunology* (2012) 1:1323–43. doi: 10.4161/onci.22009
40. Munoz-Fontela C, Mandinova A, Aaronson SA, Lee SW. Emerging Roles of P53 and Other Tumour-Suppressor Genes in Immune Regulation. *Nat Rev Immunol* (2016) 16:741–50. doi: 10.1038/nri.2016.99
41. She Y, Kong X, Ge Y, Yin P, Liu Z, Chen J, et al. Immune-Related Gene Signature for Predicting the Prognosis of Head and Neck Squamous Cell Carcinoma. *Cancer Cell Int* (2020) 20:22. doi: 10.1186/s12935-020-1104-7
42. Zhang Y, Ou DH, Zhuang DW, Zheng ZF, Lin ME. In Silico Analysis of the Immune Microenvironment in Bladder Cancer. *BMC Cancer* (2020) 20:265. doi: 10.1186/s12885-020-06740-5
43. Chang J T, Wherry EJ, Goldrath AW. Molecular Regulation of Effector and Memory T Cell Differentiation. *Nat Immunol* (2014) 15:1104–15. doi: 10.1038/ni.3031
44. Malmberg K J, Carlsten M, Bjorklund A, Sohlberg E, Bryceson YT, Ljunggren HG. Natural Killer Cell-Mediated Immunosurveillance of Human Cancer. *Semin Immunol* (2017) 31:20–9. doi: 10.1016/j.smim.2017.08.002
45. Hsu J, Hodgins JJ, Marathe M, Nicolai CJ, Bourgeois-Daigneault MC, Trevino TN, et al. Contribution of NK Cells to Immunotherapy Mediated by PD-1/PD-L1 Blockade. *J Clin Invest* (2018) 128:4654–68. doi: 10.1172/JCI99317
46. Andersen M D, Kamper P, Nielsen PS, Bendix K, Riber-Hansen R, Steiniche T, et al. Tumour-Associated Mast Cells in Classical Hodgkin's Lymphoma: Correlation With Histological Subtype, Other Tumour-Infiltrating Inflammatory Cell Subsets and Outcome. *Eur J Haematol* (2016) 96:252–9. doi: 10.1111/ejh.12583
47. Theoharides T C, Conti P. Mast Cells: The Jekyll and Hyde of Tumor Growth. *Trends Immunol* (2004) 25:235–41. doi: 10.1016/j.it.2004.02.013
48. Sakaguchi S, Yamaguchi T, Nomura T, Ono M. Regulatory T Cells and Immune Tolerance. *Cell* (2008) 133:775–87. doi: 10.1016/j.cell.2008.05.009
49. Yang T T, Song SJ, Xue HB, Shi DF, Liu CM, Liu H. Regulatory T Cells in the Pathogenesis of Type 2 Diabetes Mellitus Retinopathy by miR-155. *Eur Rev Med Pharmacol Sci* (2015) 19:2010–5.
50. Lane S W, Wang YJ, Lo Celso C, Ragu C, Bullinger L, Sykes SM, et al. Differential Niche and Wnt Requirements During Acute Myeloid Leukemia Progression. *Blood* (2011) 118:2849–56. doi: 10.1182/blood-2011-03-345165
51. Dietrich P A, Yang C, Leung HH, Lynch JR, Gonzales E, Liu B, et al. GPR84 Sustains Aberrant Beta-Catenin Signaling in Leukemic Stem Cells for Maintenance of MLL Leukemogenesis. *Blood* (2014) 124:3284–94. doi: 10.1182/blood-2013-10-532523


**Conflict of Interest:** The authors declare that the research was conducted in the absence of any commercial or financial relationships that could be construed as a potential conflict of interest.

frontiers in Immunology

REVIEW
published: 18 November 2021
doi: 10.3389/fimmu.2021.737340

# Mechanisms of Immunosuppressive Tumor Evasion: Focus on Acute Lymphoblastic Leukemia

*Silvia Jiménez-Morales*[1*], *Ivan Sammir Aranda-Uribe*[1,2], *Carlos Jhovani Pérez-Amado*[1,3], *Julian Ramírez-Bello*[4] *and Alfredo Hidalgo-Miranda*[1]

[1] Laboratorio de Genómica del Cáncer, Instituto Nacional de Medicina Genómica, Mexico City, Mexico, [2] Departamento de Farmacología, División de Ciencias de la Salud, Universidad de Quintana Roo, Quintana Roo, Mexico, [3] Programa de Doctorado en Ciencias Bioquímicas, Universidad Nacional Autónoma de México, Mexico City, Mexico, [4] Departamento de Endocrinología, Instituto Nacional de Cardiología Ignacio Chávez, Mexico City, Mexico

OPEN ACCESS

**Edited by:**
John Maher,
King's College London,
United Kingdom

**Reviewed by:**
Toshihiko Imamura,
Kyoto Prefectural University of Medicine, Japan
Rosana Pelayo,
Mexican Social Security Institute (IMSS), Mexico

***Correspondence:**
Silvia Jiménez-Morales
sjimenez@inmegen.gob.mx

**Specialty section:**
This article was submitted to Cancer Immunity and Immunotherapy, a section of the journal Frontiers in Immunology

**Received:** 06 July 2021
**Accepted:** 27 October 2021
**Published:** 18 November 2021

**Citation:**
Jiménez-Morales S, Aranda-Uribe IS, Pérez-Amado CJ, Ramírez-Bello J and Hidalgo-Miranda A (2021) Mechanisms of Immunosuppressive Tumor Evasion: Focus on Acute Lymphoblastic Leukemia. Front. Immunol. 12:737340. doi: 10.3389/fimmu.2021.737340

Acute lymphoblastic leukemia (ALL) is a malignancy with high heterogeneity in its biological features and treatments. Although the overall survival (OS) of patients with ALL has recently improved considerably, owing to the application of conventional chemotherapeutic agents, approximately 20% of the pediatric cases and 40–50% of the adult patients relapse during and after the treatment period. The potential mechanisms that cause relapse involve clonal evolution, innate and acquired chemoresistance, and the ability of ALL cells to escape the immune-suppressive tumor response. Currently, immunotherapy in combination with conventional treatment is used to enhance the immune response against tumor cells, thereby significantly improving the OS in patients with ALL. Therefore, understanding the mechanisms of immune evasion by leukemia cells could be useful for developing novel therapeutic strategies.

**Keywords: acute lymphoblastic leukemia, immunoediting, immunotherapy, tumor immune evasion, immune cells**

## INTRODUCTION

Acute lymphoblastic leukemia (ALL) is a group of lymphoid neoplasms derived from B- and T-lymphoid progenitors that are clinically and genetically heterogeneous (1–5). The incidence of ALL is rapidly growing worldwide, and it is estimated to be one in 100,000 persons/year globally (6, 7), with a peak prevalence between 1 and 4 years old (7, 8) and during the fifth decade of life (5, 9, 10). The overall survival (OS) for pediatric patients is >90% in high-income countries but is lower in middle- and low-income countries (11)—for instance, in Mexico, the global survival rate reported of children with ALL was 63.9%, the event-free survival rate was 52.3% after an average follow-up of

3.9 years (12), and it had a high rate of early mortality (12.1%) (13). Unfortunately, OS in adults with ALL is worst. Even though most adult patients can reach initial complete remission using recently developed treatments, only 40–50% (<20% in patients aged 60 years or older) of the 5-year OS is achieved (5, 14–17). Relapse, defined as the return of the disease in patients who reach initial complete remission, is one of the main obstacles in achieving improved survival rates (18) and occurs in approximately 20% of children and >50% of adults (19, 20). Most relapse incidences appear during treatment (early relapse: <30 months after diagnosis) or after treatment completion (late relapse: <2 years). Despite the use of diverse anticancer agent combinations (chemotherapy, radiotherapy, and allogeneic hematopoietic stem cell transplantation), patients who experience relapse have a higher probability of treatment failure and death (21). The survival rate of relapsed patients is approximately 50% and worse in relapsed cases where the central nervous system is affected (22–24). Cancer treatment has been based on the use of chemotherapeutic agents that are unable to differentiate between normal and cancer cells. Emerging therapeutic schemes to treat leukemia are based on the knowledge that the immune system plays an important role in tumor cell identification and elimination (25–28). In order to develop new anti-leukemic therapies, it is necessary to understand the mechanisms underlying the displacement of transformed hematopoietic cells by normal hematopoietic progenitors and the immune evasion processes by which the tumor cells hijack the immune system (25, 26). This review focuses on the mechanisms of immune system evasion of ALL cells and its potential for developing new treatments.

## IMMUNE SYSTEM AND TUMOR EVASION

The human immune system comprises leukocytes, bone marrow (BM), and other organs. Leukocytes include neutrophils, monocytes, eosinophils, basophils, dendritic cells, lymphocytes (T and B cells), and natural killer (NK) cells. By discriminating self from non-self, the human immune system is responsible for protecting the body from diseases caused by exogenous and endogenous agents. To differentiate between self or non-self, the immune system employs fundamental biochemical differences among cells, such as the absence of methylated cytosine residues in DNA and glycoprotein composition (29, 30). The two immune responses recognized are innate and acquired/adaptive (cell-mediated immunity and humoral immunity). The innate immune response, which is present from birth, activates a non-specific immune response in the presence of self-molecules, such as endogenous damage-associated molecular patterns (DAMPs), Toll-like receptor ligands, and non-self-molecules in a cytokine release-dependent manner (31). Acquired immune response involves antibody production by B cells and antigen presentation to T helper cells to stimulate cytotoxic T cells (CTLs), also known as CD8 + T cells, which induce the elimination of non-self elements and produce immune memory cells (30).

The cell-mediated immunity is activated when a specific CTL is stimulated to initiate the lysis of pathogens, infected cells, and tumor cells; thus, this protects the body against infection and tumor growth, spreading, and metastasis (31). To prevent tumor emergence, the immune system eliminates oncogenic viral infections, induces the inflammatory microenvironment, and destroys malignant cells (32, 33). Although tumor cells are self in origin, they differ from their normal counterparts in their biochemical and antigenic characteristics and biological behavior. Cancer cells express tumor-specific neoantigens that arise from an inefficient DNA damage repair system and which are presented to the CTLs by the human leukocyte antigen (HLA) system class I. Then, tumor cells are killed through a combination of direct perforin-dependent destruction and by increasing tumor immune sensitivity through the release of inflammatory cytokines, such as interferon (IFN) alpha (INF-α) and tumor necrosis factor (TNF) (30, 34, 35). However, tumor cells have an acquired mechanism to evade the immune system to avoid their destruction (**Figure 1**).

In 1908, Ehrlich proposed the role of the immune system in controlling cancer development. Later, Burnet (1957) suggested that lymphocytes are tasked with identifying and eliminating mutated cells (29, 30) and the presence of an immunological mechanism for eliminating or inactivating potentially dangerous mutant cells before tumor clinical manifestations, a concept called "immunological surveillance" (36). Currently, the role of the immune system in malignant cell elimination is unequivocally established. The quality control of the immune system to fight against tumor cells involves immune cells and their associated molecules, with the CTLs and NK cells being the major components (34, 37). These cells act as tumor suppressors by patrolling the human body and destroying transformed cells before tumor progression. The anti-tumor immune response attacks the tumor through activated lymphocytes to trigger apoptosis by producing perforin and granzyme B to damage the extracellular membrane and enter targeted tumor cells, expressing Fas-L, TNF-related apoptosis-inducing ligand, and IFN-gamma (IFN-γ) (38–40). However, tumor cells can evade immune surveillance mechanisms, and indirectly, the immune system selects tumor cells that carry mutations in genes involved in the immune detection and elimination pathways, leading to cancer progression (**Figure 1**). Despite that CTLs detect tumor cells, they frequently fail to control tumor growth (41, 42). CTL dysfunction could be induced by a continuous stimulation of the tumor antigens and by an immunosuppressive tumor microenvironment (TME), driving the T cells to a functionally exhausted state and cancer progression (42, 43). The interaction between the immune system and cancer establishment is called immunoediting.

The central assumption of immunoediting is that CTLs recognize tumor antigens and drive immunological tumor elimination or model cancer development before re-emerging. This process could select cancer cells with mutations that confer resistance to immune effectors and survival advantages in a tumorigenic environment (44, 45). Immunoediting comprises three phases: elimination, equilibrium, and evasion (30). These mechanisms have been extensively reviewed elsewhere; thus, they are briefly summarized here.

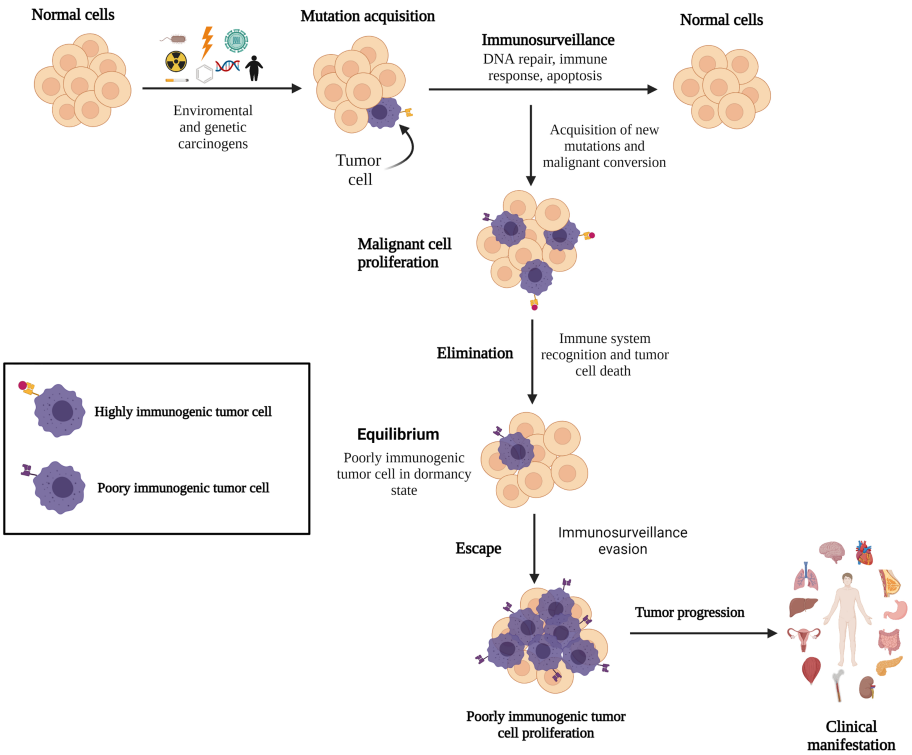


**FIGURE 1** | Immune surveillance and cancer development. Emerging malignant cells are identified and eliminated by the immune system; however, certain acquired gene mutations in tumor cells allow them to remain undetected by the immune surveillance system, resulting in cancer.

*Elimination* phase involves the recognition and killing of transformed cells and nascent tumors by the immune system through antibody production. This process starts with the recruitment of macrophages, dendritic cells, and infiltrating lymphocytes (NK and natural killer T cells) into the tumor site (46) to suppress angiogenesis and induce immunogenic necrotic tumor cell death, promote regulatory T cells (Tregs) apoptosis, and induce M1 pro-inflammatory macrophage activity to defeat tumor progression (47). Moreover, INF-γ and interleukin-12 (IL-12) enhance cytotoxic responses by NK and CTL cells, promoting tumor death by apoptosis and the release of reactive oxygen and nitrogen intermediates (47). Tumor-specific CD8+ and CD4+ T cells infiltrate the tumor site after the recognition of tumor-specific or tumor-associated antigens through HLA class I and class II molecules, respectively, which facilitate the immune mechanisms in synergy with B cells. Cancer cells that are not eradicated during the elimination phase remain in dormancy or equilibrium (**Figure 1**) (33, 43).

*Equilibrium* is the longest phase where cancer remains clinically undetectable, suggesting that tumor cells coexist with the immune system for up to several years (47, 48). Evidences have shown that immune-mediated cancer dormancy is regulated by CD8+ and CD4+ T cells and IFN-γ (49, 50). Through IFN-γ/STAT1 pathway activation, IFN-γ inhibits tumor cell proliferation and establishes tumor dormancy without destroying malignant cells (30). However, IFN-γ can facilitate tumor escape and relapse by inducing tumor antigen loss, upregulating programmed death 1 (PD1) ligand (PD-L1) in tumor cells and recruiting myeloid-derived suppressor cells (MDSCs) and tumor-associated macrophages (TAMs) to the tumor site (50).

*Escape* is the phase where tumor cells that have evaded the immune surveillance system acquired additional DNA mutations and epigenetic changes and have great effectiveness to proliferate and evade apoptotic mechanisms (51). Although new mutations could drive the expression of tumor-specific antigens that are recognized by CTL cells (52), tumor cell-intrinsic alterations and TME modifications (*e.g.*, nutrient depletion, metabolic stress, and cytokine regulation) lead to poor immune response and tumor progression (53). Long-term glucose deficiency in the TME results in low T cell response, cytokine production impairment, T cell "anergy" state, and T cell autophagy to save energy (54, 55). Lipid reduction may result in a lower tryptophan concentration in the extracellular environment, which can inhibit CTL proliferation (47, 56). Acquisition of gain-of-function mutations by tumor cells could lead to low or lack of antigenicity properties, resulting in hijacking of immune mechanisms. Mutations can also induce abnormal HLA expression or antigen processing machinery dysregulation; in fact, HLA class I downregulation is described in 40–90% of human tumors (45, 51). Altered PD-1 or PD-L1 expression on tumor and host cells is also observed, which can inhibit T cell activation and enhance the immune tolerance of malignant cells, facilitating tumor

immune escape (57, 58). Chronic PD-L1 expression, predominantly by TAMs, prolongs the immunosuppressive TME, likely by tumor-specific T cells, as if they were malignant cells (57). Studies in ALL have shown that leukemic blasts express ligands for NK cell receptors, the natural killer group 2 member D (NKG2D) and DNAX accessory molecule-1, to avoid their destruction (59). Low numbers and impaired NK-cell-mediated cytotoxicity could be due to a reduced level of activating receptors (NKp46, NKp30, NKp44, and NKG2D). Cancer cells can also alter NK cell function by modulating the NK cell surface receptors, releasing soluble factors with immunosuppressive properties such as IL-10 and transforming growth factor beta (TGF-β). The signaling lymphocytic activation molecule-associated protein adaptor, in addition to the overexpression of human leukocyte antigen G (HLA-G), which induced immune tolerance and decreased NKG2D expression in NK cells, contributes to the escape of leukemia cells from immune surveillance (60, 61). Thus, the immune system indirectly promotes tumor progression through the selection of poorly immunogenic malignant clones (44, 45). **Table 1** lists the general mechanisms involved in the evasion phase.

## IMMUNE EVASION MECHANISMS IN ALL

Several studies have shown that solid and liquid tumors share immune evasion mechanisms. Studies on B cell precursor (pre-B) ALL mouse models to analyze the cytotoxicity effect of CTLs on non-immunogenic leukemic cells revealed that leukemic blasts, which are not eliminated by the initial immune response, remain in a dormant state during immune surveillance until an immune-evasive clone emerges, which requires a loss of immunogenic antigens for immune escape (77). In addition, it was proposed that ALL displayed immunological ignorance or immune tolerance (described as poor immunogenic clones that fail to alert the immune sensing mechanisms and avoid immune response) because leukemia cells lack or only a subset of them express relevant co-stimulatory accessory molecules (CD80 and CD87, respectively), showing deficient T cell activation (78, 79). Moreover, the relatively low mutation burden in ALL in comparison to other tumors could reduce neoantigen production and induce a low immunogenic response (80–82). Nevertheless, the presence of tumor-infiltrating lymphocytes as CD8+ T cells in pediatric patients with ALL suggests a potentially robust antitumor immune response (83). In addition, by predicting mutated neoepitopes in leukemia, at least one neoepitope was found in 88% of the cases, which can be recognized by CTLs and induce an anti-tumor response (84). However, B cell leukemia fails to function as an antigen-presenting cell (APC) which, in addition to its rapid dissemination, could affect the initiation and execution of anti-leukemia immunity through non-activation of T cells, which may promote immunosuppressive TME and tumor cell survival (55, 85–87). In ALL, it has been proposed that tumor-specific T cells are never properly activated; they are instead deleted or anergized upon initial antigen presentation (80, 85). Data from pre-B cells ALL show that the T cells become anergic after interleukin-10 (IL-10) expression, which is induced by CD40 activation (80, 85). Abnormal IL-10 and CD40 expression has been found in patients with ALL (78, 79, 88–90), and polymorphisms within the *IL-10* gene promoter region (-G1082A) that influences the IL-10 plasma levels have been associated with ALL prognosis (78, 91, 92).

Immune tolerance mechanisms that protect healthy tissues are hijacked by cancer to maintain immune escape through the modulation of additional processes, such as metabolically essential amino acid (tryptophan and arginine) depletion, immunosuppressive cytokine (TGF-β and IL-10) overproduction, expansion of Tregs, MDSCs, macrophages, and expression of T cell response inhibitors and co-inhibitory ligands (*e.g.*, PD-L1) (93). Studies focused on ALL suggest that defective antigen presentation on MHC-I molecules is involved in immune evasion (94). Alterations in the expression and functionality of HLA class I (essential for CTL cytotoxicity) or II (important for CD4+ T cell response) are commonly observed in solid tumors (95, 96). The downregulation or loss of cell surface expression of HLA-I and high

**TABLE 1** | Potential mechanisms of tumor immune evasion.

| Mechanism | Features | Tumor types | References |
|---|---|---|---|
| Malignant cell selection | Low effectiveness to eliminate mutated cells<br>Gain of DNA and epigenetic mutations that increase the proliferation ability<br>Resistance to immunity-induced apoptosis (by abnormal function of IFNγ receptor or tyrosine kinases association) | ALL, breast, bladder, colorectal, CML, esophageal, endometrial, HN, hepatocellular, gastric, glioblastoma, lung, lymphoma, melanoma, pancreatic, prostate, ovarian | (62–67) |
| Altered expression of HLA antigens and co-stimulatory molecules | Reduced of HLA-I antigen expression<br>Abnormal expression of co-stimulatory molecules (CD80 or CD86)<br>Poor stimulation of T cells<br>Reduced CTL response | ALL, CLL, AML, CML, breast, cervical, colorectal, gastric, hepatocellular, lymphoma, lung, melanoma | (55, 60, 68, 69) |
| Chronic PD-L1 expression by host cells | Prolongated immunosuppressive state in the tumor microenvironment<br>Repressed T-cell function | ALL, CML, breast, colorectal, esophageal, gastric, HN, lung, melanoma, ovarian, sarcoma | (55, 57, 58, 70, 71) |
| T cell dysfunction | Reduced T-cell response<br>Cytokine production impairment<br>T-cell "anergy" and autophagy | ALL, CLL, breast, glioblastoma, lung, hepatocellular, melanoma, ovarian, sarcoma | (55, 62, 72–76) |

*ALL, acute lymphoblastic leukemia; AML, acute myeloid leukemia; CLL, chronic lymphoblastic leukemia; CML, chronic myeloid leukemia; CTLs, cytotoxic T lymphocytes; HN, head and neck; TAM, tumor-associated macrophages; APCs, antigen-presenting cells.*

resistance to NK-cell-mediated killing has been described in ALL (97–101)—for instance, the C2 epitope that is encoded by HLA-C has been found to be overrepresented in patients with ALL. Given that C2 is a high-affinity ligand of the natural killer cell inhibition receptor (KIR2DL1), it has been suggested that C2 may decrease the destruction of leukemic blasts and increase the probability of late relapse in patients with ALL (>2.5 years) by reducing the cytotoxic capacity of NK cells (99). The absence of HLA class II expression in leukemic T-cells and its regulator class II trans activator has been reported (102). Recently, HLA class II expression was associated with a better prognosis in adult T cell leukemia/lymphoma (103).

Other mechanisms, such as disrupted immune checkpoint expression and high production of suppressor factors by CTLs, alterations in the anti-inflammatory/pro-inflammatory cytokine ratio, cytotoxic abnormalities, and other cell populations with altered functions, and aberrations in the immunophenotype of the lymphoid lineage have been proposed to avoid immune surveillance by ALL cells (**Figure 2**) (85, 104).

## Disrupted Immune Checkpoint Expression and High Production of Tumor Suppressor Factors by Cytotoxic T Cells

Cytotoxic cells are the major components of the immune system that counterattack tumor cells. The overexpression of co-inhibitory ligands for specific receptors on cancer cell surfaces to disrupt T cell response is one of the primary mechanisms developed to hijack the immune system. The cell surface molecules CD28, cytotoxic T-lymphocyte-associated protein 4 (CTLA-4), inducible co-stimulator (ICOS), PD1, and PD-1L are basic ligands that induce co-stimulatory or inhibitory signals in T cells to maintain immune system homeostasis (**Figure 2A**) (105). In the early immune response stages, CD28 facilitates and maintains the CD4+ and CD8+ T cell response. CTLA-4 arrests T cell activation by triggering an inhibitory signal within the T cell, affecting critical peripheral T cell tolerance and function (106). CD28 and CTLA-4 share ligands and are necessary to avoid inappropriate or prolonged CD4+ and CD8+ T cell activation. Both molecules have been found to be constitutively expressed in acute myeloid leukemia (AML) blasts at diagnosis and have an increased expression in leukocytes from the peripheral blood of these patients compared with that of healthy controls, likely favoring AML cell escape from T cell activation and its effector functions (107). An evaluation of the CTLA-4 expression revealed that this co-inhibitory molecule was elevated in T cells in patients with high-risk ALL (108); in addition, CTLA-4 solubility was significantly elevated in 70% of B-ALL pediatric patients with active disease (109). Furthermore, CTLA-4 overexpression has been correlated with the percentage of leukemic B cells and poor prognosis in pediatric patients (108, 110), and a high serum CTLA-4 level has been detected in patients with B-ALL who died from the disease (111). Thus, the disputed CTLA-4 expression from ALL cells could be a potential mechanism of immune surveillance escape (109, 112).

PD-1 and PD-L1 overexpression has been reported to evade the host immune system in numerous cancer types (105, 110, 113). PD-L1 and PD-L2 are ligands of PD-1, which is an important inhibitory immune checkpoint that suppresses T cell activity after antigen activation. In fact, CTL function inhibition by PD-1 expression has been observed in patients with AML (113). CTLA-4 and PD-1 expression in hematological malignant cells has been suggested as an immune evasion strategy to promote leukemia blast survival and prevent efficient recognition and destruction by anti-tumor T cells (107, 110). Studies using a mouse model of disseminated AML and in transplanted patients before relapse have shown that sustained inhibitory signaling mediated by CTLA-4 and PD-1 on T cells correlates with a T cell exhaustion stage, reduced T cell effector function, and lower cytotoxicity (114, 115). Data from ALL evidenced a decrease in PD-1 expression on CD4+ and CD8+ T cells after the inhibition of myeloid–epithelial–reproductive tyrosine kinase, a gene associated with the induction of an antiapoptotic gene expression signature in B-ALL cells, leading to increased T cell activation (116). Abnormal expression of checkpoint molecule PD-1 has been reported in BM biopsies from adult patients and in T cells of pediatric cases with ALL (108, 117). In addition to the observations in ALL, upregulation of both malignant and infiltrating immune cells from B cell lymphomas and T cells of peripheral blood mononuclear cells from patients with chronic myeloid leukemia (CML) exhibits the relevance of PD-L1 in hematological malignancies (118–120). PD-L1 overexpression is correlated with poor prognosis in ALL (113) and has been found to be one of the most expressed inhibitory markers in pediatric ALL blast, whose expression is increased in relapsed patients with ALL (108, 115). Other checkpoint molecules are T cell immunoglobulin and mucin domain-containing protein 3 (TIM-3) and lymphocyte-activation gene 3 (LAG-3). TIM-3 is involved in apoptosis, and Tregs expressing TIMP3 have a higher suppressor function than Tregs negative to TIMP3 (121). LAG-3 expression has been detected in highly immunosuppressive T cells and correlates with an increased expression of IL-10 production by Tregs (122, 123). TIM-3 and LAG-3 have been found to be subexpressed in the BM of patients with ALL, in contrast to healthy subjects (117).

ICOS (CD275) is involved in maintaining immune reactions and has a relevant role in Tregs function and differentiation, which protects tumor cells from immune cells in the TME (124, 125). Significant Tregs accumulation in the BM-TME and upregulation of ICOS ligand (ICOS-L) have been observed in AML, suggesting that ICOS-L contributes to the conversion and expansion of Tregs and preserves the immunosuppressive environment. Additionally, ICOS-L and ICOS expression was found to be a predictor of OS and disease-free survival in patients with AML (126). Although there is no information regarding ICOS or ICOS-L in ALL, the relevance of ICOS in ALL immune escape is supported by studies showing that ICOS is part of the intracellular region of the signaling domain complexes that activate and induce cytotoxicity against target cells during chimeric antigen receptor (CAR) T cell immunotherapy (127).

## Alterations in the Anti-inflammatory/Pro-Inflammatory Cytokine Ratio

Inflammation is an immune response to body damage and is mediated by cytokines, which are relevant players involved in oncogenic processes, such as cell proliferation, apoptosis inhibition of mutated cells, and promotion and progression of cancer development (128). Cytokines are classified as pro-inflammatory (IL-1β, IL-6, IL-15, IL-17, IL-23, IFN-α, and

TNF-α) and anti-inflammatory (IL-4, IL-10, IL-13, and TGF-β). Interestingly, an inflammatory marker analysis of neonatal blood reported that children who developed pre-B ALL had a cytokine signature (lower concentrations of the cytokine IL-8, soluble IL-6 receptor α, and TGF-β1 and higher concentrations of IL-6, IL-17, and IL-18) (129). Increased CCL2 and IL-8 concentrations of T cell-polarizing cytokines (IFN-γ and IL-12) and cytokines associated with infectious processes, such as TNF-α and IL-6, have been detected in patients with ALL at diagnosis, suggesting a pro-inflammatory state (130–133). These findings could be associated with immune cell activation by endogenous molecules that are released after tissue injury or cell death to generate an immune response against cancer (133, 134). The pro-inflammatory environment in the BM of patients with leukemia is facilitated by hematopoietic and stromal cells. However, studies indicate that cancer cells hamper immune activation by creating an anti-inflammatory TME by overproducing anti-inflammatory cytokines and by blocking the release of pro-inflammatory cytokines, thus successfully evading immune surveillance (128, 135). In CML, AML, and ALL, cancer cells express TGF-β and IL-10 to reduce immunogenicity (136, 137). Studies in mouse models with B-ALL have shown that TNF-α is secreted by B-ALL cells, and this leads to increased invasiveness and significant prolongation of surviving leukemia cells (138), which is an important mediator of leukemia-induced NK cell dysfunction. Thus, it is fundamental for NK cell immune evasion in childhood B cell ALL (139). Although IL-4 has shown antitumor effects and ALL cell suppression (140), it has been suggested that IL-4 expression in leukemia cells could reduce immunological recognition by decreasing HLA-class II molecule expression (132).

IFN-γ and interleukin 6 (IL-6) are among the most important cytokines associated with immune response in cancer (141). IFN-γ gene expression is reduced in patients with ALL, suggesting that the immune system is disrupted and leukemia cells may take advantage of defective IFN-γ production to promote escape from immune surveillance (142, 143). IL-6 contributes to lymphocyte and monocyte differentiation and induces antibody secretion by B cells. The low antibody production and decreased cellular immunity derived from abnormal IL-6 expression detected in ALL cases (**Figure 2B**), in addition to the association between single-nucleotide polymorphisms in the *IL-6* gene and susceptibility

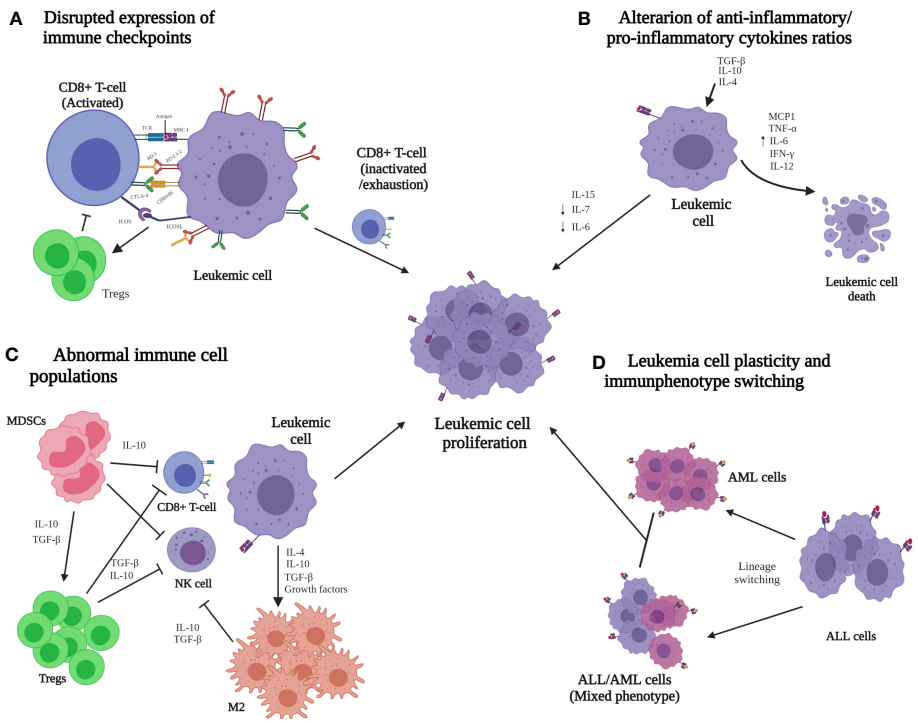


**FIGURE 2** | Immune evasion mechanisms that are potentially involved in the progression of acute lymphoid leukemia (ALL). **(A)** Low MHC-I and co-stimulatory ligands but high co-inhibitory lead to the inactivation or depletion of the CD8+ T-cell cytotoxic function. **(B)** Abnormal expression of anti-inflammatory cytokines (TGF-β, IL-4, and IL-10) reduces the cytotoxic T lymphocyte (CTL) population, and the pro-inflammatory cytokines (MCP1, TNF-α, IL-6, IL-12, and IFN-γ) are responsible for malignant cell destruction. **(C)** Immune cell enrichment, such as MDSCs, Tregs, and M2 macrophages, generates a favorable microenvironment for ALL cells and inhibits the activation and differentiation of CTLs and natural killer cells. **(D)** The plasticity of ALL cells leads to immunophenotype switching, which can reprogram immune evasion pathways. It has been proposed that these mechanisms could together contribute to the dissemination and progression of ALL. ALL, acute lymphoblastic leukemia; AML, acute myeloid leukemia; CD, cluster differentiation; CTLs, cytotoxic T lymphocytes; CTLA-4, cytotoxic T-lymphocyte-associated protein 4; ICOS, inducible co-stimulator; ICOS-L, inducible co-stimulator ligand; IFN-γ, interferon gamma; IL, interleukin; M2, M2 macrophages; MCP1, chemoattractant protein-1; MDSC, myeloid-derived suppressor cells; MHC-I, major histocompatibility complex class I; NK, natural killer; PD1, programmed death 1 ligand; PD-L1/2, programmed death 1/2 ligand; TCR, T-cell receptor; TNF-α, necrosis factor alpha; Treg, regulatory T-cell.

to ALL (the genotype of which correlated with IL-6 serum levels), are evidence of the relevance of this cytokine in this malignant disease (141, 144, 145).

Other cytokines and chemokines, such as IL-1, IL-7, IL-8, CCL2, CXC-10, and CXCL-12, could contribute to immunotolerance (112, 146). In fact, IL-1, IL-7, and CXCL12 expression favors ALL cell surveillance in the BM-TME (146, 147). Through the induction of CCL2 by periostin, this molecule stimulates the proliferation and dissemination of ALL (146, 148).

## Abnormal Cytotoxic and Other Cell Populations and Alteration of Their Functions

The abnormal proliferation of immune cell populations is another important mechanism for preventing immune attacks in cancer. Two distinct T cell subsets are involved in the immune system against cancer. The first is CTLs that kill cancer cells, and the second is cells required for the activation and proliferation of APCs.

Tregs (CD4+ CD25+ Foxp3+) are involved in tumor development and progression by inhibiting anti-tumor immunity in the TME (93, 149). Under physiological conditions, Tregs play an essential role in self-tolerance and immune homeostasis processes by suppressing normal and pathological immune responses and by eliminating a broad range of pathogenic microorganisms and malignant cells (85, 150–152). The correlation between tumor-infiltrating Treg levels and prognosis has been described in several malignancies, including ALL, suggesting that Tregs may be involved in the immune evasion process (149, 153–156). Indeed a high number of Tregs in the BM and peripheral blood of ALL cases has been associated with poor prognosis (153, 154, 157, 158). Studies in BM-TME have shown that immunosuppressive cytokines, such as IL-10 and TGF-β, are secreted by Tregs (**Figure 2C**) (159).

One of the biological features of patients with ALL is the presence of severe cytopenia and poor reconstitution of the innate and adaptive immune system. Although normal lymphoid and myeloid cells are present in ALL BM, the early compartment of progenitor hematopoietic cells is reduced in number and activity, including NK cells, MDSCs, and macrophages (93, 130, 160).

NK cells represent 5–20% of the lymphocytes in peripheral blood and are relevant in early antitumor immune response by lysing the tumor cells due to cytokine release. Based on CD56 and CD16 expression, two principal subpopulations of NK cells were identified: cytotoxic NK cells or cNK (CD56dim CD16+) and regulatory NK cells or NKregs (CD56highCd16-). cNK are abundant in peripheral blood (95% of the NK) and inflammation sites and show a higher cytotoxic capacity than NKregs, which predominate in lymphoid nodes (33). Natural cytotoxic receptor expression is a relevant mechanism to stimulate responses against tumor cells and has been observed to be downregulated in ALL BM (33). In recent years, several studies have provided evidence of the fundamental role of NK cells in the onset, development, and establishment of ALL (59, 139, 161, 162). ALL NK cells at diagnosis had an inhibitory phenotype associated with impaired function due to abnormal NK ligand expression (139). Torrelli et al. (59) observed a higher expression of the ligands for NK cell-activating receptors, Nec2, ULBP1, and UBLP3, on the surface of the blasts from children in contrast to adults with ALL, which could be associated with the worse clinical evolution of ALL in adults than in children (59). Differences in NK cell activity among molecular ALL subtypes have been described, with increased NK cell-activating ligand expression (NKG2D and DNAM1) in patients with ALL carrying the fusion gene *BCR-ABL* (Philadelphia chromosome: Ph+), in contrast to Ph negatives (59). Additionally, Ph+ cells are more susceptible to NK cell killing activity than ALL cells carrying no known molecular markers and were enhanced in Ph+ adult cases; B-ALL with *MLL-AF4* gene and T-ALL cases displayed a high density of the NKG2D ligand and UL16-binding protein (ULBP-1) (59). NK cells from child and adult patients have shown aberrant functions, such as low degranulation of granzyme B (117, 139). In a cohort of child patients with B cell ALL sampled at diagnosis, end induction, and maintenance, evidence of altered NK phenotype and function compared to age-matched controls was revealed. It should be emphasized that the NK abnormalities were partially corrected during the maintenance phase of the ALL treatment and were inducible in healthy NK cells after co-culture with ALL blasts *in vitro* by TGF-β1 release (139). In fact, leukemic cells secrete IL-10 and TGF-β in order to evade the effect of CTLs and NK cells (137). Furthermore, a direct contribution of the TME to the exhaustion of NK cell functions by the CRTAM/Necl-2 interaction was reported in ALL. Indeed the decreased NK cell content and their depleted cytotoxic capacity in peripheral blood are two of the predominant immune surveillance problems in acute leukemia (139). Current investigations focusing on *in vitro* activation and NK cell expansion protocols to treat ALL are underway.

MDSCs are a heterogeneous population of regulatory immature cells derived from monocytes or granulocytes that are involved in immunosuppression in patients with cancer (163). MDSCs consist of two main subpopulations (monocytic MDSCs—MO-MDSCs and polymorphonuclear MDSCs—PMN-MDSCs) that suppress the activation, proliferation, and cytotoxicity of effector T and NK cells and induce the differentiation and expansion of Tregs (163–165). The role of MDSCs in ALL remains incomplete. Recently, it was reported that patients with B cell ALL at diagnosis have a higher number of MDSCs than healthy subjects, which was even higher during induction chemotherapy (166). Furthermore, Zahran et al. (163) detected increased MDSCs in pediatric patients with B cell ALL compared to healthy controls. Moreover, these authors observed a relationship between PMN-MDSCs and the levels of peripheral and BM blast cells and CD34 + cells, suggesting that PMN-MDSC cells provide a suitable immune-suppressive state for B cell ALL tumor progression. A reduction in PMN-MDSC population was related to complete post-induction remission (163). The high number of these cells in pediatric patients with B cell ALL suggests that the increased levels and activity of MDSCs and Tregs could explain the immunosuppression state observed in this malignancy (163). MDSCs secrete TGF-β and IL-10 that have direct immunosuppressive effects and induce Treg

expansion, which suppressed tumor-specific T cell responses (167) (**Figure 2C**).

Macrophages are other essential immune cell populations of the host and are composed of two subtypes: M1, which has antitumor effects, and M2 (anti-inflammatory cells with protumoral properties), which supports TME through the induction of angiogenesis, metastasis, and immune suppression (168–170). Macrophages have anti-tumoral activities at the initial stages of solid and hematological tumor development; however, TME impairs macrophage function, transforming them into immunosuppressive cell types with pro-tumoral activities (171). The frequency of M1 macrophages has been reported to be notably reduced in adult patients with B-ALL compared to controls, while M2 macrophages are increased (117). M2 is divided into several subtypes, where TAMs, which are relevant in solid tumor cell invasion, are included. Knowledge about the role of macrophages in hematopoietic malignancies has been obtained mainly from the study of lymphomas, where an association between the number of TAMs in lymph node biopsy and the prognosis of patients with classical Hodgkin lymphoma (cHL) was found (172). In ALL, the production of M2 macrophages with immunosuppressive/tolerogenic properties can be induced by tumor-mediated mechanisms (tumor-derived cytokines and growth factors, *etc.*) (171). Furthermore, it has been found that spleen leukemia-associated macrophages (LAMs) stimulate the proliferation of T cell ALL and have high migration, and their functional and phenotypic characteristics are modified by an organ-specific microenvironment (169, 173). Most LAMs have an M2-like phenotype. It has been reported that this type of immune cells also secrete immunosuppressive cytokines such as IL-10 and TGF-β (159).

## Leukemia Cell Plasticity and Immunophenotype Switching

During malignant hematopoietic disorders, such as acute leukemias, intrinsic and extrinsic signals (including those participating in immune surveillance) influence the cell differentiation pathway and cooperate in abnormal fate decisions, highlighting the relevance of a continuous homeostatic control to produce elements of tumor suppression (174, 175). Switching of CML to ALL in the blast crisis, AML cases relapsing as ALL, ALL converting AML after chemotherapy, and mixed phenotypes (simultaneous expression of both myeloid and lymphoid antigens) suggest that linage-associated molecule expression contributes to immune response disruption and facilitates cancer progression (174, 176–179). Lineage switching in leukemia is more frequent in children than in adults, and most cases are ALL converting to AML (180). Studies have proposed that this process is a consequence of stem cell plasticity (capacity to cell fate conversion in defined cells adopting biological properties to the same or different lineages) since the evidence shows that cancer cells are derived from the same founder clone in leukemia lineage switching (180). Leukemias with lineage switching appear to be more common in specific genetic subtypes, such as those with *KMT2A* (*MLL*) gene rearrangements (180). The absence of *EBF1* expression in ALL allows early lymphoid progenitors to differentiate into the myeloid lineage, and deletion of *PAX5* in mature B cells can induce conversion to different fates, including macrophages and T cells (176, 181). Low *PAX5* expression has been reported in patients with ALL and very early relapse-expressing AML genes, such as *MPO* and *FLT3* (174). A single-cell RNA-seq study revealed that plasticity coexists with oncogenic and immune evasion programs in early T progenitor ALL (174), suggesting that specific features acquired during lineage conversion could contribute to immune evasion response in ALL. It has been proposed that the plasticity of leukemic blasts in early progenitor T cell ALL can modulate the treatment based on inhibitors of the Notch pathway due to the coexistence of transcriptional programs that are characteristic of lymphoid and myeloid lineages. Additionally, immunoevasion signatures were found to be activated in the TME—for example, the interaction between hepatitis A cellular virus receptor 2 and galectin 9 is associated with CD8+ T cell dysfunction (174). Studies aimed at understanding leukemic blast plasticity could contribute to the identification of potential therapeutic targets based on the reversion of T cell depletion and consequently improve OS rates in patients with ALL.

# BONE MARROW TUMOR MICROENVIRONMENT AND IMMUNE SYSTEM EVASION

Immunological evasion is due to mechanisms inherent to the TME. It is well known that malignant blasts maintain a close interaction with normal cells within the BM niche and, at the expense of normal hematopoiesis, remodel functionally and structurally the BM-TME to favor ALL development and promote tumor cell dissemination and chemotherapy resistance (43, 47, 55, 112, 118, 182–184). BM-TME favors tumor growth through polarization of host immunity to prevent anti-cancer immune responses. Alterations in immune cell populations in the TME are other mechanisms involved in the immune evasion by leukemic cells—for instance, it has been reported that the presence of leukemic cells in BM affects the CD14-expressing monocytes and non-classical CD16-expressing monocytes populations (185). Leukemic blasts have the capacity for TME remodeling during disease progression and promote monocyte differentiation into non-classical monocytes. In the BM-TME, a decrease in CTLs and NK cells has also been reported as well as an increase in suppressor immune cell populations such as Tregs, M2 macrophages, and MDSCs to support an immunosuppressive microenvironment (55). Mice models of AML revealed that those leukemic cells reduce the osteoblast population, modifying the lineage fate of hematopoietic stem cells, which increase tumor burden and reduce OS (186, 187). The interaction between leukemic blasts and the different cell types has been associated with a major surveillance of tumor cells (188). Besides this, ALL cells and the primary mesenchymal stromal cells (MSC) within the niche interact by using tunneling nanotubes (TN) that induce the secretion of prosurvival cytokines IL-8, CCL2, and CXCL10, driving stroma-mediated steroid resistance. By interruption of the TN signal, the leukemogenic processes are inhibited; thus,

pre-B-leukemic cells are resensitized with prednisolone (189, 190).

ALL blasts also express surface molecules shared with hematopoietic stem cells and interact with extracellular matrix (ECM) molecules, soluble factors, and cytokines for ALL promotion—for instance, it has been reported that integrins have a role in the retention of leukemic blasts in the BM and contribute to ALL dissemination from BM to the CNS and chemoresistance (191, 192). Otherwise, the MSC-derived ECM proteins, such as periostin and osteopontin in the niche, stimulate the proliferation and dissemination of ALL. ECM of the BM also represents a physical barrier that contributes to immune evasion in the cell niche (193).

Another important alteration in the leukemic TME is the increased levels of anti-inflammatory and immunosuppressive cytokines, such as IL-10 and TGF-β, and the high expression of PD-1 and TIGIT, which contribute to tumor progression and immune evasion (43, 47, 55, 194). IL-1, IFN-γ, TNF-α, and HLA-G in the BM-TME may induce immune tolerance and then ALL recurrence. Additionally, overexpression in BM-TME of chemotactic cytokines such as CXCL12/CXCR4 and CCL25/CCR9 (produced by stromal cells in the BM) has a role in ALL and influences the outcomes and chemoresistance. Thus, targeting the chemokine axis could significantly reduce tumor burden in ALL (182).

It is well known that the immunosuppressive microenvironment surrounding tumor cells represents a key cause of treatment failure; therefore, BM-TME is the central target for reprogramming the immune system in ALL and other hematological malignancies.

# INTO THE FRONTLINE OF ALL TREATMENT: TARGETING THE IMMUNE CELLS

Initial ALL treatment comprises induction, consolidation, and long-term maintenance therapy. The backbone of ALL therapy is chemotherapy using drugs developed during the 1950s and 1960s focused on leukemic cell eradication, normal hematopoiesis restoration, and prevention of "sanctuary site" invasion, relapse, and death (195, 196). Chemotherapy has achieved considerable success in ALL survival (9); however, relapse occurring in approximately 20% of patients with ALL is the main obstacle in improving the OS rates. Adult patients with ALL have a higher risk of relapse than pediatric patients, and the protocols used (adapted from pediatric protocols) reach less than 50% of the success rate and have lower minimal residual disease negative rates after induction therapy (197). Allogeneic hematopoietic stem cell transplantation (alloHSCT) has been an effective anti-leukemic therapy for patients with ALL (198, 199) but is a highly toxic therapy, and disease recurrences can occur within the time of immunosuppressive treatment (200, 201).

Over the last two decades, multiple studies have attempted to improve the OS of patients with ALL by incorporating new agents into the treatment protocols and exploiting the immune response against leukemia cells. Targeting of tumor cells is a promising therapeutic approach. Antibody-based therapeutic strategies are being developed to select cells of the immune system, enhance anti-tumor immune response, and reduce damage to normal tissues (93, 202). T cell signaling pathway inhibition (particularly PD-L1/PD-1), immune cell regulation, and the prevention of tryptophan depletion by indoeamine-2,3-dioxygenase are the most well-studied immunosuppressive mechanisms in liquid tumors (93). Nevertheless, few trials based on these pathways have been described for ALL treatment. Monoclonal antibodies (mAbs), immune checkpoint blockers, CAR T cells, and bispecific T-cell engagers (BiTEs) are currently used in ALL treatments approved by the USA Food and Drug Administration (FDA) (203–205). Approaches using adoptive T cell therapy (ACT) and tumor neoantigens are under investigation (93).

## Monoclonal Antibodies

Antibodies are the basis for many new anti-cancer treatment strategies due to their immunomodulatory properties and capacity to promote the induction of anti-tumor immune responses. These antibodies target self-tumor antigens or the TME to inhibit tumor growth by increasing host immune responses to antigens expressed by the tumor itself or by reducing pro-tumorigenic factors generated in the tumor stroma (206). CTLA-4-specific mAbs have been used in human cancers, such as melanoma (206). Using the anti-CTLA-4 mAb (ipilimumab) in combination with IgG4 mAb (nivolumab), which disrupts the interaction between PD-1 and PD-L1/PD-L2, in patients with relapsed/refractory cHL, non-Hodgkin lymphoma, or multiple myeloma showed no significant improvement in efficacy over single-agent nivolumab (207). The anti-PD-1 anti-leukemic treatment is based on the maintenance and expansion of tumor-specific memory T cells and NK cell activation. This approach has been explored in diverse tumors, including relapsed/refractory lymphoid malignancies; however, its clinical application in ALL remains unknown. In ALL, CD-38 and CD-52 have been identified as target antigens of mAbs for the treatment of relapsed T cell ALL. Currently, there are ongoing clinical trials testing the efficacy of anti-CD38 mAbs (isatuximab and daratumumab) and anti-CD52 mAbs (alemtuzumab) with favorable results for better disease prognosis (127).

## Bispecific T Cell Engagers

BiTEs are bispecific recombinant glycoproteins with two single-chain variable fragments (scFvs) connected by a flexible linker, whose targets are membrane molecules (costimulators, coinhibitors, adhesion, *etc.*) from both T cells and malignant cells. BiTEs favor immune responses by creating an immune synapse among tumor antigens and T cells (204). The distribution of BiTEs depends on factors such as the diffusion of the vascular endothelium, laminar flux rate, and interaction with the target. Blinatumomab (anti-CD19/anti-CD3; AMG103) is a BiTE that binds to CD3+ lymphocyte T and CD19+ B lymphocytes. Although blinatumomab induces selective lysis of tumoral cells, its half-life is short, and constant administration is necessary for effect maintenance. The Children's Oncology

Group has incorporated blinatumomab in clinical trials in patients with B cell ALL with a standard risk (1–9.99 years and leukocyte count <50,000/ml) classification. Good results and acceptable toxicity were observed; in addition, half of the population had a significant twofold improvement in median OS compared to patients with standard chemotherapy regimens (208).

Studies in patients with relapse/refractory pre-B cell ALL indicate that Treg proportion could determine the prognosis of blinatumomab treatment. It was observed that blinatumomab responders had a lower percentage of Tregs (4.82%) in peripheral blood compared to non-responders (10.25%). Additionally, the restoration of the activated T cell population was detected after the *in vitro* depletion of Tregs in leukemic blasts, thus highlighting the regulatory role of Tregs in the development of the immune response in ALL (209).

The main disadvantage of BiTEs is the induction of cytokine release syndrome (CRS) through proinflammatory cytokines and aplasia of lymphocytes B (205). Although collateral effects in clinical assays with blinatumomab have been reported (fever, nausea, headache, neurological, and hepatic adverse effects), a lower percentage of minimal residual disease in patients treated with blinatumomab in contrast to patients with high-risk ALL treated with conventional regimens was reported (204, 208, 210).

## CAR T Cells

CAR is a synthetic construct formed by an extracellular scFvc (that recognizes the tumor antigen) fused to a transmembrane domain and to intracellular activating/co-stimulator motives (CD3ζ, CD28, 4-1BB) (204, 211–213). CAR is transduced to T cells (CAR T cell), and after the recognition of the tumoral antigen, it promotes a cytotoxic effect on the target cell (205). It has been reported that CAR T cells act independently of HLA recognition. Therefore, this approach could be used in different cases to overcome the lower HLA density of ALL malignant cells. Furthermore, it is feasible to use CD4+ T and CD8+ T cells to generate CAR T cells, which increases the effector and cytotoxic potential of T cells (213).

CAR T cells have recently been approved by the FDA to treat patients with leukemia and lymphoma (203–205), and several clinical trials of CD19 CAR T cell therapy are being carried out in ALL relapse patients, which have shown favorable results with remission after 6 months in up to 90% of the patients, with 78% OS and 67% event-free survival (214). However, in a group of refractory/relapsed patients with B cell ALL, CD22 CAR T cell therapy treatment achieved a complete remission of 70.5% in comparison with those previously treated with CD19 CAR T cells without success. CD22 CAR T cell-treated patients only exhibited a moderate grade of CRS and neurotoxicity, and better results were observed in patients undergoing alloHSCT (215). An important advantage of CAR T cells is their capacity to interact with malignant cells displaying different antigens, such as CD19, CD20, and CD22 (212).

Although CAR T cell implementation in B cell ALL has obtained favorable results, its implementation in T cell ALL presents limitations because CAR T cells and malignant T cells share similar expression profiles of target antigens, which gives rise to a non-specific cytotoxic activity incapable of discriminating CAR T cells from malignant T cells, leading to T cell aplasia and eventual immunodeficiency. Notwithstanding, the identification of antigens, such as CD4, CD5, and CD7, on T cell ALL shows promise for the use of CAR T cell technology, the clinical trials of which are ongoing (127).

Limitations of CAR T cell therapy in ALL involve the following (1): poor expansion and limited persistence *in vivo* caused by defects in the design and manufacturing of CAR T cell therapy (2), internalization of the CD19 glycoprotein and resurgence in tumor cells (3), toxicity (CAR T cells present numerous cellular interactions that could promote the cytokine-mediated systemic inflammatory response), and (4) aplasia of B cells and humoral deficiency that might promote infections (204, 205, 216).

## Adoptive T Cell Therapy Using Tumor Neoantigens

ACT is based on TIL expansion and infusion in patients following lymphodepletion. ACT aims to generate a robust immune-mediated antitumor response *via* infusion of *ex vivo*-manipulated T cells. Studies have suggested that clinical outcomes correlate with tumor mutational and neoantigen load (217–219). Although ALL has been described as a malignancy with low mutational load, a recent analysis reported that it is possible to obtain immunodominant neoantigens that could be used to develop neoepitope-CD8+ T cells and treat patients with ALL (83, 220). To explore the effectiveness of this strategy, 36 putative neoantigens from the *ETV6–RUNX1* fusion were tested, and 31 neoantigens were immunogenic. The co-culture of HLA-specific APCs with neoepitopes and isolated CD8+ tumor-infiltrating lymphocytes results in TNF-α and IFN-γ production. Therefore, this strategy provides a possibility to consider the adoptive transfer of neoepitope-CD8+ T cells as immunotherapy in leukemia and could be used in the consolidation phase or subsequent treatment (83).

## Activation of Necroptosis

The suppression of cell proliferation in leukemic lineages has significant challenges. On one hand, mAb treatment ablates the main elements of the adaptive immune response, including T and B cells, which could favor infection burst or immune-mediated disease development (221, 222). On the other hand, to increase tumor-specific T cell responses, it is necessary to promote leukemic cell immunogenicity. To date, the primary goal of several research groups has been to promote apoptosis in malignant cells; however, this type of cell death is immune-tolerogenic. Recent studies have shown that a new class of targeted drugs (second mitochondrial activator of caspases, SMAC) antagonizes diverse anti-apoptotic proteins (inhibitor of apoptosis proteins) and, in combination with dexamethasone, promotes increased immunogenic cell death (necroptosis) in ALL (223, 224). Necroptosis is a regulated inflammatory mode of cell death that is caspase-independent and presents highly regulated necrotic features (225). Necroptosis produces the release of DAMPs and proinflammatory cytokines, allowing a

better cytotoxic function by tumor-specific T cells (225–227). The activation of necroptosis has been explored as an anti-leukemic therapy, and several SMAC mimetic compounds are currently in phase I or II clinical trials to treat hematological malignancies, including ALL (225, 228). The leading problem with active necroptosis in ALL therapy is its potential to induce immunogenicity. Observations from solid tumors suggest that necroptosis is not always pro-inflammatory or immunogenic; however, there are no reports of necroptosis in ALL (223, 229).

## CONCLUSION

Despite defined treatment protocols, leukemia remains a global health problem due to high relapse and treatment failure rates. ALL studies suggest that immune response evasion by leukemic cells could promote malignant cell proliferation and invasion. The identification of leukemic cell strategies to deactivate immune cells and induce an immunosuppressive TME to resist apoptosis has been suggested to have potential implications in the field of personalized immunotherapy for ALL—for example, the infusion of co-stimulatory adapted CAR T cells to increase cytotoxic T cell responses is a current option for ALL treatment. The infusion of neoepitope-specific ALL cells to increase the MHC response is also a potential alternative. Among the treatments for patients with ALL, the induction of leukemic cells to become immunogenic is a promising alternative because it promotes an immunogenic microenvironment and influences direct malignant cell elimination. Further research into the immune evasion mechanisms underlying ALL development and progression is required to gain knowledge on the molecular and cellular leukemogenesis mechanisms, which could contribute to the design of new anti-ALL therapies.

## AUTHOR CONTRIBUTIONS

SJ-M, IA-U, and CP-A participated in the preparation of the original draft. JR-B and AH-M participated in revision and editing. SJ-M took charge of conceptualization, supervision, and funding acquisition. All authors contributed to the article and approved the submitted version.

## FUNDING

This work was supported by the Consejo Nacional de Ciencia y Tecnología (CONACyT, Investigación en Fronteras de la Ciencia —2016-01-2119) and by the National Institute of Genomic Medicine (01/2018/I and 19/2019/I). ISA-U and CJP-A were supported by CONACyT with the scholarships CVU 324181 and 821714, respectively.

## REFERENCES

1. Bray F, Ferlay J, Soerjomataram I, Siegel RL, Torre LA, Jemal A. Global Cancer Statistics 2018: GLOBOCAN Estimates of Incidence and Mortality Worldwide for 36 Cancers in 185 Countries. *CA Cancer J Clin* (2018) 68 (6):394–424. doi: 10.3322/caac.21492
2. Miranda-Filho A, Pineros M, Ferlay J, Soerjomataram I, Monnereau A, Bray F. Epidemiological Patterns of Leukaemia in 184 Countries: A Population-Based Study. *Lancet Haematol* (2018) 5(1):e14–24. doi: 10.1016/S2352-3026(17)30232-6
3. Paul S, Rausch CR, Nasnas PE, Kantarjian H, Jabbour EJ. Treatment of Relapsed/Refractory Acute Lymphoblastic Leukemia. *Clin Adv Hematol Oncol* (2019) 17(3):166–75.
4. Sung H, Ferlay J, Siegel RL, Laversanne M, Soerjomataram I, Jemal A, et al. Global Cancer Statistics 2020: GLOBOCAN Estimates of Incidence and Mortality Worldwide for 36 Cancers in 185 Countries. *CA Cancer J Clin* (2021) 71(3):209–49. doi: 10.3322/caac.21660
5. Paul S, Kantarjian H, Jabbour EJ. Adult Acute Lymphoblastic Leukemia. *Mayo Clin Proc* (2016) 91(11):1645–66. doi: 10.1016/j.mayocp.2016.09.010
6. Borowitz MJ, Devidas M, Hunger SP, Bowman WP, Carroll AJ, Carroll WL, et al. Clinical Significance of Minimal Residual Disease in Childhood Acute Lymphoblastic Leukemia and Its Relationship to Other Prognostic Factors: A Children's Oncology Group Study. *Blood* (2008) 111(12):5477–85. doi: 10.1182/blood-2008-01-132837
7. Abbasi S, Maleha F, Shobaki M. Acute Lymphoblastic Leukemia Experience: Epidemiology and Outcome of Two Different Regimens. *Mediterr J Hematol Infect Dis* (2013) 5(1):e2013024. doi: 10.4084/MJHID.2013.024
8. Solomon B, Parihar N, Ayodele L, Hughes M. Hematology & Hematological Oncology. In: *Journal of Blood Disorders & Transfusion*. Las Vegas, USA (2017). p. 9864. Available from: https://www.omicsonline.org/conference-proceedings/hematology-2017-scientifictracks-abstracts.digital.
9. Dinner S, Gurbuxani S, Jain N, Stock W. Acute Lymphoblastic Leukemia in Adults. In: Hoffman R, Benz E, et al, editors. *Hematology*. Las Vegas, USA: Elsevier (2018). p. 1029.e2– 54.e2.
10. Rivera-Luna R, Velasco-Hidalgo L, Zapata-Tarres M, Cardenas-Cardos R, Aguilar-Ortiz MR. Current Outlook of Childhood Cancer Epidemiology in a Middle-Income Country Under a Public Health Insurance Program. *Pediatr Hematol Oncol* (2017) 34(1):43–50. doi: 10.1080/08880018.2016.1276236
11. Magrath I, Steliarova-Foucher E, Epelman S, Ribeiro RC, Harif M, Li CK, et al. Paediatric Cancer in Low-Income and Middle-Income Countries. *Lancet Oncol* (2013) 14(3):e104–16. doi: 10.1016/S1470-2045(13)70008-1
12. Jimenez-Hernandez E, Jaimes-Reyes EZ, Arellano-Galindo J, Garcia-Jimenez X, Tiznado-Garcia HM, Duenas-Gonzalez MT, et al. Survival of Mexican Children With Acute Lymphoblastic Leukaemia Under Treatment With the Protocol From the Dana-Farber Cancer Institute 00-01. *BioMed Res Int* (2015) 2015:576950. doi: 10.1155/2015/576950
13. Martin-Trejo JA, Nunez-Enriquez JC, Fajardo-Gutierrez A, Medina-Sanson A, Flores-Lujano J, Jimenez-Hernandez E, et al. Early Mortality in Children With Acute Lymphoblastic Leukemia in a Developing Country: The Role of Malnutrition at Diagnosis. A Multicenter Cohort MIGICCL Study. *Leuk Lymphoma* (2017) 58(4):898–908. doi: 10.1080/10428194.2016.1219904
14. Moricke A, Zimmermann M, Valsecchi MG, Stanulla M, Biondi A, Mann G, et al. Dexamethasone *vs* Prednisone in Induction Treatment of Pediatric ALL: Results of the Randomized Trial AIEOP-BFM ALL 2000. *Blood* (2016) 127(17):2101–12. doi: 10.1182/blood-2015-09-670729
15. Advani A. Acute Lymphoblastic Leukemia (ALL). *Best Pract Res Clin Haematol* (2017) 30(3):173–4. doi: 10.1016/j.beha.2017.07.004
16. O'Dwyer KM, Liesveld JL. Philadelphia Chromosome Negative B-Cell Acute Lymphoblastic Leukemia in Older Adults: Current Treatment and Novel Therapies. *Best Pract Res Clin Haematol* (2017) 30(3):184–92. doi: 10.1016/j.beha.2017.08.001
17. Jain P, Korula A, Deshpande P, Pn N, Abu Alex A, Abraham A, et al. Adult Acute Lymphoblastic Leukemia: Limitations of Intensification of Therapy in a Developing Country. *J Glob Oncol* (2018) 4:1–12. doi: 10.1200/JGO.17.00014
18. Oskarsson T, Soderhall S, Arvidson J, Forestier E, Montgomery S, Bottai M, et al. Relapsed Childhood Acute Lymphoblastic Leukemia in the Nordic

Countries: Prognostic Factors, Treatment and Outcome. *Haematologica* (2016) 101(1):68–76. doi: 10.3324/haematol.2015.131680
19. Oriol A, Vives S, Hernandez-Rivas JM, Tormo M, Heras I, Rivas C, et al. Outcome After Relapse of Acute Lymphoblastic Leukemia in Adult Patients Included in Four Consecutive Risk-Adapted Trials by the PETHEMA Study Group. *Haematologica* (2010) 95(4):589–96. doi: 10.3324/haematol.2009.014274
20. Locatelli F, Schrappe M, Bernardo ME, Rutella S. How I Treat Relapsed Childhood Acute Lymphoblastic Leukemia. *Blood* (2012) 120(14):2807–16. doi: 10.1182/blood-2012-02-265884
21. DeAngelo DJ, Jabbour E, Advani A. Recent Advances in Managing Acute Lymphoblastic Leukemia. *Am Soc Clin Oncol Educ Book* (2020) 40:330–42. doi: 10.1200/EDBK_280175
22. Parker C, Waters R, Leighton C, Hancock J, Sutton R, Moorman AV, et al. Effect of Mitoxantrone on Outcome of Children With First Relapse of Acute Lymphoblastic Leukaemia (ALL R3): An Open-Label Randomised Trial. *Lancet* (2010) 376(9757):2009–17. doi: 10.1016/S0140-6736(10)62002-8
23. Kuhlen M, Willasch AM, Dalle JH, Wachowiak J, Yaniv I, Ifversen M, et al. Outcome of Relapse After Allogeneic HSCT in Children With ALL Enrolled in the ALL-SCT 2003/2007 Trial. *Br J Haematol* (2018) 180(1):82–9. doi: 10.1111/bjh.14965
24. Kuhlen M, Klusmann JH, Hoell JI. Molecular Approaches to Treating Pediatric Leukemias. *Front Pediatr* (2019) 7:368. doi: 10.3389/fped.2019.00368
25. Phelan KW, Advani AS. Novel Therapies in Acute Lymphoblastic Leukemia. *Curr Hematol Malig Rep* (2018) 13(4):289–99. doi: 10.1007/s11899-018-0457-7
26. Zhang MY, Liu SL, Huang WL, Tang DB, Zheng WW, Zhou N, et al. Bromodomains and Extra-Terminal (BET) Inhibitor JQ1 Suppresses Proliferation of Acute Lymphocytic Leukemia by Inhibiting C-Myc-Mediated Glycolysis. *Med Sci Monit* (2020) 26:e923411. doi: 10.12659/MSM.923411
27. Inaba H, Pui CH. Immunotherapy in Pediatric Acute Lymphoblastic Leukemia. *Cancer Metastasis Rev* (2019) 38(4):595–610. doi: 10.1007/s10555-019-09834-0
28. Witkowski MT, Lasry A, Carroll WL, Aifantis I. Immune-Based Therapies in Acute Leukemia. *Trends Cancer* (2019) 5(10):604–18. doi: 10.1016/j.trecan.2019.07.009
29. Blair GE, Cook GP. Cancer and the Immune System: An Overview. *Oncogene* (2008) 27(45):5868. doi: 10.1038/onc.2008.277
30. Abbott M, Ustoyev Y. Cancer and the Immune System: The History and Background of Immunotherapy. *Semin Oncol Nurs* (2019) 35(5):150923. doi: 10.1016/j.soncn.2019.08.002
31. Beatty GL, Gladney WL. Immune Escape Mechanisms as a Guide for Cancer Immunotherapy. *Clin Cancer Res* (2015) 21(4):687–92. doi: 10.1158/1078-0432.CCR-14-1860
32. Swann JB, Smyth MJ. Immune Surveillance of Tumors. *J Clin Invest* (2007) 117(5):1137–46. doi: 10.1172/JCI31405
33. Ramirez-Ramirez D, Padilla-Castaneda S, Galan-Enriquez CS, Vadillo E, Prieto-Chavez JL, Jimenez-Hernandez E, et al. CRTAM(+) NK Cells Endowed With Suppressor Properties Arise in Leukemic Bone Marrow. *J Leukoc Biol* (2019) 105(5):999–1013. doi: 10.1002/JLB.MA0618-231R
34. Kearney CJ, Vervoort SJ, Hogg SJ, Ramsbottom KM, Freeman AJ, Lalaoui N, et al. Tumor Immune Evasion Arises Through Loss of TNF Sensitivity. *Sci Immunol* (2018) 3(23):1–14. doi: 10.1126/sciimmunol.aar3451
35. Pardoll D. Cancer and the Immune System: Basic Concepts and Targets for Intervention. *Semin Oncol* (2015) 42(4):523–38. doi: 10.1053/j.seminoncol.2015.05.003
36. Sharma P, Hu-Lieskovan S, Wargo JA, Ribas A. Primary, Adaptive, and Acquired Resistance to Cancer Immunotherapy. *Cell* (2017) 168(4):707–23. doi: 10.1016/j.cell.2017.01.017
37. Cheng M, Chen Y, Xiao W, Sun R, Tian Z. NK Cell-Based Immunotherapy for Malignant Diseases. *Cell Mol Immunol* (2013) 10(3):230–52. doi: 10.1038/cmi.2013.10
38. Jorgovanovic D, Song M, Wang L, Zhang Y. Roles of IFN-Gamma in Tumor Progression and Regression: A Review. *Biomark Res* (2020) 8:49. doi: 10.1186/s40364-020-00228-x
39. Takeda K, Nakayama M, Hayakawa Y, Kojima Y, Ikeda H, Imai N, et al. IFN-Gamma Is Required for Cytotoxic T Cell-Dependent Cancer Genome Immunoediting. *Nat Commun* (2017) 8:14607. doi: 10.1038/ncomms14607
40. Aqbi HF, Wallace M, Sappal S, Payne KK, Manjili MH. IFN-Gamma Orchestrates Tumor Elimination, Tumor Dormancy, Tumor Escape, and Progression. *J Leukoc Biol* (2018) 22:1–5. doi: 10.1002/JLB.5MIR0917-351R
41. Crispin JC, Tsokos GC. Cancer Immunosurveillance by CD8 T Cells. *F1000Res* (2020) 9:1–7. doi: 10.12688/f1000research.21150.1
42. Philip M, Schietinger A. CD8(+) T Cell Differentiation and Dysfunction in Cancer. *Nat Rev Immunol* (2021). doi: 10.1038/s41577-021-00574-3
43. Anderson KG, Stromnes IM, Greenberg PD. Obstacles Posed by the Tumor Microenvironment to T Cell Activity: A Case for Synergistic Therapies. *Cancer Cell* (2017) 31(3):311–25. doi: 10.1016/j.ccell.2017.02.008
44. Teng MW, Galon J, Fridman WH, Smyth MJ. From Mice to Humans: Developments in Cancer Immunoediting. *J Clin Invest* (2015) 125(9):3338–46. doi: 10.1172/JCI80004
45. Vinay DS, Ryan EP, Pawelec G, Talib WH, Stagg J, Elkord E, et al. Immune Evasion in Cancer: Mechanistic Basis and Therapeutic Strategies. *Semin Cancer Biol* (2015) 35 Suppl:S185–98. doi: 10.1016/j.semcancer.2015.03.004
46. Tugues S, Burkhard SH, Ohs I, Vrohlings M, Nussbaum K, Vom Berg J, et al. New Insights Into IL-12-Mediated Tumor Suppression. *Cell Death Differ* (2015) 22(2):237–46. doi: 10.1038/cdd.2014.134
47. Cassim S, Pouyssegur J. Tumor Microenvironment: A Metabolic Player That Shapes the Immune Response. *Int J Mol Sci* (2019) 21(1):1–23. doi: 10.3390/ijms21010157
48. Dunn GP, Old LJ, Schreiber RD. The Immunobiology of Cancer Immunosurveillance and Immunoediting. *Immunity* (2004) 21(2):137–48. doi: 10.1016/j.immuni.2004.07.017
49. Romero I, Garrido C, Algarra I, Collado A, Garrido F, Garcia-Lora AM. T Lymphocytes Restrain Spontaneous Metastases in Permanent Dormancy. *Cancer Res* (2014) 74(7):1958–68. doi: 10.1158/0008-5472.CAN-13-2084
50. Wang HF, Wang SS, Huang MC, Liang XH, Tang YJ, Tang YL. Targeting Immune-Mediated Dormancy: A Promising Treatment of Cancer. *Front Oncol* (2019) 9:498. doi: 10.3389/fonc.2019.00498
51. Palucka AK, Coussens LM. The Basis of Oncoimmunology. *Cell* (2016) 164(6):1233–47. doi: 10.1016/j.cell.2016.01.049
52. Chalmers ZR, Connelly CF, Fabrizio D, Gay L, Ali SM, Ennis R, et al. Analysis of 100,000 Human Cancer Genomes Reveals the Landscape of Tumor Mutational Burden. *Genome Med* (2017) 9(1):34. doi: 10.1186/s13073-017-0424-2
53. Chen J, Zhang H, Zhou L, Hu Y, Li M, He Y, et al. Enhancing the Efficacy of Tumor Vaccines Based on Immune Evasion Mechanisms. *Front Oncol* (2020) 10:584367. doi: 10.3389/fonc.2020.584367
54. Zheng Y, Delgoffe GM, Meyer CF, Chan W, Powell JD. Anergic T Cells are Metabolically Anergic. *J Immunol* (2009) 183(10):6095–101. doi: 10.4049/jimmunol.0803510
55. Dander E, Palmi C, D'Amico G, Cazzaniga G. The Bone Marrow Niche in B-Cell Acute Lymphoblastic Leukemia: The Role of Microenvironment From Pre-Leukemia to Overt Leukemia. *Int J Mol Sci* (2021) 22(9):1–24. doi: 10.3390/ijms22094426
56. Howie D, Ten Bokum A, Necula AS, Cobbold SP, Waldmann H. The Role of Lipid Metabolism in T Lymphocyte Differentiation and Survival. *Front Immunol* (2017) 8:1949. doi: 10.3389/fimmu.2017.01949
57. Noguchi T, Ward JP, Gubin MM, Arthur CD, Lee SH, Hundal J, et al. Temporally Distinct PD-L1 Expression by Tumor and Host Cells Contributes to Immune Escape. *Cancer Immunol Res* (2017) 5(2):106–17. doi: 10.1158/2326-6066.CIR-16-0391
58. Jiang X, Wang J, Deng X, Xiong F, Ge J, Xiang B, et al. Role of the Tumor Microenvironment in PD-L1/PD-1-Mediated Tumor Immune Escape. *Mol Cancer* (2019) 18(1):10. doi: 10.1186/s12943-018-0928-4
59. Torelli GF, Peragine N, Raponi S, Pagliara D, De Propris MS, Vitale A, et al. Recognition of Adult and Pediatric Acute Lymphoblastic Leukemia Blasts by Natural Killer Cells. *Haematologica* (2014) 99(7):1248–54. doi: 10.3324/haematol.2013.101931
60. Alkhouly N, Shehata I, Ahmed MB, Shehata H, Hassan S, Ibrahim T. HLA-G Expression in Acute Lymphoblastic Leukemia: A Significant Prognostic Tumor Biomarker. *Med Oncol* (2013) 30(1):460. doi: 10.1007/s12032-013-0460-8
61. Valenzuela-Vazquez L, Nunez-Enriquez JC, Sanchez-Herrera J, Jimenez-Hernandez E, Martin-Trejo JA, Espinoza-Hernandez LE, et al. Functional Characterization of NK Cells in Mexican Pediatric Patients With Acute

Lymphoblastic Leukemia: Report From the Mexican Interinstitutional Group for the Identification of the Causes of Childhood Leukemia. *PloS One* (2020) 15(1):e0227314. doi: 10.1371/journal.pone.0227314
62. Montironi C, Munoz-Pinedo C, Eldering E. Hematopoietic *Versus* Solid Cancers and T Cell Dysfunction: Looking for Similarities and Distinctions. *Cancers (Basel)* (2021) 13(2):1–20. doi: 10.3390/cancers13020284
63. Xu J, Xu W, Xuan Y, Liu Z, Sun Q, Lan C. Pancreatic Cancer Progression Is Regulated by IPO7/p53/LncRNA MALAT1/MiR-129-5p Positive Feedback Loop. *Front Cell Dev Biol* (2021) 9:630262. doi: 10.3389/fcell.2021.630262
64. Shimada K, Yoshida K, Suzuki Y, Iriyama C, Inoue Y, Sanada M, et al. Frequent Genetic Alterations in Immune Checkpoint-Related Genes in Intravascular Large B-Cell Lymphoma. *Blood* (2021) 137(11):1491–502. doi: 10.1182/blood.2020007245
65. Rosenthal R, Cadieux EL, Salgado R, Bakir MA, Moore DA, Hiley CT, et al. Neoantigen-Directed Immune Escape in Lung Cancer Evolution. *Nature* (2019) 567(7749):479–85. doi: 10.1038/s41586-019-1032-7
66. Vidotto T, Nersesian S, Graham C, Siemens DR, Koti M. DNA Damage Repair Gene Mutations and Their Association With Tumor Immune Regulatory Gene Expression in Muscle Invasive Bladder Cancer Subtypes. *J Immunother Cancer* (2019) 7(1):148. doi: 10.1186/s40425-019-0619-8
67. Kobayashi Y, Lim SO, Yamaguchi H. Oncogenic Signaling Pathways Associated With Immune Evasion and Resistance to Immune Checkpoint Inhibitors in Cancer. *Semin Cancer Biol* (2020) 65:51–64. doi: 10.1016/j.semcancer.2019.11.011
68. Meyer S, Handke D, Mueller A, Biehl K, Kreuz M, Bukur J, et al. Distinct Molecular Mechanisms of Altered HLA Class II Expression in Malignant Melanoma. *Cancers (Basel)* (2021) 13(15):1–18. doi: 10.3390/cancers13153907
69. Xu HH, Gan J, Xu DP, Li L, Yan WH. Comprehensive Transcriptomic Analysis Reveals the Role of the Immune Checkpoint HLA-G Molecule in Cancers. *Front Immunol* (2021) 12:614773. doi: 10.3389/fimmu.2021.614773
70. Mimura K, Teh JL, Okayama H, Shiraishi K, Kua LF, Koh V, et al. PD-L1 Expression is Mainly Regulated by Interferon Gamma Associated With JAK-STAT Pathway in Gastric Cancer. *Cancer Sci* (2018) 109(1):43–53. doi: 10.1111/cas.13424
71. Sivori S, Della Chiesa M, Carlomagno S, Quatrini L, Munari E, Vacca P, et al. Inhibitory Receptors and Checkpoints in Human NK Cells, Implications for the Immunotherapy of Cancer. *Front Immunol* (2020) 11:2156. doi: 10.3389/fimmu.2020.02156
72. Jansen JA, Omuro A, Lucca LE. T Cell Dysfunction in Glioblastoma: A Barrier and an Opportunity for the Development of Successful Immunotherapies. *Curr Opin Neurol* (2021). doi: 10.1097/WCO.0000000000000988
73. Vlachonikola E, Stamatopoulos K, Chatzidimitriou A. T Cell Defects and Immunotherapy in Chronic Lymphocytic Leukemia. *Cancers (Basel)* (2021) 13(13):1–16. doi: 10.3390/cancers13133255
74. Qiu Y, Yang Y, Yang R, Liu C, Hsu JM, Jiang Z, et al. Activated T Cell-Derived Exosomal PD-1 Attenuates PD-L1-Induced Immune Dysfunction in Triple-Negative Breast Cancer. *Oncogene* (2021) 40(31):4992–5001. doi: 10.1038/s41388-021-01896-1
75. Hung MH, Lee JS, Ma C, Diggs LP, Heinrich S, Chang CW, et al. Tumor Methionine Metabolism Drives T-Cell Exhaustion in Hepatocellular Carcinoma. *Nat Commun* (2021) 12(1):1455. doi: 10.1038/s41467-021-21804-1
76. Abiko K, Mandai M, Hamanishi J, Yoshioka Y, Matsumura N, Baba T, et al. PD-L1 on Tumor Cells is Induced in Ascites and Promotes Peritoneal Dissemination of Ovarian Cancer Through CTL Dysfunction. *Clin Cancer Res* (2013) 19(6):1363–74. doi: 10.1158/1078-0432.CCR-12-2199
77. Jo S, Lee JH, Mattei JJ, Barrett DM, van den Elzen P, Grupp SA, et al. Generation of a Multi-Antigen-Directed Immune Response for Durable Control of Acute Lymphoblastic Leukemia. *Leukemia* (2018) 32(2):574. doi: 10.1038/leu.2017.312
78. Kebelmann-Betzing C, Korner G, Badiali L, Buchwald D, Moricke A, Korte A, et al. Characterization of Cytokine, Growth Factor Receptor, Costimulatory and Adhesion Molecule Expression Patterns of Bone Marrow Blasts in Relapsed Childhood B Cell Precursor All. *Cytokine* (2001) 13(1):39–50. doi: 10.1006/cyto.2000.0794
79. Luczynski W, Stasiak-Barmuta A, Ilendo E, Kovalchuk O, Krawczuk-Rybak M, Malinowska I, et al. Low Expression of Costimulatory Molecules and mRNA for Cytokines are Important Mechanisms of Immunosuppression in Acute Lymphoblastic Leukemia in Children? *Neoplasma* (2006) 53(4):301–4.
80. D'Amico G, Vulcano M, Bugarin C, Bianchi G, Pirovano G, Bonamino M, et al. CD40 Activation of BCP-ALL Cells Generates IL-10-Producing, IL-12-Defective APCs That Induce Allogeneic T-Cell Anergy. *Blood* (2004) 104(3):744–51. doi: 10.1182/blood-2003-11-3762
81. Feng YY, Griffith OL, Griffith M. Clinical Implications of Neoepitope Landscapes for Adult and Pediatric Cancers. *Genome Med* (2017) 9(1):77. doi: 10.1186/s13073-017-0470-9
82. Zamora AE, Crawford JC, Thomas PG. Hitting the Target: How T Cells Detect and Eliminate Tumors. *J Immunol* (2018) 200(2):392–9. doi: 10.4049/jimmunol.1701413
83. Zamora AE, Crawford JC, Allen EK, Guo XJ, Bakke J, Carter RA, et al. Pediatric Patients With Acute Lymphoblastic Leukemia Generate Abundant and Functional Neoantigen-Specific CD8(+) T Cell Responses. *Sci Transl Med* (2019) 11(498):1–29. doi: 10.1126/scitranslmed.aat8549
84. Chang TC, Carter RA, Li Y, Li Y, Wang H, Edmonson MN, et al. The Neoepitope Landscape in Pediatric Cancers. *Genome Med* (2017) 9(1):78. doi: 10.1186/s13073-017-0468-3
85. Curran EK, Godfrey J, Kline J. Mechanisms of Immune Tolerance in Leukemia and Lymphoma. *Trends Immunol* (2017) 38(7):513–25. doi: 10.1016/j.it.2017.04.004
86. Vardhana S, Younes A. The Immune Microenvironment in Hodgkin Lymphoma: T Cells, B Cells, and Immune Checkpoints. *Haematologica* (2016) 101(7):794–802. doi: 10.3324/haematol.2015.132761
87. Cardoso AA, Schultze JL, Boussiotis VA, Freeman GJ, Seamon MJ, Laszlo S, et al. Pre-B Acute Lymphoblastic Leukemia Cells may Induce T-Cell Anergy to Alloantigen. *Blood* (1996) 88(1):41–8. doi: 10.1182/blood.V88.1.41.41
88. Spencer HC, Masaba SC, Kiaraho D. Sensitivity of Plasmodium Falciparum Isolates to Chloroquine in Kisumu and Malindi, Kenya. *Am J Trop Med Hyg* (1982) 31(5):902–6. doi: 10.4269/ajtmh.1982.31.902
89. Bien E, Balcerska A, Adamkiewicz-Drozynska E, Rapala M, Krawczyk M, Stepinski J. Pre-Treatment Serum Levels of Interleukin-10, Interleukin-12 and Their Ratio Predict Response to Therapy and Probability of Event-Free and Overall Survival in Childhood Soft Tissue Sarcomas, Hodgkin's Lymphomas and Acute Lymphoblastic Leukemias. *Clin Biochem* (2009) 42(10-11):1144–57. doi: 10.1016/j.clinbiochem.2009.04.004
90. Knaus HA, Kanakry CG, Luznik L, Gojo I. Immunomodulatory Drugs: Immune Checkpoint Agents in Acute Leukemia. *Curr Drug Targets* (2017) 18(3):315–31. doi: 10.2174/1389450116666150518095346
91. de Deus DM, Lugo KA, Muniz MT. Influence of IL10 (G1082A) and TNFalpha (G308A) Polymorphisms on the Survival of Pediatric Patients With ALL. *Leuk Res Treat* (2012) 2012:692348. doi: 10.1155/2012/692348
92. Hiroki CH, Amarante MK, Petenuci DL, Sakaguchi AY, Trigo FC, Watanabe MA, et al. IL-10 Gene Polymorphism and Influence of Chemotherapy on Cytokine Plasma Levels in Childhood Acute Lymphoblastic Leukemia Patients: IL-10 Polymorphism and Plasma Levels in Leukemia Patients. *Blood Cells Mol Dis* (2015) 55(2):168–72. doi: 10.1016/j.bcmd.2015.06.004
93. Andersen MH. The Targeting of Immunosuppressive Mechanisms in Hematological Malignancies. *Leukemia* (2014) 28(9):1784–92. doi: 10.1038/leu.2014.108
94. Green MR, Monti S, Rodig SJ, Juszczynski P, Currie T, O'Donnell E, et al. Integrative Analysis Reveals Selective 9p24.1 Amplification, Increased PD-1 Ligand Expression, and Further Induction *via* JAK2 in Nodular Sclerosing Hodgkin Lymphoma and Primary Mediastinal Large B-Cell Lymphoma. *Blood* (2010) 116(17):3268–77. doi: 10.1182/blood-2010-05-282780
95. Liu Z, Derkach A, Yu KJ, Yeager M, Chang YS, Chen CJ, et al. Patterns of Human Leukocyte Antigen Class I and Class II Associations and Cancer. *Cancer Res* (2021) 81(4):1148–52. doi: 10.1158/0008-5472.CAN-20-2292
96. Wang SS, Carrington M, Berndt SI, Slager SL, Bracci PM, Voutsinas J, et al. HLA Class I and II Diversity Contributes to the Etiologic Heterogeneity of Non-Hodgkin Lymphoma Subtypes. *Cancer Res* (2018) 78(14):4086–96. doi: 10.1158/0008-5472.CAN-17-2900
97. Brouwer RE, van der Heiden P, Schreuder GM, Mulder A, Datema G, Anholts JD, et al. Loss or Downregulation of HLA Class I Expression at the Allelic Level in Acute Leukemia Is Infrequent But Functionally Relevant, and can be Restored by Interferon. *Hum Immunol* (2002) 63(3):200–10. doi: 10.1016/s0198-8859(01)00381-0

98. Liu L, Chang YJ, Xu LP, Zhang XH, Wang Y, Liu KY, et al. T Cell Exhaustion Characterized by Compromised MHC Class I and II Restricted Cytotoxic Activity Associates With Acute B Lymphoblastic Leukemia Relapse After Allogeneic Hematopoietic Stem Cell Transplantation. *Clin Immunol* (2018) 190:32–40. doi: 10.1016/j.clim.2018.02.009
99. Babor F, Manser AR, Fischer JC, Scherenschlich N, Enczmann J, Chazara O, et al. KIR Ligand C2 Is Associated With Increased Susceptibility to Childhood ALL and Confers an Elevated Risk for Late Relapse. *Blood* (2014) 124(14):2248–51. doi: 10.1182/blood-2014-05-572065
100. Reusing SB, Manser AR, Enczmann J, Mulder A, Claas FH, Carrington M, et al. Selective Downregulation of HLA-C and HLA-E in Childhood Acute Lymphoblastic Leukaemia. *Br J Haematol* (2016) 174(3):477–80. doi: 10.1111/bjh.13777
101. Pende D, Marcenaro S, Falco M, Martini S, Bernardo ME, Montagna D, et al. Anti-Leukemia Activity of Alloreactive NK Cells in KIR Ligand-Mismatched Haploidentical HSCT for Pediatric Patients: Evaluation of the Functional Role of Activating KIR and Redefinition of Inhibitory KIR Specificity. *Blood* (2009) 113(13):3119–29. doi: 10.1182/blood-2008-06-164103
102. Holling TM, Schooten E, Langerak AW, van den Elsen PJ. Regulation of MHC Class II Expression in Human T-Cell Malignancies. *Blood* (2004) 103 (4):1438–44. doi: 10.1182/blood-2003-05-1491
103. Takeuchi M, Miyoshi H, Asano N, Yoshida N, Yamada K, Yanagida E, et al. Human Leukocyte Antigen Class II Expression Is a Good Prognostic Factor in Adult T-Cell Leukemia/Lymphoma. *Haematologica* (2019) 104(8):1626–32. doi: 10.3324/haematol.2018.205567
104. Mannelli F SI. Immunophenotyping of Acute Leukemias – From Biology to Clinical Application. In: *Flow Cytometry*. Rijeka: IntechOpen (2016). p. Ch. 6. doi: 10.5772/62332
105. Yang K, Xu J, Liu Q, Li J, Xi Y. Expression and Significance of CD47, PD1 and PDL1 in T-Cell Acute Lymphoblastic Lymphoma/Leukemia. *Pathol Res Pract* (2019) 215(2):265–71. doi: 10.1016/j.prp.2018.10.021
106. Brunner-Weinzierl MC, Rudd CE. CTLA-4 and PD-1 Control of T-Cell Motility and Migration: Implications for Tumor Immunotherapy. *Front Immunol* (2018) 9:2737. doi: 10.3389/fimmu.2018.02737
107. Ramzi M, Iravani Saadi M, Yaghobi R, Arandi N. Dysregulated Expression of CD28 and CTLA-4 Molecules in Patients With Acute Myeloid Leukemia and Possible Association With Development of Graft *Versus* Host Disease After Hematopoietic Stem Cell Transplantation. *Int J Organ Transplant Med* (2019) 10(2):84–90.
108. Kang SH, Hwang HJ, Yoo JW, Kim H, Choi ES, Hwang SH, et al. Expression of Immune Checkpoint Receptors on T-Cells and Their Ligands on Leukemia Blasts in Childhood Acute Leukemia. *Anticancer Res* (2019) 39 (10):5531–9. doi: 10.21873/anticanres.13746
109. Simone R, Tenca C, Fais F, Luciani M, De Rossi G, Pesce G, et al. A Soluble Form of CTLA-4 is Present in Paediatric Patients With Acute Lymphoblastic Leukaemia and Correlates With CD1d+ Expression. *PloS One* (2012) 7(9): e44654. doi: 10.1371/journal.pone.0044654
110. Austin R, Smyth MJ, Lane SW. Harnessing the Immune System in Acute Myeloid Leukaemia. *Crit Rev Oncol Hematol* (2016) 103:62–77. doi: 10.1016/j.critrevonc.2016.04.020
111. Mansour A, Elkhodary T, Darwish A, Mabed M. Increased Expression of Costimulatory Molecules CD86 and sCTLA-4 in Patients With Acute Lymphoblastic Leukemia. *Leuk Lymphoma* (2014) 55(9):2120–4. doi: 10.3109/10428194.2013.869328
112. Pastorczak A, Domka K, Fidyt K, Poprzeczko M, Firczuk M. Mechanisms of Immune Evasion in Acute Lymphoblastic Leukemia. *Cancers (Basel)* (2021) 13(7):1–25. doi: 10.3390/cancers13071536
113. Four M, Cacheux V, Tempier A, Platero D, Fabbro M, Marin G, et al. PD1 and PDL1 Expression in Primary Central Nervous System Diffuse Large B-Cell Lymphoma Are Frequent and Expression of PD1 Predicts Poor Survival. *Hematol Oncol* (2017) 35(4):487–96. doi: 10.1002/hon.2375
114. Zhou Q, Munger ME, Veenstra RG, Weigel BJ, Hirashima M, Munn DH, et al. Coexpression of Tim-3 and PD-1 Identifies a CD8+ T-Cell Exhaustion Phenotype in Mice With Disseminated Acute Myelogenous Leukemia. *Blood* (2011) 117(17):4501–10. doi: 10.1182/blood-2010-10-310425
115. Feucht J, Kayser S, Gorodezki D, Hamieh M, Doring M, Blaeschke F, et al. T-Cell Responses Against CD19+ Pediatric Acute Lymphoblastic Leukemia Mediated by Bispecific T-Cell Engager (BiTE) are Regulated Contrarily by PD-L1 and CD80/CD86 on Leukemic Blasts. *Oncotarget* (2016) 7 (47):76902–19. doi: 10.18632/oncotarget.12357
116. Lee-Sherick AB, Jacobsen KM, Henry CJ, Huey MG, Parker RE, Page LS, et al. MERTK Inhibition Alters the PD-1 Axis and Promotes Anti-Leukemia Immunity. *JCI Insight* (2018) 3(21):1–17. doi: 10.1172/jci.insight.97941
117. Hohtari H, Bruck O, Blom S, Turkki R, Sinisalo M, Kovanen PE, et al. Immune Cell Constitution in Bone Marrow Microenvironment Predicts Outcome in Adult ALL. *Leukemia* (2019) 33(7):1570–82. doi: 10.1038/s41375-018-0360-1
118. Chiarini F, Lonetti A, Evangelisti C, Buontempo F, Orsini E, Evangelisti C, et al. Advances in Understanding the Acute Lymphoblastic Leukemia Bone Marrow Microenvironment: From Biology to Therapeutic Targeting. *Biochim Biophys Acta* (2016) 1863(3):449–63. doi: 10.1016/j.bbamcr.2015.08.015
119. Choi DC, Tremblay D, Iancu-Rubin C, Mascarenhas J. Programmed Cell Death-1 Pathway Inhibition in Myeloid Malignancies: Implications for Myeloproliferative Neoplasms. *Ann Hematol* (2017) 96(6):919–27. doi: 10.1007/s00277-016-2915-4
120. Christiansson L, Soderlund S, Svensson E, Mustjoki S, Bengtsson M, Simonsson B, et al. Increased Level of Myeloid-Derived Suppressor Cells, Programmed Death Receptor Ligand 1/Programmed Death Receptor 1, and Soluble CD25 in Sokal High Risk Chronic Myeloid Leukemia. *PloS One* (2013) 8(1):e55818. doi: 10.1371/journal.pone.0055818
121. Ju Y, Shang X, Liu Z, Zhang J, Li Y, Shen Y, et al. The Tim-3/Galectin-9 Pathway Involves in the Homeostasis of Hepatic Tregs in a Mouse Model of Concanavalin A-Induced Hepatitis. *Mol Immunol* (2014) 58(1):85–91. doi: 10.1016/j.molimm.2013.11.001
122. Gagliani N, Magnani CF, Huber S, Gianolini ME, Pala M, Licona-Limon P, et al. Coexpression of CD49b and LAG-3 Identifies Human and Mouse T Regulatory Type 1 Cells. *Nat Med* (2013) 19(6):739–46. doi: 10.1038/nm.3179
123. Solinas C, Migliori E, De Silva P, Willard-Gallo K. LAG3: The Biological Processes That Motivate Targeting This Immune Checkpoint Molecule in Human Cancer. *Cancers (Basel)* (2019) 11(8):1–16. doi: 10.3390/cancers11081213
124. Lee HJ, Kim SN, Jeon MS, Yi T, Song SU. ICOSL Expression in Human Bone Marrow-Derived Mesenchymal Stem Cells Promotes Induction of Regulatory T Cells. *Sci Rep* (2017) 7:44486. doi: 10.1038/srep44486
125. Li DY, Xiong XZ. ICOS(+) Tregs: A Functional Subset of Tregs in Immune Diseases. *Front Immunol* (2020) 11:2104. doi: 10.3389/fimmu.2020.02104
126. Han Y, Dong Y, Yang Q, Xu W, Jiang S, Yu Z, et al. Acute Myeloid Leukemia Cells Express ICOS Ligand to Promote the Expansion of Regulatory T Cells. *Front Immunol* (2018) 9:2227. doi: 10.3389/fimmu.2018.02227
127. Bayon-Calderon F, Toribio ML, Gonzalez-Garcia S. Facts and Challenges in Immunotherapy for T-Cell Acute Lymphoblastic Leukemia. *Int J Mol Sci* (2020) 21(20):1–35. doi: 10.3390/ijms21207685
128. Zappavigna S, Cossu AM, Grimaldi A, Bocchetti M, Ferraro GA, Nicoletti GF, et al. Anti-Inflammatory Drugs as Anticancer Agents. *Int J Mol Sci* (2020) 21(7):1–29. doi: 10.3390/ijms21072605
129. Soegaard SH, Rostgaard K, Skogstrand K, Wiemels JL, Schmiegelow K, Hjalgrim H. Neonatal Inflammatory Markers Are Associated With Childhood B-Cell Precursor Acute Lymphoblastic Leukemia. *Cancer Res* (2018) 78(18):5458–63. doi: 10.1158/0008-5472.CAN-18-0831
130. Balandran JC, Purizaca J, Enciso J, Dozal D, Sandoval A, Jimenez-Hernandez E, et al. Pro-Inflammatory-Related Loss of CXCL12 Niche Promotes Acute Lymphoblastic Leukemic Progression at the Expense of Normal Lymphopoiesis. *Front Immunol* (2016) 7:666. doi: 10.3389/fimmu.2016.00666
131. Fleischhack G, Cipic D, Juettner J, Hasan C, Bode U. Procalcitonin-A Sensitive Inflammation Marker of Febrile Episodes in Neutropenic Children With Cancer. *Intensive Care Med* (2000) 26 Suppl 2:S202–11. doi: 10.1007/BF02900739
132. Park HH, Kim M, Lee BH, Lim J, Kim Y, Lee EJ, et al. Intracellular IL-4, IL-10, and IFN-Gamma Levels of Leukemic Cells and Bone Marrow T Cells in Acute Leukemia. *Ann Clin Lab Sci* (2006) 36(1):7–15.
133. Perez-Figueroa E, Sanchez-Cuaxospa M, Martinez-Soto KA, Sanchez-Zauco N, Medina-Sanson A, Jimenez-Hernandez E, et al. Strong Inflammatory Response and Th1-Polarization Profile in Children With Acute Lymphoblastic Leukemia Without Apparent Infection. *Oncol Rep* (2016) 35(5):2699–706. doi: 10.3892/or.2016.4657

134. Castellheim A, Brekke OL, Espevik T, Harboe M, Mollnes TE. Innate Immune Responses to Danger Signals in Systemic Inflammatory Response Syndrome and Sepsis. *Scand J Immunol* (2009) 69(6):479–91. doi: 10.1111/j.1365-3083.2009.02255.x
135. Naka K, Hoshii T, Muraguchi T, Tadokoro Y, Ooshio T, Kondo Y, et al. TGF-Beta-FOXO Signalling Maintains Leukaemia-Initiating Cells in Chronic Myeloid Leukaemia. *Nature* (2010) 463(7281):676–80. doi: 10.1038/nature08734
136. Bernasconi P, Borsani O. Immune Escape After Hematopoietic Stem Cell Transplantation (HSCT): From Mechanisms to Novel Therapies. *Cancers (Basel)* (2019) 12(1):1–25. doi: 10.3390/cancers12010069
137. Wu S, Gessner R, von Stackelberg A, Kirchner R, Henze G, Seeger K. Cytokine/cytokine Receptor Gene Expression in Childhood Acute Lymphoblastic Leukemia: Correlation of Expression and Clinical Outcome at First Disease Recurrence. *Cancer* (2005) 103(5):1054–63. doi: 10.1002/cncr.20869
138. Verma D, Zanetti C, Godavarthy PS, Kumar R, Minciacchi VR, Pfeiffer J, et al. Bone Marrow Niche-Derived Extracellular Matrix-Degrading Enzymes Influence the Progression of B-Cell Acute Lymphoblastic Leukemia. *Leukemia* (2020) 34(6):1540–52. doi: 10.1038/s41375-019-0674-7
139. Rouce RH, Shaim H, Sekine T, Weber G, Ballard B, Ku S, et al. The TGF-Beta/SMAD Pathway Is an Important Mechanism for NK Cell Immune Evasion in Childhood B-Acute Lymphoblastic Leukemia. *Leukemia* (2016) 30(4):800–11. doi: 10.1038/leu.2015.327
140. Srivannaboon K, Shanafelt AB, Todisco E, Forte CP, Behm FG, Raimondi SC, et al. Interleukin-4 Variant (BAY 36-1677) Selectively Induces Apoptosis in Acute Lymphoblastic Leukemia Cells. *Blood* (2001) 97(3):752–8. doi: 10.1182/blood.v97.3.752
141. Allahbakhshian Farsani M, Kamel M, Mehrpouri M, Heris RS, Hamidpour M, Salari S, et al. The Expression of Interferon Gamma (IFN-Gamma) and Interleukin 6 (IL6) in Patients With Acute Lymphoblastic Leukemia (ALL). *Pathol Oncol Res* (2020) 26(1):461–6. doi: 10.1007/s12253-018-0536-z
142. Cloppenborg T, Stanulla M, Zimmermann M, Schrappe M, Welte K, Klein C. Immunosurveillance of Childhood ALL: Polymorphic Interferon-Gamma Alleles are Associated With Age at Diagnosis and Clinical Risk Groups. *Leukemia* (2005) 19(1):44–8. doi: 10.1038/sj.leu.2403553
143. Zhang XL, Komada Y, Chipeta J, Li QS, Inaba H, Azuma E, et al. Intracellular Cytokine Profile of T Cells From Children With Acute Lymphoblastic Leukemia. *Cancer Immunol Immunother* (2000) 49(3):165–72. doi: 10.1007/s002620050616
144. Eber SW, Morris SA, Schroter W, Gratzer WB. Interactions of Spectrin in Hereditary Elliptocytes Containing Truncated Spectrin Beta-Chains. *J Clin Invest* (1988) 81(2):523–30. doi: 10.1172/JCI113350
145. Zhao H, Zhou H, Cao Q, Wang C, Bai J, Lv P, et al. Effect of Allogeneic Blood Transfusion on Levels of IL-6 and sIL-R2 in Peripheral Blood of Children With Acute Lymphocytic Leukemia. *Oncol Lett* (2018) 16(1):849–52. doi: 10.3892/ol.2018.8760
146. Juarez J, Baraz R, Gaundar S, Bradstock K, Bendall L. Interaction of Interleukin-7 and Interleukin-3 With the CXCL12-Induced Proliferation of B-Cell Progenitor Acute Lymphoblastic Leukemia. *Haematologica* (2007) 92(4):450–9. doi: 10.3324/haematol.10621
147. Scupoli MT, Perbellini O, Krampera M, Vinante F, Cioffi F, Pizzolo G. Interleukin 7 Requirement for Survival of T-Cell Acute Lymphoblastic Leukemia and Human Thymocytes on Bone Marrow Stroma. *Haematologica* (2007) 92(2):264–6. doi: 10.3324/haematol.10356
148. Ma Z, Zhao X, Deng M, Huang Z, Wang J, Wu Y, et al. Bone Marrow Mesenchymal Stromal Cell-Derived Periostin Promotes B-ALL Progression by Modulating CCL2 in Leukemia Cells. *Cell Rep* (2019) 26(6):1533–43.e4. doi: 10.1016/j.celrep.2019.01.034
149. El-Maadawy EA, Elshal MF, Bakry RM, Moussa MM, El-Naby S, Talaat RM. Regulation of CD4(+)CD25(+)FOXP3(+) Cells in Pediatric Acute Lymphoblastic Leukemia (ALL): Implication of Cytokines and miRNAs. *Mol Immunol* (2020) 124:1–8. doi: 10.1016/j.molimm.2020.05.002
150. Hiroki ER, Erthal RP, Pereira APL, Pacholak LM, Fujita TC, Marinello PC, et al. Acute Lymphoblastic Leukemia and Regulatory T Cells: Biomarkers and Immunopathogenesis. *Curr Immunol Rev* (2016) 12:14–9. doi: 10.2174/1573395511666150923234547
151. Sakaguchi S, Yamaguchi T, Nomura T, Ono M. Regulatory T Cells and Immune Tolerance. *Cell* (2008) 133(5):775–87. doi: 10.1016/j.cell.2008.05.009
152. Wu CP, Qing X, Wu CY, Zhu H, Zhou HY. Immunophenotype and Increased Presence of CD4(+)CD25(+) Regulatory T Cells in Patients With Acute Lymphoblastic Leukemia. *Oncol Lett* (2012) 3(2):421–4. doi: 10.3892/ol.2011.499
153. An F, Wang H, Liu Z, Wu F, Zhang J, Tao Q, et al. Influence of Patient Characteristics on Chimeric Antigen Receptor T Cell Therapy in B-Cell Acute Lymphoblastic Leukemia. *Nat Commun* (2020) 11(1):5928. doi: 10.1038/s41467-020-19774-x
154. Idris SZ, Hassan N, Lee LJ, Md Noor S, Osman R, Abdul-Jalil M, et al. Increased Regulatory T Cells in Acute Lymphoblastic Leukaemia Patients. *Hematology* (2016) 21(4):206–12. doi: 10.1080/10245332.2015.1101965
155. Jacobs JF, Nierkens S, Figdor CG, de Vries IJ, Adema GJ. Regulatory T Cells in Melanoma: The Final Hurdle Towards Effective Immunotherapy? *Lancet Oncol* (2012) 13(1):e32–42. doi: 10.1016/S1470-2045(11)70155-3
156. Niedzwiecki M, Budzilo O, Adamkiewicz-Drozynska E, Pawlik-Gwozdecka D, Zielinski M, Maciejka-Kemblowska L, et al. CD4(+)CD25(high)CD127(low/-)FoxP3 (+) Regulatory T-Cell Population in Acute Leukemias: A Review of the Literature. *J Immunol Res* (2019) 2019:2816498. doi: 10.1155/2019/2816498
157. Beyer M, Kochanek M, Darabi K, Popov A, Jensen M, Endl E, et al. Reduced Frequencies and Suppressive Function of CD4+CD25hi Regulatory T Cells in Patients With Chronic Lymphocytic Leukemia After Therapy With Fludarabine. *Blood* (2005) 106(6):2018–25. doi: 10.1182/blood-2005-02-0642
158. Bhattacharya K, Chandra S, Mandal C. Critical Stoichiometric Ratio of CD4 (+) CD25(+) FoxP3(+) Regulatory T Cells and CD4(+) CD25(-) Responder T Cells Influence Immunosuppression in Patients With B-Cell Acute Lymphoblastic Leukaemia. *Immunology* (2014) 142(1):124–39. doi: 10.1111/imm.12237
159. Chen Z, Zheng Y, Yang Y, Kang J, You MJ, Tian C. Abnormal Bone Marrow Microenvironment: The "Harbor" of Acute Lymphoblastic Leukemia Cells. *Blood Sci* (2021) 3(2):29–34. doi: 10.1097/bs9.0000000000000071
160. Purizaca J, Contreras-Quiroz A, Dorantes-Acosta E, Vadillo E, Arriaga-Pizano L, Fuentes-Figueroa S, et al. Lymphoid Progenitor Cells From Childhood Acute Lymphoblastic Leukemia Are Functionally Deficient and Express High Levels of the Transcriptional Repressor Gfi-1. *Clin Dev Immunol* (2013) 2013:349067. doi: 10.1155/2013/349067
161. Makanga DR, Da Rin de Lorenzo F, David G, Willem C, Dubreuil L, Legrand N, et al. Genetic and Molecular Basis of Heterogeneous NK Cell Responses Against Acute Leukemia. *Cancers (Basel)* (2020) 12(7):1–18. doi: 10.3390/cancers12071927
162. Foley B, Ta C, Barnes S, de Jong E, Nguyen M, Cheung LC, et al. Identifying the Optimal Donor for Natural Killer Cell Adoptive Therapy to Treat Paediatric B- and T-Cell Acute Lymphoblastic Leukaemia. *Clin Transl Immunol* (2020) 9(7):e1151. doi: 10.1002/cti2.1151
163. Zahran AM, Shibl A, Rayan A, Mohamed M, Osman AMM, Saad K, et al. Increase in Polymorphonuclear Myeloid-Derived Suppressor Cells and Regulatory T-Cells in Children With B-Cell Acute Lymphoblastic Leukemia. *Sci Rep* (2021) 11(1):15039. doi: 10.1038/s41598-021-94469-x
164. Parker KH, Beury DW, Ostrand-Rosenberg S. Myeloid-Derived Suppressor Cells: Critical Cells Driving Immune Suppression in the Tumor Microenvironment. *Adv Cancer Res* (2015) 128:95–139. doi: 10.1016/bs.acr.2015.04.002
165. Labib Salem M, Zidan AA, Ezz El-Din El-Naggar R, Attia Saad M, El-Shanshory M, Bakry U, et al. Myeloid-Derived Suppressor Cells and Regulatory T Cells Share Common Immunoregulatory Pathways-Related microRNAs That Are Dysregulated by Acute Lymphoblastic Leukemia and Chemotherapy. *Hum Immunol* (2021) 82(1):36–45. doi: 10.1016/j.humimm.2020.10.009
166. Salem ML, El-Shanshory MR, Abdou SH, Attia MS, Sobhy SM, Zidan MF, et al. Chemotherapy Alters the Increased Numbers of Myeloid-Derived Suppressor and Regulatory T Cells in Children With Acute Lymphoblastic Leukemia. *Immunopharmacol Immunotoxicol* (2018) 40(2):158–67. doi: 10.1080/08923973.2018.1424897
167. Lee CR, Lee W, Cho SK, Park SG. Characterization of Multiple Cytokine Combinations and TGF-Beta on Differentiation and Functions of Myeloid-

Derived Suppressor Cells. *Int J Mol Sci* (2018) 19(3):1–12. doi: 10.3390/ijms19030869
168. Bingle L, Brown NJ, Lewis CE. The Role of Tumour-Associated Macrophages in Tumour Progression: Implications for New Anticancer Therapies. *J Pathol* (2002) 196(3):254–65. doi: 10.1002/path.1027
169. Chen SY, Yang X, Feng WL, Liao JF, Wang LN, Feng L, et al. Organ-Specific Microenvironment Modifies Diverse Functional and Phenotypic Characteristics of Leukemia-Associated Macrophages in Mouse T Cell Acute Lymphoblastic Leukemia. *J Immunol* (2015) 194(6):2919–29. doi: 10.4049/jimmunol.1400451
170. Li Y, You MJ, Yang Y, Hu D, Tian C. The Role of Tumor-Associated Macrophages in Leukemia. *Acta Haematol* (2020) 143(2):112–7. doi: 10.1159/000500315
171. Valencia J, MF-S L, Fraile-Ramos A, Sacedon R, Jimenez E, Vicente A, et al. Acute Lymphoblastic Leukaemia Cells Impair Dendritic Cell and Macrophage Differentiation: Role of BMP4. *Cells* (2019) 8(7):1–14. doi: 10.3390/cells8070722
172. Steidl C, Lee T, Shah SP, Farinha P, Han G, Nayar T, et al. Tumor-Associated Macrophages and Survival in Classic Hodgkin's Lymphoma. *N Engl J Med* (2010) 362(10):875–85. doi: 10.1056/NEJMoa0905680
173. Chen S, Yang X, Feng W, Yang F, Wang R, Chen C, et al. Characterization of Peritoneal Leukemia-Associated Macrophages in Notch1-Induced Mouse T Cell Acute Lymphoblastic Leukemia. *Mol Immunol* (2017) 81:35–41. doi: 10.1016/j.molimm.2016.11.014
174. Anand P, Guillaumet-Adkins A, Dimitrova V, Yun H, Drier Y, Sotudeh N, et al. Single-Cell RNA-Seq Reveals Developmental Plasticity With Coexisting Oncogenic States and Immune Evasion Programs in ETP-ALL. *Blood* (2021) 137(18):2463–80. doi: 10.1182/blood.2019004547
175. Nuñez-Enriquez JC, Barcenas-Lopez DA, Hidalgo-Miranda A, Jimenez-Hernandez E, Bekker-Mendez VC, Flores-Lujano J, et al. Gene Expression Profiling of Acute Lymphoblastic Leukemia in Children With Very Early Relapse. *Arch Med Res* (2016) 47(8):644–55. doi: 10.1016/j.arcmed.2016.12.005
176. Dorantes-Acosta E, Pelayo R. Lineage Switching in Acute Leukemias: A Consequence of Stem Cell Plasticity? *Bone Marrow Res* (2012) 2012:406796. doi: 10.1155/2012/406796
177. Goardon N, Marchi E, Atzberger A, Quek L, Schuh A, Soneji S, et al. Coexistence of LMPP-Like and GMP-Like Leukemia Stem Cells in Acute Myeloid Leukemia. *Cancer Cell* (2011) 19(1):138–52. doi: 10.1016/j.ccr.2010.12.012
178. Park BG, Park CJ, Jang S, Seo EJ, Chi HS, Lee JH. Erythroleukemia Relapsing as Precursor B-Cell Lymphoblastic Leukemia. *Korean J Lab Med* (2011) 31 (2):81–5. doi: 10.3343/kjlm.2011.31.2.81
179. Schmidt CA, Przybylski GK. What can We Learn From Leukemia as for the Process of Lineage Commitment in Hematopoiesis? *Int Rev Immunol* (2001) 20(1):107–15. doi: 10.3109/08830180109056725
180. Horgan C, Kartsios C, Nikolousis E, Shankara P, Kishore B, Lovell R, et al. First Case of Near Haploid Philadelphia Negative B-Cell Acute Lymphoblastic Leukaemia Relapsing as Acute Myeloid Leukemia Following Allogeneic Hematopoietic Stem Cell Transplantation. *Leuk Res Rep* (2020) 14:100213. doi: 10.1016/j.lrr.2020.100213
181. Nutt SL, Heavey B, Rolink AG, Busslinger M. Commitment to the B-Lymphoid Lineage Depends on the Transcription Factor Pax5. *Nature* (1999) 401(6753):556–62. doi: 10.1038/44076
182. Hong Z, Wei Z, Xie T, Fu L, Sun J, Zhou F, et al. Targeting Chemokines for Acute Lymphoblastic Leukemia Therapy. *J Hematol Oncol* (2021) 14(1):48. doi: 10.1186/s13045-021-01060-y
183. Gaggero S, Witt K, Carlsten M, Mitra S. Cytokines Orchestrating the Natural Killer-Myeloid Cell Crosstalk in the Tumor Microenvironment: Implications for Natural Killer Cell-Based Cancer Immunotherapy. *Front Immunol* (2020) 11:621225. doi: 10.3389/fimmu.2020.621225
184. Pinho S, Frenette PS. Haematopoietic Stem Cell Activity and Interactions With the Niche. *Nat Rev Mol Cell Biol* (2019) 20(5):303–20. doi: 10.1038/s41580-019-0103-9
185. Witkowski MT, Dolgalev I, Evensen NA, Ma C, Chambers T, Roberts KG, et al. Extensive Remodeling of the Immune Microenvironment in B Cell Acute Lymphoblastic Leukemia. *Cancer Cell* (2020) 37(6):867–82 e12. doi: 10.1016/j.ccell.2020.04.015
186. Krevvata M, Silva BC, Manavalan JS, Galan-Diez M, Kode A, Matthews BG, et al. Inhibition of Leukemia Cell Engraftment and Disease Progression in Mice by Osteoblasts. *Blood* (2014) 124(18):2834–46. doi: 10.1182/blood-2013-07-517219
187. Anderson D, Skut P, Hughes AM, Ferrari E, Tickner J, Xu J, et al. The Bone Marrow Microenvironment of Pre-B Acute Lymphoblastic Leukemia at Single-Cell Resolution. *Sci Rep* (2020) 10(1):19173. doi: 10.1038/s41598-020-76157-4
188. Shafat MS, Gnaneswaran B, Bowles KM, Rushworth SA. The Bone Marrow Microenvironment - Home of the Leukemic Blasts. *Blood Rev* (2017) 31 (5):277–86. doi: 10.1016/j.blre.2017.03.004
189. Polak R, de Rooij B, Pieters R, den Boer ML. B-Cell Precursor Acute Lymphoblastic Leukemia Cells Use Tunneling Nanotubes to Orchestrate Their Microenvironment. *Blood* (2015) 126(21):2404–14. doi: 10.1182/blood-2015-03-634238
190. Soundara Rajan T, Gugliandolo A, Bramanti P, Mazzon E. Tunneling Nanotubes-Mediated Protection of Mesenchymal Stem Cells: An Update From Preclinical Studies. *Int J Mol Sci* (2020) 21(10):1–10. doi: 10.3390/ijms21103481
191. Scharff B, Modvig S, Marquart HV, Christensen C. Integrin-Mediated Adhesion and Chemoresistance of Acute Lymphoblastic Leukemia Cells Residing in the Bone Marrow or the Central Nervous System. *Front Oncol* (2020) 10:775. doi: 10.3389/fonc.2020.00775
192. Berrazouane S, Doucet A, Boisvert M, Barabe F, Aoudjit F. VLA-4 Induces Chemoresistance of T Cell Acute Lymphoblastic Leukemia Cells *via* PYK2-Mediated Drug Efflux. *Cancers (Basel)* (2021) 13(14):1–15. doi: 10.3390/cancers13143512
193. Klamer S, Voermans C. The Role of Novel and Known Extracellular Matrix and Adhesion Molecules in the Homeostatic and Regenerative Bone Marrow Microenvironment. *Cell Adh Migr* (2014) 8(6):563–77. doi: 10.4161/19336918.2014.968501
194. Xu L, Liu L, Yao D, Zeng X, Zhang Y, Lai J, et al. PD-1 and TIGIT Are Highly Co-Expressed on CD8(+) T Cells in AML Patient Bone Marrow. *Front Oncol* (2021) 11:686156. doi: 10.3389/fonc.2021.686156
195. Kato M, Manabe A. Treatment and Biology of Pediatric Acute Lymphoblastic Leukemia. *Pediatr Int* (2018) 60(1):4–12. doi: 10.1111/ped.13457
196. Malard F, Mohty M. Acute Lymphoblastic Leukaemia. *Lancet* (2020) 395 (10230):1146–62. doi: 10.1016/S0140-6736(19)33018-1
197. Terwilliger T, Abdul-Hay M. Acute Lymphoblastic Leukemia: A Comprehensive Review and 2017 Update. *Blood Cancer J* (2017) 7(6): e577. doi: 10.1038/bcj.2017.53
198. Giebel S, Labopin M, Socie G, Beelen D, Browne P, Volin L, et al. Improving Results of Allogeneic Hematopoietic Cell Transplantation for Adults With Acute Lymphoblastic Leukemia in First Complete Remission: An Analysis From the Acute Leukemia Working Party of the European Society for Blood and Marrow Transplantation. *Haematologica* (2017) 102(1):139–49. doi: 10.3324/haematol.2016.145631
199. Merli P, Algeri M, Del Bufalo F, Locatelli F. Hematopoietic Stem Cell Transplantation in Pediatric Acute Lymphoblastic Leukemia. *Curr Hematol Malig Rep* (2019) 14(2):94–105. doi: 10.1007/s11899-019-00502-2
200. Mamcarz E, Madden R, Qudeimat A, Srinivasan A, Talleur A, Sharma A, et al. Improved Survival Rate in T-Cell Depleted Haploidentical Hematopoietic Cell Transplantation Over the Last 15 Years at a Single Institution. *Bone Marrow Transplant* (2020) 55(5):929–38. doi: 10.1038/s41409-019-0750-7
201. Yanir AD, Martinez CA, Sasa G, Leung K, Gottschalk S, Omer B, et al. Current Allogeneic Hematopoietic Stem Cell Transplantation for Pediatric Acute Lymphocytic Leukemia: Success, Failure and Future Perspectives-A Single-Center Experience, 2008 to 2016. *Biol Blood Marrow Transplant* (2018) 24(7):1424–31. doi: 10.1016/j.bbmt.2018.03.001
202. Shang Y, Zhou F. Current Advances in Immunotherapy for Acute Leukemia: An Overview of Antibody, Chimeric Antigen Receptor, Immune Checkpoint, and Natural Killer. *Front Oncol* (2019) 9:917. doi: 10.3389/fonc.2019.00917
203. Shah NN, Fry TJ. Mechanisms of Resistance to CAR T Cell Therapy. *Nat Rev Clin Oncol* (2019) 16(6):372–85. doi: 10.1038/s41571-019-0184-6
204. Slaney CY, Wang P, Darcy PK, Kershaw MH. CARs *Versus* BiTEs: A Comparison Between T Cell-Redirection Strategies for Cancer Treatment. *Cancer Discov* (2018) 8(8):924–34. doi: 10.1158/2159-8290.CD-18-0297
205. Tomuleasa C, Fuji S, Berce C, Onaciu A, Chira S, Petrushev B, et al. Chimeric Antigen Receptor T-Cells for the Treatment of B-Cell Acute Lymphoblastic Leukemia. *Front Immunol* (2018) 9:239. doi: 10.3389/fimmu.2018.00239

206. Weiner LM, Surana R, Wang S. Monoclonal Antibodies: Versatile Platforms for Cancer Immunotherapy. *Nat Rev Immunol* (2010) 10(5):317–27. doi: 10.1038/nri2744
207. Armand P, Lesokhin A, Borrello I, Timmerman J, Gutierrez M, Zhu L, et al. A Phase 1b Study of Dual PD-1 and CTLA-4 or KIR Blockade in Patients With Relapsed/Refractory Lymphoid Malignancies. *Leukemia* (2021) 35 (3):777–86. doi: 10.1038/s41375-020-0939-1
208. McNeer JL, Rau RE, Gupta S, Maude SL, O'Brien MM. Cutting to the Front of the Line: Immunotherapy for Childhood Acute Lymphoblastic Leukemia. *Am Soc Clin Oncol Educ Book* (2020) 40:1–12. doi: 10.1200/EDBK_278171
209. Duell J, Dittrich M, Bedke T, Mueller T, Eisele F, Rosenwald A, et al. Frequency of Regulatory T Cells Determines the Outcome of the T-Cell-Engaging Antibody Blinatumomab in Patients With B-Precursor ALL. *Leukemia* (2017) 31(10):2181–90. doi: 10.1038/leu.2017.41
210. Bosse KR, Majzner RG, Mackall CL, Maris JM. Immune-Based Approaches for the Treatment of Pediatric Malignancies. *Annu Rev Cancer Biol* (2020) 4:353–70. doi: 10.1146/annurev-cancerbio-030419-033436
211. Caliendo F, Dukhinova M, Siciliano V. Engineered Cell-Based Therapeutics: Synthetic Biology Meets Immunology. *Front Bioeng Biotechnol* (2019) 7:43. doi: 10.3389/fbioe.2019.00043
212. Shah NN, Maatman T, Hari P, Johnson B. Multi Targeted CAR-T Cell Therapies for B-Cell Malignancies. *Front Oncol* (2019) 9:146. doi: 10.3389/fonc.2019.00146
213. Zhang X, Li JJ, Lu PH. Advances in the Development of Chimeric Antigen Receptor-T-Cell Therapy in B-Cell Acute Lymphoblastic Leukemia. *Chin Med J (Engl)* (2020) 133(4):474–82. doi: 10.1097/CM9.0000000000000638
214. Biondi A, Magnani CF, Tettamanti S, Gaipa G, Biagi E. Redirecting T Cells With Chimeric Antigen Receptor (CAR) for the Treatment of Childhood Acute Lymphoblastic Leukemia. *J Autoimmun* (2017) 85:141–52. doi: 10.1016/j.jaut.2017.08.003
215. Pan J, Niu Q, Deng B, Liu S, Wu T, Gao Z, et al. CD22 CAR T-Cell Therapy in Refractory or Relapsed B Acute Lymphoblastic Leukemia. *Leukemia* (2019) 33(12):2854–66. doi: 10.1038/s41375-019-0488-7
216. Lischka A, Popow C, Simbruner G. [Can Muscle Relaxation Prevent the Development of Pneumothorax in Artificially Ventilated Newborn Infants]? *Wien Klin Wochenschr* (1987) 99(18):636–8.
217. Kristensen NP, Heeke C, Tvingsholm SA, Bjerregaard A-M, Draghi A, Bentzen AK, et al. Neoepitope-Specific CD8+ T Cells in Adoptive T-Cell Transfer [abstract]. In: *Proceedings of the AACR Special Conference on Tumor Immunology and Immunotherapy; 2019 Nov 17-20; Boston, MA. Philadelphia (PA): AACR. Cancer Immunol Res* (2020) 8(3 Suppl):Abstract nr A14.
218. Met O, Jensen KM, Chamberlain CA, Donia M, Svane IM. Principles of Adoptive T Cell Therapy in Cancer. *Semin Immunopathol* (2019) 41(1):49–58. doi: 10.1007/s00281-018-0703-z
219. Vormehr M, Reinhard K, Blatnik R, Josef K, Beck JD, Salomon N, et al. A non-Functional Neoepitope Specific CD8(+) T-Cell Response Induced by Tumor Derived Antigen Exposure *In Vivo*. *Oncoimmunology* (2019) 8 (3):1553478. doi: 10.1080/2162402X.2018.1553478
220. Maleki Vareki S. High and Low Mutational Burden Tumors *Versus* Immunologically Hot and Cold Tumors and Response to Immune Checkpoint Inhibitors. *J Immunother Cancer* (2018) 6(1):157. doi: 10.1186/s40425-018-0479-7
221. Guedan S, Ruella M, June CH. Emerging Cellular Therapies for Cancer. *Annu Rev Immunol* (2019) 37:145–71. doi: 10.1146/annurev-immunol-042718-041407
222. Saghafian-Hedengren S, Soderstrom I, Sverremark-Ekstrom E, Nilsson A. Insights Into Defective Serological Memory After Acute Lymphoblastic Leukaemia Treatment: The Role of the Plasma Cell Survival Niche, Memory B-Cells and Gut Microbiota in Vaccine Responses. *Blood Rev* (2018) 32(1):71–80. doi: 10.1016/j.blre.2017.08.009
223. Dougan SK, Dougan M. Regulation of Innate and Adaptive Antitumor Immunity by IAP Antagonists. *Immunotherapy* (2018) 10(9):787–96. doi: 10.2217/imt-2017-0185
224. Rohde K, Kleinesudeik L, Roesler S, Lowe O, Heidler J, Schroder K, et al. A Bak-Dependent Mitochondrial Amplification Step Contributes to Smac Mimetic/Glucocorticoid-Induced Necroptosis. *Cell Death Differ* (2017) 24 (1):83–97. doi: 10.1038/cdd.2016.102
225. Mezzatesta C, Bornhauser BC. Exploiting Necroptosis for Therapy of Acute Lymphoblastic Leukemia. *Front Cell Dev Biol* (2019) 7:40. doi: 10.3389/fcell.2019.00040
226. Frank D, Vince JE. Pyroptosis *Versus* Necroptosis: Similarities, Differences, and Crosstalk. *Cell Death Differ* (2019) 26(1):99–114. doi: 10.1038/s41418-018-0212-6
227. Li KP, Shanmuganad S, Carroll K, Katz JD, Jordan MB, Hildeman DA. Dying to Protect: Cell Death and the Control of T-Cell Homeostasis. *Immunol Rev* (2017) 277(1):21–43. doi: 10.1111/imr.12538
228. F G. *A Phase I-II Open Label Non-Randomized Study Using TL32711 for Patients With Acute Myelogenous Leukemia, Myelodysplastic Syndrome and Acute Lymphoblastic Leukemia*. Philadelphia, Pennsylvania, United States (2021).
229. Lohmann C, Muschaweckh A, Kirschnek S, Jennen L, Wagner H, Hacker G. Induction of Tumor Cell Apoptosis or Necrosis by Conditional Expression of Cell Death Proteins: Analysis of Cell Death Pathways and *In Vitro* Immune Stimulatory Potential. *J Immunol* (2009) 182(8):4538–46. doi: 10.4049/jimmunol.0803989

**Conflict of Interest:** The authors declare that the research was conducted in the absence of any commercial or financial relationships that could be construed as a potential conflict of interest.

**Publisher's Note:** All claims expressed in this article are solely those of the authors and do not necessarily represent those of their affiliated organizations, or those of the publisher, the editors and the reviewers. Any product that may be evaluated in this article, or claim that may be made by its manufacturer, is not guaranteed or endorsed by the publisher.

## GLOSSARY

| | |
|---|---|
| ACT | adoptive T cell therapy |
| ALL | acute lymphoblastic leukemia |
| alloHSCT | allogeneic hematopoietic stem cell transplantation |
| AML | acute myeloid leukemia |
| APCs | antigen-presenting cells |
| BiTEs | bispecific T-cell engagers |
| CAR | chimeric antigen receptor |
| cHL | classical Hodgkin lymphoma |
| CML | chronic myeloid leukemia |
| CTLA-4 | cytotoxic T-lymphocyte-associated protein 4 |
| CTLs | cytotoxic T cells |
| CXCL | IFNγ-inducible chemokine (C-X-C motif) ligands |
| DAMPs | damage-associated molecular patterns |
| EBF1 | EBF transcription factor 1 |
| ETV6 | ETS variant transcription factor 6 |
| FDA | Food and Drug Administration |
| FLT3 | Fms-related receptor tyrosine kinase 3 |
| HLA | human leukocyte antigen |
| HLA-G | human leukocyte antigen G |
| IAP: ICOS | inducible co-stimulator |
| ICOS-L | ICOS ligand |
| IFN-γ | interferon gamma |
| IL | interleukin |
| INF-α | interferon alpha |
| KIR2DL1 | natural killer cell inhibition receptor |
| KMT2A | lysine methyltransferase 2A |
| LAG-3 | lymphocyte-activation gene 3 |
| LAMs | leukemia-associated macrophages |
| mAbs | monoclonal anti-bodies |
| MSCs | mesenchymal stromal cells |
| MDSCs | myeloid-derived suppressor cells |
| MHC | major histocompatibility complex |
| MLL | lysine methyltransferase 2A |
| MPO | myeloperoxidase |
| NHL | non-Hodgkin lymphoma |
| NK | natural killer |
| NKG2D | natural killer group 2 member D |
| NKT | natural killer T |
| OS | overall survival |
| PAX5 | paired box 5 |
| PD1 | programmed death 1 |
| PD-L1 | programmed death 1 ligand |
| pre-B | B cell precursor |
| RUNX1 | RUNX family transcription factor 1 |
| SAP | (SLAM)-associated protein |
| scFvs | single-chain variable fragment |
| SMAC | second mitochondrial activator of caspases |
| TAMs | tumor-associated macrophages |
| TIM-3 | T-cell immunoglobulin and mucin domain-containing protein 3 |
| Tregs | regulatory T cells |
| TILs | tumor-infiltrating lymphocytes |
| TME | tumor microenvironment |
| TNF | tumor necrosis factor |
| TRAIL | TNF-related apoptosis-inducing ligand |
| TN | tunneling nanotubes |
| ULBP-1 | UL16-binding protein |

frontiers in Immunology

ORIGINAL RESEARCH
published: 02 December 2021
doi: 10.3389/fimmu.2021.804408

# Tryptase Regulates the Epigenetic Modification of Core Histones in Mast Cell Leukemia Cells

*Sultan Alanazi, Fabio Rabelo Melo* and Gunnar Pejler**

*Department of Medical Biochemistry and Microbiology, Uppsala University, Uppsala, Sweden*

Mast cells are immune cells that store large amounts of mast cell-restricted proteases in their secretory granules, including tryptase, chymase and carboxypeptidase A3. In mouse mast cells, it has been shown that tryptase, in addition to its canonical location in secretory granules, can be found in the nuclear compartment where it can impact on core histones. Here we asked whether tryptase can execute core histone processing in human mast cell leukemia cells, and whether tryptase thereby can affect the epigenetic modification of core histones. Our findings reveal that triggering of cell death in HMC-1 mast cell leukemia cells is associated with extensive cleavage of core histone 3 (H3) and more restricted cleavage of H2B. Tryptase inhibition caused a complete blockade of such processing. Our data also show that HMC-1 cell death was associated with a major reduction of several epigenetic histone marks, including H3 lysine-4-mono-methylation (H3K4me1), H3K9me2, H3 serine-10-phosphorylation (H3S10p) and H2B lysine-16-acetylation (H2BK16ac), and that tryptase inhibition reverses the effect of cell death on these epigenetic marks. Further, we show that tryptase is present in the nucleus of both viable and dying mast cell leukemia cells. In line with a role for tryptase in regulating nuclear events, tryptase inhibition caused increased proliferation of the mast cell leukemia cells. Altogether, the present study emphasizes a novel principle for how epigenetic modification of core histones is regulated, and provides novel insight into the biological function of human mast cell tryptase.

**Keywords: tryptase, histones, mast cells, epigenetics, apoptosis**

OPEN ACCESS

***Edited by:***
*Giovanna Schiavoni,*
*National Institute of Health (ISS), Italy*

***Reviewed by:***
*Giuliano Zabucchi,*
*University of Trieste, Italy*
*Igor Bucchwalow,*
*Institute For Hematopathology*
*Hamburg, Germany*

****Correspondence:***
*Fabio Rabelo Melo*
*fabio.melo@imbim.uu.se*
*Gunnar Pejler*
*Gunnar.Pejler@imbim.uu.se*

***Specialty section:***
*This article was submitted to Cancer Immunity and Immunotherapy, a section of the journal Frontiers in Immunology*

***Received:*** *29 October 2021*
***Accepted:*** *17 November 2021*
***Published:*** *02 December 2021*

***Citation:***
*Alanazi S, Rabelo Melo F and Pejler G (2021) Tryptase Regulates the Epigenetic Modification of Core Histones in Mast Cell Leukemia Cells. Front. Immunol. 12:804408. doi: 10.3389/fimmu.2021.804408*

## INTRODUCTION

Mast cells are hematopoietic cells of the immune system. They are implicated in various pathological conditions, including allergic conditions, autoimmune disorders, cancer and cardiovascular diseases (1–3). In addition, mastocytosis is a pathological condition in which the mast cell population is expanded. Typically, the latter occurs through a D816E mutation in KIT, i.e., the receptor for stem cell factor. This mutation results in constitutive KIT activation,

**Abbreviations:** MC, mast cell; LLME, H-Leu-Leu-OMe; H, histone.

and since stem cell factor is a critical growth factor for mast cells, constant KIT signaling will result in excessive mast cell proliferation (4). Mastocytosis is a rare disorder and is subclassified into cutaneous and systemic forms, with the systemic form being further subclassified into indolent and advanced variants, the latter encompassing aggressive systemic mastocytosis and mast cell leukemia (4).

A hallmark feature of mast cells is their high content of secretory granules. These contain vast amounts of preformed bioactive inflammatory mediators, including various amines (e.g., histamine, serotonin), proteoglycans of serglycin type, lysosomal hydrolases, cytokines (e.g., TNF), growth factors (e.g., VEGF), and a panel of mast cell-restricted proteases (5). The latter category encompasses tryptase, chymase and carboxypeptidase A3 (CPA3), and these proteases are stored in remarkably high amounts (5, 6). The mast cell proteases have been shown to account for the detrimental impact of mast cells in various pathological settings (5–9), but they also have beneficial functions, in particular in host defense against various toxins (10–12).

Among the mast cell proteases, tryptase has a unique macromolecular organization, being built up as a tetrameric enzyme with all of its active sites facing a central, narrow pore (13). Due to this organization, tryptase is completely resistant to the action of endogenous, macromolecular protease inhibitors. Moreover, since most macromolecular substrates are not able to enter the central pore of tryptase, the enzyme has a relatively narrow substrate cleavage repertoire (13, 14).

In a previous study, we noted that tryptase expressed by mouse primary mast cells has the capacity to execute N-terminal cleavage of nuclear core histones in mast cells undergoing apoptotic cell death (15). We also demonstrated that tryptase, in addition to its canonical location within the mast cell secretory granules, also can be found in the nucleus of primary, cultured mouse mast cells (15). It is now well established that the N-terminal portions of nuclear core histones are important sites for deposition of epigenetic marks, including acetylation, phosphorylation and methylation (16, 17). N-terminal cleavage of core histones by tryptase could potentially serve to remove such epigenetic histone marks. Hence, any biological effects mediated by the respective marks will be erased though the action of tryptase. In support of this notion, we found previously that murine mast cells lacking tryptase expression display an elevation in the levels of histone 2B (H2B) lysine-5 acetylation (H2BK5ac) (18).

Although an effect of tryptase on core histones has been detected in primary mouse mast cells, the possibility that tryptase has an effect on the processing and epigenetic modification of core histones in human mast cells has not been explored. In this study we addressed this possibility by examining the effects of tryptase on core histone processing and epigenetic modification in human mast cell leukemia cells undergoing cell death. Moreover, we investigated whether tryptase can be found in the nucleus of mast cell leukemia cells and if tryptase can have an impact on mast cell leukemia cell proliferation.

# RESULTS

## H-Leu-Leu-OMe (LLME), Staurosporine and Histone Methyltransferase Inhibitors Are Cytotoxic for HMC-1 Mast Cells

To investigate the impact of tryptase on histone integrity during mast cell death, we first evaluated cell death responses of HMC-1 cells to various cytotoxic agents. To this end, HMC-1 cells were treated with either H-Leu-Leu-OMe (LLME) [a lysosomotropic agent with mast cell granule-permeabilizing properties (19)], staurosporine (an agent known to cause caspase-dependent apoptosis), UNC-0638 or UNC-1999; the latter compounds represent histone methyltransferase inhibitors with known ability to induce cell death in transformed mast cells (20). These analyses revealed that all of the employed agents were cytotoxic to the HMC-1 cells (**Supplementary Figure 1A**). A further analysis showed that all agents caused cell death with signs of both apoptosis (Annexin $V^+$/$Draq7^-$) and necrosis/late apoptosis (Annexin $V^+$/$Draq7^+$) (**Supplementary Figure 1B, C**). Notably, apoptotic cell death dominated in response to LLME, in agreement with previous findings in which LLME was shown to cause apoptosis in primary mouse mast cells (19, 21).

## LLME, Staurosporine and Histone Methyltransferase Inhibitors Cause Histone 3 Processing in HMC-1 Mast Cells

To investigate the impact of cell death on core histone processing in the HMC-1 cells, we performed Western blot analysis. As shown in **Figure 1A**, the intensities of the bands corresponding to the respective core histones (H3, H2B, H4, H2A) were generally reduced in response to UNC-0638 or UNC-1999 (**Figure 1A**), most likely reflecting a general decline in cellular protein levels during the cell death process; this was supported by a general reduction in β-actin levels (**Figure 1A**). Interestingly, limited cleavage of H3 was seen in response to UNC-0638, and also to some extent in response to UNC-1999 (**Figure 1A**; quantification of band intensities is shown in the right part of the panel), suggesting that histone processing may accompany cell death in response to these agents. Cleavage of H2B, H2A or H4 was not observed. Limited H3 cleavage was also seen in response to staurosporine (**Figure 1B**), and profound H3 cleavage was seen in response to LLME (**Figure 1B**); LLME also caused cleavage of H2B. Altogether, these findings indicate that cell death of HMC-1 cells, in response to various cytotoxic agents, is accompanied by histone cleavage. Moreover, out of the assessed cytotoxic agents, LLME had the most extensive effects on core histone cleavage in the HMC-1 cells.

## Cell Death in HMC-1 Cells Is Associated With a Reduction in the H3K4me1, H3K9me2 and H3K27me3 Epigenetic Marks

Next, we assessed whether cell death in HMC-1 cells is accompanied by effects on the levels of epigenetic histone marks, based on the notion that apoptosis is associated with extensive histone modifications (22). For this purpose,

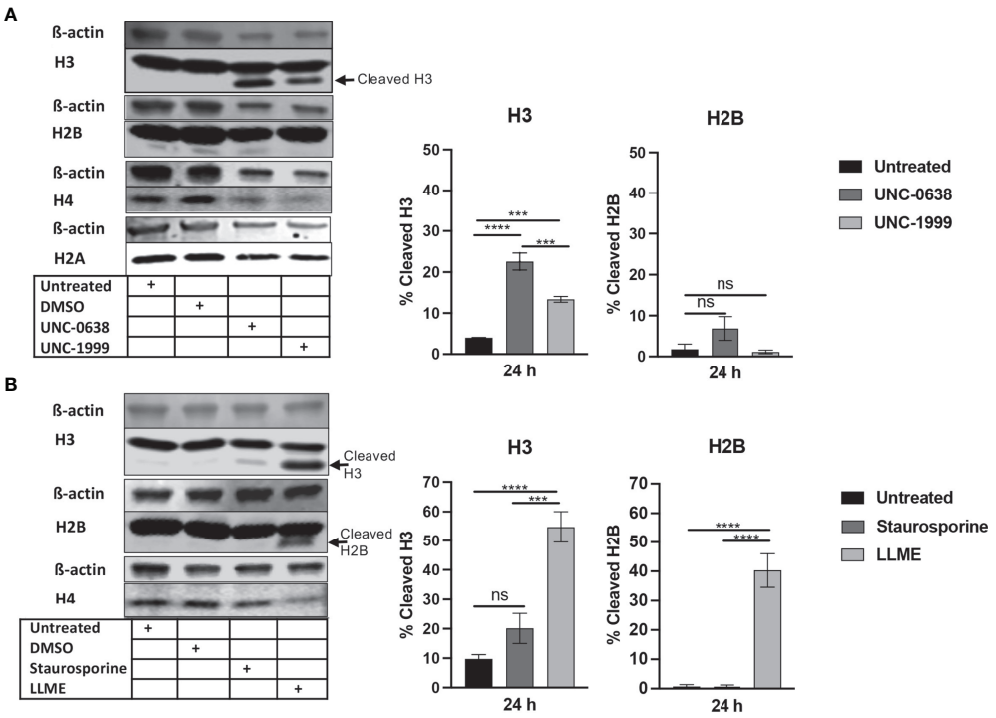


**FIGURE 1** | Histone 3 (H3) is cleaved in human mast cell leukemia cells in response to cytotoxic agents. HMC-1 cells (0.5 x $10^6$ cells/ml) were either left untreated or incubated for 24 h with either **(A)** UNC-0638 (25 μM), UNC-1999 (50 μM), **(B)** staurosporine (1 μM) or H-Leu-Leu-OMe (LLME) (400 μM). Samples corresponding to equal numbers of cells were subjected to Western blot analysis for histone 3 (H3), H2B, H4 and H2A, with ß-actin as loading control. Quantification of the signal intensity for cleaved H3 and H2B, as % of total H3 and H2B, is shown in the right part of the panels. The presented data are representative of at least two independent experiments and are given as mean values ± SEM (n=3). ***p ≤ 0.001; ****p ≤ 0.0001. ns, not significant.

we examined the effects of LLME, staurosporine, UNC-0638 or UNC-1999 on the levels of the H3 lysine-4 mono-methylation (H3K4me1), H3 lysine-9 di-methylation (H3K9me2) and H3 lysine-27 tri-methylation (H3K27me3) epigenetic marks. As shown in **Figure 2A**, a robust reduction of H3K4me1 and H3K27me3, as well as a minor rection of H3K9me2, was seen in response to both UNC-0638 and UNC-1999. Moreover, a profound reduction in the levels of H3K4me1 and H3K9me2 was seen in response to LLME (**Figure 2B**). A more limited reduction of H3K4me1 and H3K9me2 was seen in response to staurosporine, whereas neither LLME nor staurosporine caused a reduction of H3K27me3 levels.

## Tryptase Inhibition Causes Increased Late Apoptosis/Necrosis Over Apoptosis in HMC-1 Cells

The findings above reveal that cell death in HMC-1 cells is accompanied by extensive core histone processing and alterations in the levels of epigenetic histone marks. Considering that tryptase has previously been shown to regulate such processes in primary murine mast cells (15, 18), we next considered the possibility that the effects on core histone processing/epigenetic modification in HMC-1 cells could be dependent on tryptase. To approach this issue, we first assessed whether the inhibition of tryptase, by using either a general seine protease inhibitor (Pefabloc SC) or a potent tryptase inhibitor (nafamostat) (23), could have an impact on the cell death process in HMC-1 cells. Moreover, since we noted above that cell death-induced core histone cleavage and epigenetic modification was most profound in response to LLME, we focused in the following on LLME out of the assessed cytotoxic agents.

As seen in **Figures 3A, B** and **Supplementary Figure 1**, LLME caused predominantly apoptotic cell death in HMC-1 cells. However, in the presence of either Pefabloc SC (**Figure 3A**) or nafamostat (**Figure 3B**), a profound reduction in the proportion of apoptotic (Annnexin $V^+$/$Draq7^-$) cells was seen, and this was accompanied by a corresponding increase in the population of late apoptotic/necrotic (Annexin $V^+$/$Draq7^+$) cells. Nafamostat was not cytotoxic to the HMC-1 cells (**Figure 3B**), whereas limited cytotoxicity of Pefabloc SC was seen (**Figure 3A**). Hence, these findings reveal that tryptase impacts on the mechanism of cell death of HMC-1 cells in response to LLME.

## Tryptase Inhibition Blocks H3 Cleavage in HMC-1 Cells

Next, we sought to investigate whether the LLME-induced cleavage of H3 was dependent on tryptase. As seen in **Figures 4A, B**, extensive cleavage of H3 was seen in response to LLME, confirming our findings above. However, when cells had been treated with either Pefabloc SC or nafamostat, the H3

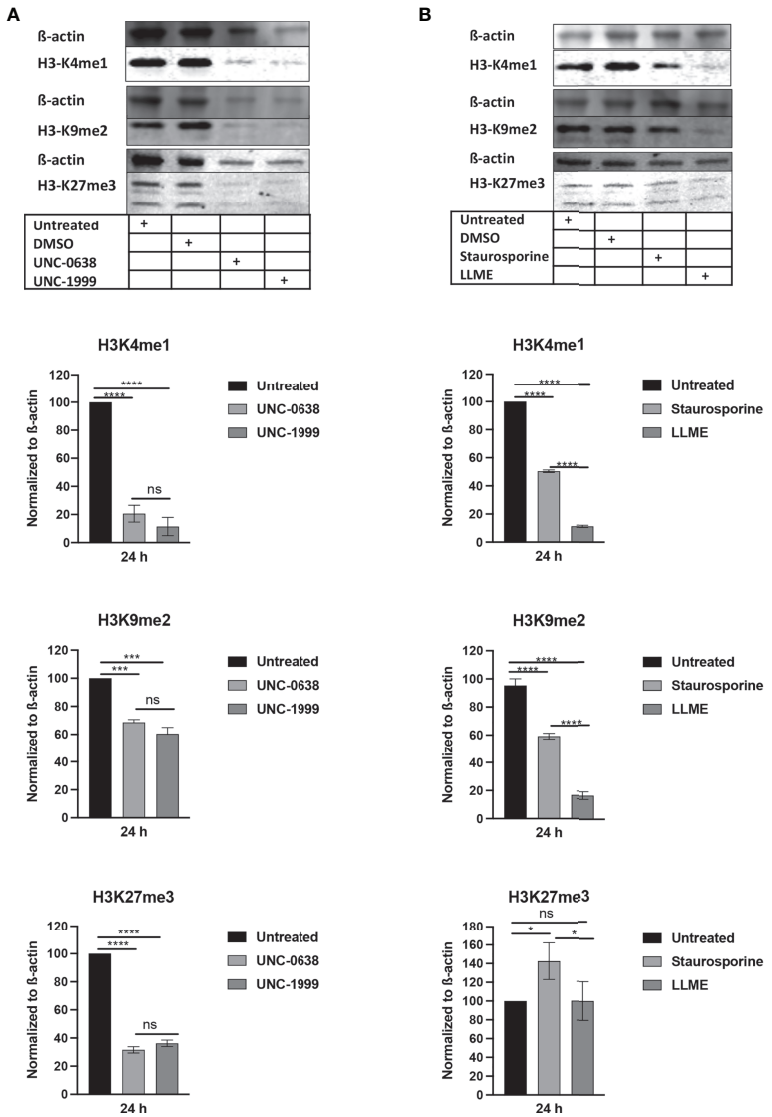


**FIGURE 2** | Cytotoxic agents cause reductions in the levels of epigenetic histone marks in mast cell leukemia cells. HMC-1 cells ($0.5 \times 10^6$ cells/ml) were incubated for 24 hours with **(A)** UNC-0638 (25 μM), UNC-1999 (50 μM), **(B)** staurosporine (1 μM) or H-Leu-Le (400 μM), followed by Western blot analysis for the levels of the H3K4me1, H3K9me2 and H3K27me3 marks, with ß-actin as loading control. Quantification of H3K4me1, H3K9me2 and H3K27me3 levels by densitometry is shown in the lower part of the panels. Data are representative of three independent experiments and are given as mean values ± SEM (n=3). *p ≤ 0.05; ***p ≤ 0.001; ****p ≤ 0.0001. ns, not significant.

processing was completely abolished. In contrast, the H3 cleavage was not affected in the presence of general inhibitors of cysteine proteases (E-64d), aspartic acid proteases (Pepstatin A) or metalloproteases (EDTA). Hence, these findings indicate that tryptase has a major role in executing H3 cleavage in the context of cell death in HMC-1 cells.

## Tryptase Inhibition Modulates Epigenetic Histone Modification in HMC-1 Cells

Extending from the observation that tryptase causes H3 cleavage in HMC-1 cells during cell death, we then proceeded to investigate whether tryptase thereby could modify the pattern of epigenetic H3 marks in the HMC-1 cells. First, we investigated the impact of tryptase inhibition on the levels of the H3K4me1 and H3K9me2 marks, considering that the levels of both of these are affected during LLME-induced cell death (see **Figure 2**). As seen in **Figures 5A, B**, tryptase inhibition by either Pefabloc SC or nafamostat completely reversed the effect of LLME on the levels of both these marks. Moreover, both Pefabloc SC and nafamostat caused a slight increase in the levels of the H3K4me1 and H3K9me2 marks also at baseline conditions, i.e., in the absence of cell death-inducing agent (**Figures 5A, B**).

To extend these findings, we also analyzed whether tryptase inhibition could impact on the levels of the H2B serine-14

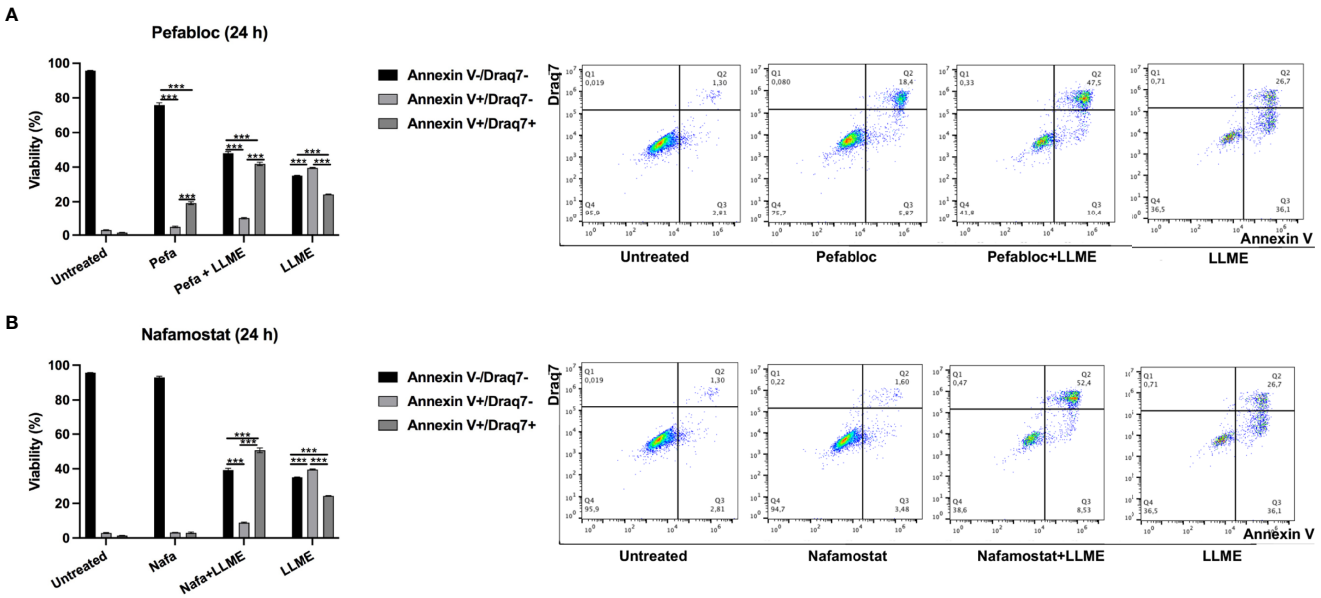


**FIGURE 3** | Tryptase inhibition alters the mode of cell death in human mast cell leukemia cells subjected to cytotoxic agent. HMC-1 cells (0.5 x $10^6$ cells/ml) were incubated with either Pefabloc SC (**A**; 100 μM) or nafamostat (**B**; 20 μM) for 30 min prior to treating the cells with LLME (400 μM) for 24 h. Cells were analyzed by flow cytometry for Annexin V/Draq7 positivity. Dot plots are shown with representative samples showing staining with Annexin V-FITC (FL-1) and Draq7 (FL-3), with the % of cells indicated within each quadrant. Quantification of the data is shown to the left. Data are representative of at least two independent experiments and are given as mean values ± SEM (n = 3). ***p ≤ 0.001.

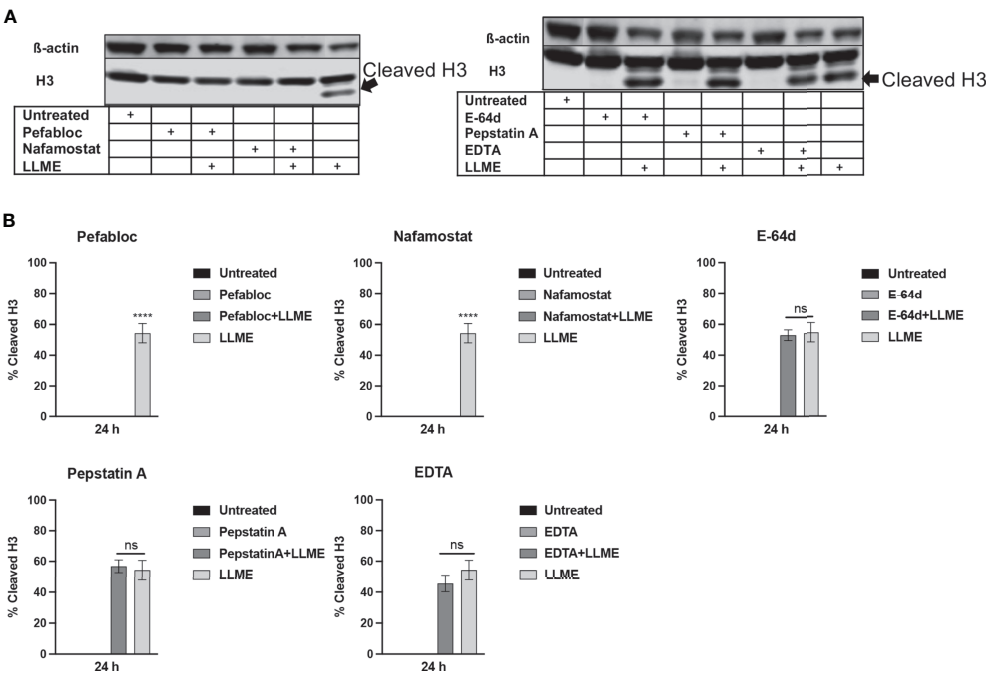


**FIGURE 4** | Treatment of mast cell leukemia cells with tryptase inhibitor abrogates H3 cleavage in response to cytotoxic agents. **(A)** HMC-1 cells (0.5 x $10^6$ cells/ml) were incubated with protease inhibitors: Pefabloc SC (Pefa; 0.1 mM), nafamostat (Nafa; 20 μM), E-64d (15 μM), Pepstatin A (Pep A; 50 μM) or EDTA (20 μM) for 30 min prior to treating the cells with LLME (400 μM) for 24 h. Subsequently, samples corresponding to equal numbers of cells were subjected to Western blot analysis for histone 3 (H3), with ß-actin as loading control. **(B)** Quantification of the signal intensity for cleaved H3, as % of total H3. The presented data are representative of at least two independent experiments, and are given as mean values ± SEM (n=3). ****p ≤ 0.0001. ns, not significant.

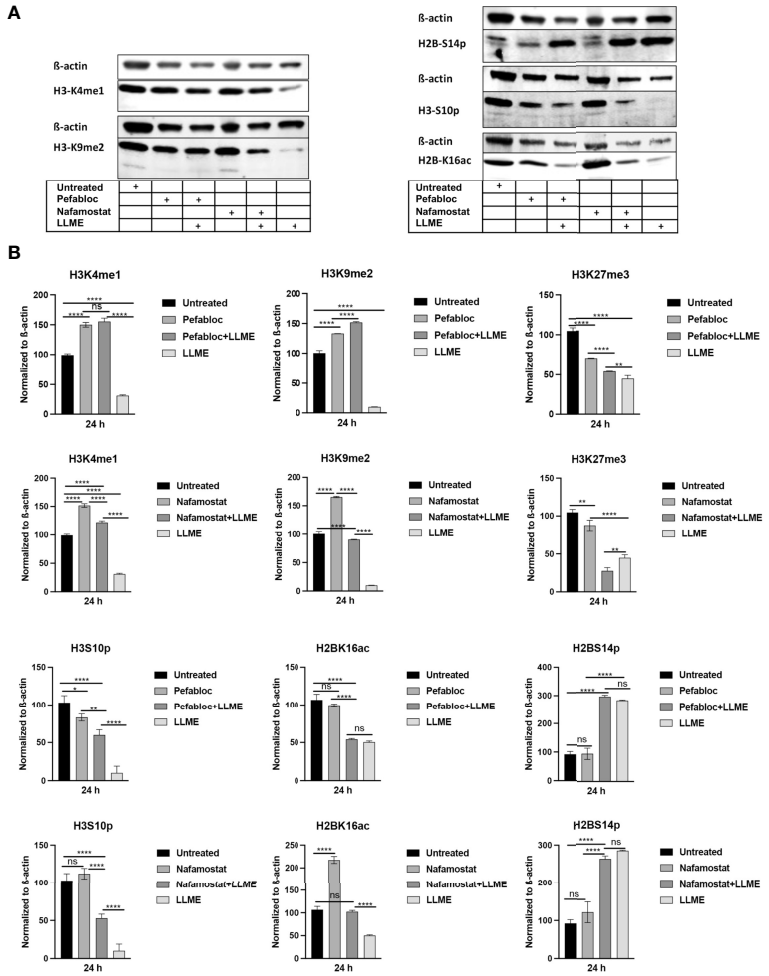


**FIGURE 5** | Tryptase inhibition blocks the effect of cytotoxic agents on the levels of epigenetic histone marks in mast cell leukemia cells. **(A)** HMC-1 cells (0.5 x $10^6$ cells/ml) were either left untreated or treated with either Pefabloc SC (Pefa; general serine protease inhibitor) or nafamostat (Nafa; tryptase inhibitor) for 30 min prior to incubation with LLME (400 μM) for 24 h. Samples corresponding to equal numbers of cells were subjected to Western blot analysis for levels of the H3K4me1, H3K9me2, H3K27me3, H2BS14p, H3S10p and H2BK16ac marks, with ß-actin used as loading control. **(B)** Quantification of the levels of the H3K4me1, H3K9me2, H3K27me3, H2BS14p, H3S10p, and H2BK16ac marks, normalized to the loading control. The presented data are representative of at least two independent experiments and are given as mean values ± SEM (n=3). *p ≤ 0.05; **p ≤ 0.01; ****p ≤ 0.0001. ns, not significant.

phosphorylation (H2BS14p), H3 serine-10 phosphorylation (H3S10p) and H2B lysine-16 acetylation (H2BK16ac) marks. Out of these, the H2BS14p mark has a documented role in apoptosis, typically being upregulated in response to cell death (24–26). The H3S10p mark has an important role in chromatin remodeling during the mitotic process (27) but is also implicated in apoptosis (28). Further, the H2BK16ac mark has been shown to be involved in regulation of the cell cycle (29). As depicted in **Figures 5A, B**, cell death induced by LLME caused a robust reduction in the levels of the H3S10p mark, and it was also seen that tryptase inhibition by either Pefabloc SC or nafamostat attenuated the effect of LLME on H3S10p levels. LLME also caused a reduction in the levels of the H2BK16ac mark, and this effect was blunted in the presence of nafamostat, whereas Pefabloc SC was not capable of reverting the effects of LLME on H2BK16ac levels. Further, cell death in response to LLME was accompanied by a robust increase in the levels of the H2BS14p mark. However, neither nafamostat nor Pefabloc SC had the capacity to reverse the effect of LLME on the levels of this epigenetic mark.

## Tryptase Is Found in the Nucleus of HMC-1 Cells

The observed impact of tryptase on nuclear histones implies that tryptase is physically associated with these proteins, either at baseline conditions or as a consequence of the apoptotic process. To address this, we stained the HMC-1 cells for tryptase, both at baseline conditions and after treatment with LLME. As seen in **Figures 6A, B**, HMC-1 cells showed strong cytoplasmic staining for tryptase, in agreement with the large quantities of tryptase

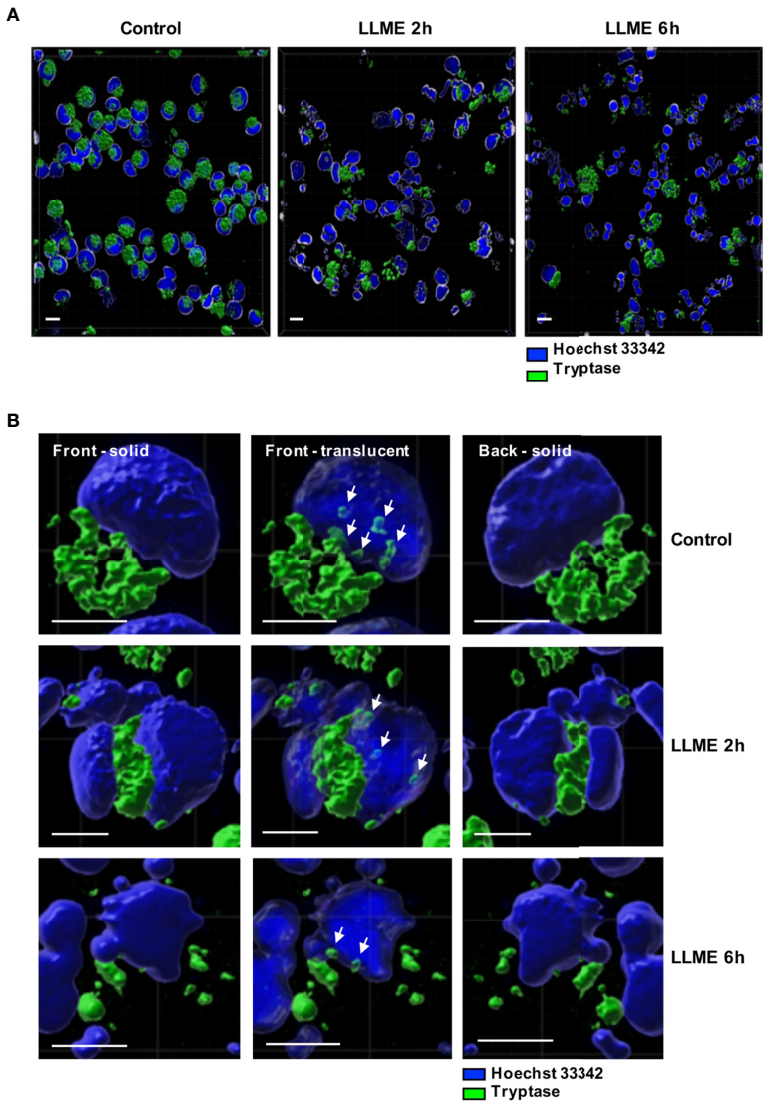


**FIGURE 6** | Tryptase is found in the nucleus of HMC-1 cells. HMC-1 cells (0.5 x $10^6$ cell/ml) were either left untreated or treated with 400 μM LLME for 2 or 6 hours. Cells were stained for tryptase and nuclear DNA (Hoechst 33342), followed by confocal microscopy analysis. **(A)** 3-D view generated from Z-stack sections. Note the abundant tryptase staining in the cytoplasm of control cells and a gradual decline in tryptase staining after LLME treatment; bar scale = 10 μm. **(B)** The left and right panels show solid front and back views of the same control cell or cells treated with LLME for either 2 or 6 hours. The middle panels show translucent nuclear structure. Note that the translucent depiction of nuclei reveals the presence of tryptase within the nuclear compartment of both control- and LLME-treated cells (indicated by white arrows); bar scale = 5 μm.

typically found in the secretory granules. Tryptase positivity was also seen after LLME-induced cell death. However, a gradual decline in tryptase staining was seen after induction of cell death, most likely reflecting the release or degradation of tryptase during the cell death process. In accordance with previous finding in mouse mast cells (15), tryptase staining was also seen in the nuclear compartment. This was observed both at baseline conditions and after induction of cell death by LLME. As expected, LLME treatment caused extensive disintegration of the nuclear compartment of the HMC-1 cells, and it was also seen that the levels and distribution of nuclear tryptase was relatively similar at baseline vs. cell death conditions.

## Tryptase Inhibition Causes Increased HMC-1 Cell Proliferation

Our findings above reveal that tryptase has an impact on events occurring during cell death, and our data also demonstrate that tryptase is found in the HMC-1 cell nucleus, both at baseline conditions and in the context of cell death. Intriguingly, our findings also suggest that tryptase has an impact on the levels of certain epigenetic marks at baseline conditions. Altogether, this introduces the possibility that tryptase might impact on nuclear events even at baseline conditions, a notion that is supported by previous studies showing that the knockout of tryptase in murine primary mast cells results in loss of proliferative control (18). To

assess whether tryptase could have an impact on proliferation also in transformed, human mast cells, we next investigated whether tryptase inhibition has an effect on the ability of HMC-1 cells to proliferate. For this purpose, HMC-1 cells were cultured in the absence or presence of nafamostat, followed by assessment of cell death (Annexin V/Draq7 staining) and quantification of cell numbers. This analysis revealed that nafamostat was not cytotoxic to the HMC-1 cells (**Figure 7A**), and also revealed a more rapid increase in cell numbers when cells were cultured in the presence of the tryptase inhibitor (**Figure 7B**). To assess whether the increased growth rate was due to increased proliferation, we adopted EdU staining. Indeed, this analysis revealed a markedly higher portion of proliferating cells in the presence of nafamostat (**Figure 7C**), suggesting that tryptase inhibition has a stimulatory impact on HMC-1 cell proliferation.

## DISCUSSION

Tryptase is one of the established biomarkers for mastocytosis, with an increase in tryptase levels being one out several criteria for diagnosing a patient with mastocytosis (30). Tryptase is also a

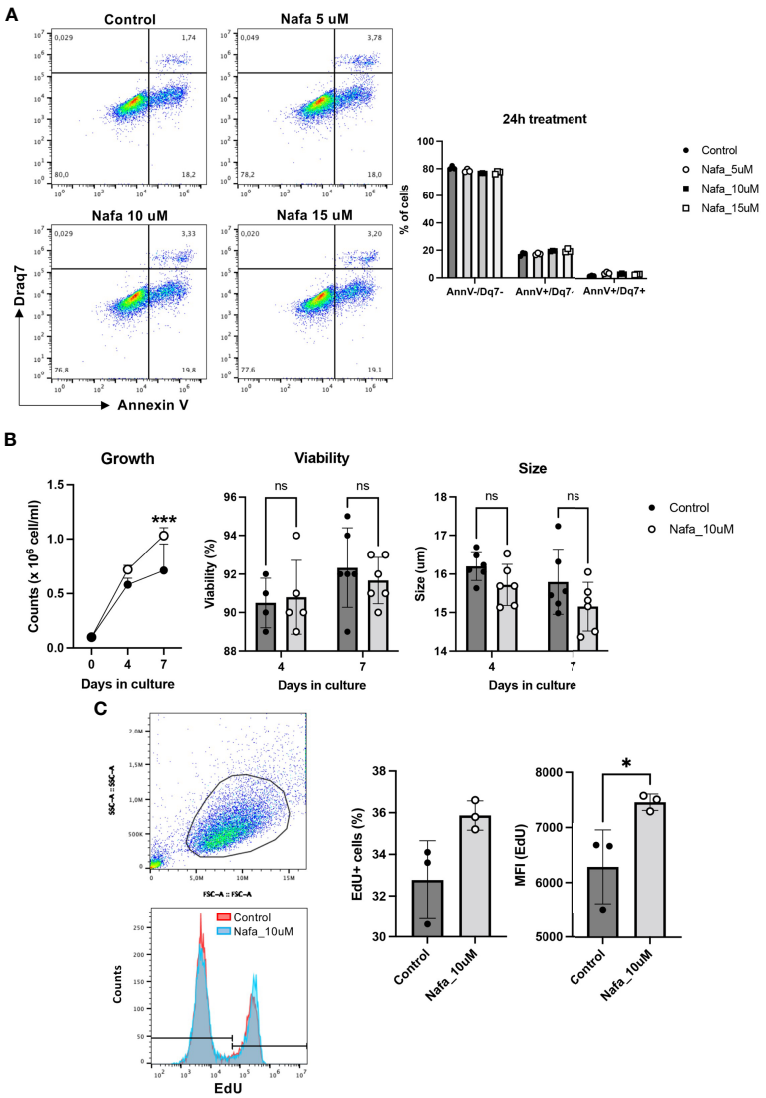


**FIGURE 7** | Nafamostat increases proliferation of HMC-1 cells. HMC-1 (0.1 x $10^6$ cell/ml) were left untreated or cultured in presence of nafamostat. **(A)** Flow cytometry analysis showing representative dot plots and cell viability of HMC-1 cells after 24h treatment with different concentrations of nafamostat; quantification is shown in the right panel. **(B)** Cell counts in control cultures and in cultures containing 10 μM nafamostat. Note the increase in cell numbers when cells are cultured in the presence of nafamostat. No effect of nafamostat was seen on cell viability as measured by trypan-blue staining or on cell size. **(C)** Cells were assessed for proliferation by EdU staining and flow cytometry analysis. Representative dot blot shows gated alive cells (upper left panel) and merged representative histograms for the EdU staining (left lower panel). Quantification of the EdU staining as % $EdU^+$ cells and mean fluorescence intensity (MFI) is depicted in the right panel. Data are represented as mean values ± SEM and analyzed with 2-way ANOVA and unpaired *t* test. $*p \leq 0.05$, $***p \leq 0.0001$. ns, not significant.

well-established biomarker for anaphylaxis, in which a dramatic increase in serum tryptase levels can be attained (31). Further, tryptase is considered as a potential biomarker for a range of additional pathologies, including asthma (8) and melanoma (32). On a different angle, it has been found that certain individuals harbor an increased copy number of the tryptase alpha gene, which leads to elevated basal tryptase levels, associated with a complex pathology denoted hereditary alpha tryptasemia syndrome (33).

Altogether, tryptase is thus implicated as a diagnostic tool in a wide range of disorders. However, beyond its diagnostic value, there is more limited insight as to whether tryptase has a functional impact on any of these settings. In this study we provide novel insight into this issue, by examining the functional impact of tryptase on mast cell leukemia cells. Our findings reveal that tryptase has a profound effect on the processing of nuclear core histones, in the context of cell death induced in response to a variety of triggers. Notably, the extent of histone processing was most profound in cells where cell death was triggered by exposure to LLME. LLME is a lysosomotropic agent that has the capacity to induce mast cell secretory granule permeabilization. This will lead to the release of tryptase from the granules into the cytosol, and it would thus be expected that cell death in response to such a mechanism would lead to more evident effects on histone processing vs. triggering of cell death by other mechanisms (which may not cause granule permeabilization to the same extent). It was also notable that, out of the various core histones, H3 was most susceptible, being degraded in response into each of the adopted cell death-triggering agents. This probably reflects that H3 has a more extended N-terminal tail than the other core histones, protruding outside of the nucleosomes. Most likely, the N-terminal tail of H3 is thereby highly susceptible to the proteolytic action of tryptase. Moreover, since the H3 N-terminal tail is structurally flexible, it is likely that it can enter the central pore of tryptase without major steric hindrance.

We also noted that cell death induced by LLME was accompanied by a reduction in several epigenetic marks deposited on H3, including H3K9me2 and H3K4me1. H3K9me2 is strongly associated with transcriptional repression (34), whereas H3K4me1 is enriched at active enhancers (35). The reduction of these marks in HMC-1 cells exposed to cytotoxic agents may thus reflect effects on regulation of the transcriptional program. Intriguingly, the reduction in the levels of these marks was completely abolished in cells treated with tryptase inhibitor, introducing the notion that tryptase can regulate transcriptional events mediated through these epigenetic marks. These marks are found close to the N-terminus of H3, and a likely explanation for the observed effects would be that tryptase executes proteolytical cleavage in the N-terminal tail of H3, such that these marks are erased.

In addition to influencing H3K9me2 and H3K4me1, our data also indicate that tryptase has the capacity to remove H3S10p and H2BK16ac marks in response to triggering of cell death. The H3S10p mark is known to have a role in the regulation of cell apoptosis (28), and our data thus suggest that tryptase has the capacity to modulate apoptotic responses mediated by this epigenetic mark. In line with this, we noted that tryptase inhibition has a strong impact on the mechanism of cell death, with tryptase inhibition causing a diversion of the cell death mode from apoptosis to late apoptosis/necrosis. However, further investigations are needed to determine if this diversion is a direct effect of the altered epigenetic landscape induced by proteolytic effects of tryptase on core histone tails.

An interesting observation was that tryptase inhibition caused an increase in the levels of certain histone marks (H3K4me1 and H3K9me2) even at baseline conditions, i.e., in the absence of cell death-triggering agent. This implies that tryptase may have an impact in the nuclear compartment even in viable cells. In line with this, we found here that tryptase, in addition to its location within secretory granules, also is found within the nuclear compartment of the human mast cell leukemia cells, and there is also previous evidence that tryptase can be found in the nucleus of non-transformed mast cells (36, 37). Hence, tryptase can impact on core histones not only during cell death, when large amounts of tryptase are released from granules, but also at steady state. Indeed, our data show that tryptase inhibition caused an increased expansion of the HMC-1 cultures under baseline conditions, and that this was attributed to an enhanced rate of proliferation. Potentially, this increase in proliferation could be due to tryptase-mediated effects on the epigenetic landscape in the HMC-1 nucleus, such as our observed increase in the H3K4me1 and H3K9me2 marks in HMC-1 cells treated with tryptase inhibitor. However, further investigations will be needed to establish the causative relationship between tryptase inhibition and regulation of cellular proliferation.

# MATERIALS AND METHODS

## Reagents

UNC-0638 (cat no U4885) was from Sigma-Aldrich (Steinheim, Germany), UNC-1999 (cat no S7165) from Selleckchem (Houston, TX), H-Leu-Leu-OMe (LLME) (cat no 4000725.0005) from Bachem (Bubendorf, Switzerland). Nafamostat mesylate (cat no N0289), staurosporine (cat no S4400), mefloquine (cat no M2319), Pefabloc SC (cat no 11429868001), pepstatin A (cat no 516481) and E-64d (cat no E8640) were from Sigma-Aldrich (Steinheim, Germany). Rabbit anti-H3K9me2 antibody (cat no 07-441) was from EMD-Millipore (Darmstadt, Germany). Rabbit anti-H3K4me1 (cat no 5323S) monoclonal antibody was from Cell Signaling Technology (Danvers, MA). Rabbit anti-histone 2A (H2A) (cat no ab177308), H2B (cat no ab1790), H3 (cat no ab1791) and H4 (cat no ab177840) antibodies, mouse anti-H3K27me3 (cat no ab6002) monoclonal antibody and rabbit anti-H3S10p (cat no ab272166) polyclonal antibody were from Abcam (Cambridge, UK). A mouse monoclonal antibody to β-actin (cat no sc-517582) was from Santa Cruz Biotechnology (Santa Cruz, CA). Rabbit anti-H2BS14p polyclonal antibody (cat no PA5-105775)

was from Invitrogen (Eugene, OR). Rabbit anti-H2BK16ac (cat no 39121) was from Active Motif (Carlsbad, CA).

## Culture of Mast Cell Leukemia Cells

The human mast cell line (HMC-1) was cultured in Iscove's Modified Dulbecco's medium (IMDM) (cat no 11504556; Invitrogen, Carlsbad, CA) supplemented with 10% heat-inactivated fetal bovine serum (FBS) (cat no 11573397; Invitrogen, Carlsbad, CA), 2 mM L-glutamine (cat no 59202C; Sigma Aldrich), 100 µg/mL streptomycin (Sigma Aldrich), 100 IU/mL penicillin (Sigma Aldrich; cat no P4333) and 1.2 mM 1-thioglycerol (cat no M6145; Sigma Aldrich). The medium was replaced every third day; cells were cultured at 0.3 x $10^6$ cells/ml at 37°C with 5% $CO_2$ and used for at most 10 passages after initial thawing.

## Cell Viability Assessment

To evaluate the effects of different inhibitors on cell viability, cells were preincubated with or without inhibitors. The Cell Titer-Blue cell viability assay (cat no G8080; Promega, Carlsbad, CA) was used to assess cytotoxicity. Triplicates of 0.5 x $10^6$ cells/ml were resuspended in complete culture medium, transferred into a 24-well flat-bottomed plates and incubated overnight at 37°C with 5% $CO_2$. The next day, cells were either treated with inhibitors or left non-treated and incubated at 37°C with 5% $CO_2$. After 24 h incubation, 90 µl of the cell suspensions were transferred into 96-well flat-bottomed plates, followed by adding 10 µl of cell viability reagent, and incubation for 1 h at 37°C (5% $CO_2$) followed by measuring of fluorescence using a microplate reader (M200-Infinite; Tecan, Männedorf, Switzerland) at 560 nm for excitation and 590 nm for emission.

## Flow Cytometry Assessment of Cell Death

Cells were treated with UNC-0638 (25 µM), UNC-1999 (50 µM), LLME (400 µM), staurosporine (1 µM) or left untreated prior to incubation for 24h (at 37°C, 5% $CO_2$). Subsequently, cells were centrifuged (400 x g, 5 min), washed with cold PBS and cell death was assessed by staining with Annexin V-FITC (BD Biosciences, Franklin Lakes, NJ) and Draq7™ (Biostatus, Shepshed, UK) diluted in Annexin V binding buffer (BD Biosciences). Cells were analyzed with a BD Accuri™ C6 Plus Flow Cytometer (BD Biosciences), and the FlowJo software (BD Biosciences) was used for data analysis. Cells were counted using a Countess II FL automated cell counter (Thermo Fisher Scientific, Waltham, MA). Protease inhibitors (Pefabloc SC, Nafamostat, E-64d, EDTA and pepstatin A) were preincubated for 30 min before adding the UNC-0638, UNC-1999, LLME or Staurosporine.

## Western Blot

Western blot analysis was performed as previously described (38). Equal amounts of cells were diluted in 100 µl of Laemmli sample buffer and boiled for 10 min at 95°C in a heating-block. Thereafter, samples were separated by SDS-PAGE (Novex WedgeWell 4-20% Tris-Glycine Gels, Thermo Fisher Scientific). Gels were transferred onto Immobilon-FL PVDF membranes (EMD-Millipore), followed by blocking in Odyssey Blocking buffer (LI-COR, Lincoln, NE) mixed with an equal volume of TBS or PBS, prior to overnight-incubation at 4°C with one of the following primary antibodies (1:1000; in blocking buffer): anti-histone 2A (H2A), H2B, H4, H3K4me, H3K9me3, H3K27me3, H2B-S14p or H3-S10p antibody. Thereafter, membranes were washed (3 × 10 min) with PBS or TBS/0.1% Tween-20, followed by a final wash (10 min) with PBS or TBS and then by incubation with secondary fluorescent antibodies (1:15,000; in TBS or PBS). The secondary antibodies were from LI-COR (IRDye 800 CW Donkey Anti-Rabbit IgG, IRDye 680 CW Donkey Anti-Mouse IgG, and IRDye 800 Donkey; LI-COR). After one hour of incubation at room temperature, the membranes were washed and scanned by using the Odyssey CLx Imaging System (LI-COR). Western blots were quantified and analyzed using Image Studio Lite Software (LI-COR). The targeted proteins were normalized to the loading control (β-actin).

## Confocal Microscopy

Aliquots of 200 µl with 0.3 x $10^6$ cells were dropped into round areas on microscopic glasses made with liquid-repellent pen. Suspensions were kept for 15 min and liquid was removed carefully with filter paper. The remaining cells were left to dry for 15 min. Samples were fixed and permeabilized with methanol for 10 min, followed by a 15 min drying step. On the top of each area, 100 µl of the mouse monoclonal human mast cell tryptase antibody (Abcam, Cambridge, UK) (1:500) in Tris-buffered saline (TBS)/1% bovine serum albumin (BSA) and/or isotype control at the same concentration were left overnight at 4°C, followed by 3 x washing with TBS-T. 100 µl of anti-mouse Alexa-488 conjugated antibody in TBS/1% BSA was added to each slide. The slides were kept at room temperature in the dark for 2 h and then washed three x with TBS-T. NucBlue (Life Technologies, Carlsbad, CA) was added, followed by 3 x washing with TBS-T. The slides were mounted with SlowFade™ diamond antifade mounting medium (Invitrogen, Eugene, OR) and cover glasses. Samples were analyzed using a laser-scanning microscope equipped with ZEN 2009 software (LSM 710, Carl Zeiss, Berlin, Germany).

## Cell Growth in the Presence of Nafamostat

HMC-1 cells were initially diluted to 0.1 x $10^6$ cells/ml and 1 ml cell suspensions were distributed in triplicates into 24-well plates. Nafamostatat mesylate was added at different concentrations and cells were incubated at 37°C with 5% $CO_2$ for different time periods. Cell viability was accessed using Annexin-V and Draq7 (Biostatus, Shepshed, UK) 24 h after nafamostat treatment to evaluate toxicity. Samples were analyzed by flow cytometry using a BD Accuri C6 plus flow cytometer (BD Biosciences). Cells left under culture conditions were subcultured for 4 and 7 days. Cell counts, viability and size were measured using the Countess II FL automated cells counter (Life Technologies).

## EdU Labeling

1 ml of 0.1 x $10^6$ cells/ml were distributed into 24-well plates. Cells were treated with 10 µM nafamostat and kept at 37°C in 5% $CO_2$ for 48 h. Two hours before harvesting the cells, 10 µM EdU was added. Cells were then stained using the Click-iT™ EdU Alexa 488 flow cytometry kit (Life Technologies). Flow cytometry analysis was performed (BD Accuri C6 plus). Data from 10,000 events/sample were collected and analyzed by the Flow Jo software (Ashland, OR).

## Statistical Analysis

Statistically significant differences between groups were determined by using one-way ANOVA with *post hoc* Dunnett's multiple comparison test. All graphs were prepared, and statistics calculated using GraphPad Prism 8.0 (GraphPad software Inc., San Diego, CA). A *P*-value of less than 0.05 was considered significant.

## DATA AVAILABILITY STATEMENT

The original contributions presented in the study are included in the article/**Supplementary Material**. Further inquiries can be directed to the corresponding authors.

## AUTHOR CONTRIBUTIONS

SA designed and performed experiments, and wrote the paper. FR designed, supervised and performed experiments, interpreted data and contributed to the writing of the paper. GP designed and planned the study, and wrote the paper. All authors contributed to the article and approved the submitted version.

## FUNDING

This study was supported by grants from The Swedish Research Council, The Swedish Heart and Lung Foundation, The Swedish Research Council, The Swedish Cancer Foundation, Knut & Alice Wallenberg Foundation and the Saudi Arabian Ministry of Education.

## SUPPLEMENTARY MATERIAL

The Supplementary Material for this article can be found online at: https://www.frontiersin.org/articles/10.3389/fimmu.2021.804408/full#supplementary-material

## REFERENCES

1. Voehringer D. Protective and Pathological Roles of Mast Cells and Basophils. *Nat Rev Immunol* (2013) 13:362–75. doi: 10.1038/nri3427
2. Dahlin JS, Maurer M, Metcalfe DD, Pejler G, Sagi-Eisenberg R, Nilsson G. The Ingenious Mast Cell: Contemporary Insights Into Mast Cell Behavior and Function. *Allergy* (2021). doi: 10.1111/all.14881
3. Galli SJ, Gaudenzio N, Tsai M. Mast Cells in Inflammation and Disease: Recent Progress and Ongoing Concerns. *Annu Rev Immunol* (2020) 38:49–77. doi: 10.1146/annurev-immunol-071719-094903
4. Valent P, Akin C, Hartmann K, Nilsson G, Reiter A, Hermine O, et al. Advances in the Classification and Treatment of Mastocytosis: Current Status and Outlook Toward the Future. *Cancer Res* (2017) 77:1261–70. doi: 10.1158/0008-5472.CAN-16-2234
5. Wernersson S, Pejler G. Mast Cell Secretory Granules: Armed for Battle. *Nat Rev Immunol* (2014) 14:478–94. doi: 10.1038/nri3690
6. Pejler G, Ronnberg E, Waern I, Wernersson S. Mast Cell Proteases: Multifaceted Regulators of Inflammatory Disease. *Blood* (2010) 115:4981–90. doi: 10.1182/blood-2010-01-257287
7. Pejler G. Novel Insight Into the *In Vivo* Function of Mast Cell Chymase: Lessons From Knockouts and Inhibitors. *J Innate Immun* (2020) 12:357–72. doi: 10.1159/000506985
8. Pejler G. The Emerging Role of Mast Cell Proteases in Asthma. *Eur Respir J* (2019) 54:1900685. doi: 10.1183/13993003.00685-2019
9. Pejler G, Knight SD, Henningsson F, Wernersson S. Novel Insights Into the Biological Function of Mast Cell Carboxypeptidase A. *Trends Immunol* (2009) 30:401–8. doi: 10.1016/j.it.2009.04.008
10. Akahoshi M, Song CH, Piliponsky AM, Metz M, Guzzetta A, Abrink M, et al. Mast Cell Chymase Reduces the Toxicity of Gila Monster Venom, Scorpion Venom, and Vasoactive Intestinal Polypeptide in Mice. *J Clin Invest* (2011) 121:4180–91. doi: 10.1172/JCI46139
11. Metz M, Piliponsky AM, Chen CC, Lammel V, Abrink M, Pejler G, et al. Mast Cells can Enhance Resistance to Snake and Honeybee Venoms. *Science* (2006) 313:526–30. doi: 10.1126/science.1128877
12. Anderson E, Stavenhagen K, Kolarich D, Sommerhoff CP, Maurer M, Metz M. Human Mast Cell Tryptase Is a Potential Treatment for Snakebite Envenoming Across Multiple Snake Species. *Front Immunol* (2018) 9:1532. doi: 10.3389/fimmu.2018.01532
13. Pereira PJ, Bergner A, Macedo-Ribeiro S, Huber R, Matschiner G, Fritz H, et al. Human Beta-Tryptase Is a Ring-Like Tetramer With Active Sites Facing a Central Pore. *Nature* (1998) 392:306–11. doi: 10.1038/32703
14. Sommerhoff CP, Bode W, Pereira PJ, Stubbs MT, Sturzebecher J, Piechottka GP, et al. The Structure of the Human betaII-Tryptase Tetramer: Fo(U)R Better or Worse. *Proc Natl Acad Sci USA* (1999) 96:10984–91. doi: 10.1073/pnas.96.20.10984
15. Melo FR, Vita F, Berent-Maoz B, Levi-Schaffer F, Zabucchi G, Pejler G. Proteolytic Histone Modification by Mast Cell Tryptase, a Serglycin Proteoglycan-Dependent Secretory Granule Protease. *J Biol Chem* (2014) 289:7682–90. doi: 10.1074/jbc.M113.546895
16. Kouzarides T. Chromatin Modifications and Their Function. *Cell* (2007) 128:693–705. doi: 10.1016/j.cell.2007.02.005
17. Strahl BD, Allis CD. The Language of Covalent Histone Modifications. *Nature* (2000) 403:41–5. doi: 10.1038/47412
18. Melo FR, Wallerman O, Paivandy A, Calounova G, Gustafson AM, Sabari BR, et al. Tryptase-Catalyzed Core Histone Truncation: A Novel Epigenetic Regulatory Mechanism in Mast Cells. *J Allergy Clin Immunol* (2017) 140:474–85. doi: 10.1016/j.jaci.2016.11.044
19. Melo FR, Lundequist A, Calounova G, Wernersson S, Pejler G. Lysosomal Membrane Permeabilization Induces Cell Death in Human Mast Cells. *Scand J Immunol* (2011) 74:354–62. doi: 10.1111/j.1365-3083.2011.02589.x
20. Alanazi S, Melo FR, Pejler G. Histone Methyltransferase Inhibition Has a Cytotoxic Impact on Transformed Mast Cells: Implications for Mastocytosis. *Anticancer Res* (2020) 40:2525–36. doi: 10.21873/anticanres.14223
21. Melo FR, Waern I, Ronnberg E, Abrink M, Lee DM, Schlenner SM, et al. A Role for Serglycin Proteoglycan in Mast Cell Apoptosis Induced by a Secretory Granule-Mediated Pathway. *J Biol Chem* (2011) 286:5423–33. doi: 10.1074/jbc.M110.176461
22. Fullgrabe J, Hajji N, Joseph B. Cracking the Death Code: Apoptosis-Related Histone Modifications. *Cell Death Differ* (2010) 17:1238–43. doi: 10.1038/cdd.2010.58
23. Mori S, Itoh Y, Shinohata R, Sendo T, Oishi R, Nishibori M. Nafamostat Mesilate Is an Extremely Potent Inhibitor of Human Tryptase. *J Pharmacol Sci* (2003) 92:420–3. doi: 10.1254/jphs.92.420
24. Ajiro K. Histone H2B Phosphorylation in Mammalian Apoptotic Cells. An Association With DNA Fragmentation. *J Biol Chem* (2000) 275:439–43. doi: 10.1074/jbc.275.1.439
25. Cheung WL, Ajiro K, Samejima K, Kloc M, Cheung P, Mizzen CA, et al. Apoptotic Phosphorylation of Histone H2B Is Mediated by Mammalian Sterile Twenty Kinase. *Cell* (2003) 113:507–17. doi: 10.1016/S0092-8674(03)00355-6
26. Pefani DE, Tognoli ML, Pirincci Ercan D, Gorgoulis V, O'Neill E. MST2 Kinase Suppresses rDNA Transcription in Response to DNA Damage by

Phosphorylating Nucleolar Histone H2B. *EMBO J* (2018) 37:e98760. doi: 10.15252/embj.201798760
27. Komar D, Juszczynski P. Rebelled Epigenome: Histone H3S10 Phosphorylation and H3S10 Kinases in Cancer Biology and Therapy. *Clin Epigenet* (2020) 12:147. doi: 10.1186/s13148-020-00941-2
28. Park CH, Kim KT. Apoptotic Phosphorylation of Histone H3 on Ser-10 by Protein Kinase Cdelta. *PloS One* (2012) 7:e44307. doi: 10.1371/journal.pone.0044307
29. Gatta R, Mantovani R. NF-Y Affects Histone Acetylation and H2A.Z Deposition in Cell Cycle Promoters. *Epigenetics* (2011) 6:526–34. doi: 10.4161/epi.6.4.14852
30. Zanotti R, Bonifacio M, Lucchini G, Sperr WR, Scaffidi L, van Anrooij B, et al. Refined Diagnostic Criteria for Bone Marrow Mastocytosis: A Proposal of the European Competence Network on Mastocytosis. *Leukemia* (2021). doi: 10.1038/s41375-021-01406-y
31. Schwartz LB. Diagnostic Value of Tryptase in Anaphylaxis and Mastocytosis. *Immunol Allergy Clin North Am* (2006) 26:451–63. doi: 10.1016/j.iac.2006.05.010
32. Crincoli E, Moliterni E, Catania F, Didona D, Calvieri S, Paolino G. Correlation of Serum Tryptase Levels With Total Number of Nevi, Breslow Thickness, Ulceration, and Mitotic Index in Melanoma Patients: Evaluation of a Promising Prognostic Marker. *Melanoma Res* (2018) 29:621–5. doi: 10.1097/CMR.0000000000000561
33. Lyons JJ, Yu X, Hughes JD, Le QT, Jamil A, Bai Y, et al. Elevated Basal Serum Tryptase Identifies a Multisystem Disorder Associated With Increased TPSAB1 Copy Number. *Nat Genet* (2016) 48:1564–9. doi: 10.1038/ng.3696
34. Scheer S, Zaph C. The Lysine Methyltransferase G9a in Immune Cell Differentiation and Function. *Front Immunol* (2017) 8:429. doi: 10.3389/fimmu.2017.00429
35. Rada-Iglesias A. Is H3K4me1 at Enhancers Correlative or Causative? *Nat Genet* (2018) 50:4–5. doi: 10.1038/s41588-017-0018-3
36. Atiakshin D, Samoilova V, Buchwalow I, Tiemann M. Expression of CD38 in Mast Cells: Cytological and Histotopographic Features. *Cells* (2021) 10:2511. doi: 10.3390/cells10102511
37. Alanazi S, Grujic M, Lampinen M, Rollman O, Sommerhoff CP, Pejler G, et al. Mast Cell Beta-Tryptase Is Enzymatically Stabilized by DNA. *Int J Mol Sci* (2020) 21:5065. doi: 10.3390/ijms21145065
38. Rönnberg E, Pejler G. Serglycin: The Master of the Mast Cell. *Methods Mol Biol* (2012) 836:201–17. doi: 10.1007/978-1-61779-498-8_14

**Conflict of Interest:** The authors declare that the research was conducted in the absence of any commercial or financial relationships that could be construed as a potential conflict of interest.

**Publisher's Note:** All claims expressed in this article are solely those of the authors and do not necessarily represent those of their affiliated organizations, or those of the publisher, the editors and the reviewers. Any product that may be evaluated in this article, or claim that may be made by its manufacturer, is not guaranteed or endorsed by the publisher.

frontiers in Immunology

ORIGINAL RESEARCH
published: 07 January 2022
doi: 10.3389/fimmu.2021.731435

# Chimeric Antigens Receptor T Cell Therapy Improve the Prognosis of Pediatric Acute Lymphoblastic Leukemia With Persistent/Recurrent Minimal Residual Disease in First Complete Remission

*Guan-hua Hu[1†], Yi-fei Cheng[1†], Ying-xi Zuo[2], Ying-jun Chang[1], Pan Suo[1], Jun Wu[2], Yue-ping Jia[2], Ai-dong Lu[2], Ying-chun Li[3], Yu Wang[3], Shun-chang Jiao[4], Long-ji Zhang[5], Xiang-yu Zhao[1], Chen-hua Yan[1], Lan-ping Xu[1], Xiao-hui Zhang[1], Kai-yan Liu[1], Yu Wang[1], Le-ping Zhang[2*] and Xiao-jun Huang[1*]*

[1] Peking University People's Hospital, Peking University Institute of Hematology, National Clinical Research Center for Hematologic Disease, Beijing Key Laboratory of Hematopoietic Stem Cell Transplantation, Peking-Tsinghua Center for Life Science, Research Unit of Key Technique for Diagnosis and Treatment of Hematologic Malignancies, Chinese Academic of Medical Sciences, Beijing, China, [2] Department of Pediatrics, Peking University People's Hospital, Peking University, Beijing, China, [3] Beijing Yongtai Reike Biotechnology Company Ltd, Beijing, China, [4] Chinese People Liberation Army (PLA) General Hospital, Beijing, China, [5] Shenzhen Geno-immune Medical Institute, Shenzhen, China

**Background:** The presence of minimal residual disease (MRD) is an independent risk factor for poor prognosis in patients with acute lymphoblastic leukemia (ALL). Moreover, the role of chimeric antigen receptor T-cell (CAR-T) therapy in patients with MRD is currently unclear.

**Methods:** We conducted a prospective study to investigate the role of CAR-T therapy in patients with persistent/recurrent MRD-positive ALL in first remission.

**Results:** A total of 77 patients who had persistent/recurrent MRD were included. Of these patients, 43 were enrolled in the CAR-T group, 20 received chemotherapy as a bridge to allogeneic hematopoietic cell transplantation (allo-HSCT), and 14 patients received intensified chemotherapy. MRD negativity was achieved in 90.7% of the patients after CAR-T infusion. Patients who received CAR-T therapy had a higher 3-year leukemia-free survival (LFS) than patients who did not (77.8% *vs.* 51.1%, P = 0.033). Furthermore, patients in the CAR-T group had a higher 3-year LFS than those in the chemotherapy bridge-to-allo-HSCT group [77.8% (95% CI, 64.8–90.7%) *vs.* 68.7% (95% CI, 47.7–89.6%), P = 0.575] and had a significantly higher 3-year LFS than those in the intensified chemotherapy group [77.8% (95% CI, 64.8–90.7%) *vs.* 28.6% (95% CI, 4.9–52.3%), P = 0.001]. Among the patients who received CAR-T therapy, eight were not bridged to allo-HSCT, and six (75%) remained in remission with a median follow-up of 23.0 months after CAR-T infusion.

OPEN ACCESS

**Edited by:**
*Rayne Rouce, Baylor College of Medicine, United States*

**Reviewed by:**
*Di Yu, Uppsala University, Sweden*
*Xi Zhang, Xinqiao Hospital, China*

***Correspondence:**
*Le-ping Zhang*
*zhangleping@pkuph.edu.cn*
*Xiao-jun Huang*
*huangxiaojun@bjmu.edu.cn*

*[†]These authors have contributed equally to this work*

**Specialty section:**
*This article was submitted to Cancer Immunity and Immunotherapy, a section of the journal Frontiers in Immunology*

**Received:** *27 June 2021*
**Accepted:** *15 December 2021*
**Published:** *07 January 2022*

**Citation:**
*Hu G-h, Cheng Y-f, Zuo Y-x, Chang Y-j, Suo P, Wu J, Jia Y-p, Lu A-d, Li Y-c, Wang Y, Jiao S-c, Zhang L-j, Zhao X-y, Yan C-h, Xu L-p, Zhang X-h, Liu K-y, Wang Y, Zhang L-p and Huang X-j (2022) Chimeric Antigens Receptor T Cell Therapy Improve the Prognosis of Pediatric Acute Lymphoblastic Leukemia With Persistent/Recurrent Minimal Residual Disease in First Complete Remission. Front. Immunol. 12:731435. doi: 10.3389/fimmu.2021.731435*

**Conclusions:** Our findings show that CAR-T therapy can effectively eliminate MRD and improve survival in patients with a suboptimal MRD response.

**Keywords: measurable residual disease, chimeric antigen receptor T-cell, pre-empty therapy, acute lymphocyte leukemia, pediatrics**

## BACKGROUND

Acute lymphoblastic leukemia (ALL) is the most common pediatric cancer. Despite remarkable improvements in the prognosis of ALL over the past decades, treating relapsed ALL remains challenging. Many studies have shown that eliminating minimal residual disease (MRD), which is one of the most important criteria for risk stratification, reduces relapse (1, 2). The US Food and Drug Administration claimed that the persistence of MRD is associated with poor prognosis, regardless of trial approach and detection methods, and highlighted the need for interventions for patients in first complete remission (CR1) (3). A previous study in our institute also showed that persistent/recurrent MRD was the most significant adverse prognostic indicator in pediatric ALL (4). Thus, eradicating MRD in CR1 is essential.

Allogeneic hematopoietic stem cell transplantation (allo-HSCT) is recommended as a frontline treatment for high-risk and relapsed ALL. Several studies have suggested that allo-HSCT is associated with lower relapse risk than chemotherapy in patients with MRD in CR1 (5, 6). However, Zhao et al. indicated that the 3-year cumulative incidence of relapse was significantly lower in patients with pre-HSCT MRD negativity than in those with pre-HSCT MRD positivity (16% *vs.* 31%, $P < 0.001$). St. Jude Children's Research Hospital also reported that persistent MRD at the time of HSCT was associated with high relapse rates and transplant-related mortality (TRM) (7). HSCT and intensification of chemotherapy to decrease pre-HSCT MRD carry a substantial risk of morbidity and mortality in the presence of MRD. Therefore, novel therapeutic approaches that can effectively eliminate MRD are urgently needed.

Recently, chimeric antigen receptor T-cell (CAR-T) therapy has been reported to be the most promising approach for the treatment of refractory/relapsed (R/R) B-cell ALL (8). In the ELIANA trial, which included children and young adults with R/R B-ALL, the response rate was 81%, and the leukemia-free survival (LFS) among responders was 62% at 24 months (9). Several groups have shown that most of patients become MRD-negative and maintain their status for several months after CAR-T infusion. Moreover, a previous study in our institute showed that CAR-T infusion was effective in patients with MRD and with no responsive to donor lymphocytes infusion after allo-HSCT (10), suggesting that CAR-T therapy has the potential to induce deeper remission while reducing toxicity. However, the short-term and long-term effects of CAR-T on patients with MRD have not been assessed. Several issues that need to be explored include whether CAR-T therapy can efficiently eradicate MRD and reach a satisfactory response rate similar to those of previous reports on R/R ALL, whether CAR-T therapy can improve the long-term survival of patients with MRD, and whether sustained remission can be achieved with the application of CAR-T therapy without allo-HSCT. To the best of our knowledge, this study is the first prospective study to explore the role of CAR-T therapy in patients with persistent/recurrent MRD in CR1.

## METHODS

### Patients

In this single-center, prospective study, a total of 525 patients who were newly diagnosed with Philadelphia chromosome-negative B-ALL between January 2015 and September 2019 were included (**Figure 1**). The inclusion criteria were (1) age of 1–18 years (2), achieved complete remission (CR) after induction chemotherapy (3), persistent positive MRD within three months from the start of treatment, and (4) achieved MRD negativity and the conversion of negative to positive MRD during consolidation chemotherapy. The exclusion criteria included (1) morphological relapse within two months of recurrent MRD and (2) severe heart, kidney, or liver disease. This study was approved by the Peking University People's Hospital review board. All patients' legal guardians provided written informed consent documents in accordance with the Declaration of Helsinki.

### CAR-T Protocols

The lymphodepleting chemotherapy before CAR-T therapy included fludarabine (25 mg/m$^2$/d on days –5 to –3) and cyclophosphamide (250 mg/m2/d on days –5 to –3). Multiple up-to-date CAR-T engineering technologies have been summarized (11). Anti-CD19 CAR-T cells constructed with a 4-1BB (79%) or CD28 (21%) costimulatory domain were generated *via* lentiviral vector from fresh leukapheresis material in this study.

For the CAR-T with a 4-1BB costimulatory domain, peripheral blood mononuclear cells (PBMCs) were collected from patients and stimulated with dynabeads coated with anti-CD3 and anti-CD28 mAbs (Thermo Fisher Scientific). Activated T cells were transduced with lentiviral vector encoding the anti-CD19 CAR construct consisting of CD19 recognition domain, transmembrane link domain, 4-1BB intracellular domain, CD3ζ intracellular domain. After lentiviral transduction, the 4-1BB CAR-T-19 cells were cultured in medium supplemented with 500 IU/ml IL-2 at 37°C/5% CO2 for approximately 5 to 11 days to obtain sufficient cells for infusion.

For the CAR-T with a CD28 costimulatory domain, peripheral blood mononuclear cells (PBMCs) were acquired through apheresis from the patients at relapses with sufficient lymphocyte counts, and the T cells were selected using CD3 magnetic beads. CD28 monoclonal antibodies were added for T cell activation *in vitro*. The activated T cells were

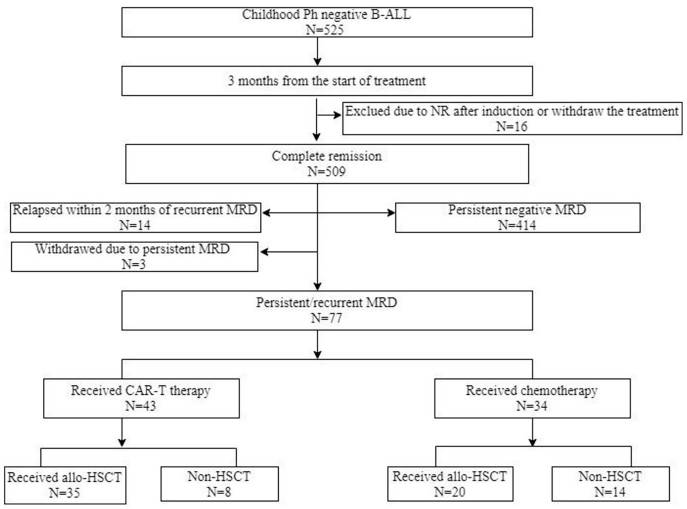


**FIGURE 1** | Diagram of patients enrolled in this study. CAR-T, chimeric antigen receptor T cells; ALL, acute lymphoblastic leukemia; allo-HSCT, allogeneric haematopoietic stem cell transplantation; MRD, measurable residual disease; NR, non-remission; Ph, Philadelphia chromosome.

transduced with the 4SCAR19 lentiviral vector encoding the CD19 CAR carrying a "safety switch"—iCasp9 for 3-5 days. The CAR-T cells were cultured in AIM-V (Invitrogen, San Diego, CA, USA) medium supplemented with IL-2, IL-7, and IL-15 at 37°C/5% CO2 for approximately 5–7 days to obtain sufficient cells for infusion.

Real-time quantitative polymerase chain reaction was used to quantify the level of the CAR gene (<100 copies/μg DNA was defined as negative). Flow cytometry (FCM) was performed to determine the transduction efficiency and the ratio of B cells in peripheral blood and bone marrow after CAR-T infusion. For patients who chose to be enrolled in the observation group after CAR-T infusion, the levels of the CAR gene and B cells were assessed every month, and maintenance chemotherapy was administered if CAR T cells were not detected *in vivo* and/or B cells were recovered.

## Transplant Protocols

The conditioning regimen for allo-HSCT was in accordance with previous reports (12, 13). Patients who received an HLA-mismatched HSCT received a regimen that included cytarabine (4 g/m2/day IV, days −10 and −9), busulfan (3.2 mg/kg/day IV, days −8 to −6), cyclophosphamide (1.8 g/m2/day IV, days −5 and −4), semustine (250 mg/m2 PO, day −3), and antithymocyte globulin (ATG) (2.5 mg/kg/day IV, days −5 to −2). Patients who received an HLA-identical HSCT were treated with a regimen identical to that of the patients who received an HLA-mismatched HSCT, but without ATG. All patients received acute graft-versus-host disease (aGVHD) prophylaxis consisting of cyclosporine A, mycophenolate mofetil, and a short-term methotrexate regimen.

## Chemotherapy Protocols

The intensified chemotherapy regimens were in accordance with a previous report (14). These regimens included (1) an induction therapy (2), a consolidation therapy with two cycles of a re-induction block in between, and (3) a maintenance therapy. The induction and re-induction chemotherapy regimens consisted of vincristine, idarubicin, cyclophosphamide, and L-asparaginase. The consolidation chemotherapy regimens were comprised of methotrexate (MTX), vincristine, and peg-aspargase; and cytarabine (Ara-c), idarubicin, fosfamide, etoposide, and vincristine. The maintenance chemotherapy regimens included mercaptopurine (50 mg/m2/d PO, daily) and methotrexate (20 mg/m2/d IM, weekly). Patients in the chemotherapy bridge-to-allo-HSCT group received MTX (2–3 g/m2/d IV) and/or Ara-c (2 g/m2/d IV, days 1 to 3) based chemotherapy regimens.

## Detection of MRD

A panel of eight antibody combinations, which included cCD3, mCD3, CD2, CD5, CD7, CD10, CD19, CD20, CD34, CD38, CD45, CD58, CD99, CD123, and cTDT, were used for MRD detection. The standardized assays and quality controls were consistent with those of previous reports (15). Any MRD level was considered positive. MRD was assessed every month until MRD negativity, every two to three months during consolidation chemotherapy, and every six months during maintenance chemotherapy for patients in the chemotherapy group. MRD was assessed every month until one year of CAR-T therapy and every two to three months until two years of CAR-T therapy for patients in the CAR-T group. MRD was assessed at 1, 2, 3, 4.5, 6, 9, and 12 months post-HSCT and at six-month intervals thereafter for patients in the HSCT group.

## Definitions

CR was defined as the presence of <5% blasts in the bone marrow, an absolute neutrophil count of >1 × $10^9$/L, a platelet count of >100 × 109/L, and the absence of extramedullary disease. Recurrence of ≥5% bone marrow blasts and/or the

development of extramedullary disease were defined as a relapse. Recurrent MRD was defined as two MRD-positive samples at an interval of one month in a patient who was previously MRD-negative. Non-relapse-related mortality (NRM), aGVHD, and chronic GVHD (cGVHD) were defined as previously described (12). Cytokine release syndrome (CRS) grading was based on the National Cancer Institute (NCI) consensus CRS scoring system.

## End Points and Statistical Analysis

The primary endpoint is LFS. The secondary endpoints are MRD negativity rate, overall survival (OS), and safety. LFS was measured from the time when CR was achieved; events of LFS included death in CR1 or relapse. MRD negativity was associated with an undetectable MRD by FCM. The event of OS was death at the date of the last follow-up. The patients' characteristics were compared using the chi-square test or Fisher's exact test for categorical variables and the Mann–Whitney rank test or Student's t-test for continuous variables. The Kaplan-Meier method was used to analyze the LFS and OS. Comparisons between different LFS and OS probabilities were performed using the log-rank test. Multivariate analysis was performed using the Cox proportional hazards regression model. Statistical significance was set at $P < 0.05$. SPSS version 23.0 (SPSS Inc., Chicago, IL, USA) and R version 3.5.3 (R Foundation for Statistical Computing, Vienna, Austria) were used for data analysis.

# RESULTS

## Patients' Characteristics

A total of 525 patients diagnosed with Philadelphia chromosome-negative B-ALL were included in this study; 448 patients were excluded due to persistent negative MRD (n = 414), relapse within two months of recurrent MRD (n = 14), withdrawal due to personal reasons (n = 12), failure to achieve CR after induction chemotherapy (n = 6), and loss to follow-up (n = 2). Of the 77 patients with persistent/recurrent MRD who were screened and encouraged to receive CAR-T therapy, 43 patients were enrolled in the CAR-T group. The remaining patients were divided into the chemotherapy bridge-to-allo-HSCT group (n = 20) and the intensified chemotherapy group (n = 14) according to their personal willingness, economic background, and donor availability. After a month of CAR-T infusion, patients who failed to achieve MRD negativity received allo-HSCT (n = 4), and patients who achieved MRD negativity were divided into the bridge-to-allo-HSCT group (n = 31) and the observation group (n = 8). **Tables 1** and **2** show the characteristics of the patients, and the baseline characteristics of the patients who received CAR-T therapy and those who did not were comparable.

## CAR-T Therapy

In this study, 43 patients received CAR-T therapy. The median dose of infused CAR T cells was $3.85 \times 10^6$ ($0.45–8.45 \times 10^6$)/kg. The viability of CAR-T pre-infusion was 93.4% (75.0-99.1%), transduction efficiency of CAR-T pre-infusion was 29.5% (8.7-83.8%). CAR T cells rapidly expanded during the first month in 42 (97.6%) patients. The mean CAR-T count at peak expansion was 303,238 (1,250–1,890,000), and the median time to peak expansion was 11.6 (7–17) days. One patient had unsatisfactory peak CAR-T counts (1,250 copies at peak expansion).

The median MRD level pre-lymphodepletion was 0.22% (0.01–2.86%), and the rate of patients who achieved MRD negativity after a month of CAR-T infusion was 90.7%. Patients who achieved MRD negativity and those who did not received comparable doses of CAR T cells ($3.9 \times 10^6$/kg *vs.* $5.0 \times 10^6$/kg, P = 0.65), but the peak CAR-T counts of patients who achieved MRD negativity were significantly higher than those of patients who failed to achieve MRD negativity (362,350 copies *vs.* 70,323 copies, P = 0.02). Among the patients who failed to achieve MRD negativity after a month of CAR-T infusion (n = 4), one had unsatisfactory peak CAR-T counts, and another had undetectable CAR-T counts at 1 month after CAR T-cell infusion.

Among the patients who received CAR-T therapy, 23 (53.8%) had CRS of any grade, and six (13.9%) had severe CRS (grades 3 and 4). Neurological adverse events occurred in six (13.9%) patients, of which four experienced headache and confusion, one had seizures, and another had encephalopathy. No CAR-T-related mortality was observed.

All patients who failed to achieve MRD negativity after CAR-T therapy received allo-HSCT. Among the patients who achieved MRD negativity after CAR-T infusion (n = 39), 31 were bridged to allo-HSCT after CAR-T therapy, while eight were not (**Table 3**). Among patients who bridged to allo-HSCT after CAR-T therapy, 26 of them received 4-1 BB CAR-T, CAR-T cell can be detected before allo-HSCT in 24 patients who received 4-1 BB CAR-T. Among patients who bridged to allo-HSCT after CAR-T therapy, 9 of them received CD28 CAR-T (**Table 4**), the level of CAR-T cell after infusion was not monitored.

In patients who were not bridged to allo-HSCT after CAR-T therapy, the median dose of infused CAR T cells was $3.96 \times 10^6$ ($0.45–5.3 \times 10^6$)/kg, the median persistence time of CAR T cells was 5.0 (2–12) months, and the median recovery time of B cells was 3.9 (1.5–7.5) months. B cells were not recovered in two patients until the last follow-up. One of them remained in CR after 23 months of CAR-T infusion, while the other patient with CD19 negativity relapsed.

## Allo-HSCT

In this study, 55 patients received allo-HSCT. A total of 35 patients received CAR-T therapy before allo-HSCT, and the median time from CAR-T therapy to allo-HSCT was 67 days. The other 20 patients received chemotherapy before allo-HSCT. Thirty (85.7%) patients in the CAR-T bridge-to-allo-HSCT group were MRD-negative pre-HSCT, while the other five patients were MRD-positive with a median MRD level of 0.17% (0.01–0.77%). Fifteen (75%) patients in the chemotherapy bridge-to-allo-HSCT group were MRD-negative pre-HSCT, while the other five patients were MRD-positive with a median MRD level of 0.44% (0.01–1.5%).

Of the patients who received allo-HSCT, five received allo-HSCT from matched sibling donors, while the others received haplo-HSCT. Patients achieved neutrophil engraftment at a

**TABLE 1 |** Characteristics of patients stratified by CAR-T and non-CAR-T group.

| Characteristics | CAR-T Group | Non-CAR-T Group | P value |
|---|---|---|---|
| Number of patients | 43 | 34 | |
| Median age (range), years | 8.3 (1–17) | 8.2 (1–17) | 0.978 |
| Male sex, n (%) | 23 (53.5) | 22 (64.7) | 0.359 |
| Cytogenetic risk group | | | |
| Low-risk, n (%) | 29 (67.4) | 19 (55.8) | 0.348 |
| High-risk, n (%) | 14 (32.6) | 15 (44.2) | 0.348 |
| Fusion genes, n (%) | | | |
| *MLL-AF4* | 2 (4.6) | 4 (11.7) | 0.251 |
| *E2A-PBX1* | 2 (4.6) | 2 (5.8) | 0.810 |
| *TEL-AML1* | 6 (13.9) | 2(5.8) | 0.252 |
| *E2A-HLF* | 1 (2.3) | 1 (2.9) | 0.867 |
| High hyperdiploid | 6 (13.9) | 3 (8.8) | 0.489 |
| High risk gene mutation, n (%) | 14 (32.5) | 13 (38.2) | 0.604 |
| *IKZF1* | 6 (13.9) | 8 (23.4) | |
| *JAK2* | 3 (6.9) | 4 (11.7) | |
| *CRLF2* | 3(6.9) | 1 (2.9) | |
| *PDGFRB* | 2 (4.6) | 0 (0.0) | |
| Extramedullary infiltration, n (%) | 5 (11.6) | 4 (11.7) | 0.628 |
| Persistent positive MRD, n (%) | 17 (39.5) | 16 (47.0) | 0.259 |
| Recurrent positive MRD, n (%) | 26 (60.5) | 18 (53.0) | 0.488 |
| MRD > 0.1% at any checking points, n (%) | 29 (67.4) | 27 (79.4) | 0.307 |
| MRD > 1% at any checking points, n (%) | 15 (34.8) | 9 (26.4) | 0.467 |
| Levels of recurrent MRD (%) | 0.52 (0.01-5.09) | 0.58 (0.004-3.3) | 0.843 |
| Follow-up time (range), months | 37.4 (7.0-70.0) | 45.0 (7.0-70.0) | 0.518 |

*CAR-T, chimeric antigen receptor T cells; MRD, minimal residual disease.*

**TABLE 2 |** Characteristics of patients stratified by CAR-T bridge to allo-HSCT and chemotherapy bridge to allo-HSCT.

| Characteristics | CAR-T Bridge to Allo-HSCT | Chemotherapy Bridge to Allo-HSCT | P value |
|---|---|---|---|
| Number of patients | 35 | 20 | |
| Median age (range), years | 8.4 (1–17) | 9.3 (1–17) | 0.546 |
| Male sex, n (%) | 17(48.6) | 11 (55.0) | 0.781 |
| Median level of pre-HSCT MRD (range), % | 0.04 (0.00-0.77) | 0.06 (0.00-1.5) | 0.754 |
| Median time from diagnosis to allo-HSCT (range), months | 8.2 (3–14) | 7.5 (4–20) | 0.348 |
| Donor-recipient sex match grafts, n (%) | | | |
| Male-male | 17 (48.5) | 12 (60) | 0.575 |
| Male-female | 11 (31.4) | 7 (35.0) | 0.786 |
| Female-male | 3 (8.5) | 0 (0.0) | 0.182 |
| Female-female | 4 (11.4) | 1 (5.0) | 0.429 |
| Donor-recipient relationship, n (%) | | | |
| Father-child | 26 (74.2) | 18 (90.0) | 0.165 |
| Mother-child | 3 (8.6) | 1 (5.0) | 0.627 |
| Brother-brother | 3 (8.6) | 0(0.0) | 0.182 |
| Sister-brother | 3 (8.6) | 1 (5.0) | 0.627 |
| ABO matched grafts, n (%) | | | |
| Matched | 17 (48.6) | 12 (60.0) | 0.575 |
| Major mismatch | 5 (14.3) | 3 (15.0) | 0.943 |
| Minor mismatch | 11 (31.4) | 4 (20.0) | 0.364 |
| Bidirectional mismatch | 2 (5.7) | 1 (5.0) | 0.911 |
| Cell compositions in grafts, mean (range) | | | |
| Infused nuclear cells, $10^8$/kg, mean (range) | 9.5 (7.0-14.0) | 9.5 (6.6-13.91) | 0.792 |
| infused $CD34^+$cells, $10^6$/kg, mean (range) | 3.4 (1.2-9.8) | 2.8 (0.9-4.7) | 0.543 |
| Median time of neutrophil engraftment (range), days | 13.1 (10–18) | 13.9 (10–19) | 0.965 |
| Median time of platelet engraftment (range), days | 15.6 (9–46) | 20.3 (10–43) | 0.687 |
| Grade II-IV aGVHD, % | 22 | 21 | 0.758 |
| Chronic GVHD, % | 43 | 40 | 0.810 |
| Moderate to severe cGVHD, % | 19 | 21 | 0.897 |
| 3-years probability of LFS, % | 75.0 | 68.7 | 0.586 |
| 3-years probability of OS, % | 85.6 | 73.3 | 0.920 |

*CAR-T, chimeric antigen receptor T cells; GVHD, graft-versus-host disease; HSCT, allogeneic hematopoietic stem cell transplantation; LFS, leukemia-free survival; MRD, minimal residual disease; OS, overall survival.*

**TABLE 3 |** Clinical features and outcomes of patients who did not bridge to allo-HSCT after CAR-T therapy.

| Patient | Cyto/mol abn | MRD Before Lymphodepletion (%) | Total CAR-T cells/kg infused | Time of Persistence of CAR-T Cell (months) | Time of B Cell Recovery (months) | Treatment After CAR-T Disappeared | Outcome After CAR-T |
|---|---|---|---|---|---|---|---|
| 1 | No | 0.08 | $3.4\times10^6$ | 4 | 2.5 | 6-MP; MTX | CCR for 29 months |
| 2 | hypodiploid | 0.02 | $5.0\times10^6$ | 2.5 | 1.5 | 6-MP; MTX | CD19+relapse |
| 3 | No | 0.03 | $3.0\times10^6$ | 2.5 | 6 | 6-MP; MTX | CCR for 21 months |
| 4 | TEL/AML1 | 0.3 | $5.3\times10^6$ | 4 | 4 | 6-MP; MTX | CCR for 12 months |
| 5 | hyperdiploid | 0.98 | $0.45\times10^6$ | 12 | 7.5 | 6-MP; MTX | CCR for 14 months |
| 6 | IKZF1 | 0.56 | $5.0\times10^6$ | 8 | without B cell recovery | 6-MP; MTX | CCR for 23 months |
| 7 | TEL/AML1 | 0.06 | $4.6\times10^6$ | 2 | 2 | CD22-CAR-T | CCR for 14 months |
| 8 | IKZF1; complex chromosome | 0.28 | $5.0\times10^6$ | 5 | without B cell recovery | Chinese medicine | CD19-relapse |

*CAR-T, chimeric antigen receptor T cells; Cyto/mol abn, cytogenetic/molecular abnormalities; CCR, continuous complete remission; 6-MP, mercaptopurine; MRD, minimal residual disease; MTX, methotrexate.*

median time of 13 (10–35) days, and all patients achieved platelet engraftment at a median time of 14 (7–58) days. The cumulative 100-day incidence of aGVHD grades II–IV and grades III–IV in the CAR-T bridge-to-allo-HSCT group were similar to those of the chemotherapy bridge-to-allo-HSCT group [24% (95% CI, 17–27%) *vs.* 23% (95% CI, 12–32%), P = 0.956; 8% (95% CI, 4–12%) *vs.* 6% (95% CI, 3–11%), P = 0.818]. The cumulative 3-year incidence of total cGVHD and severe cGVHD in the CAR-T bridge-to-allo-HSCT group were also similar to those of the chemotherapy bridge-to-allo-HSCT group [56% (95% CI, 38–65%) *vs.* 49% (95% CI, 39–55%), P = 0.687; 12% (95% CI, 6–19%) *vs.* 11% (95% CI, 5–15%), P = 0.918]. The cumulative 3-year incidence of NRM was 3% (95% CI, 1–6%).

## Chemotherapy

Of the patients who received intensified chemotherapy without allo-HSCT, nine (64.2%) achieved MRD negativity. No serious treatment-related toxicity or TRM was observed.

## Relapse, LFS, and OS

Between January 1, 2015 and December 31, 2020, the median follow-up time for surviving patients was 44.0 (18.0–70.0) months. Of patients in the CAR-T group, 10 (23.2%) relapsed (four withdrew, three achieved second CR with allo-HSCT, two achieved second CR with CD22-CAR-T therapy, and one abandoned further treatment after no response to CD22-CAR-T therapy). Relapse occurred at a median time of 9.6 (4–17) months after CAR-T infusion. Nine (20.9%) patients experienced a CD19-positive relapse, while one (2.3%) patient experienced a CD19-negative relapse. Of the patients in the chemotherapy bridge-to-allo-HSCT group, six (30%) relapsed (four withdrew and two achieved second CR with allo-HSCT). Of the patients who received intensified chemotherapy, 10 (71.4%) relapsed (five withdrew, three achieved second CR with allo-HSCT, and two failed to achieve second CR with salvage chemotherapy). At the last follow-up, 17 (22.0%) patients died of relapse, and two (2.5%) patients died of transplant-related complications.

**TABLE 4 |** Characteristics of patients stratified by 4-1 BB CAR-T and CD28 CAR-T.

| Characteristics | 4-1BB CAR-T | CD28 CAR-T | P value |
|---|---|---|---|
| Number of patients | 34 | 9 | |
| Median age (range), years | 8.0 (2–16) | 9.0 (1–17) | 0.613 |
| Male sex, n (%) | 19 (55.8) | 2 (22.2) | 0.076 |
| Cytogenetic risk group | | | |
| Low-risk, n (%) | 23 (67.6) | 6 (66.7) | |
| High-risk, n (%) | 11 (32.4) | 3 (33.3) | 0.956 |
| MRD negativity after one month of CAR-T infusion, n (%) | 33 (97.0) | 6 (66.7) | 0.006 |
| Bridge to allo-HSCT, n (%) | 26 (76.5) | 9 (100) | 0.111 |
| 3-years probability of LFS, % | 80.7 | 66.7 | 0.426 |
| 3-years probability of OS, % | 91.1 | 66.7 | 0.138 |
| CRS of any grade, n (%) | 21 (61.7) | 2 (22.2) | 0.037 |
| Severe CRS (grade 3 and 4), n(%) | 6 (17.6) | 0 (0) | 0.179 |

*CAR-T, chimeric antigen receptor T cells; CRS, cytokine release syndrome; HSCT, allogeneic hematopoietic stem cell transplantation; LFS, leukemia-free survival; MRD, minimal residual disease; OS, overall survival.*

Patients who received CAR-T therapy (n = 43) had a higher 3-year LFS [77.8% (95% CI, 65.6–89.9%) *vs.* 51.1% (95% CI, 33.8–68.3), P = 0.033, **Figure 2A**] and a trend of higher OS [86.0% (95% CI, 93.4–75.6%) *vs.* 62.6% (95% CI, 45.5–76.5%), P = 0.059, **Figure 2B**] than those who did not (n = 34). Patients in the CAR-T group (n = 43) also had a trend of higher 3-year LFS than those in the chemotherapy bridge-to-allo-HSCT group (n = 20) [77.8% (95% CI, 64.8–90.7%) *vs.* 68.7% (95% CI, 47.7–89.6%), P = 0.575] and had a significantly higher 3-year LFS than those in the intensified chemotherapy group (n = 14) [77.8% (95% CI, 64.8–90.7%) *vs.* 28.6% (95% CI, 4.9–52.3%), P = 0.001) (**Figure 2C**). The 3-year OS of patients in the CAR-T group (n = 43) tented to be higher than that in the chemotherapy bridge-to-allo-HSCT group (n = 20) [86.0% (95% CI, 75.6–96.3%) *vs.* 73.3% (95% CI, 52.9–93.6%), P = 0.470] and was significantly higher than that in the intensified chemotherapy group (n = 14) [86.0% (95% CI, 75.6–96.3%) *vs.* 49.0% (95% CI, 22.3–75.6%), P = 0.010] (**Figure 2D**).

Multivariate Cox regression modeling showed that MRD ≥1% at any checking point and non-CAR-T therapy were independent risk factors associated with inferior LFS in all patients (**Table 5**).

## Subgroup Analysis for Patients Who Received CAR-T Therapy

In patients who received CAR-T therapy (n = 43), the LFS and OS of patients who were bridged to allo-HSCT after CAR-T infusion (n = 35) were comparable with those of patients who were not (n = 8) [75.0% (95% CI, 59.9–90.0%)*vs.* 75.0% (95% CI, 45.0–104.9%), P = 0.765, **Figure 2E**; 85.2% (95% CI, 73.2–97.1%) *vs.* 75.0% (95% CI, 45.0–104.9%), P = 0.470, **Figure 2F**]. MRD ≥1% at any checking point pre-CAR-T therapy (n = 15) tended to lower the LFS of the CAR-T group, but the trend was not statistically significant [65.5% (95% CI, 40.8–90.1%) *vs.* 82.9% (95% CI, 67.6–98.1%), P = 0.236], indicating that the negative impact of high-level MRD can be abrogated by CAR-T therapy to some extent. Multivariate Cox regression modeling showed that high-risk cytogenetics was an independent risk factor

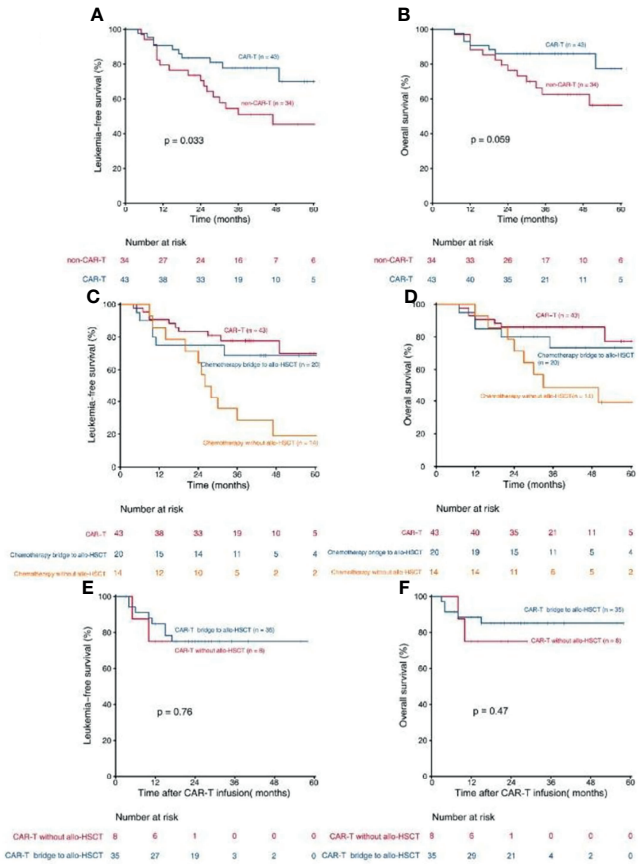


**FIGURE 2** | Kaplan- Meier estimates for patients with persistent/recurrent MRD. **(A)** LFS rates for patients received CAR-T therapy and patients did not receive CAR-T theraphy; **(B)** OS rates for patients received CAR-T therapy and patients did not receive CAR-T therapy; **(C)** LFS rates for patients received CAR-T therapy, patients received chemotherapy bridge to allo-HSCT and patients received chemotherapy without allo-HSCT; **(D)** OS rates for patients received CAR-T therapy, patients received chemotherapy bridge to allo-HSCT and patients received chemotherapy without allo-HSCT; **(E)** LFS rates for CAR-T patients who bridge to allo-HSCT and who did not; **(F)** Os rates for CAR-T patients who bridge to allo-HSCT and who did not.

**TABLE 5** | Multivariate analysis of factors associated with survival outcomes.

| | LFS | | OS | |
|---|---|---|---|---|
| **Variable** | **HR (95%CI)** | **P** | **HR (95%CI)** | **P** |
| **Overall patients** | | | | |
| Cytogenetic risk group (high-risk *vs.* non-high-risk) | 1.326 (0.753-2.335) | 0.328 | 1.781 (0.894-3.631) | 0.112 |
| Level of MRD (≥1% *vs.*<1%) | 3.659 (1.642-8.155) | 0.002 | 2.424 (0.947-6.203) | 0.065 |
| CAR-T therapy (no *vs.* yes) | 2.409 (0.999-5.812) | 0.049 | 2.112 (0.733-6.086) | 0.166 |
| HSCT (no *vs.* yes) | 2.075 (0.890-4.838) | 0.091 | 2.249 (0.832-6.077) | 0.110 |
| **Recurrent MRD group** | | | | |
| Cytogenetic risk group (high-risk *vs.* non-high-risk) | 0.783 (0.160-3.831) | 0.763 | 2.546 (0.613-10.572) | 0.198 |
| Median time of MRD recurred (<18 months *vs.* ≥18 months) | 1.001 (1.095-1.718) | 0.430 | 2.714 (0.537-8.323) | 0.044 |
| Level of recurred MRD (≥1% *vs.*<1%) | 1.605 (1.895-2.981) | 0.000 | 0.428 (0.069-2.641) | 0.361 |
| CAR-T therapy (no *vs.* yes) | 9.456 (2.087-42.848) | 0.004 | 4.736 (0.872-25.718) | 0.072 |
| HSCT (no *vs.* yes) | 6.642 (1.116-39.519) | 0.037 | 23.503 (2.633-209.791) | 0.005 |
| **Persistence positive MRD** | | | | |
| Cytogenetic risk group (high-risk *vs.* non-high-risk) | 1.994 (0.547-7.268) | 0.295 | 2.669 (0.669-10.785) | 0.168 |
| Level of MRD (≥1% *vs.*<1%) | 2.907 (0.804-10.503) | 0.104 | 1.239 (0.296-5.188) | 0.769 |
| CAR-T therapy (no *vs.* yes) | 1.674 (0.407-6.892) | 0.476 | 0.671 (0.154-2.934) | 0.596 |
| HSCT (no *vs.* yes) | 3.160 (0.720-13.808) | 0.127 | 1.899 (0.331-10.902) | 0.472 |
| **CAR-T therapy group** | | | | |
| Cytogenetic risk group (high-risk *vs.* non-high-risk) | 1.384 (0.305-6.281) | 0.674 | 12.413 (1.275-120.851) | 0.030 |
| Level of MRD (≥1% *vs.*<1%) | 2.291 (0.560-9.377) | 0.249 | 1.787 (0.304-10.510) | 0.521 |
| MRD after CAR-T (positive *vs.* negative) | 1.236 (0.206-7.436) | 0.817 | 3.677 (0.497-27.193) | 0.202 |
| Bridge to HSCT (no *vs.* yes) | 0.633 (0.069-5.816) | 0.686 | 2.528 (0.189-33.717) | 0.483 |
| **Allo-HSCT group** | | | | |
| Cytogenetic risk group (high-risk *vs.* non-high-risk) | 0.647 (0.193-2.164) | 0.479 | 1.649 (0.359-7.570) | 0.520 |
| Level of MRD (≥1% *vs.*<1%) | 5.848 (1.753-19.514) | 0.004 | 5.054 (1.127-22.669) | 0.034 |
| Pre-HSCT MRD (negative *vs.* positive) | 0.651 (0.168-2.521) | 0.534 | 0.838 (0.512-4.630) | 0.840 |
| CAR-T pre-HSCT (no *vs.* yes) | 3.010 (0.860-10.466) | 0.083 | 3.425 (0.732-16.022) | 0.118 |
| cGVHD (no *vs.* yes) | 6.506 (1.518-27.884) | 0.012 | 1.908 (0.401-9.080) | 0.417 |
| **Chemotherapy group** | | | | |
| Cytogenetic risk group (high-risk *vs.* non-high-risk) | 1.290 (0.310-5.366) | 0.726 | 1.870 (0.389-8.992) | 0.435 |
| Level of MRD (≥1% *vs.*<1%) | 4.014 (0.860-18.673) | 0.076 | 9.881 (0.312-11.355) | 0.491 |
| Recurrent MRD (yes *vs.* no) | 2.771 (0.616-12.474) | 0.184 | 7.875 (0.820-75.640) | 0.074 |

*CAR-T, chimeric antigen receptor T cells; CI, confidence interval; GVHD, graft-versus-host disease; HR, hazard ratio; HSCT, allogeneic hematopoietic stem cell transplantation; LFS, leukemia-free survival; MRD, minimal residual disease; OS, overall survival.*

associated with inferior OS in patients who received CAR-T therapy (**Table 5**).

## Subgroup Analysis for Patients Who Received Allo-HSCT

In patients who received allo-HSCT (n = 55), the 3-year LFS and OS of patients who received CAR-T therapy pre-HSCT (n = 35) were higher than those of patients who did not (n = 20) [75.0% (95% CI, 59.7–90.2%) *vs.* 68.7% (95% CI, 47.7–89.6%), P = 0.586; 85.6% (95% CI, 69.9–97.3%) *vs.* 73.3% (95% CI, 52.9–93.6%), P = 0.382]. MRD ≥1% at any checking point pre-HSCT (n = 16) significantly lowered the LFS and OS of the allo-HSCT group [46.1% (95% CI, 20.2–71.9%) *vs.* 85.5% (95% CI, 73.7–97.2%), P = 0.006; 61.4% (95% CI, 33.9–88.8%) *vs.* 88.7% (95% CI, 78.3–99.0), P = 0.045]. The 3-year LFS of patients with cGVHD (n = 29) [85.9% (95% CI, 71.0–100.7%)] was higher than that of patients without cGVHD (n = 26) [61.4% (95% CI, 41.9–80.8%)] (P = 0.045). Multivariate Cox regression modeling revealed that MRD ≥1% and not having cGVHD were independent risk factors associated with inferior LFS, and MRD ≥1% was also an independent risk factor associated with inferior OS.

## Subgroup Analysis for Patients Who Received Intensified Chemotherapy

In patients who received intensified chemotherapy (n = 14), the 3-year LFS of patients with recurrent MRD (n = 9) was lower than that of patients with persistent MRD (n = 5) [0.0% *vs.* 40.0% [95% CI, 9.0–69.0%], P = 0.350). MRD ≥1% at any checking point (n = 4) tended to lower the LFS (0.0% *vs.* 40.0% [95% CI, 9.6–70.3], P = 0.125).

# DISCUSSION

Multiple studies have demonstrated the effectiveness of CAR-T therapy in treating R/R B-ALL, with consistently high response

rates (83–94.3%) (16–19). However, the patients enrolled in previous trials were those who relapsed and were in morphological non-remission (20–22). In a retrospective study, CAR-T therapy was effective in patients with refractory ALL, of which nine had positive MRD (23). However, the survival analysis of patients with MRD was not performed, and the median follow-up time was only seven months. Thus, whether CAR-T therapy can eliminate MRD and improve outcomes in patients with MRD remains unknown. In this study, with a median follow-up of 44.0 months for all patients and 37.4 months for patients who received CAR-T therapy, we observed that MRD negativity after one month of CAR-T infusion was achieved by 90.7% of patients. This proportion was higher than that in patients who did not receive CAR-T infusion (90.7% *vs.* 70.5%, P = 0.036), proving the effectiveness of CAR-T therapy in eliminating MRD. Patients who received CAR-T therapy had a higher 3-year LFS (77.8% *vs.* 51.1%, P = 0.033) than patients who did not, and only one (2.3%) experienced a CD19-negative relapse. Patients who received CAR-T therapy also tended to be a higher 3-year LFS and OS than patients who received chemotherapy as a bridge to allo-HSCT. Eight patients were not bridged to allo-HSCT after CAR-T infusion, and six (75%) of them remained in remission with a median follow-up of 23.0 months after CAR-T infusion. This observation indicates the effectiveness of CAR-T therapy in improving long-term survival. In this study, the incidence of CRS was 53.8%, which is lower than that reported by Maude et al. (77–93%) (9), suggesting the possible correlation between CRS incidence and severity with tumor burden (24). As present, this study is the first prospective trial to prove the effectiveness of CAR-T therapy in patients with MRD.

The high MRD negativity and survival rates demonstrate that CAR-T therapy is effective in patients with low tumor loads. In patients with MRD, the LFS of patients who were bridged to allo-HSCT was similar to that of patients who were not (n = 8) (75.0% *vs.* 75.0%, P = 0.765). Six (75%) of patients who received CAR-T therapy without bridging to allo-HSCT remained in remission with a median follow-up of 23.0 months after CAR-T infusion. Thus, CAR-T therapy alone with improved CAR-T structure and risk stratification to achieve long-term survival may be feasible in patients with MRD in CR1. The role of allo-HSCT in patients receiving CAR-T therapy for R/R ALL is controversial. In a single-center phase I trial conducted by the University of Pennsylvania, only 10% of MRD-negative patients in CR underwent allo-HSCT post-CAR-T treatment (22). Similarly, in the multicenter ELIANA trial, 14% (n = 8) of the patients in CR underwent allo-HSCT (9); an updated analysis of the trial showed that the OS was nearly identical irrespective of whether patients were censored during allo-HSCT. In an analysis from Seattle Children's Hospital, the 28% of patients who underwent allo-HSCT after CAR-T therapy had a lower relapse rate than those who did not (18% *vs.* 55%) at a median follow-up of 12.2 months (25). Consistently, an NCI phase I cohort study revealed that most patients (83%) who received CAR-T therapy achieved MRD-negative CR after allo-HSCT, and all HSCT recipients were in remission at the last follow-up (18). Moreover, Hay et al. found that the intervention involving CAR-T therapy with HSCT was associated with improved LFS compared with the non-HSCT intervention (HR 0.39) (26). The American Society for Transplantation and Cellular Therapy recommended that conducting allo-HSCT after CAR-T therapy should be based on patient (physical condition and donor availability), disease (MRD status and B cell aplasia), and CAR T cell (costimulatory domain and potential persistence of CAR T cells) factors (27). Certainly, whether patients with MRD should receive allo-HSCT after CAR-T therapy remains unclear. The present study showed that allo-HSCT might not be necessary in patients with MRD after CAR-T therapy, especially in patients who achieved MRD negativity after CAR-T infusion.

## CONCLUSIONS

This prospective study showed that CAR-T therapy could effectively and safely eliminate MRD and significantly improve survival in children with persistent/recurrent MRD in CR1. In some patients, improve survival through CAR-T alone may be possible; however, further multicenter, prospective clinical trials are needed.

## DATA AVAILABILITY STATEMENT

The original contributions presented in the study are included in the article/supplementary material. Further inquiries can be directed to the corresponding authors.

## ETHICS STATEMENT

This study was approved by the Peking University People's Hospital Review Board. All patients' legal guardians provided written informed consent documents in accordance with the Declaration of Helsinki.

## AUTHOR CONTRIBUTIONS

LZ and XH designed the research and revised the paper. GH and YFC analyzed the data and wrote the paper. YZ, YJC, PS, JW, YJ, AL, YL, YW (10th author), SJ, LZ, XZ, CY, LX, XZ, KL, and YW (18th author) collected and analyzed data. All authors contributed to the article and approved the submitted version.

## FUNDING

This work was supported by the Foundation of 2018 Beijing Key Clinical Specialty Construction Project-Pediatrics (2199000726) and the Foundation of CAMS Innovation Fund for Medical Sciences (CIFMS) (grant number: 2019-I2M-5-034).

## ACKNOWLEDGMENTS

The authors thank all the doctors at the institute who participated in this study for providing the follow-up samples and information.

## REFERENCES


1. Malard F, Mohty M. Acute Lymphoblastic Leukaemia. *Lancet* (2020) 395:1146–62. doi: 10.1016/S0140-6736(19)33018-1
2. Inaba H, Mullighan CG. Pediatric Acute Lymphoblastic Leukemia. *Haematologica* (2020) 105:2524–39. doi: 10.3324/haematol.2020.247031
3. Berry DA, Zhou S, Higley H, Mukundan L, Fu S, Reaman GH, et al. Association of Minimal Residual Disease With Clinical Outcome in Pediatric and Adult Acute Lymphoblastic Leukemia: A Meta-Analysis. *JAMA Oncol* (2017) 3:e170580. doi: 10.1001/jamaoncol.2017.0580
4. Xue YJ, Wang Y, Jia YP, Zuo YX, Wu J, Lu AD, et al. The Role of Minimal Residual Disease in Specific Subtypes of Pediatric Acute Lymphoblastic Leukemia. *Int J Hematol* (2021) 113:547–55. doi: 10.1007/s12185-020-03063-w
5. Dhedin N, Huynh A, Maury S, Tabrizi R, Beldjord K, Asnafi V, et al. Role of Allogeneic Stem Cell Transplantation in Adult Patients With Ph-Negative Acute Lymphoblastic Leukemia. *Blood* (2015) 125:2486–96; quiz 2586. doi: 10.1182/blood-2014-09-599894
6. Giebel S, Labopin M, Socie G, Beelen D, Browne P, Volin L, et al. Improving Results of Allogeneic Hematopoietic Cell Transplantation for Adults With Acute Lymphoblastic Leukemia in First Complete Remission: An Analysis From the Acute Leukemia Working Party of the European Society for Blood and Marrow Transplantation. *Haematologica* (2017) 102:139–49. doi: 10.3324/haematol.2016.145631
7. Leung W, Pui CH, Coustan-Smith E, Yang J, Pei D, Gan K, et al. Detectable Minimal Residual Disease Before Hematopoietic Cell Transplantation is Prognostic But Does Not Preclude Cure for Children With Very-High-Risk Leukemia. *Blood* (2012) 120:468–72. doi: 10.1182/blood-2012-02-409813
8. Inaba H, Pui CH. Immunotherapy in Pediatric Acute Lymphoblastic Leukemia. *Cancer Metastasis Rev* (2019) 38:595–610. doi: 10.1007/s10555-019-09834-0
9. Maude SL, Laetsch TW, Buechner J, Rives S, Boyer M, Bittencourt H, et al. Tisagenlecleucel in Children and Young Adults With B-Cell Lymphoblastic Leukemia. *N Engl J Med* (2018) 378:439–48. doi: 10.1056/NEJMoa1709866
10. Chen Y, Cheng Y, Suo P, Yan C, Wang Y, Chen Y, et al. Donor-Derived CD19-Targeted T Cell Infusion Induces Minimal Residual Disease-Negative Remission in Relapsed B-Cell Acute Lymphoblastic Leukaemia With No Response to Donor Lymphocyte Infusions After Haploidentical Haematopoietic Stem Cell Transplantation. *Br J Haematol* (2017) 179:598–605. doi: 10.1111/bjh.14923
11. Huang R, Li X, He Y, Zhu W, Gao L, Liu Y, et al. Recent Advances in CAR-T Cell Engineering. *J Hematol Oncol* (2020) 13:86. doi: 10.1186/s13045-020-00910-5
12. Wang Y, Liu QF, Xu LP, Liu KY, Zhang XH, Ma X, et al. Haploidentical *vs*.Identical-Sibling Transplant for AML in Remission: A Multicenter, Prospective Study. *Blood* (2015) 125:3956–62. doi: 10.1182/blood-2015-02-627786
13. Huang XJ, Liu DH, Liu KY, Xu LP, Chen H, Han W, et al. Haploidentical Hematopoietic Stem Cell Transplantation Without *In Vitro* T-Cell Depletion for the Treatment of Hematological Malignancies. *Bone Marrow Transplant* (2006) 38:291–7. doi: 10.1038/sj.bmt.1705445
14. Xue YJ, Suo P, Huang XJ, Lu AD, Wang Y, Zuo YX, et al. Superior Survival of Unmanipulated Haploidentical Haematopoietic Stem Cell Transplantation Compared With Intensive Chemotherapy as Post-Remission Treatment for Children With Very High-Risk Philadelphia Chromosome Negative B-Cell Acute Lymphoblastic Leukaemia in First Complete Remission. *Br J Haematol* (2020) 188:757–67. doi: 10.1111/bjh.16226
15. Chang YJ, Wang Y, Xu LP, Zhang XH, Chen H, Chen YH, et al. Haploidentical Donor is Preferred Over Matched Sibling Donor for Pre-Transplantation MRD Positive ALL: A Phase 3 Genetically Randomized Study. *J Hematol Oncol* (2020) 13:27. doi: 10.1186/s13045-020-00860-y
16. Yang X, Wang GX, Zhou JF. CAR T Cell Therapy for Hematological Malignancies. *Curr Med Sci* (2019) 39:874–82. doi: 10.1007/s11596-019-2118-z
17. Grupp SA, Kalos M, Barrett D, Aplenc R, Porter DL, Rheingold SR, et al. Chimeric Antigen Receptor-Modified T Cells for Acute Lymphoid Leukemia. *N Engl J Med* (2013) 368:1509–18. doi: 10.1056/NEJMoa1215134
18. Lee DW, Kochenderfer JN, Stetler-Stevenson M, Cui YK, Delbrook C, Feldman SA, et al. T Cells Expressing CD19 Chimeric Antigen Receptors for Acute Lymphoblastic Leukaemia in Children and Young Adults: A Phase 1 Dose-Escalation Trial. *Lancet* (2015) 385:517–28. doi: 10.1016/S0140-6736(14)61403-3
19. Heng G, Jia J, Li S, Fu G, Wang M, Qin D, et al. Sustained Therapeutic Efficacy of Humanized Anti-CD19 Chimeric Antigen Receptor T Cells in Relapsed/Refractory Acute Lymphoblastic Leukemia. *Clin Cancer Res* (2020) 26:1606–15. doi: 10.1158/1078-0432.CCR-19-1339
20. Park JH, Riviere I, Gonen M, Wang X, Senechal B, Curran KJ, et al. Long-Term Follow-Up of CD19 CAR Therapy in Acute Lymphoblastic Leukemia. *N Engl J Med* (2018) 378:449–59. doi: 10.1056/NEJMoa1709919
21. Cappell KM, Sherry RM, Yang JC, Goff SL, Vanasse DA, McIntyre L, et al. Long-Term Follow-Up of Anti-CD19 Chimeric Antigen Receptor T-Cell Therapy. *J Clin Oncol* (2020) 38:3805–15. doi: 10.1200/JCO.20.01467
22. Maude SL, Frey N, Shaw PA, Aplenc R, Barrett DM, Bunin NJ, et al. Chimeric Antigen Receptor T Cells for Sustained Remissions in Leukemia. *N Engl J Med* (2014) 371:1507–17. doi: 10.1056/NEJMoa1407222
23. Pan J, Yang JF, Deng BP, Zhao XJ, Zhang X, Lin YH, et al. High Efficacy and Safety of Low-Dose CD19-Directed CAR-T Cell Therapy in 51 Refractory or Relapsed B Acute Lymphoblastic Leukemia Patients. *Leukemia* (2017) 31:2587–93. doi: 10.1038/leu.2017.145
24. Gust J, Hay KA, Hanafi LA, Li D, Myerson D, Gonzalez-Cuyar LF, et al. Endothelial Activation and Blood-Brain Barrier Disruption in Neurotoxicity After Adoptive Immunotherapy With CD19 CAR-T Cells. *Cancer Discov* (2017) 7:1404–19. doi: 10.1158/2159-8290.CD-17-0698
25. Gardner RA, Finney O, Annesley C, Brakke H, Summers C, Leger K, et al. Intent-To-Treat Leukemia Remission by CD19 CAR T Cells of Defined Formulation and Dose in Children and Young Adults. *Blood* (2017) 129:3322–31. doi: 10.1182/blood-2017-02-769208
26. Hay KA, Gauthier J, Hirayama AV, Voutsinas JM, Wu Q, Li D, et al. Factors Associated With Durable EFS in Adult B-Cell ALL Patients Achieving MRD-Negative CR After CD19 CAR T-Cell Therapy. *Blood* (2019) 133:1652–63. doi: 10.1182/blood-2018-11-883710
27. Kansagra AJ, Frey NV, Bar M, Laetsch TW, Carpenter PA, Savani BN, et al. Clinical Utilization of Chimeric Antigen Receptor T Cells in B Cell Acute Lymphoblastic Leukemia: An Expert Opinion From the European Society for Blood and Marrow Transplantation and the American Society for Blood and Marrow Transplantation. *Biol Blood Marrow Transplant* (2019) 25:e76–85. doi: 10.1016/j.bbmt.2018.12.068


**Conflict of Interest:** Authors YL and YW (10th author) were employed by Beijing Yongtai Reike Biotechnology Company Ltd.

The remaining authors declare that the research was conducted in the absence of any commercial or financial relationships that could be construed as a potential conflict of interest.

frontiers in Immunology

ORIGINAL RESEARCH
published: 28 February 2022
doi: 10.3389/fimmu.2022.781364

# A Specific CD44lo CD25lo Subpopulation of Regulatory T Cells Inhibits Anti-Leukemic Immune Response and Promotes the Progression in a Mouse Model of Chronic Lymphocytic Leukemia

*Agnieszka Goral[1], Malgorzata Firczuk[1], Klaudyna Fidyt[1], Marta Sledz[1], Francesca Simoncello[2], Karolina Siudakowska[1], Giulia Pagano[3], Etienne Moussay[3], Jérôme Paggetti[3], Patrycja Nowakowska[1], Stefania Gobessi[4], Joanna Barankiewicz[5], Aleksander Salomon-Perzynski[5], Federica Benvenuti[2], Dimitar G. Efremov[4], Przemyslaw Juszczynski[5], Ewa Lech-Maranda[5] and Angelika Muchowicz[1]**

[1] Department of Immunology, Medical University of Warsaw, Warsaw, Poland, [2] Cellular Immunology, International Centre for Genetic Engineering and Biotechnology, Trieste, Italy, [3] Tumor-Stroma Interactions, Department of Cancer Research, Luxembourg Institute of Health, Luxembourg, Luxembourg, [4] Molecular Hematology, International Centre for Genetic Engineering and Biotechnology, Trieste, Italy, [5] Department of Experimental Hematology, Institute of Hematology and Transfusion Medicine, Warsaw, Poland

OPEN ACCESS

**Edited by:**
Eyad Elkord,
University of Salford, United Kingdom

**Reviewed by:**
Daniel Gray,
Walter and Eliza Hall Institute of Medical Research, Australia
Mingfeng Zhao,
Tianjin First Central Hospital, China

***Correspondence:**
Angelika Muchowicz
angelika.muchowicz@wum.edu.pl

**Specialty section:**
This article was submitted to Cancer Immunity and Immunotherapy, a section of the journal Frontiers in Immunology

**Received:** 22 September 2021
**Accepted:** 07 February 2022
**Published:** 28 February 2022

**Citation:**
Goral A, Firczuk M, Fidyt K, Sledz M, Simoncello F, Siudakowska K, Pagano G, Moussay E, Paggetti J, Nowakowska P, Gobessi S, Barankiewicz J, Salomon-Perzynski A, Benvenuti F, Efremov DG, Juszczynski P, Lech-Maranda E and Muchowicz A (2022) A Specific CD44lo CD25lo Subpopulation of Regulatory T Cells Inhibits Anti-Leukemic Immune Response and Promotes the Progression in a Mouse Model of Chronic Lymphocytic Leukemia. Front. Immunol. 13:781364. doi: 10.3389/fimmu.2022.781364

Regulatory T cells (Tregs) are capable of inhibiting the proliferation, activation and function of T cells and play an important role in impeding the immune response to cancer. In chronic lymphocytic leukemia (CLL) a dysfunctional immune response and elevated percentage of effector-like phenotype Tregs have been described. In this study, using the Eμ-TCL1 mouse model of CLL, we evaluated the changes in the Tregs phenotype and their expansion at different stages of leukemia progression. Importantly, we show that Tregs depletion in DEREG mice triggered the expansion of new anti-leukemic cytotoxic T cell clones leading to leukemia eradication. In TCL1 leukemia-bearing mice we identified and characterized a specific Tregs subpopulation, the phenotype of which suggests its role in the formation of an immunosuppressive microenvironment, supportive for leukemia survival and proliferation. This observation was also confirmed by the gene expression profile analysis of these TCL1-specific Tregs. The obtained data on Tregs are consistent with those described so far, however, above all show that the changes in the Tregs phenotype described in CLL result from the formation of a specific, described in this study Tregs subpopulation. In addition, functional tests revealed the ability of Tregs to inhibit T cells that recognize model antigens expressed by leukemic cells. Moreover, inhibition of Tregs with a MALT1 inhibitor provided a therapeutic benefit, both as monotherapy and also when combined with an immune checkpoint inhibitor. Altogether, activation of Tregs appears to be crucial for CLL progression.

**Keywords: Tregs, CLL, Eμ-TCL1, MALT1, TCR repertoire, anti-leukemic immune response**

## INTRODUCTION

Despite the extensive research and the development of new treatment modalities, the number of chronic lymphocytic leukemia (CLL) cases with clinical resistance to therapy is constantly rising (1). The newest achievement in immunotherapy – chimeric antigen receptor T cells (CAR-T cells) – are less effective in CLL as compared to other B cell malignancies, including B cell acute lymphoblastic leukemia or diffuse large B cell lymphoma (2–4). Similarly, immune checkpoint inhibitors have a limited efficacy in relapsed/refractory CLL (3). In preclinical studies, antibodies against lymphocyte activation gene 3 (LAG-3), programmed cell death protein 1 (PD-1) or programmed death-ligand 1 (PD-L1) are only effective when administrated in the initial stage of leukemia development (5–7). Importantly, the immune system dysfunctions observed in CLL patients, suggest that CLL cells modulate the microenvironment to their own benefit (8–10). The exhausted phenotype of T cells that display high expression of PD-1, LAG-3, or T cell immunoglobulin domain and mucin domain (TIM-3) is a hallmark of CLL (11, 12). In order to improve the therapeutic strategies for CLL, it is crucial to understand the mechanisms that shape the leukemia microenvironment.

Naturally occurring, thymic, Forkhead box protein P3 $(FoxP3)^+$, $CD4^+$ regulatory T cells (Tregs), are sensitive to activation by self-antigens and tumor neoantigens, and are main players of the neoplastic microenvironment (13). Tregs can affect T cells in all stages of immune response development: priming, proliferation, and T cell effector functions (14). Increased frequency of Tregs correlates with poor prognosis of CLL patients (15). The expression patterns of Tregs-associated markers (CD25, LAG-3, killer cell lectin like receptor G1, CD69, Eomesodermin - EOMES) that determines their suppressive functions was recently presented in both CLL patients and leukemia-bearing mice (5, 16, 17). Nevertheless, the function of Tregs in CLL has not been elucidated and the approaches for Tregs elimination have shown to be insufficient. For instance, the administration of anti-CD25 antibodies or phosphoinositide 3-kinase δ (PI3Kδ) inhibitors affected not only Tregs but also abrogated the activation and function of $CD8^+$ lymphocytes (18).

In order to evaluate the role of Tregs in the development and shaping of immunosuppressive microenvironment of CLL, in this work we used Eμ-TCL1 transgenic mice model (19, 20). We characterized a novel, TCL1-derived Tregs subpopulation and assessed Tregs suppressive activity in functional tests. Furthermore, TCR sequencing allowed us to better understand the influence of leukemia on Tregs and $CD8^+$ T lymphocytes activation and clonality. Finally, we used the inhibitor of mucosa-associated lymphoid tissue lymphoma translocation protein 1 (MALT1) to block the activation of Tregs. MALT1 protease is a component of CARMA1-BCL10-MALT1 (CBM) complex which was shown to be crucial for Tregs activity (21). The results obtained in this study provide the evidence that Tregs are essential for leukemia progression in immunocompetent mice and can be efficiently targeted to block CLL progression.

## MATERIALS AND METHODS

### Reagents

MI-2 (Malt1 inhibitor, Selleckchem.com) was dissolved in DMSO (Sigma-Aldrich, St Louis, MA, USA), aliquoted and stored at -20°C. Albumin from chicken egg white (OVA, Sigma-Aldrich, St Louis, MA, USA) and Poly (I:C) (HMW) (*In vivo*Gen, San Diego, CA, USA) were aliquoted and stored at -20°C. Diphtheria Toxin (DT) from *Corynebacterium diphtheriae* (Sigma-Aldrich, St Louis, MA, USA) was aliquoted and stored at -80°C. Anti-mouse PD-L1 antibody InVivoPlus (B7-H1) (BioXcell, Lebanon, NH, USA) and InVivoPlus rat IgG2b isotype control, (BioXcell, Lebanon, NH, USA) were stored at 4°C.

### Animals Studies

All *in vivo* studies were performed in accordance with the EU Directive 2010/63/EU and the Polish legislation for animal experiments of the Polish Ministry of Science and Higher Education (February 26, 2015) and approved by the Local Ethics Committee for the Animal Experimentation in Warsaw. The *in vivo* experiments were carried out in Animal Facility of the Medical University of Warsaw.

For the study, 6-12 weeks old female or male (never mixed in one experiment) mice were used. Mouse strains include: C57BL6/J (wild-type, immunocompetent mice) (Medical University of Bialystok or Mossakowski Medical Research Centre), B6.Cg-Foxp3tm2(EGFP)Tch/J (B6 $Foxp3^{EGFP}$, Tregs express GFP) (University of Warsaw), C57BL/6-Tg(Foxp3-DTR/EGFP)23.2Spar/Mmjax (DEREG, Tregs express GFP and receptor for diphtheria toxin) (The International Centre for Genetic Engineering and Biotechnology, Trieste, Italy) B6(Cg)-Rag2tm1.1Cgn/J (RAG2-KO, immunodeficient mice) and C57BL/6-Tg(TcraTcrb)1100Mjb/J (OT-1) (Medical University of Warsaw). Splenocytes or leukemic $CD5^+CD19^+$ TCL1 cells ($5\times10^6$ – $1\times10^7$) isolated from spleens of female Eμ-TCL1 transgenic mice (The International Centre for Genetic Engineering and Biotechnology, Trieste, Italy) were adoptively transferred *via* tail vein injection. In described experiments we used cells isolated from two different Eμ-TCL1 transgenic mice, either TCL1-1159 or TCL1-1013. These cells were propagated in mice maximally twice, with the exception of genetically modified TCL1 cells expressing OVA (due to the procedure of generating modified cells, they required additional propagation in RAG2-KO mice).

### *In Vivo* Treatments

Eμ-TCL1 mice model of CLL was used in this study. To monitor leukemia development and progression, the percentage of leukemic TCL1 cells ($CD5^+CD19^+$) among white blood cells (WBC) in the peripheral blood (PB) collected from cheek vein was assessed by flow cytometry. The consistency in the assessment of leukemia was ensured and blinding practice was not applicable. Mice with detected leukemia were randomly selected and further used in the experiments. The sample size was calculated with power analysis test (22).

DEREG mice were treated with DT (50 μg/kg) administered intraperitoneally (i.p.) every four days. MI-2 was administered

i.p. daily, at dose 20 mg/kg and the control mice were injected with the DMSO as a solvent. Anti-PD-L1 antibody or the appropriate isotype control were administered i.p. every second day at a dose 200 μg/mouse. The schemes of the treatments are presented in details in the appropriate figures.

## Cell Isolation

In order to prepare a single cell suspension, spleens (SPL) or lymph nodes (LNs) were cut in small pieces and passed through a 150 μm cell strainer. To remove red blood cells the isolated splenocytes were lysed with ACK Lysing Buffer (Thermofisher Scientific, Waltham, MA, USA) according to the manufacturer's instructions. $CD19^+$, $CD4^+$ and $CD8^+$ cell subpopulations were isolated by immunomagnetic negative selection using EasySep™ Mouse B Cell Isolation Kit, EasySep™ Mouse $CD4^+$ T cell Isolation Kit and EasySep™ Mouse $CD8^+$ Cell Isolation Kit (STEMCELL Technologies, Vancouver, Canada), respectively, according to the manufacturer's protocols. The efficacy of the isolation was over 90%.

## $CD8^+$ Cells Proliferation Assay

$CD8^+$ cells isolated from spleens were incubated with CellTrace™ Violet Cell Proliferation kit (CT) (Invitrogen/Thermo Fisher Scientific, Waltham, MA, USA) for 20 min at 37°C, washed with cell culture medium and seeded onto 96-well U-bottom plates coated with anti-CD3 antibody (eBioscience, San Diego, CA, USA) together with sorted Tregs-GFP (either all $GFP^+$ or $GFP^+$ $CD69^{high}$ $CD44^{-/low}$) in various ratios (1:0.125, 1:0.25, 1:0.5, 1:1 and 1:2). For stimulation, anti-CD28 (eBioscience, San Diego, CA, USA) antibody was added to the culture medium. The proliferation of $CD8^+$ cells was evaluated upon 72h using BD FACSCanto™ II Flow Cytometer and BD FACSDiva Software (v8.0.1) (BD Biosciences, La Jolla, CA, USA).

## TCL1 OVA-Expressing Cells

The sequence encoding ovalbumin (Addgene, cat. number 25097) was inserted into mammalian expression vector pCDH-EF1-MCS-T2A-copGFP (System Biosciences). The pCDH-EF1-OVA-GFP and a packaging (psPAX2) and an envelope (pMD2.G) plasmids (gifts from prof. Didier Trono, École Polytechnique Fédérale de Lausanne, Switzerland) were introduced into HEK-293T cells using Polyethylenimine (Polysciences). Then freshly isolated TCL1 cells ($CD5^+CD19^+$) from mouse spleens were seeded into 24-well plates with M2-10B4 murine stroma cells. Next, medium containing lentiviral particles was added into TCL1 and M2-10B4 cells co-culture. Then TCL1 cells were washed and inoculated into RAG2-KO mice for leukemic cells propagation. Finally, $OVA^+$ $GFP^+$ cells were sorted and used for further experiments. In all performed experiments at least 60% of injected leukemic cells exerted $OVA^+$ $GFP^+$ phenotype as evaluated by flow cytometry.

## *In Vivo* Functional Assays

Two weeks following TCL1 cells adoptive transfer, leukemia-bearing DEREG transgenic mice were treated with DT and on the following day, injected with CT-positive $CD8^+$ T cells isolated from spleens and lymph nodes of OT-1 mice. 4-5 hours later, the mice were i.v. inoculated with OVA protein (50 μg). The proliferation of $CD8^+$ OT-1 cells isolated from spleens was assessed upon 3 days using flow cytometry. In the second approach, DEREG mice were injected with genetically modified TCL1 leukemic cells expressing OVA-GFP (TCL1-OVA). Three days later, the mice were treated with DT and on the following day, injected with CT-positive $CD8^+$ OT-1 T cells. The proliferation of $CD8^+$ OT-1 cells was evaluated following 3 or 4 days using flow cytometry. The schemes of described experiments are presented in detail on appropriate figures.

## Flow Cytometry

The isolated cells were stained with Zombie NIR™ Fixable Viability kit or Zombie Violet™ Fixable Viability Kit (BioLegend, San Diego, CA, USA) for 20 min at room temperature (RT) and washed with PBS. Next, the cells were incubated with Purified Rat Anti-Mouse CD16/CD32 (Mouse BD Fc Block™; clone 2.4G2, BD Biosciences, La Jolla, CA, USA) for 15 min at RT and stained for surface markers with proper fluorochrome-conjugated antibodies (all antibodies used in this study are listed in **Supplementary Table 1**) for 20-30 min at RT. After final washing with PBS, the cells were analysed using BD FACS Canto™ II Flow Cytometer and BD FACS Diva Software (v8.0.1)(BD Biosciences, La Jolla, CA, USA). For further analyses, including t-SNE (with markers: CD44, CD25, LAG-3, CD69), FlowJo Software (v. 10.6.1) (FlowJo LLC, Ashland, OR, USA) was used.

## Cell Sorting

In order to sort Tregs ($CD4^+$, $GFP^+$) from spleens of B6 $Foxp3^{EGFP}$ or DEREG mice, $CD4^+$ cell subpopulation was enriched prior to sorting. To this end, isolated splenocytes were subjected to immunomagnetic positive selection for $CD19^+$ using EasySep™ Mouse CD19 Positive Selection Kit II (STEMCELL Technologies) and then the negative fraction was subsequently subjected to negative selection using EasySep™ Mouse $CD4^+$ T cell Isolation Kit (STEMCELL Technologies). When needed, $CD4^+$ cells were additionally stained with anti-CD69-PE and anti-CD44-PE-Cy7 monoclonal antibodies as described above. To sort $CD8^+$ cells, the fraction of splenocytes devoid of $CD19^+$ cells was stained with anti-CD8a-PerCP-Cy5.5 monoclonal antibody. Then the cells were sorted using BD FACS Aria™ III Cell Sorter (BD Biosciences).

## DNA Isolation and Analysis of TCRβ Repertoire

Tregs A ($GFP^+$, $CD69^{high}$, $CD44^{-/low}$, gated as presented in **Figure 5** CD69/CD44 right panel) and $CD8^+$ cells were sorted as described above. Then the genomic DNA was isolated from the sorted cells using DNA Micro Kit (QIAGEN, Hilden, Germany) according to the manufacturer's instructions. The concentration and purity of extracted DNA was assessed using NanoDrop 2000 Spectrophotometer (Thermo Fisher Scientific). Immunosequencing of the CDR3 regions of TCRβ chains was performed with immunoSEQ® Assay and analysed by immunoSEQ® Analyzer (Adaptive Biotechnologies, Seatlle, WA, USA).

## RNA Sequencing

When percentage of leukemic cells in mouse blood reached at least 20% of all PBMC, the GFP$^+$ Tregs: A (GFP$^+$, CD69$^{high}$, CD44$^{-/low}$) and B (GFP$^+$ excluding fraction A) were sorted from TCL1 leukemia-injected DEREG mice. Additionally, GFP$^+$ Tregs were also sorted from control DEREG mice. The mRNA was isolated from $4.5 \times 10^5$ cells with the RNeasy Micro Kit (Qiagen, Hilden, Germany). Libraries were prepared with the QuantSeq 3' mRNA-Seq Library Prep Kit FWD for Illumina (Lexogen), according to manufacturer's instructions, with the addition of UMI. Barcoded samples were pooled, diluted, loaded onto a NextSeq 500/550 Mid Output flowcell (130M reads, Illumina) and single-end 150bp sequencing was performed on a NextSeq 550 (Illumina).

After initial QCs using FastQC (https://www.bioinformatics.babraham.ac.uk/projects/fastqc/) and FastQ Screen (https://www.bioinformatics.babraham.ac.uk/projects/fastq_screen/), fastq files were processed using a local Snakemake workflow including the following main steps. First, raw reads were trimmed from their UMI index, poly A and adapter sequences using a combination of dedicated scripts and cutadapt (v2.10). Next, filtered reads were submitted for mapping (STAR v2.5.3a) on the Mouse Reference genome (GRCm38). Collapsing of reads originating from the same fragment was achieved with umi_tools (v 1.0.0) and counting was performed with featureCounts (subread v2.0.0).

Counts were filtered and transformed with edgeR (cpm > 5 and presence in at least 3 samples). For data visualization, heatmaps, sample distance matrix, and volcano plots were drawn with EdgeR, heatmap, and EnhancedVolcano R packages. For differential expression of genes across samples (DEGs), FDR < 0.05 and log2 fold change cut-off of 1 were imposed. For clustering, DEGs were selected as important for immune functions in Tregs. Gene expression values were z-scored and subjected to correlation-based clustering with complete linkage. Raw and processed data were deposited at the NCBI GEO database (GSE179121). The following secure token has been created to allow review of record GSE179121 while it remains in private status: qlchuysazpinjed. To better understand the nature of Tregs A and Tregs B, we re-analyzed the public dataset GSE72494 describing the transcriptome of naive, activated, and effector Treg (23) and performed a Gene Set Enrichment Analysis (GSEA, Hallmark and curated gene sets) with the stand-alone software (GSEA v4.2.1, Broad Institute, Boston, MA). Normalized enrichment scores (NES) and p-values < 0.05 were taken into consideration.

## Statistical Analysis

GraphPad Prism 6 Software (GraphPad Software Inc., San Diego, CA, USA) was used for data analysis. The statistical significance was calculated by Mann-Whitney U test. The mice survival rate was analyzed by log-rank survival test. For gene expression data (RNA sequencing), one-way ANOVA with multiple comparisons was calculated for single genes and histograms were drawn with GraphPad Prism 9 Software.

Additional experimental procedures are described in details in the **Supplementary Material**.

# RESULTS

## Depletion of Tregs in Mice With Adoptively Transferred TCL1 Leukemia Results in the Expansion of Functional CD8$^+$ Cells and Leukemia Clearance

To evaluate the significance of Tregs for CLL progression we used DEREG transgenic mice with depletion of FoxP3$^+$ CD4$^+$ Tregs by treatment with diphtheria toxin (DT) (**Figure 1** and **Supplementary Figure 1A, B**). DEREG mice were treated with DT one day prior to adoptive transfer of malignant (CD5$^+$CD19$^+$) B cells, isolated from an Eμ-TCL1 transgenic mouse. Effective depletion of Tregs was observed in spleens and peripheral blood of DEREG mice and was maintained by additional DT injections every four days (**Figure 1A** and **Supplementary Figure 1A**). As monitored in peripheral blood twice a week, injection of DT did not affect the progression of leukemia during the first fifteen days of experiments. However, starting from day 18$^{th}$ after TCL1 leukemia inoculation, we detected a significant decrease in the percentage of leukemic cells (CD5$^+$CD19$^+$), in the peripheral blood, of DT-treated mice as compared to untreated TCL1 leukemia-bearing animals (**Figure 1B**, left panel). In line with these results, we observed a significant reduction of previously established leukemia in the spleens of Tregs-depleted mice (**Figure 1B**, right panel). The same observations were made when DEREG mice were injected with TCL1 leukemia isolated from another transgenic mouse (**Supplementary Figure 1B**). The decrease in the percentage of leukemic cells in spleens of DT-treated mice was accompanied by the extensive increase of the percentage in both CD4$^+$ and CD8$^+$ T lymphocytes (**Figure 1C**). These observations prompted us to investigate the putative changes in the phenotype of splenic CD4$^+$ and CD8$^+$ T cells mediated by Tregs-depletion. We observed the enrichment of effector (EFF; CD44$^+$CD62L$^-$) and central memory (CM; CD44$^+$CD62L$^+$) cells in both CD4$^+$ and CD8$^+$ T cell subpopulations in mice deprived of Tregs (**Figures 1D, E**). A significant increase in the percentage of effector (CD4$^+$ and CD8$^+$) and central memory (CD8$^+$) T cells was also observed in lymph nodes (axillary, brachial, inguinal) of DT-treated mice (**Figure 1F**). Depletion of Tregs resulted in the elevation of CD69 on both, CD4$^+$ and CD8$^+$ T cells in the lymph nodes, and reduced the percentage of naïve cells, suggesting the activation of a systemic immune response. Nevertheless, the depletion of Tregs, performed at an advanced stage of the disease (first dose of DT was administered when 30% of malignant B cells were detected among all white blood cells in peripheral blood) did not affect the progression of leukemia (**Supplementary Figure 1C**). Tregs depletion at an advanced stage of leukemia progression increased the percentage of effector and IFN-γ-positive CD4$^+$ and CD8$^+$ T lymphocytes, significantly elevated IFN-γ concentration and reduced the concentration of IL-10 in the sera (**Supplementary Figure 1D, E**). Importantly, three weeks of DT injections of control (without leukemia) DEREG mice lead to a minor activation of T cells, mostly CD4$^+$ T cell subpopulation (**Supplementary Figure 1F**, upper panel). However, no changes were observed in the level of CD69 in lymphatic T cells upon

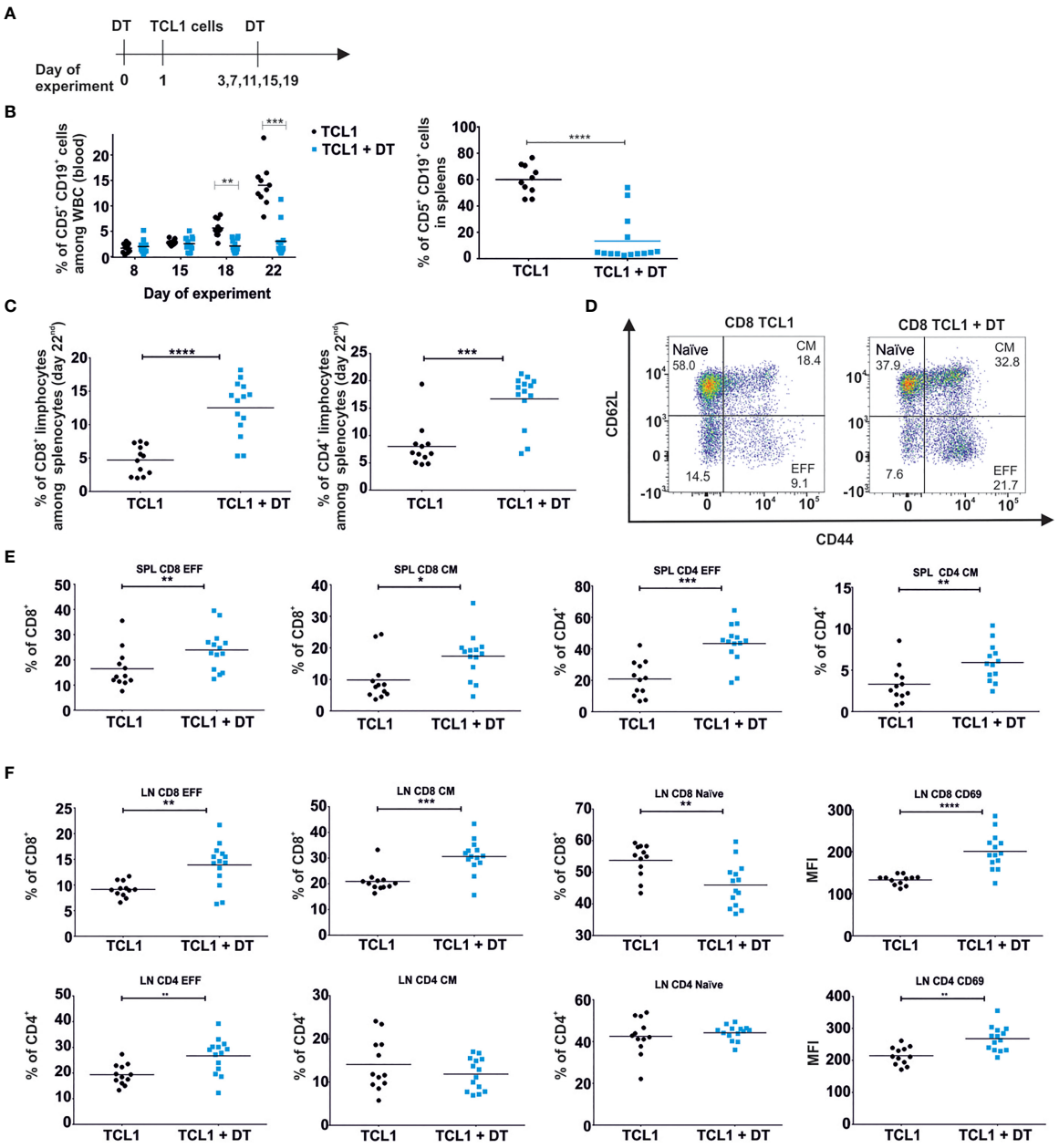


**FIGURE 1** | Depletion of Tregs diminishes the progression of leukemia in DEREG mice and affects the relative frequency of conventional T cell subpopulations. **(A)** The graph presenting a scheme of the experiment. Tregs were depleted with DT and on the next day mice were injected with TCL1 CD19$^+$ leukemic cells. The depletion of Tregs (DT administration) was repeated every 4 days. **(B)** The percentage of leukemic cells (CD5$^+$CD19$^+$) among all white blood cells (WBC) assessed by flow cytometry in blood (at indicated time points of the experiment, left) and spleens (day 22$^{nd}$ of experiment, right) of untreated (TCL1) and DT-treated (TCL1+DT) TCL1 leukemia-bearing mice. The graphs represent mean results from two independent experiments. Each dot represents an individual sample (mouse), n = 10-12, Mann-Whitney U test *p ≤ 0.05. **(C)** The Percentage of CD8$^+$ (left) and CD4$^+$ (right) T cells in spleens of untreated and DT-treated TCL1 leukemia-bearing mice. The graphs present mean results from two independent experiments. Each dot represents an individual sample (mouse), n = 12-14, Mann-Whitney U test ***p ≤ 0.001, ****p < 0.0001. **(D–F)** The percentage of CD4$^+$ and CD8$^+$ T cells with phenotype of naïve, effector (EFF) and central memory (CM) subpopulations according to the expression of CD44 and CD62L surface markers. Representative dot plots with a gating strategy **(D)** and the graphs present the results from spleens (SPL) **(E)** and lymph nodes (LN) **(F)** of untreated and DT-treated TCL1 leukemia-bearing mice. In **(F)** the graphs presenting the expression of CD69 surface marker on CD4$^+$ and CD8$^+$ T cells in LN are also shown. The data from two independent experiments are showing mean values. Each dot represents an individual sample (mouse), n = 12-14, Mann-Whitney U test *p ≤ 0.05, **p ≤ 0.01, ***p ≤ 0.001, ****p < 0.0001.

DT-treatment (**Supplementary Figure 1F**, lower panel). The activation of $CD4^+$ T cells may be the result of anti-DT immune response as it was described before (24).

To understand more deeply the anti-leukemia immune response induced by Tregs depletion, we investigated the impact of $CD8^+$ T lymphocytes derived from the mice after DT injections on leukemia progression. We limited these experiments to the subset of $CD8^+$ T cells as it was shown that these cells play a superior role in anti-leukemia immune response over $CD4^+$ T lymphocytes (25). Importantly, an effective Tregs depletion in DEREG mice is transient. At day 22 after TCL1 injection we observed that the Tregs population was restored in murine blood despite continuous injections of DT (**Supplementary Figure 1A**, right panel), as was also reported by others (26). Thus, to examine the impact of the $CD8^+$ lymphocytes on leukemia progression and mice survival, the cells were isolated from spleens of untreated or DT-treated TCL1 leukemia-bearing mice (the same scheme of experiment as shown in **Figure 1A**), and adoptively transferred into TCL1-injected RAG2-KO mice (**Figure 2A**). Next, the expansion of TCL1 leukemic cells was monitored in murine blood twice a week. Interestingly, $CD8^+$ T lymphocytes, isolated from Tregs-depleted mice effectively prevented leukemia progression, and in some mice even lead to complete elimination of TCL1 cells (**Figures 2B, C**). In contrast, the $CD8^+$ T lymphocytes adoptively transferred from mice with intact Tregs population did not significantly affect the progression of the disease in RAG2-KO mice. Consequently, in TCL1-injected RAG2-KO mice, the adoptive transfer of $CD8^+$ T cells isolated from DEREG mice after Tregs depletion, translated into prolonged survival and complete leukemia eradication in three out of nine mice. (**Figure 2D**).

The results obtained from the experiments described above revealed that the lack of Tregs in the leukemia microenvironment triggers the expansion of anti-leukemic $CD8^+$ T cells. To address the differences in the investigated T cells, the $CD8^+$ T cells from spleens of TCL1-injected DEREG mice treated with DT or untreated were sorted for DNA isolation and the T cell receptor beta chain (TCRβ) third complementarity-determining regions (CDR3) sequences analysis. An increase of $CD8^+$ T cell clonality was observed in three out of five TCL1 leukemia-bearing mice with Tregs depletion, but overall, the observed differences were not statistically significant between the two examined groups (**Figure 2E**). Strikingly though, we observed distinct amino acid sequences of TCRβ CDR3 regions in the tested $CD8^+$ T cells, suggesting different specificity of the T cells among untreated and DT-treated mice (**Figure 2F**). Indeed, only one sequence is shared in the top fifteen rearrangements between both analyzed $CD8^+$ T cell populations (**Figure 2F**). Altogether, these data indicate that the elimination of Tregs from the TCL1 leukemia microenvironment resulted in the expansion of a distinct set of cytotoxic $CD8^+$ T effector cells, capable of clearing leukemia in DEREG and RAG2-KO mice.

## CLL Leads to the Formation of a Specific Population of Tregs

We analyzed the phenotype and function of Tregs in TCL1-injected B6 $FoxP3^{EGFP}$ transgenic mice that express *EGFP* and *FOXP3* under the control of endogenous promoter. Based on the results of phenotyping with a set of markers (FoxP3, LAG-3, CD69, CD44, CD25), we performed t-distributed stochastic neighbor embedding (tSNE) analysis, which allowed us to distinguish a specific Tregs subpopulation that exerts the phenotype characteristic only for Tregs isolated from TCL1 leukemia-bearing mice (Tregs A) (**Figure 3A**). This particular Tregs A subpopulation can be defined by high level of CD69, LAG-3 and low of CD44 and CD25 on their surface.

In order to investigate whether the observed changes in Tregs phenotype are mediated by the interactions with malignant B cells, we co-cultured the control Tregs-$GFP^+$ (sorted from spleens of control B6 $Foxp3^{EGFP}$ mice) with leukemic (TCL1) or normal (CD19) B cells. After three days, significantly higher level of LAG-3 was observed on Tregs-$GFP^+$ co-cultured with TCL1 cells, but not with the control $CD19^+$ cells (**Supplementary Figure 2A**). The elevated expression of LAG-3 was achieved only when Tregs-GFP+ and TCL1 leukemia cells were cultured in direct contact. On contrary, the level of CD44 in Tregs-$GFP^+$ co-cultured with TCL1 leukemia cells (but not normal $CD19^+$ cells) was reduced regardless the separation of the cells by transwells (**Supplementary Figure 2B**).

Next, the clonality of Tregs A subpopulation was examined, based on the TCRβ CDR3 region sequences. Importantly, the TCL1-associated Tregs A subpopulation sorted from spleens of TCL1-leukemia bearing DEREG mice exhibits increased clonality and elevated frequency of particular clones, compared to whole Treg-$GFP^+$ subpopulation sorted from the control animals (CTR Tregs) (**Figures 3B, C**).

Finally, in order to characterize the TCL1-associated Tregs at the transcriptomic level, we performed RNA sequencing on two subpopulations of Tregs sorted from the spleens of TCL1-injected DEREG mice: Tregs A (specific to Eμ-TCL1 model, sorted as $GFP^+$ $CD44^{-/lo}$ and $CD69^{hi}$) and Tregs B (the remaining $GFP^+$ Tregs, which did not meet the criteria of subpopulation A). The transcriptome of both TCL1-associated subpopulations was compared with Tregs-$GFP^+$ population sorted from spleens of control mice. Interestingly, the analysis of differentially expressed genes (DEGs), showed that Tregs A subpopulation was markedly different from both Tregs B as well as control Tregs populations (**Supplementary Figure 3, 4**). This data suggests that the specific Tregs A cells signature might be selectively induced within the conditions of leukemia progression. In Tregs A, we observed increased expression of genes responsible for immunosuppressive activity (*Gzmb, Prf1, Gzmk, Il10*), checkpoints (*Havcr 2, Lag-3, Tigit*), chemokines that may support leukemia progression and its microenvironment (*Ccl3, Csf1, Ccl5*), as well as genes that have been recently reported as unique for CLL-Tregs (*EOMES*) (**Figure 3D**). Importantly, the gene expression profile was in line with the phenotype observed in flow cytometry, apart from CD69, which seemed to be regulated post-transcriptionally (**Figure 3E**). Additionally, the elevated level of *Ikzf2* encoding Helios transcription factor suggests enhanced suppressive capacity of Tregs A subpopulation (27).

Next, we compared the gene expression profiles of Tregs A and B with a public dataset [GSE72494 (23)] describing the transcription profiles of naive, activated, and effector Tregs. We used a gene signature reported in that study (23), and built heat maps to

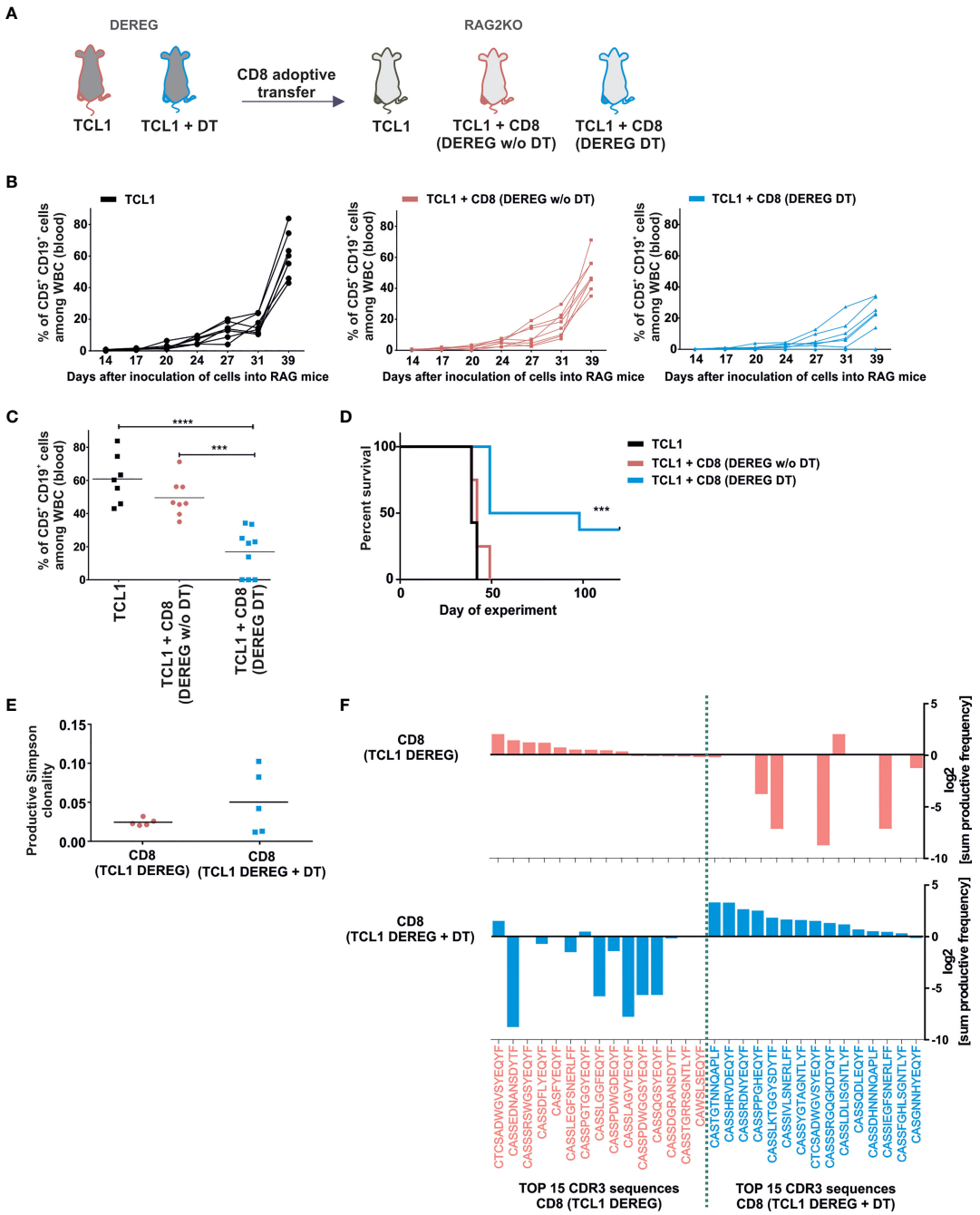


**FIGURE 2** | Depletion of Tregs in TCL1 leukemia-bearing DEREG mice results in the expansion of CD8+ lymphocytes capable of eradicating leukemic cells. **(A)** The graph presenting a scheme of the experiment. DEREG mice were treated according to scheme from Fig1A. Then 5 x $10^6$ of splenic $CD8^+$ T cells isolated with magnetic beads from untreated (DEREG w/o DT) or DT-treated (DEREG DT) leukemic DEREG mice were injected to RAG2-KO mice following the injection of TCL1 ($CD5^+CD19^+$) cells. **(B, C)** The percentage of leukemic cells ($CD5^+CD19^+$) assessed at indicated time points in the peripheral blood of RAG2-KO mice: TCL1 leukemia-injected mice (black lines), TCL1- and $CD8^+$-injected mice ($CD8^+$ isolated from TCL1 leukemia bearing-DEREG w/o DT, pink lines), and TCL1- and $CD8^+$-injected mice ($CD8^+$ isolated from leukemia-bearing DEREG treated with DT, blue lines). Each line represents an individual sample (mouse), **(B)** and on day 39$^{th}$ **(C)**, each dot represents an individual sample (mouse). The graphs represent mean results from two independent experiments, n = 7-9, Mann-Whitney U test ***$p \leq 0.001$, ****$p < 0.0001$. **(D)** The survival plot summarizing the results from two independent experiments, n = 7-9, log-rank survival test ***$p \leq 0.001$. **(E)** The productive Simpson clonality of $CD8^+$ lymphocytes sorted from untreated or DT-treated mice analyzed in immunoSEQ Analyzer (from Adaptive Biotechnologies), n = 5. **(F)** The top 15 amino acid sequences of CDR3 TCRβ with the highest sum frequency (total amount of clones with a given sequence in all tested mice), of $CD8^+$ lymphocytes sorted from untreated (pink) or DT-treated TCL1 leukemia-bearing DEREG mice (blue). The Graphs present log2 transformation of % sum frequency of a given sequence in untreated (pink, upper graph) and DT- treated TCL1- injected DEREG mice (blue, lower graph), n = 5.

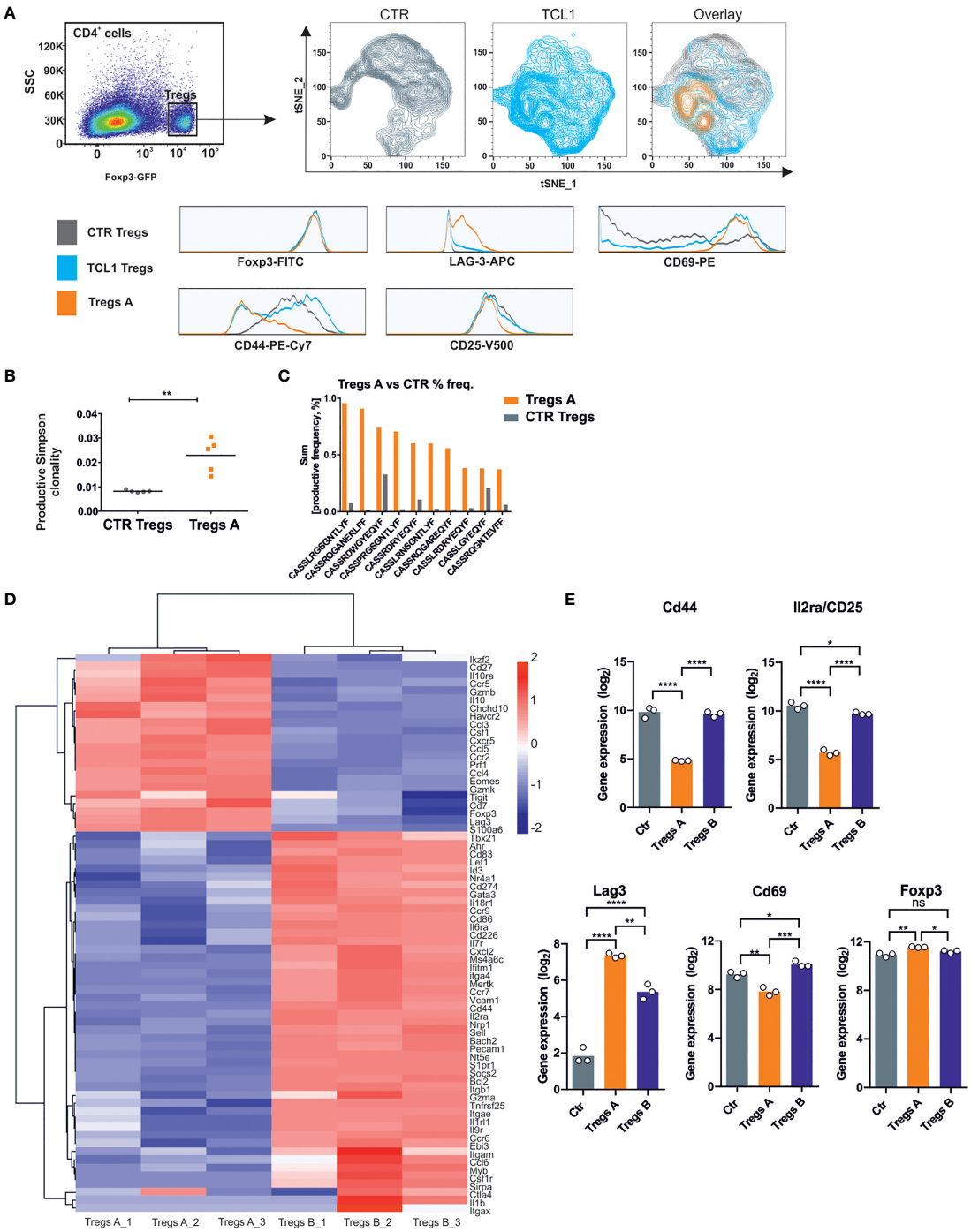


**FIGURE 3** | A specific Tregs population is formed during the progression of TCL1 leukemia. **(A)** tSNE analysis of Tregs phenotype isolated from control (grey) and TCL1 leukemia-bearing (blue) B6 Foxp3$^{EGFP}$ mice 14 days after injections with leukemic cells. The overlay of counterplots presents the Tregs subpopulation, specific for TCL1 leukemia-bearing mice (Tregs A, orange). The Tregs GFP$^{+}$-were plot on the graphs according to the expression of CD44, CD69, CD25, and LAG-3 that are presented on the histograms. The counter plots show representative analysis of Tregs from 2 control and 4 TCL1 leukemia-injected mice. **(B)** The productive Simpson clonality of Tregs sorted from control (all Tregs, CTR Tregs) and TCL1 leukemia-bearing (the specific TCL1-associated Tregs subpopulation, Tregs A) DEREG mice, n = 5. **(C)** The productive sum frequency of top 10 amino acid sequences of CDR3 TCRβ of Tregs A which were present in all of tested TCL1 leukemia-bearing DEREG mice, n = 5. **(D)** Clustering of selected DEGs between Tregs A and Tregs B (RNA sequencing with FDR < 0.05 and $\log_2$FC > 1) by correlation with complete linkage, n = 3. **(E)** Gene expression (log2, RNA sequencing) of genes from panel A in Tregs from CTR and TCL1 leukemia-bearing mice, n = 3. One-way ANOVA * p≤ 0.05, ** p< 0.01, *** p< 0.001.

compare Tregs subsets. The gene expression profiles indicated that our Ctrl Tregs population resembles naive Tregs and that Treg A and Tregs B exert similar expression patterns to effector Tregs and activated Tregs, respectively (**Supplementary Figure 4C**). Similar gene sets were identified as enriched in Tregs A (vs Treg B) and Effector Tregs (vs Activated Treg) (**Supplementary Tables 2** and **3**). Although Tregs A exhibited comparable transcription changes as compared to Effector Tregs (up-regulation of *Il10* and *Havcr2/Tim3* and down-regulation of *Sell* and *Ccr7*), we identified important differences suggesting a particular gene modulation in this specific Tregs population found in CLL (e.g. *Eomes, Prf1, Itgae, Cxcl10*) (**Supplementary Figure 4D**).

## The TCL1-Induced Tregs Are Functionally Active

Next, we determined the ability of splenic Tregs population, sorted from control and TCL1 leukemia-bearing B6 FoxP3$^{EGFP}$ mice to inhibit CD8$^+$ T cell proliferation in an antigen unspecific test, where T cells were activated *via* anti-CD3 and anti-CD28 antibodies. The obtained results indicated that whole Tregs population isolated from spleens of TCL1 leukemia-bearing mice is prone to inhibit CD8$^+$ T cells proliferation similarly to control Tregs (**Figure 4A**). Similarly, in a test with OVA peptide presented by the bone marrow-derived dendritic cells, Tregs isolated from leukemic mice inhibited CD8$^+$ OT1 cells proliferation as effectively as Tregs from control mice (**Supplementary Figure 5**). This data suggest that the effectiveness of antigen-independent suppression of Tregs from TCL leukemia-baring mice is similar to control Tregs.

In order to explore whether TCL1-associated Tregs suppress CD8$^+$ T cells in an antigen specific manner, we generated OVA-expressing TCL1 by means of lentiviral transduction. DEREG mice were inoculated with TCL1-OVA cells, and 3 days later, Tregs were depleted with DT in one group. On the following day, mice were injected with Cell Trace (CT)-positive OT1 CD8$^+$ T cells and the proliferation of these cells in the spleen was subsequently analyzed (**Figures 4B–D**). Interestingly, although the T cells were effectively activated in all tested TCL1 leukemia-bearing mice, in the group treated with DT, the proliferation was more efficient, suggesting that the Tregs population impeded OT1 CD8$^+$ T cells proliferation to some extent. Moreover, a significant drop in the percentage of leukemic cells in blood and spleens of DT-treated mice was observed after injection of OT1 CD8$^+$ T lymphocytes (**Figure 4B**). Conversely, when mice were inoculated with TCL1 cells (without OVA expression) and subsequently injected with OVA protein, no impact of Tregs depletion was observed on OT1 CD8$^+$ T cells proliferation (**Figure 4C**). Altogether, these results suggest that Tregs inhibit proliferation of leukemia-specific CD8$^+$ T cells in an antigen-dependent manner.

## Treatment With MALT1 Inhibitor Disturbs the Formation of Tregs A Subpopulation in TCL1 Leukemia-Bearing Mice and Enhances the Effect of Immunotherapy

The analysis of Tregs phenotype at the various stages of leukemia revealed significant changes in the expression levels of Tregs surface proteins. The shift of Tregs into Tregs A phenotype escalated during leukemia progression and was accompanied by an increase in the percentage of splenic Tregs in leukemic mice (**Figure 5A**). Importantly, the Tregs A subpopulation was clearly formed at an advanced stage of the disease (when more than 40% of leukemic cells among all white blood cells were present in the spleens).

MI-2 has been described as a para-caspase MALT1 inhibitor that can selectively prevent the conversion of naïve Tregs into effector cells by decreasing the NFκB activity (21). MI-2 revealed its cytotoxic effect on primary CLL cells *in vitro* (28). Moreover, RNA sequencing analysis indicated elevated expression of NFκB-related genes in Tregs of TCL1-injected mice (**Supplementary Figure 4B**). In order to verify the influence of MI-2 on development of Tregs subpopulations, the inhibitor was administered intraperitoneally to the control and TCL1 leukemia-bearing B6 FoxP3$^{EGFP}$ mice for two weeks starting from day 5 following TCL1 leukemic cells inoculation (**Figure 5B**). Administration of MI-2 impeded the change of Tregs into Tregs A phenotype and elevated the percentage of naïve Tregs (CD62L$^+$ CD44$^-$) (**Figure 5C**). MI-2 inhibited the progression of leukemia and increased significantly the percentage of central memory and effector CD4$^+$ and CD8$^+$ T lymphocytes (**Figures 5C–E**). Importantly, the effectiveness of MI-2 treatment was impaired in TCL1 leukemia-bearing RAG2-KO mice as compared to immunocompetent, wild type mice, suggesting a key role of T cells in the mechanism of action of this drug (**Supplementary Figures 6A, B**).

Since the PD1/PD-L1 axis was already shown to contribute to T cells dysregulations in both human and mouse models of CLL, we used MI-2 therapy as a pretreatment for checkpoint blockade with anti-PD-L1 antibody in immunocompetent TCL1-leukemia bearing mice (6, 29). Considering that long-term inhibition of Tregs functions can lead to autoimmune pathology (30), MI-2 inhibitor was used only before anti-PD-L1 therapy (**Figure 6A**). The anti-PD-L1 therapy did not affect the percentage of T cells already elevated by MI-2 (**Figure 6B**). However, the combined treatment decreased the percentage of naive cells and increased the percentage of effector cells of both CD4$^+$ and CD8$^+$ T lymphocytes (**Figure 6B**) Anti-PD-L1 antibodies administered 16 days post TCL1 inoculation decreased the percentage of leukemic cells in blood and spleen when applied after treatment with MI-2 (**Figure 6C**). These results indicate that the combination of Tregs inhibition with anti-PD-L1 antibody can bring beneficial treatment outcome in leukemia.

# DISCUSSION

The anti-tumor strategy reducing the number of Tregs has been reported since 1999 (31). Nevertheless, targeting Tregs can yield differential responses in cancer models (32). In this study, we revealed that in the CLL mouse model, the depletion of Tregs population can lead to the expansion of CD8$^+$ T cells with the ability to completely eradicate leukemia.

Published studies have consistently demonstrated elevated levels of Tregs in the peripheral blood collected from CLL

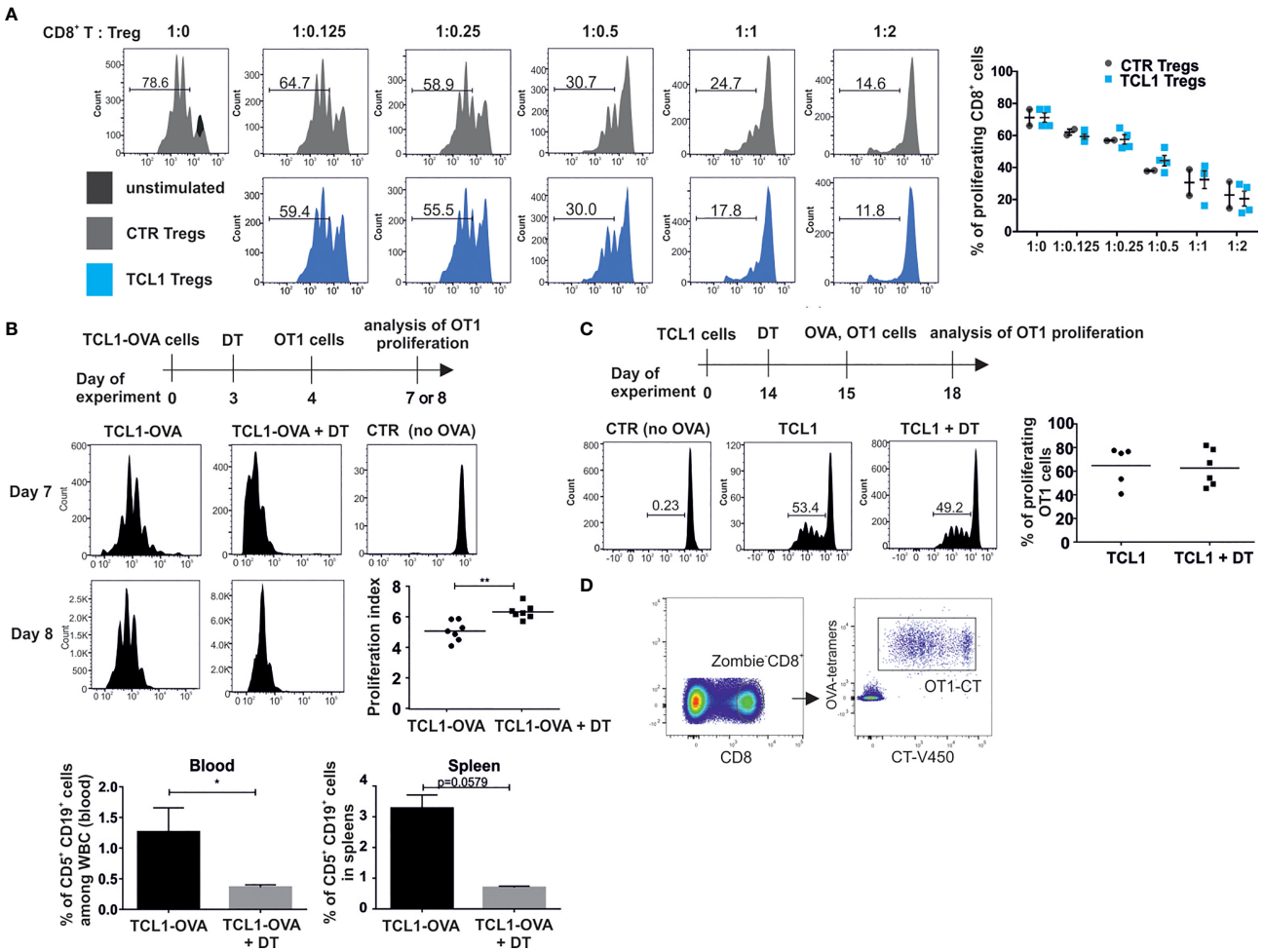


**FIGURE 4** | Tregs from TCL1 leukemia-bearing mice are capable of inhibiting T cells proliferation. **(A)** All Tregs-GFP$^+$ sorted from spleens of control (CTR Tregs) and TCL1-injected (TCL1 Tregs) B6-Foxp3$^{EGFP}$ mice, were added to the Cell Trace Violet (CT) stained CD8$^+$ lymphocytes isolated from control mice and activated with αCD3 and αCD28 antibodies. The proliferation of – CT-stained CD8$^+$ T cells was assessed by flow cytometry. Graphs show the results from two independent experiments, mean ± SD, n = 2-4 **(B)** OT1 CD8$^+$ cell proliferation in mice injected with TCL1-OVA cells. After TCL1-OVA cells inoculation the mice were treated with DT and injected with CT-positive OT1 CD8$^+$ lymphocytes (scheme of the experiment, upper panel). The proliferation of OT1 CD8$^+$ cells from untreated or DT-treated mice was evaluated on the same day (7$^{th}$ or 8$^{th}$). The representative histograms of proliferation measured on days 7$^{th}$ and 8$^{th}$ are shown (left panel) and the proliferation index, from two independent experiments, is shown on the graph (middle right panel), n = 7 **p ≤ 0.01. Proliferation index was calculated by FlowJo software as the total number of divisions divided by the number of cells that went into division. The percentage of leukemic cells was assessed in blood and spleens of DEREG mice on day 8th of the experiment (lower panel), data is presented as mean ± SD, n = 3-4, Mann-Whitney U test * p ≤ 0.05. **(C)** OT1 CD8$^+$ cell proliferation in mice injected with TCL1 cells and vaccinated with OVA protein. The representative histograms (left panel) and graph summarizing the results from two independent experiments (right panel), n = 5-6. **(D)** Gating strategy incorporated for analysis of CT-positive OT1 CD8$^+$ T cells proliferation in functional *in vivo* tests.

patients compared to healthy subjects (33). The phenotype of analyzed Tregs was described as effector-like in both CLL patients and the Eμ-TCL1 mouse model of CLL (5, 16, 18). Our results indicate that the phenotype of Tregs changes during the course of leukemia to establish a subpopulation of CD4$^+$, FoxP3$^+$, LAG-3$^+$, CD69$^{hi}$, and surprisingly, CD44$^{lo}$ and CD25$^{lo}$ cells. A low expression of CD25 in Tregs has been already reported by another group (34), yet the CD44$^{lo}$ phenotype is rather a characteristic feature of naïve lymphocytes. Our *ex vivo* experiments revealed that the level of cell-surface glycoprotein CD44 decreased in Tregs as a result of leukemia progression. At the transcriptomic level, however, the reduced amount of mRNA for CD44 was seen only in Tregs A, a specific TCL1-associated Tregs subpopulation distinguished for the first time in this study. Interestingly, the Tregs A subpopulation is positive for already reported markers of CLL-related Tregs, including IL-10, LAG-3, granzyme B, EOMES, as well as share a unique gene expression signature of chemokines that may support leukemia progression and formation of leukemic microenvironment (35, 36). Moreover, the overexpression of mRNA encoding HELIOS, TIGIT, TIM-3 and CD27 suggests that TCL1-related Tregs may possess immunosuppressive activity (27, 37–39).

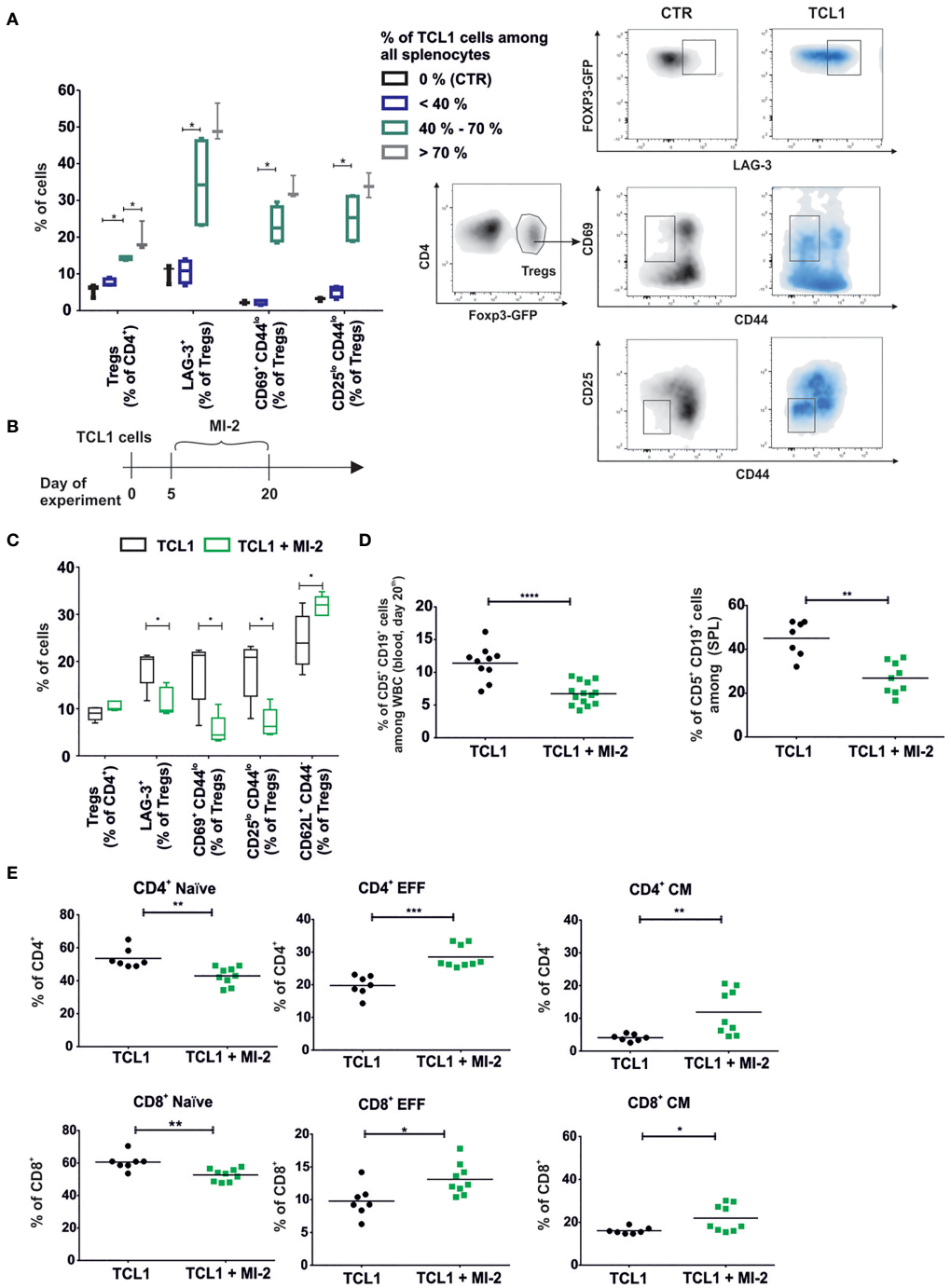


**FIGURE 5** | Development of a specific TCL1-related Tregs (Tregs A) population is correlated with the stage of the disease and can be blocked by MALT-1 inhibitor. **(A)** The box plot min-max graph (left panel) and density plots with gating strategy (right panel) present phenotype of Tregs in relation to the percentage of leukemic cells ($CD5^+CD19^+$) in the spleens. Mean ± SD, n=11, Mann-Whitney U test *p ≤ 0.05. **(B)** The graph presenting a scheme of the experiment. MI-2 was administered daily at dose 20 mg/kg *via* intraperitoneal injections for two weeks. **(C)** The phenotype of Tregs collected from spleens of TCL1 leukemia-bearing B6 $Foxp3^{EGFP}$ mice, untreated (TCL1) or treated with MI-2(TCL1 + MI-2). Mean ± SD, Mann-Whitney U test n = 5, *p ≤ 0.05. **(D)** Percentage of leukemic cells ($CD5^+CD19^+$) assessed by flow cytometry in blood (left graph) and spleens (right graph) on day $21^{st}$ of the experiment. The graph presents data from three (blood, n = 10-14) or two (spleens, n = 7-8) independent experiments. Each dot represents an individual sample (mouse), means, Mann-Whitney U test **p ≤ 0.01, ***p ≤ 0.001, **** p < 0.0001. **(E)** The percent of naïve, effector (EFF), central memory (CM), subpopulations of $CD4^+$ and $CD8^+$ T cells. Cells were collected from spleens of untreated and MI-2-treated TCL1 leukemia-bearing B6 $Foxp3^{EGFP}$ mice in two independent experiments, n = 7-12. Each dot represents an individual sample (mouse), means, Mann-Whitney U test *p ≤ 0.05, **p ≤ 0.01, ***p ≤ 0.001.

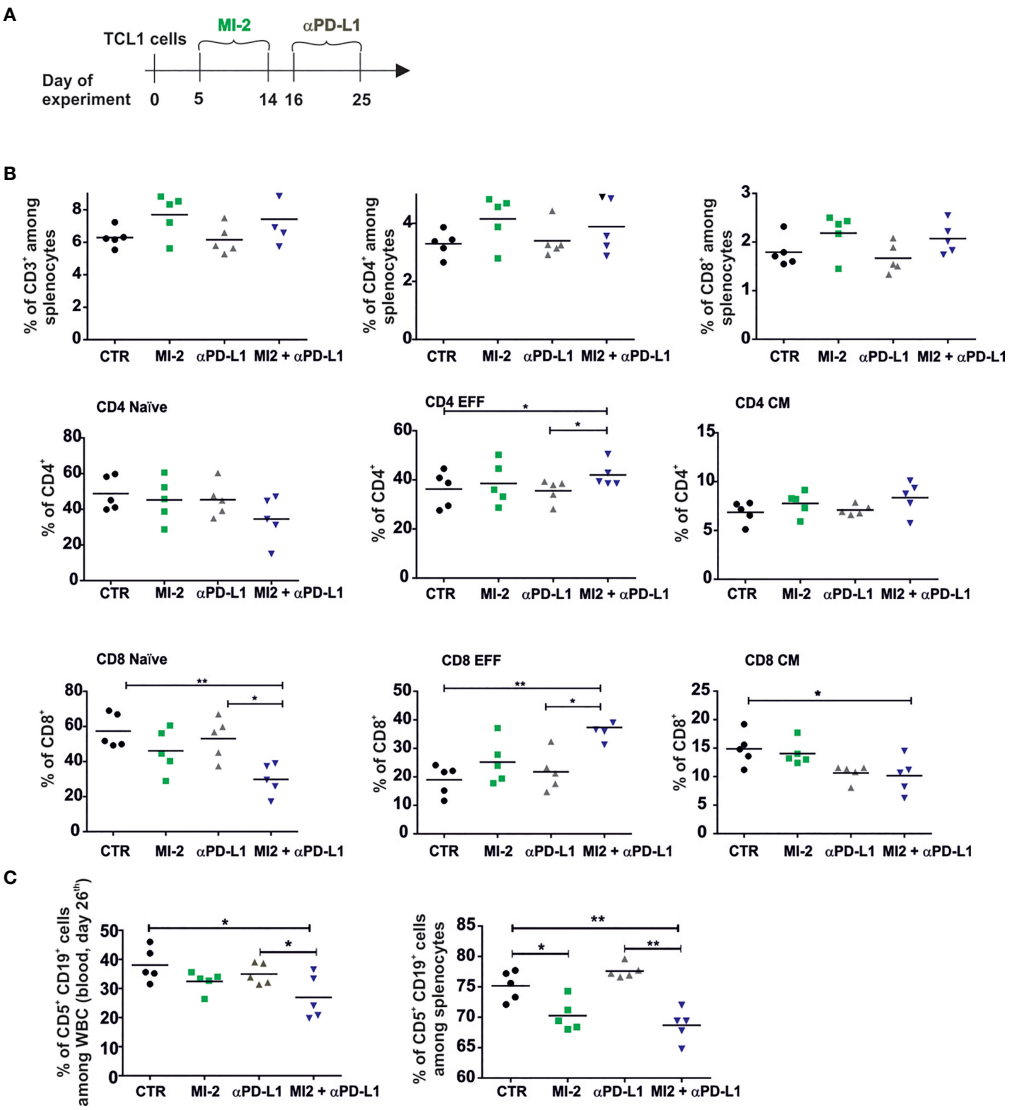


**FIGURE 6** | The pretreatment with MALT-1 inhibitor sensitizes leukemia to the therapy with anti-PD-L1 at the advanced stage of the disease. **(A)** The graphs presenting a scheme of the experiment. **(B)** The percentage of $CD3^+$, $CD4^+$, $CD8^+$ and naïve, effector (EFF), and central memory (CM) subpopulations of $CD4^+$ and $CD8^+$. Cells were collected from spleens of untreated (CTR), MI-2 and/or aPD-L1-treated TCL1 leukemia-bearing mice, n = 4-5, each dot represents an individual sample (mouse), means, Mann-Whitney U test *p ≤ 0.05, **p ≤ 0.01. **(C)** The Percentage of leukemic cells ($CD5^+CD19^+$) assessed by flow cytometry in blood (left panel) and spleens (right panel) at day 26th of the experiment, n = 5, each dot represents an individual sample (mouse), means, Mann-Whitney U test *p ≤ 0.05, **p ≤ 0.01.

Importantly, our results prove that the observed change in the Tregs phenotype occurring during the progression of CLL results from the formation of a specific Tregs subpopulation (Tregs A).

Mpakou and colleagues show that Tregs isolated from CLL patients have an ability to inhibit $CD8^+$ T cell proliferation (34). Likewise, according to our results, TCL1-derived Tregs are able to inhibit proliferation of T cells *ex vivo*. In *ex vivo* assays, T cells were activated in unspecific and specific manner, accordingly with the cognate antigen or by OVA peptide presented by dendritic cells thus the observed effect was not related to leukemia-specific antigens. The CLL-related Tregs functionality was finally confirmed in the *in vivo* experiment with TCL1-OVA cells, indicating that Tregs inhibit the proliferation of $CD8^+$ cells upon recognition of tumor-expressed antigen.

The variable CDR3 regions of TCR interact with the peptide presented by MHC. The analysis of CDR3 sequence provides information about the diversity and clonality of investigated T cell populations and has become a valuable research tool in immunology (40). Thus, the higher oligoclonal composition of TCL1-derived Tregs compared to Tregs sorted from control mice, suggests that only selected clones of Tregs have undergone the expansion in TCL1 leukemia-bearing mice.

The expansion of exhausted T cells is a hallmark of human CLL and is also recapitulated in the Eμ-TCL1 mouse model (11).

The $CD8^+$ lymphocytes, which are present in spleens of TCL1 leukemia-bearing mice, have been described as antigen-experienced, oligoclonal cells that expand during the progression of the disease (12). In our experiments, upon depletion of Tregs, the $CD8^+$ T cells became more oligoclonal and were effective in the elimination of leukemic cells. Surprisingly, anti-leukemic $CD8^+$ T cells expressed different CDR3 sequences compared to the CDR3 sequences of lymphocytes from non-DT-treated, leukemia-bearing mice. It has been reported that in some tumors, based on the TCR sequences functional T cells formed a distinct group from dysfunctional, transitional tumor - infiltrating lymphocytes (41). Our results suggest that the depletion of Tregs in leukemia-bearing mice triggers the expansion of functional $CD8^+$ T cell clones through the presentation of different epitopes than those used for splenic, exhausted $CD8^+$ T cells. Elimination of Tregs primed the activation of T cells not only in spleens but also in the lymph nodes. The expansion of $CD8^+$ T lymphocytes capable of killing leukemic cells occurred due to Tregs depletion, thus revealing their role in the maintenance of tumor antigen tolerance in CLL. The limitation of these studies is the fact that the antigens that led to the activation of anti-leukemic T lymphocytes were not identified yet. However, we suspect that these antigens could be associated with mutations typical for CLL. Importantly, we cannot rule out the possibility that these antigens are of other origins, for example derived due to genetic differences between mouse strains. Nevertheless, the depletion of Tregs seems to be a trigger for the expansion of effector T lymphocytes.

As it was also shown for other malignances, the inhibition of Tregs activation must occur early in the course of the disease to bring the beneficial outcome (42, 43). It has also been shown that the efficacy of adoptive T cell therapy is dependent on the tumor burden and is high in the early stages of tumor development or after chemotherapy (44, 45). To address this observation we conducted treatment with the MALT1 inhibitor, MI-2, when the leukemic cells were already detectable in blood but at a low level. MI-2 disrupted Tregs activation, prevented the formation of the specific TCL1-derived Tregs A subpopulation and inhibited the progression of leukemia in immunocompetent mice. Since the MI-2 was shown to exert a cytotoxic effect on leukemic cells (28), it is difficult to conclude from our experiments, whether it affects Tregs directly or only delays their activation due to the inhibition of leukemia progression. Though, the relatively small anti-leukemia efficacy of MI-2 obtained in RAG2-KO mice model may bring to the conclusion that T cells are important component in anti-leukemic MI-2 mechanism of action. Moreover, the decrease in the frequency of activated Tregs provided the therapeutic window to reduce the percentage of leukemic cells in mouse blood even two weeks after inoculation of leukemic cells.

Our results underline the role of Tregs in the progression of CLL and more importantly suggest that reactivation of the existing, exhausted T cell populations with anti-PD-L1 therapy, might be insufficient to block the disease progression. Notably, the presented results indicate that one approach to obtain an effective anti-leukemia immune response is to reorganize the CLL microenvironment, in order to create an opportunity for the expansion of a population of cytotoxic $CD8^+$ T cells.

## DATA AVAILABILITY STATEMENT

The datasets presented in this study can be found in online repositories. The names of the repository/repositories and accession number(s) can be found below: https://www.ncbi.nlm.nih.gov/, GSE179121.

## ETHICS STATEMENT

The animal study was reviewed and approved by The Local Ethics Committee for the Animal Experimentation in Warsaw, Warsaw University of Life Sciences, Warsaw, Poland.

## AUTHOR CONTRIBUTIONS

Conceptualization, AM, AG, and MF. Investigation, AG, KF, MS, KS, PN, FS, GP, JP, and EM. Resources, JB, AS-P, SG, EL-M, and DE. Writing and visualization AM, AG, KF, JP, and EM. Critical revision, SG, FB, DE, PJ, MF, JP, and EM. Supervision, project administration AM. All authors contributed to the article and approved the submitted version.

## FUNDING

This work was supported by: the Polish National Science Centre grants 2018/29/B/NZ6/01962 (AM) and 2016/21/B/NZ7/02041 (MF) and the Ministry of Science and Higher Education within "Regional Initiative of Excellence" program in the years 2019-2022 - 013/RID/2018/19, the FNRS "Télévie" 7.6518.20 (GP), and the Fonds National de la Recherche Luxembourg TIME-CLL: C20/BM/14582635 (EM).

## ACKNOWLEDGMENTS

We wish to thank Ewa Kozlowska from University of Warsaw for providing Treg-Foxp3EGFP mice, Serena Zacchigna and Simone Vodret from ICGEB, Trieste for their support with DEREG mice experiments and sharing the DEREG colony, and Nathalie Nicot, Elise Mommaerts, Arnaud Muller (LUXGEN Platform, LIH) for RNA sequencing.

## SUPPLEMENTARY MATERIAL

The Supplementary Material for this article can be found online at: https://www.frontiersin.org/articles/10.3389/fimmu.2022.781364/full#supplementary-material

## REFERENCES


1. Sedlarikova L, Petrackova A, Papajik T, Turcsanyi P, Kriegova E. Resistance-Associated Mutations in Chronic Lymphocytic Leukemia Patients Treated With Novel Agents. *Front Oncol* (2020) 10:894. doi: 10.3389/fonc.2020.00894
2. Lemal R, Tournilhac O. State-Of-the-Art for CAR T-Cell Therapy for Chronic Lymphocytic Leukemia in 2019. *J Immunother Cancer* (2019) 7 (1):202. doi: 10.1186/s40425-019-0686-x
3. Cox MJ, Lucien F, Sakemura R, Boysen JC, Kim Y, Horvei P, et al. Leukemic Extracellular Vesicles Induce Chimeric Antigen Receptor T Cell Dysfunction in Chronic Lymphocytic Leukemia. *Mol Ther J Am Soc Gene Ther* (2020) 29 (4):1529–40. doi: 10.1016/j.bbmt.2019.12.137
4. June CH, Sadelain M. Chimeric Antigen Receptor Therapy. *N Engl J Med* (2018) 379(1):64–73. doi: 10.1056/NEJMra1706169
5. Wierz M, Pierson S, Guyonnet L, Viry E, Lequeux A, Oudin A, et al. Dual PD1/LAG3 Immune Checkpoint Blockade Limits Tumor Development in a Murine Model of Chronic Lymphocytic Leukemia. *Blood* (2018) 131 (14):1617–21. doi: 10.1182/blood-2017-06-792267
6. McClanahan F, Hanna B, Miller S, Clear AJ, Lichter P, Gribben JG, et al. PD-L1 Checkpoint Blockade Prevents Immune Dysfunction and Leukemia Development in a Mouse Model of Chronic Lymphocytic Leukemia. *Blood* (2015) 126(2):203–11. doi: 10.1182/blood-2015-01-622936
7. Wierz M, Janji B, Berchem G, Moussay E, Paggetti J. High-Dimensional Mass Cytometry Analysis Revealed Microenvironment Complexity in Chronic Lymphocytic Leukemia. *Oncoimmunology* (2018) 7(8):e1465167. doi: 10.1080/2162402X.2018.1465167
8. Archibald WJ, Meacham PJ, Williams AM, Baran AM, Victor AI, Barr PM, et al. Management of Melanoma in Patients With Chronic Lymphocytic Leukemia. *Leukemia Res* (2018) 71:43–6. doi: 10.1016/j.leukres.2018.07.003
9. Falchi L, Vitale C, Keating MJ, Lerner S, Wang X, Elhor Gbito KY, et al. Incidence and Prognostic Impact of Other Cancers in a Population of Long-Term Survivors of Chronic Lymphocytic Leukemia. *Ann Oncol* (2016) 27 (6):1100–6. doi: 10.1093/annonc/mdw072
10. Teh BW, Tam CS, Handunnetti S, Worth LJ, Slavin MA. Infections in Patients With Chronic Lymphocytic Leukaemia: Mitigating Risk in the Era of Targeted Therapies. *Blood Rev* (2018) 32(6):499–507. doi: 10.1016/j.blre.2018.04.007
11. Palma M, Gentilcore G, Heimersson K, Mozaffari F, Nasman-Glaser B, Young E, et al. T Cells in Chronic Lymphocytic Leukemia Display Dysregulated Expression of Immune Checkpoints and Activation Markers. *Haematologica* (2017) 102(3):562–72. doi: 10.3324/haematol.2016.151100
12. Llao Cid L, Hanna BS, Iskar M, Roessner PM, Ozturk S, Lichter P, et al. CD8 (+) T-Cells of CLL-Bearing Mice Acquire a Transcriptional Program of T-Cell Activation and Exhaustion. *Leuk Lymphoma* (2020) 61(2):351–6. doi: 10.1080/10428194.2019.1660972
13. Han S, Toker A, Liu ZQ, Ohashi PS. Turning the Tide Against Regulatory T Cells. *Front Oncol* (2019) 9:279. doi: 10.3389/fonc.2019.00279
14. Gajewski TF, Meng Y, Blank C, Brown I, Kacha A, Kline J, et al. Immune Resistance Orchestrated by the Tumor Microenvironment. *Immunol Rev* (2006) 213:131–45. doi: 10.1111/j.1600-065X.2006.00442.x
15. D'Arena G, Vitale C, Coscia M, Festa A, Di Minno NMD, De Feo V, et al. Regulatory T Cells and Their Prognostic Relevance in Hematologic Malignancies. *J Immunol Res* (2017) 2017:1832968. doi: 10.1155/2017/1832968
16. De Matteis S, Molinari C, Abbati G, Rossi T, Napolitano R, Ghetti M, et al. Immunosuppressive Treg Cells Acquire the Phenotype of Effector-T Cells in Chronic Lymphocytic Leukemia Patients. *J Transl Med* (2018) 16(1):172. doi: 10.1186/s12967-018-1545-0
17. Roessner PM, Llao Cid L, Lupar E, Roider T, Bordas M, Schifflers C, et al. EOMES and IL-10 Regulate Antitumor Activity of T Regulatory Type 1 CD4 (+) T Cells in Chronic Lymphocytic Leukemia. *Leukemia* (2021) 35:2311–24. doi: 10.1101/2020.03.09.983098
18. Hanna BS, Roessner PM, Scheffold A, Jebaraj BMC, Demerdash Y, Ozturk S, et al. PI3Kdelta Inhibition Modulates Regulatory and Effector T-Cell Differentiation and Function in Chronic Lymphocytic Leukemia. *Leukemia* (2019) 33(6):1427–38. doi: 10.1038/s41375-018-0318-3
19. Bichi R, Shinton SA, Martin ES, Koval A, Calin GA, Cesari R, et al. Human Chronic Lymphocytic Leukemia Modeled in Mouse by Targeted TCL1 Expression. *Proc Natl Acad Sci USA* (2002) 99(10):6955–60. doi: 10.1073/pnas.102181599
20. Johnson AJ, Lucas DM, Muthusamy N, Smith LL, Edwards RB, De Lay MD, et al. Characterization of the TCL-1 Transgenic Mouse as a Preclinical Drug Development Tool for Human Chronic Lymphocytic Leukemia. *Blood* (2006) 108(4):1334–8. doi: 10.1182/blood-2005-12-011213
21. Rosenbaum M, Gewies A, Pechloff K, Heuser C, Engleitner T, Gehring T, et al. Bcl10-Controlled Malt1 Paracaspase Activity Is Key for the Immune Suppressive Function of Regulatory T Cells. *Nat Commun* (2019) 10 (1):2352. doi: 10.1038/s41467-019-10203-2
22. Charan J, Kantharia ND. How to Calculate Sample Size in Animal Studies? *J Pharmacol Pharmacother* (2013) 4(4):303–6. doi: 10.4103/0976-500X.119726
23. Dias S, D'Amico A, Cretney E, Liao Y, Tellier J, Bruggeman C, et al. Effector Regulatory T Cell Differentiation and Immune Homeostasis Depend on the Transcription Factor Myb. *Immunity* (2017) 46(1):78–91. doi: 10.1016/j.immuni.2016.12.017
24. Wang J, Siffert M, Spiliotis M, Gottstein B. Repeated Long-Term DT Application in the DEREG Mouse Induces a Neutralizing Anti-DT Antibody Response. *J Immunol Res* (2016) 2016:1450398. doi: 10.1155/2016/1450398
25. Hanna BS, Roessner PM, Yazdanparast H, Colomer D, Campo E, Kugler S, et al. Control of Chronic Lymphocytic Leukemia Development by Clonally-Expanded CD8(+) T-Cells That Undergo Functional Exhaustion in Secondary Lymphoid Tissues. *Leukemia* (2019) 33(3):625–37. doi: 10.1038/s41375-018-0250-6
26. Lahl K, Sparwasser T. *In Vivo* Depletion of FoxP3+ Tregs Using the DEREG Mouse Model. *Methods Mol Biol* (2011) 707:157–72. doi: 10.1007/978-1-61737-979-6_10
27. Thornton AM, Lu J, Korty PE, Kim YC, Martens C, Sun PD, et al. Helios(+) and Helios(-) Treg Subpopulations Are Phenotypically and Functionally Distinct and Express Dissimilar TCR Repertoires. *Eur J Immunol* (2019) 49 (3):398–412. doi: 10.1002/eji.201847935
28. Saba NS, Wong DH, Tanios G, Iyer JR, Lobelle-Rich P, Dadashian EL, et al. MALT1 Inhibition Is Efficacious in Both Naive and Ibrutinib-Resistant Chronic Lymphocytic Leukemia. *Cancer Res* (2017) 77(24):7038–48. doi: 10.1158/0008-5472.CAN-17-2485
29. Brusa D, Serra S, Coscia M, Rossi D, D'Arena G, Laurenti L, et al. The PD-1/PD-L1 Axis Contributes to T-Cell Dysfunction in Chronic Lymphocytic Leukemia. *Haematologica* (2013) 98(6):953–63. doi: 10.3324/haematol.2012.077537
30. Martin K, Junker U, Tritto E, Sutter E, Rubic-Schneider T, Morgan H, et al. Pharmacological Inhibition of MALT1 Protease Leads to a Progressive IPEX-Like Pathology. *Front Immunol* (2020) 11:745. doi: 10.3389/fimmu.2020.00745
31. Onizuka S, Tawara I, Shimizu J, Sakaguchi S, Fujita T, Nakayama E. Tumor Rejection by *In Vivo* Administration of Anti-CD25 (Interleukin-2 Receptor Alpha) Monoclonal Antibody. *Cancer Res* (1999) 59(13):3128–33.
32. Hu G, Li Z, Wang S. Tumor-Infiltrating FoxP3(+) Tregs Predict Favorable Outcome in Colorectal Cancer Patients: A Meta-Analysis. *Oncotarget* (2017) 8 (43):75361–71. doi: 10.18632/oncotarget.17722
33. D'Arena G, Simeon V, D'Auria F, Statuto T, Sanzo PD, Martino LD, et al. Regulatory T-Cells in Chronic Lymphocytic Leukemia: Actor or Innocent Bystander? *Am J Blood Res* (2013) 3(1):52–7.
34. Mpakou VE, Ioannidou HD, Konsta E, Vikentiou M, Spathis A, Kontsioti F, et al. Quantitative and Qualitative Analysis of Regulatory T Cells in B Cell Chronic Lymphocytic Leukemia. *Leukemia Res* (2017) 60:74–81. doi: 10.1016/j.leukres.2017.07.004
35. Sivina M, Hartmann E, Kipps TJ, Rassenti L, Krupnik D, Lerner S, et al. CCL3 (MIP-1alpha) Plasma Levels and the Risk for Disease Progression in Chronic Lymphocytic Leukemia. *Blood* (2011) 117(5):1662–9. doi: 10.1182/blood-2010-09-307249
36. Patterson SJ, Pesenacker AM, Wang AY, Gillies J, Mojibian M, Morishita K, et al. T Regulatory Cell Chemokine Production Mediates Pathogenic T Cell Attraction and Suppression. *J Clin Invest* (2016) 126(3):1039–51. doi: 10.1172/JCI83987
37. Arroyo Hornero R, Georgiadis C, Hua P, Trzupek D, He LZ, Qasim W, et al. CD70 Expression Determines the Therapeutic Efficacy of Expanded Human Regulatory T Cells. *Commun Biol* (2020) 3(1):375. doi: 10.1038/s42003-020-1097-8
38. Gautron AS, Dominguez-Villar M, de Marcken M, Hafler DA. Enhanced Suppressor Function of TIM-3+ FoxP3+ Regulatory T Cells. *Eur J Immunol* (2014) 44(9):2703–11. doi: 10.1002/eji.201344392

39. Joller N, Lozano E, Burkett PR, Patel B, Xiao S, Zhu C, et al. Treg Cells Expressing the Coinhibitory Molecule TIGIT Selectively Inhibit Proinflammatory Th1 and Th17 Cell Responses. *Immunity* (2014) 40 (4):569–81. doi: 10.1016/j.immuni.2014.02.012
40. De Simone M, Rossetti G, Pagani M. Single Cell T Cell Receptor Sequencing: Techniques and Future Challenges. *Front Immunol* (2018) 9:1638. doi: 10.3389/fimmu.2018.01638
41. Li H, van der Leun AM, Yofe I, Lubling Y, Gelbard-Solodkin D, van Akkooi ACJ, et al. Dysfunctional CD8 T Cells Form a Proliferative, Dynamically Regulated Compartment Within Human Melanoma. *Cell* (2019) 176(4):775–89.e18. doi: 10.1016/j.cell.2018.11.043
42. Teng MW, Ngiow SF, von Scheidt B, McLaughlin N, Sparwasser T, Smyth MJ. Conditional Regulatory T-Cell Depletion Releases Adaptive Immunity Preventing Carcinogenesis and Suppressing Established Tumor Growth. *Cancer Res* (2010) 70(20):7800–9. doi: 10.1158/0008-5472.CAN-10-1681
43. Fisher SA, Aston WJ, Chee J, Khong A, Cleaver AL, Solin JN, et al. Transient Treg Depletion Enhances Therapeutic Anti-Cancer Vaccination. *Immun Inflammation Dis* (2017) 5(1):16–28. doi: 10.1002/iid3.136
44. Prato S, Zhan Y, Mintern JD, Villadangos JA. Rapid Deletion and Inactivation of CTLs Upon Recognition of a Number of Target Cells Over a Critical Threshold. *J Immunol* (2013) 191(7):3534–44. doi: 10.4049/jimmunol.1300803
45. Segal G, Prato S, Zehn D, Mintern JD, Villadangos JA. Target Density, Not Affinity or Avidity of Antigen Recognition, Determines Adoptive T Cell Therapy Outcomes in a Mouse Lymphoma Model. *J Immunol* (2016) 196 (9):3935–42. doi: 10.4049/jimmunol.1502187

**Conflict of Interest:** The authors declare that the research was conducted in the absence of any commercial or financial relationships that could be construed as a potential conflict of interest.

**Publisher's Note:** All claims expressed in this article are solely those of the authors and do not necessarily represent those of their affiliated organizations, or those of the publisher, the editors and the reviewers. Any product that may be evaluated in this article, or claim that may be made by its manufacturer, is not guaranteed or endorsed by the publisher.

frontiers in Immunology

ORIGINAL RESEARCH
published: 18 March 2022
doi: 10.3389/fimmu.2022.832263

# Indoleamine 2, 3-Dioxygenase 1 Mediates Survival Signals in Chronic Lymphocytic Leukemia *via* Kynurenine/Aryl Hydrocarbon Receptor-Mediated MCL1 Modulation

*Claudio Giacinto Atene[1], Stefania Fiorcari[1], Nicolò Mesini[1], Silvia Alboni[2,3], Silvia Martinelli[1,4], Monica Maccaferri[4], Giovanna Leonardi[4], Leonardo Potenza[1,4], Mario Luppi[1,4], Rossana Maffei[4†] and Roberto Marasca[1,4*†]*

[1] Hematology Section, Department of Medical and Surgical Sciences, University of Modena and Reggio Emilia, Modena, Italy, [2] Center for Neuroscience and Neurotechnology, University of Modena and Reggio Emilia, Modena, Italy, [3] Department of Life Sciences, University of Modena and Reggio Emilia, Modena, Italy, [4] Hematology Section, Policlinico, Department of Oncology and Hematology, Azienda Ospedaliero-Universitaria (A.O.U.) of Modena, Modena, Italy

The indoleamine 2,3-dioxygenase 1 (IDO1) metabolic circuitry, comprising the first tryptophan (Trp) catabolite L-kynurenine (Kyn) and the aryl hydrocarbon receptor (AHR), has emerged as a mechanism of cancer immune evasion. Here, we investigated the functional role of the IDO1/Kyn/AHR axis in chronic lymphocytic leukemia (CLL). Our data show that CLL cells expressed an active form of the IDO1 enzyme and microenvironmental stimuli can positively modulate its expression. Interferon (IFN)-γ induces IDO1 expression through the Jak/STAT1 pathway and mediates Kyn production concomitantly with Trp consumption in CLL-conditioned media, while INCB018424 (ruxolitinib), a JAK1/2 inhibitor, impaired both effects. To characterize the involvement of IDO1 in leukemic cell maintenance, we overexpressed IDO1 by vector transfection measuring enhanced resistance to spontaneous apoptosis. IDO1 pro-survival influence was confirmed by treating CLL cells with Kyn, which mediated the increase of induced myeloid leukemia cell differentiation protein (MCL1). Conversely, AHR silencing or its blockade *via* CH-223191 improved the apoptosis of leukemic clones and mitigated MCL1 expression. Moreover, Kyn-treated CLL cells are less affected by the pro-apoptotic effect of ABT-199 (venetoclax), while CH-223191 showed synergistic/additive cytotoxicity with this drug. Lastly, targeting directly MCL1 in CLL cells with AMG-176, we abrogate the pro-survival effect of Kyn. In conclusion, our data identify IDO1/Kyn/AHR signaling as a new therapeutic target for CLL, describing for the first time its role in CLL pathobiology.

**Keywords: chronic lymphocytic leukemia (CLL), tumor microenvironment, indoleamine 2, 3-dioxygenase 1, target therapy, aryl hydrocarbon receptor (AHR)**

OPEN ACCESS

***Edited by:***
*Antonio Macchiarulo, University of Perugia, Italy*

***Reviewed by:***
*Han Yu, Roswell Park Comprehensive Cancer Center, United States*
*Ciriana Orabona, University of Perugia, Italy*
*Nagaja Capitani, University of Siena, Italy*

****Correspondence:***
*Roberto Marasca*
*roberto.marasca@unimore.it*

*†These authors share last authorship*

***Specialty section:***
*This article was submitted to Cancer Immunity and Immunotherapy, a section of the journal Frontiers in Immunology*

***Received:*** *09 December 2021*
***Accepted:*** *21 February 2022*
***Published:*** *18 March 2022*

***Citation:***
*Atene CG, Fiorcari S, Mesini N, Alboni S, Martinelli S, Maccaferri M, Leonardi G, Potenza L, Luppi M, Maffei R and Marasca R (2022) Indoleamine 2, 3-Dioxygenase 1 Mediates Survival Signals in Chronic Lymphocytic Leukemia via Kynurenine/Aryl Hydrocarbon Receptor-Mediated MCL1 Modulation. Front. Immunol. 13:832263. doi: 10.3389/fimmu.2022.832263*

## INTRODUCTION

Chronic lymphocytic leukemia (CLL) is the most common leukemia in the western world, usually affecting the elderly (1). CLL is a dynamic disease in which proliferation of the antigen-experienced B cell clone in pseudofollicular centers of lymphoid tissues is combined with a reduced cell turnover of quiescent B cells that accumulate in peripheral blood (2). The survival of leukemic cells is closely linked to the presence of a specific tumor microenvironment (TME). Malignant cells are able to manipulate surrounding supportive cells by forcing them to create a niche in which they can receive survival stimuli, escape immunosurveillance, and protect themselves from the action of drugs (3). Moreover, CLL cells play an active role in establishing progressive immunosuppression, demonstrated by the presence of an expanded population of regulatory and exhausted T cells, myeloid-derived suppressor cells (MDSCs), and macrophages with the M2 phenotype, called nurse-like cells (NLCs). Several treatments available for CLL exert a long-term control of the disease in the majority of CLL patients, as novel tyrosine kinase inhibitors and the B-cell lymphoma 2 (BCL2) inhibitor ABT-199 (venetoclax) (4), but CLL still remains largely incurable due to frequent relapses and the emergence of drug resistance or intolerance (5).

Indoleamine 2,3-dioxygenase 1 (IDO1) is the rate-limiting and first enzyme of the kynurenine pathway that converts the essential amino acid L-tryptophan (Trp) to produce bioactive metabolites in mammalian extrahepatic tissues (6). Since its discovery, IDO1 was described as an immunomodulatory molecule, able to promote immune tolerance in mammalian pregnancy (7), chronic infection, autoimmunity, and allergic inflammation (8). Inflammatory mediators, in particular interferon (IFN)-γ (9), induce and sustain IDO1 production in a variety of cells as a feedback mechanism to control inflammation and dampen overactivation of cytotoxic T responses (10). The first Trp catabolite, L-kynurenine (Kyn), is a key signaling molecule that directly affects antigen-specific T-cell proliferation (11, 12) and induces T-cell death indirectly through the aryl hydrocarbon receptor (AHR), also known as the dioxin receptor (13, 14). IDO1 is overexpressed in a wide variety of human hematologic malignancies and solid tumors as a part of concerted mechanisms of evading immunosurveillance (15–17). In addition, many cells belonging to the TME—fibroblasts, macrophages, MDSCs, and dendritic cells, including endothelial cells—are coerced by cancer cells to express IDO1, collectively supporting the immune escape (12). Besides, IDO1 expression is correlated with a poor prognosis, shorter overall survival, and chemoresistance in different cancers (18–24), corroborating the concept that a treatment strategy of IDO1 blockade may have antitumor effects. To date, a large number of IDO1 inhibitors have been reported, some of them including epacadostat, BMS986205, and indoximod, have advanced into clinical trials for cancer treatment (25).

In CLL, the activity of IDO1, measured as the plasma kynurenine-to-tryptophan ratio ([Kyn]/[Trp]), is reported to be increased (26). The expression of IDO1 is reduced in peripheral blood mononuclear cells (26), while NLCs (27) and $CD14^+HLA\text{-}DR^{lo}$ MDSCs (28) expressed high levels of this catabolic enzyme, and IDO1 inhibition may restore T cell proliferation. Even in studies on Eμ-TCL1 mice with a CLL-like disease, the enhanced expression of IDO1 in tumor-associated myeloid cells was observed (29). Interestingly, IDO1 expression was significantly higher in malignant $CD19^+$ B cells of Eμ-TCL1 mice compared to $CD19^+$ B cells of wild-type (WT) mice (29). However, the functional role of IDO1 in the leukemic clones from CLL patients is unknown. Here, we evaluated whether the IDO1/Kyn/AHR signaling pathway may be involved in CLL pathobiology. Our findings illustrate for the first time a role of the IDO1 metabolic pathway in CLL-prolonged survival and impaired drug sensitivity. The effects are mediated by the autocrine/paracrine action of Kyn that activates AHR. Interestingly, the blockade of AHR *via* CH-223191 interferes with the pro-survival signal and MCL1 induction triggered by IDO1. We also demonstrated that IDO1 metabolic activity affects the response to ABT-199, while CH-223191 treatment synergizes with the BCL2 inhibitor to kill leukemic CLL cells. Collectively, our findings suggest that the IDO1/Kyn/AHR axis may represent a novel therapeutic target in CLL.

## MATERIALS AND METHODS

### Patients

Blood samples from untreated patients that matched standard diagnostic criteria for CLL were obtained from the Hematology Section of Modena Hospital, Italy, with a protocol approved by the Institutional Review Board. All patients provided written informed consent in accordance with the declaration of Helsinki. Peripheral blood mononuclear cells were isolated by density gradient centrifugation with Lymphoprep medium (Pharmacia LKB Biotechnology, Piscataway, NY, USA) and used fresh or cryopreserved in RPMI-1640 medium, 50% FBS, and 10% DMSO and stored in liquid nitrogen until use. To enrich for CLL cells, peripheral blood mononuclear cells were incubated with CD19-specific microbeads (Miltenyi Biotech, Auburn, CA, USA) and separated by autoMACS (Miltenyi Biotec).

### *In Vitro* CLL Stimulation and Drug Treatments

To analyze basal IDO1 levels, $CD19^+$ CLL cells were serum starved for 1 h in RPMI-1640 at 37°C prior to RNA extraction. In all other experiments, $CD19^+$ CLL cells were resuspended in RPMI-1640 medium + 10% FBS. To mimic microenvironmental stimulation, CLL cells were treated with one of the following soluble factors: IFN-γ 500 U/ml (PeproTech Cat# 300-02, Rocky Hill, NJ, USA); LPS 5 μg/ml (Sigma-Aldrich Cat# L5293, St. Louis, MO, USA); goat F(AB′)2 fragment to human IgM (5FCμ) 10 μg/ml (Thermo Fisher Scientific Cat# ICN55055, Waltham, MA, USA); Type B CpG oligonucleotides 1 μg/ml (ODN 2006) (InvivoGen Cat# tlrl-2006, San Diego, CA, USA); and CD40L 200 ng/ml + interleukin (IL)-4 20 ng/ml (both from PeproTech Cat# 310-02 and 200-04) or tumor necrosis factor (TNF)-α 5 ng/ml (PeproTech Cat# 300-01A). Control cells were cultured in

parallel without stimulation. L-Kynurenine (Sigma-Aldrich Cat# K8625) was used at 100 µM. INCB018424 (ruxolitinib) (SelleckChem Cat# S1378, Houston, TX, USA) was used at 0.1 and 1 µM as previously described (30). CH-223191 (MedChemExpress Cat# HY-12684, Princeton, NJ, USA) was used at 10 µM. ABT-199 (venetoclax) (SelleckChem Cat# S8048) was used at 1 nM. AMG-176 (MedChemExpress Cat# HY-101565) was used at 100 or 300 nM.

## Real-Time PCR

Total RNA was extracted with the RNeasy Plus Mini Kit (Qiagen Cat# 74134) and reverse transcribed using SS VILO Master Mix (Life Technologies Cat# 11755050, Carlsbad, CA, USA). Twenty nanograms per reaction of cDNA was analyzed in real-time PCR on LightCycler 480 v.2 (Roche) using SYBR Green Master Mix (Applied Biosystems Cat# 4309155, Foster City, CA, USA). Specific primers designed for *IDO1*, *CYP1A1*, and *MCL1* are listed in **Supplementary Table 1**. Amplification of the sequence of interest was normalized to an endogenous reference control (*GAPDH*) and analyzed by the relative quantification method.

## Immunoblottings

Purified $CD19^+$ CLL cells were lysed for 20 min on ice with lysis buffer supplemented with dithiothreitol and protease inhibitor cocktail (BioVision Cat# K269, Milpitas, CA, USA). Proteins (70 µg/lane) were electrophoresed on 4 to 20% of SDS-polyacrylamide gradient gels (Bio-Rad Laboratories Cat# 4561094, Hercules, CA, USA). Membranes were immunoblotted with primary antibodies listed in **Supplementary Table 2**. Then, membranes were incubated with a species-specific horseradish peroxidase (HRP)-conjugated secondary antibody (diluted 1:20,000) (Bethyl Cat# A120-101P, and Cat# A90-116) and developed using HRP conjugates Western Bright Sirius (Advasta, Menlo Park, CA, USA). Images were acquired by ChemiDoc XRS+ (Bio-Rad Laboratories) and analyzed using Image Lab Software v.3.0 (Bio-Rad Laboratories).

## Immunofluorescence

Expression levels of IDO1 protein in $CD19^+$ CLL cells were also evaluated by intracytoplasmic immunofluorescence staining. $CD19^+$ CLL cells were plated in RPMI-1640 medium + 10% FBS on coverslips in a 24-well plate and pretreated (or not) with INCB018424 for 1 h before the incubation with IFN-γ for 20 h. After stimulation, cells were fixed and permeabilized on coverslips. After washes, the primary IDO1 antibody was loaded on coverslips and incubated overnight at +4°C. The day after, CLL cells were washed and incubated with Alexa-Fluor 488 conjugated secondary antibody (Thermo Fisher Scientific Cat# A-11034) for 1 h at room temperature. Finally, DAPI Antifade ES (CytoCell Cat# DES500L, Cambridge, UK) was added to stain cell nuclei. Immunofluorescent images were visualized with EVOS™ M5000 Imaging System (Thermo Fisher Scientific).

## Flow Cytometry

A flow cytometric evaluation of IDO1 expression in CLL cells was assessed treating $CD19^+$ cells isolated from CLL patients with IFN-γ for 24 h. Then, cells were fixed and permeabilized overnight. The following day, cells were washed and incubated with the anti-human IDO1-PE antibody (Cell Signaling Technology Cat# 10312) for 1 h on ice. For each sample, an isotype control was prepared in parallel.

## Sample Preparation for Metabolite Analysis

To assess the effect of IFN-γ on IDO1 activity, purified $CD19^+$ CLL cells were resuspended in 0.5 ml of RPMI-1640 medium + 10% FBS and cultured at a density of $12 \times 10^6$/well in 12-well plates. Cells were pretreated (or not) with INCB018424 1 µM for 1 h before the incubation with IFN-γ for 24 h. Similarly, 0.5 ml of conditioned media was collected from $5 \times 10^6$ CLL cells 24 h post transfection with the IDO1 vector, or the corresponding empty vector. Conditioned media were collected by centrifugation at 2,000 × g for 15 min and stored at −80°C until assayed. Fifty µl of these supernatants was added with an equal volume of ice-cold 1 M perchloric acid ($HClO_4$) fortified with a mix of the following stable isotope-labeled internal standard (final concentration 1 µM): L-kynurenine-d4 (Buchem BV, Apeldoorn, Netherlands) and L-tryptophan-d5 (Sigma-Aldrich). Samples were centrifuged (15,000 × g, 15 min), and the supernatants were collected and directly injected into LC-MS/MS.

## Liquid Chromatography and Chemicals

LC-MS/MS analyses were performed as previously described (31), with a few changes. The analyses were performed using an Agilent HP 1200 liquid chromatograph (Agilent, Santa Clara, CA, USA) consisting of a binary pump, an autosampler, and a thermostated column compartment. Chromatographic separations were carried out using a Discovery® HS-F5-3 column (150 × 2.1 mm, 3 µm, Supelco Cat# 567503-U, Bellefonte, PA, USA) using 0.1% formic acid in water (solvent A) and acetonitrile (solvent B) as mobile phase. The HPLC analyses were performed using a linear elution profile of 15 min from 5% to 90% of acetonitrile (ACN). The column was then washed with 90% of ACN for 3.5 min followed by the equilibration of the column for 5 min with 5% ACN. The flow rate was 0.5 ml/min. The injection volume was 20 µl. An Agilent 6410 triple quadrupole-mass spectrometer with an electrospray ion source (ESI) operating in positive mode was used for detection. L-Tryptophan, HPLC-grade acetonitrile, and methanol were obtained from Sigma-Aldrich. Analytical grade formic acid, acetonitrile, and perchloric acid were obtained from Carlo Erba. Water was purified using the Milli-Q water purification system (Millipore).

## B-CLL Cell Transfection Strategy

CLL cells were transfected using either a plasmid vector or small interfering RNAs (siRNAs). The transfections were carried out in a Nucleofector instrument (Lonza, Basel, Switzerland) with the P3 primary cell solution kit using the program EO-117. Briefly, $5 \times 10^6$ $CD19^+$ CLL cells were transfected with 10 µg of IDO1 plasmid vector (Cat# HG11650-NF) or the corresponding empty vector pCMV3-Negative Control (Cat# CV020) (all from Sino

Biological Inc., Shanghai, China). The expression of AHR was silenced using TriFECTa® Kit DsiRNA Duplex (IDT Design ID# hs.Ri.AHR.13) at a concentration of 200 nM. Non-targeted negative control siRNA was used as negative control in all experiments. Transfected cells were subsequently plated in RPMI-1640 medium supplemented with 10% FBS and analyzed at indicated time points.

## CLL Cell Viability

The apoptotic cell death of CLL cells was analyzed using Annexin V-FITC and propidium iodide (PI) staining (Thermo Fisher Scientific Cat# BMS500FI/100). Viability was defined as the percentage of Annexin V-/PI- cells, while apoptosis was defined as the percentage of Annexin V+/PI- cells. Events were acquired using the BD Accuri™ C6 Plus Flow Cytometer System (Becton Dickinson) and then analyzed by FlowJo Software (Tree Star).

## Statistical Analyses

Data were analyzed using GraphPad Prism 6 (GraphPad Software) or R 3.6.3 software (The R Foundation for Statistical Computing). In some experiments, results were normalized on control (100%) (vehicle-treated samples). Normalization was performed by dividing the value of a particular treated sample to the value of the corresponding sample treated with vehicle. p values were calculated by Student paired t test, and repeated-measure two- or three-way ANOVA (*$p < 0.05$, **$p < 0.01$, ***$p < 0.001$). When applicable, experiments followed a complete factorial design with two or three experimental factors. Data from each experiment were analyzed with a repeated-measure approach. Firstly, a full model was estimated, including all pairwise and—if the case—higher-order interaction terms. When interaction terms were not statistically significant, they were removed from the models and only the main effects for each factor were estimated. Main effects were reported as the mean difference (MD) with 95% confidence intervals (CI). Repeated-measure analyses were carried out with linear mixed models with a random intercept for each individual and random slope terms for each factor (without interactions). Data are presented as mean and standard error of the mean (SEM) is depicted as error bars.

# RESULTS

## IDO1 Is Expressed in CLL and Modulated by Stimuli That Mimic Tumor Microenvironment

Firstly, we characterized IDO1 expression in CLL. $CD19^+$ cells were purified from peripheral blood of untreated patients and inspected for IDO1 mRNA expression, detecting a variable amount in all samples (data not shown). These data were confirmed analyzing the expression level of IDO1 protein as shown in **Figure 1A**. After exposure to IFN-γ, a known inducer of IDO1, $CD19^+$ leukemic cells strongly upregulated IDO1 protein (**Figure 1B**). Given the pivotal role of TME in CLL progression and clonal evolution, we decided to evaluate the impact of microenvironmental signaling on IDO1 regulation in CLL. Purified $CD19^+$ cells were treated with different stimuli to trigger the B cell receptor (BCR), toll-like receptor (TLR) 4, TLR 7-9, CD40, and TNF receptor, in order to mimic the CLL microenvironment. After 4 h of stimulation, we observed a significant increase in IDO1 mRNA level in samples treated with IFN-γ ( $p = 0.037$), with LPS ($p = 0.028$), with anti-IgM ($p = 0.021$), with CpG DNA ($p = 0.032$), with CD40L + IL-4 ($p = 0.049$), and with TNF-α ($p = 0.003$) (**Figure 1C**). Accordingly, we also detected significantly higher IDO1 protein in CLL cells following each stimulation if compared to controls after 24 h, as reported in **Figure 1D**.

## IFN-γ/Jak/STAT1 Pathway Regulates the Production of Enzymatically Active IDO1 in CLL

We investigated whether overexpressed IDO1 was mediated by the Jak/STAT1 pathway and was enzymatically active. Firstly, we pretreated CLL cells with a JAK1/2 inhibitor, INCB018424, leading to the blockade of the intracellular signaling molecules downstream to IFN-γ. A dose escalation of INCB018424 (0.1–1 μM) significantly impaired the expression of IDO1 in a dose-dependent manner with a concomitant reduction of phosphorylated and total STAT1 protein levels induced by IFN-γ stimulation (**Figure 2A**, both $p < 0.05$). The reduction of IDO1 level by the most effective dose of INCB018424 (1 μM) was also confirmed by immunofluorescence (**Figure 2B**, $p = 0.046$). Because IDO1 activity can be indirectly estimated by determining the ratio between the amount of metabolites produced to the degraded substrate (32), we quantified the Kyn and Trp levels in the conditioned media of cultured CLL cells. Treatment of $CD19^+$ cells with IFN-γ induced a significant production of Kyn (from 0.7 μM ± 0.1 μM to 4.2 μM ± 0.50 μM, $p = 0.002$) with a concomitant depletion of Trp (from 14.0 μM ± 0.3 μM to 8.1 μM ± 0.6 μM, $p < 0.001$) if compared to control. Again, treatment with INCB018424 1 μM significantly affected the production of Kyn (1.0 ± 0.4 μM, $p = 0.018$) (**Figure 2C**). As a result, the [Kyn]/[Trp] ratio calculated after IFN-γ stimulation increased considerably (from 0.05 ± 0.003 to 0.54 ± 0.083, $p = 0.004$) indicating the full activity of the IDO1 enzyme. A minimal IDO1 activity was observed in INCB018424-treated CLL cells, in which the [Kyn]/[Trp] ratio was significantly decreased (0.09 ± 0.054, $p = 0.028$) (**Figure 2C**). Overall, these findings showed that CLL cells respond to IFN-γ stimulation upregulating an active form of IDO1 protein, confirming that this enzyme is active and inducible in CLL.

## IDO1 Is Involved in Preserving CLL Survival

To specifically investigate the functional role of IDO1 in CLL cells, transfection of the IDO1 vector or empty vector as control was performed. We detected a significant IDO1 overexpression comparable to the induction previously obtained with IFN-γ stimulation (**Figure 3A**, $p = 0.018$). We used the LC-MS/MS procedure for Kyn and Trp dosage in conditioned media of IDO1-transfected $CD19^+$ cells, confirming the increased activity

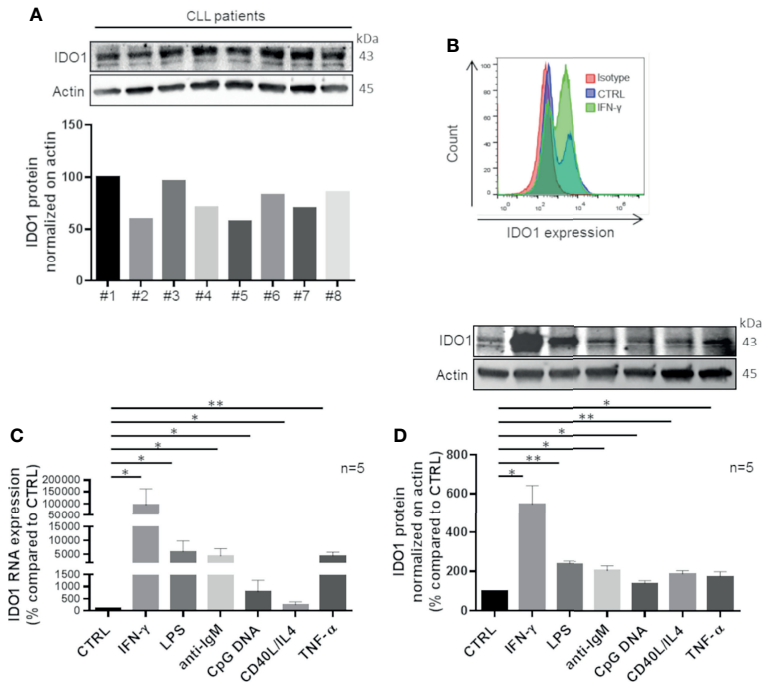


**FIGURE 1** | CLL cells up-regulate IDO1 in response to stimuli that mimic microenvironmental signals. **(A)** Purified leukemic CD19$^+$ cells from CLL patients were serum starved for 1 h. Then the basal level of IDO1 was inspected by Western blot (n = 8) and illustrated by a bar diagram. **(B)** Flow cytometric histograms represent a high IDO1 level in CD19$^+$ cells treated for 24 h with IFN-γ compared to the untreated control sample and isotype sample. **(C)** Bar diagram represents *IDO1* expression in CD19$^+$ CLL measured by real-time PCR. Samples were treated for 4 h with one of microenvironment stimuli individually (Student paired t test, *p < 0.05, **p < 0.01; n = 5). **(D)** Immunoblots represent IDO1 protein induction after 24 h of stimulation with the abovementioned factors. Histograms below represent the densitometric quantifications (Student paired t test, *p < 0.05, **p < 0.01; n = 5).

of the overexpressed enzyme compared to the control (Kyn from 0.3 μM ± 0.02 μM to 0.6 μM ± 0.06 μM, p = 0.002; Trp from 15.7 μM ± 1.0 μM to 12.7 μM ± 0.5 μM, p = 0.028; [Kyn]/[Trp] ratio from 0.02 ± 0.003 to 0.05 ± 0.005, p = 0.005; **Figure 3B**). The genetic modulation of IDO1 determined an increase of CLL survival (from 66.9% ± 2.4% to 73.5% ± 2.7% of viable cells, p = 0.015) (**Figure 3C**). This result was also confirmed by measuring a decrease in the apoptotic rate after transfection with the IDO1 vector, as shown in **Supplementary Figure 1A**. Moreover, we treated purified CD19$^+$ cells with exogenous Kyn to mimic the effect of IDO1 enzymatic action. As expected, Kyn promoted a significant increase in CLL cell viability (from 33.7% ± 3.8% to 41.1% ± 3.4%, p = 0.002) (**Figure 3D**) and a decrease in CLL cell apoptosis (**Supplementary Figure 1B**). These data confirmed the involvement of IDO1 and its derived metabolite in preserving CLL cell survival.

## AHR Promotes Cell Survival Modulating MCL1 in CLL Cells

Kyn is a potent endogenous activator of AHR (33), a ligand-controlled transcription factor that regulates enzymes metabolizing xenobiotic chemicals, such as cytochrome P450s (34). Therefore, we inspected if Kyn produced by CLL cells could act through an autocrine and/or paracrine loop on AHR. We observed that Kyn treatment is able to induce the transcription of *CYP1A1*, a known target of AHR (**Figure 4A**, p = 0.021). Then, we silenced AHR expression by siRNA transfection observing its significant impairment (**Figure 4B**, p = 0.02). Accordingly, CYP1A1 expression was decreased by AHR silencing (**Supplementary Figure 2A**). In this context, we detected a significant reduction of MCL1 expression in CLL cells consequent to the decreased AHR level (**Figure 4B**, p = 0.004). Of note, reduction of AHR determined a significant decrease in CLL cell viability (from 53.0% ± 4.1% to 42.3% ± 4.8%, p = 0.003) (**Figure 4C**). As a consequence, the apoptotic rate of AHR-silenced CLL cells was increased (**Supplementary Figure 2A**). Accordingly, we pretreated isolated CD19$^+$ cells with CH-223191, an AHR antagonist, and then we analyzed the expression of MCL1. Inhibition of AHR was able to affect MCL1 expression induced by Kyn stimulation, both at transcriptional (from 137.1% ± 2.7% to 120.5% ± 0.4%, p = 0.028) (**Figure 4D**) and protein levels (from 128.6% ± 3.4% to 109.4% ± 4.2%, p = 0.002) (**Figure 4E**).

## MCL1 Induction by the IDO1/Kyn/AHR Axis Affects the Response to ABT-199 in CLL

A high expression of B-cell lymphoma-extra large (BCL-xL) and MCL1 has reported to contribute to reduced response to ABT-199 in CLL (35). Therefore, to evaluate the effect of IDO1-induced survival on CLL cell sensitivity to ABT-199 treatment,

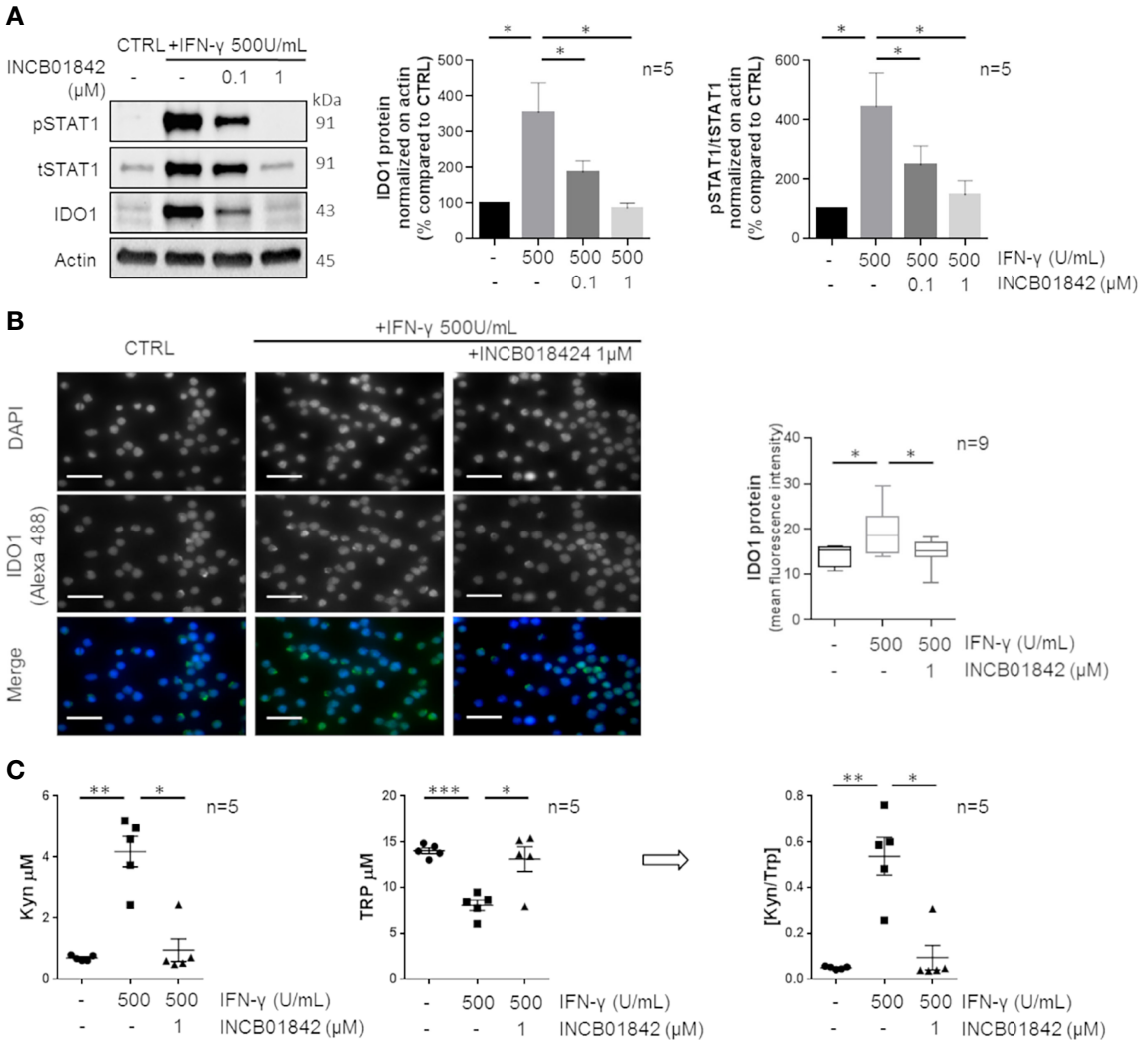


**FIGURE 2** | IDO1 protein induction and activity can be regulated by IFN-γ in CLL. **(A)** Purified CLL cells were pretreated with two doses (0.1–1 μM) of INCB018424 for 1 h prior to IFN-γ stimulation for 24 h. Immunoblots depict IDO1, tSTAT1, and pSTAT1 protein levels in a representative case. Histograms on the right represent the densitometric quantifications of IDO1 and pSTAT1/tSTAT1 in 5 CLL samples (Student paired t test, *p < 0.05; n = 5). **(B)** Immunofluorescence staining shows the ability of INCB018424 1 μM to reduce IDO1 expression induced by IFN-γ. Scale bar is 20 μm. Box plots summarize the fluorescent levels in DMSO, IFN-γ, or IFN-γ + INCB018424-treated CLL cells (Student paired t test, *p < 0.05; n = 9). **(C)** Conditioned media were collected after INCB018424 pretreatment (or not) and IFN-γ incubation for 24 h. Dot plots on the left represent the mean of the Kyn concentration measured by LC-MS/MS analytical technique in 5 separated experiments (Student paired t test, *p < 0.05, **p < 0.01; n = 5). The central dot plots represent the mean of the Trp concentration (Student paired t test, *p < 0.05, ***p < 0.001; n = 5). The resultant [Kyn]/[Trp] ratio calculated is depicted in the right dot plot (Student paired t test, *p < 0.05, **p < 0.01; n = 5).

we treated CD19$^+$ cells with Kyn, and then we added or not ABT-199 1 nM. We found that the killing effect of the BCL2 inhibitor was impaired in CLL because of the Kyn-mediated survival signal. Indeed, Kyn pre-incubation improved the percentage of viable cells in both settings, with or without ABT-199 treatment, from 54.7% ± 1.6% to 58.4% ± 1.6% and from 68.0% ± 1.4% to 71.8% ± 1.3%, respectively (**Figure 5A**). The interaction effect was not significant. The main effects were MD = 3.76, [95% CI = 2.12; 5.40], p = 0.001, for Kyn treatment and MD = -13.32, [95% CI = -20.73; -5.92], p = 0.006, for ABT-199 treatment. Given the important role of the IDO1/Kyn/AHR axis in the induction of MCL1 documented above, we pretreated CD19$^+$ cells with CH-223191 to block the signaling downstream to Kyn prior to ABT-199 1-nM addition. AHR inhibition promoted apoptotic cell death because CH-22311 showed an additive effect with ABT-199 in CLL (cell viability from 56.6% ± 2.1% to 48.8% ± 3.0%) (**Figure 5B**) as deduced from the main effects obtained for the three treatments (MD = 3.80, [95% CI = 0.88; 6.73], p = 0.043; MD = -4.81, [95% CI = -7.00; -2.62], p = 0.003; MD = -16.63, [95% CI = -26.79; -6.46], p = 0.019 for Kyn, Ch-223291 and ABT-199 treatments, respectively). Since inhibition of MCL1 is effective in CLL cells and the MCL1 antagonist, AMG-176, has been demonstrated to induce apoptosis in the CLL setting (36), we wanted to evaluate if AMG-176 could impair Kyn-mediated

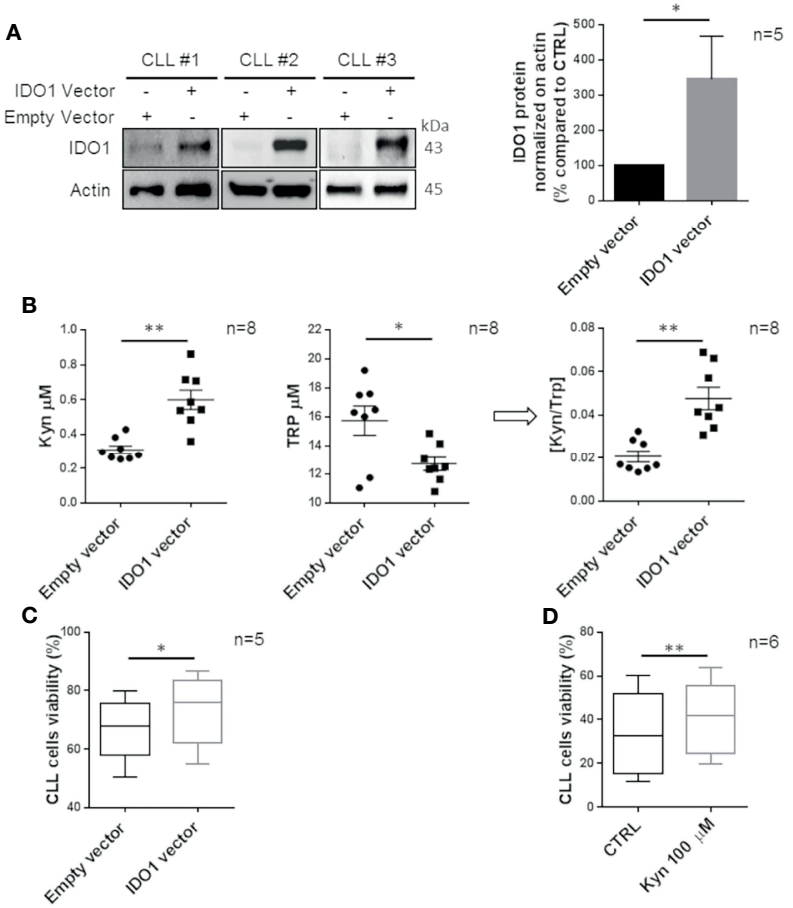


**FIGURE 3** | CLL cell survival is promoted by IDO1 overexpression. **(A)** CLL cells were transfected with an IDO1-expressing vector or an empty vector. After 24 h from transfection, the IDO1 protein level was measured by Western blot. Bar diagrams represent the densitometric quantifications of IDO1 (Student paired t test, *p < 0.05; n = 5). **(B)** Conditioned media were collected 24 h post transfection with the IDO1 vector or empty vector. Dot plots on the left represent the mean of the Kyn concentration measured by HPLC in 8 separated experiments (Student paired t test, **p < 0.01; n = 8). The central dot plots represent the mean of the Trp concentration (Student paired t test, *p < 0.05; n = 8). The resultant [Kyn]/[Trp] ratio calculated is depicted in the right dot plot (Student paired t test, **p < 0.01; n = 8). **(C)** Box plots represent the percentage of viable CLL cells after 24 h of transfection with IDO1-expressing vector or empty vector (Student paired t test, *p < 0.05; n = 5). **(D)** Box plots represent the percentage of CLL cell viability measured after 48 h of stimulation with Kyn 100 µM (Student paired t test, **p < 0.01; n = 6).

survival of CLL cells. Hence, isolated $CD19^+$ cells were pre-incubated with Kyn and then two doses of AMG-176 (100–300 nM) were tested. After 5 h of culture with AMG-176, we detected in all our conditions a significant induction of apoptosis (**Figure 5C**). Since the interaction effect was not significant, the main effects were MD = -1.238, [95% CI = -2.966; 0.4911], p = 0.14, and MD = 15.45, [95% CI = 10.76; 20.15], p < 0.001, for Kyn and AMG-176 100 nM treatment; MD = -0.7250, [95% CI = -2.215; 0.7651], p = 0.31, and MD = 29.68, [95% CI = 21.29; 38.06], p < 0.001, for Kyn and AMG-176 300 nM treatment, respectively. However, directly inhibiting MCL1, AMG-176 completely nullified the survival effect of Kyn, as no difference in cell viability was found in the comparison between samples treated with Kyn and AMG-176 or the MCL1 inhibitor alone. Summarizing, these data showed that the IDO1/Kyn/AHR axis induces survival in CLL leukemic cell through the maintenance of high levels of MCL1.

## DISCUSSION

IDO1 is an intracellular enzyme that initiates the first and rate-limiting step of Trp breakdown along the kynurenine pathway. In different tumors, IDO1 is constitutively expressed by the tumor cells themselves and also by tumor-associated cells, such as dendritic cells or endothelial cells (17).

Here, we demonstrated for the first time that CLL cells express an active and functional form of IDO1 enzyme and that microenvironmental stimuli, as inflammatory and pro-survival factors, are able to strongly induce a positive modulation of IDO1 expression. In line with previous literature, IFN-γ strongly induces IDO1 expression through the Jak/STAT1 signaling pathway in CLL. The kynurenine-to-tryptophan ratio is frequently used to measure or reflect the activity of IDO1. The elevated plasma level of the [Kyn]/[Trp] ratio was detected in patients diagnosed with various solid

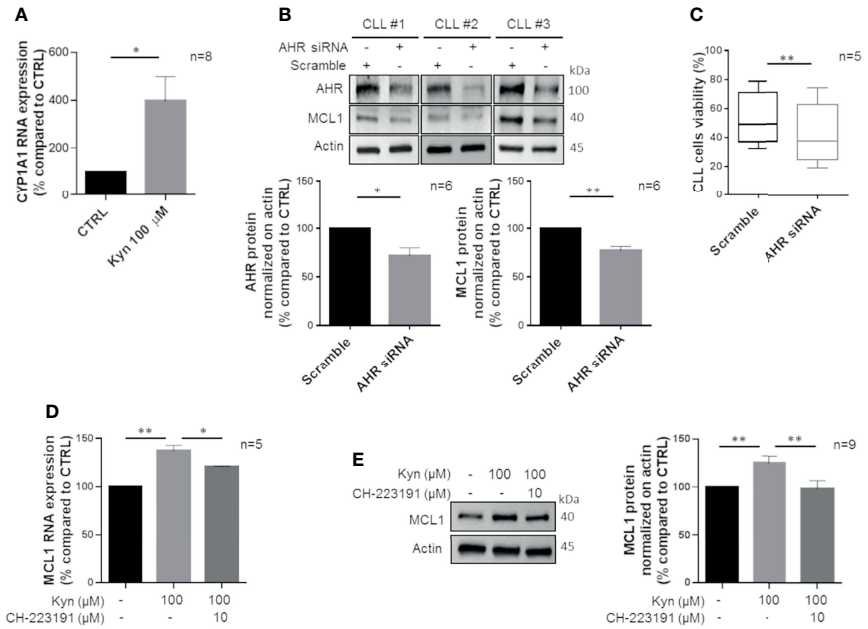


**FIGURE 4** | Kyn enhances MCL1 levels by activating AHR. **(A)** Bar diagram displays *CYP1A1* mRNA levels that were measured by real-time PCR in $CD19^+$ cells treated with 100 µM Kyn, for 3 h (Student paired t test, *p < 0.05; n = 8). **(B)** Immunoblots show expression of AHR and MCL1 48 h after transfection with scramble or AHR siRNA in 3 representative CLL samples. Histograms show densitometric quantification of AHR and MCL1 protein level (Student paired t test, *p < 0.05, **p < 0.01; n = 6). **(C)** Box plots represent the percentage of viable CLL cells after 48 h from transfection with AHR siRNA or scramble (Student paired t test, **p < 0.01; n = 5). **(D)** *MCL1* mRNA levels were measured by real-time PCR in CLL cells pretreated for 90 min with 10 µM CH-223191 prior to addition of 100 µM Kyn. Histogram depicts the inhibition of MCL1 induction by CH-223191 (Student paired t test, *p < 0.05, **p < 0.01; n = 5). **(E)** Immunoblot depicts MCL1 protein levels in a representative case. On the right, histogram represents the densitometric quantifications of CLL samples (Student paired t test, **p < 0.01; n = 9).

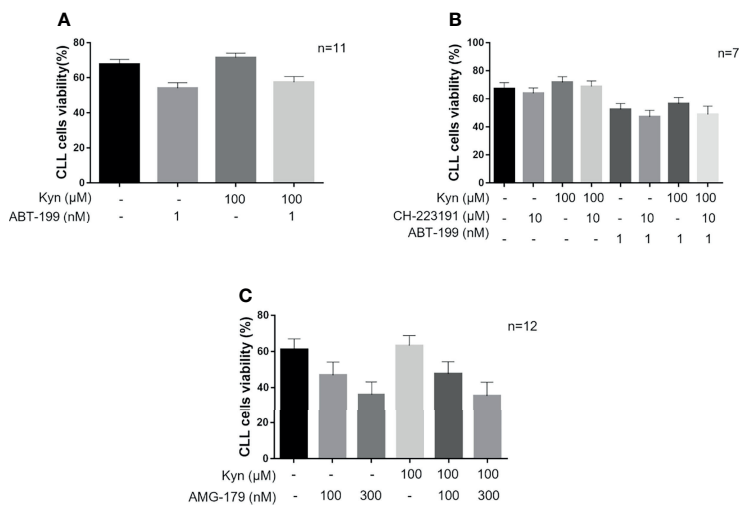


**FIGURE 5** | The activity of IDO1/Kyn/AHR axis impairs CLL cells response to ABT-199. **(A)** Histograms show comparison on viability rate of CLL cells treated with 1 nM ABT-199 for 5 h after overnight stimulation with 100 µM Kyn (repeated-measure two-way ANOVA with Kyn and CH-223191 treatment groups as the two factors; n = 11). **(B)** CLL cells were pretreated for 90 min with 10 µM CH-223191 and cultured overnight with Kyn. Then, 1 nM ABT-199 was added to culture for 5 h prior to cell viability assessment. Histograms illustrate the synergistic effect of CH-223191 with ABT-199 in CLL cells (repeated-measure three-way ANOVA with Kyn, ABT-199, and CH-223191 treatment groups as the three factors; n = 7). **(C)** CD19+ cells were cultured overnight with 100 µM Kyn, and then 100 or 300 nM AMG-176 was added to culture for 5 h. Cell viability was measured and depicted in histograms (repeated-measure two-way ANOVA with Kyn and AMG-176 treatment groups as the two factors; n = 12).

tumors but also in CLL cases and often correlate with poor prognosis (18–24, 26). High levels of Kyn concomitantly with consumption of Trp were detected in conditioned media collected from $CD19^+$ CLL cells stimulated with IFN-γ, confirming that the overexpressed IDO1 enzyme was active in CLL cells. Accordingly, we found that blocking IFN-γ signaling *via* INCB018424 interferes with IDO1 induction, STAT1 phosphorylation, and Kyn production. Overall, our findings suggested that IDO1 may be abnormally produced and activated in leukemic cells in response to signals known to be present inside the tissue microenvironment.

Nowadays, attention has been focused on the effects of IDO1, because in addition to immune regulation, activation of the IDO1/Kyn/AHR axis affects tumor cell viability, proliferation, and apoptosis *in vitro*. It was demonstrated that blockade of IDO1 activity in cancer cells could reduce β-catenin activation and inhibit cell proliferation (37). IDO1 silencing in melanoma cells inhibited cancer cell proliferation and induced cell apoptosis (38). We argued whether the IDO1 pathway may trigger survival stimuli on CLL cells by establishing an autocrine loop and/or by acting throughout the microenvironment. We observed an enhanced resistance to spontaneous apoptosis in CLL cells when IDO1 expression was forced with the plasmid vector. This pro-survival influence induced by IDO1 is also confirmed by treating CLL cells with Kyn, the main metabolite of the IDO1 enzyme. Accordingly, we demonstrated that Kyn activates AHR transcriptional activity in CLL cells. AHR is involved in the formation of tumors as its activation enhanced clonogenic survival and motility of tumor cells (39, 40) and as transgenic mice with a constitutively active AHR spontaneously develop tumors (41). As a consequence, we argued whether AHR may have a role in CLL survival and maintenance. Although the study of Gonder and colleagues showed that the conditional knockout of AHR in $CD19^+$ B cells of the Eμ-TCL1 mouse model seems to have no impact on CLL progression or survival *in vivo* (42), we demonstrated that AHR silencing on CLL cells significantly increased apoptosis of $CD19^+$ clones *in vitro*. These conflicting findings keep open the debate about AHR's active involvement in CLL leukemogenesis and maintenance, which requires further investigation.

The BCL2 family proteins are well-known modulators of apoptosis. B-cell malignancies, such as CLL and follicular lymphomas, are functionally dependent on BCL2 for survival (43). Surprisingly, CLL cells treated with AHR agonist Kyn showed increased MCL1 transcript and protein. Conversely, we found that blocking AHR *via* CH-223191 or by AHR silencing abrogates MCL1 expression. Our data suggest that AHR blocking interferes with the survival of CLL cells by limiting the expression of MCL1. Here, we also evaluated whether IDO1/Kyn/AHR signaling may determine protection against drug-induced apoptosis as reported in solid tumors (44, 45). Mature B-cells, both normal and leukemic (CLL), are highly sensitive to BCL2 inhibition by ABT-199, which induces BAX/BAK-mediated apoptosis triggered mainly by BIM (46), but ABT-199 is much less effective against CLL cells that have received survival signals from the microenvironment (47). Sustained engagement of the BCR induces MCL1 (48), and high levels of MCL1 have been shown to protect CLL, other hematological malignancies, and certain solid tumors from ABT-199 (47). We found that Kyn-treated CLL cells are less affected by the pro-apoptotic effect of ABT-199. AHR blockade by the CH-223191 antagonist inhibited the Kyn-mediated protection against ABT-199-induced apoptosis. Moreover, at low concentrations of ABT-199, CH-223191 showed synergistic or additive cytotoxicity to CLL lymphocytes. Finally, we wanted to confirm that the IDO1/Kyn/AHR axis improves CLL survival through MCL1 induction, targeting MCL1 itself. AMG-176 is a selective and direct antagonist of MCL1, which has shown efficacy in several hematological malignancies, including CLL (36). As expected, $CD19^+$ cells rapidly went into apoptosis after AMG-176 treatment even if treated with Kyn. Indeed, AMG-176 completely neutralized the survival effect of the IDO1/Kyn/AHR pathway in CLL. In this scenario, the IDO1 pathway activated in CLL cells by stimuli from other cell types, such as endothelial cells, NLCs, MDSCs, and T cells inside microenvironmental niches, could interfere with the effect of novel targeted drugs currently used for CLL patients' management. The results support the notion that the activation status of the IDO1/Kyn/AHR axis may be of relevance in CLL clinical outcome.

Several issues concerning the role of IDO1 in CLL remain to be explored. First, multiple mechanisms at both transcriptional (i.e., Bridging integrator 1, Bin1) and posttranslational levels (i.e., suppressor of cytokine signaling 3, SOCS3) may be implicated in the abnormal levels of IDO1. Second, the mechanisms underlying AHR induction of MCL1 are not fully elucidated. Upon ligand binding, AHR translocates to the nucleus and the formation of AHR-AHR nuclear translocator (ARNT) heterodimer leads to the transcription of dioxin-responsive element-containing genes (49). In addition to the canonical pathway characterized by AHR nuclear translocation through which AHR regulates target gene expression, AHR influences many biological processes through non-genomic signaling mechanisms (45). Further studies are needed to clarify the molecular cascade that links IDO1 activity to MCL1 expression through not only Kyn and AHR. On this line, we have planned to confirm our findings in an adoptive transfer mouse model of CLL. An *in vivo* study will allow (i) to evaluate the effects of the IDO1/Kyn/AHR axis on the complexity of the leukemic microenvironment; (ii) to consider the impact of the known deregulation of nicotinate/nicotinamide pathways and purine metabolism by the action of IDO1 (50); and (iii) to analyze the effects of IDO1 and AHR inhibitors on the leukemic population evaluating the disease dynamics (insurgence, aggressiveness, progression and remission).

In conclusion, our data show for the first time that CLL cells express an active IDO1 enzyme that produces high levels of Kyn consuming Trp *via* the kynurenine pathway. The results also demonstrate that the IDO1/Kyn/AHR axis plays a role in survival and drug resistance of leukemic cells. The observed ability of the AHR selective antagonist to interfere with protective signals of CLL cells may be explored, both experimentally and clinically, as a possible novel therapeutic approach in CLL.

## DATA AVAILABILITY STATEMENT

The original contributions presented in the study are included in the article/**Supplementary Material**. Further inquiries can be directed to the corresponding author.

## ETHICS STATEMENT

The studies involving human participants were reviewed and approved by 1003/2018/SPER/AOUMO – IDO in CLL-"Indoleamina-2,3-diossigenasi come mediatore della tolleranza immunitaria nella leucemia linfatica cronica – IDO". The patients/participants provided their written informed consent to participate in this study.

## AUTHOR CONTRIBUTIONS

RMaf and RMar conceived and coordinated the research and interpreted the results. CA performed the *in vitro* experiments, performed the statistical analyses, interpreted the results, and wrote the manuscript. SF acquired and analyzed the flow cytometric data. NM performed molecular analyses and contributed to Western blot analyses. SA performed LC-MS/MS analyses. MM and GL provided patient samples and clinical data. SM managed the biological samples. LP, ML, RMaf, and RMar revised and approved the final version of the manuscript. All authors contributed to the article and approved the submitted version.

## FUNDING

This work was supported by Associazione Italiana per la Ricerca sul Cancro (IG21436 RMar) and Progetto Dipartimenti di Eccellenza 2018–2022. SF was supported by an annual fellowship from Fondazione Umberto Veronesi, Italy.

## ACKNOWLEDGMENTS

We would like to thank Federico Banchelli and the Medical Statistics Unit directed by Prof. Roberto D'Amico (Department of Medical and Surgical Sciences, University of Modena and Reggio Emilia) for providing their expertise with statistical analysis.

## SUPPLEMENTARY MATERIAL

The Supplementary Material for this article can be found online at: https://www.frontiersin.org/articles/10.3389/fimmu.2022.832263/full#supplementary-material

**Supplementary Figure 1 |** IDO1 overexpression and Kyn treatment reduce apoptosis of CLL cells. **(A)** Box plots represent the percentage of apoptotic CLL cells after 24 h of transfection with IDO1-expressing vector or empty vector (Student paired t test, $*p < 0.05$; n = 5). **(B)** Apoptotic CLL cells measured after 48 h of stimulation with Kyn 100 μM are depicted in box plots (Student paired t test, $**p < 0.01$; n = 6).

**Supplementary Figure 2 |** Silencing of AHR in CLL cells reduces CYP1A1 protein expression and enhances apoptosis. **(A)** Immunoblots show expression of CYP1A1 48 h after transfection with scramble or AHR siRNA in 3 representative CLL samples. Histograms show densitometric quantification of CYP1A1 protein level (Student paired t test, $*p < 0.05$; n = 6). **(B)** Box plots represent the percentage of apoptotic CLL cells after 48 h from transfection with AHR siRNA or scramble (Student paired t test, $***p < 0.001$; n = 5).

**Supplementary Table 1 |** List of primers used for Real Time PCR.

**Supplementary Table 2 |** List of primary antibodies used in this study.

## REFERENCES

1. Hallek M. Chronic Lymphocytic Leukemia: 2020 Update on Diagnosis, Risk Stratification and Treatment. *Am J Hematol* (2019) 94:1266–87. doi: 10.1002/ajh.25595
2. Defoiche J, Debacq C, Asquith B, Zhang Y, Burny A, Bron D, et al. Reduction of B Cell Turnover in Chronic Lymphocytic Leukaemia. *Br J Haematol* (2008) 143:240–7. doi: 10.1111/j.1365-2141.2008.07348.x
3. Cutucache CE. Tumor-Induced Host Immunosuppression: Special Focus on CLL. *Int Immunopharmacol* (2013) 17:35–41. doi: 10.1016/j.intimp.2013.05.021
4. Kater AP, Wu JQ, Kipps T, Eichhorst B, Hillmen P, D'Rozario J, et al. Venetoclax Plus Rituximab in Relapsed Chronic Lymphocytic Leukemia: 4-Year Results and Evaluation of Impact of Genomic Complexity and Gene Mutations From the MURANO Phase III Study. *J Clin Oncol Am Soc Clin Oncol* (2020) 38:4042–54. doi: 10.1200/JCO.20.00948
5. Haselager MV, Kater AP, Eldering E. Proliferative Signals in Chronic Lymphocytic Leukemia; What Are We Missing? *Front Oncol* (2020) 10:592205. doi: 10.3389/fonc.2020.592205
6. Moffett JR, Namboodiri MA. Tryptophan and the Immune Response. *Immunol Cell Biol* (2003) 81:247–65. doi: 10.1046/j.1440-1711.2003.t01-1-01177.x
7. Munn DH, Zhou M, Attwood JT, Bondarev I, Conway SJ, Marshall B, et al. Prevention of Allogeneic Fetal Rejection by Tryptophan Catabolism. *Science* (1998) 281:1191–3. doi: 10.1126/science.281.5380.1191
8. Grohmann U, Fallarino F, Puccetti P. Tolerance, DCs and Tryptophan: Much Ado About IDO. *Trends Immunol* (2003) 24:242–8. doi: 10.1016/S1471-4906(03)00072-3
9. Burke F, Knowles RG, East N, Balkwill FR. The Role of Indoleamine 2,3-Dioxygenase in the Anti-Tumour Activity of Human Interferon-γ *In Vivo*. *Int J Cancer* (1995) 60:115–22. doi: 10.1002/ijc.2910600117
10. Mbongue JC, Nicholas DA, Torrez TW, Kim NS, Firek AF, Langridge WHR. The Role of Indoleamine 2, 3-Dioxygenase in Immune Suppression and Autoimmunity. *Vaccines* (2015) 3:703–29. doi: 10.3390/vaccines3030703
11. Frumento G, Rotondo R, Tonetti M, Damonte G, Benatti U, Ferrara GB. Tryptophan-Derived Catabolites Are Responsible for Inhibition of T and Natural Killer Cell Proliferation Induced by Indoleamine 2,3-Dioxygenase. *J Exp Med* (2002) 196:459–68. doi: 10.1084/jem.20020121
12. Uyttenhove C, Pilotte L, Théate I, Stroobant V, Colau D, Parmentier N, et al. Evidence for a Tumoral Immune Resistance Mechanism Based on Tryptophan Degradation by Indoleamine 2,3-Dioxygenase. *Nat Med* (2003) 9:1269–74. doi: 10.1038/nm934
13. Kewley RJ, Whitelaw ML, Chapman-Smith A. The Mammalian Basic Helix-Loop-Helix/PAS Family of Transcriptional Regulators. *Int J Biochem Cell Biol* (2004) 36:189–204. doi: 10.1016/S1357-2725(03)00211-5
14. Cheong JE, Sun L. Targeting the IDO1/TDO2–KYN–AhR Pathway for Cancer Immunotherapy – Challenges and Opportunities. *Trends Pharmacol Sci* (2018) 39:307–25. doi: 10.1016/j.tips.2017.11.007
15. Liu X, Shin N, Koblish HK, Yang G, Wang Q, Wang K, et al. Selective Inhibition of IDO1 Effectively Regulates Mediators of Antitumor

Immunity. *Blood* (2010) 115:3520–30. doi: 10.1182/blood-2009-09-246124
16. Pilotte L, Larrieu P, Stroobant V, Colau D, Dolušić E, Frédérick R, et al. Reversal of Tumoral Immune Resistance by Inhibition of Tryptophan 2,3-Dioxygenase. *Proc Natl Acad Sci USA* (2012) 109:2497–502. doi: 10.1073/pnas.1113873109
17. Munn DH, Mellor AL. IDO in the Tumor Microenvironment: Inflammation, Counter-Regulation, and Tolerance. *Trends Immunol* (2016) 37:193–207. doi: 10.1016/j.it.2016.01.002
18. Corm S, Berthon C, Imbenotte M, Biggio V, Lhermitte M, Dupont C, et al. Indoleamine 2,3-Dioxygenase Activity of Acute Myeloid Leukemia Cells Can be Measured From Patients' Sera by HPLC and Is Inducible by IFN-γ. *Leuk Res* (2009) 33:490–4. doi: 10.1016/j.leukres.2008.06.014
19. Ninomiya S, Hara T, Tsurumi H, Goto N, Saito K, Seishima M, et al. Indoleamine 2,3-Dioxygenase Expression and Serum Kynurenine Concentrations in Patients With Diffuse Large B-Cell Lymphoma. *Leuk Lymphoma* (2012) 53:1143–5. doi: 10.3109/10428194.2011.643472
20. Chen JY, Li CF, Kuo CC, Tsai KK, Hou MF, Hung WC. Cancer/stroma Interplay *via* Cyclooxygenase-2 and Indoleamine 2,3-Dioxygenase Promotes Breast Cancer Progression. *Breast Cancer Res* (2014) 16:1–14. doi: 10.1186/s13058-014-0410-1
21. Ferns DM, Kema IP, Buist MR, Nijman HW, Kenter GG, Jordanova ES. Indoleamine-2,3-Dioxygenase (IDO) Metabolic Activity Is Detrimental for Cervical Cancer Patient Survival. *OncoImmunology* (2015) 4:1–7. doi: 10.4161/2162402X.2014.981457
22. Wainwright DA, Balyasnikova IV, Chang AL, Ahmed AU, Moon KS, Auffinger B, et al. IDO Expression in Brain Tumors Increases the Recruitment of Regulatory T Cells and Negatively Impacts Survival. *Clin Cancer Res* (2012) 18:6110–21. doi: 10.1158/1078-0432.CCR-12-2130
23. Speeckaert R, Vermaelen K, Van Geel N, Autier P, Lambert J, Haspeslagh M, et al. Indoleamine 2,3-Dioxygenase, a New Prognostic Marker in Sentinel Lymph Nodes of Melanoma Patients. *Eur J Cancer* (2012) 48:2004–11. doi: 10.1016/j.ejca.2011.09.007
24. Inaba T, Ino K, Kajiyama H, Yamamoto E, Shibata K, Nawa A, et al. Role of the Immunosuppressive Enzyme Indoleamine 2,3-Dioxygenase in the Progression of Ovarian Carcinoma. *Gynecologic Oncol* (2009) 115:185–92. doi: 10.1016/j.ygyno.2009.07.015
25. Tang K, Wu YH, Song Y, Yu B. Indoleamine 2,3-Dioxygenase 1 (IDO1) Inhibitors in Clinical Trials for Cancer Immunotherapy. *J Hematol Oncol* (2021) 14:1–21. doi: 10.1186/s13045-021-01080-8
26. Lindström V, Aittoniemi J, Jylhävä J, Eklund C, Hurme M, Paavonen T, et al. Indoleamine 2,3-Dioxygenase Activity and Expression in Patients With Chronic Lymphocytic Leukemia. *Clin Lymphoma Myeloma Leuk* (2012) 12:363–5. doi: 10.1016/j.clml.2012.06.001
27. Giannoni P, Pietra G, Travaini G, Quarto R, Shyti G, Benelli R, et al. Chronic Lymphocytic Leukemia Nurse-Like Cells Express Hepatocyte Growth Factor Receptor (C-MET) and Indoleamine 2,3-Dioxygenase and Display Features of Immunosuppressive Type 2 Skewed Macrophages. *Haematologica* (2014) 99:1078–87. doi: 10.3324/haematol.2013.091405
28. Jitschin R, Braun M, Büttner M, Dettmer-Wilde K, Bricks J, Berger J, et al. CLL-Cells Induce IDOhi CD14+HLA-DRlo Myeloid-Derived Suppressor Cells That Inhibit T-Cell Responses and Promote TRegs. *Blood* (2014) 124:750–60. doi: 10.1182/blood-2013-12-546416
29. Öztürk S, Kalter V, Roessner PM, Sunbul M, Seiffert M. Ido1-Targeted Therapy Does Not Control Disease Development in the Eμ-Tcl1 Mouse Model of Chronic Lymphocytic Leukemia. *Cancers* (2021) 13:1–12. doi: 10.3390/cancers13081899
30. Maffei R, Fiorcari S, Benatti S, Atene CG, Martinelli S, Zucchini P, et al. IRF4 Modulates the Response to BCR Activation in Chronic Lymphocytic Leukemia Regulating IKAROS and SYK. *Leukemia* (2021) 35:1330–43. doi: 10.1038/s41375-021-01178-5
31. Borsini A, Alboni S, Horowitz MA, Tojo LM, Cannazza G, Su K-P, et al. Rescue of IL-1β-Induced Reduction of Human Neurogenesis by Omega-3 Fatty Acids and Antidepressants. *Brain Behav Immun* (2017) 65:230–8. doi: 10.1016/j.bbi.2017.05.006
32. Badawy AAB, Guillemin G. The Plasma [Kynurenine]/[Tryptophan] Ratio and Indoleamine 2,3-Dioxygenase: Time for Appraisal. *Int J Tryptophan Res* (2019) 12:1–10. doi: 10.1177/1178646919868978
33. Mezrich JD, Fechner JH, Zhang X, Johnson BP, Burlingham WJ, Bradfield CA. An Interaction Between Kynurenine and the Aryl Hydrocarbon Receptor Can Generate Regulatory T Cells. *J Immunol (Baltimore Md : 1950)* (2010) 185:3190. doi: 10.4049/JIMMUNOL.0903670
34. Sogawa K, Fujii-Kuriyama Y. Ah Receptor, a Novel Ligand-Activated Transcription Factor. *J Biochem* (1997) 122:1075–9. doi: 10.1093/OXFORDJOURNALS.JBCHEM.A021864
35. Choudhary GS, Al-Harbi S, Mazumder S, Hill BT, Smith MR, Bodo J, et al. MCL-1 and BCL-xL-Dependent Resistance to the BCL-2 Inhibitor ABT-199 Can be Overcome by Preventing PI3K/AKT/mTOR Activation in Lymphoid Malignancies. *Cell Death Dis* (2015) 6:e1593–12. doi: 10.1038/cddis.2014.525
36. Yi X, Sarkar A, Kismali G, Aslan B, Ayres M, Iles LKR, et al. AMG-176, an Mcl-1 Antagonist, Shows Preclinical Efficacy in Chronic Lymphocytic Leukemia. *Clin Cancer Res Off J Am Assoc Cancer Res* (2020) 26:6856–67. doi: 10.1158/1078-0432.CCR-19-1397
37. Thaker AI, Rao MS, Bishnupuri KS, Kerr TA, Foster L, Marinshaw JM, et al. IDO1 Metabolites Activate β-Catenin Signalin. *Gastroenterology* (2013) 145:416–25. doi: 10.1053/j.gastro.2013.05.002.IDO1
38. Liu Y, Zhang Y, Zheng X, Zhang X, Wang H, Li Q, et al. Gene Silencing of Indoleamine 2,3-Dioxygenase 2 in Melanoma Cells Induces Apoptosis Through the Suppression of NAD+ and Inhibits *In Vivo* Tumor Growth. *Oncotarget* (2016) 7:32329–40. doi: 10.18632/oncotarget.8617
39. Opitz CA, Litzenburger UM, Sahm F, Ott M, Tritschler I, Trump S, et al. An Endogenous Tumour-Promoting Ligand of the Human Aryl Hydrocarbon Receptor. *Nature* (2011) 478:197–203. doi: 10.1038/NATURE10491
40. Gramatzki D, Pantazis G, Schittenhelm J, Tabatabai G, Köhle C, Wick W, et al. Aryl Hydrocarbon Receptor Inhibition Downregulates the TGF-B/Smad Pathway in Human Glioblastoma Cells. *Oncogene* (2009) 28:2593–605. doi: 10.1038/onc.2009.104
41. Andersson P, McGuire J, Rubio C, Gradin K, Whitelaw ML, Pettersson S, et al. A Constitutively Active Dioxin/Aryl Hydrocarbon Receptor Induces Stomach Tumors. *Proc Natl Acad Sci USA* (2002) 99:9990. doi: 10.1073/PNAS.152706299
42. Gonder S, Largeot A, Gargiulo E, Pierson S, Botana IF, Pagano G, et al. The Tumor Microenvironment-Dependent Transcription Factors Ahr and Hif-1α Are Dispensable for Leukemogenesis in the Eμ-Tcl1 Mouse Model of Chronic Lymphocytic Leukemia. *Cancers* (2021) 13:1–18. doi: 10.3390/cancers13184518
43. Zhu H, Almasan A. Development of Venetoclax for Therapy of Lymphoid Malignancies. *Drug Design Dev Ther* (2017) 11:685–94. doi: 10.2147/DDDT.S109325
44. Ye M, Zhang Y, Gao H, Xu Y, Jing P, Wu J, et al. Activation of the Aryl Hydrocarbon Receptor Leads to Resistance to EGFR TKIs in Non–Small Cell Lung Cancer by Activating Src-Mediated Bypass Signaling. *Clin Cancer Res* (2018) 24:1227–39. doi: 10.1158/1078-0432.CCR-17-0396
45. Xiong J, Zhang X, Zhang Y, Wu B, Fang L, Wang N, et al. Aryl Hydrocarbon Receptor Mediates Jak2/STAT3 Signaling for Non-Small Cell Lung Cancer Stem Cell Maintenance. *Exp Cell Res* (2020) 396:112288. doi: 10.1016/j.yexcr.2020.112288
46. Khaw SL, Mérino D, Anderson MA, Glaser SP, Bouillet P, Roberts AW, et al. Both Leukaemic and Normal Peripheral B Lymphoid Cells Are Highly Sensitive to the Selective Pharmacological Inhibition of Prosurvival Bcl-2 With ABT-199. *Leukemia* (2014) 28:1207–15. doi: 10.1038/leu.2014.1
47. Bojarczuk K, Sasi BK, Gobessi S, Innocenti I, Pozzato G, Laurenti L, et al. BCR Signaling Inhibitors Differ in Their Ability to Overcome Mcl-1-Mediated Resistance of CLL B Cells to ABT-199. *Blood* (2016) 127:3192–201. doi: 10.1182/blood-2015-10-675009
48. Petlickovski A, Laurenti L, Li X, Marietti S, Chiusolo P, Sica S, et al. Sustained Signaling Through the B-Cell Receptor Induces Mcl-1 and Promotes Survival of Chronic Lymphocytic Leukemia B Cells. *Blood* (2005) 105:4820–7. doi: 10.1182/blood-2004-07-2669
49. Gutiérrez-Vázquez C, Quintana FJ. Regulation of the Immune Response by the Aryl Hydrocarbon Receptor. *Immunity* (2018) 48:19–33. doi: 10.1016/j.immuni.2017.12.012
50. Amobi-McCloud A, Muthuswamy R, Battaglia S, Yu H, Liu T, Wang J, et al. IDO1 Expression in Ovarian Cancer Induces PD-1 in T Cells *via* Aryl

Hydrocarbon Receptor Activation. *Front Immunol* (2021) 12:678999. doi: 10.3389/fimmu.2021.678999

**Conflict of Interest:** The authors declare that the research was conducted in the absence of any commercial or financial relationships that could be construed as a potential conflict of interest.

**Publisher's Note:** All claims expressed in this article are solely those of the authors and do not necessarily represent those of their affiliated organizations, or those of the publisher, the editors and the reviewers. Any product that may be evaluated in this article, or claim that may be made by its manufacturer, is not guaranteed or endorsed by the publisher.

frontiers | Frontiers in Immunology

ORIGINAL RESEARCH
published: 04 April 2022
doi: 10.3389/fimmu.2022.809261

# Notch-Signaling Deregulation Induces Myeloid-Derived Suppressor Cells in T-Cell Acute Lymphoblastic Leukemia

*Paola Grazioli[1†], Andrea Orlando[2,3†], Nike Giordano[2], Claudia Noce[2], Giovanna Peruzzi[3], Behnaz Abdollahzadeh[2], Isabella Screpanti[2*] and Antonio Francesco Campese[2*]*

[1] Department of Experimental Medicine, Sapienza University, Rome, Italy, [2] Department of Molecular Medicine, Sapienza University, Rome, Italy, [3] Center for Life Nano- and Neuro-Science, Fondazione Istituto Italiano di Tecnologia (IIT), Rome, Italy

OPEN ACCESS

**Edited by:**
Sergei Kusmartsev,
University of Florida, United States

**Reviewed by:**
Barbara A. Osborne,
University of Massachusetts Amherst, United States
Fokhrul Hossain,
Louisiana State University, United States

***Correspondence:**
Antonio Francesco Campese
antonello.campese@uniroma1.it
Isabella Screpanti
isabella.screpanti@uniroma1.it

[†]These authors have contributed equally to this work and share first authorship

**Specialty section:**
This article was submitted to Cancer Immunity and Immunotherapy, a section of the journal Frontiers in Immunology

**Received:** 04 November 2021
**Accepted:** 09 March 2022
**Published:** 04 April 2022

**Citation:**
Grazioli P, Orlando A, Giordano N, Noce C, Peruzzi G, Abdollahzadeh B, Screpanti I and Campese AF (2022) Notch-Signaling Deregulation Induces Myeloid-Derived Suppressor Cells in T-Cell Acute Lymphoblastic Leukemia. Front. Immunol. 13:809261. doi: 10.3389/fimmu.2022.809261

Notch receptors deeply influence T-cell development and differentiation, and their dysregulation represents a frequent causative event in "T-cell acute lymphoblastic leukemia" (T-ALL). "Myeloid-derived suppressor cells" (MDSCs) inhibit host immune responses in the tumor environment, favoring cancer progression, as reported in solid and hematologic tumors, with the notable exception of T-ALL. Here, we prove that Notch-signaling deregulation in immature T cells promotes $CD11b^{+}Gr\text{-}1^{+}$ MDSCs in the Notch3-transgenic murine model of T-ALL. Indeed, aberrant T cells from these mice can induce MDSCs *in vitro*, as well as in immunodeficient hosts. Conversely, anti-Gr1-mediated depletion of MDSCs in T-ALL-bearing mice reduces proliferation and expansion of malignant T cells. Interestingly, the coculture with Notch-dependent T-ALL cell lines, sustains the induction of human $CD14^{+}HLA\text{-}DR^{low/neg}$ MDSCs from healthy-donor PBMCs that are impaired upon exposure to gamma-secretase inhibitors. Notch-independent T-ALL cells do not induce MDSCs, suggesting that Notch-signaling activation is crucial for this process. Finally, in both murine and human models, IL-6 mediates MDSC induction, which is significantly reversed by treatment with neutralizing antibodies. Overall, our results unveil a novel role of Notch-deregulated T cells in modifying the T-ALL environment and represent a strong premise for the clinical assessment of MDSCs in T-ALL patients.

**Keywords: MDSC, T-ALL, Notch, IL-6, tumor microenvironment**

## INTRODUCTION

The signaling of Notch receptors is simple and conserved, although many levels of regulation exist and its outcomes are strictly context-dependent (1–3). In mammals, it starts with the interaction between receptors (Notch1 to Notch4) and ligands (Jagged or Delta family) expressed on neighboring cells. Two sequential proteolytic cuts then lead to the release of the functional intracellular domain of Notch (ICN), which translocates into the nucleus to activate the CSL transcription factor. Notch exerts essential roles in T-cell development and differentiation (4–6),

and ICN constitutive activation drives the development of "T-cell acute lymphoblastic leukemia" (T-ALL) (7), as demonstrated in murine models (8–10) and reported in patients (11, 12). Many efforts have been produced to dissect the oncogenic role of Notch inside T-ALL cells. However, the effects of T-cell-targeted deregulation of Notch signaling on tumor environment remain underexplored.

"Myeloid-derived suppressor cells" (MDSCs) represent a small and heterogeneous group of immature/progenitor myeloid cells. In mice, they are broadly identified as $CD11b^+Gr\text{-}1^+$ cells (13) and are expanded/activated in the tumor environment, where they suppress host immune responses, facilitating cancer progression (14). MDSCs have been described in detail in solid tumors (15, 16). Instead, studies are limited and with conflicting results in hematological malignancies, and nothing has been reported for T-ALL (17, 18), so far.

Notch may regulate MDSC behavior in a different context (19, 20). Notch-signaling inhibition in $Gr\text{-}1^+$ cells facilitates the aberrant production of MDSCs in tumor-bearing mice and cancer patients (21, 22). In contrast, other groups reported that Notch-signaling inhibition, by using GSI or anti-jagged antibodies, limits the function of MDSCs in cancer settings, thus suggesting a positive role of Notch activation (23, 24). The non-cell autonomous influence of Notch activation on the myeloid compartment was already reported in T-ALL. Indeed, the constitutive expression of ICN1 in murine bone marrow (BM) progenitors, by retroviral vectors, induces the expansion of $CD11b^+Gr\text{-}1^+$ cells in non-transduced populations (25, 26). On the other hand, myeloid cells may directly influence the onset and progression of T-ALL (27). Nonetheless, the possible arising of MDSCs in T-ALL, their crosstalk with leukemic T cells, and the underlying mechanism/s remain largely undetermined.

Here, we demonstrate that functional $CD11b^+Gr\text{-}1^+$ MDSCs accumulate in a transgenic murine model of Notch3-dependent T-ALL (*N3-tg* mice), bearing an *lck*-driven constitutive expression of ICN3 in T cells (9). The aberrant $CD4^+CD8^+$ [double positive (DP)] T cells from *N3-tg* mice drive the generation of MDSCs in a coculture system with BM progenitors of *wt* mice, as well as in NSG hosts, upon their adoptive transfer. Furthermore, we suggest that induced MDSCs facilitate, in turn, the proliferation and expansion of DP T-ALL cells. We also show that MDSC induction is IL-6-dependent. Finally, we start extending our observations to humans, showing that Notch-deregulated T-ALL cell lines promote *in vitro* the generation of $CD14^+HLA\text{-}DR^{low/neg}$ MDSCs from healthy-donor PBMCs, through a mechanism that depends on both Notch and IL-6.

In summary, our preclinical studies and preliminary observations in humans could pave the way for exploring MDSCs as a potential target of therapy for Notch-dependent T-ALL.

# MATERIALS AND METHODS

## Flow Cytometry and Cell Sorting

Single-cell suspensions of thymus, spleen, BM, or peripheral blood from *N3-tg* or *wt* mice were resuspended in PBS; 2% FBS and erythrocytes were lysed with ammonium-chloride–potassium lysing buffer, as described (28); then, cells were stained with surface markers for 30 min on ice, using anti-CD4-PerCPCy5.5 (RM4-5), anti-CD8-APC (53-6.7), anti-CD11b-FITC (M1/70), and anti-Gr-1-PE (RB6-8C5) antibodies, all from BD Bioscience (La Jolla, CA, USA). For IL-6 detection, freshly isolated BM or thymus cells were stimulated for 4 h with PMA 50 ng/ml and ionomycin 1 μg/ml (Sigma Aldrich, St Louis, MA, USA), in the presence of brefeldin A (Golgi Plug, BD Bioscience, La Jolla, CA, USA). Samples were stained with the appropriate surface markers, followed by the intracellular staining with anti-IL-6-PE (MP5-20F3) antibody or isotype control, performed by using Cytofix/Cytoperm kit (BD Bioscience, La Jolla, CA, USA), according to manufacturer's instructions. For arginase-1 intracellular detection, samples were stained with the appropriate surface markers, followed by the intracellular staining with anti-arginase1-APC (A1exF5) antibody or isotype control (both from Invitrogen/eBiosciences, San Diego, CA, USA), performed by using the FoxP3/Transcription Factor Buffer set (Invitrogen/eBiosciences, San Diego, CA, USA), according to manufacturer's instructions. Samples were run on FacsCalibur, equipped with CellQuestPro software (BD Bioscience, La Jolla, CA, USA).

Human MDSCs were assessed by using antibodies against CD33-FITC (HIM3-4), CD11b-PE (ICRF44), CD14-PerCPCy5.5 (M5E2), HLA-DR-APC (G46-6), and Fixable-Viability Stain 780 to discriminate dead cells, all from BD Bioscience (La Jolla, CA, USA). The samples were run on a BD-LSRFortessa cytometer and analyzed with the FlowJo software (Tree Star). For IL-6 intracellular detection in human T-ALL cell lines, the cells were cultured 5 h in the presence of brefeldin A (Golgi Plug, BD Bioscience, La Jolla, CA, USA). The cells were then stained with 0.25 μg of anti-IL-6-PE (MQ2-13A5) antibody by using Cytofix/Cytoperm kit (BD Bioscience, La Jolla, CA, USA). To discriminate specific staining from artifactual staining, we used ligand blocking control where anti-IL-6 antibodies (0.25 μg) were preblocked for 30 min with an excess of human recombinant IL-6 (1 μg), prior to the addition to sample, according to manufacturer's instructions.

For cell sorting, cell suspensions of thymus, spleen, or BM from *N3-tg* or *wt* mice were stained with anti-CD4, anti-CD8, anti-CD11b, and anti-Gr-1 antibodies, as above. $CD4^+CD8^+$ (DP) T, non-DP T (that includes $CD4^+CD8^-$, $CD4^-CD8^+$, and $CD4^-CD8^-$ T cells, sorted from pre-enriched pan T-cell samples), $CD4^-CD8^+$ or $CD11b^+Gr1^+$ subsets were isolated (purity level ≥97%) with a FACSAriaIII cell sorter, equipped with the FACSDiva software (BD Bioscience, La Jolla, CA, USA).

## RNA Isolation and RT-qPCR

Total RNA was extracted with TRIzol reagent (Invitrogen/ThermoFisher, Waltham, MA, USA), and reverse-transcription was performed with High-Capacity cDNA Reverse-Transcription Kit (ThermoFisher, Waltham, MA, USA). The mRNA expression levels of murine Arginase-1 and IL-6 (Mm00475988_m1 and Mm00446190_m1 assay, respectively, by ThermoFisher, Waltham, MA, USA) were determined by TaqMan quantitative real-time RT-PCR performed on cDNA, using the StepOn ePlus™ Real-Time PCR System (ThermoFisher, Waltham, MA, USA),

following the manufacturer's instructions. Data were analyzed by the ΔΔCt method; murine HPRT was used as reference.

## ELISA

BM supernatants were obtained by flushing bones in 500 µl of ice-cold PBS; after centrifugation, the supernatants were kept and frozen. For serum isolation, whole blood was allowed to clot and supernatant (serum) was collected after centrifugation at 1,000×*g* for 15 min at +4°C. All samples were stored at −80°C. The IL-6 concentration was measured using mouse IL-6 Quantikine ELISA kit (R&D Systems, Minneapolis, MN, USA), according to manufacturer's instructions.

## Detection of ROS Production and pSTAT3 Expression

Freshly isolated cells from BM or spleen of 12-week-old *N3-tg* and *wt* mice were obtained, and ROS production staining was performed upon incubation with MitoSOX Red 5 µM (Molecular Probes/Invitrogen/ThermoFisher, Waltham, MA, USA) for 30 min at 37°C. For the intracellular staining with anti-pSTAT3/pY705-PE (4/P-STAT3) antibody or relative isotype control (both from BD, Bioscience, La Jolla, CA, USA), BM cells were treated with Lyse Fix Buffer and Perm Buffer III (both from BD, Bioscience, La Jolla, CA, USA), according to the manufacturer's recommendations, and then, samples were stained and processed for FACS analysis.

## Western Blotting

Total protein extracts were prepared from human cell line samples, and Western blotting analysis was conducted, as described elsewhere (28), using anti-Notch1-ICD Val1744 (D3B8) antibody (from Cell Signaling, Danvers, MA, USA). Anti-β-actin antibody (Sigma-Aldrich, St Louis, MA, USA) was used to normalize protein expression levels.

## Mice

Eight- to 12-week-old *N3-tg* mice (C57Bl/6 background) (9) and *wt* littermates were used. Immunodeficient nonobese diabetic/severe combined immunodeficient NOD.Cg-*Prkdc*$^{scid}$ *Il2rg*$^{tm1Wjl}$/SzJ (NSG) (29) mice were obtained from Charles River Laboratories (Calco, Italy). Mice were bred and housed in the Institute's Animal Care Facilities. All mice were monitored daily and euthanized upon disease detection (9), as evidenced by an enlarged spleen, hunched posture, ruffled fur, reduced mobility, and/or labored breathing. Experimental groups were based on the age and genotype of mice. The number of mice used in each experiment was reported in figure legends. All procedures involving animals were approved by the local Animal Welfare Committee and conducted in accordance with the recommendations of the Italian national guidelines for experimental animal care and use (D.lgs 26/2014).

## *In Vitro* Suppression Assay and Induction of Murine MDSCs

*wt* T splenocytes were isolated by negative selection (PanT-Cell Isolation KitII, Miltenyi Biotec, Bergisch Gladbach, Germany) and stained with 2.5 µM CFSE (Sigma Aldrich, St Louis, MA, USA). CFSE-labeled T cells were activated with coated 3 µg/ml anti-CD3 and 2 µg/ml anti-CD28 (BD Bioscience , La Jolla, CA, USA), and $3.0 \times 10^5$ cells/well ("responders") were cocultured with graded numbers of CD11b$^+$Gr1$^+$ splenocytes ("suppressors"), sorted from the spleen of *wt* or *N3-tg* mice. Cocultures were performed for 72 h in 96-well plates. Samples were then harvested and stained, and proliferating cell percentage was evaluated as CFSE dilution by FACS analysis on gated CD4$^-$CD8$^+$ T cells. To induce MDSCs from BM myeloid progenitors (30), $3.5 \times 10^6$/well of total cells from *wt* BM were placed in 6-well plates and cocultured for 5 days at a 1:1 ratio with sorted BM DP T cells from 12-week-old *N3-tg* mice by using transwell inserts (pore diameter, 0.4 µm, Falcon/Corning, NY, USA). The Gr1$^+$ cells (suppressors) that were also CD11b$^+$ at 99.0% (not shown) were then selected from the harvested samples (purity ≥93%) by using biotin-anti-Gr1 antibody and streptavidin magnetic microbeads (Miltenyi Biotec, Bergisch Gladbach, Germany) and were cultured with activated and CFSE-labeled *wt* T splenocytes (responders), to assess their function, as above. We used Gr1$^+$ fractions from *wt* BM cells cultured alone or supplemented with GM-CSF 40 ng/ml (STEMCELL Technologies, Vancouver, Canada) as negative and positive controls. For IL-6 neutralization, we performed MDSC induction assay in the presence of anti-IL-6 (MP5-20F3) antibodies or isotype controls (BD Bioscience, La Jolla, CA, USA) at 2 µg/ml.

## Treatment of *N3-tg* Mice With Anti-IL-6 or Anti-Gr-1 Antibodies

To neutralize IL-6, we used 300 µg/mouse of anti-mouse IL-6 (MP5-20F3) antibodies or RatIgG anti-horseradish peroxidase (HRPN) isotype controls (both *in vivo*MAb from BioXCell, Lebanon, NH, USA). To deplete Gr-1$^+$ cells, we used 250 µg/mouse of anti-mouse Ly6G/Ly6C (Gr-1, RB6-8C5 clone) antibodies or RatIgG2b (LTF-2 clone) isotype controls (both *in vivo*Plus from BioXCell, Lebanon, NH, USA). In another set of experiments, mice were treated with both anti-IL-6 and anti-Gr-1 antibodies. We treated 8-week-old *N3-tg* mice with intraperitoneal injections of the relevant antibodies, resuspended in 200 µl/mouse of PBS1×, twice a week for 4 weeks. Mice were then sacrificed and characterized by FACS analysis, as above. Some of the mice were also intraperitoneally injected with BrdU (1.5 mg/mouse; BD Bioscience, La Jolla, CA, USA), 24 h before the sacrifice. Single-cell suspensions from the spleen and BM were then stained with the BrdU-flow kit (BD Bioscience, La Jolla, CA, USA), according to the manufacturer's instructions, and Gr-1$^+$BrdU$^+$ and CD4$^+$CD8$^+$BrdU$^+$ cell percentages were assessed by FACS analysis. At the end of the assay, Gr-1$^+$ cell fractions were magnetically purified from spleens and tested by suppression assay, as above.

## Adoptive Transfer of CD4$^+$CD8$^+$ (DP) T Cells

We intravenously injected 6–10-week-old NSG female mice with $2–4 \times 10^6$ of DP T cells sorted from the BM of 8-week-old *N3-tg* mice or thymus of *wt* littermates and resuspended in 200 µl/mouse of PBS1×. Each of the *N3-tg* or *wt* donors had two NSG recipients that were sacrificed at 3–5- and 9–11-week posttransplantation, respectively, and analyzed by FACS procedures. CD11b$^+$Gr-1$^+$ BM cells from NSG recipients at 9–11-week posttransplantation were sorted and assessed by suppression assay, as above.

## Cell Lines

The human cell lines of Notch1-dependent T-ALL, KE-37 (11) and of Notch3-dependent T-ALL, TALL-1 (31), and the human Notch-independent T-ALL cell line, Loucy (12, 32), were cultured at 37°C and 5% $CO_2$ in RPMI-1640 (GIBCO/ThermoFisher, Waltham, MA, USA) complete medium, supplemented with 10% FBS, 10 U/ml penicillin and streptomycin, and 2 mM glutamine. The Loucy cell line was purchased from the ATCC (#CRL-2629). Cells were routinely verified to be mycoplasma free by using a PCR detection kit (Mycoplasma #G238, Abm Inc., Richmond, Canada).

## Induction of Human MDSCs

Human PBMCs from healthy donors were isolated by density gradient centrifugation on Ficoll-PaquePLUS (GE Healthcare-Amersham, GB). We put $5 \times 10^6$/well of PBMCs in 6-well plates and cocultured with $2.5 \times 10^6$ of KE-37 or TALL-1 cell lines, in transwell inserts (pore diameter, 0.4 μm, Falcon/Corning, NY, USA), for 6 days. Autologous PBMCs cultured in medium alone were run in parallel, as a control. The T-ALL cells were then removed, and all the remaining cells were collected. Adherent cells were harvested by using the Accutase detachment solution (BD Bioscience, La Jolla, CA, USA). In some cases, the cocultures were conducted in the presence of neutralizing anti-IL-6 (MQ2-13A5) antibodies or isotype controls (BD Bioscience, La Jolla, CA, USA), at 10 μg/ml, or with GSI IX (DAPT, Calbiochem/Sigma Aldrich, St Louis, MA, USA), at 10 μM. In another set of experiments, GSIs and anti-IL-6 antibodies were used together. The $CD33^+$ cell fractions were isolated from the harvested samples above, by using anti-CD33 magnetic microbeads (Miltenyi Biotec, Bergisch Gladbach, Germany; purity ≥92%), and evaluated by their ability to inhibit the proliferation of $CD4^-CD8^+$ T-gated cells from CFSE-stained autologous PBMCs, upon activation with coated anti-CD3 and soluble anti-CD28 (at 1 and 5 μg/ml, respectively, BD Bioscience, La Jolla, CA, USA), at 72 h of culture. Blood samples from healthy donors were obtained upon written informed consent, and all the human investigations were conducted in accordance with the Declaration of Helsinki, and approval was obtained from the Institutional Ethics Committee.

## Statistical Analysis

Data were reported as mean ± SD from at least three independent experiments unless otherwise specified. Statistical analysis was performed using unpaired 2-tailed Student's *t*-test to analyze the difference between two groups, using GraphPad software (San Diego, CA, USA). *p*-values of ≤0.05 are considered statistically significant. $^*p \le 0.05$, $^{**}p \le 0.01$, $^{***}p \le 0.001$, and $^{****}p \le 0.0001$ are significant differences between the indicated groups; not significant (ns), $p > 0.05$.

# RESULTS

## MDSCs Populate the T-ALL Environment of *N3-tg* Mice

In murine models of Notch-dependent T-ALL, aberrant immature T cells, including $CD4^+CD8^+$ (DP) T cells, infiltrate the BM (8, 10, 28, 33). Immature T cells from Notch-dependent T-ALL-bearing mice are also able to induce non-cell autonomous expansion of the myeloid compartment (25, 26). In particular, *N3-tg* mice develop an aggressive form of T-ALL. The typical disease signs (enlarged spleen, hunched posture, ruffled fur, reduced mobility, and/or labored breathing) become evident starting at 6–8 weeks of age and 95% of animals have died by 16 weeks of age (9). They develop tumors with heterogeneous phenotypes, regarding the expression of CD4 and CD8 markers, including some in which peripheral tumor T cells display a prevalent $CD4^-CD8^-$ or $CD4^+CD8^-$ or $CD4^-CD8^+$ phenotype (9). However, more than 90% of *N3-tg* transgenic mice show the presence of aberrant DP T cells in the BM and spleen (AFC and PG, unpublished data), and their accumulation in the periphery raises along with the disease progression and represents a pathognomonic feature (33–35).

We have already shown that aberrant DP T cells massively colonize the BM of *N3-tg* mice and that their numbers increase with age (33). Now, we report a marked expansion of the $CD11b^+Gr\text{-}1^+$ myeloid subset in the spleen (**Figure 1A**), as well as in peripheral blood (PB) and BM (**Figure 1B**) of *N3-tg* mice, when compared with *wt* littermates.

In mice, $CD11b^+Gr\text{-}1^+$ MDSCs express a high level of "reactive species of oxygen" (ROS) and arginase-1, which are related to the immunosuppressive function (36), and STAT3-signaling activation is crucial during their expansion/activation phase (37). We found a significant increase of arginase-1 expression, at mRNA and protein levels (**Supplementary Figures S1A, B**, respectively), and of the proportion of both ROS-producing cells (**Supplementary Figure S1C**) and phosphorylated STAT3 (pSTAT3) protein-expressing cells (**Supplementary Figures S1D, E**), inside the $Gr\text{-}1^+$ subset from *N3-tg* mice, with respect to *wt* counterparts. However, the immunosuppressive function remains one of the most important features of MDSCs (13). Strikingly, we observed that $CD11b^+Gr\text{-}1^+$ splenocytes from *N3-tg* mice do exert *in vitro* a dose-dependent suppressive activity on proliferating *wt* $CD4^-CD8^+$ T cells, which is significantly higher than that of *wt* controls (**Figures 1C, D**).

Overall, our results demonstrate that functional $CD11b^+Gr\text{-}1^+$ MDSCs are present in the tumor environment of Notch3-dependent T-ALL.

## $CD4^+CD8^+$ (DP) T Cells from *N3-tg* Mice Induce MDSCs *In Vitro*, Through an IL-6-Dependent Mechanism

To start shedding light on the mechanism of Notch-driven MDSC induction, we explored the potential role of the proinflammatory cytokine IL-6, a remarkable factor in the expansion/activation of MDSCs (37). The IL-6 concentration in blood serum is undetectable in *wt* controls, whereas it increases with age in *N3-tg* mice (**Figure 2A**). IL-6 concentration is also higher in the BM supernatants of *N3-tg* mice, compared with *wt* littermates (**Figure 2B**). Furthermore, DP T cells from transgenic animals express more IL-6 at mRNA level (**Figure 2C**) and present a greater percentage of IL-6 protein-expressing cells (**Figure 2D**) when compared with

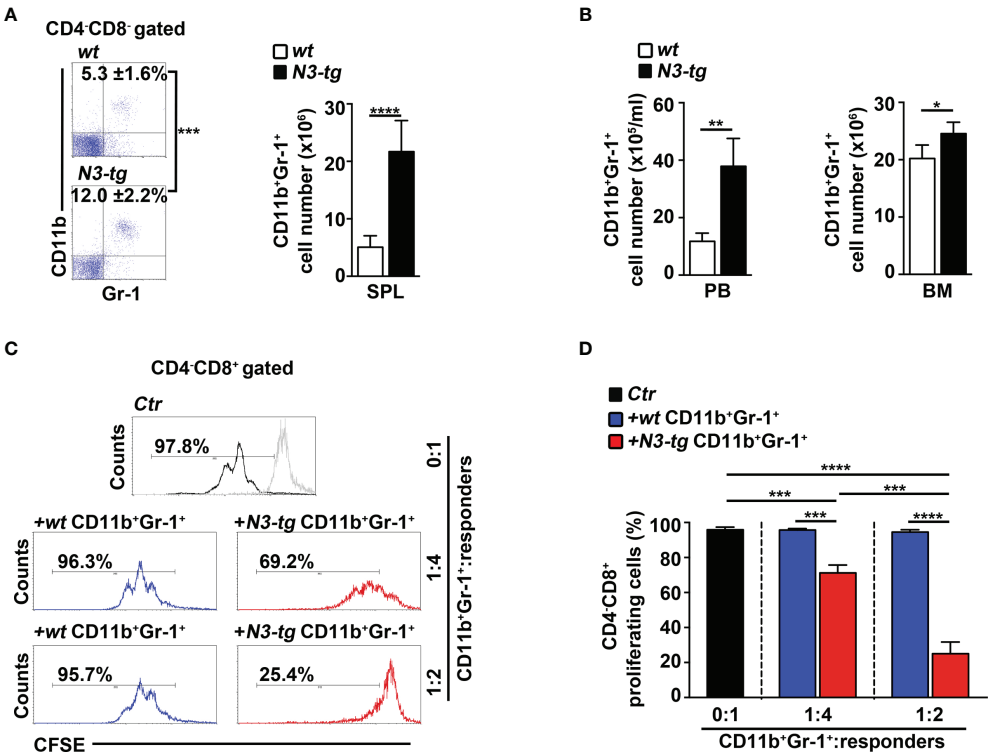


**FIGURE 1** | CD11b$^+$Gr-1$^+$ MDSCs expand in *N3-tg* mice. **(A)** Percentages and absolute numbers of CD11b$^+$Gr-1$^+$ cells, as assessed by FACS analysis distribution of CD4 vs. CD8 vs. CD11b vs Gr-1 markers in spleen (SPL) of *N3-tg* and *wt* mice. Numbers inside cytograms indicate mean percentages ± SD of CD11b$^+$Gr-1$^+$ cells. The cytograms in this panel illustrate the percentages of CD11b$^+$Gr-1$^+$ splenocytes inside the CD4$^-$CD8$^-$ subset, to avoid any possible dilution effect due to the presence of DP T cells in transgenic mice. **(B)** CD11b$^+$Gr-1$^+$ numbers in peripheral blood (PB) and BM from *N3-tg* vs. *wt* mice, assessed by FACS analysis, as in **(A)**. In **(A, B)**, the values are presented as mean ± SD of four independent experiments ($n$ = 6 mice per group). **(C)** Representative FACS analysis of suppression assay with CFSE-labeled/activated *wt* T splenocytes ("responders"), cultured either alone (Ctr), as a control, or in combination with CD11b$^+$Gr-1$^+$ "putative" MDSCs ("suppressors"). Numbers inside cytograms represent percentages of proliferating CD4$^-$CD8$^+$ responder cells. Similar results were obtained by analyzing the proliferation rate of gated *wt* CD4$^+$CD8$^-$ T responder cells (not shown). CD11b$^+$Gr-1$^+$ cells were sorted from spleen of *N3-tg* or *wt* mice and used at the indicated CD11b$^+$Gr-1$^+$:responders ratio. The gray line represents nonactivated negative controls. In **(D)**, results of suppression test, as in **(C)**, are illustrated as mean values ± SD from three independent experiments ($n$ = 3 mice per group), with two technical replicates per experiment. All the mice were analyzed at 12 weeks of age. $^*p \le 0.05$, $^{**}p \le 0.01$, $^{***}p \le 0.001$, and $^{****}p \le 0.0001$ represent significant differences between the indicated groups.

control *wt* DP thymocytes. We hypothesized that *N3-tg* DP T cells could contribute to inducing MDSCs through IL-6. It is important to note that literature shows that it is possible to drive *in vitro* the differentiation of MDSCs from their *wt* BM precursors, through their exposure to cytokines, including IL-6 (30), but also in coculture with tumor cell lines (38). Thus, we performed coculture experiments of total BM cells from *wt* mice with DP T cells from the BM of *N3-tg* mice, in the presence of neutralizing anti-IL-6 antibodies or isotype controls and by using transwell inserts. At the end of the assay, we selected Gr-1$^+$ fractions from the harvested coculture samples and controls and used them in a suppression test. We observed that Gr-1$^+$ cells selected from *wt* BM cocultured with *N3-tg* DP T cells are functional MDSCs, whereas inhibitory activity is greatly impaired by the addition of anti-IL-6 antibodies during the coculturing time (**Figures 3A, B**). The suppressive function of control Gr1$^+$ cells selected from *wt* BM cultured in medium alone (**Figure 3C**, white bars), as well as in the presence of anti-IL-6 antibodies or isotype controls (**Supplementary Figure S2A**), was instead negligible. We also used Gr1$^+$ cells selected from *wt BM* cells cultured in medium supplemented with GM-CSF, as positive controls (**Figure 3C**, grey bars). Furthermore, Gr1$^+$ cells from *wt* BM cultured with recombinant IL-6 or cocultured with *wt* DP thymocytes, in the presence or not of IL-6, are not suppressive (**Supplementary Figure S2B**), suggesting that induction of MDSCs requires *N3-tg* DP T cells. As stated above, aberrant DP T cells colonize the periphery in the vast majority of *N3-tg* animals, and thus, we focused our observations and experiments on them. However, other T-cell subsets from *N3-tg* mice may include tumor cells and could exert similar effects on MDSCs. Indeed, *N3-tg* non-DP T cells (defined as a mixture of CD4$^+$CD8$^-$, CD4$^-$CD8$^+$, and CD4$^-$CD8$^-$ T cells, sorted from pre-enriched pan T-cell samples), as well as CD4$^-$CD8$^+$ cells from *N3-tg* mice are comparable with transgenic DP T cells in inducing MDSCs (**Supplementary Figure S2B**).

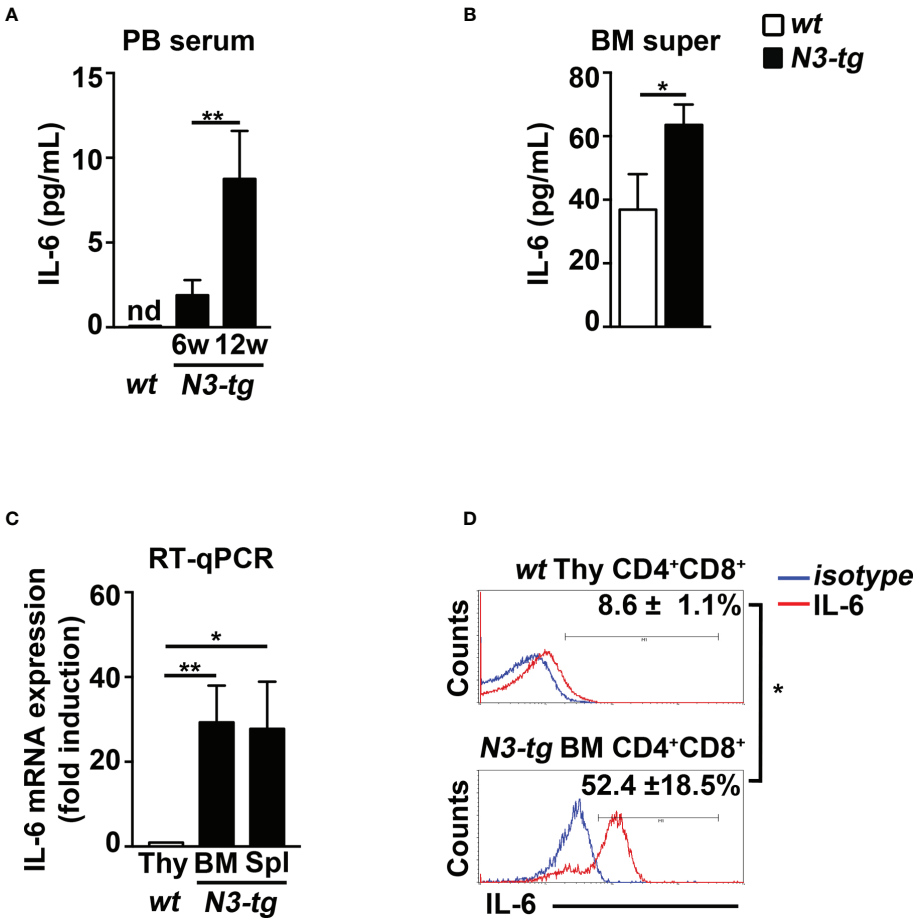


**FIGURE 2** | *N3-tg* mice display high levels of IL-6. IL-6 protein concentration assessed by ELISA **(A)** in blood serum (PB serum), from *N3-tg* vs. *wt* mice at 6 and 12 weeks of age, and **(B)** in BM supernatant (BM super), from *N3-tg* vs. *wt* mice at 12 weeks of age. **(C)** RT-qPCR of relative IL-6 mRNA expression in DP T cells sorted from BM or spleen (Spl) of *N3-tg* mice or from *wt* thymus (Thy), as a control, at 12 weeks of age. IL-6 mRNA expression levels in *wt* DP thymocytes are set as 1. **(D)** Representative FACS analysis of intracellular IL-6 staining in DP T cells from *N3-tg* BM or from *wt* thymus (Thy), at 12 weeks of age, upon 4 h of PMA/ionomycin stimulation (red lines). Blue lines, isotype controls. Numbers inside cytograms represent mean percentages ± SD of IL-6$^+$ cells inside CD4$^+$CD8$^+$ subset. The values are presented as mean ± SD from three independent experiments ($n$ = 4 mice per group), and in **(A–C)** with three technical replicates per experiment. nd, not detectable; *$p \leq 0.05$ and **$p \leq 0.01$ represent significant differences between the indicated groups.

In summary, our data show that aberrant DP T cells from the BM of T-ALL-bearing *N3-tg* mice induce MDSCs, through a mechanism that is IL-6-dependent.

## CD4$^+$CD8$^+$ (DP) T Cells From *N3-tg* Mice Drive the Expansion of CD11b$^+$Gr-1$^+$ MDSCs in NSG Host Mice

To corroborate *in vivo* our conclusions above, we performed adoptive transfer experiments of DP T cells from the BM of *N3-tg* mice or the thymus of *wt* mice, as a control. We used immunodeficient NSG hosts, which are devoid of T, B, and NK cells, but retain the CD11b$^+$Gr-1$^+$ subset (29). This model allows us to test if aberrant *N3-tg* DP T cells are able to drive the generation of MDSCs, by acting directly on their precursors, avoiding any possible interference by other immune-cell populations. We reported that *N3-tg* DP T cells (DP*tg*) efficiently engraft the BM of NSG recipients (**Supplementary Figure S3**), compared with what was observed with control *wt* DP thymocytes (*DPwt*). Notably, transplanted DP*tg* cells induce the expansion of the myeloid compartment in the BM of their NSG hosts; in fact, in the BM of these recipients, the CD11b$^+$Gr-1$^+$ absolute numbers progressively increase and are always significantly higher, with respect to those observed in NSG control mice, transplanted with DP*wt* control cells (**Figure 4A**). We then sorted CD11b$^+$Gr-1$^+$ cells from NSG-transplanted mice and tested them in an *in vitro* suppression test (**Figures 4B, C**). We observed that the CD11b$^+$Gr-1$^+$ cells from the NSG recipients of DP*tg* cells (CD11b$^+$Gr-1$^+$/DP*tg*) are functional MDSCs, whereas the suppressive ability of control counterparts (CD11b$^+$Gr-1$^+$/DP*wt*), is negligible. Overall, our data prove that N3-*tg* DP T cells can induce MDSCs *in vivo*. However, the NSG model has some limitations, and it will be interesting in the future to perform our adoptive transfer experiments in immunocompetent mice in order

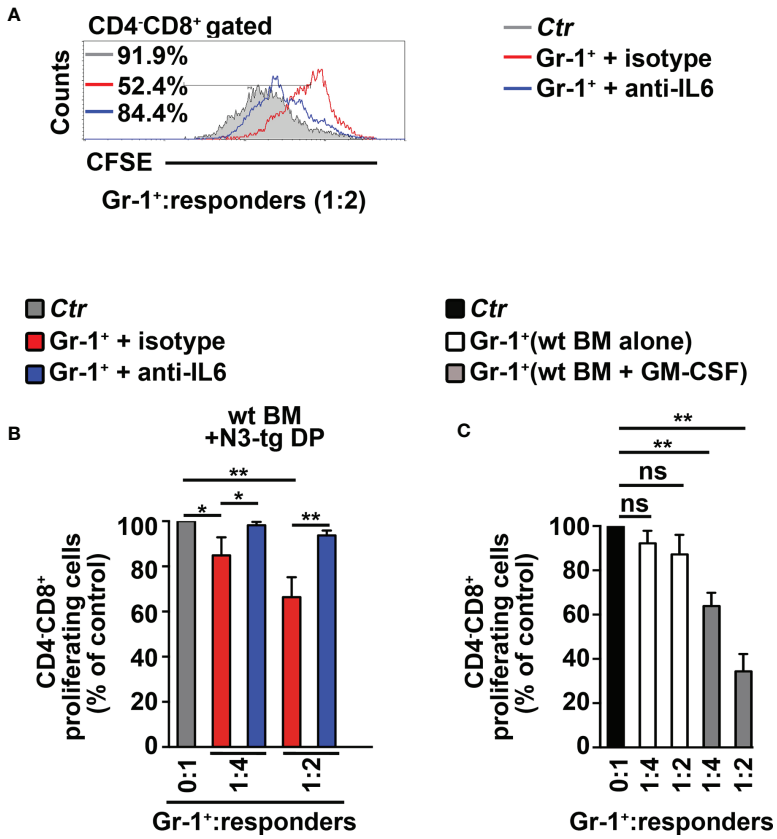


**FIGURE 3** | $CD4^+CD8^+$ (DP) T cells from *N3-tg* mice drive *in vitro* differentiation of MDSCs through IL-6. **(A)** Representative FACS analysis of suppression assay with CFSE/activated *wt* T splenocytes ("responders"), cultured either alone (Ctr), as a control, or in combination with Gr-$1^+$ cells (Gr-$1^+$), at the indicated Gr-$1^+$/responders ratio. Numbers inside cytograms indicate the percentages of proliferating *wt* $CD4^-CD8^+$ T responder cells. Gr-$1^+$ cells were magnetically selected from 5-day cocultures of total *wt* BM cells with DP T cells from BM of *N3-tg*, in the presence of anti-IL-6-neutralizing antibodies (blue line) or isotype controls (red line), and by using transwell inserts. In **(B)**, the results of the same suppression test, as in **(A)**, are illustrated as mean values ± SD from multiple experiments, see below. **(C)** The suppression test was performed by using *wt* T responder cells cultured either alone (black bar), as a control, or in combination with Gr-$1^+$ cells (Gr-$1^+$), selected, as above, from total *wt* BM cells cultured in medium alone or supplemented with GM-CSF (white bars and gray bars, respectively), for 5 days, and used at the indicated Gr-$1^+$:responders ratios. In **(B, C)**, the results are calculated as the ratio between percentages of proliferating $CD4^-CD8^+$ T responder cells in Gr-$1^+$-containing cultures and in controls, set up in the absence of Gr-$1^+$ cells, and are expressed as % of control. The results represent the mean values ± SD from three independent experiments ($n$ = 3 mice per group), with two technical replicates per experiment. ns, not significant, $p > 0.05$; $^*p \leq 0.05$, and $^{**}p \leq 0.01$ represent significant differences between the indicated groups.

to conduct a more comprehensive analysis of T-ALL cell interactions with the immune system during MDSC induction.

## The Inhibition of IL-6 Impairs MDSCs in *N3-tg* Mice

To confirm the role of IL-6 in mediating the Notch-dependent induction of MDSCs, we treated *N3-tg* mice with repeated *i.p.* injections of neutralizing anti-IL-6 antibodies or isotype controls. The anti-IL-6-treated *N3-tg* mice reveal a significant decrease of $CD11b^+$Gr-$1^+$ cell count proportions (**Figure 5A**), and of the proliferating Gr-$1^+$$BrdU^+$ cell percentages (**Figure 5B**) in BM and spleen, when compared with controls, with no significant variation of total numbers of DP T- or other T-cell subsets (not shown), thus excluding that effects of neutralizing antibodies on $Gr1^+$ subset are indirect. The *in vitro* suppression activity exerted by $CD11b^+$Gr-$1^+$ MDSCs from the spleen of *N3-tg* mice is impaired upon treatment with anti-IL-6 antibodies (**Figures 5C, D**). Thus, our *in vivo* experiments confirm the significant contribution of IL-6 in promoting the accumulation of MDSCs.

## MDSCs Sustain Expansion and Proliferation of $CD4^+CD8^+$ (DP) T Cells in *N3-tg* Mice

We aimed to study the impact of MDSCs on T-ALL cell behavior. Thus, we performed experiments of i.p. injections with the RB6-8C5 antibody (39) that significantly deplete Gr-$1^+$ cells in spleen and peripheral blood (**Supplementary Figures S4A, B**) and impair their suppressive function in BM (**Supplementary Figure S4C**) of *N3-tg* mice. Notably, this treatment leads to a significant decrease of the percentages and cell count proportions of DP T cells (**Figures 6A, B**), as well as of

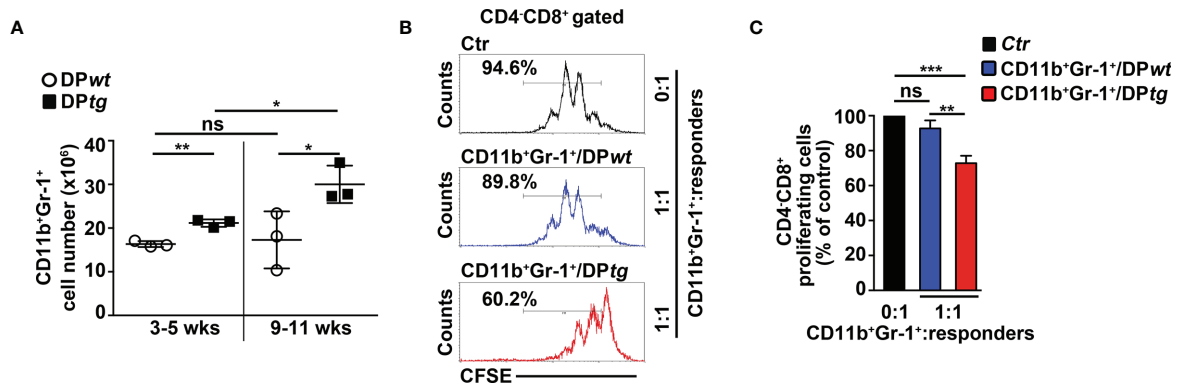


**FIGURE 4** | $CD4^+CD8^+$ (DP) T cells from *N3-tg* mice induce $CD11b^+Gr\text{-}1^+$ MDSCs in NSG hosts. NSG recipients were transplanted *i.v.* with $CD4^+CD8^+$ (DP) T cells sorted from BM of *N3-tg* mice (DP*tg*; $n = 3$ donors) or from thymus of *wt* mice (DP*wt*; $n = 3$ donors), as a control. Each of the donors has two recipients. NSG recipients were sacrificed at 3–5 weeks ($n = 3$ NSG recipients per group) and 9–11 weeks ($n = 3$ NSG recipients per group) posttransplantation and analyzed by FACS. **(A)** Absolute numbers of $CD11b^+Gr\text{-}1^+$ cells in BM of NSG mice, recipients of DP*wt* or DP*tg* cells, assessed by FACS analysis, at 3–5 and 9–11 weeks posttransplantation. **(B)** Representative FACS analysis of *in vitro* suppression assay of activated/CFSE-labeled *wt* T splenocytes ("responders"), cultured either alone (Ctr), as a control, or in combination with $CD11b^+Gr\text{-}1^+$ cells (as putative "suppressors"), at the indicated $CD11b^+Gr\text{-}1^+$/responders ratio. Numbers inside cytograms indicate the percentages of proliferating *wt* $CD4^-CD8^+$ T responder cells. $CD11b^+Gr\text{-}1^+$ cells were sorted from BM of NSG hosts, at 9–11 posttransplantation with DP*wt* ($CD11b^+Gr\text{-}1^+$/DP*wt*) or DP*tg* ($CD11b^+Gr\text{-}1^+$/DP*tg*) cells. In **(C)**, the results of suppression test, as in **(B)**, are calculated as ratio between percentages of proliferating *wt* $CD4^-CD8^+$ T cells in $CD11b^+Gr\text{-}1^+$-containing cultures ($CD11b^+Gr\text{-}1^+$/DP*wt* or $CD11b^+Gr\text{-}1^+$/DP*tg*) and in control cultures set up in the absence of $CD11b^+Gr\text{-}1^+$ (Ctr) and are expressed as % of control. Data represent the mean values ± SD from three independent experiments ($n = 3$ mice per group), with two technical replicates per experiment in **(C)**. ns, not significant, $p > 0.05$; $^*p \le 0.05$, $^{**}p \le 0.01$, and $^{***}p \le 0.001$ represent significant differences between the indicated groups.

the $CD4^+CD8^+BrdU^+$ cell percentages (**Figures 6C, D**), in the BM of anti-Gr-1-treated *N3-tg* mice, when compared with controls, with more limited effects on DP T splenocytes. We also reported that IL-6 protein levels in PB serum of anti-Gr1 *N3-tg*-treated mice decrease (**Supplementary Figure S4D**). This could be related to the reduction of IL-6-producing DP T cells in treated mice. However, we cannot rule out that it also derives from the depletion of IL-6-producing MDSCs/myeloid cells (40, 41).

Finally, we tried to improve the effects of MDSC depletion on disease progression by treating *N3-tg* mice with both anti-Gr-1 and neutralizing anti-IL-6 antibodies. Notably, we observed significant reductions of important parameters of disease progression in our model (9, 33–35), such as total splenocyte and DP T-cell numbers, as well as of $Brdu^+$ DP T-cell percentages, in the spleen of *double-treated* mice, when compared with RB6-8C5-treated mice or controls (**Figure 6E**). In summary, our results show that MDSCs sustain the accumulation and proliferation of aberrant DP T cells from Notch3-dependent T-ALL.

## Human Notch-Dependent T-ALL Cell Lines Induce MDSCs From Healthy PBMCs

We tried to extend our remarks above to humans, by performing coculture experiments of PBMCs from healthy donors with human Notch-dependent T-ALL cell lines. First, we used the Notch1-activated KE-37 cell line, being Notch1 a frequent target of oncogenic gain-of-function mutations in T-ALL patients (11). Interestingly, KE-37 cells are GSI resistant and Notch3 negative (42) and express intracellular IL-6 (**Supplementary Figure S5A**). The harvested PBMCs/KE-37 coculture samples reveal a significant increase of $CD14^+HLA\text{-}DR^{low/neg}$ "putative" MDSCs, both in percentages (**Figures 7A, B**, left panel) and absolute numbers (**Figure 7B**, right panel), when compared with samples of autologous PBMCs cultured alone. At the end of the culture, we selected the $CD33^+$ fractions from all the harvested samples and assessed their suppressive function on autologous $CD4^-CD8^+$ T cells. We revealed that $CD33^+$ cells from PBMCs/KE-37 cocultures are highly suppressive MDSCs (**Figure 7C**) when compared with those from PBMCs cultured alone. Importantly, the KE-37 line is part of a group of human T-ALL cell lines in which the growth is not inhibited by GSI treatment, probably due to a lack in the expression of the *PTEN* gene, although GSI is effective in blocking Notch1 activation [(43) and references therein]. Indeed, we confirmed the expression of Notch1 intracellular domain in KE-37 cells and its downmodulation upon GSI treatment, during cocultures with PBMCs (**Supplementary Figure S6A**). We then repeated the PBMCs/KE-37 coculture experiments in the presence of gamma-secretase inhibitors or neutralizing anti-IL-6 antibodies. We observed that the inhibition of Notch activation or the block of IL-6 signals induces significant reductions of MDSC expansion (**Figures 7D, E**, respectively).

We measured the expression of IL-6 protein by FACS analysis in T-ALL cells, as well as in cell subsets of human PBMCs in our experiments of cocultures. At day 6, KE-37 cells produce IL-6 when cultured alone and also upon cocultures with PBMCs, showing no significant variation between the two conditions (**Supplementary Figure S6B**, left panel). Conversely, the expression of IL-6 appears very low in both T-cell and myeloid cell compartments of PBMCs

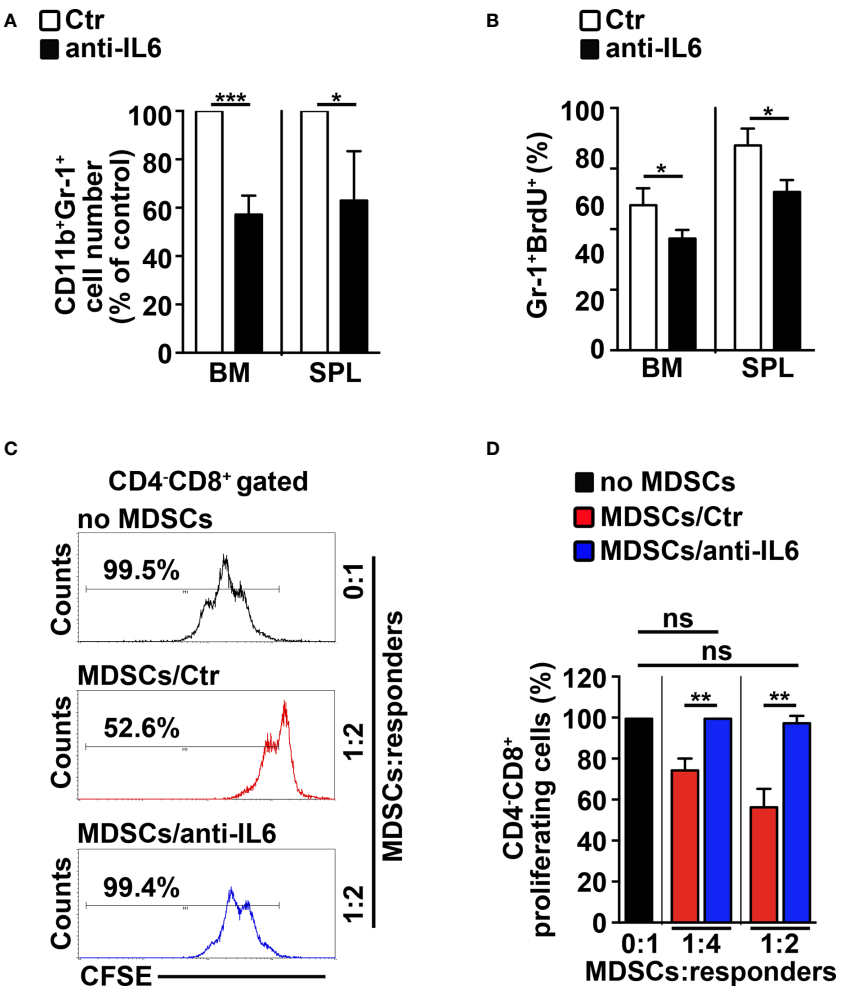


**FIGURE 5** | IL-6 neutralization impairs MDSCs in *N3-tg* mice. *N3-tg* mice were injected *i.p.* with neutralizing anti-IL-6 antibodies (anti-IL-6) or isotype controls (Ctr), twice a week and sacrificed/analyzed after 4 weeks of treatment; some of the mice were also injected *i.p.* with BrdU solution 1 day before the sacrifice. **(A)** The graph reports the ratio between the $CD11b^+Gr\text{-}1^+$ cell counts in anti-IL-6-treated *N3-tg* mice and in control mice, expressed as % of control, measured by FACS analysis in the BM and spleen (SPL) and presented as mean value ± SD from three independent experiments ($n$ = 4 mice per group). **(B)** The percentages of $Gr\text{-}1^+BrdU1^+$ cells in the BM and SPL of anti-IL-6-treated *N3-tg* mice vs. controls are shown, assessed by FACS analysis. The data are presented as the mean value ± SD from two independent experiments ($n$ = 3 mice per group). **(C)** Representative FACS analysis of suppression assay of CFSE-labeled/activated *wt* T splenocytes ("responders"), cultured either alone (no MDSC), as a control, or in combination with $Gr\text{-}1^+$ MDSCs ("suppressors"), at the indicated MDSCs/responders ratio. Numbers inside cytograms indicate the percentages of proliferating *wt* $CD4^-CD8^+$ T responder cells. The $Gr\text{-}1^+$ MDSCs were magnetically selected from spleen of *N3-tg* mice, treated with isotype control antibodies (MDSCs/Ctr) or anti-IL-6-neutralizing antibodies (MDSCs/anti-IL-6). In **(D)**, the results of the same suppression test, as in **(C)**, are illustrated as the percentage of proliferating $CD4^-CD8^+$ responder cells in MDSC-containing cultures (MDSCs/Ctr or MDSCs/anti-IL-6) and in control cultures set up in the absence of MDSCs (no MDSCs), at the indicated MDSCs:responders ratio. The results represent mean values ± SD from two independent experiments ($n$ = 3 mice per group), with two technical replicates per experiment. ns, not significant, $p > 0.05$; $^*p \leq 0.05$; $^{**}p \leq 0.01$, $^{***}p \leq 0.001$ represent significant differences between the indicated groups.

cultured either alone or with KE-37 line (**Supplementary Figure S6B**, middle and right panels, respectively). Our results suggest that T-ALL cells may represent the main producer of IL-6 during MDSC induction, at least *in vitro*.

Furthermore, we performed experiments above with the Notch3-activated T-ALL cell line, TALL-1 (31) that is $IL\text{-}6^+$ (**Supplementary Figure S5A**) and Notch1-negative (42). TALL-1 cells promote the induction of suppressive MDSCs (**Supplementary Figures S5B–D**) that is inhibited by exposure to GSIs or anti-IL-6 antibodies (**Supplementary Figures S5E, F**, respectively). Collectively, our results indicate that Notch3 deregulation, as well as Notch1 deregulation, is capable of inducing MDSCs. In other words, it seems that the activation of Notch pathway in a T-ALL context induces MDSCs no matter which Notch receptor is activated.

We then tried to better clarify the Notch/IL-6 crosstalk during the induction of MDSCs, by using both GSIs and neutralizing anti-IL-6 antibodies, compared with GSIs alone, in our coculture

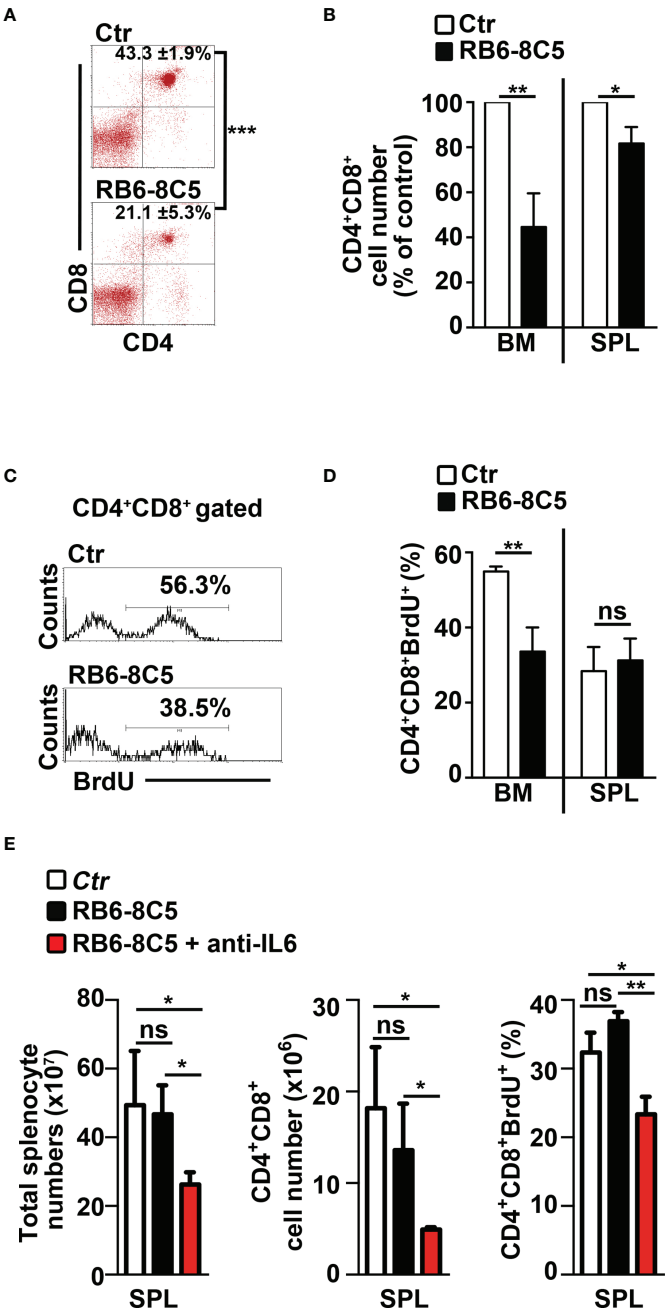


**FIGURE 6** | Gr-1 depletion affects $CD4^+CD8^+$ (DP) T cells in *N3-tg* mice. *N3-tg* mice were injected *i.p.* with anti-Gr-1 depleting antibodies (RB6-8C5) or isotype controls (Ctr), twice a week and sacrificed/analyzed after 4 weeks of treatment; some of the mice were also injected *i.p* with BrdU solution 1 day before the sacrifice. **(A)** Percentages of $CD4^+CD8^+$ cells are shown, as measured by FACS analysis in the BM of *N3-tg* mice, treated as above. Numbers inside cytograms indicate the mean percentages ± SD of $CD4^+CD8^+$ cells. **(B)** The graph reports the ratio between the $CD4^+CD8^+$ cell counts in RB6-8C5-treated *N3-tg* mice and in relative controls, expressed as % of control, and calculated in the BM and spleen (SPL), by the same FACS analysis, as in **(A)**. In **(A, B)**, the data are presented as the mean value ± SD from three independent experiments ($n$ = 4 mice per group). **(C)** Representative FACS analysis of $BrdU^+$ cells inside the $CD4^+CD8^+$ subset in the BM of *N3-tg* mice, treated as above, with isotype control antibodies (Ctr) or anti-Gr-1 depleting antibodies (RB6-8C5). Numbers inside cytograms indicate the percentages of $CD4^+CD8^+BrdU^+$ cells. **(D)** The graphs show the $CD4^+CD8^+BrdU^+$ cell percentages in the BM and spleen (SPL) of *N3-tg* mice, treated as above, and measured by the same FACS analysis, as in **(C)**. We have not observed any effects of anti-Gr-1 treatment on T-cell compartment of *wt* mice (not shown). **(E)** The graphs report total cell counts (left panel), absolute numbers of DP T cells (middle panel), and percentages of $BrdU^+$DP T cells (right panel), in mice injected with RB6-8C5 antibodies alone (black bars), or in combination with anti-IL-6 antibodies (red bars), compared with controls (white bars). In **(D, E)**, the results are presented as the mean value ± SD from two independent experiments ($n$ = 3 mice per group). ns, not significant, $p > 0.05$; $^*p \leq 0.05$; $^{**}p \leq 0.01$, and $^{***}p \leq 0.001$ represent significant differences between the indicated groups.

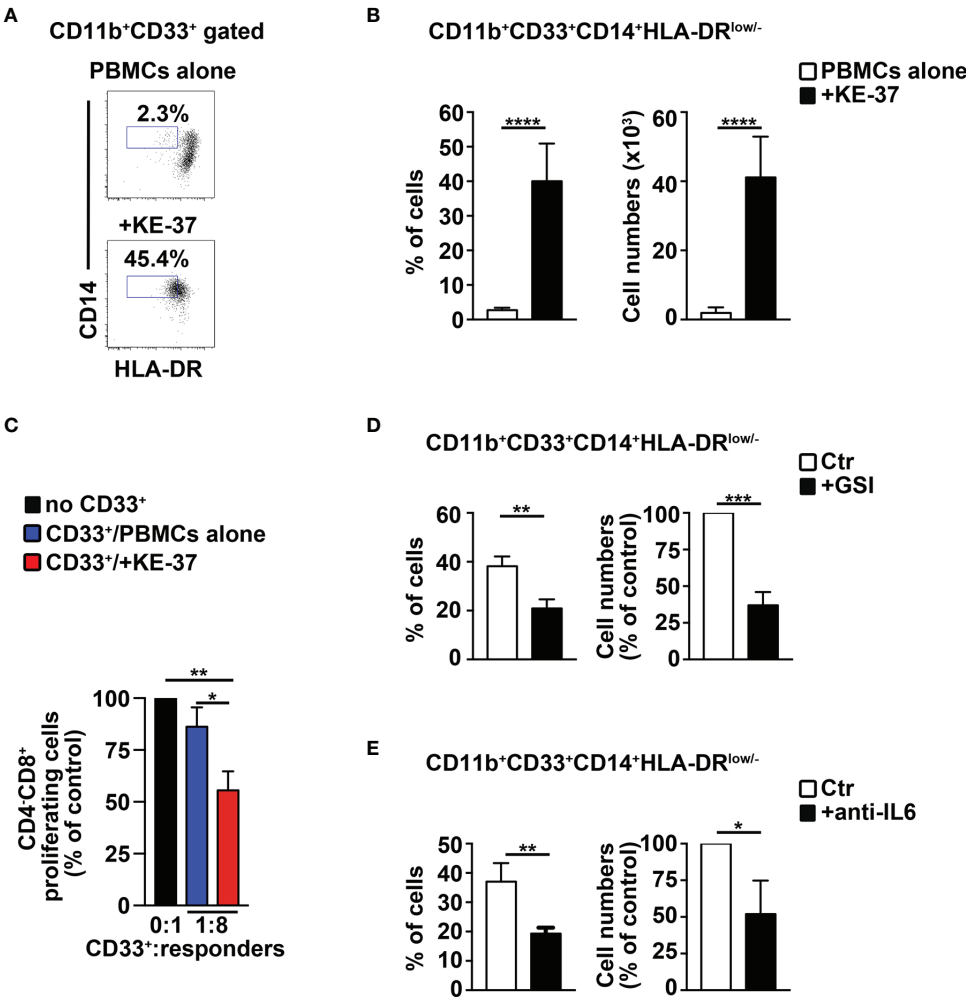


**FIGURE 7** | The Notch1-active T-ALL cell line, KE-37 induces MDSCs from healthy PBMCs. PBMCs from healthy donors were cocultured with the human Notch1-dependent T-ALL cell line, KE-37, or were cultured in medium alone, as a control, for 6 days, by using transwell inserts. The data shown are relative to the end of the culture. **(A)** Representative dot plot of $CD14^+HLA\text{-}DR^{low/neg}$ cells inside $CD11b^+CD33^+$ subset, as measured by FACS analysis in harvested PBMCs/KE-37 coculture samples (+KE-37), *versus* samples of autologous PBMCs cultured alone (PBMCs alone). Numbers inside cytograms indicate the percentages of $CD11b^+CD33^+CD14^+HLA\text{-}DR^{low/neg}$ cells. **(B)** Percentages and absolute numbers of $CD11b^+CD33^+CD14^+HLA\text{-}DR^{low/neg}$ cells, measured by the same FACS analysis, as in **(A)**. The values are presented as mean ± SD from four independent experiments ($n$ = 6 samples per group, donors $n$ = 6), each in triplicates. **(C)** At the end of the coculture assay above, $CD33^+$ fractions were magnetically selected from harvested samples and used as "putative" suppressors ($CD33^+$) in a suppression test on proliferating $CD4^-CD8^+$-gated cells ("responders"), from CFSE-labeled/activated autologous PBMCs, at the indicated $CD33^+$:responder ratios. $CD33^+$ cells were selected from PBMCs cultured either in medium alone ($CD33^+$/PBMCs alone) or with KE-37 cells ($CD33^+$/+KE-37). The results are illustrated as the ratio between the percentages of proliferating $CD4^-CD8^+$-gated cells in cultures containing $CD33^+$ and in control cultures set up in the absence of $CD33^+$ (no $CD33^+$) and expressed as % of control. In **(D, E)**, the graphs report percentages and cell count proportions of $CD11b^+CD33^+CD14^+HLA\text{-}DR^{low/neg}$ cells in harvested PBMCs/KE-37 cocultures, assessed by the same FACS analysis, as in **(A)**. The samples in **(D)** were cultured in the absence (CTR) or presence of GSI (+GSI), and the samples in **(E)** were cultured in the absence (CTR) or presence of anti-IL-6-neutralizing antibodies (+anti-IL-6). The cell count proportions were calculated as the ratio between the $CD11b^+CD33^+CD14^+HLA\text{-}DR^{low/neg}$ absolute numbers in PBMCs/KE-37 treated cocultures and in relative untreated controls and expressed as % of control. In **(C–E)**, the values represent the mean ± SD from three independent experiments ($n$ = 3 samples per group, donors $n$ = 3), each in triplicates. $^*p \le 0.05$, $^{**}p \le 0.01$, $^{***}p \le 0.001$, and $^{****}p \le 0.0001$ represent significant differences between the indicated groups.

assay of healthy PBMCs with TALL-1 cells. We have observed no significant difference between the two treatment conditions regarding the inhibition of MDSC induction (**Supplementary Figure S5G**); similar results were obtained with PBMCs/KE-37 cocultures (not shown). These data sustain the hypothesis that IL-6 cooperates with Notch-signaling activation in inducing MDSCs, but the last one represents the necessary condition to observe this induction.

Finally, we performed coculture experiments of healthy PBMCs with the human T-ALL cell line, Loucy, that does not express Notch1- or Notch3-activated protein (12, 32). Notably, we have not observed any evident induction of MDSCs

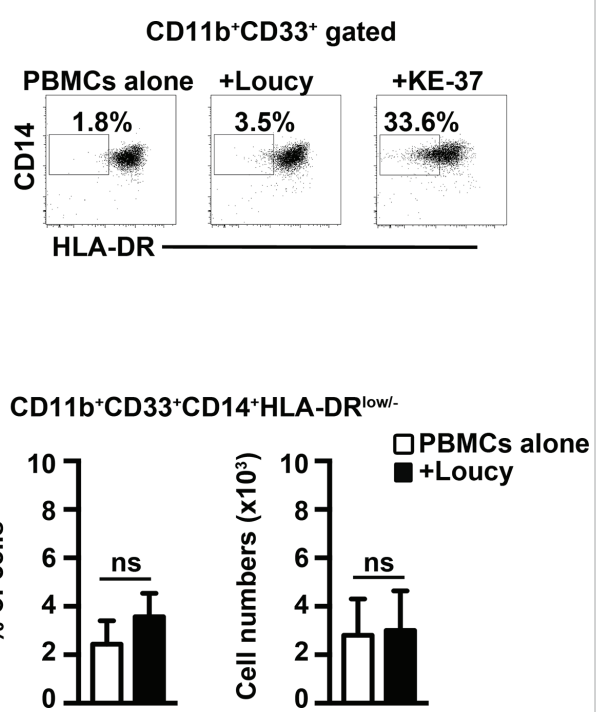


**FIGURE 8** | The Notch-inactive T-ALL cell line, Loucy, does not induce MDSCs from healthy PBMCs. **(A)** Representative dot plot of $CD14^{+}HLA\text{-}DR^{low/neg}$ cells inside $CD11b^{+}CD33^{+}$ subset, as measured by FACS analysis in harvested PBMCs/Loucy coculture samples (+Loucy), vs. samples of autologous PBMCs cultured alone (PBMCs alone). PBMCs/KE-37 coculture samples (+KE-37) were also included as positive controls of MDSC induction. Numbers inside cytograms indicate the percentages of $CD11b^{+}CD33^{+}CD14^{+}HLA\text{-}DR^{low/neg}$ cells. **(B)** Percentages (left panel) and absolute numbers (right panel) of $CD11b^{+}CD33^{+}CD14^{+}HLA\text{-}DR^{low/neg}$ cells, as measured by the same FACS analysis, as in **(A)**. In **(B)**, the values represent the mean ± SD from three independent experiments ($n$ = 4 samples per group, donors $n$ = 4), each in duplicates. ns, not significant.

(**Figure 8**). In summary, we show that Notch-dependent T-ALL cells promote human MDSCs *in vitro*, through a mechanism that depends on both Notch and IL-6, consistently with findings in our mouse model.

## DISCUSSION

T-ALL accounts for 10%–15% of pediatric and 25% of adult ALL cases. Despite the efficacy of current chemotherapy protocols, 25%–30% of children and up to 60% of adults among T-ALL patients still relapse (44, 45). Bone marrow is the most common site of T-ALL recurrence, and BM relapse often represents a feature of worse prognosis (46, 47). Similarly, the BM of murine models of Notch-dependent T-ALL reveals precocious invasion of immature T cells (8, 10, 28, 33) that perturb stromal niches and hematopoiesis (25, 26). Here, we report that aberrant T cells from Notch3-dependent T-ALL participate in shaping the leukemia environment, through the control exerted on MDSCs. Indeed, we observed that $CD4^{+}CD8^{+}$(DP) T cells from the bone marrow of our murine model of Notch3-dependent T-ALL induce functional MDSCs *in vitro*, as well as in immunodeficient hosts.

Regarding the mechanism of MDSC induction, it has been well established that the development/activation of MDSCs depends on the production/release of proinflammatory cytokines, such as IL-6 (37). IL-6 expression is elevated in tumor cell lines that induce MDSCs (30) and in plasma of cancer patients, where its concentration positively correlates with the level of circulating MDSCs (48). In many tumors, including T-ALL, Notch signaling promotes IL-6 production by stromal components (26, 49). However, malignant cells themselves may represent the source of IL-6 (50, 51). We observed that IL-6 concentration is very high in blood serum and BM supernatant of *N3-tg* mice and that transgenic DP T cells express considerable levels of IL-6. Moreover, we reported that MDSC induction is significantly attenuated *via* neutralizing anti-IL-6 antibody exposure, *in vitro* and *in vivo*. These results emphasize the hypothesis that Notch-signaling deregulation in the T-cell compartment of T-ALL could contribute to inducing MDSCs, through an IL-6-dependent pathway. The use of transwell inserts in our *in vitro* coculture experiments supports a prevalent role of diffusible factors in Notch-driven induction of MDSCs. However, we cannot exclude that *in vivo* Notch activation may promote MDSCs, through other mechanism/s, such as those based on ligand/receptor interactions (23), and that other cell subsets may participate in releasing IL-6 in the tumor microenvironment.

Our *in vivo* Gr-1 depletion experiments suggest that MDSCs from *N3-tg* T-ALL mice limit significantly the expansion and proliferation of aberrant DP T cells, and then, they may eventually affect the disease outcome. Interestingly, by treating *N3-tg* mice with both anti-Gr1 and neutralizing anti-IL-6 antibodies, we observed a significant reduction of parameters that specifically mark the disease progression in our model, such as total numbers of splenocytes and splenic DP T-cell numbers (9, 33–35).

We need more efforts to elucidate the target/s and precise mechanism/s of MDSC action in T-ALL. However, summarizing our *in vivo* data, we can suggest some hypotheses (**Supplementary Figure S7**): it is very likely that alternative pathways are involved, besides the "classical" suppression of T-cell antitumor responses. MDSCs may act through the *de novo* generation of Tregs (36), including in cancer settings (52, 53), and Treg expansion has been described in the BM of T-ALL patients (54). In this regard, we demonstrated that Notch3 activation improves the generation and suppressive function of Tregs in *N3-tg* mice (55–57). MDSCs could also impinge on pathways that are underinvestigated in hematological malignancies, to date. They may target "innate" subsets engaged in cancer immune responses, such as NK cells (58), and/or exploit suppression *via* alternative signalings, such as the PD-1/PDL-1 axis (59, 60), with a potential impact on cancer immunotherapy (61, 62). In line with our hypothesis, a recent paper reports that myeloid cells can directly support T-ALL cell survival, independently from suppression of T-cell response (27).

Thus, MDSCs may sustain T-ALL cell proliferation and/or survival and, eventually, tumor progression, either directly and, more likely, indirectly by blocking antitumor immune responses of NKs, besides that of CTL/Th1 subsets, as well as through the generation of immunosuppressive Tregs.

We start extending our preclinical observations to humans. We demonstrated that human Notch-dependent T-ALL cell lines sustain the expansion of functional MDSCs from normal PBMCs, in a coculture assay. Interestingly, by the exposure of cocultures above to GSIs or neutralizing anti-IL-6 antibodies or both, we suggested that Notch and IL-6 are both able to influence the MDSC induction; however, Notch-signaling activation remains the crucial event in this process, at least in our *in vitro* model with human T-ALLs.

Notably, the induction of MDSCs is not observed using a model of Notch-independent T-ALL, such as the Loucy cell line, suggesting that this process is specific for Notch-dependent T-ALL. Moreover, both Notch1 and Notch3 deregulation seems able to generate MDSCs from human PBMCs, as suggested by our observations on MDSC induction with human T-ALL cell lines, KE-37 and TALL-1, that overexpress in a mutually exclusive way active-Notch1 and active-Notch3, respectively. Notch1 has a prominent role in T-ALL development, and its activation by gain-of-function mutations has been reported in more than the 60% of T-ALL patients (11). Notch3 is often assumed as a target of Notch1 [ (63), and references therein], and it has been shown that Notch1 and Notch3 have common oncogenomic programs (64). On the other hand, aberrant Notch3 deregulation occurs in T-ALL cases lacking Notch1 activation (12, 63), and then, a specific Notch3-dependent subset of T-ALL patients may exist. Thus, we can speculate that, whatever the case, our preclinical conclusions in *N3-tg* mice, together with observations in humans, could have clinical relevance. It is important to note that, in the retroviral-vector-induced murine model of Notch1-dependent T-ALL, the expansion of $CD11b^{+}Gr\text{-}1^{+}$ myeloid cells was described in non-transduced populations (25, 26), and Notch3 was reported as a transcriptional target of Notch1 in transduced DP T cells from the BM (10). Based on these premises, it is likely that also in murine models of T-ALL, Notch1- and Notch3-signaling deregulation converge on the final effect of inducing MDSCs. However, this point deserves confirmation and detailed examination mainly focused on the mechanism/s involved. Remarkably, human T-ALL originates in the thymus and then infiltrates into the BM and peripheral blood [ (65) and references therein], and these features are well reproduced in the *N3-tg* model (9), which is based on the genetic alteration of this pathway at the level of immature thymocytes. In the Notch1 murine model, instead, deregulation of the Notch1 signal is already active in the BM where it is able to sustain T-cell development until the stage of DP T cells (8, 10).

Overall, we believe that our results represent the necessary premise for the analysis of MDSCs in T-ALL patients, with the final aim of defining them as a new target of therapy and/or as an innovative prognostic biomarker. Moreover, the *N3-tg* model could serve as a proof-of-concept system to deepen the studies on the bidirectional crosstalk between leukemic T cells, MDSCs, and other cell subsets, inside the T-ALL environment.

## DATA AVAILABILITY STATEMENT

The raw data supporting the conclusions of this article will be made available by the authors, without undue reservation.

## ETHICS STATEMENT

The studies involving human participants were reviewed and approved by the Institutional Ethics Committee. The patients/participants provided their written informed consent to participate in this study. The animal study was reviewed and approved by the local animal welfare committee and conducted in accordance with the recommendations of the Italian national guidelines for experimental animal care and use (D.lgs 26/2014).

## AUTHOR CONTRIBUTIONS

PG and AO designed and performed research, analyzed the data, and wrote the first draft of the paper. NG, CN, and BA performed the research. GP analyzed the data. IS critically revised the manuscript. AC supervised the experiments, analyzed the data, and wrote the manuscript. All authors listed have made a substantial, direct, and intellectual contribution to the work and approved it for publication.

## FUNDING

This work was supported by the Italian Association for Cancer Research (AIRC, IG13214) to IS, the FIRB Program (RBAP11WCRZ) to IS, the Sapienza University grants PH118164340087CF to IS and RM11715C7C626BAB to AC and by the Italian Ministry of Education, University and Research - Dipartimenti di Eccellenza - L. 232/2016.

## ACKNOWLEDGMENTS

Dedicated to the memory of Prof. Alberto Gulino. We thank Prof. Giovanni Bernardini, Prof. Helena Stabile, Dr. Laura Fasano, Mr. Alessandro Martini, Mr. Fernando Duranti, and Mrs. Dina Milana for technical assistance.

## SUPPLEMENTARY MATERIAL

The Supplementary Material for this article can be found online at: https://www.frontiersin.org/articles/10.3389/fimmu.2022.809261/full#supplementary-material

## REFERENCES


1. Hori K, Sen A, Artavanis-Tsakonas S. Notch Signaling at a Glance. *J Cell Sci* (2013) 126(Pt 10):2135–40. doi: 10.1242/jcs.127308
2. South AP, Cho RJ, Aster JC. The Double-Edged Sword of Notch Signaling in Cancer. *Semin Cell Dev Biol* (2012) 23(4):458–64. doi: 10.1016/j.semcdb.2012.01.017
3. Palermo R, Checquolo S, Bellavia D, Talora C, Screpanti I. The Molecular Basis of Notch Signaling Regulation: A Complex Simplicity. *Curr Mol Med* (2014) 14(1):34–44. doi: 10.2174/1566524013666131118105216
4. Bellavia D, Campese AF, Vacca A, Gulino A, Screpanti I. Notch3, Another Notch in T Cell Development. *Semin Immunol* (2003) 15(2):107–12. doi: 10.1016/s10445323(03)00007-1
5. Yashiro-Ohtani Y, Ohtani T, Pear WS. Notch Regulation of Early Thymocyte Development. *Semin Immunol* (2010) 22(5):261–69. doi: 10.1016/j.smim.201
6. Amsen D, Helbig C, Backer RA. Notch in T Cell Differentiation: All Things Considered. *Trends Immunol* (2015) 36(12):802–14. doi: 10.1016/j.it.2015.10.007
7. Aster JC, Blacklow SC, Pear WS. Notch Signaling in T-Cell Lymphoblastic Leukaemia/Lymphoma and Other Haematological Malignancies. *J Pathol* (2011) 223(2):262–73. doi: 10.1002/path.2789
8. Pear WS, Aster JC, Scott ML, Hasserjian RP, Soffer B, Sklar J, et al. Exclusive Development of T Cell Neoplasms in Mice Transplanted With Bone Marrow Expressing Activated Notch Alleles. *J Exp Med* (1996) 183(5):2283–91. doi: 10.1084/jem.183.5.2283
9. Bellavia D, Campese AF, Alesse E, Vacca A, Felli MP, Balestri A, et al. Constitutive Activation of NF-kappaB and T-Cell Leukemia/Lymphoma in Notch3 Transgenic Mice. *EMBO J* (2000) 19(13):3337–48. doi: 10.1093/emboj/19.13.3337
10. Campese AF, Garbe AI, Zhang F, Grassi F, Screpanti I, von Boehmer H. Notch1-Dependent Lymphomagenesis is Assisted by But Does Not Essentially Require Pre-TCR Signaling. *Blood* (2006) 108(1):305–10. doi: 10.1182/blood-2006-01-0143
11. Weng AP, Ferrando AA, Lee W, Morris JP4, Silverman LB, Sanchez-Irizarry C, et al. Activating Mutations of NOTCH1 in Human T Cell Acute Lymphoblastic Leukemia. *Science* (2004) 306(5694):269–71. doi: 10.1126/science.1102160
12. Bernasconi-Elias P, Hu T, Jenkins D, Firestone B, Gans S, Kurth E, et al. Characterization of Activating Mutations of NOTCH3 in T-Cell Acute Lymphoblastic Leukemia and Anti-Leukemic Activity of NOTCH3 Inhibitory Antibodies. *Oncogene* (2016) 35(47):6077–86. doi: 10.1038/onc.2016.133
13. Bronte V, Brandau S, Chen SH, Colombo MP, Frey AB, Greten TF, et al. Recommendations for Myeloid-Derived Suppressor Cell Nomenclature and Characterization Standards. *Nat Commun* (2016) 7:12150. doi: 10.1038/ncomms12150
14. Marvel D, Gabrilovich DI. Myeloid-Derived Suppressor Cells in the Tumor Microenvironment: Expect the Unexpected. *J Clin Invest* (2015) 125(9):3356–64. doi: 10.1172/JCI80005
15. Solito S, Marigo I, Pinton L, Damuzzo V, Mandruzzato S, Bronte V. Myeloid-Derived Suppressor Cell Heterogeneity in Human Cancers. *Ann N Y Acad Sci* (2014) 1319:47–65. doi: 10.1111/nyas.12469
16. Messmer MN, Netherby CS, Banik D, Abrams SI. Tumor-Induced Myeloid Dysfunction and its Implications for Cancer Immunotherapy. *Cancer Immunol Immunother* (2015) 64(1):1–13. doi: 10.1007/s00262-014-1639-3
17. De Veirman K, Van Valckenborgh E, Lahmar Q, Geeraerts X, De Bruyne E, Menu E, et al. Myeloid-Derived Suppressor Cells as Therapeutic Target in Hematological Malignancies. *Front Oncol* (2014) 4:349. doi: 10.3389/fonc.2014.00349
18. Lv M, Wang K, Huang XJ. Myeloid-Derived Suppressor Cells in Hematological Malignancies: Friends or Foes. *J Hematol Oncol* (2019) 12 (1):105. doi: 10.1186/s13045-019-0797-3
19. Grazioli P, Felli MP, Screpanti I, Campese AF. The Mazy Case of Notch and Immunoregulatory Cells. *J Leukoc Biol* (2017) 102(2):361–8. doi: 10.1189/jlb.1VMR1216-505R
20. Hossain F, Majumder S, Ucar DA, Rodriguez PC, Golde TE, Minter LM, et al. Notch Signaling in Myeloid Cells as a Regulator of Tumor Immune Responses. *Front Immunol* (2018) 9:1288. doi: 10.3389/fimmu.2018.01288
21. Cheng P, Kumar V, Liu H, Youn JI, Fishman M, Sherman S, et al. Effects of Notch Signaling on Regulation of Myeloid Cell Differentiation in Cancer. *Cancer Res* (2014) 74(1):141–52. doi: 10.1158/0008-5472.CAN-13-1686
22. Wang SH, Lu QY, Guo YH, Song YY, Liu PJ, Wang YC. . The Blockage of Notch Signaling Promoted the Generation of Polymorphonuclear Myeloid-Derived Suppressor Cells With Lower Immunosuppression. *Eur J Cancer* (2016) 68:90–105. doi: 10.1016/j.ejca.2016.08.019
23. Sierra RA, Trillo-Tinoco J, Mohamed E, Yu L, Achyut BR, Arbab A, et al. Anti-Jagged Immunotherapy Inhibits MDSCs and Overcomes Tumor-Induced Tolerance. *Cancer Res* (2017) 77(20):5628–38. doi: 10.1158/0008-5472.CAN-17-0357
24. Mao L, Zhao ZL, Yu GT, Wu L, Deng WW, Li YC, et al. γ-Secretase Inhibitor Reduces Immunosuppressive Cells and Enhances Tumour Immunity in Head and Neck Squamous Cell Carcinoma. *Int J Cancer* (2018) 142(5):999–1009. doi: 10.1002/ijc.31115
25. Kawamata S, Du C, Li K, Lavau C. Notch1 Perturbation of Hemopoiesis Involves Non-Cell- Autonomous Modifications. *J Immunol* (2002) 168 (4):1738–45. doi: 10.4049/jimmunol.168.4.1738
26. Wang W, Zimmerman G, Huang X, Yu S, Myers J, Wang Y, et al. Aberrant Notch Signaling in the Bone Marrow Microenvironment of Acute Lymphoid Leukemia Suppresses Osteoblast-Mediated Support of Hematopoietic Niche Function. *Cancer Res* (2016) 76(6):1641–52. doi: 10.1158/0008-5472.CAN-15-2092
27. Lyu A, Triplett TA, Nam SH, Hu Z, Arasappan D, Godfrey WH, et al. Tumor-Associated Myeloid Cells Provide Critical Support for T-ALL. *Blood* (2020) 136(16):1837–50. doi: 10.1182/blood.2020007145
28. Grazioli P, Orlando A, Giordano N, Noce C, Peruzzi G, Scafetta G, et al. NF-κb1 Regulates Immune Environment and Outcome of Notch-Dependent T-Cell Acute Lymphoblastic Leukemia. *Front Immunol* (2020) 11:541. doi: 10.3389/fimmu.2020.00541
29. Shultz LD, Lyons BL, Burzenski LM, Gott B, Chen X, Chaleff S, et al. Human Lymphoid and Myeloid Cell Development in NOD/LtSz-Scid IL2R Gamma Null Mice Engrafted With Mobilized Human Hemopoietic Stem Cells. *J Immunol* (2005) 174(10):6477–89. doi: 10.4049/jimmunol.174.10.6477
30. Marigo I, Bosio E, Solito S, Mesa C, Fernandez A, Dolcetti L, et al. Tumor-Induced Tolerance and Immune Suppression Depend on the C/EBPbeta Transcription Factor. *Immunity* (2010) 32(6):790–802. doi: 10.1016/j.immuni.2010.05.010
31. Miyoshi I, Hiraki S, Tsubota T, Kubonishi I, Matsuda Y, Nakayama T, et al. Human B Cell, T Cell and Null Cell Leukaemic Cell Lines Derived From Acute Lymphoblastic Leukaemias. *Nature* (1977) 267(5614):843–4. doi: 10.1038/267843a0
32. O'Neil J, Grim J, Strack P, Rao S, Tibbitts D, Winter C, et al. FBW7 Mutations in Leukemic Cells Mediate NOTCH Pathway Activation and Resistance to Gamma-Secretase Inhibitors. *J Exp Med* (2007) 204(8):1813–24. doi: 10.1084/jem.20070876
33. Ferrandino F, Bernardini G, Tsaouli G, Grazioli P, Campese AF, Noce C, et al. Intrathymic Notch3 and CXCR4 Combinatorial Interplay Facilitates T-Cell Leukemia Propagation. *Oncogene* (2018) 37(49):6285–98. doi: 10.1038/s41388-018-0401-2
34. Franciosa G, Diluvio G, Gaudio FD, Giuli MV, Palermo R, Grazioli P, et al. Prolyl-Isomerase Pin1 Controls Notch3 Protein Expression and Regulates T-ALL Progression. *Oncogene* (2016) 35(36):4741–51. doi: 10.1038/onc.2016.5
35. Palermo R, Checquolo S, Giovenco A, Grazioli P, Kumar V, Campese AF, et al. Acetylation Controls Notch3 Stability and Function in T-Cell Leukemia. *Oncogene* (2012) 31(33):3807–17. doi: 10.1038/onc.2011.533
36. Gabrilovich DI, Nagaraj S. Myeloid-Derived Suppressor Cells as Regulators of the Immune System. *Nat Rev Immunol* (2009) 9(3):162–74. doi: 10.1038/nri2506
37. Condamine T, Mastio J, Gabrilovich D. Transcriptional Regulation of Myeloid-Derived Suppressor Cells. *J Leukoc Biol* (2015) 98(6):913–22. doi: 10.1189/jlb.4RI0515-204R
38. Fleming V, Hu X, Weller C, Weber R, Groth C, Riester Z, et al. Melanoma Extracellular Vesicles Generate Immunosuppressive Myeloid Cells by Upregulating PD-L1 *via* TLR4 Signaling. *Cancer Res* (2019) 79(18):4715–28. doi: 10.1158/0008-5472.CAN-19-0053
39. Kumar V, Cheng P, Condamine T, Mony S, Languino LR, McCaffrey JC, et al. CD45 Phosphatase Inhibits STAT3 Transcription Factor Activity in Myeloid

Cells and Promotes Tumor-Associated Macrophage Differentiation. *Immunity* (2016) 44(2):303–15. doi: 10.1016/j.immuni.2016.01.014
40. Peng D, Tanikawa T, Li W, Zhao L, Vatan L, Szeliga W, et al. Myeloid-Derived Suppressor Cells Endow Stem-Like Qualities to Breast Cancer Cells Through IL6/STAT3 and NO/NOTCH Cross-Talk Signaling. *Cancer Res* (2016) 76 (11):3156–65. doi: 10.1158/00085472.CAN-15-2528
41. Smith AD, Lu C, Payne D, Paschall AV, Klement JD, Redd PS, et al. Autocrine IL6-Mediated Activation of the STAT3-DNMT Axis Silences the Tnfα-RIP1 Necroptosis Pathway to Sustain Survival and Accumulation of Myeloid-Derived Suppressor Cells. *Cancer Res* (2020) 80(15):3145–56. doi: 10.1158/0008-5472.CAN-19-3670
42. Giuli MV, Diluvio G, Giuliani E, Franciosa G, Di Magno L, Pignataro MG, et al. Notch3 Contributes to T-Cell Leukemia Growth *via* regulation of the unfolded protein response. *Oncogenesis* (2020) 9(10):93. doi: 10.1038/s41389-020-00279-7
43. Dastur A, Choi A, Costa C, Yin X, Williams A, McClanaghan J, et al. NOTCH1 Represses MCL-1 Levels in GSI-Resistant T-ALL, Making Them Susceptible to ABT-263. *Clin Cancer Res* (2019) 25(1):312–24. doi: 10.1158/1078-0432.CCR-18-0867
44. Pui CH, Evans WE. Treatment of Acute Lymphoblastic Leukemia. *N Engl J Med* (2006) 354(2):166–78. doi: 10.1056/NEJMra052603
45. Pui CH, Mullighan CG, Evans WE, Relling MV. Pediatric Acute Lymphoblastic Leukemia: Where are We Going and How do We Get There? *Blood* (2012) 120(6):1165–74. doi: 10.1182/blood-2012-05-378943
46. Rivera GK, Zhou Y, Hancock ML, Gajjar A, Rubnitz J, Ribeiro RC, et al. Bone Marrow Recurrence After Initial Intensive Treatment for Childhood Acute Lymphoblastic Leukemia. *Cancer* (2005) 103(2):368–76. doi: 10.1002/cncr.20743
47. Nguyen K, Devidas M, Cheng SC, La M, Raetz EA, Carroll WL, et al. Factors Influencing Survival After Relapse From Acute Lymphoblastic Leukemia: A Children's Oncology Group Study. *Leukemia* (2008) 22(12):2142–50. doi: 10.1038/leu.2008.251
48. Chen MF, Kuan FC, Yen TC, Lu MS, Lin PY, Chung YH, et al. IL-6-Stimulated CD11b+CD14+HLA-DR- Myeloid-Derived Suppressor Cells, are Associated With Progression and Poor Prognosis in Squamous Cell Carcinoma of the Esophagus. *Oncotarget* (2014) 5(18):8716–28. doi: 10.18632/oncotarget.2368
49. Sethi N, Dai X, Winter CG, Kang Y. Tumor-Derived JAGGED1 Promotes Osteolytic Bone Metastasis of Breast Cancer by Engaging Notch Signaling in Bone Cells. *Cancer Cell* (2011) 19(2):192–205. doi: 10.1016/j.ccr.2010.12.022
50. Reynaud D, Pietras E, Barry-Holson K, Mir A, Binnewies M, Jeanne M, et al. IL-6 Controls Leukemic Multipotent Progenitor Cell Fate and Contributes to Chronic Myelogenous Leukemia Development. *Cancer Cell* (2011) 20(5):661–73. doi: 10.1016/j.ccr.2011.10.012
51. Kim SW, Kim JS, Papadopoulos J, Choi HJ, He J, Maya M, et al. Consistent Interactions Between Tumor Cell IL-6 and Macrophage TNF-α Enhance the Growth of Human Prostate Cancer Cells in the Bone of Nude Mouse. *Int Immunopharmacol* (2011) 11(7):862–72. doi: 10.1016/j.intimp.2011.01.004
52. Huang B, Pan PY, Li Q, Sato AI, Levy DE, Bromberg J, et al. Gr-1+CD115+ Immature Myeloid Suppressor Cells Mediate the Development of Tumor-Induced T Regulatory Cells and T-Cell Anergy in Tumor-Bearing Host. *Cancer Res* (2006) 66(2):1123–31. doi: 10.1158/0008-5472.CAN-05-1299
53. Yang R, Cai Z, Zhang Y, Yutzy WH4, Roby KF, Roden RB. CD80 in Immune Suppression by Mouse Ovarian Carcinoma-Associated Gr-1+CD11b+ Myeloid Cells. *Cancer Res* (2006) 66(13):6807–15. doi: 10.1158/0008-5472.CAN-05-3755
54. Wu CP, Qing X, Wu CY, Zhu H, Zhou HY. Immunophenotype and Increased Presence of CD4(+)CD25(+) Regulatory T Cells in Patients With Acute Lymphoblastic Leukemia. *Oncol Lett* (2012) 3(2):421–4. doi: 10.3892/ol.2011.499
55. Anastasi E, Campese AF, Bellavia D, Bulotta A, Balestri A, Pascucci M, et al. Expression of Activated Notch3 in Transgenic Mice Enhances Generation of T Regulatory Cells and Protects Against Experimental Autoimmune Diabetes. *J Immunol* (2003) 171(9):4504–11. doi: 10.4049/jimmunol.171.9.4504
56. Campese AF, Grazioli P, Colantoni S, Anastasi E, Mecarozzi M, Checquolo S, et al. Notch3 and Ptalpha/Pre-TCR Sustain the *In Vivo* Function of Naturally Occurring Regulatory T Cells. *Int Immunol* (2009) 21(6):727–43. doi: 10.1093/intimm/dxp042
57. Barbarulo A, Grazioli P, Campese AF, Bellavia D, Di Mario G, Pelullo M, et al. Notch3 and Canonical NF-kappaB Signaling Pathways Cooperatively Regulate Foxp3 Transcription. *J Immunol* (2011) 186(11):6199–206. doi: 10.4049/jimmunol.1002136
58. Bruno A, Mortara L, Baci D, Noonan DM, Albini A. Myeloid Derived Suppressor Cells Interactions With Natural Killer Cells and Pro-Angiogenic Activities: Roles in Tumor Progression. *Front Immunol* (2019) 10:771. doi: 10.3389/fimmu.2019.00771
59. Azzaoui I, Uhel F, Rossille D, Pangault C, Dulong J, Le Priol J, et al. T-Cell Defect in Diffuse Large B-Cell Lymphomas Involves Expansion of Myeloid-Derived Suppressor Cells. *Blood* (2016) 128(8):1081–92. doi: 10.1182/blood-2015-08-662783
60. Vari F, Arpon D, Keane C, Hertzberg MS, Talaulikar D, Jain S, et al. Immune Evasion *via* PD-1/PD-L1 on NK Cells and Monocyte/Macrophages is More Prominent in Hodgkin Lymphoma Than DLBCL. *Blood* (2018) 131(16):1809–19. doi: 10.1182/blood-2017-07-796342
61. Weber R, Fleming V, Hu X, Nagibin V, Groth C, Altevogt P, et al. Myeloid-Derived Suppressor Cells Hinder the Anti-Cancer Activity of Immune Checkpoint Inhibitors. *Front Immunol* (2018) 9:1310. doi: 10.3389/fimmu.2018.01310
62. Hou A, Hou K, Huang Q, Lei Y, Chen W. Targeting Myeloid-Derived Suppressor Cell, a Promising Strategy to Overcome Resistance to Immune Checkpoint Inhibitors. *Front Immunol* (2020) 11:783. doi: 10.3389/fimmu.2020.00783
63. Tottone L, Zhdanovskaya N, Carmona Pestaña Á, Zampieri M, Simeoni F, Lazzari S, et al. Histone Modifications Drive Aberrant Notch3 Expression/Activity and Growth in T-ALL. *Front Oncol* (2019) 9:198. doi: 10.3389/fonc.2019.00198
64. Choi SH, Severson E, Pear WS, Liu XS, Aster JC, Blacklow SC. The Common Oncogenomic Program of NOTCH1 and NOTCH3 Signaling in T-Cell Acute Lymphoblastic Leukemia. *PloS One* (2017) 2(10):e0185762. doi: 10.1371/journal.pone.0185762
65. Tan SH, Bertulfo FC, Sanda T. Leukemia-Initiating Cells in T-Cell Acute Lymphoblastic Leukemia. *Front Oncol* (2017) 7:218. doi: 10.3389/fonc.2017.00218

**Conflict of Interest:** The authors declare that the research was conducted in the absence of any commercial or financial relationships that could be construed as a potential conflict of interest.

frontiers | Frontiers in Immunology

ORIGINAL RESEARCH
published: 26 April 2022
doi: 10.3389/fimmu.2022.879030

# Impact of Consolidative Unrelated Cord Blood Transplantation on Clinical Outcomes of Patients With Relapsed/Refractory Acute B Lymphoblastic Leukemia Entering Remission Following CD19 Chimeric Antigen Receptor T Cells

*Qianwen Xu[1†], Lei Xue[1†], Furun An[2], Hui Xu[1], Li Wang[1], Liangquan Geng[1], Xuhan Zhang[1], Kaidi Song[1], Wen Yao[1], Xiang Wan[1], Juan Tong[1], Huilan Liu[1], Xin Liu[1], Xiaoyu Zhu[1], Zhimin Zhai[2], Zimin Sun[1] and Xingbing Wang[1*]*

[1] Department of Hematology, The First Affiliated Hospital of University of Science and Technology of China (USCT) (Anhui Provincial Hospital), Division of Life Sciences and Medicine, University of Science and Technology of China, Hefei, China, [2] Hematology Department, The Second Hospital of Anhui Medical University (SHAMU), Hefei, China

**Background:** While chimeric antigen receptor (CAR)-T cell therapy is becoming widely used in hematological malignancies with remarkable remission rate, their high recurrence remains an obstacle to overcome. The role of consolidative transplantation following CAR-T cell-mediated remission remains controversial. We conducted a retrospective study to explore whether bridging to unrelated cord blood transplantation (UCBT) could improve the prognosis of patients entering remission after CAR-T therapy with different characteristics through subgroup analyses.

**Methods:** We reviewed 53 patients with relapsed/refractory (R/R) B-cell acute lymphoblastic leukemia (B-ALL) successfully infused with CD19 CAR-T cells and achieved complete remission (CR). In this study, 25 patients received consolidative UCBT (UCBT group) and 28 patients did not accept any intervention until relapse (non-UCBT group). Subgroup analysis on prognosis was then performed according to gender, age, number of previous relapses, tumor burden, presence of poor prognostic markers, and structure of CAR.

**Results:** Compared with the non-UCBT group, patients who underwent consolidative UCBT had better median event-free survival (EFS; 12.3 months vs. 6.2 months; P = 0.035) and relapse-free survival (RFS; 22.3 months vs. 7.2 months; P = 0.046), while no significant difference was found in overall survival (OS; 30.8 months vs. 15.3 months; P = 0.118). Subsequent multivariate analysis revealed that bridging to UCBT was a protective factor for RFS (P = 0.048) but had no significant effect on EFS (P = 0.205) or OS (P = 0.541). In the subgroup analysis, UCBT has an added benefit in patients with specific characteristics.

OPEN ACCESS

**Edited by:**
*Trent Spencer, Emory University, United States*

**Reviewed by:**
*Xiao-Dong Mo, Peking University People's Hospital, China*
*Kunming Qi, Xuzhou Medical University, China*

***Correspondence:**
*Xingbing Wang*
*wangxingbing@ustc.edu.cn*

*[†]These authors have contributed equally to this work and share first authorship*

**Specialty section:**
*This article was submitted to Cancer Immunity and Immunotherapy, a section of the journal Frontiers in Immunology*

**Received:** *18 February 2022*
**Accepted:** *28 March 2022*
**Published:** *26 April 2022*

**Citation:**
*Xu Q, Xue L, An F, Xu H, Wang L, Geng L, Zhang X, Song K, Yao W, Wan X, Tong J, Liu H, Liu X, Zhu X, Zhai Z, Sun Z and Wang X (2022) Impact of Consolidative Unrelated Cord Blood Transplantation on Clinical Outcomes of Patients With Relapsed/Refractory Acute B Lymphoblastic Leukemia Entering Remission Following CD19 Chimeric Antigen Receptor T Cells. Front. Immunol. 13:879030. doi: 10.3389/fimmu.2022.879030*

Patients who experienced ≥2 relapses or with sustained non-remission (NR) showed better RFS (P = 0.025) after UCBT. Better EFS was seen in patients with poor prognostic markers (P = 0.027). In the subgroup with pre-infusion minimal residual disease (MRD) ≥5% or with extramedullary disease (EMD), UCBT significantly prolonged EFS (P = 0.009), RFS (P = 0.017), and OS (P = 0.026). Patients with occurrence of acute graft-versus-host disease (aGVHD) appeared to have a longer duration of remission (P = 0.007).

**Conclusion:** Consolidative UCBT can, to some extent, improve clinical outcomes of patients with R/R B-ALL entering remission following CD19 CAR-T therapy, especially in patients with more recurrences before treatment, patients with poor prognostic markers, and patients with a higher tumor burden. The occurrence of aGVHD after UCBT was associated with better RFS.

**Keywords: chimeric antigen receptor (CAR), unrelated cord blood transplantation, acute B lymphoblastic leukemia, CD19, prognosis**

## 1 INTRODUCTION

Chimeric antigen receptor (CAR)-T cell therapy has been proven to have remarkable efficacy in hematological malignancies in recent years and is considered one of the most promising targeted therapies for tumors. CD19-targeted CAR-T cell therapy has led to a paradigm shift in the treatment of relapsed and refractory (R/R) B-cell acute lymphoblastic leukemia (B-ALL). Numerous clinical trials revealed that patients treated with CD19 CAR-T cells can achieve a complete remission (CR) rate of 75%–93%. Despite the impressive results, however, approximately 38%–61% of patients eventually relapsed during long-term follow-up (1–8). Researchers have proposed a series of solutions to reduce the recurrence rate after CAR-T cell therapy such as optimizing CAR structure (7, 8), designing artificial antigen-presenting cells (AAPCs) (9), binding immunological checkpoint inhibitors (10), sequentially administering two groups of CAR-T cells (11), and bridging to transplantation. Some studies speculated that the combination of CAR-T therapy and transplantation prolonged survival and provided patients with more opportunities (12–14).

However, the role of consolidative transplantation following CAR-T therapy remains controversial while the effect can be influenced by pretreatment patient characteristics, lymphodepletion regimen, structure of CAR, and post-CAR-T therapy parameters (12). In some groups, it increases the economic burden and risk of death related to transplantation. It is necessary to weigh the advantages and disadvantages.

Equally important, which source of stem cells for transplantation to choose is inconclusive. Current studies emphasize the interface between allogeneic hematopoietic stem cell transplantation (allo-HSCT) and CAR-T cell therapy, as allo-HSCT is considered the only recognized curative cellular therapy for patients with B-ALL. Few studies have focused on unrelated cord blood transplantation (UCBT) following CAR-T therapy. Umbilical cord blood (UCB) is gradually being considered as an alternative source of peripheral blood progenitor cells (PBPCs) or bone marrow (BM) transplantation, particularly when a human leukocyte antigen (HLA)-matched donor is not available. A retrospective study determined the optimal role of UCBT in adults with acute leukemia, and showed that leukemia-free survival (LFS) in patients after UCBT was equivalent to that after PBPC or BM transplantation (15). Thus, UCBT may also be considered as an option to improve the prognosis of patients who have undergone CAR-T therapy. Another study conducted at our center showed that patients who received consolidative UCBT after CAR-T-induced remission had a 26.7% 2-year cumulative incidence of relapse (CIR) (16), so it is worth exploring if UCBT can benefit patients who have obtained remission after CAR-T therapy. Our research aims to explore the role of consolidative UCBT in patients receiving CD19 CAR-T cells and which characteristics of patients can influence the effect of UCBT more obviously.

## 2 MATERIALS AND METHODS

### 2.1 Patients

From January 2016 to April 2021, we reviewed patients with R/R B-ALL who were successfully infused with CD19 CAR-T cells at the First Affiliated Hospital of USCT (Anhui Provincial Hospital) and the Second Hospital of Anhui Medical University (SHAMU). The medical ethics committee of the two hospitals reviewed and approved the study protocols. Fifty-three patients were consecutively enrolled in this non-randomized clinical study according to exclusion criteria including the following: 1) unable to evaluate the effectiveness of CAR-T cell therapy, (2) failure to achieve CR after CAR-T cell therapy, (3) contraindications in terms of critical organ insufficiency and uncontrollable infections, and (4) a history of transplantation before CAR-T therapy. Twenty-five patients received consolidative UCBT at our center selectively, depending on pre-UCBT assessment including disease features, treatment history, comorbidities, and personal reasons including patient preference and economic considerations. In conformity with the Declaration of Helsinki, informed consent was provided from each participant.

## 2.2 Procedures

### 2.2.1 Chimeric Antigen Receptor-T Cell Therapy Protocol

All included patients were treated with conditioning chemotherapy including fludarabine (FLU, 30 mg/m$^2$ × 3 days) in combination with cyclophosphamide (CY, 300 mg/m$^2$ × 3 days) before the intravenous infusion of cryopreserved CD19 CAR-T cells at a dose of 1 × 10$^6$ cells/kg body weight. The CAR in this study consists of an CD19-specific single-chain antibody fragment (scFv) derived from FMC63 fused to a modified IgG4-hinge spacer, a costimulatory molecule including CD28 alone or both CD28 and CD137 (4-1BB), and a CD3ζ signaling domain. Enrichment of CAR-T cells from patient's PBMCs was done using CD4-magnetic beads (Miltenyi Biotec GmbH) and CD8-magnetic beads (Miltenyi Biotec GmbH).

### 2.2.2 Unrelated Cord Blood Transplantation Procedures

The selection of cord blood and HLA typing have been previously described (17). Concisely, molecular techniques with minimum antigenic segmentation level resolution for HLA-A and HLA-B and allele-level resolution for DRB1 were used when performing HLA typing. All recipients obtained single-unit cord blood from the Chinese Cord Blood Bank. Each unit of cord blood was high-resolution matched to the recipient's HLA-A and HLA-B antigens and HLA-DRB1 and had a minimum of 3.0 × 10$^7$ total nucleated cells (TNCs)/kg of body weight and 1.2 × 10$^5$ CD34$^+$ cells/kg of body weight until frozen. All recipients were given myeloablative regimen including FLU/BU/CY (FLU, 30 mg/m$^2$ per day for 4 days; busulfan, total 12.8 mg/kg, 0.8 mg/kg every 6 h for 4 days; CY, 60 mg/kg daily for 2 days), FLU/BU/CY plus carmustine (BCNU) (250 mg/m$^2$), FLU/CY plus total body irradiation (TBI; total 12 Gy, 4 fractions) or FLU/BU/CY plus semustine (320 mg/m$^2$). A co-application of mycophenolate mofetil and cyclosporin A was used as prophylaxis for graft-versus-host disease (GVHD).

## 2.3 Definitions

Bone marrow morphology with ≤5% blasts, no evidence of circulating blasts, and no extramedullary infiltration were considered as CR. Minimal residual disease (MRD)-negative CR was characterized as no immunophenotypically abnormal blasts detected in peripheral blood (PB)/BM by multiparametric flow cytometry (FCM). MRD status was assessed by 10-color FCM with a sensitivity of 10$^4$ nucleated cells. Disease relapse was defined as ≥5% of blasts in BM, reappearance of blasts in the PB, or extramedullary infiltration after CR. The endpoints were event-free survival (EFS), relapse-free survival (RFS), and overall survival (OS). We calculated EFS as the time interval from CAR-T cell infusion to disease progression (including MRD-positive and gene recurrence), relapse, or death, whichever came first, or last visit. RFS was calculated from the date of CAR-T cell infusion to the date of relapse, death, or last visit. For OS, death as the final endpoint was caused by any factor or the final follow-up date could be used. Acute GVHD (aGVHD) was assessed according to the Mount Sinai Acute GvHD International Consortium (MAGIC) criterion (18), and chronic GVHD (cGVHD) was assessed according to the consensus criteria of the National Institutes of Health (19).

## 2.4 Statistical Analysis

Descriptive statistics were used to present the characteristics of the patients. The difference in non-relapse mortality (NRM) rate between two groups was determined by Fisher's exact test. Kaplan–Meier analysis and Cox regression model were applied to perform univariate and multivariate analysis on factors affecting the survival of overall patients, respectively. The median EFS, RFS, and OS were demonstrated by Kaplan–Meier curves and were compared by log-rank test. The hazard ratio (HR) and 95% CI for EFS, PFS, and OS for subgroup analysis were estimated using a stratified Cox regression model and visualized by a forest plot. A two-tailed P value <0.05 was considered statistically significant. All statistical analyses were conducted using Statistical Product and Service Solutions (SPSS) 26.0, and GraphPad Prism 8.00 software (GraphPad Software, La Jolla, CA, USA) was used to create figures.

# 3 RESULTS

## 3.1 Patients

A total of 53 patients with B-ALL treated with CD19 CAR-T cells were consecutively enrolled. Characteristics of patients with a median age of 28 (range 3–66 years) years are presented in **Table 1**. Twenty-two (41.5%) patients experienced less than 2 relapses, and 31 (58.5%) patients experienced ≥2 relapses or remain in non-remission (NR). Thirty-six (67.9%) patients had poor prognostic markers including *TP53*, *BCR-ABL1*, *E2A-PBX1*, and *MLL-AF4* and complex karyotype before CAR-T therapy. Furthermore, 43 (81.1%) patients had MRD >5% or with extramedullary disease (EMD) before CAR-T treatment, and 10 (18.9%) patients had MRD <5%. Thirty-eight (71.7%) patients were infused with CAR-T cells incorporating a CD28 co-stimulation domain, and 15 (28.3%) patients with CAR-T cells contained both CD28 and 4-1BB. All patients achieved CR before transplant, while 3 patients remained MRD-positive.

Twenty-five patients received UCBT after CAR-T cell therapy (the UCBT group); 28 patients did not accept any treatment until relapse (the non-UCBT group). The median interval from CAR-T therapy to UCBT was 66 (range 30–268 days) days; 17 patients received UCBT within 3 months following CAR-T therapy. The median infused TNC count and CD34$^+$ cells were 2.79 (range, 1.24–9.80) × 10$^7$/kg and 1.97 (range, 0.69–7.15) × 10$^5$/kg, respectively. Among the patients who underwent UCBT after CAR-T therapy, 11 (44.0%) patients had aGVHD and one patient had cGVHD in the follow-up. Pre-engraftment syndrome (PES) was observed in 19 (76.0%) patients (**Table 1**).

## 3.2 Overall Outcomes

Disease status of 53 patients from the day of CAR-T cell infusion to the end of follow-up was shown in **Figure 1A**. The NRM rates in the UCBT and non-UCBT groups were 33.3% and 5%,

**TABLE 1** | Characteristics of the 53 patients.

| Characteristics | Overall number (%) |
|---|---|
| **Bridging to UCBT** | |
| Yes | 25 (47.2) |
| No | 28 (52.8) |
| **Age (years)** | 28 (3-66) |
| **Gender** | |
| Men | 20 (37.7) |
| Women | 33 (62.3) |
| **Number of relapses** | |
| <2 | 22 (41.5) |
| ≥2 or NR | 31 (58.5) |
| **Poor prognostic markers*** | 36 (67.9) |
| **Previous EMD** | 12 (22.6) |
| **Pre-infusion tumor burden** | |
| MRD ≥5% or with EMD | 43 (81.1) |
| MRD <5% | 10 (18.9) |
| **CAR structure** | |
| CD28 | 38 (71.7) |
| CD28/4-1BB | 15 (28.3) |
| **Pre-transplant BM-MRD** | |
| MRD negative CR | 22 (88.0) |
| MRD positive CR | 3 (12.0) |
| **Transplant-related complications** | |
| aGVHD | 11 (44.0) |
| cGVHD | 1 (4.0) |
| PES | 19 (76.0) |
| TRM | 4 (16.0) |

*Data are presented as the median (range) or count (percentage).*
*UCBT, unrelated cord blood transplantation; EMD, extramedullary disease; MRD, minimal residual disease; CAR, chimeric antigen receptor; BM, bone marrow; CR, complete remission; aGVHD, acute graft-versus-host disease; cGVHD, chronic graft-versus-host disease; PES, pre-engraftment syndrome; TRM, transplantation-related mortality.*
**Include: Complex karyotype, BCR-ABL1, MLL-AF4, TP53, E2A-PBX1.*

respectively; no significant difference was found by Fisher's exact test (P = 0.128) between the two groups. In the UCBT group, 10 (40.0%) patients relapsed at a median time of 6.2 months (range 1.4–22.3 months) including one CD19-negative relapse and one central nervous system leukemia (CNSL), and one patient underwent transformation from ALL to myelodysplastic syndrome (MDS) and eventually progressed to acute myeloid leukemia (AML). Ten (40.0%) patients remained disease-free until the end of follow-up; one patient was lost to follow-up at 5.6 months of remission. Four patients died because of transplant-related complications including GVHD, thrombotic microangiopathy (TMA), and severe infection. Among the patients who relapsed after UCBT, eight patients received reinfusions of CAR-T cells after relapse, five patients achieved CR again, and two of them remained in MRD-negative remission until the end of follow-up. The remaining two patients who received only chemotherapy or supportive therapy showed poor prognosis and died of primary disease in the short term. In the non-UCBT group, 18 (64.3%) patients experienced relapses at a median time of 6.5 months (range 1.4–58.9 months). Six patients achieved sustained MRD-negative remission without other interventions after CAR-T cell infusion until the end of follow up, one patient remained in MRD-negative remission and was lost to follow-up at 34.3 months, one patient showed a positive MRD at 36.5 months, and one patient showed a positive *P210* at 17.7 months.

## 3.3 Survival Analysis

Initially, we performed an analysis of the factors associated with overall prognosis (**Table 2**). Univariate analysis indicated a

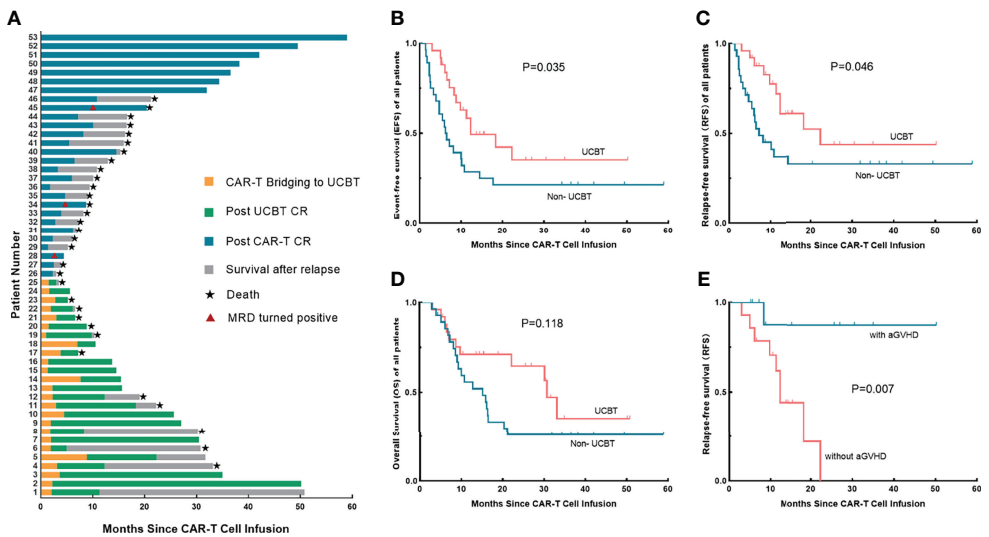


**FIGURE 1** | Treatment responses and long-term survival of each patient, survival analysis between the UCBT group and the non-UCBT group, and the association between aGVHD and RFS in the UCBT group. **(A)** Disease status from CAR-T cell infusion to the end of follow-up of each patient. **(B–D)** Differences of EFS **(B)**, RFS **(C),** and OS **(D)** between the UCBT group and the non-UCBT group in overall patients. **(E)** The association between the occurrence of aGVHD and RFS of patients underwent consolidative UCBT after entering remission by CAR-T therapy. UCBT, unrelated cord blood transplantation; aGVHD, acute graft-versus-host disease; EFS, event-free survival; RFS, relapse-free survival; OS, overall survival; CAR, chimeric antigen receptor.

**TABLE 2** | Factors affecting EFS, RFS, and OS in overall patients.

| Items | EFS | | | RFS | | | OS | | |
|---|---|---|---|---|---|---|---|---|---|
| | Median/mean | Log-rank $\chi^2$ | P | Median/mean | Log-rank $\chi^2$ | P | Median/mean | Log-rank $\chi^2$ | P |
| **Univariate analysis** | | | | | | | | | |
| Bridging to UCBT | | | | | | | | | |
| No | 6.2 | 4.456 | 0.035* | 7.2 | 3.990 | 0.046* | 15.3 | 2.522 | 0.112 |
| Yes | 12.3 | | | 22.3 | | | 30.8 | | |
| CAR structure | | | | | | | | | |
| CD28 | 10.0 | 0.084 | 0.772 | 12.3 | 0.113 | 0.737 | 16.6 | 0.155 | 0.694 |
| CD28/4-1BB | 9.8 | | | 12.3 | | | 30.8 | | |
| Age (years) | | | | | | | | | |
| <25 | 18.3 | 3.362 | 0.067 | 22.3 | 1.198 | 0.274 | 33.2 | 3.090 | 0.079 |
| ≥25 | 7.2 | | | 10.1 | | | 15.3 | | |
| Poor prognostic markers* | | | | | | | | | |
| No | 22.3 | 2.985 | 0.084 | 6.5 | 1.946 | 0.163 | 38.0 | 3.610 | 0.057 |
| Yes | 8.2 | | | 2.7 | | | 19.3 | | |
| Number of relapses | | | | | | | | | |
| <2 | 14.5 | 0.817 | 0.366 | 18.3 | 0.788 | 0.375 | 22.2 | 0.531 | 0.466 |
| ≥2 or NR | 8.3 | | | 11.3 | | | 16.5 | | |
| Tumor burden | | | | | | | | | |
| MRD ≥5%/EMD | 8.8 | 0.001 | 0.979 | 6.1 | 0.514 | 0.474 | 16.5 | 0.099 | 0.754 |
| MRD <5% | 10.8 | | | 4.1 | | | 16.6 | | |
| **Multivariate analysis** | | | | | | | | | |
| **Items** | **HR (95% CI)** | | **P** | **HR (95% CI)** | | **P** | **HR (95% CI)** | | **P** |
| Bridging to UCBT | 0.562 (0.232–1.370) | | 0.205 | 0.456 (0.210–0.992) | | 0.048* | 0.737 (0.276–1.964) | | 0.541 |
| Age (years) | 1.293 (0.521–3.205) | | 0.580 | 1.865 (0.788–4.413) | | 0.156 | 1.679 (0.612–4.601) | | 0.314 |
| Poor prognostic markers | 2.033 (0.945–4.375) | | 0.069 | – | | – | 2.411 (1.022–5.688) | | 0.045* |

*EFS, event-free survival; RFS, relapse-free survival; OS, overall survival; UCBT, unrelated cord blood transplantation; CAR, chimeric antigen receptor; NR, non-remission; MRD, minimal residual disease; EMD, extramedullary disease; HR, hazard ratio; CI, confidence interval.*
**Include: Complex karyotype, BCR-ABL1, MLL-AF4, TP53, E2A-PBX1.*

significant difference in survival between the two groups, the estimated median EFS (12.3 months vs. 6.2 months; P = 0.035) and RFS (22.3 months vs. 7.2 months; P = 0.046) were better in the UCBT group than those in the non-UCBT group, while the OS showed no difference (30.8 months vs. 15.3 months; P = 0.118) (**Figures 1B–D**). Subsequent multivariate analysis for factors with P < 0.2 in the univariate analysis showed that consolidative UCBT was an independent protective factor for RFS (P = 0.048), but with no significant effect on overall EFS (P = 0.205) or OS (P = 0.541). Multivariate analysis also showed a worse EFS (P = 0.069) and OS (P = 0.045) in patients with poor prognostic markers.

Comparison of baseline characteristics of the two groups revealed no significant differences in gender, number of relapses, poor prognostic markers, pre-infusion tumor burden, and CAR structure; however, there were differences in the age distribution (**Table 3**). Considering if those factors may potentially associate with the influence of consolidative UCBT on the prognosis of patients, we subsequently subgrouped the patients to determine which group of patients were more likely to benefit from consolidative UCBT (**Figure 2**). In patients who experienced ≥2 relapses or sustained NR, UCBT prolonged RFS (P = 0.025) compared to non-UCBT. Consolidative UCBT had significant influences in EFS (P = 0.027) of patients with poor prognostic markers including *MLL-AF4*, *BCR-ABL1*, *TP53*, *E2A-PBX1*, and complex karyotype, while no significant effect was shown in patients without those markers. In the subgroup with MRD ≥5% or with EMD before infusion, UCBT prolonged EFS (P = 0.009), RFS (P = 0.017), and OS (P = 0.026) independent of poor prognostic markers; the improvement was not observed in patients with pre-infusion MRD <5%. No significant effect of UCBT was seen in either group subdivided according to gender (men and women), CAR structure (CD28 and CD28/4-1BB), and age (<25 years and ≥25 years).

In our study, time between CAR-T cell infusion and UCBT did not influence EFS (P = 0.360), RFS (P = 0.413), or OS (P = 0.204) of the patients. Four patients bridging to UCBT at 3 months after CAR-T therapy still showed sustained remission. Our further exploration suggested a correlation between aGVHD after UCBT and prognosis, which showed that patients who had aGVHD tend to have a better RFS (P = 0.007) (**Figure 1E**), although EFS (P = 0.113) and OS (P = 0.593) did not significantly prolong, and the results need to be further confirmed by a large sample.

## 4 DISCUSSION

While CAR-T cell therapy increases the remission rate of patients diagnosed with R/R B-cell hematological malignancies, the limited duration of remission and unsatisfactory long-term survival present challenges for CAR-T cell therapy. The two relapse patterns after CAR-T therapy include CD19-positive relapse and CD19-negative relapse. CD19-positive relapses are commonly associated with decreased CAR-T cell persistence, low potency and poor response of CAR, and transient B-cell aplasia (20).

**TABLE 3** | Patient characteristics among the two groups.

| Characteristics | Non-UCBT group (N = 27) | UCBT group (N = 29) | P value (Non-UCBT vs. UCBT) |
|---|---|---|---|
| Age (years) | | | <0.001** |
| <25 | 4 (14.3) | 19 (76.0) | |
| ≥25 | 24 (85.7) | 6 (24.0) | |
| Gender | | | 0.145 |
| Men | 8 (28.6) | 12 (48.0) | |
| Women | 20 (71.4) | 13 (52.0) | |
| Number of relapses | | | 0.833 |
| <2 | 12 (42.9) | 10 (40.0) | |
| ≥2 or NR | 16 (57.1) | 15 (60.0) | |
| Poor prognostic markers* | | | 0.991 |
| No | 9 (32.1) | 8 (32.0) | |
| Yes | 19 (67.9) | 17 (68.0) | |
| Pre-infusion tumor burden | | | 0.842 |
| MRD <5% | 5 (17.9) | 5 (20.0) | |
| MRD ≥5% or with EMD | 23 (82.1) | 20 (80.0) | |
| CAR structure | | | 0.572 |
| CD28 | 21 (75.0) | 17 (68.0) | |
| CD28/4-1BB | 7 (25.0) | 8 (32.0) | |

*Data are presented as count (percentage).*
**P < 0.05 (bilateral); **P < 0.01 (bilateral).*
*UCBT, unrelated cord blood transplantation; NR, non-remission; MRD, minimal residual disease; EMD, extramedullary disease; CAR, chimeric antigen receptor.*
**Include: Complex karyotype, BCR-ABL1, MLL-AF4, TP53, E2A-PBX1.*

The mechanism of this kind of relapse may be related to CD19 gene mutation leading to CD19 loss (21), selection and lineage switch by immune pressure (22, 23), and trogocytosis and cooperative killing (24). Prevention for relapse after CAR-T therapy includes improving the structure of CAR (7, 25), optimizing lymphodepletion regimen (26), dual/multi-targeted CAR-T cells (23, 27), sequential infusion of two groups of CAR-T cells (11, 28), CAR-T cell combined with immune checkpoint inhibitor (10), and consolidative transplantation after CAR-T therapy (12–14, 29–33). HSCT has been chosen in several centers to consolidate remission after CAR-T treatment. Clinical studies by Lee et al. (14) demonstrated a decline in relapse rate in pediatric patients who were consolidated with HSCT. Hay et al. (34) reported a phase I/II data investigating the role of 4-1BB CD19 CAR-T cells in adult ALL, demonstrating prolonged EFS in patients who received HSCT after CAR-T therapy. A clinical study by Shalabi et al. (29) showed that CAR-T cell therapy combined with HSCT could synergistically improve LFS. However, whether to consolidate with transplantation after CAR-T is still a critical question, since treatment-related morbidity and mortality need to be balanced against the risk of relapse. Functional CAR-T cells that persisted in patients may be destroyed by transplantation and losing their antitumor activity. And there are some studies showing that no difference in prognosis was seen in patients who did and did not receive consolidative transplantation after fusion of CD28-based CD19 CAR-T therapy (6, 35).

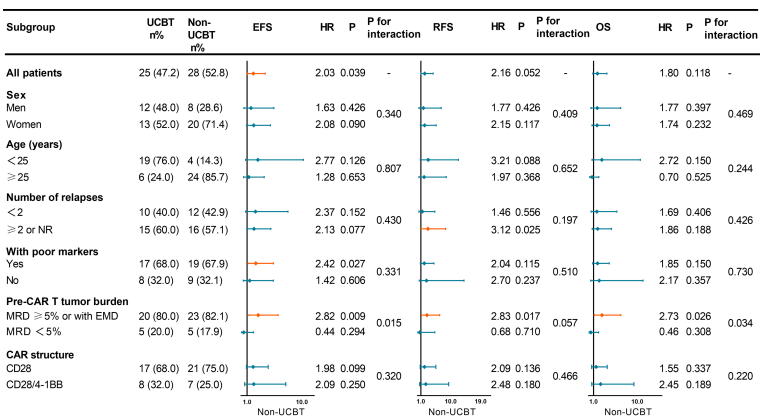


**FIGURE 2** | Forest plot showing the hazard ratios for EFS, RFS, and OS of various subgroups. UCBT, unrelated cord blood transplantation; EFS, event-free survival; RFS, relapse-free survival; OS, overall survival; CAR, chimeric antigen receptor; NR, non-remission; MRD, minimal residual disease; EMD, extramedullary disease; HR, hazard ratio.

Another issue to be addressed is which source of transplantation should be chosen. Current studies have focused on consolidative HSCT after CAR-T therapy, with fewer studies on UCBT. Stem cells can be obtained from BM, PB, or UCB. UCB offers benefits such as rapid acquisition, less constricted HLA matching, and lower rates of GVHD (36–38). A comparative analysis of UCB and BM in children with acute leukemia demonstrated that 4-6/6 HLA-matched UCB provided a similar probability of LFS to matched BM (39). Thus, we assumed that UCBT may serve as an alternative for patients without a compatible donor. However, there is still a deficiency of data on the outcomes of CAR-T therapy bridging to UCBT. Another study in our center showed a relatively high 2-year CIR in patients who received consolidative UCBT following CAR-T-mediated remission (16), so it is worth exploring whether UCBT can benefit patients who achieved remission after CAR-T therapy or not.

In this retrospective study, 25 of the 53 patients received subsequent UCBT after CAR-T therapy, and the other 28 received CAR-T therapy alone. In overall patients, the NRM rate appeared to be higher in the UCBT group, but there was no statistical difference between the two groups, and UCBT contributed a significant improvement in RFS, while there was no significant effect on EFS and OS. In studies focusing on consolidative allo-HSCT after CAR-T, the effect of HSCT was influenced by many potential factors including complex karyotypes, certain genes associated with poor prognosis, leukemia burden, number of relapses, high lactate dehydrogenase (LDH) levels, lymphodepletion regimen, and constructure of CARs (12). Therefore, we conducted a subgroup analysis to explore factors influencing the effect of UCBT.

A high pre-infusion tumor burden had been reported to increase the relapse rate after CAR-T therapy (6, 13, 40). A clinical trial showed that consolidative HSCT significantly prolonged EFS and RFS in patients with a high leukemia burden (13). In our study, we observed a pronounced influence of consolidative UCBT on patients with MRD ≥5% or with EMD, suggesting that patients with a higher tumor burden would be more likely to benefit from consolidative UCBT. Some studies have found that surface CAR expression was inversely correlated with tumor burden due to receptor internalization (41–43); this may contribute to a higher probability of relapse in patients with a high tumor burden. Those findings demonstrate the necessity of consolidative transplantation for patients with a high tumor burden after CAR-T therapy. In addition, we found that the number of relapses can influence the effect of UCBT, patients who experienced fewer than 2 relapses did not benefit from consolidative UCBT, while in patients with recurrent relapses or sustainable NR, consolidative UCBT improved their RFS significantly. As for patients with poor prognosis markers, while worse overall EFS and OS were observed in multivariate analysis, those patients showed an improved EFS after bridging to UCBT. *MLL/AF4*, *BCR/ABL1*, *TP53*, and *E2A/PBX1* complex karyotypes are reported to indicate an inferior prognosis in B-ALL patients (44–48). Consolidative UCBT after CAR-T therapy may achieve a longer molecular response.

According to criteria published by Gökbuget et al. (49) age is the most important prognostic factor for ALL, and the prognosis of patients deteriorates with increasing age. Apart from that, some studies showed that adult patients are more likely to benefit from consolidative allo-HSCT, while younger patients can achieve durable remission without a consolidating allo-HSCT (4, 8). As the younger patients took a larger proportion in the UCBT group in our study, we further grouped the patients according to age (<25 years vs. ≥25 years) to reduce the influence of the confounding variable; the results showed that consolidative UCBT did not affect survival of patients in either group.

Another factor that can affect prognosis is the co-stimulatory structural domain of CAR. Preclinical studies indicated a relatively short duration after infusion of CAR-T cells with CD28 co-stimulatory domain (50, 51); moreover, numerous investigations have revealed that 4-1BB-based CAR-T cells exhibited more durable persistence than CAR-T cells that contained CD28 co-stimulatory domain (20, 32, 33, 52, 53). However, the outcomes of CAR-T cell containing CD28 co-stimulatory domains varied significantly among different studies. A retrospective analysis showed no improvement in EFS or OS in patients using CD28-based CD19 CAR-T cells bridged with HSCT (6). A study in pediatric patients using CD28 co-stimulatory CD19 CAR-T cells (54) suggested that HSCT leads to better EFS. Several reports of treating patients with 4-1BB-based CD19 CAR-T cells (13, 34) exhibited better RFS with consolidative HSCT, whereas patients receiving 4-1BB-containing CD19 CAR-T cells in the global ELIANA trial show no benefit in OS (8). It is unscrupulous to conclude the influence of different CAR structures on the effect of post-CAR-T transplantation. In our study, we did not observe an improvement in prognosis by consolidative UCBT in patients receiving CD28-based CAR nor in those receiving CD28/4-1BB-based CAR. Considering the limited sample size and confounding factors, a comparative study is needed.

Our study demonstrated that consolidative UCBT after CAR-T therapy can improve the clinical outcomes in specific groups of patients; however, the recurrence rate after transplantation was relatively high (40.0%, 10/25). Patients without occurrence of aGVHD appeared to have a shorter duration of remission. The occurrence of aGVHD after UCBT may indicate better RFS. A study showed that time from CAR-T cell application to transplantation associated with the risk of death (55). Some researchers recommended early consolidative UCBT to maximize the benefit, considering that approximately 10% of patients relapsed after CAR-T therapy within 3 months (12). However, our study did not show a correlation between the interval and long-term survival; among the 10 patients in the UCBT group who achieved sustained remission, four patients had an interval ≥3 months from CAR-T infusion to transplantation. Thus, the optimal time for consolidative transplantation needs to be determined by multicenter and large-sample studies. It is imperative to seek a treatment option for patients who relapse after transplantation because these patients generally have a poor prognosis. Eight patients

accepted re-infusion of CAR-T cells in this study, five of them achieved CR and the median OS after relapse was 21.9 months (range 9.4–39.5 months), the remaining two patients who did not receive a second CAR-T therapy died rapidly after relapse. Comparative studies with larger samples are necessary to explore the role of re-infusion of CAR-T cells.

Our study has its shortcomings due to its retrospective nature and the uniformity in baseline characteristics of patients; election bias on transplantation may also exist. However, the results from real-world data by subgroup analysis are still informative. Large-sample studies with consistent patient baseline characteristics are still needed.

## 5 CONCLUSION

To conclude, our study showed that consolidative UCBT provides an option for post-CAR-T consolidation. In patients with a history of ≥2 relapses or sustained NR, with poor prognostic markers, or with MRD ≥5% or EMD, long-term survival was significantly improved by consolidative UCBT. In contrast, UCBT does not necessarily result in a better prognosis for patients with a lower number of recurrences, no prognostic markers, and a lower tumor burden. For posttransplantation relapse, re-infusion of CAR-T cells may be an option to consider.

## DATA AVAILABILITY STATEMENT

The original contributions presented in the study are included in the article/supplementary material. Further inquiries can be directed to the corresponding author.

## ETHICS STATEMENT

This study was approved by the medical ethics committee of the First Affiliated Hospital of USTC (Anhui Provincial Hospital), Hefei, China (2016-101), and the Second Hospital of Anhui Medical University (SHAMU). All patients gave their written informed consent in accordance with the Declaration of Helsinki.

## AUTHOR CONTRIBUTIONS

QX, LX, and XBW analyzed the data and wrote the paper. FA, HX, LW, LG, XHZ, KS, WY, XW, JT, HL, XL, XYZ, ZZ, ZS, and XBW provided the study patients. XBW designed the research and edited the article. All authors contributed to the article and approved the submitted version.

## FUNDING

This study received funding from the National Natural Science Foundation of China #1 under Grant 82170221. The funder was not involved in the study design, collection, analysis, interpretation of data, the writing of this article or the decision to submit it for publication. All authors declare no other competing interests.

## ACKNOWLEDGMENTS

The authors would like to thank all members of the study team and the patients and their families.

## REFERENCES

1. Neelapu SS, Locke FL, Bartlett NL, Lekakis LJ, Miklos DB, Jacobson CA, et al. Axicabtagene Ciloleucel CAR T-Cell Therapy in Refractory Large B-Cell Lymphoma. *N Engl J Med* (2017) 377(26):2531–44. doi: 10.1056/NEJMoa1707447
2. June CH, Sadelain M. Chimeric Antigen Receptor Therapy. *N Engl J Med* (2018) 379(1):64–73. doi: 10.1056/NEJMra1706169
3. Pan J, Yang JF, Deng BP, Zhao XJ, Zhang X, Lin YH, et al. High Efficacy and Safety of Low-Dose CD19-Directed CAR-T Cell Therapy in 51 Refractory or Relapsed B Acute Lymphoblastic Leukemia Patients. *Leukemia* (2017) 31 (12):2587–93. doi: 10.1038/leu.2017.145
4. Gardner RA, Finney O, Annesley C, Brakke H, Summers C, Leger K, et al. Intent-To-Treat Leukemia Remission by CD19 CAR T Cells of Defined Formulation and Dose in Children and Young Adults. *Blood* (2017) 129 (25):3322–31. doi: 10.1182/blood-2017-02-769208
5. Wang M, Munoz J, Goy A, Locke FL, Jacobson CA, Hill BT, et al. KTE-X19 CAR T-Cell Therapy in Relapsed or Refractory Mantle-Cell Lymphoma. *N Engl J Med* (2020) 382(14):1331–42. doi: 10.1056/NEJMoa1914347
6. Park JH, Riviere I, Gonen M, Wang X, Senechal B, Curran KJ, et al. Long-Term Follow-Up of CD19 CAR Therapy in Acute Lymphoblastic Leukemia. *N Engl J Med* (2018) 378(5):449–59. doi: 10.1056/NEJMoa1709919
7. Cao J, Wang G, Cheng H, Wei C, Qi K, Sang W, et al. Potent Anti-Leukemia Activities of Humanized CD19-Targeted Chimeric Antigen Receptor T (CAR-T) Cells in Patients With Relapsed/Refractory Acute Lymphoblastic Leukemia. *Am J Hematol* (2018) 93(7):851–8. doi: 10.1002/ajh.25108
8. Maude SL, Laetsch TW, Buechner J, Rives S, Boyer M, Bittencourt H, et al. Tisagenlecleucel in Children and Young Adults With B-Cell Lymphoblastic Leukemia. *N Engl J Med* (2018) 378(5):439–48. doi: 10.1056/NEJMoa1709866
9. Singh H, Figliola MJ, Dawson MJ, Olivares S, Zhang L, Yang G, et al. Manufacture of Clinical-Grade CD19-Specific T Cells Stably Expressing Chimeric Antigen Receptor Using Sleeping Beauty System and Artificial Antigen Presenting Cells. *PloS One* (2013) 8(5):e64138. doi: 10.1371/journal.pone.0064138
10. Li AM, Hucks GE, Dinofia AM, Seif AE, Teachey DT, Baniewicz D, et al. Checkpoint Inhibitors Augment CD19-Directed Chimeric Antigen Receptor (CAR) T Cell Therapy in Relapsed B-Cell Acute Lymphoblastic Leukemia. *Blood* (2018) 132(Supplement 1):556–6. doi: 10.1182/blood-2018-99-112572
11. Huang L, Wang N, Cao Y, Li C, Xiao Y, Xiao M, et al. CAR22/19 Cocktail Therapy for Patients With Refractory/Relapsed B-Cell Malignancies. *Blood* (2018) 132(Supplement 1):1408–8. doi: 10.1182/blood-2018-99-113714
12. Jiang H, Hu Y, Mei H. Consolidative Allogeneic Hematopoietic Stem Cell Transplantation After Chimeric Antigen Receptor T-Cell Therapy for Relapsed/Refractory B-Cell Acute Lymphoblastic Leukemia: Who? When? Why? *biomark Res* (2020) 8(1):66. doi: 10.1186/s40364-020-00247-8
13. Jiang H, Li C, Yin P, Guo T, Liu L, Xia L, et al. Anti-CD19 Chimeric Antigen Receptor-Modified T-Cell Therapy Bridging to Allogeneic Hematopoietic Stem Cell Transplantation for Relapsed/Refractory B-Cell Acute Lymphoblastic Leukemia: An Open-Label Pragmatic Clinical Trial. *Am J Hematol* (2019) 94(10):1113–22. doi: 10.1002/ajh.25582
14. Lee DW, Stetler-Stevenson M, Yuan CM, Shah NN, Delbrook C, Yates B, et al. Long-Term Outcomes Following CD19 CAR T Cell Therapy for B-ALL Are Superior in Patients Receiving a Fludarabine/Cyclophosphamide Preparative

Regimen and Post-CAR Hematopoietic Stem Cell Transplantation. *Blood* (2016) 128(22):218–8. doi: 10.1182/blood.V128.22.218.218
15. Eapen M, Rocha V, Sanz G, Scaradavou A, Zhang M-J, Arcese W, et al. Effect of Graft Source on Unrelated Donor Haemopoietic Stem-Cell Transplantation in Adults With Acute Leukaemia: A Retrospective Analysis. *Lancet Oncol* (2010) 11(7):653–60. doi: 10.1016/s1470-2045(10)70127-3
16. Sun G, Tang B, Wan X, Yao W, Song K, Tu M, et al. CAR-T Cell Therapy Followed by Unrelated Cord Blood Transplantation for the Treatment of Relapsed/Refractory B-Cell ALL in Children and Young Adults: Superior Survival But Relatively High Posttransplant Relapse. *Transplant Cell Ther* (2021) 28(2):71.e1–8. doi: 10.1016/j.jtct.2021.11.011
17. Zhu X, Huang L, Zheng C, Tang B, Liu H, Geng L, et al. European Group for Blood and Marrow Transplantation Risk Score Predicts the Outcome of Patients With Acute Leukemia Receiving Single Umbilical Cord Blood Transplantation. *Biol Blood Marrow Transplant* (2017) 23(12):2118–26. doi: 10.1016/j.bbmt.2017.08.011
18. Schoemans HM, Lee SJ, Ferrara JL, Wolff D, Levine JE, Schultz KR, et al. EBMT-NIH-CIBMTR Task Force Position Statement on Standardized Terminology & Guidance for Graft-Versus-Host Disease Assessment. *Bone Marrow Transplant* (2018) 53(11):1401–15. doi: 10.1038/s41409-018-0204-7
19. Jagasia MH, Greinix HT, Arora M, Williams KM, Wolff D, Cowen EW, et al. National Institutes of Health Consensus Development Project on Criteria for Clinical Trials in Chronic Graft-Versus-Host Disease: I. The 2014 Diagnosis and Staging Working Group Report. *Biol Blood Marrow Transplant* (2015) 21 (3):389–401.e381. doi: 10.1016/j.bbmt.2014.12.001
20. Maude SL, Frey N, Shaw PA, Aplenc R, Barrett DM, Bunin NJ, et al. Chimeric Antigen Receptor T Cells for Sustained Remissions in Leukemia. *N Engl J Med* (2014) 371(16):1507–17. doi: 10.1056/NEJMoa1407222
21. Sotillo E, Barrett DM, Black KL, Bagashev A, Oldridge D, Wu G, et al. Convergence of Acquired Mutations and Alternative Splicing of CD19 Enables Resistance to CART-19 Immunotherapy. *Cancer Discov* (2015) 5 (12):1282–95. doi: 10.1158/2159-8290.CD-15-1020
22. Grupp SA, Kalos M, Barrett D, Aplenc R, Porter DL, Rheingold SR, et al. Chimeric Antigen Receptor-Modified T Cells for Acute Lymphoid Leukemia. *N Engl J Med* (2013) 368(16):1509–18. doi: 10.1056/NEJMoa1215134
23. Jacoby E, Nguyen SM, Fountaine TJ, Welp K, Gryder B, Qin H, et al. CD19 CAR Immune Pressure Induces B-Precursor Acute Lymphoblastic Leukaemia Lineage Switch Exposing Inherent Leukaemic Plasticity. *Nat Commun* (2016) 7:12320. doi: 10.1038/ncomms12320
24. Hamieh M, Dobrin A, Cabriolu A, van der Stegen SJC, Giavridis T, Mansilla-Soto J, et al. CAR T Cell Trogocytosis and Cooperative Killing Regulate Tumour Antigen Escape. *Nature* (2019) 568(7750):112–6. doi: 10.1038/s41586-019-1054-1
25. Guedan S, Posey AD Jr, Shaw C, Wing A, Da T, Patel PR, et al. Enhancing CAR T Cell Persistence Through ICOS and 4-1BB Costimulation. *JCI Insight* (2018) 3(1):e96976. doi: 10.1172/jci.insight.96976
26. Tengfei Z, Ling C, Jing X, Ni S, Zhen Z, Zhenzhen L, et al. Efficiency of CD19 Chimeric Antigen Receptor-Modified T Cells for Treatment of B Cell Malignancies in Phase I Clinical Trials a Meta-Analysis. *Oncotarget* (2015) 6(32):33961–71. doi: 10.18632/oncotarget.5582
27. Gardner R, Annesley C, Finney O, Summers C, Lamble AJ, Rivers J, et al. Early Clinical Experience of CD19 X CD22 Dual Specific CAR T Cells for Enhanced Anti-Leukemic Targeting of Acute Lymphoblastic Leukemia. *Blood* (2018) 132(Supplement 1):278–8. doi: 10.1182/blood-2018-99-113126
28. Huang L, Wang N, Li C, Cao Y, Xiao Y, Xiao M, et al. Sequential Infusion of Anti-CD22 and Anti-CD19 Chimeric Antigen Receptor T Cells for Adult Patients With Refractory/Relapsed B-Cell Acute Lymphoblastic Leukemia. *Blood* (2017) 130(Supplement 1):846–6. doi: 10.1182/blood.V130.Suppl_1.846.846
29. Shalabi H, Delbrook C, Stetler-Stevenson M, Yuan C, Steinberg SM, Yates B, et al. Chimeric Antigen Receptor T-Cell (CAR-T) Therapy can Render Patients With ALL Into PCR-Negative Remission and can be an Effective Bridge to Transplant (HCT). *Biol Blood Marrow Transplantation* (2018) 24 (3):S25–6. doi: 10.1016/j.bbmt.2017.12.018
30. Yang J, Li J, Zhang X, LV F, Guo X, Wang Q, et al. A Feasibility and Safety Study of CD19 and CD22 Chimeric Antigen Receptors-Modified T Cell Cocktail for Therapy of B Cell Acute Lymphoblastic Leukemia. *Blood* (2018) 132(Supplement 1):277–7. doi: 10.1182/blood-2018-99-114415
31. Gardner R, Wu D, Cherian S, Fang M, Hanafi L-A, Finney O, et al. Acquisition of a CD19-Negative Myeloid Phenotype Allows Immune Escape of MLL-Rearranged B-ALL From CD19 CAR-T-Cell Therapy. *Blood* (2016) 127(20):2406–10. doi: 10.1182/blood-2015-08-665547
32. Brentjens RJ, Davila ML, Riviere I, Park J, Wang X, Cowell LG, et al. CD19-Targeted T Cells Rapidly Induce Molecular Remissions in Adults With Chemotherapy-Refractory Acute Lymphoblastic Leukemia. *Sci Transl Med* (2013) 5(177):177ra138. doi: 10.1126/scitranslmed.3005930
33. Lee DW, Kochenderfer JN, Stetler-Stevenson M, Cui YK, Delbrook C, Feldman SA, et al. T Cells Expressing CD19 Chimeric Antigen Receptors for Acute Lymphoblastic Leukaemia in Children and Young Adults: A Phase 1 Dose-Escalation Trial. *Lancet* (2015) 385(9967):517–28. doi: 10.1016/s0140-6736(14)61403-3
34. Hay KA, Gauthier J, Hirayama AV, Voutsinas JM, Wu Q, Li D, et al. Factors Associated With Durable EFS in Adult B-Cell ALL Patients Achieving MRD-Negative CR After CD19 CAR T-Cell Therapy. *Blood* (2019) 133(15):1652–63. doi: 10.1182/blood-2018-11-883710
35. Shah BD, Ghobadi A, Oluwole OO, Logan AC, Boissel N, Cassaday RD, et al. KTE-X19 for Relapsed or Refractory Adult B-Cell Acute Lymphoblastic Leukaemia: Phase 2 Results of the Single-Arm, Open-Label, Multicentre ZUMA-3 Study. *Lancet* (2021) 398(10299):491–502. doi: 10.1016/s0140-6736(21)01222-8
36. Ruggeri A, Volt F, Locatelli F, Michel G, Diaz de Heredia C, Abecasis M, et al. Unrelated Cord Blood Transplantation for Acute Leukemia Diagnosed in the First Year of Life: Outcomes and Risk Factor Analysis. *Biol Blood Marrow Transplant* (2017) 23(1):96–102. doi: 10.1016/j.bbmt.2016.10.014
37. Rocha V, Cornish J, Sievers EL, Filipovich A, Locatelli F, Peters C, et al. Comparison of Outcomes of Unrelated Bone Marrow and Umbilical Cord Blood Transplants in Children With Acute Leukemia. *Blood* (2001) 97 (10):2962–71. doi: 10.1182/blood.V97.10.2962
38. Zhang H, Chen J, Que W. A Meta-Analysis of Unrelated Donor Umbilical Cord Blood Transplantation Versus Unrelated Donor Bone Marrow Transplantation in Acute Leukemia Patients. *Biol Blood Marrow Transplant* (2012) 18(8):1164–73. doi: 10.1016/j.bbmt.2012.01.015
39. Eapen M, Rubinstein P, Zhang MJ, Stevens C, Kurtzberg J, Scaradavou A, et al. Outcomes of Transplantation of Unrelated Donor Umbilical Cord Blood and Bone Marrow in Children With Acute Leukaemia: A Comparison Study. *Lancet* (2007) 369(9577):1947–54. doi: 10.1016/S0140-6736(07)60915-5
40. Kebriaei P, Singh H, Huls MH, Figliola MJ, Bassett R, Olivares S, et al. Phase I Trials Using Sleeping Beauty to Generate CD19-Specific CAR T Cells. *J Clin Invest* (2016) 126(9):3363–76. doi: 10.1172/JCI86721
41. Kalos M, Levine BL, Porter DL, Katz S, Grupp SA, Bagg A, et al. T Cells With Chimeric Antigen Receptors Have Potent Antitumor Effects and can Establish Memory in Patients With Advanced Leukemia. *Sci Transl Med* (2011) 3 (95):95ra73. doi: 10.1126/scitranslmed.3002842
42. Ghosh A, Smith M, James SE, Davila ML, Velardi E, Argyropoulos KV, et al. Donor CD19 CAR T Cells Exert Potent Graft-Versus-Lymphoma Activity With Diminished Graft-Versus-Host Activity. *Nat Med* (2017) 23(2):242–9. doi: 10.1038/nm.4258
43. Eyquem J, Mansilla-Soto J, Giavridis T, van der Stegen SJ, Hamieh M, Cunanan KM, et al. Targeting a CAR to the TRAC Locus With CRISPR/Cas9 Enhances Tumour Rejection. *Nature* (2017) 543(7643):113–7. doi: 10.1038/nature21405
44. Gleißner B, Gökbuget N, Bartram CR, Janssen B, Rieder H, Janssen JWG, et al. Leading Prognostic Relevance of the BCR-ABL Translocation in Adult Acute B-Lineage Lymphoblastic Leukemia: A Prospective Study of the German Multicenter Trial Group and Confirmed Polymerase Chain Reaction Analysis. *Blood* (2002) 99(5):1536–43. doi: 10.1182/blood.V99.5.1536
45. Schlieben S, Borkhardt A, Reinisch I, Ritterbach J, Janssen JW, Ratei R, et al. Incidence and Clinical Outcome of Children With BCR/ABL-Positive Acute Lymphoblastic Leukemia (ALL). A Prospective RT-PCR Study Based on 673 Patients Enrolled in the German Pediatric Multicenter Therapy Trials ALL-BFM-90 and CoALL-05-92. *Leukemia (Basingstoke)* (1996) 10(6):957–63.
46. Iqbal Z, Akhtar T, Awan T, Aleem A, Sabir N, Rasool M, et al. High Frequency and Poor Prognosis of Late Childhood BCR-ABL-Positive and MLL-AF4-Positive ALL Define the Need for Advanced Molecular Diagnostics and Improved Therapeutic Strategies in Pediatric B-ALL in Pakistan. *Mol Diagn Ther* (2015) 19(5):277–87. doi: 10.1007/s40291-015-0149-0

47. Forero-Castro M, Robledo C, Benito R, Bodega-Mayor I, Rapado I, Hernandez-Sanchez M, et al. Mutations in TP53 and JAK2 are Independent Prognostic Biomarkers in B-Cell Precursor Acute Lymphoblastic Leukaemia. *Br J Cancer* (2017) 117(2):256–65. doi: 10.1038/bjc.2017.152
48. Foa R, Vitale A, Mancini M, Cuneo A, Mecucci C, Elia L, et al. E2A-PBX1 Fusion in Adult Acute Lymphoblastic Leukaemia: Biological and Clinical Features. *Br J Haematol* (2003) 120(3):484–7. doi: 10.1046/j.1365-2141.2003.04113.x
49. Gökbuget N, Hoelzer D. Treatment of Adult Acute Lymphoblastic Leukemia. *Semin Hematol* (2009) 46(1):64–75. doi: 10.1053/j.seminhematol.2008.09.003
50. Long AH, Haso WM, Shern JF, Wanhainen KM, Murgai M, Ingaramo M, et al. 4-1BB Costimulation Ameliorates T Cell Exhaustion Induced by Tonic Signaling of Chimeric Antigen Receptors. *Nat Med* (2015) 21(6):581–90. doi: 10.1038/nm.3838
51. Zhao Z, Condomines M, van der Stegen SJC, Perna F, Kloss CC, Gunset G, et al. Structural Design of Engineered Costimulation Determines Tumor Rejection Kinetics and Persistence of CAR T Cells. *Cancer Cell* (2015) 28 (4):415–28. doi: 10.1016/j.ccell.2015.09.004
52. Davila ML, Riviere I, Wang X, Bartido S, Park J, Curran K, et al. Efficacy and Toxicity Management of 19-28z CAR T Cell Therapy in B Cell Acute Lymphoblastic Leukemia. *Sci Transl Med* (2014) 6(224):224ra25. doi: 10.1126/scitranslmed.3008226
53. Jacoby E, Bielorai B, Avigdor A, Itzhaki O, Hutt D, Nussboim V, et al. Locally Produced CD19 CAR T Cells Leading to Clinical Remissions in Medullary and Extramedullary Relapsed Acute Lymphoblastic Leukemia. *Am J Hematol* (2018) 93(12):1485–92. doi: 10.1002/ajh.25274
54. Shah NN, Lee DW, Yates B, Yuan CM, Shalabi H, Martin S, et al. Long-Term Follow-Up of CD19-CAR T-Cell Therapy in Children and Young Adults With B-ALL. *J Clin Oncol* (2021) 39(15):1650–9. doi: 10.1200/JCO.20
55. Shadman M, Gauthier J, Hay KA, Voutsinas JM, Milano F, Li A, et al. Safety of Allogeneic Hematopoietic Cell Transplant in Adults After CD19-Targeted CAR T-Cell Therapy. *Blood Adv* (2019) 3(20):3062–9. doi: 10.1182/bloodadvances.2019000593

**Conflict of Interest:** The authors declare that the research was conducted in the absence of any commercial or financial relationships that could be construed as a potential conflict of interest.

frontiers | Frontiers in Immunology

TYPE Original Research
PUBLISHED 02 September 2022
DOI 10.3389/fimmu.2022.953644



OPEN ACCESS

EDITED BY
Fabio Malavasi,
University of Turin, Italy

REVIEWED BY
Nicholas Chiorazzi,
Feinstein Institute for Medical Research, United States
Xin Wang,
Shandong Provincial Hospital, China

*CORRESPONDENCE
Regina Michelis
ReginaM@gmc.gov.il

†These authors have contributed equally to this work

SPECIALTY SECTION
This article was submitted to Cancer Immunity and Immunotherapy, a section of the journal Frontiers in Immunology

RECEIVED 12 June 2022
ACCEPTED 08 August 2022
PUBLISHED 02 September 2022

CITATION
Michelis R, Milhem L, Galouk E, Stemer G, Aviv A, Tadmor T, Shehadeh M, Shvidel L, Barhoum M and Braester A (2022) Increased serum level of alpha-2 macroglobulin and its production by B-lymphocytes in chronic lymphocytic leukemia. *Front. Immunol.* 13:953644. doi: 10.3389/fimmu.2022.953644



# Increased serum level of alpha-2 macroglobulin and its production by B-lymphocytes in chronic lymphocytic leukemia

Regina Michelis[1*], Lama Milhem[1,2], Evleen Galouk[1,2], Galia Stemer[2,3], Ariel Aviv[4], Tamar Tadmor[5,6], Mona Shehadeh[7], Lev Shvidel[8,9], Masad Barhoum[2†] and Andrei Braester[2,3†]

[1]The Institute for Medical Research, Galilee Medical Center, Nahariya, Israel, [2]Azrieli Faculty of Medicine, Bar Ilan University, Safed, Israel, [3]Institute of Hematology, Galilee Medical Center, Nahariya, Israel, [4]Department of Hematology, Emek Medical Center, Afula, Israel, [5]Hematology Unit, Bnai Zion Medical Center, Haifa, Israel, [6]The Ruth and Bruce Rappaport Faculty of Medicine, Technion, Haifa, Israel, [7]Biochemistry Laboratory, Galilee Medical Center, Nahariya, Israel, [8]Hematology Institute, Kaplan Medical Center, Rehovot, Israel, [9]Faculty of Medicine, Hebrew University, Jerusalem, Israel

Chronic lymphocytic leukemia (CLL), the most common adult's leukemia in the western world, is caused in 95% of the cases by uncontrolled proliferation of monoclonal B-lymphocytes. The complement system in CLL is chronically activated at a low level *via* the classical pathway (CP). This chronic activation is induced by IgG-hexamers, which are formed after binding to alpha-2-macroglobulin (A2M). The study investigated for the first time the serum levels of A2M in CLL patients, their association with the disease severity, and A2M production by the malignant B-lymphocytes. Blood samples were collected from 65 CLL patients and 30 normal controls (NC) subjects, and used for quantifications of the A2M levels, the complement activation marker (sC5b-9), the complement components C2, C3 and C4, and clinical biochemistry and hematology parameters. The production of A2M was studied in B-lymphocytes isolated from blood samples as well as in CLL and non-CLL cell lines.The serum A2M levels were significantly higher in CLL patients vs NCs, showing values of 3.62 $\pm$ 0.22 and 1.97 $\pm$ 0.10 mg/ml, respectively. Within the CLL group, A2M levels correlated significantly with the disease stage, with sC5b-9, and with clinical indicators of the disease severity. Increased A2M production was showed in three out of four CLL B-lymphocytic lines that were studied, as compared to non-CLL lines, to a non-lymphocytic line, and to blood-derived primary B-lymphocytes. A2M production was further increased both in primary cells and in the CLL cell-line after incubation with CLL sera, compared to NC sera. This study shows for the first time that serum A2M levels in CLL are significantly increased, likely due to A2M production by the malignant B-lymphocytes, and are correlated with the disease severity and with chronic complement activation. The moderate change in A2M production after incubation with NC sera *in-vitro* supports the hypothesis that inhibition of excess A2M production can be achieved, and that

this may potentially down-regulate the IgG-hexamerization and the resulting chronic CP activation. This may also help restore complement system activity, and eventually improve complement activity and immunotherapy outcomes in CLL.

KEYWORDS

alpha-2-macroglobulin (A2M), B-lymphocytes, chronic lymphocytic leukemia, complement system, classical pathway of complement

# 1 Introduction

Alpha-2-Macroglobulin (A2M), the largest major non-immunoglobulin protein in human plasma, is a broad-spectrum protease inhibitor that can inhibit all proteinase families, including serine-, cysteine-, aspartic- and metalloproteinases (1). Each A2M molecule contains a macroglobulin domain, a thioester (TE) containing domain and a receptor-binding domain (2). Its protease-inhibitory functions are executed *via* a conformational change that traps the attacking protease after binding to a TE motif, GCGEQ, also called "the bait" within the A2M protein (3). Similar to other members of the thioester-containing proteins (TEPs) family, named after their active site that functions by forming covalent bonds with specific molecular targets, A2M plays an important role in clearance of proteases from the circulation, regulation of fibrinolysis, coagulation and complement activation (3). A2M also participates, with IgG molecules, in formation of immune complexes that generate aggregated/hexameric structures (A2M-IgG-hexamers) and activate the classical pathway (CP) of the complement system in patients with Chronic Lymphocytic Leukemia (CLL) (4).

A2M is an acute-phase protein, produced primarily by the liver and lungs, and secreted into the bloodstream and extracellular environments (5). It is also produced locally by macrophages, fibroblasts, and epithelial cells (5). A2M is formed by the assembly of four 182kDa subunits into two disulfide-linked dimers, which non-covalently associate to complete the tetrameric structure of A2M (1). However, several studies showed that A2M is present in the circulation in either a dimeric or tetrameric form (6, 7).

Mutations in the A2M gene play a role in the pathogenesis of Alzheimer's disease, Parkinson's disease, and prostate cancer (1), while increased serum concentrations were shown to be associated with nephrotic syndrome, diabetes (type 1 and type 2), chronic liver disease and acute lymphoblastic leukemia (8–10). In patients with CLL, A2M has rarely been studied, and the serum levels of A2M have not yet been reported.

CLL is the most common leukemia, comprising 25-30% of all adult leukemia patients in the western world. It affects the B-type lymphocytes in the bone marrow in 95% of the patients, and is characterized by increased numbers of monoclonal B-lymphocytes (>5x10$^3$/μl) that express specific antigens (CD5, CD19, CD20, CD23) on their surface. A2M is involved in the chronic CP activation in CLL (4), which decreases the CP activity in these patients. This decrease in CP activity compromises the CP dependent mechanisms activated by the immunotherapeutic drugs, such as the complement dependent cytotoxicity (CDC), and may eventually affect the outcomes of the immunotherapy. Thus, the aims of the study were to measure A2M levels in CLL sera in various stages of the disease and to assess its production by the malignant B-lymphocytes.

# 2 Materials and methods

## 2.1 Subjects

Blood samples were collected from 65 un-treated (naïve) CLL patients and 30 normal (non-malignant) controls (NC). As CLL patients are normally ~69 years old, many of them also suffer from chronic diseases such as type 2 Diabetes mellitus and/or hypertension, which were not used as exclusion criteria. Accordingly, the NC group included subjects who were matched with the CLL group for gender, chronic diseases and age (as possible). NC exclusion: any type of malignancy in the past or present, and any type of severe infection or hospitalization within the past 6 months. Plasma and sera were separated and frozen at -80°C. The study was approved by the Helsinki Committee (Institutional Review Board) of Galilee Medical Center (Nahariya, Israel), and all subjects signed informed consent.

## 2.2 Measurement of A2M levels

### 2.2.1 ELISA

To measure the A2M and C2 levels, commercial ELISA kits were used (human A2M and human C2 ELISA kits, both from Elabscience), according to the manufacturers' instructions. The results were measured using an ELISA reader (CARIOSKAN LUX, Thermo scientific).

## 2.3 Analysis of A2M production by B-lymphocytes

### 2.3.1 Cell culture

The following CLL B-lymphocytes cell lines were used: MEC-2 (CSC-C0511 from Creative-Bioarray, USA), JVM-2 (CRL-3002 from American Type Culture Collection, USA/ATCC), JVM-13 (CRL-3003 from ATCC) and HG-3 (ACC 765 from DSMZ-German Collection of Microorganisms and Cell Cultures GmbH, Germany). All cell lines were cultured at 37°C in a humidified 5% $CO_2$ atmosphere. JVM-2, JVM-13 and HG-3 were cultured with RPMI 1640 medium (ATCC) and MEC-2 in IMDM medium (Biological Industries). The medium for MEC-2 and HG-3 was supplemented with 10% heat-inactivated fetal bovine serum (hi FBS, Biological Industries, Israel) and non-hi FBS for JVM-2 and JVM-13. The monocytic cell line THP-1 (TIB-202 from ATCC) as well as two B-lymphocytes cell lines from non-CLL origin (from patients with Diffuse Large B-cell Lymphoma (DLBCL): SU-DHL-4 and SU-DHL-5 (CRL-2957 and CRL-2958, respectively, from ATCC) were used as controls. THP-1 cells were cultured in RPMI 1640 medium and 20% hi FBS, while SU-DHL-4 and SU-DHL-5 cells were cultured in RPMI 1640 medium and 10% non-hi FBS. All growth media were supplemented with 0.1% penicillin-streptomycin (ATCC) and the growth media of MEC-2 and JVM-2 were also supplemented with 1% glutamine (Biological Industries, except for THP-1), and all cell lines were cultured for <8 passages.

### 2.3.2 Isolation of primary B-lymphocytes from peripheral blood

Primary B-lymphocytes were isolated from peripheral blood as described previously (11) except that the isolation procedure was performed under sterile conditions. Blood was obtained from patients and NC subjects in EDTA-containing tubes and used immediately for separation of peripheral blood mononuclear cells (PBMCs) by Lymphoprep (Axis-shield) density gradient centrifugation in SepMate™ PBMC Isolation Tubes (STEMCELL Technologies Inc.). Cell numbers were counted in a hemocytometer and $10^7$ PBMCs were further used for B-lymphocyte isolation, based on negative selection, using magnetic-activated cell sorting (MACS) bead Isolation kits (Miltenyi Biotec). B-lymphocytes from CLL and NC subjects were isolated with B-Cell Isolation B-CLL Kit (130–103–466) and B Cell Isolation Kit II (130–091–151), respectively. In order to validate the purity of separated primary B-cells, they were studied by flow-cytometry, using CD19 and CD20 antibodies. Cell suspensions ($10^5$ cells) were washed twice with PBS, and stained for 10 min with the fluorescent antibodies anti-CD19-Phycoerythrin Cyanin 7 (CD19-PC7, Beckman) and anti-CD20-Allophycocyanin (CD20-APC, protein-tech), that bind to B-lymphocytes. All incubations were performed at room temperature (RT), in the dark. The staining of the cells was assessed by a Flow cytometer (Navios, Beckman Coulter).

### 2.3.3 A2M production in B-lymphocytes

Cells of the CLL B-lymphocyte cell lines were centrifuged at 120g for 7min at RT, re-suspended in fresh culture medium at a concentration of 20,000 cells/100µl, and incubated in triplicates in a 96 well plate, in the 37°C incubator. After 12-72 hrs, depending on the cell type (12 hrs for lines MEC-2, HG-3, JVM-13, SU-DHL-4 and SU-DHL-5; 24 hrs for the THP-1 line; 72 hrs for the JVM-2 line), the triplicates were combined, centrifuged at 5000 g for 5 min at RT to remove the cells, and the supernatants were stored at -20°C until the A2M analysis (by ELISA) was performed. The incubation time for each cell type were selected after evaluation of several time points (data not shown).

In parallel, cells were centrifuged at 120g for 7min at RT and re-suspended in fresh medium at a concentration of 20,000 cells/80µl. Sera of CLL patients or NC subjects, with known A2M levels, were added to a final concentration of 20%, and 100µl of the mixture was incubated in triplicates in a 96 well plate, and processed as described above. A2M levels were measured in the cell's medium, and the production of A2M by the cells was calculated as the change in A2M amount (ΔA2M in µg) after subtracting the level contributed by the serum, and the levels produced by the cells without any added serum.

For examination of A2M production in primary B-lymphocytes, B-cells isolated from peripheral blood of CLL patients and NC subjects were centrifuged at 120g for 7min at RT, re-suspended in fresh culture medium (RPMI 1640 and 10% non-hi FBS) at a concentration of 20,000 cells/100µl or 20,000 cells/80µl and incubated with or without 20% human serum as described above for the cell-line cells. After 24 hrs the triplicates were combined, centrifuged at 5000g for 5min at RT to remove the cells and the supernatants were frozen for later A2M analysis (by ELISA). The ΔA2M was calculated, in µg, as described above.

## 2.4 Statistical analysis

Data were analyzed by unpaired, two tailed, student t-test. Data from the *in-vitro* experiments were analyzed by Mann-Whitney tests (two tailed), as appropriate. $P<0.05$ was considered significant.

# 3 Results

## 3.1 Characteristics of the subjects' groups

The Clinical parameters of patients and NCs are shown in Table 1. As expected, all the hematological parameters in CLL

patients were significantly different from the values in the NC group, so that WBC, lymphocyte counts, and lymphocyte percentage were higher while RBC, Hb, and platelets counts were lower, relative to NC. The mean patient's age was higher relative to the NC group, however A2M levels were not influenced by age (Supplementary Figure S1). One liver function indicator, ALT, was significantly decreased in the patients, although within the normal range. Two lipid profile parameters, the HDL and total cholesterol levels, were significantly decreased in the patients, as reported previously (12). No significant differences were observed in all other parameters.

## 3.2 A2M levels in patients and NC subjects – association with CLL stage and mutation status

The serum levels of A2M were significantly higher ($p<0.0001$) in patients vs. NCs, showing values of 3.62 ± 0.22 and 1.97 ± 0.10 mg/ml, respectively (Figure 1A). Within the CLL group, A2M levels did not correlate with age, and was similar in males and females (Supplementary Figure S1).

When the patients cohort was divided into subgroups according to the disease stage (Binet staging), the serum A2M levels showed clear association with the disease stage, as can be seen in the gradual increase in A2M values along with the CLL stages (Figure 1B). The values of A2M in patients at stage A, B and C were 2.86 ± 0.18, 3.76 ± 0.26 and 5.61 ± 0.83 mg/ml, respectively, and were significantly different ($p<0.01$) between the groups (Figure 1B).

Genetic analysis of CLL-associated genes was available from 36 out of the 65 patients included in the study. This analysis is not a routine test in the care of CLL patients with indolent disease, and is usually performed when the disease advances and the patient may face intervention. Therefore, the distribution of CLL stages in these 36 patients differed from the stage distribution in the original cohort, with relatively decreased proportion of patients in stage A (only 19% vs. 44% in the 65 patients cohort) and increased proportion of patients at stages B (53% vs. 38%) and C (28% vs. only 18%).

Among these 36 patients with available genetic data, 12 (33%) had normal karyotype, 7 (19%) had trisomy 12, 3 (8%) had 11q deletion, 11 (31%) had 13q deletion, and only one patient (3%) had 17p deletion and 2 patients (6%) had both 17p and 11q deletions. When A2M levels were compared between the CLL subgroups divided according to the genetic abnormalities (Figure 1C), high levels (4.2 ± 0.5 mg/ml) were found in patients with normal karyotype, and lower A2M levels, although significantly higher compared with NCs, were found in patients with Trisomy 12 (2.6 ± 0.32 mg/ml) or with deletions of the 11q or 13q (2.9 and 4.0 mg/ml, respectively). The high A2M

TABLE 1 Characteristics of the subjects' groups.

| Clinical parameter | CLL patients | Normal controls | p-value |
|---|---|---|---|
| n | 65 | 30 | |
| Gender (male/female) | 41/24 | 19/11 | |
| Age (years) | 67.6 ± 1.3* | 59.6 ± 1.9 | **0.001** |
| ALP U/L (40-150) | 87.6 ± 6.7 | 74.2 ± 3.6 | 0.105 |
| ALT U/L (<55) | 20.0 ± 1.4* | 27.9 ± 2.1 | **0.002** |
| AST U/L (5-34) | 23.3 ± 1.0 | 24.4 ± 0.8 | 0.502 |
| Cholesterol mg/dl (<200) | 161.5 ± 6.3* | 196.9 ± 8.4 | **0.001** |
| Triglycerides mg/dl (<150) | 151.0 ± 10.7 | 147.8 ± 17.9 | 0.932 |
| HDL mg/dl (>40) | 35.1 ± 1.9* | 47.3 ± 2.8 | **<0.001** |
| LDL mg/dl (<100) | 96.4 ± 6.1* | 120.8 ± 7.9 | **0.016** |
| Non-HDL chol. mg/dl (<130) | 125.7 ± 6.5* | 149.6 ± 8.3 | **0.023** |
| Serum C3 mg/dl (82-185) | 127.8 ± 6.1 | 119.5 ± 3.6 | 0.320 |
| Serum C4 mg/dl (15-53) | 26.5 ± 1.6 | 31.5 ± 1.5 | 0.052 |
| WBC x10e$^3$/μl (4-10) | 49.5 ± 8.8* | 6.9 ± 0.3 | **0.002** |
| Lymph. abs x10e$^3$/μl (1.5-8) | 44.9 ± 9.6* | 2.2 ± 0.1 | **0.001** |
| Lymph. % (19-48) | 69.0 ± 2.5* | 30.9 ± 1.2 | **<0.001** |
| Platelets x 10e$^3$/μl (130-400) | 159.2 ± 9.2* | 243.4 ± 9.3 | **<0.001** |
| RBC x 10e$^6$/μl (4-5.5) | 4.3 ± 0.1* | 4.8 ± 0.1 | **0.003** |
| Hb g/dl (13-18) | 12.9 ± 0.3* | 14.1 ± 0.3 | **0.006** |

The results of subjects' characteristics are shown as mean ± SEM. ALP, alkaline phosphatase; AST, aspartate transaminase; ALT, alanine transaminase; HDL, high density lipoprotein; LDL, low-density lipoprotein; non-HDL Chol., Non-HDL Cholesterol; C3, complement component 3; C4, complement component 4; WBC, white blood cells; Lymph. abs., absolute lymphocytes count; Lymph.%, lymphocytes percentage; RBC, red blood cells; Hb, hemoglobin. * indicates significant p value ($p<0.05$) as indicated by t-test.
Significant p values (<0.05) are indicated by bold text.

level in the only patient with the 17p deletion (6.5 mg/ml), should be further verified in order to establish this observation, particularly since 17p deletion, as a sole abnormality is associated with poor prognosis: short survival and the shortest treatment-free interval (13). The prognosis for patients with normal karyotype, however, is better relative to CLL patients with one or more genetic abnormalities (13).

Overall, the data in Figure 1 show that A2M levels are increased in CLL and are associated with indicators for aggravation of the patient's condition (CLL stage), but it is unclear if they are also associated with genetic indicators for poor prognosis.

## 3.3 Association of A2M levels with hematological parameters

The association of serum A2M levels with hematological parameters was analyzed and the resulting correlation data is given in Table 2. The graph for each correlation analysis is given in Supplementary Figure S2. The data showed significant positive correlations with WBC, lymphocytes numbers and % of CD38+ B-cells (in patients with CD38+ staining), and significant negative correlations with RBC, platelet counts and hemoglobin levels (Table 2). The data indicate, again, that A2M levels in CLL are associated with indicators for disease severity, including high WBC and lymphocyte counts, and low RBC, Hb and platelet counts.

## 3.4 Association of A2M levels with biochemical parameters

The associations of serum A2M levels with biochemical parameters are provided in Table 3. The graph for each correlation analysis is given in Supplementary Figure S3. The data showed significant positive correlations with alkaline phosphatase (ALP), aspartate aminotransferase (AST), glucose and b2M levels, and a significant negative correlation with HDL. Among the biochemical parameters that were used for correlation analyses, b2M and abnormal liver function are known to be associated with the CLL staging (14). Thus, the data in Table 3 support the association of A2M levels with indicators for aggravation of the CLL disease.

## 3.5 Association of A2M levels with complement-related parameters

We recently showed the involvement of A2M in the formation of cell-free aggregates that act as activators of the CP (4). Therefore, the correlation of serum A2M levels with complement-related parameters was studied. The correlations with the levels of C2 and C4, that are essential components of the CP and can presumably be exhausted by chronic CP activation, were studied, as well as the correlation with the levels of C3. Also, the baseline levels of sC5b-9, the final product of complement activation and a marker of complement activity, are associated with chronic activation of the CP (15), and therefore its correlation with the A2M levels were assessed as well. The correlation data, presented in Figure 2, did not show significant correlation with either C2, C3 or C4 (Figures 2A–C). However, a significant positive correlation was found in the CLL patients with the baseline levels of sC5b-9 (Figure 2D), supporting a link between A2M levels and chronic activation of the CP.

Interestingly, although the correlation of A2M and C4 did not reach a significant p value ($p=0.063$), the data in Figure 2C shows that among the 4 patients with C4 values below the normal range (i.e. <15 mg/dL), 3 patients had very high A2M levels, clearly above (>twice) the normal A2M average (which is $1.97 \pm 0.10$ mg/ml). Alas, examination of the A2M values in the subgroup of 4 patients with sub-normal C4 values vs the rest of the CLL patients indicated a p value of 0.052. Yet, this result suggests that analysis of a larger group of patients with sub-normal C4 values may eventually indicate significant differences that can further support the link between A2M levels and chronic activation of the CP. This assumption is supported by a correlation analysis of A2M with C2-C4, which was performed in a larger cohort, including both CLL and NC subjects, and showed significant correlation with the levels of C4, but not with C2 or C3 (Supplementary Figure S4).

Altogether, the data indicate that A2M levels in CLL are not only associated with the disease severity, but are also significantly associated with sC5b-9, which is a marker of chronic complement activation.

## 3.6 Production of A2M in B-lymphocytes

A2M is produced primarily in the liver and lungs, but local production by macrophages, fibroblasts, and epithelial cells was also reported (5). The increased levels of A2M in CLL serum and the association with WBC and particularly with lymphocytes counts, encouraged us to explore the possibility that in CLL patients, A2M levels may be increased in the circulation due to local production by B-lymphocytes. This was first examined in the CLL cell lines MEC-2, JVM-2, JVM-13 and HG-3 that were compared with the non-CLL B-lymphocytic cell lines SU-DHL-4 and SU-DHL-5, and with a monocytic cell line, THP-1 (Figure 3). When compared with non-CLL or monocytic lines, the data clearly indicated higher production of A2M in the CLL B-lymphocytic cell lines that were examined, particularly in the MEC-2 and JVM-2 lines (Figure 3). In one CLL cell line, the JVM-13, the increase in A2M production was not as pronounced as in the other CLL lines.

10.3389/fimmu.2022.953644

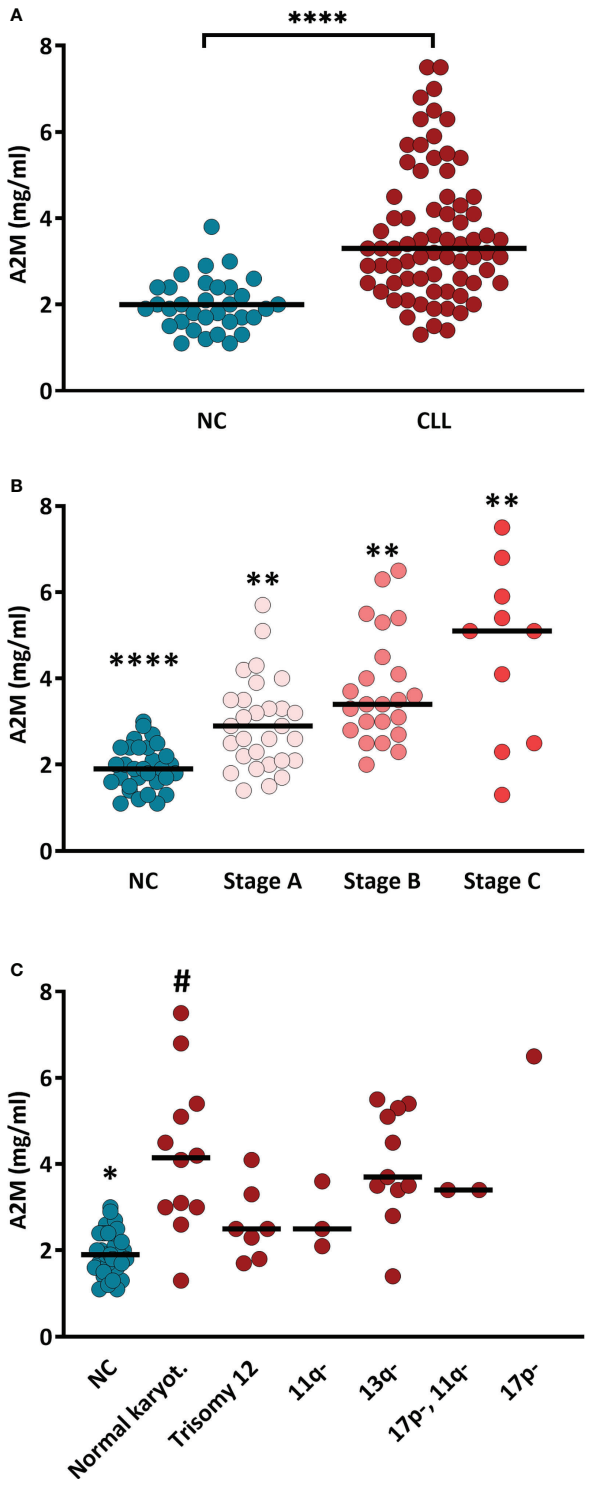


FIGURE 1
Serum A2M levels in CLL patients and NC subjects. **(A)** A2M levels were determined (using ELISA) in sera of CLL patients (n = 65) and NC subjects (n = 30). **** indicates p<0.0001 by t-test. **(B)** A2M levels in sera of CLL patients divided according to the CLL stage (Binet staging; stage A: n=29, stage B: n=23, stage C: n=12). **** and ** indicate p<0.0001 and p<0.02, respectively, vs. each other group. **(C)** Serum A2M levels in CLL patients divided according to the mutation associated with CLL. * indicates p<0.05 vs. each other group, # indicates p<0.05 vs. the NCs and vs. the CLL groups with 11q- and trisomy 12, as determined by the Mann-Whitney test.

TABLE 2 Association of serum A2M levels with hematological parameters.

| Clinical parameters | R value | p value |
|---|---|---|
| WBC | 0.29 | **0.02** |
| Lymph. abs. | 0.42 | **0.004** |
| Lymph. % | 0.09 | 0.056 (ns) |
| Platelets | -0.48 | **0.0001** |
| RBC | -0.42 | **0.0045** |
| Hb | -0.44 | **0.0004** |
| CD38+ % | 0.56 | **0.024** |

The results of linear correlation analysis between serum A2M levels and hematological parameters are shown. WBC, white blood cells; Lymph. abs., absolute lymphocytes count; Lymph%., lymphocytes percentage; RBC, red blood cells; Hb, hemoglobin; % CD38+, percentage of CD38 positive B-lymphocytes; ns, non-significant p value. P value <0.05 was considered significant.
Significant p values (<0.05) are indicated by bold text.

The A2M production was further studied in primary B-lymphocytes, isolated from peripheral blood of CLL patients and NC subjects. These experiments utilized separated B-cells with a ~99% purity (validated by flow-cytometry; showing 1.1 ± 0.7% and 1.1 ± 0.5% of non-B-cells for separations from CLL and NC, respectively), and were performed in order to verify the findings in primary cells, as well as to examine A2M production by B-lymphocytes from NC subjects. The results indicated nearly no A2M production by primary B-lymphocytes from both patients and NC subjects (Figure 3). Clearly, the production of A2M by primary B-lymphocytes was lower than its production by the CLL cell lines.

## 3.7 Production of A2M in B-lymphocytes depends on serum factor/s

The data from CLL cell lines indicated that B-lymphocytes have the ability to produce A2M, so we next focused on initial characterization of the factor/s that may cause or influence A2M production in CLL, by studying whether A2M production depends on the cells' surroundings. This was examined in primary B-lymphocytes from peripheral blood and in the CLL cell line MEC-2, since MEC-2 showed the highest A2M production rate among the four CLL cell lines that were examined. In these experiments MEC-2 cells were incubated for 12 hrs with NC or CLL sera and the A2M levels were measured in the culture medium. The production of A2M by the cells was calculated as the change in A2M levels (ΔA2M) after subtraction of the A2M contributed by the added serum, and the levels self-produced by the cells (i.e. without any added serum). The average ΔA2M levels after incubation of MEC-2 cells with NC sera was -5 ± 19 μg, indicating no change or a very small decrease in A2M levels, while incubation with CLL sera resulted in significantly (p=0.0011) higher ΔA2M, with an average of 65 ± 12 μg (Figure 4A).

In the next set of experiments, primary B-lymphocytes were isolated, incubated with identical sera samples (CLL and NC sera) for 24 hrs, and the A2M levels in the incubation media were quantified. The data in Figure 4B showed increases in A2M production after incubation of the primary cells with sera. However, the increases in A2M production was significantly greater when cells were incubated with patients' sera, relative to incubations with NC sera. This was observed in both NC and patients' lymphocytes (Figure 4B). Interestingly, the responsiveness of CLL cells to the sera was lower than that of NC cells, so that upon incubation, CLL cells were unable to increase their A2M production to the extent seen with NC cells (Figure 4B).

Altogether, these data suggest that the increased A2M production by CLL B-lymphocytes probably depends both on factor/s that exist in the CLL serum (such as IL-6-type cytokines), as well as on the capability of the cells to respond to these factors, an ability that appears to exist in both CLL and NC B-lymphocytes.

TABLE 3 Association of serum A2M levels with biochemical parameters.

| Clinical parameters | R value | p value |
|---|---|---|
| ALP | 0.53 | **0.0007** |
| AST | 0.43 | **0.0074** |
| ALT | -0.22 | 0.180 (ns) |
| Glucose | 0.47 | **0.0026** |
| HDL | -0.47 | **0.0018** |
| Non-HDL Chol. | 0.083 | 0.63 (ns) |
| LDL | 0.007 | 0.99 (ns) |
| Cholesterol | -0.104 | 0.52 (ns) |
| Triglycerides | 0.21 | 0.186 (ns) |
| b2M | 0.62 | **0.0033** |

The results of linear correlation analysis between A2M levels and biochemical parameters are shown. ALP, alkaline phosphatase; AST, aspartate aminotransferase; ALT, alanine transaminase; HDL, high density lipoprotein; LDL, low-density lipoprotein; non-HDL Chol., Non-HDL Cholesterol; B2M, beta-2-microglobulin; ns, non-significant p value. P value <0.05 was considered significant.
Significant p values (<0.05) are indicated by bold text.

# 4 Discussion

This study shows for the first time that the serum levels of A2M in CLL are significantly increased compared to normal control subjects, and are correlated with the disease stage, with various biochemical and hematological parameters associated with the severity of the disease, and with chronic complement activation. Moreover, increased serum levels of A2M may be, at least partially, due to A2M production by the malignant B-lymphocytes.

Our previous studies that focused on the chronic CP activation in CLL included characterization of the cell-free IgG-aggregates that exist in CLL serum and act as a CP activator (4, 16). In the initiation of CP activation, IgG-hexamers bind C1, the first component of the CP, and activate a cascade of events until C5b-9 (MAC), the final complement

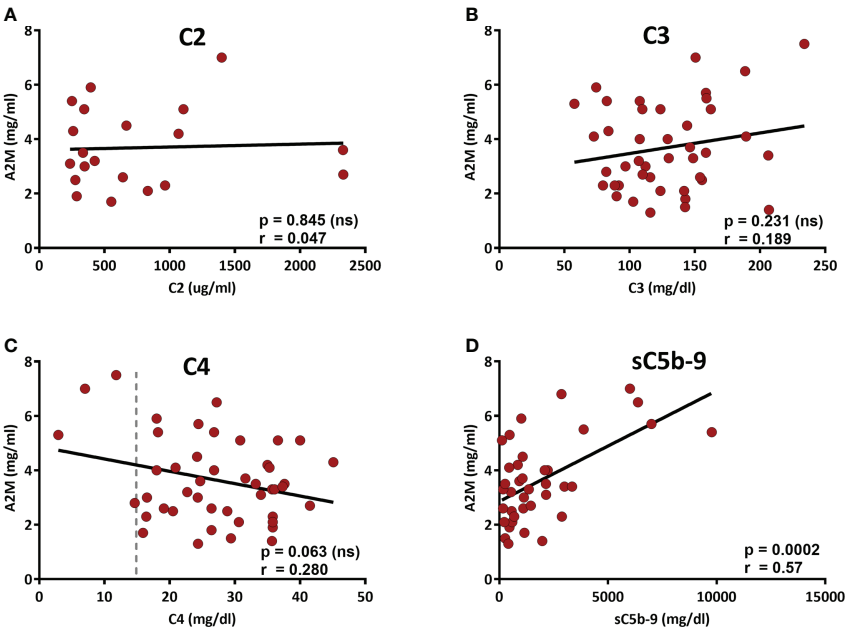


FIGURE 2
Correlation of the serum A2M levels with complement components. The levels of the complement components C2-C4 and the complement activity marker sC5b-9 (the final product of complement activation) were measured in patients' sera. A2M levels were correlated with C2 **(A)**, C3 **(B)**, C4 **(C)** and sC5b-9 **(D)**. The dashed line indicates 15 mg/dL, which is the lower level of the normal range (15-57 mg/dL).

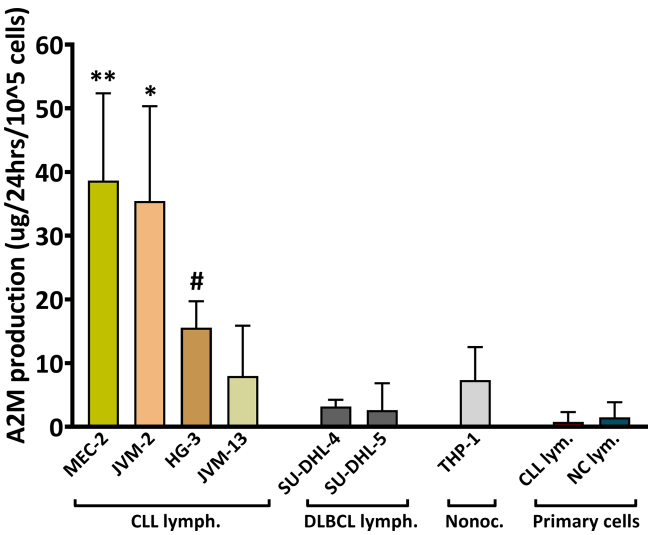


FIGURE 3
A2M production in B-Cells. The production of A2M was studied in the CLL cell lines MEC-2, JVM-2, JVM-13, HG-3, in the non-CLL B-lymphocytic cell lines SU-DHL-4 and SU-DHL-5, and in one monocytic cell line, THP-1. The assay was repeated ≥3 times for each cell line (n = 5 for MEC-2 and HG-3, n = 4 for JVM-13). A2M production was also studied in B-lymphocytes (primary cells) separated from peripheral blood of CLL patients (CLL lym.; n = 4) and NC subjects (NC lym.; n = 4). Cells were incubated in triplicates at a density of 20,000-40,000 cells per 100µl in the appropriate medium for each line, for 12-72 hrs and the ΔA2M levels were calculated for 100,000 cells for 24 hrs. ** indicates significant p values < 0.01 compared to each of the other cell lines, except for JVM-2; * indicates significant p values < 0.05 compared to each of the other cell lines, except for MEC-2; # indicates significant p values (p< 0.05) compared to each of the other cell lines, except for JVM-13 and THP-1.

product, is generated. IgG-aggregates are assembled in the form of hexamers after an antigen binds to each IgG monomer and non-covalent Fc-Fc interactions occur (17). In CLL patients, A2M was found to be the antigen causing the hexamerization and the assembly of the cell-free IgG-aggregates (4). The factors that control the cell-free hexamerization process in CLL plasma are not yet discovered, however one can assume that this process requires the existence of anti-A2M IgG molecules, along with available A2M, hypothetically at levels that are increased above normal, at least for one of these two factors. The present study demonstrates one of these conditions in CLL patients, showing A2M levels that are increased by 84% in the entire CLL patient's cohort, and by up to 185% in patients with stage C CLL.

The correlation analyses with different hematological parameters also suggest the association of A2M levels with the CLL disease severity, as shown by the correlations with the established CLL parameters (18): RBC, platelet counts, lymphocyte counts and Hb levels. Moreover, this observation is also supported by the correlation data of A2M with various biochemical parameters that were shown to increase with CLL severity, such as abnormal liver function tests (LFT) (14), b2M (19), blood glucose levels/Diabetes mellitus (DM, 20), and HDL that is decreased in CLL and particularly in the advanced CLL stages (12). Normal karyotype is a not an indicator of poor prognosis for CLL patients (13), unlike the immunoglobulin gene heavy-chain variable region (IGHV) gene, where absence of

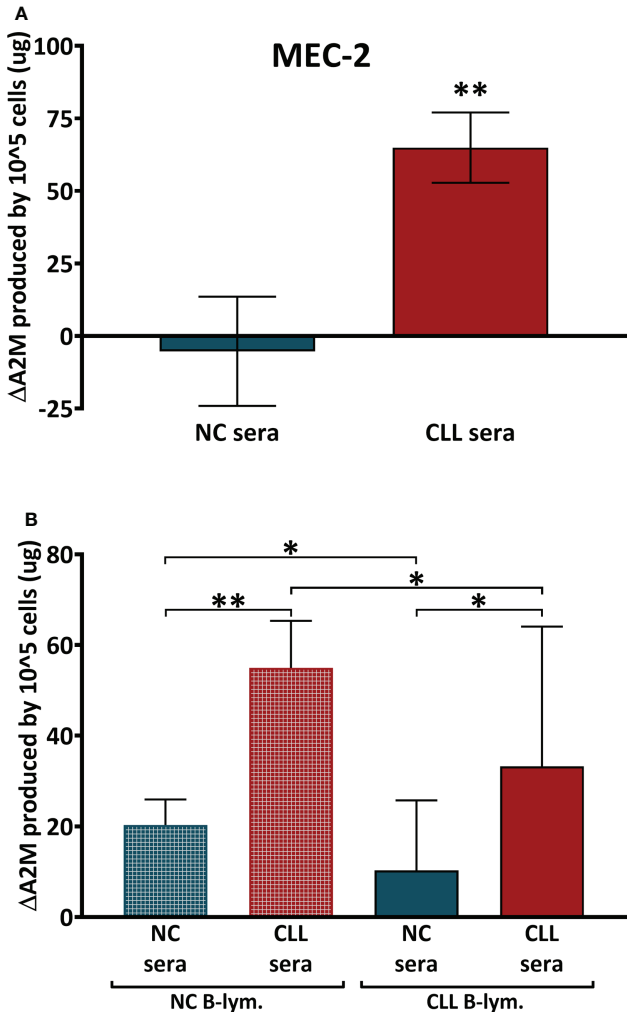


FIGURE 4
A2M production in B-Cells after incubation with sera. **(A)** The production of A2M was studied in the CLL cell line MEC-2 (n = 25) and in primary B-lymphocytes **(B)** that were separated from peripheral blood of CLL patients (CLL B-lym.) and NC subjects (NC B-lym.);. Cells were incubated with NC sera (n = 10 with MEC-2 cells, n=11 with NC-lym. and n = 12 with CLL lym.) or with CLL sera (n = 15 with MEC-2 cells, n = 12 with NC-lym. and n = 11 with CLL lym.), A2M levels were measured and the ΔA2M levels were calculated for 100,000 cells per 24 hrs. ** indicates significant p values < 0.01 and * indicates significant p values < 0.05.

mutations (unmutated IGHV) is associated with poor outcomes (21, 22). The increased level of A2M in patients with normal karyotype compared to patients with genetic aberrations should be further investigated in order to clarify whether serum A2M levels are associated with the disease prognosis.

Since A2M is produced by several human tissues, the excess A2M levels in the circulation of CLL patients may originate from various cells/organs. In this study, we have evaluated the possibility that the B-lymphocytes in CLL may produce A2M and thus contribute to the increase in serum A2M levels. We demonstrated that circulating B-lymphocytes have the ability to produce significant amounts of A2M in response to factors that exist in CLL serum. After incubation with sera, the A2M production capacity of CLL-B-lymphocytes was somewhat decreased (~40%) compared with NC-B-lymphocytes. However, it is reasonable to assume that the huge numbers of B-lymphocytes in CLL circulation, 20 times higher than in NC (Table 1), can certainly overcome the 40% difference in production capacity of the B-cells and eventually result in significantly increased A2M levels in CLL serum. The significant correlation of A2M levels with the lymphocyte counts also supports this possibility.

A2M production in primary B-lymphocytes exposed to CLL sera or NC sera showed an increase of 23 μg A2M per $10^5$ cells (33 vs 10 μg A2M/$10^5$ cells, for incubation with CLL vs. NC sera, respectively). Based on these data, and on the essential condition of at least 5000 monoclonal lymphocytes per μl that is requisite to fulfill the criteria for CLL diagnosis, the minimal amount of excess A2M produced by the B-lymphocytes was calculated to be 1.15 mg/ml. This value is in very good agreement with the data showing an increase of ~1.6 mg/ml in A2M values in CLL vs. NC subjects (from 1.97 ± 0.10 to 3.6 ± 0.22 mg/ml in NC and CLL subjects, respectively). For the majority of CLL patients, the numbers of monoclonal lymphocytes per μl are considerably above 5000 and normally reach ~67% (56-78%) of the total lymphocyte count (23), hence the amounts of A2M produced are presumably increased accordingly. This is particularly evident at advanced CLL stages. Although some of the A2M molecules bind to T-lymphocytes and to the B-lymphocytes *via* the CD91 receptor (24) and the GRP78 receptor (4, 25, 26), respectively, the increased amounts of A2M produced, yield serum levels that correlate very well with the lymphocytes' counts in the circulation. In the experiments assessing A2M production by B-cells, the potential binding to the CD91 receptor on T-lymphocytes is irrelevant, since these experiments were performed using only B-cells (in case of cell lines) or 99% pure primary B-cells preparations. The potential binding to the GRP78 receptor exists, and definitely deserves further studies. If some of the produced A2M molecules bind to the GRP78 receptor, it would mean that the actual amount of A2M produced by the B-cells is higher than the measured values.

The study also showed that most cell-lines of CLL B-lymphocytes that were analyzed are capable of producing A2M even in absence of the CLL-serum-factors. Altogether, the data suggest that the excess A2M in CLL patients' sera may be, at least partly, due to production by the numerous B-lymphocytes in the circulation.

Study limitations: Although the study was conducted on an adequate size of CLL patient's population, karyotype information was available only from a limited number of patients, only 36 out of the 65 patients included in the study. As a result, the distribution of CLL stages in these 36 patients differed from the stage distribution in the original cohort and may not be representative of the stage distribution, or the mutational status in the entire patient's cohort. Also, due to this limitation, some mutations were only observed in one (17p deletion) or two (17p and 11q deletions) patients, making statistical analysis irrelevant for some CLL subgroups categorized by these specific mutations. Thus, this data set should be analyzed with caution, and the apparently high level of A2M found in the only patient with 17p deletion, for example, should be further validated in additional patients with a similar karyotype.

Also, although the study was not limited only to descriptive data and correlation indices, and the mechanisms that affect A2M production were assessed, we have not yet fully described the CLL-serum-factor/s that trigger A2M production in B-lymphocytes. The data available from studies in hepatocytes indicate the involvement of cytokines that are released during inflammatory processes, with IL-1- and IL-6-type cytokines as leading regulators of the acute phase response (27). These cytokines show additive, inhibitory, or synergistic regulatory effects on A2M expression. A2M production by B-cells has not yet been studied, however autocrine IL-6 production by CLL B-cells has been described (28), and was shown to be associated with poor clinical outcome in CLL (29) due to IL-6-mediated survival mechanisms that provide resistance of CLL cells to chemotherapy. In primary CLL B-cells, IL-6 activated both STAT3 and NF-κB, similar to the cascade described in hepatocytes (29), and we believe that this IL-6 mediated control mechanism can potentially control A2M production in CLL B-lymphocytes.

From a translational perspective, we believe that the results may be useful for following the severity of the CLL disease, before and potentially during immunotherapy treatments. The data may also be used for developing advanced immunotherapy treatments, combined with inhibitors of excess A2M production (such as IL-1β or an IL-1β-agonist), and thus the IgG-hexamerization and the resulting chronic CP activation may be down-regulated, helping the complement system attain maximal capacity. Such A2M inhibitors may improve the patients' complement system activity against infections, as well as their response to immunotherapy.

## Data availability statement

The raw data supporting the conclusions of this article will be made available by the authors, without undue reservation.

## Ethics statement

The studies involving human participants were reviewed and approved by Institutional Review Board of Galilee Medical Center, Nahariya, Israel. The patients/participants provided their written informed consent to participate in this study.

## Author contributions

RM: conceptualization, data curation, data analysis, methodology, project administration, supervision, validation, writing – original draft, writing – review and editing. LM: data curation, methodology. EG: data curation, methodology. GS: resources, review and editing. TT: resources. AA: resources. MS: methodology. LS: resources. MB: project administration, supervision. AB: supervision, resources, project administration, methodology, funding, conceptualization, review and editing. All authors contributed to the article and approved the submitted version.

## Funding

The study was funded by the the Health Corporation of Galilee Medical Center, Nahariya, Israel.

## Acknowledgments

The authors thank Prof. Chaim Putterman and Dr. Adi Litmanovich for their help in editing and proofreading of the manuscript.

## Conflict of interest

The authors declare that the research was conducted in the absence of any commercial or financial relationships that could be construed as a potential conflict of interest.

## Publisher's note



## Supplementary material

The Supplementary Material for this article can be found online at: https://www.frontiersin.org/articles/10.3389/fimmu.2022.953644/full#supplementary-material

SUPPLEMENTARY FIGURE 1
Association of serum A2M levels with gender and age.The levels of A2M in sera of male and female **(A)** and the correlation between serum A2M and age **(B)** were studied in the CLL patients. Abbreviations: ns: non-significant p value. P value <0.05 was considered significant.

SUPPLEMENTARY FIGURE 2
Association of serum A2M levels with hematological parameters.The results of linear correlation analysis between serum A2M levels and hematological parameters are shown. WBC: white blood cells; Hb: hemoglobin; CD38(%): percentage of CD38 positive B-lymphocytes; RBC, red blood cells; Lymph.#., absolute lymphocytes count; Lymph%., lymphocytes percentage; ns, non-significant p value. P value <0.05 was considered significant.

SUPPLEMENTARY FIGURE 3
Association of serum A2M levels with biochemical parameters.The results of linear correlation analysis between A2M levels and biochemical parameters are shown. ALP, alkaline phosphatase; AST, aspartate aminotransferase; ALT, alanine transaminase; HDL, high density lipoprotein; LDL, low-density lipoprotein; non-HDL Chol., Non-HDL Cholesterol; b2M, beta-2-microglobulin; ns, non-significant p value. P value <0.05 was considered significant.

SUPPLEMENTARY FIGURE 4
Correlation of serum A2M levels with complement components in CLL and NC. The levels of the complement components C2-C4 were measured in sera of CLL patients and NC subjects. A2M levels were correlated with C2 **(A)**, C3 **(B)** and C4 **(C)**. The dashed line indicates 15 mg/dL, which is the lower level of the normal range (15-57 mg/dL). ● indicate CLL patients and ○ indicate NC subjects.

## References

1. Cater JH, Wilson MR, Wyatt AR. Alpha-2-Macroglobulin, a hypochlorite-regulated chaperone and immune system modulator. *Oxid Med Cell Longev* (2019) 2019:5410657. doi: 10.1155/2019/5410657

2. Doan N, Gettins PG. Human alpha2-macroglobulin is composed of multiple domains, as predicted by homology with complement component C3. *Biochem J* (2007) 407:23–30. doi: 10.1042/BJ20070764

3. Shokal U, Eleftherianos I. Evolution and function of thioester-containing proteins and the complement system in the innate immune response. *Front Immunol* (2017) 8:759. doi: 10.3389/fimmu.2017.00759

4. Naseraldeen N, Michelis R, Barhoum M, Chezar J, Tadmor T, Aviv A, et al. The role of alpha 2 macroglobulin in IgG-aggregation and chronic activation of the complement system in patients with chronic lymphocytic leukemia. *Front Immunol* (2021) 11:603569. doi: 10.3389/fimmu.2020.603569

5. Available at: https://atlasgeneticsoncology.org/gene/42923/a2m-(alpha-2-macroglobulin).

6. Garcia-Ferrer I, Marrero A, Gomis-Rüth FX, Goulas T. α2-macroglobulins: Structure and function. *Subcell Biochem* (2017) 83:149–83. doi: 10.1007/978-3-319-46503-6_6

7. Pitekova B, Kupcova V, Uhlikova E, Mojto V, Turecky L. Alpha-2-macroglobulin and hyaluronic acid as fibromarkers in patients with chronic hepatitis c. *Bratisl Lek Listy* (2017) 118:658–61. doi: 10.4149/BLL_2017_125

8. Housley J. Alpha-2-macroglobulin levels in disease in man. *J Clin Pathol* (1968) 21:27–31. doi: 10.1136/jcp.21.1.27

9. Yoshino S, Fujimoto K, Takada T, Kawamura S, Ogawa J, Kamata Y, et al. Molecular form and concentration of serum α2-macroglobulin in diabetes. *Sci Rep* (2019) 9:12927. doi: 10.1038/s41598-019-49144-7

10. Cavalcante Mde S, Torres-Romero JC, Lobo MD, Moreno FB, Bezerra LP, Lima DS, et al. A panel of glycoproteins as candidate biomarkers for early diagnosis and treatment evaluation of b-cell acute lymphoblastic leukemia. *Biomark Res* (2016) 4:1. doi: 10.1186/s40364-016-0055-6

11. Moore DK, Motaung B, du Plessis N, Shabangu AN, Loxton AGSU-IRG Consortium. Isolation of b-cells using miltenyi MACS bead isolation kits. *PloS One* (2019) 14:e0213832. doi: 10.1371/journal.pone.0213832

12. Yavasoglu I, Sargin G, Yilmaz F, Altındag S, Akgun G, Tombak A, et al. Cholesterol levels in patients with chronic lymphocytic leukemia. *J Natl Med Assoc* (2017) 109:23–7. doi: 10.1016/j.jnma.2016.11.006

13. Döhner H, Stilgenbauer S, Benner A, Leupolt E, Kröber A, Bullinger L, et al. Genomic aberrations and survival in chronic lymphocytic leukemia. *N Engl J Med* (2000) 343:1910–6. doi: 10.1056/NEJM200012283432602

14. Hampel PJ, Chaffee KG, King RL, Simonetto D, Larson MC, Achenbach S, et al. Liver dysfunction in chronic lymphocytic leukemia: Prevalence, outcomes, and pathological findings. *Am J Hematol* (2017) 92:1362–9. doi: 10.1002/ajh.24915

15. Michelis R, Tadmor T, Barhoum M, Shehadeh M, Shvidel L, Aviv A, et al. A C5a-immunoglobulin complex in chronic lymphocytic leukemia patients is associated with decreased complement activity. *PLoS One* (2019) 14:1–17. doi: 10.1371/journal.pone.0209024

16. Michelis R, Tadmor T, Aviv A, Stemer G, Majdob R, Shvidel L, et al. Cell-free IgG-aggregates in plasma of patients with chronic lymphocytic leukemia cause chronic activation of the classical complement pathway. *PLoS One* (2020) 15: e0230033. doi: 10.1371/journal.pone.0230033

17. Strasser J, de Jong RN, Beurskens FJ, Wang G, Heck AJR, Schuurman J, et al. Unraveling the macromolecular pathways of IgG oligomerization and complement activation on antigenic surfaces. *Nano Lett* (2019) 19:4787–96. doi: 10.1021/acs.nanolett.9b02220

18. Hallek M, Al-Sawaf O. Chronic lymphocytic leukemia: 2022 update on diagnostic and therapeutic procedures. *Am J Hematol* (2021) 96:1679–705. doi: 10.1002/ajh.26367

19. Di Giovanni S, Valentini G, Carducci P, Giallonardo P. Beta-2-microglobulin is a reliable tumor marker in chronic lymphocytic leukemia. *Acta Haematol* (1989) 81:181–5. doi: 10.1159/000205558

20. Gao R, Man TS, Liang JH, Wang L, Zhu HY, Wu W, et al. Diabetes mellitus is associated with inferior prognosis in patients with chronic lymphocytic leukemia: A propensity score-matched analysis. *Cancer Res Treat* (2020) 52:189–206. doi: 10.4143/crt.2019.122

21. Jondreville L, Krzisch D, Chapiro E, Nguyen-Khac F. The complex karyotype and chronic lymphocytic leukemia: Prognostic value and diagnostic recommendations. *Am J Hematol* (2020) 95:1361–7. doi: 10.1002/ajh.25956

22. Sun C, Chen YC, Martinez AZ, Baptista MJ, Pittaluga S, Liu D, et al. The immune microenvironment shapes transcriptional and genetic heterogeneity in chronic lymphocytic leukemia. *Blood Adv* (2022) 31. doi: 10.1182/bloodadvances.2021006941

23. Shanafelt TD, Kay NE, Jenkins G, Call TG, Zent CS, Jelinek DF, et al. B-cell count and survival: Differentiating chronic lymphocytic leukemia from monoclonal b-cell lymphocytosis based on clinical outcome. *Blood* (2009) 113:4188–96. doi: 10.1182/blood-2008-09-176149

24. Binder RJ, Karimeddini D, Srivastava PK. Adjuvanticity of alpha 2-macroglobulin, an independent ligand for the heat shock protein receptor CD91. *J Immunol* (2001) 166:4968–72. doi: 10.4049/jimmunol.166.8.4968

25. Ni M, Zhang Y, Lee AS. Beyond the endoplasmic reticulum: Atypical GRP78 in cell viability, signalling and therapeutic targeting. *Biochem J* (2011) 434:181–8. doi: 10.1042/BJ20101569

26. Huergo-Zapico L, Gonzalez-Rodriguez AP, Contesti J, Gonzalez E, López-Soto A, Fernandez-Guizan A, et al. Expression of ERp5 and GRP78 on the membrane of chronic lymphocytic leukemia cells: Association with soluble MICA shedding. *Cancer Immunol Immunother* (2012) 61:1201–10. doi: 10.1007/s00262-011-1195-z

27. Bode JG, Albrecht U, Häussinger D, Heinrich PC, Schaper F. Hepatic acute phase proteins–regulation by IL-6- and IL-1-type cytokines involving STAT3 and its crosstalk with NF-κB-dependent signaling. *Eur J Cell Biol* (2012) 91:496–505. doi: 10.1016/j.ejcb.2011.09.008

28. Robak T, Wierzbowska A, Błasińska-Morawiec M, Korycka A, Błoński JZ. Serum levels of IL-6 type cytokines and soluble IL-6 receptors in active b-cell chronic lymphocytic leukemia and in cladribine induced remission. *Mediators Inflamm* (1999) 8:277–86. doi: 10.1080/09629359990289

29. Wang HQ, Jia L, Li YT, Farren T, Agrawal SG, Liu FT. Increased autocrine interleukin-6 production is significantly associated with worse clinical outcome in patients with chronic lymphocytic leukemia. *J Cell Physiol* (2019) 234:13994–4006. doi: 10.1002/jcp.28086

frontiers | Frontiers in Immunology

TYPE Original Research
PUBLISHED 23 September 2022
DOI 10.3389/fimmu.2022.985280



OPEN ACCESS

EDITED BY
Anne Marit Sponaas,
Norwegian University of Science and Technology, Norway

REVIEWED BY
Andrea Patriarca,
Azienda Ospedaliero Universitaria Maggiore della Carità, Italy
Xin Wang,
Shandong Provincial Hospital, China

*CORRESPONDENCE
Qingsong Yin
jnyinqingsong@163.com

SPECIALTY SECTION
This article was submitted to Cancer Immunity and Immunotherapy, a section of the journal Frontiers in Immunology

RECEIVED 03 July 2022
ACCEPTED 08 September 2022
PUBLISHED 23 September 2022

CITATION
Liang T, Wang X, Liu Y, Ai H, Wang Q, Wang X, Wei X, Song Y and Yin Q (2022) Decreased TCF1 and BCL11B expression predicts poor prognosis for patients with chronic lymphocytic leukemia. *Front. Immunol.* 13:985280. doi: 10.3389/fimmu.2022.985280



# Decreased TCF1 and BCL11B expression predicts poor prognosis for patients with chronic lymphocytic leukemia

Taotao Liang, Xiaojiao Wang, Yanyan Liu, Hao Ai, Qian Wang, Xianwei Wang, Xudong Wei, Yongping Song and Qingsong Yin*

Department of Hematology, The Affiliated Cancer Hospital of Zhengzhou University and Henan Cancer Hospital, Zhengzhou, China

T cell immune dysfunction is a prominent characteristic of chronic lymphocytic leukemia (CLL) and the main cause of failure for immunotherapy and multi-drug resistance. There remains a lack of specific biomarkers for evaluating T cell immune status with outcome for CLL patients. T cell factor 1 (TCF1, encoded by the *TCF7* gene) can be used as a critical determinant of successful anti-tumor immunotherapy and a prognostic indicator in some solid tumors; however, the effects of TCF1 in CLL remain unclear. Here, we first analyzed the biological processes and functions of TCF1 and co-expressing genes using the GEO and STRING databases with the online tools Venny, Circos, and Database for Annotation, Visualization, and Integrated Discovery (DAVID). Then the expression and prognostic values of TCF1 and its partner gene B cell leukemia/lymphoma 11B (BCL11B) were explored for 505 CLL patients from 6 datasets and validated with 50 CLL patients from Henan cancer hospital (HNCH). TCF1 was downregulated in CLL patients, particularly in CD8+ T cells, which was significantly correlated with poor time-to-first treatment (TTFT) and overall survival (OS) as well as short restricted mean survival time (RMST). Function and pathway enrichment analysis revealed that TCF1 was positively correlated with BCL11B, which is involved in regulating the activation and differentiation of T cells in CLL patients. Intriguingly, BCL11B was highly consistent with TCF1 in its decreased expression and prediction of poor prognosis. More importantly, the combination of TCF1 and BCL11B could more accurately assess prognosis than either alone. Additionally, decreased TCF1 and BCL11B expression serves as an independent risk factor for rapid disease progression, coinciding with high-risk indicators, including unmutated IGHV, TP53 alteration, and advanced disease. Altogether, this study demonstrates that decreased TCF1 and BCL11B expression is significantly correlated with poor prognosis, which may be due to decreased TCF1+CD8+ T cells, impairing the effector CD8+ T cell differentiation regulated by TCF1/BCL11B.

KEYWORDS

**chronic lymphocytic leukemia, T cell immune, TCF1, BCL11B, TTFT, prognosis**

# Background

Chronic lymphocytic leukemia (CLL) is a heterogenous B cell malignancy that is the most common adult leukemia in Western countries (1, 2). CLL cell survival depends on the tumor microenvironment in which B cell receptor (BCR) signaling is highly activated by crosstalk between CLL cells and microenvironment-supporting cells, particularly T cells (3–5). T cells are the main effector cells involved in anti-tumor immunity, and several studies have shown enrichment of CD4+ and CD8+ T cells in CLL (6). Nevertheless, CD4+ T cells could stimulate CLL cell survival and proliferation *via* cytokine secretion and direct contact (5, 6), and CD8+ T cells are persistently stimulated in the CLL microenvironment and gradually become exhausted, finally losing effector function, particularly during disease progression (7). Exhaustion has been suggested to be causative of the poor response to chimeric antigen receptor T cell (CAR-T) therapies for CLL patients (5, 8, 9). However, little is known about specific indicators for evaluating the T cell immune status and its correlation with the prognosis of patients with CLL.

T cell factor-1 (TCF1) is a transcription factor encoded by the transcription factor 7 (*TCF7*) gene (10). As one of the critical master regulators for T cell commitment in the thymus, TCF1 is the first T cell-specific transcription factor induced and activated by Notch signaling in the successive stage of T lineage specification, and it maintains a high expression level until T cell maturation (11, 12). Activated TCF1 positively regulates two major target genes, B cell leukemia/lymphoma 11B (BCL11B) and GATA binding protein 3 (GATA3), to sustain T cell commitment and proliferation (13–17). Additionally, as pivotal T cell-specific transcription factors, TCF1 and BCL11B also participate in T cell activation and expansion (15, 18–20). More importantly, TCF1 and BCL11B are crucial for maintaining the stem-like properties of CD8+ T cells (21–24). Upon stimulation, TCF1 promotes CD8+ T cells to differentiate into TCF1+CD8+ T cells that participate in effective antitumor immunity (24, 25). Recently, infiltration of TCF1+CD8+ T cells into tumor tissues has been reported in several solid tumors (23, 24, 26). TCF1+ tumor-infiltrating lymphocytes (TILs) have been positively correlated with tumor regression, successful response to anti-PD-1 treatment, and longer overall survival (OS) (27, 28). Multiple studies have also found that decreased BCL11B expression predicts inferior clinical outcome in adult standard risk T cell acute lymphoblastic leukemia and myelodysplastic syndrome (29, 30). However, the effects of TCF1 and BCL11B expression on the prognosis of CLL patients remain unclear.

In this study, we first performed a variety of bioinformatic analysis of TCF1 expression and examined the effects of TCF1 on the time-to-first treatment (TTFT), overall survival (OS) and restricted mean survival time (RMST) for patients with CLL from public datasets. Furthermore, a protein-protein interaction (PPI) network of co-expressing genes was constructed using STRING, and we performed KEGG pathway and biological process analysis of significant, *TCF7*-related co-expressing genes using the Database for Annotation, Visualization, and Integrated Discovery (DAVID) database. Lastly, the above findings were validated with 50 CLL patients from our clinical center Henan Cancer Hospital (HNCH), revealing that both TCF1 and BCL11B participate in the regulation of T cell immunity and further determine the prognosis of patients with CLL.

# Methods

## Patients and clinical data collection

Peripheral blood samples from 50 patients with CLL, including 32 newly diagnosed patients and 18 refractory/relapsed (R/R) patients, and 8 age-matched healthy individuals (HIs) were analyzed after obtaining informed consent according to the hospital Medical Ethical Committee. Peripheral blood mononuclear cells (PBMCs) were isolated using Human Mononuclear Cell Separation Medium 1.077 (Bio-Processing System, 25610) density-gradient centrifugation, and they were cryopreserved until analysis. Clinical characteristics of 50 patients with CLL in the HNCH were listed in Table S1.

## Flow cytometry

Cells were washed in phosphate-buffered saline containing 2% FBS and incubated at 4°C for 30 min with combinations of the following antibodies: CD3-APC-A750 (A94680, Beckman Coulter), CD4-KrO (A96417, Beckman Coulter), CD8-APC-A700 (B49181, Beckman Coulter), and TCF1-PE (655208, Biolegend). Relevant isotype control mAbs were purchased from BD Biosciences. After two washes in phosphate-buffered saline containing 2% FBS, cells were analyzed by FACS Calibur (Becton Dickinson, San Jose, CA). Data were processed with Navios Flow Cytometer software (Beckman Coulter, Brea, CA, USA).

## GEO database analysis

The gene expression profiles of CLL cells and HIs were queried in the Gene Expression Omnibus (GEO) database, and the GSE19147 (31), GSE66425 (32), and GSE50006 datasets (33) were obtained. The GSE19147 dataset included 25 CLL patients and 8 HIs. GSE66425 included 30 PBMC samples from CLL

patients and 5 samples of PBMCs from HIs, and GSE50006 included 32 B cell samples from HIs and 188 CLL samples. Differences in expression between CLL patients and HIs were compared using GEO2R.

## mRNA expression analysis

To verify the data from the public datasets, total RNA was prepared from CLL patients and HIs using TRIzol Reagent (Invitrogen, Carlsbad, CA, USA) according to the manufacturer's instructions. cDNA was synthesized from equal amounts of total RNA (1 μg) using HiScript® III RT SuperMix for real-time quantitative PCR (qPCR) (+gDNA wiper) (Vazyme, Q711-02, China) and analyzed by ChamQ Universal SYBR qPCR Master Mix. Table S2 lists the primers used for PCR, which was performed using the ABI 7500 FAST real-time PCR system. The levels of transcripts were quantified by the $2^{-\Delta\Delta CT}$ (cycle threshold) method.

## TTFT and OS analysis of CLL patients

The TTFT of CLL patients was queried in the GSE39671 dataset (34), which included 130 CLL patients and their TTFT information. In addition, we collected samples from 43 CLL patients from HNCH to confirm the TTFT results. The TTFT and OS for CLL patients is shown in Kaplan-Meier (KM) survival curves and analyzed by the log-rank Kaplan-Meier method using the "survival" package in R software (version 4.1.0). CLL prognoses were queried in the GSE22762 dataset (35), which included 107 CLL patients and OS information. CLL patients were segregated into 2 distinct categories according to TCF1 expression. The cutpoint value was calculated by the "survminer" package in R, and the RMST was obtained by the "survRM2" package in R. All cutpoint values are shown in Figure S1.

## Co–expressed gene calculation and analysis

The genes differentially expressed in correlation with *TCF7* in the GSE39671 and GSE22762 datasets were analyzed by the Spearman correlation coefficient. Additionally, the Venny 2.1.0 program was used to screen for common genes in the two databases ($R > 0.3$ and $P < 0.05$), and the DAVID version 6.8 (36) was used to conduct corresponding biological process and KEGG pathway enrichment analysis, and a bubble plot was drawn with the "ggplot2" package in R.

## PPI network construction and cluster identification

A PPI network for co-expressing genes was constructed using the Search Tool for the Retrieval of Interacting Genes (STRING) database (https://string-db.org/cgi/) (37), and the results were visualized using Cytoscape software (version 3.4.0) (38). The cutoff criterion for the confidence score was the default setting (> 0.7). In addition, the closely connected protein-interactive regions were obtained by the Molecular Complex Detection (MCODE) plug-in, and the correlation of hub genes in GSE39671 and GSE22762 was plotted with the Circos online tool, and the biological process results were also shown in a PPI network by the STRING database. Further, the hub genes from MCODE were filtered again using the Markov Clustering (MCL) algorithm.

## Statistical analysis

Data were analyzed using GraphPad Prism 8.2.1. Results are presented as the mean ± SD. Student's unpaired t-test was used for differential expression analysis, the log-rank test was used to indicate the statistical significance of survival or TTFT correlation between groups, and the correlation of two genes was tested by the Spearman correlation coefficient. Survival curves were analyzed by the log-rank Kaplan-Meier method. Cox regression analysis was constructed to determine the hazard ratio (HR). All statistically significant variables ($P < 0.05$), as found in the univariate analyses, were included in multivariate analysis based on a Cox proportional hazards model. $P < 0.05$ was considered statistically significant.

# Results

## TCF1 expression significantly decreases in CLL patients

To investigate the effects of TCF1 in CLL, we developed the research plan shown in the study flow chart (Figure 1). We first analyzed the expression of the TCF1, in PBMCs, CLL cells, T cells, and normal B cells in CLL patients from the GEO database and HNCH, respectively. The expression of TCF1 in PBMCs was mainly concentrated in T cells, it was quite low in CLL cells, and it was lower in normal B cells (Figures S2A, S2B). Moreover, TCF1 expression in PBMCs from CLL patients was lower than that in HIs in the GSE66425 dataset ($P = 0.012$; Figure 2A). Although there was no significant difference compared with HIs in the GSE19147 dataset, the proportion of TCF1+CD3+ T cells

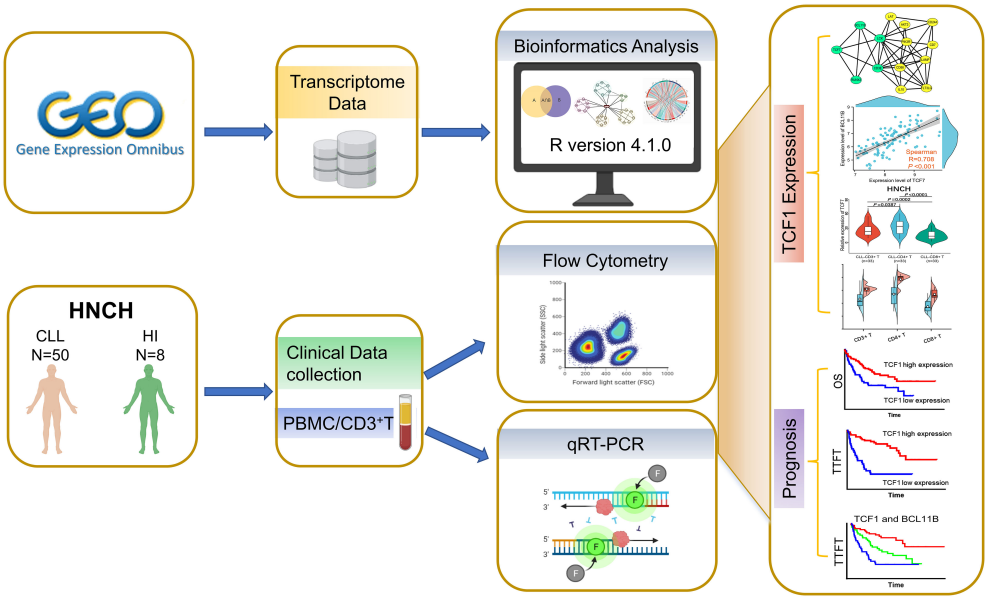


FIGURE 1
Study flow chart. The expression, biological function, and effects of TCF1 and its co-expressing genes were analyzed in the GEO and STRING databases. Then, the above findings were validated in 50 CLL patients from Henan Cancer Hospital (HNCH).

in CLL patients displayed a clear downward trend ($P$ = 0.098; Figure 2B). We verified the above results in 50 patients with CLL from HNCH. Amazingly, TCF1 had low expression not only in PBMCs as determined by qPCR ($P$ = 0.011; Figure 2C) but also in CD3+ T cells as determined by FCM ($P$ = 0.004; Figure 2D) in CLL patients compared with HIs, which is highly consistent with the above findings from the GEO databases. Therefore, compared with HIs, TCF1 was significantly downregulated in the PBMCs of CLL patients, particularly in CD3+ T cells.

## Decreased TCF1 expression predicts short TTFT and OS for CLL patients

Most patients with CLL are diagnosed at the early stage of asymptomatic disease and are not treated until treatment indicators appear. TTFT is an important index that evaluates disease stability in patients with CLL like lymphocyte doubling time (39). Thus, we explored the predictive effects of TCF1 on the TTFT and OS of patients with CLL using the GSE39671 and GSE22762 datasets, respectively. The results demonstrated that CLL patients with low TCF1 expression have a shorter TTFT (5-year TTFT rate: 36% *vs.* 57%, $P$ = 0.009; Figure 2E) and OS (5-year OS rate: 28% *vs.* 98%, $P$ < 0.001; Figure 2F) than those with high TCF1 expression. Next, we confirmed the above findings in 43 CLL patients from HNCH and found that low TCF1 expression appeared to be correlated with short TTFT (5-year TTFT rate: 11% *vs.* 57%, $P$ < 0.001; Figure 2G). Furthermore, we employed RMST to confirm the TTFT and OS data and found that patients with low TCF1 expression have a shorter RMST than those with high TCF1 expression (Figures 2E–G, right panel). Collectively, there was a clear trend where patients with low TCF1 expression have rapid disease progression and a short survival time. Thus, TCF1 can be used as a predictive biomarker of inferior prognosis for CLL patients.

## Construction of a *TCF7* co–expressing gene PPI network

The 114 genes commonly co-expressed with *TCF7* in the GSE39671 (592 genes) and GSE22762 datasets (903 genes) (Figure 3A, left panel) were filtered by Venny and then built into a protein-protein network using the STRING database. Cytoscape (MCODE plug-in) was used to establish the most important module, which is highlighted in yellow (Figure 3A, middle panel). Based on the degree score, we selected the module with the highest score that included 14 genes: *TCF7*, *BCL11B*, *RUNX3*, *LCK*, *CD3E*, *LAT*, *AKT3*, *PIK3R1*, *CD86*, *IL10*, *FLT3LG*, *SLAMF1*, *CD7*, and *CD244*. These genes were identified as potential hub genes, and the expression levels of the 14 hub genes were plotted by the Circos webtool for the GSE22762 and GSE39671 datasets (Figure 3A, right panel).

10.3389/fimmu.2022.985280

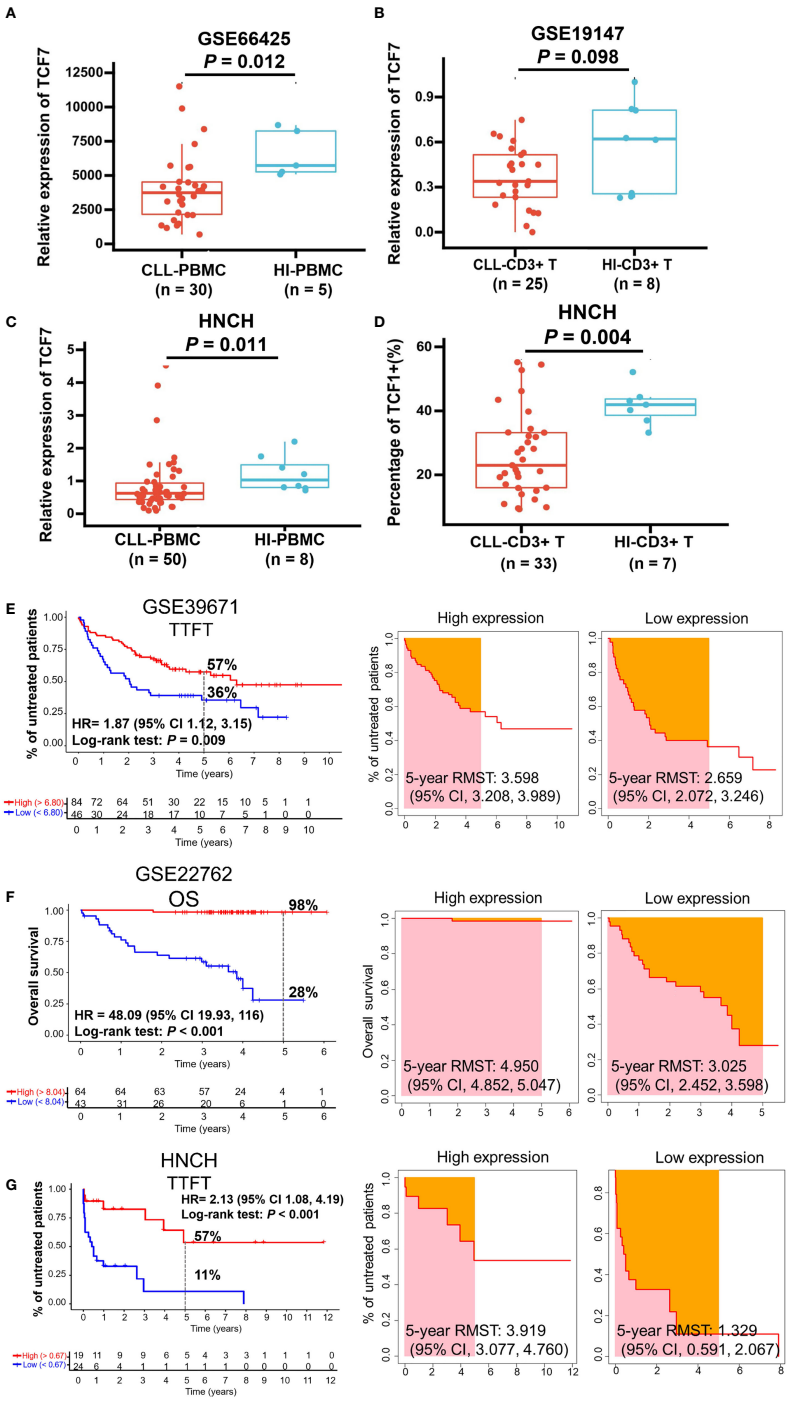


FIGURE 2
The expression and predictive effects of TCF1 on the TTFT and OS for patients with CLL. The expression of TCF1 in PBMCs and CD3+ T cells from CLL patients and healthy individuals (HIs) in the GSE66425 **(A)** and GSE19147 **(B)** datasets. **(C)** qPCR and **(D)** FCM verified the results of TCF1 expression in PBMCs and CD3+ T cells from CLL patients and HIs in the HNCH. **(E)** The TTFT (left panel) and RMST (right panel) for the high and low TCF1 expression groups in the GSE39671 dataset. **(F)** The OS (left panel) and RMST (right panel) for the high and low TCF1 expression groups in the GSE22762 dataset. **(G)** The TTFT (left panel) and RMST (right panel) for the high and low TCF1 expression groups in the HNCH. Error bars indicate SE.

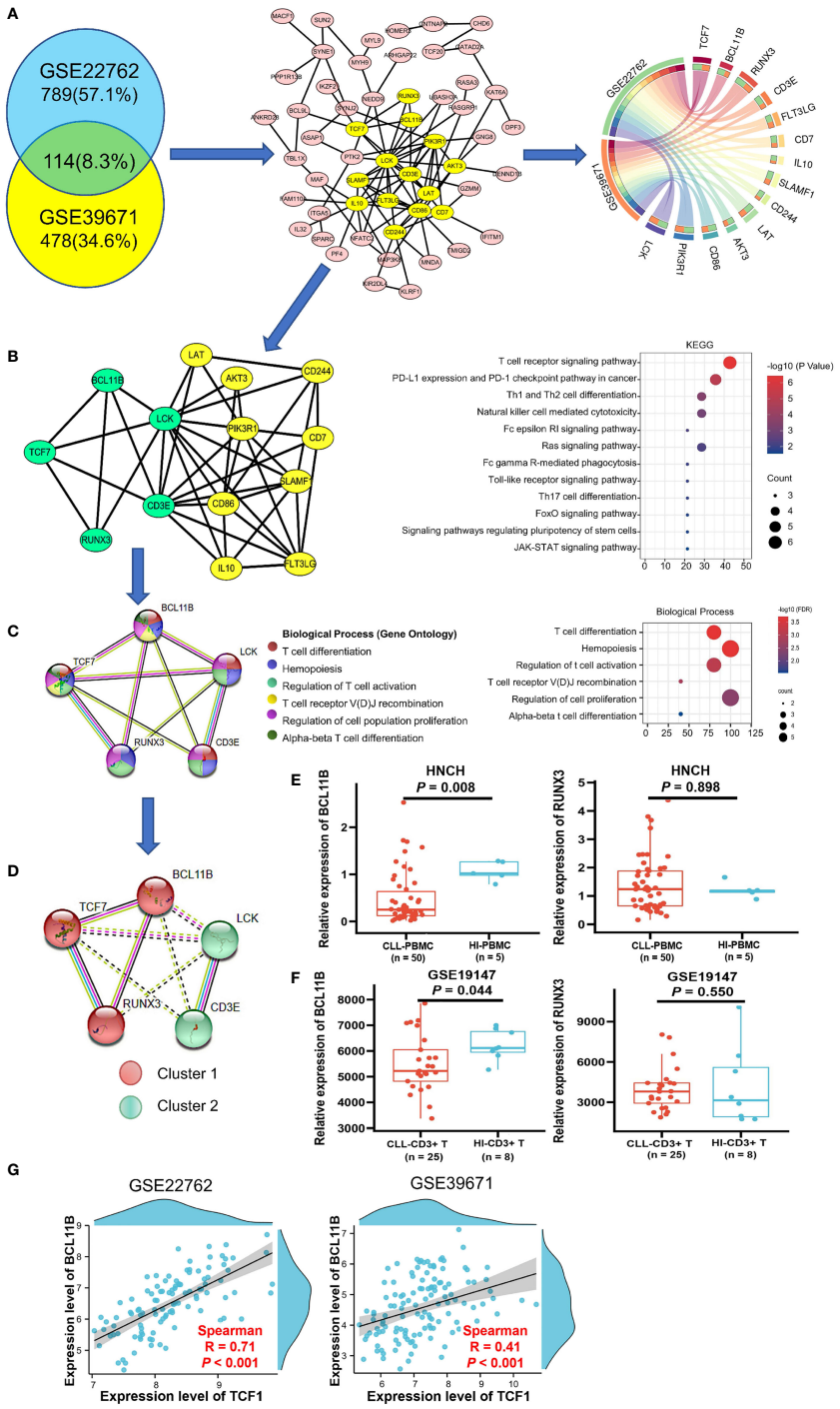


FIGURE 3
Biological process and KEGG pathway analysis of *TCF7* co-expressing genes and partner gene screening in patients with CLL. **(A)** The 114 common co-expressing genes (R > 0.3 P < 0.05) in the GSE22762 and GSE39671 datasets were filtered by the Venny online tool (left panel). Then, the STRING online tool was used to create the PPI network, MCODE analysis (middle panel) identified the 14 hub genes (highlighted in yellow), and the correlations of the 14 hub genes in the GSE2276 and GSE39671 datasets were plotted by the Circos web tool (right panel). **(B)** The PPI network of the 14 hub genes and their KEGG pathway annotation. **(C)** The PPI network and biological processes of 5 hub genes was directly related to *TCF7*. **(D)** MCL clustering analysis demonstrated a close relationship among *TCF7*, *BCL11B*, and *RUNX3* in CLL patients in the GSE22762 and GSE39671 datasets. The expression of *BCL11B* and *RUNX3* was measured in CLL patients from the HNCH **(E)** and GSE19147 **(F)** dataset, respectively. **(G)** The correlation between *TCF7* and *BCL11B* in the GSE39671 and GSE22762 datasets, respectively. R, Spearman correlation coefficient. Error bars indicate SE.

## Functional and KEGG pathway analysis of the 14 hub genes in CLL

The results of KEGG pathway analysis, which was performed using the DAVID database and plotted by R, indicated that the 14 hub genes mainly participate in T cell receptor signaling and T cell differentiation (Figure 3B, right panel). Notably, we found that, of the 14 genes in the PPI network, *BCL11B*, *RUNX3*, *CD3E*, and *LCK* are directly related to *TCF7* gene (highlighted in green) (Figure 3B, left panel). We next reconstructed the PPI network of these five genes using the STRING database (Figure 3C, left panel). The biological process category of each gene is displayed in different colors and mainly include regulation of T cell activation, T cell differentiation, and T cell receptor recombination (Figure 3C, right panel), which is highly consistent with the above KEGG analysis results. These data indicate that *TCF7* coordinates with hub genes in regulating T cell immunity.

To determine genes closely related to *TCF7*, we clustered the 5 genes using the MCL method. Remarkably, the 5 genes divided into 2 clusters, cluster 1 (including *TCF7*, *RUNX3*, and *BCL11B*) and cluster 2 (including *LCK* and *CD3E*). It was evident that the genes in cluster 1 were closely related to *TCF7* (Figure 3D). We further verified the expression of *BCL11B* and *RUNX3* in PBMCs from CLL patients (HNCH) and HIs by qPCR. Intriguingly, *BCL11B* expression was significantly decreased in CLL patients compared with that in HIs ($P = 0.008$; Figure 3E, left panel), but there was no significant difference in *RUNX3* between CLL patients and HIs ($P = 0.898$, Figure 3E, right panel). Likewise, we found that *BCL11B* expression in CD3+ T cells was significantly decreased in CLL-CD3+ T cells compared to HI-CD3+ T cells in the GSE19147 dataset ($P = 0.044$ Figure 3F, left panel), but *RUNX3* did not demonstrate a difference between CLL and HIs ($P = 0.550$, Figure 3F, right panel). In addition, there was a high positive correlation between *TCF7* and *BCL11B* expression in the GSE22762 ($R = 0.71$, $P < 0.001$) and GSE39671 ($R = 0.41$ $P < 0.001$) datasets (Figure 3G). Therefore, among the genes co-expressed with *TCF7* in CLL patients, *BCL11B* may be the closest partner gene for *TCF7* involved in T cell immune regulation.

## Decreased BCL11B expression predicts short TTFT and OS for CLL patients

To investigate the effects of BCL11B alone or in combination with TCF1 on the prognosis of patients with CLL, we further analyzed the effects of BCL11B on TTFT and OS for CLL patients in the GSE39671 and GSE22762 datasets, respectively (Figures S3A, S3B). Low expression of BCL11B was significantly associated with shorter TTFT and poorer OS compared with high expression (5-year TTFT: 28% *vs.* 77%; 5-year OS: 33% *vs.* 98%) (Figures 4A, B, left panel). Similarly, patients with low BCL11B expression had shorter RMST than those with high expression (Figures 4A, B, right panel). As expected, the above findings were confirmed with 50 patients with CLL from HNCH (5-year TTFT: 0% *vs.* 28%) (Figure 4C). Next, we analyzed the effects of BCL11B in combination with TCF1 on prognosis, compared with those who were $TCF1^{high}BCL11B^{high}$, CLL patients who were $TCF1^{low}BCL11B^{low}$ had a poorer TTFT and OS (Figures 4D, E, left panel) as well as shorter RMST (Figures 4D, E, right panel). Specifically, the 5-year TTFT was 26% and 74%, and the 5-year OS was ≤ 17% and 100%, respectively. Similarly, those results also were validated in HNCH, the 5-year TTFT and for $TCF1^{low}BCL11B^{low}$ and $TCF1^{high}BCL11B^{high}$ was 0% and 37%, respectively (Figure 4F). Therefore, BCL11B can be used as a predictive biomarker for inferior prognosis for CLL patients. More importantly, the combination of TCF1 and BCL11B expression could more accurately assess the prognosis of CLL patients compared with either alone.

## Correlation between TCF1 expression and clinical factors for CLL patients

To explore the correlation between TCF1 expression and the characteristics of patients with CLL, we next integrated a series of clinical characteristics, including disease state, Rai stage, β2 microglobulin (β2M) level, lactate dehydrogenase (LDH) level, gender, age, lymphocyte percentage, IGHV mutation status, cytogenetic abnormalities such as del(17p) or P53 mutation (TP53 aberration), del(11q), del(13q) and trisomy12, absolute lymphocyte count (ALC), and bulky disease (≥ 5 cm) (Figures 5A–N). Notably, decreased TCF1 expression was significantly associated with relapsed and refractory disease ($P = 0.001$; Figure 5A), Rai stage 3-4 ($P = 0.012$; Figure 5B), and β2M ≥ 3.5 (mg/L) ($P = 0.009$; Figure 5C), which mainly serve as clinical indexes for disease progression and adverse prognosis. In relapsed and refractory CLL patients, we found there was no significant difference in the effect of first-line treatment regimens on TCF1 expression except for a slight upward trend in the ibrutinib group, which may be related to the small number of cases in different groups (Table S1).

Cox regression analysis demonstrated that low TCF1 and BCL11B expression are independent predictive factors for short TTFT of CLL patients (Table 1). Specifically, in univariate analysis, ≥ 65 years old, female, high β2M level, high LDH level, unmutated IGHV, TP53 aberration, del(11q), trisomy12, Rai stage 3-4, R/R, low TCF1, and low BCL11B were significant risk factors for short TTFT. Statistically significant factors for TTFT ($P < 0.05$) were included in the multivariate analysis, revealing that unmutated IGHV, TP53 aberration, trisomy12, Rai stage 3-4, R/R, low TCF1, and low BCL11B were independent risk factors for shortened TTFT. Thus, TCF1 is a

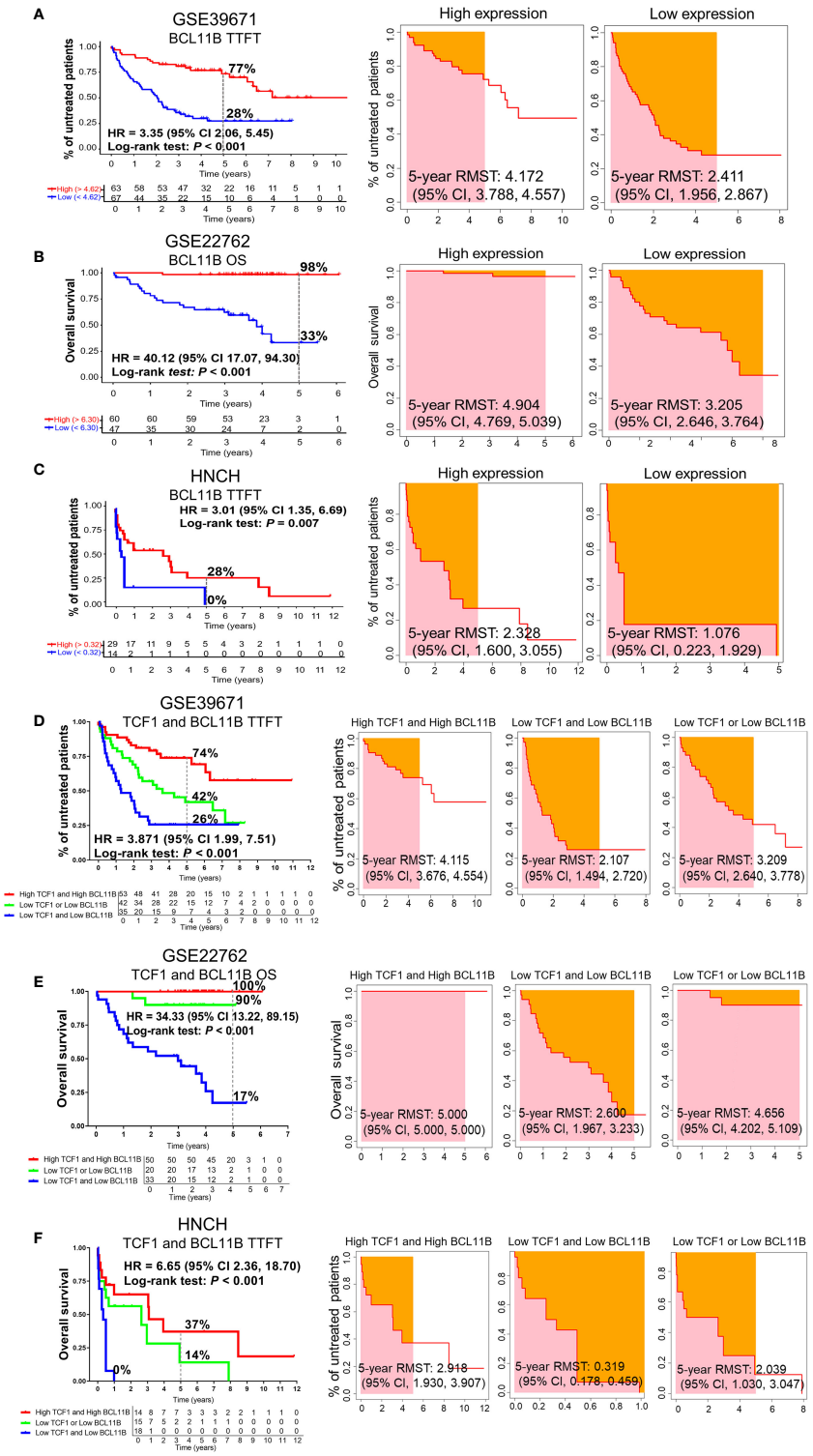


FIGURE 4
The predictive effects of BCL11B alone and in combination with TCF1 on the TTFT and OS of patients with CLL. **(A)** The TTFT (left panel) and RMST (right panel) for the high and low BCL11B expression groups in the GSE39671 dataset. **(B)** The OS (left panel) and RMST (right panel) for the high and low BCL11B expression groups in the GSE22762 dataset. **(C)** The TTFT (left panel) and RMST (right panel) for the high and low BCL11B expression groups in the HNCH. **(D)** The effects of TCF1 combined with BCL11B on TTFT (left panel) and RSMT (right panel) in the GSE39671 dataset. **(E)** The effects of TCF1 combined with BCL11B on OS (left panel) and RSMT (right panel) in the GSE22762 dataset. **(F)** The effects of TCF1 combined with BCL11B on TTFT (left panel) and RSMT (right panel) in the HNCH.

10.3389/fimmu.2022.985280

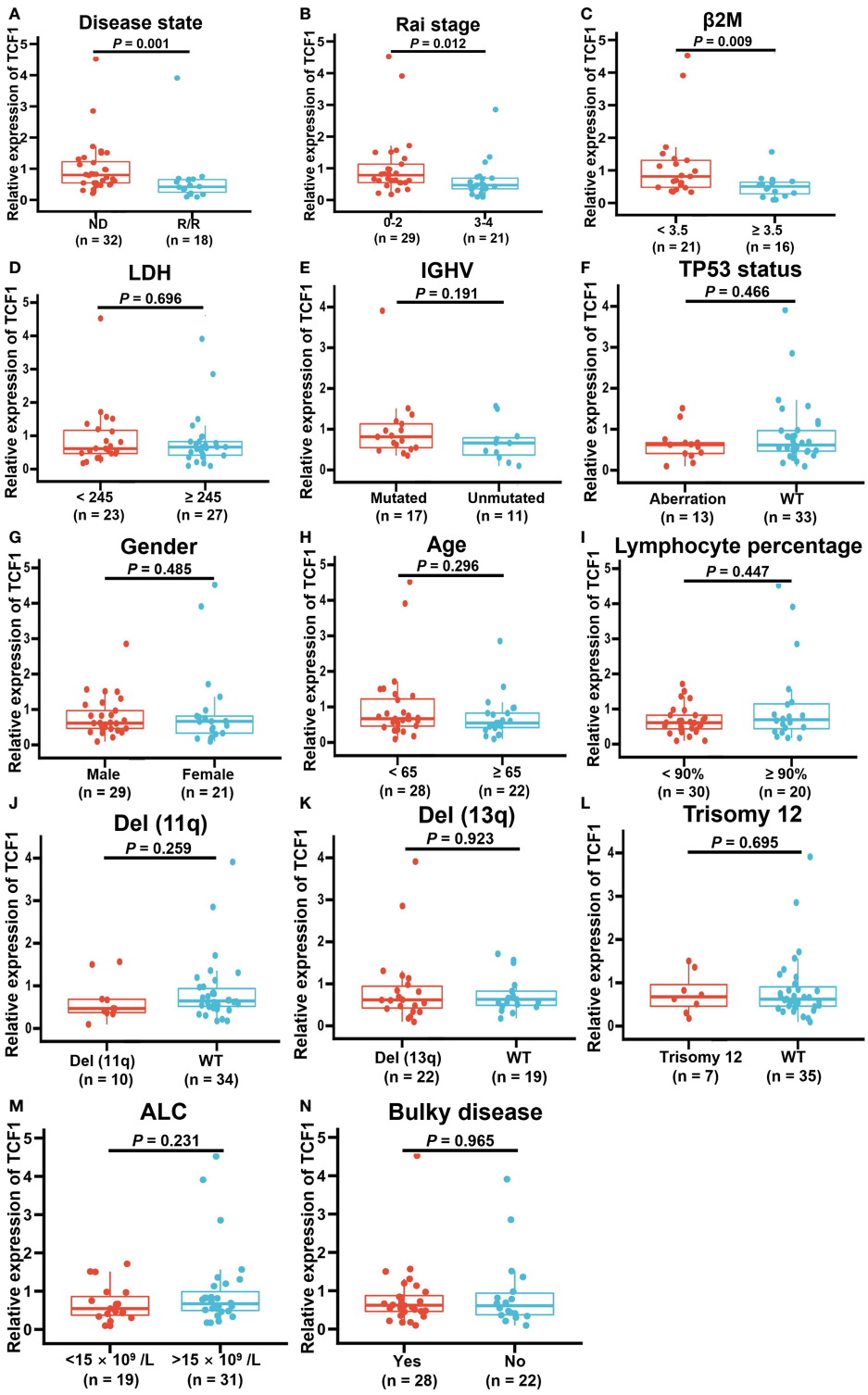


FIGURE 5
Correlation between decreased TCF1 expression and clinical factors in CLL patients. The correlation of TCF1 expression and various clinical characteristics, such as **(A)** newly diagnosed (ND) and relapsed/refractory (R/R) patients, **(B)** Rai stage 0-2 and 3-4, **(C)** β2M < 3.5 or ≥ 3.5 (mg/L), **(D)** LDH < 245 or ≥ 245 (IU/L), **(E)** IGHV mutated and unmutated, **(F)** TP53 aberration or WT, **(G)** Male or female CLL patients, **(H)** < 65 or ≥ 65 years old, **(I)** Lymphocyte percentage, **(J)** Del(11q) or WT, **(K)** Del(13q) or WT, **(L)** Trisomy12 or WT, **(M)** ALC < 15 $\times 10^9$/L or >15 $\times 10^9$/L, and **(N)** Bulky or no. WT means wild type. Del means deletion. Error bars indicate SE.

10.3389/fimmu.2022.985280

TABLE 1 Univariate and multivariate Cox regression analysis of risk factors associated with TTFT.

| VARIABLES | UNIVARIATE COX | | MULTIVARIATE COX | |
|---|---|---|---|---|
| | HR (95% CI) | *P* value | HR (95% CI) | *P* value |
| Age (< 65 vs. ≥ 65) | 0.37 (0.17 - 0.83) | 0.001 | 0.90 (0.72 - 1.14) | 0.385 |
| Gender (Male vs. Female) | 0.24 (0.10 - 0.58) | 0.001 | 1.47 (0.09 - 23.08) | 0.785 |
| β2M (< 3.5 vs. ≥ 3.5) | 0.36 (0.15 - 0.85) | 0.002 | 0.01 (0.00 - 1.02) | 0.051 |
| LDH (< 245 vs. ≥ 245) | 0.49 (0.22 - 1.07) | 0.041 | 0.07 (0.00 - 8.10) | 0.268 |
| IGHV (Unmut vs. Mut) | 3.29 (1.03 - 10.56) | 0.004 | 0.00 (0.00 - 0.28) | 0.020 |
| TP53 aberration (No vs. Yes) | 0.47 (0.20 - 1.12) | 0.030 | 0.00 (0.00 - 0.14) | 0.008 |
| Lymphocyte Percentage (< 90% vs. ≥ 90%) | 1.14 (0.58 - 2.23) | 0.703 | | |
| Del(13q) (No vs. Yes) | 1.63 (0.74 - 3.59) | 0.178 | | |
| Del(11q) (No vs. Yes) | 0.48 (0.18 - 1.24) | 0.040 | 1.57 (0.01 - > 50) | 0.877 |
| Trisomy 12 (No vs. Yes) | 0.35 (0.11 - 1.08) | 0.006 | 45.99 (1.69 - > 50) | 0.023 |
| Rai stage (0-2 vs. 3-4) | 0.36 (0.17 - 0.75) | < 0.001 | 30.81 (2.59 - > 50) | 0.007 |
| Disease status (ND vs. R/R) | 0.37 (0.17 - 0.83) | 0.001 | > 50 (5.85 - > 50) | 0.007 |
| ALC (< 15 × $10^9$/L *vs.* > 15 ×$10^9$/L) | 0.61 (0.31 - 1.20) | 0.141 | | |
| Bulky Disease (Yes or No) | 1.12 (0.57 - 2.19) | 0.737 | | |
| TCF1 (Low vs. High) | 4.18 (1.8 - 9.85) | < 0.001 | 0.00 (0.00 - 0.13) | 0.006 |
| BCL11B (Low vs. High) | 2.37 (1.06 - 5.27) | 0.007 | > 50 (1.79 - > 50) | 0.028 |

CI, confidence interval; HR, hazard ratio.

potential clinical biomarker for predicting disease progression for CLL patients.

## Percentage of TCF1+ cells in the CD3+, CD4+, and CD8+ T cell subgroups from CLL patients

To explore the reduced expression of TCF1 in various T cell subgroups, we subsequently detected the percentage of TCF1+ cells in the CD3+, CD3+CD4+, and CD3+CD8+ T cell subgroups of 33 CLL patients and compared these with HIs. We restricted all analyses to CD3+ T cells (Figure 6A). The results demonstrated that the percentages of TCF1+ cells in the CD3+, CD3+CD4+, and CD3+CD8+ T cell populations from CLL patients were significantly lower than that in corresponding T cell subgroups from HIs (*P* values are 0.004, < 0.001 and < 0.001, respectively), particularly for CD3+CD8+ T cells (Figures 6B, C). We further compared the percentages of TCF1+ cells among the different T subgroups and found that TCF1+ cells had a higher percentage in CD3+CD4+ T cells irrespective of CLL patients or HIs (Figure 6C). Notably, the percentage of TCF1+ cells in the CD3+CD8+ T cell population was significantly lower than that in the CD3+CD4+ T cell population, particularly in CLL patients. It has been reported that TCF1+CD8+ T cells promote effective antitumor immunity (40). Based on previous studies and our current findings, decreased TCF1+CD8+ T cells in CLL patients indicates T cell immune dysfunction. Therefore, TCF1 has the potential to be a biomarker for T cell immune status and a therapeutic target in CLL patients.

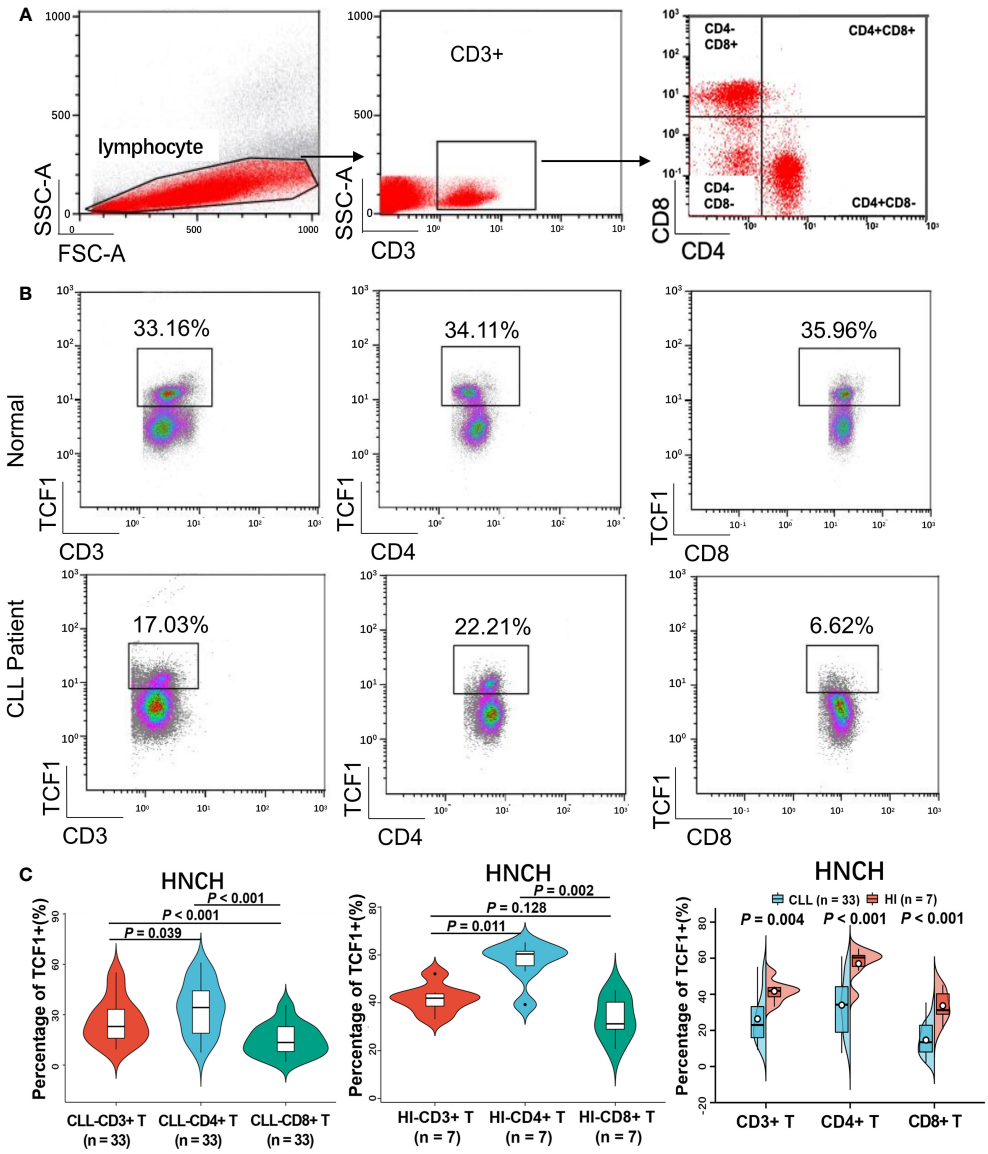


FIGURE 6
The percentage of TCF1+ cells on various T cell subgroups of CLL and HIs. **(A)** Flow cytometry gating strategy. **(B)** Representative profiles of TCF1 expression on CD3+, CD3+CD4+, and CD3+CD8+ T cells in HIs (top) and CLL patients (bottom). **(C)** The expression of TCF1 in CD3+, CD3+CD4+, and CD3+CD8+ T cells from CLL patients and HIs in the HNCH. Error bars indicate SE.

## Discussion

Accumulating studies have illustrated that TCF1 is a key regulator for maintaining the stem-like properties of central memory CD8+ T cells and the cytotoxicity of effector CD8+ T cells (22, 41). TCF1+CD8+ T cells reportedly serve as a positive biomarker for prolonged survival and effective response to anti-PD-1 treatment in solid tumors (24, 27). However, little is known about the role of TCF1 in assessing the immune function with clinical outcome of CLL patients. In this study, TCF1 and BCL11B downregulation is a discernable event where decreased expression of these genes in CLL patients was significantly correlated with short TTFT and poor OS, particularly with the two combined. This lower expression may be due to the decrease in TCF1+CD8+ T cells, which thus impairs the differentiation of effector CD8+ T cells regulated by TCF1 and BCL11B.

In recent years, research on the role of TCF1 in evaluating efficacy and prognosis has exhibited an upward trend (21–24, 27, 41). Previous studies have claimed that infiltration of TCF1+CD8+ T

cells contributes to the induction of tumor regression but not that of TCF1+CD4+ T cells (23). Herein, our findings demonstrate that the proportion of TCF1+ T cells, particularly in CD8+ T cells, is significantly decreased in CLL patients. As previously reported, TCF1 was highly expressed in naïve T cells and downregulated during effector differentiation, and low TCF1 expression was a characteristic of terminally differentiated T cells (42, 43). A recent study has also demonstrated that the terminally exhausted T cells generated in response to chronic viral infection lacked TCF1 expression and were TCF1 negative (41). Therefore, in this study, the decrease in TCF1 expression and proportion of TCF1+CD8+ T cells indicates the accumulation of terminally differentiated and exhausted T cells and T cell immunodeficiency, which is consistent with clinical findings for CLL patients (44), which in turn drives the CLL progression (3). In addition, it was reported that TCF1+CD8+ T cells contribute to broadening the diversity of the TCR repertoire (45). These decreased TCF1+CD8+ T cells suggest skewed T cell compartments and disordered T cell immunity, which explains the deficient anti-tumor effects of CD8+ T cells in CLL patients. Therefore, it is not surprising that low TCF1 expression indicates rapid progression and inferior prognosis for CLL patients.

To further explore the mechanism by which TCF1 regulates CLL prognosis and the partner molecules interacting with TCF1, functional and pathway enrichment analysis revealed that TCF1 is positively correlated with BCL11B, which is mainly involved in T cell differentiation and activation and immune regulation in CLL patients, in accordance with the literature (20, 22). Moreover, BCL11B was highly consistent with TCF1 in terms of decreased expression and the prediction of poor prognosis based on analysis of public datasets and HNCH data. Importantly, combination of the two genes could more accurately predict disease progression and prognosis for CLL patients compared with either alone. Cox regression analysis also demonstrated that both TCF1 and BCL11B downregulation could serve as an independent risk factor for rapid disease progression. Therefore, BCL11B may be a close partner for TCF1, and both may be used as indicators of T cell immunity to regulate the prognosis of CLL patients.

We additionally explored evidence that BCL11B cooperates with TCF1 to participate in immune regulation. Previous studies have reported that BCL11B plays an important role in mature T cell activation and proliferation (18, 21). In addition, BCL11B is a downstream target of TCF1 (15, 16), and TCF1 deficiency results in BCL11B downregulation (15, 16, 46). Moreover, another study demonstrated that BCL11B deficiency in virus-specific CD8+ T cells results in decreased memory precursor effector cells, and the effector cells skewed toward short-lived effector cells, resulting in a reduced ability to secrete cytotoxic granules (21). These data suggest an impairment in effector CD8+ T cell differentiation. These findings indicated that BCL11B is highly correlated with TCF1 and coordinates with this gene to maintain the stem-like properties and cytotoxicity of effector CD8+ T cells (22, 24, 41). Unfortunately, we found that TCF1 and BCL11B expression was decreased in CLL patients, and this resulted in impaired differentiation potential for effector CD8+ T cells (21, 22), which clinically manifested as the accumulation of terminally differentiated T cells (44), immune function dysfunction, and further rapid CLL progression. Although the data were not yet significant enough, this, to some extent, explains why decreased TCF1 and BCL11B expression leads to poor prognosis for patients with CLL. TCF1 and BCL11B may be promising biomarkers for T cell immune status and therapeutic targets in CLL patients.

Additionally, it is worth noting that, as an independent risk factor for rapid disease progression of CLL patients, decreased TCF1 and BCL11B expression coincided with high-risk indicators for CLL, including unmutated IGHV and TP53 aberration. Moreover, decreased TCF1 expression was significantly correlated with clinical indicators for CLL disease advancement (1), such as relapsed and refractory disease, Rai stage 3-4, and high β2M level. It has been reported that with the progression of CLL disease, T cell immune dysfunction is aggravated, which further leads to poor efficacy and treatment resistance (8, 9). Collectively, reduced TCF1 and BCL11B expression can be used as a clinical indicator for T cell immune function to assess the disease progression and prognosis of patients with CLL in the clinic.

## Conclusions

This study demonstrated for the first time that reduced TCF1 and BCL11B expression is significantly correlated with the poor prognosis of patients with CLL. TCF1 co-expression analysis revealed that TCF1 is positively associated with BCL11B, which is mainly involved in regulating the activation and differentiation of T cells. Downregulation of TCF1 and BCL11B, particularly in CD8+ T cells, in CLL patients may impair the stem-like differentiation potential of memory CD8+ T cells, leading to T cell immune dysfunction, and this may provide insight into the mechanism by which TCF1 and BCL11B regulates the prognosis of CLL patients. Therefore, manipulating the effects of TCF1 and BCL11B on T cell immunity will contribute to further designing combined therapies for T cell-based immunotherapy in the future.

## Data availability statement

Publicly available datasets were analyzed in this study. This data can be found here: https://www.ncbi.nlm.nih.gov/geo/. The original contributions presented in the study are included in the article/Supplementary Material. Further inquiries can be directed to the corresponding author.

## Ethics statement

The studies involving human participants were reviewed and approved by The ethics committees of the Affiliated Cancer Hospital of Zhengzhou University. The patients/participants provided their written informed consent to participate in this study.

## Author contributions

TTL analyzed the data, designed the figures, performed statistical analysis, and wrote the manuscript. XJW and YYL did flow cytometry and qPCR analysis. HA and QW collected the patient information and literature information. XWW carried out bioinformatics analysis. XDW and YPS designed and participated in editing the manuscript. QSY designed the study, analyzed the data, and wrote and revised the manuscript. All authors read and approved the final manuscript.

## Funding

This study was supported by the Natural Science Foundation of Henan province (162300410280), the Foundation for Young Teachers' Basal Research of Zhengzhou University (jc202050015), and the Medical Science and Technology Research Project of Henan Province (LHGJ20220185).

## Acknowledgments

We are very thankful to Prof. Yangqiu Li (Jinan University, Guangzhou) for outstanding manuscript edits and her advice on bioinformatics analyses.

## Conflict of interest

The authors declare that the research was conducted in the absence of any commercial or financial relationships that could be construed as a potential conflict of interest.

## Publisher's note

All claims expressed in this article are solely those of the authors and do not necessarily represent those of their affiliated organizations, or those of the publisher, the editors and the reviewers. Any product that may be evaluated in this article, or claim that may be made by its manufacturer, is not guaranteed or endorsed by the publisher.

## Supplementary material

The Supplementary Material for this article can be found online at: https://www.frontiersin.org/articles/10.3389/fimmu.2022.985280/full#supplementary-material

## References

1. Patel K, Pagel JM. Current and future treatment strategies in chronic lymphocytic leukemia. *J Hematol Oncol* (2021) 14(1):69. doi: 10.1186/s13045-021-01054-w

2. Agathangelidis A, Chatzidimitriou A, Gemenetzi K, Giudicelli V, Karypidou M, Plevova K, et al. Higher-order connections between stereotyped subsets: implications for improved patient classification in CLL. *Blood* (2021) 137 (10):1365–76. doi: 10.1182/blood.2020007039

3. van Attekum MH, Eldering E, Kater AP. Chronic lymphocytic leukemia cells are active participants in microenvironmental cross-talk. *Haematologica* (2017) 102(9):1469–76. doi: 10.3324/haematol.2016.142679

4. Jiménez I, Tazón-Vega B, Abrisqueta P, Nieto JC, Bobillo S, Palacio-García C, et al. Immunological and genetic kinetics from diagnosis to clinical progression in chronic lymphocytic leukemia. *biomark Res* (2021) 9(1):37. doi: 10.1186/s40364-021-00290-z

5. Roessner PM, Seiffert M. T-Cells in chronic lymphocytic leukemia: Guardians or drivers of disease? *Leukemia* (2020) 34(8):2012–24. doi: 10.1038/s41375-020-0873-2

6. Elston L, Fegan C, Hills R, Hashimdeen SS, Walsby E, Henley P, et al. Increased frequency of CD4(+) PD-1(+) HLA-DR(+) T cells is associated with disease progression in CLL. *Br J Haematol* (2020) 188(6):872–80. doi: 10.1111/bjh.16260

7. Kurachi M. CD8(+) T cell exhaustion. *Semin Immunopathol* (2019) 41 (3):327–37. doi: 10.1007/s00281-019-00744-5

8. Lemoine J, Ruella M, Houot R. Born to survive: how cancer cells resist CAR T cell therapy. *J Hematol Oncol* (2021) 14(1):199. doi: 10.1186/s13045-021-01209-9

9. Yin Z, Zhang Y, Wang X. Advances in chimeric antigen receptor T-cell therapy for b-cell non-Hodgkin lymphoma. *Biomark Res* (2021) 9(1):58. doi: 10.1186/s40364-021-00309-5

10. Yu S, Zhou X, Steinke FC, Liu C, Chen SC, Zagorodna O, et al. The TCF-1 and LEF-1 transcription factors have cooperative and opposing roles in T cell development and malignancy. *Immunity* (2012) 37(5):813–26. doi: 10.1016/j.immuni.2012.08.009

11. Germar K, Dose M, Konstantinou T, Zhang J, Wang H, Lobry C, et al. T-Cell factor 1 is a gatekeeper for T-cell specification in response to notch signaling. *Proc Natl Acad Sci USA* (2011) 108(50):20060–5. doi: 10.1073/pnas.1110230108

12. Weber BN, Chi AW, Chavez A, Yashiro-Ohtani Y, Yang Q, Shestova O, et al. A critical role for TCF-1 in T-lineage specification and differentiation. *Nature* (2011) 476(7358):63–8. doi: 10.1038/nature10279

13. Li L, Leid M, Rothenberg EV. An early T cell lineage commitment checkpoint dependent on the transcription factor Bcl11b. *Science* (2010) 329 (5987):89–93. doi: 10.1126/science.1188989

14. Hosoya T, Kuroha T, Moriguchi T, Cummings D, Maillard I, Lim KC, et al. GATA-3 is required for early T lineage progenitor development. *J Exp Med* (2009) 206(13):2987–3000. doi: 10.1084/jem.20090934

15. Garcia-Perez L, Famili F, Cordes M, Brugman M, van Eggermond M, Wu H, et al. Functional definition of a transcription factor hierarchy regulating T cell lineage commitment. *Sci Adv* (2020) 6(31):eaaw7313. doi: 10.1126/sciadv.aaw7313

16. Gounari F, Khazaie K. TCF-1: A maverick in T cell development and function. *Nat Immunol* (2022) 23(5):671–8. doi: 10.1038/s41590-022-01194-2

17. Chiara VD, Daxinger L, Staal F. The route of early T cell development: Crosstalk between epigenetic and transcription factors. *Cells* (2021) 10(5):1074. doi: 10.3390/cells10051074

18. Chen S, Huang X, Chen S, Yang L, Shen Q, Zheng H, et al. The role of BCL11B in regulating the proliferation of human naive T cells. *Hum Immunol* (2012) 73(5):456–64. doi: 10.1016/j.humimm

19. Avram D, Califano D. The multifaceted roles of bcl11b in thymic and peripheral T cells: Impact on immune diseases. *J Immunol* (2014) 193(5):2059–65. doi: 10.4049/jimmunol.1400930

20. Zhang S, Rozell M, Verma RK, Albu DI, Califano D, VanValkenburgh J, et al. Antigen-specific clonal expansion and cytolytic effector function of CD8+ T lymphocytes depend on the transcription factor bcl11b. *J Exp Med* (2010) 207 (8):1687–99. doi: 10.1084/jem.20092136

21. Abboud G, Stanfield J, Tahiliani V, Desai P, Hutchinson TE, Lorentsen KJ, et al. Transcription factor Bcl11b controls effector and memory CD8 T cell fate decision and function during poxvirus infection. *Front Immunol* (2016) 7:425. doi: 10.3389/fimmu.2016.00425

22. Jung S, Baek JH. The potential of T cell factor 1 in sustaining CD8(+) T lymphocyte-directed anti-tumor immunity. *Cancers (Basel)* (2021) 13(3):515. doi: 10.3390/cancers13030515

23. Jansen CS, Prokhnevska N, Master VA, Sanda MG, Carlisle JW, Bilen MA, et al. An intra-tumoral niche maintains and differentiates stem-like CD8 T cells. *Nature* (2019) 576(7787):465–70. doi: 10.1038/s41586-019-1836-5

24. Siddiqui I, Schaeuble K, Chennupati V, Fuertes Marraco SA, Calderon-Copete S, Pais Ferreira D, et al. Intratumoral Tcf1(+)PD-1(+)CD8(+) T cells with stem-like properties promote tumor control in response to vaccination and checkpoint blockade immunotherapy. *Immunity* (2019) 50(1):195–211. doi: 10.1016/j.immuni.2018.12.021

25. Hudson WH, Gensheimer J, Hashimoto M, Wieland A, Valanparambil RM, Li P, et al. Proliferating transitory T cells with an effector-like transcriptional signature emerge from PD-1(+) stem-like CD8(+) T cells during chronic infection. *Immunity* (2019) 51(6):1043–58.e4. doi: 10.1016/j.immuni.2019.11.002

26. Pagliarulo F, Cheng PF, Brugger L, van Dijk N, van den Heijden M, Levesque MP, et al. Molecular, immunological, and clinical features associated with lymphoid neogenesis in muscle invasive bladder cancer. *Front Immunol* (2022) 12:793992. doi: 10.3389/fimmu.2021.793992

27. Miller BC, Sen DR, Al Abosy R, Bi K, Virkud YV, LaFleur MW, et al. Subsets of exhausted CD8(+) T cells differentially mediate tumor control and respond to checkpoint blockade. *Nat Immunol* (2019) 20(3):326–36. doi: 10.1038/s41590-019-0312-6

28. Ma L, Sun L, Zhao K, Dong Z, Huang Z, Meng X. The prognostic value of TCF1+CD8+T in primary small cell carcinoma of the esophagus. *Cancer Sci* (2021) 112(12):4968–76. doi: 10.1111/cas.15167

29. Huang X, Chen C, Zhong M, Geng S, Zhao Y, Li M, et al. Lower BCL11B expression is associated with adverse clinical outcome for patients with myelodysplastic syndrome. *biomark Res* (2021) 9(1):46. doi: 10.1186/s40364-021-00302-y

30. Li K, Chen C, Gao R, Yu X, Huang Y, Chen Z, et al. Inhibition of BCL11B induces downregulation of PTK7 and results in growth retardation and apoptosis in T-cell acute lymphoblastic leukemia. *biomark Res* (2021) 9(1):17. doi: 10.1186/s40364-021-00270-3

31. Göthert JR, Eisele L, Klein-Hitpass L, Weber S, Zesewitz ML, Sellmann L, et al. Expanded CD8+ T cells of murine and human CLL are driven into a senescent KLRG1+ effector memory phenotype. *Cancer Immunol Immunother* (2013) 62 (11):1697–709. doi: 10.1007/s00262-013-1473-z

32. Cornet E, Debliquis A, Rimelen V, Civic N, Docquier M, Troussard X, et al. Developing molecular signatures for chronic lymphocytic leukemia. *PloS One* (2015) 10(6):e0128990. doi: 10.1371/journal.pone.0128990

33. Landau DA, Carter SL, Stojanov P, McKenna A, Stevenson K, Lawrence MS, et al. Evolution and impact of subclonal mutations in chronic lymphocytic leukemia. *Cell* (2013) 152(4):714–26. doi: 10.1016/j.cell.2013.01.019

34. Chuang HY, Rassenti L, Salcedo M, Licon K, Kohlmann A, Haferlach T, et al. Subnetwork-based analysis of chronic lymphocytic leukemia identifies pathways that associate with disease progression. *Blood* (2012) 120(13):2639–49. doi: 10.1182/blood-2012-03-416461

35. Herold T, Jurinovic V, Metzeler KH, Boulesteix AL, Bergmann M, Seiler T, et al. An eight-gene expression signature for the prediction of survival and time to treatment in chronic lymphocytic leukemia. *Leukemia* (2011) 25(10):1639–45. doi: 10.1038/leu.2011.125

36. Huang da W, Sherman BT, Lempicki RA. Systematic and integrative analysis of large gene lists using DAVID bioinformatics resources. *Nat Protoc* (2009) 4(1):44–57. doi: 10.1038/nprot.2008.211

37. Szklarczyk D, Franceschini A, Wyder S, Forslund K, Heller D, Huerta-Cepas J, et al. STRING v10: protein-protein interaction networks, integrated over the tree of life. *Nucleic Acids Res* (2015) 43(Database issue):D447–52. doi: 10.1093/nar/gku1003

38. Shannon P, Markiel A, Ozier O, Baliga NS, Wang JT, Ramage D, et al. Cytoscape: a software environment for integrated models of biomolecular interaction networks. *Genome Res* (2003) 13(11):2498–504. doi: 10.1101/gr.1239303

39. Baumann T, Moia R, Gaidano G, Delgado J, Condoluci A, Villamor N, et al. Lymphocyte doubling time in chronic lymphocytic leukemia modern era: a real-life study in 848 unselected patients. *Leukemia* (2021) 35(8):2325–31. doi: 10.1038/s41375-021-01149-w

40. Hanna BS, Llaó-Cid L, Iskar M, Roessner PM, Klett LC, Wong JKL, et al. Interleukin-10 receptor signaling promotes the maintenance of a PD-1(int) TCF-1 (+) CD8(+) T cell population that sustains anti-tumor immunity. *Immunity* (2021) 54(12):2825–41. doi: 10.1016/j.immuni.2021.11.004

41. Zhao X, Shan Q, Xue HH. TCF1 in T cell immunity: a broadened frontier. *Nat Rev Immunol* (2022) 22(3):147–57. doi: 10.1038/s41577-021-00563-6

42. Kim C, Jin J, Weyand CM, Goronzy JJ. The transcription factor TCF1 in T cell differentiation and aging. *Int J Mol Sci* (2020) 21(18):6497. doi: 10.3390/ijms21186497

43. Kratchmarov R, Magun AM, Reiner SL. TCF1 expression marks self-renewing human CD8(+) T cells. *Blood Adv* (2018) 2(14):1685–90. doi: 10.1182/bloodadvances.2018016279

44. Solman IG, Blum LK, Hoh HY, Kipps TJ, Burger JA, Barrientos JC, et al. Ibrutinib restores immune cell numbers and function in first-line and relapsed/refractory chronic lymphocytic leukemia. *Leuk Res* (2020) 97:106432. doi: 10.1016/j.leukres.2020.106432

45. Welten SPM, Yermanos A, Baumann NS, Wagen F, Oetiker N, Sandu I, et al. Tcf1(+) cells are required to maintain the inflationary T cell pool upon MCMV infection. *Nat Commun* (2020) 11(1):2295. doi: 10.1038/s41467-020-16219-3

46. Kueh HY, Yui MA, Ng KK, Pease SS, Zhang JA, Damle SS, et al. Asynchronous combinatorial action of four regulatory factors activates Bcl11b for T cell commitment. *Nat Immunol* (2016) 17(8):956–65. doi: 10.1038/ni.3514

frontiers | Frontiers in Immunology

TYPE Case Report
PUBLISHED 26 September 2022
DOI 10.3389/fimmu.2022.965932



OPEN ACCESS

EDITED BY
Trent Spencer,
Emory University, United States

REVIEWED BY
Satiro De Oliveira,
University of California, Los Angeles, United States
Marcin Jasinski,
Medical University of Warsaw, Poland

*CORRESPONDENCE
Keshu Zhou
drzhouks77@163.com

SPECIALTY SECTION
This article was submitted to Cancer Immunity and Immunotherapy, a section of the journal Frontiers in Immunology

RECEIVED 10 June 2022
ACCEPTED 07 September 2022
PUBLISHED 26 September 2022

CITATION
Han L, Zhao R, Yang JY, Zu YL, Liu YY, Zhou J, Li LL, Huang ZH, Zhang JS, Gao QL, Song YP and Zhou KS (2022) Case Report: Successful engraftment of allogeneic hematopoietic stem cells using CAR-T cell therapy as the conditioning regimen in R/R $Ph^+$ B cell acute lymphoblastic leukemia. *Front. Immunol.* 13:965932. doi: 10.3389/fimmu.2022.965932



# Case Report: Successful engraftment of allogeneic hematopoietic stem cells using CAR-T cell therapy as the conditioning regimen in R/R $Ph^+$ B cell acute lymphoblastic leukemia

Lu Han[1], Ran Zhao[2], Jingyi Yang[2], Yingling Zu[2], Yanyan Liu[2], Jian Zhou[2], Linlin Li[1], Zhenghua Huang[2], Jishuai Zhang[3], Quanli Gao[1], Yongping Song[2] and Keshu Zhou[2]

[1]Department of Immunology, The Affiliated Cancer Hospital of Zhengzhou University & Henan Cancer Hospital, Zhengzhou, China, [2]Department of Hematology, The Affiliated Cancer Hospital of Zhengzhou University & Henan Cancer Hospital, Zhengzhou, China, [3]Department of Research and Development, The Shenzhen Pregene Biopharma Company, Ltd., Shenzhen, China

**Background:** Consolidative allogeneic hematopoietic stem cells (allo-HSCs) after chimeric antigen receptor T cells (CAR-T) therapy is an emerging modality in hematologic malignancies. Knowledge about the success of allogeneic hematopoietic stem cell transplantation (allo-HSCT) after CAR-T therapy without a conditioning regimen is limited.

**Case presentation:** We report a patient with relapsed/refractory (R/R) $Ph^+$ B-cell acute lymphoblastic leukemia (ALL) who underwent anti-CD19 CAR-T immunotherapy. After 1 month of treatment, bone marrow hyperplasia remained reduced with no hematopoietic improvements. In line with this, allogeneic hematopoietic stem cells (HSCs) were extracted from an HLA-matched sibling donor and administered to the patient on day 33 after CAR-T cell therapy to support hematopoiesis. On day 40, the level of immature bone marrow lymphocytes was at 0% and minimal residual disease-negative, and the fusion gene *BCR/ABL* 190 was negative. Chimerism analysis showed full donor chimerism. Three months after CAR-T cells infusion, the patient was still in complete remission with full donor chimerism. However, decreased liver function with skin pigmentation and festering, indicative of acute graft versus host disease, was noted. The treatment was halted owing to financial reasons.

10.3389/fimmu.2022.965932

**Conclusion:** We report the successful engraftment of allogeneic HSCs using CAR-T cell therapy as a conditioning regimen for R/R B-ALL patients.

KEYWORDS

B-cell acute lymphoblastic leukemia, CAR-T, allogeneic hematopoietic stem cell transplantation, conditioning regimen, CD19

## Introduction

Treatment with CD19 targeting chimeric antigen receptor (CAR) T cells has significantly improved the prognosis of patients with R/R B-cell acute lymphoblastic leukemia (B-ALL) (1–7). However, post-CAR-T cell therapy recurrence remains a significant obstacle. Some studies found that allogeneic hematopoietic stem cell transplantation (allo-HSCT) after anti-CD19 CAR-T therapy was associated with an improved leukemia-free survival (LFS) (8–10). Usually, after CAR-T cell therapy, patients undergo conditioning regimens such as myeloablative (cyclophosphamide and busulfan-based and total body irradiation-based) or nonmyeloablative regimens prior to allo-HSCT (11, 12). However, this treatment protocol will lead to a relatively long treatment cycle and more adverse reactions for patients. Knowledge about the successful engraftment of allogeneic hematopoietic stem cell (allo-HSC) after CAR-T therapy without a conditioning regimen is limited. We described a R/R B-ALL patient who received an allo-HSC infusion to support hematopoiesis due to CAR-T cell therapy, and the HSCs were successfully engrafted, which suggest CAR-T cell therapy not only induced disease remission but also directly as a pretreatment regimen for HSC implantation.

## Case presentation

A 36-year-old man was diagnosed with $Ph^+$ B-ALL. He received ten courses of chemotherapy and relapsed after four lines of therapy. In relation to the evaluation criteria, morphology complete remission (CR) was achieved after one course of vincristine, daunorubicin, cyclophosphamide, and prednisone (VDCP) plus imatinib. Then two courses of cyclophosphamide, cytarabine, and 6-mercaptopurine (CAM) plus imatinib were performed. The patient remained in morphology CR, but *BCR-ABL 190* was positive. The patient proceeded with two courses of high-dose methotrexate (HD-MTX) plus dasatinib and one course of VDCP plus dasatinib. Morphology CR persisted, but *BCR-ABL 190* did not become negative even with dasatinib. After one course of CAM plus dasatinib, the percentage of lymphoblasts and prolymphocytes in the bone marrow increased to 11%. Moreover, the fusion gene showed that *BCR-ABL 190/ABL* was 0.4, and flow cytometry (FCM) analysis revealed minimal residual disease (MRD) with 10.5% abnormal lymphocytes. Subsequently, one course of dexamethasone, vincristine, cytarabine, mitoxantrone, and etoposide (DOAME) plus dasatinib was conducted, and molecular CR was achieved. Unfortunately, the patient progressed to molecular relapse within 2 weeks. DOAME plus dasatinib was administered again, but *BCR-ABL 190/ABL* ascended to 0.29 with 20.2% lymphoblasts in the bone marrow. Subsequently, a T315I mutation was detected, and dasatinib was discontinued. Finally, the patient was administered a course of cytarabine, aclacinomycin, granulocyte colony-stimulating factor (CAG) in combination with prednisone and L-asparaginase, whereas the disease continued to progress with 68% lymphoblasts in the bone marrow (the WBC count was $1.92 \times 10^9$/L; LDH was 227 U/L; *BCR-ABL 190* was not detected). During the above treatment process, the patient received nine intrathecal injections of dexamethasone, cytarabine and methotrexate and did not develop central nervous system invasion.

Owing to the presence of R/R disease, anti-CD19 CAR-T cell therapy was initiated. The anti-CD19 CAR-T cells were cultured for 8 days before infusion. The CAR transduction efficiency was 41%. The conditioning regimen was administered to the patient using a standard lymphodepleting regimen (fludarabine 30 mg/$m^2$ and cyclophosphamide 600 mg/$m^2$) on day −5 to −3. The CAR-T cell infusion was administered as follows: $4 \times 10^6$ cells/kg of anti-CD19 CAR-T cells were divided into three infusions on day 0 to day +2 (Figure 1A). Following the infusion, the patient experienced grade 4 cytokine release syndrome (CRS) with elevated IL-6, IL-10, IFN-γ, and ferritin levels, as well as grade 3 CAR-T cell-related encephalopathy syndrome according to Lee's grading system (13). The levels of IL-6, IL-10, IFN-γ, and ferritin gradually returned to baseline 3 weeks after treatment with tocilizumab (monoclonal antibody against the IL-6 receptor) (8 mg/kg, qd, +3 and +5 days), dexamethasone (20 mg, qd, +6 to +8 days, +12 to +15 days, +19 to +21 days), and plasma exchange (14, 15) (2000 mL per time, +10 days, +11 days and +17 days) (Figures 1B, C). One month later, the white blood cell (WBC) and lymphocyte counts remained below $1.0 \times 10^9$/L, except for a brief increase on days 6 and 7 post-CAR-T cell infusion. The dynamic changes of WBC and lymphocyte counts

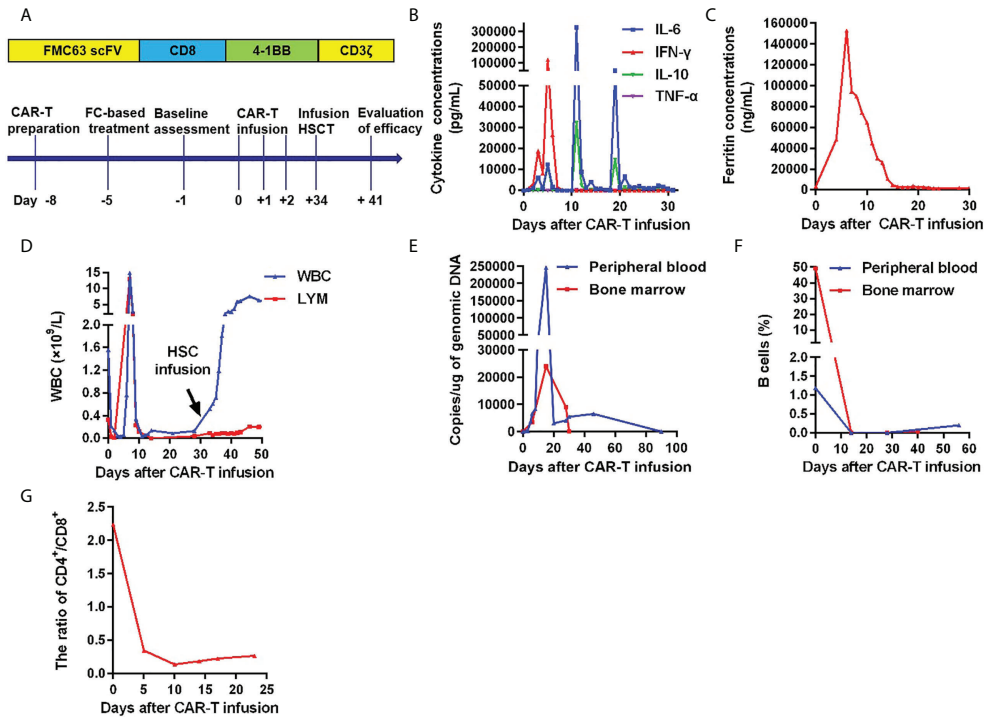


FIGURE 1
Infusion of anti-CD19 CAR-T cells and allo-HSC. **(A)** Anti-CD19 CAR design and the schematic clinical treatment protocol for anti-CD19 CAR-T cell therapy. The scFv region that recognizes CD19 was derived from the FMC63 monoclonal antibody. The CAR contained a 4-1BB costimulatory domain and a CD3ζ T-cell activation domain (top panel). Clinical treatment protocol (bottom panel). **(B)** Levels of cytokines after CAR-T cell therapy. **(C)** Levels of ferritin after CAR-T cell therapy. **(D)** Dynamic white blood cell and lymphocyte numbers after CAR-T cell therapy. **(E)** Copies of lentivirus-containing CAR-T cells in the peripheral blood and bone marrow after CAR-T cell therapy. **(F)** CAR-T cells and B-cells after CAR-T cell therapy. **(G)** Ratio of $CD4^+/CD8^+$ T cells in the peripheral blood after CAR-T cell therapy.

after CAR-T cell therapy were depicted in Figure 1D. Furthermore, lentivirus copies with the polymerase chain reaction test to reflect CAR-T cell infusion increased in relation to the B lymphocyte decline, suggesting that the CAR-T cells reached peak levels after 2 weeks (Figures 1E, F). In addition, the $CD4^+/CD8^+$ T cell ratio in the peripheral blood was significantly below normal 2–3 weeks after the CAR-T cell infusion (Figure 1G).

After CAR-T cell therapy, bone marrow morphology revealed 0% immature lymphocytes, and severe bone marrow suppression with no hematopoietic recovery, granulocyte colony-stimulating factor (G-CSF) was administered to promote granulocyte recovery. Antibiotics and intravenous immunogloblin (IVIG) were administered because the patient developed infections (*Escherichia coli*) during myelosuppression. There was no evidence of viral infection. To support hematopoietic recovery, allogeneic HSCs were harvested by apheresis from a 6/6 HLA-matched sibling donor. Furthermore, 100 mL of HLA-homologous donor peripheral HSCs (mononuclear cells [MNC] $1.8\times10^8$/kg and $CD34^+$ cells $0.95\times10^6$/kg) (16, 17) were infused on day 34 following the CAR-T cell infusion. Before allogeneic HSCs on day 33 after the CAR-T cell infusion, the WBC count was $0.61\times10^9$/L, the neutrophil count was $0.53\times10^9$/L, lymphocyte count was $0.06\times10^9$/L, and the platelet count was $20\times10^9$/L. The engraftment time of neutrophils was +36 days, and the engraftment time of platelets was +42 days after CAR-T cells infusion (Figure 1D). On day 40, bone marrow morphology revealed 0% immature lymphocytes and negative MRD by FCM. The expression of the fusion gene *BCR/ABL 190* was negative. Chimeric analysis showed full donor chimerism. Three months after CAR-T cell therapy, bone marrow morphology, and fusion gene expression level suggested molecular CR. However, decreased liver function with skin pigmentation and a festering skin rash was noted (Figure 2). The level of donor chimerism was 100%. According to the consensus criteria for acute graft versus host disease (aGVHD), grade III aGVHD was highly likely (18). Unfortunately, we did not expect allogeneic HSCs to engraft successfully for patient and did not realize that aGVHD would occur, therefore, no prophylaxis for aGVHD was administered. Treatment was halted owing to financial reasons, and the patient abandoned the treatment and eventually may be died of aGVHD combined with infection. A brief chronology of this case's key clinical events is depicted in Table 1.

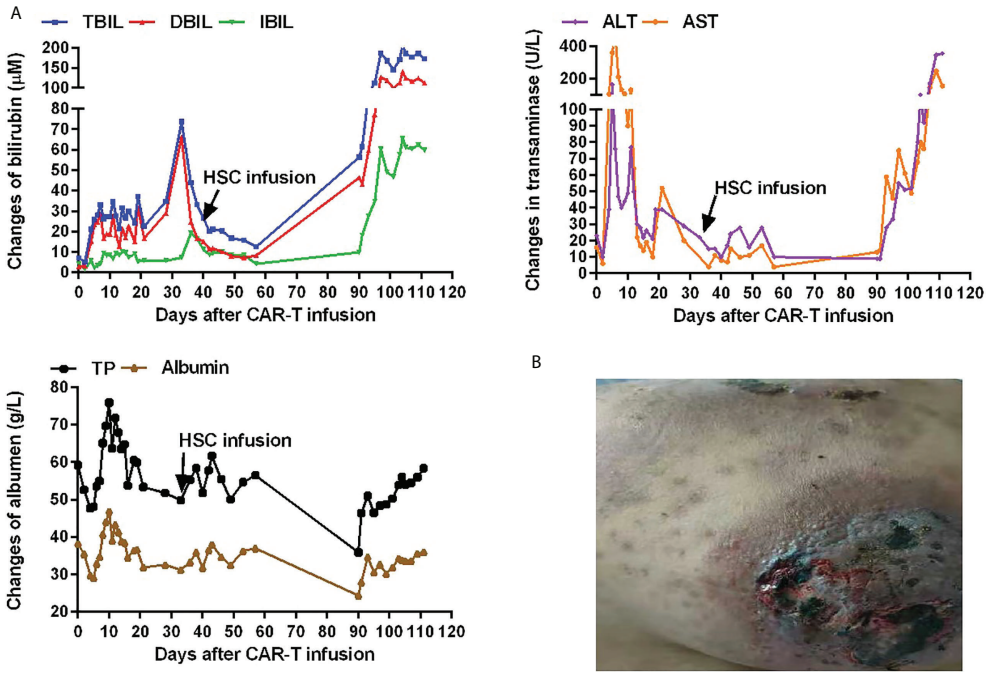


FIGURE 2
Hepatic function and skin changes after CAR-T cell infusion. **(A)** Hepatic function after CAR-T cell infusion. Expression of total bilirubin (TBIL; normal range, 0–21 μM), direct bilirubin (DBIL; normal range, 0–5 μM), indirect bilirubin (IBIL; normal range, 0–15 μM), alanine transaminase (ALT; normal range, 5–40 U/L), aspartate transaminase (AST; normal range, 8–40 U/L), total protein (TP; normal range, 64–83 g/L), and albumin (normal range, 34–48 g/L) after CAR-T cell infusion. **(B)** Skin pigmentation and a festering skin rash after CAR-T cell infusion.

## Discussion

Notably, consolidative allo-HSCT after CAR-T therapy is still a controversial option for improving long-term LFS. Park et al. reported that of seventeen patients who underwent allo-HSCT after CAR-T therapy. Relapse and transplantation-associated complications were the main causes of death for those who received CAR-T therapy before allo-HSCT, and the patients seemed not to benefit from allo-HSCT after CAR-T treatment. However, some studies have shown allo-HSCT after CAR-T cell therapy can reduce the risk of relapse and improve long-term OS and LFS (8, 10, 19). Jiang et al. summarized the data of several clinical trials in which some R/R B-ALL patients received consolidative allo-HSCT after CAR-T cell therapy (19). In total, 429 R/R B-ALL patients achieved CR/CRi after CAR-T cell therapy. A total of 203 of these responding patients underwent allo-HSCT subsequently, and only 27 (13.3%) relapsed. In comparison, 116/226 (51.3%) of the patients who did not proceed with allo-HSCT relapsed finally. Generally, for patients who received consolidative allo-HSCT after CAR-T cell therapy, high-dose conditioning chemotherapy or total body irradiation are administered before allo-HSCT. The aims of pre-treatment are to (1) eliminate abnormal clonal cells from the body, (2) inhibit the immune system to prevent the rejection of foreign cells, and (3) allow the transplanted cells to settle in the bone marrow.

CAR-T cell therapy has emerged as a potential induction therapy for patients with R/R ALL, chronic lymphocytic leukemia, and non-Hodgkin's lymphoma. Clinical studies have reported favorable outcomes (4, 20, 21). The main adverse effects of CAR-T cell therapy include CRS, B-cell aplasia, neurotoxicity, and bone marrow depression (22, 23). Moreover, myelosuppression is the most common reported adverse reaction of CAR-T cell therapy. Fried et al. analyzed the persistent severe hematologic toxicity after anti-CD19 CAR-T cell therapy in patients with R/R leukemia and lymphoma (21). Severe myelosuppression was more commonly reported in patients with high-grade CRS. Wang et al. reported the kinetics of immune reconstitution after anti-CD19 CAR-T cell therapy and found that neutrophils, platelets, lymphocytes returned to a normal level with a median time of recovery on day 28 (14-44), 28 (3-45), 42 (3-125), respectively (24). In the present case, the bone marrow suppression remained persistent with no hematopoietic recovery after 1 month of CAR-T cell therapy, consistent with the previous literature. Considering the severe myelosuppression of the patient and referring to the report by Rejeski K et al (17), HSCs were infused to support hematopoietic recovery. Fortunately, the

TABLE 1 Key clinical events in this case.

| Lines of therapy | Time before or after CAR-T cell therapy | Date of regime | Regime | Date of BM aspiration | Blasts in BM | MRD | *BCR-ABL 190* (copies/mL) | Response |
|---|---|---|---|---|---|---|---|---|
| | -290 days | 2016/3/9 | VDCP+Imatinib | 2016/4/7 | 0.0% | - | $6.70\times10^3$ | Morphology CR |
| 1 | -259 days | 2016/4/9 | CAM+Imatinib | 2016/5/9 | 0.0% | - | $6.39\times10^2$ | Morphology CR |
| | -227 days | 2016/5/11 | CAM+Imatinib | 2016/6/9 | 0.0% | 0.26% | $2.75\times10^3$ | Molecular relapse |
| | -194 days | 2016/6/13 | HD-MTX+Dasatinib | - | - | - | - | - |
| 2 | -183 days | 2016/6/24 | HD-MTX+Dasatinib | 2016/7/18 | 0.8% | Negative | $3.47\times10^2$ | Morphology CR |
| | -157 days | 2016/7/20 | VDCP+Dasatinib | 2016/8/18 | 0.0% | Negative | $4.78\times10^3$ | Morphology CR |
| | -126 days | 2016/8/20 | CAM+Dasatinib | 2016/9/21 | 11.0% | 10.50% | $2.5\times10^6$ | Relapse |
| | -89 days | 2016/9/26 | DOAME+Dasatinib | 2016/10/14 | 0.6% | - | Negative | Molecular CR |
| | | | | 2016/10/25 | 2.6% | 2.70% | $1.37\times10^5$ | Molecular relapse |
| 3 | -52 days | 2016/11/2 | DOAME+Dasatinib | 2012/11/23 | 12.0% | 20.20% | $1.69\times10^6$ | Relapse |
| | -26 days | 2016/11/28 | T315I mutation was detected, withdraw Dasatinib | 2016/11/28 | 33.0% | - | - | Progression |
| 4 | -24 days | 2016/11/30 | CAG+Pred+L-Asp | 2016/12/7 | 68.0% | - | - | Progression |
| | -5 to -3 days | 2016/12/19 to 2016/12/21 | Standard lymphodepleting regimen | | | | | |
| | 0 to +2 days | 2016/12/24 to 2016/12/26 | Anti-CD19 CAR-T cells infusion | 2017/1/22 | 0% with myelosuppression | | | - |
| | +34 days | 2017/1/26 | HSCs infusion | 2017/2/4 | 0% | Negative | Negative | Molecular CR |
| | +90 days | 2017/3/23 | Symptomatic and supportive treatment | 2017/3/27 | 0% | Negative | Negative | Molecular CR |
| | +113 days | 2017/4/15 | The patient abandoned the treatment | 2017/4/15 | 0% | Negative | Negative | Molecular CR |

BM, bone marrow; MRD, minimal residual disease; CR, complete response; VDCP, vincristine, daunorubicin, cyclophosphamide, and prednisone; CAM, cyclophosphamide, cytarabine, and 6-mercaptopurine; HD-MTX, high-dose methotrexate; DOAME, dexamethasone, vincristine, cytarabine, mitoxantrone, and etoposide; CAG+Pred+L-Asp, cytarabine, aclacinomycin, granulocyte colony-stimulating factor, prednisone, and l-asparaginase; HSCs, hematopoietic stem cells; -: not available.

HSCs were successfully implanted into the patient. This indicates the possibility of direct transfusion of allogeneic HSCs without any conditioning regimen, during the period of bone marrow suppression after CAR-T cell therapy. Potential reasons for the HSCs were successfully implanted into the patient were: (a) clearance of abnormal tumor cells and reduction of tumor load and (b) inhibition of the body's systemic immunity, similar to the pre-transplant effect. Concerning the eligibility of the patients or the degree of bone marrow suppression for which HSCs may be successfully implanted, further studies are needed.

So far, there have been no previous reports of HSCs successful engraftment without a conditioning regimen. In this case, the initial purpose of apply allogeneic HSCs was to restore hematopoietic function temporarily, and we did not expect allogeneic HSCs to engraft successfully for patient. aGVHD was a common complication in the allo-HSCT setting, thus, we did not realize that aGVHD would occur, which led to no prophylaxis and treatment being initiated. Multiple laboratory parameters and careful clinical observations may be useful for the early detection the occurrence of aGVHD in the future. CAR-T cell therapy not only induced disease remission but also as a conditioning regimen enabled the successful implantation of HSCs in R/R $Ph^+$ B-cell ALL patient is well-documented. But, how many the HSCs required for successful engraftment would be a more important discussion.

In summary, CAR-T cell therapy induced disease remission simultaneously as a pretreatment protocol enabling successful implantation of allo-HSCs in a patient with R/R $Ph^+$ B-cell ALL, which greatly simplified treatment process and reduce the injury to patient. However, further research is required to assess the viability of CAR-T cell therapy as an allo-HSCT pre-emptive treatment. Additional data should be collected to confirm the best time of infusing allogeneic HSCs after CAR-T cell therapy.

## Data availability statement

The original contributions presented in the study are included in the article/supplementary material. Further inquiries can be directed to the corresponding author.

## Ethics statement

The studies involving human participants were reviewed and approved by Medical Ethics Committee of Henan Cancer Hospital. The patients/participants provided their written informed consent to participate in this study. Written informed consent was obtained from the patient's brother for the publication of any potentially identifiable images or data included in the article.

## Author contributions

LH, YYL and KSZ provided and interpreted data. LH, KSZ, YPS, and JZ provided design input and analyzed the data. LH drafted the final manuscript. All authors reviewed and approved the final manuscript.

## Funding

This study received funding from the National Natural Science Foundation (grant number 81470336); Henan Provincial Scientific and Technological Project (grant number 222102310250).

## Conflict of interest

Author JSZ is employed by The Shenzhen Pregene Biopharma Company, Ltd.

The remaining authors declare that the research was conducted in the absence of any commercial or financial relationships that could be construed as a potential conflict of interest.

## Publisher's note



## References

1. Gökbuget N, Stanze D, Beck J, Diedrich H, HorstHA, Hüttmann A, et al. Outcome of relapsed adult lymphoblastic leukemia depends on response to salvage chemotherapy, prognostic factors, and performance of stem cell transplantation. *Blood* (2012) 120(10):2032–41. doi: 10.1182/blood-2011-12-399287

2. Inagaki J, Fukano R, Noguchi M, Kurauchi K, Tanioka S, Okamura J. Hematopoietic stem cell transplantation following unsuccessful salvage treatment for relapsed acute lymphoblastic leukemia in children. *Pediatr Blood Cancer* (2015) 62(4):674–9. doi: 10.1002/pbc.25353

3. Davila ML, Riviere I, Wang X, Bartido S, Park J, Curran K, et al. Efficacy and toxicity management of 19-28z CAR T cell therapy in b cell acute lymphoblastic leukemia. *Sci Transl Med* (2014) 6(224):224ra225. doi: 10.1126/scitranslmed.3008226

4. Maude SL, Frey N, Shaw PA, Aplenc R, Barrett DM, Bunin NJ, et al. Chimeric antigen receptor T cells for sustained remissions in leukemia. *N Engl J Med* (2014) 371(16):1507–17. doi: 10.1056/NEJMoa1407222

5. Hu Y, Wu Z, Luo Y, Shi J, Yu J, Pu C, et al. Potent anti-leukemia activities of chimeric antigen receptor-modified T cells against CD19 in Chinese patients with Relapsed/Refractory acute lymphocytic leukemia. *Clin Cancer Res* (2017) 23 (13):3297–306. doi: 10.1158/1078-0432.CCR-16-1799

6. Hollyman D, Stefanski J, Przybylowski M, Bartido S, Borquez-Ojeda O, Taylor C, et al. Manufacturing validation of biologically functional T cells targeted to CD19 antigen for autologous adoptive cell therapy. *J Immunother* (2009) 32 (2):169–80. doi: 10.1097/CJI.0b013e318194a6e8

7. Kochenderfer JN, Feldman SA, Zhao Y, Xu H, Black MA, Morgan RA, et al. Construction and preclinical evaluation of an anti-CD19 chimeric antigen receptor. *J Immunother* (2009) 32(7):689–702. doi: 10.1097/CJI.0b013e3181ac6138

8. Hay KA, Gauthier J, Hirayama AV, Voutsinas JM, Wu Q, Li D, et al. Factors associated with durable EFS in adult b-cell ALL patients achieving MRD-negative CR after CD19 CAR T-cell therapy. *Blood* (2019) 133(15):1652–63. doi: 10.1182/blood-2018-11-883710

9. Zhang Y, Chen H, Song Y, Tan X, Zhao Y, Liu X, et al. Chimeric antigens receptor T cell therapy as a bridge to haematopoietic stem cell transplantation for refractory/relapsed b-cell acute lymphomalastic leukemia. *Br J Haematol* (2020) 189(1):146–52. doi: 10.1111/bjh.16339

10. Jiang H, Li C, Yin P, Guo T, Liu L, Xia L, et al. Anti-CD19 chimeric antigen receptor-modified T-cell therapy bridging to allogeneic hematopoietic stem cell transplantation for relapsed/refractory b-cell acute lymphoblastic leukemia: An open-label pragmatic clinical trial. *Am J Hematol* (2019) 94(10):1113–22. doi: 10.1002/ajh.25582

11. Bazarbachi AH, Al Hamed R, Labopin M, Afanasyev B, Hamladji RM, Beelen D, et al. Allogeneic stem-cell transplantation with sequential conditioning in adult patients with refractory or relapsed acute lymphoblastic leukemia: A report from the EBMT acute leukemia working party. *Bone Marrow Transplant* (2020) 55 (3):595–602. doi: 10.1038/s41409-019-0702-2

12. Peters C, Dalle JH, Locatelli F, Poetschger U, Sedlacek P, Buechner J, et al. Total body irradiation or chemotherapy conditioning in childhood ALL: A multinational, randomized, noninferiority phase III study. *J Clin Oncol* (2021) 39 (4):295–307. doi: 10.1200/JCO.20.02529

13. Lee DW, Gardner R, Porter DL, Louis CU, Ahmed N, Jensen M, et al. Current concepts in the diagnosis and management of cytokine release syndrome. *Blood* (2014) 124(2):188–95. doi: 10.1182/blood-2014-05-552729

14. Xiao X, He X, Li Q, Zhang H, Meng J, Jiang Y, et al. Plasma exchange can be an alternative therapeutic modality for severe cytokine release syndrome after chimeric antigen receptor-T cell infusion: A case report. *Clin Cancer Res* (2019) 25 (1):29–34. doi: 10.1158/1078-0432.CCR-18-1379

15. Heng G, Jia J, Li S, Fu G, Wang M, Qin D, et al. Sustained therapeutic efficacy of humanized anti-CD19 chimeric antigen receptor T cells in Relapsed/Refractory acute lymphoblastic leukemia. *Clin Cancer Res* (2020) 26(7):1606–15. doi: 10.1158/1078-0432.CCR-19-1339

16. Lin Q, Liu X, Han L, Liu L, Fang B, Gao Q, et al. Autologous hematopoietic stem cell infusion for sustained myelosuppression after BCMA-CAR-T therapy in patient with relapsed myeloma. *Bone Marrow Transplant* (2020) 55(6):1203–5. doi: 10.1038/s41409-019-0674-2

17. Rejeski K, Burchert A, Iacoboni G, Sesques P, Fransecky L, Bücklein V, et al. Safety and feasibility of stem cell boost as a salvage therapy for severe

hematotoxicity after CD19 CAR T-cell therapy. *Blood Adv* (2022) 6(16):4719–25. doi: 10.1182/bloodadvances.2022007776

18. Przepiorka D, Weisdorf D, Martin P, Klingemann HG, Beatty P, Hows J, et al. 1994 Consensus conference on acute GVHD grading. *Bone Marrow Transplant* (1995) 15(6):825–8.

19. Jiang H, Hu Y, Mei H. Consolidative allogeneic hematopoietic stem cell transplantation after chimeric antigen receptor T-cell therapy for relapsed/refractory b-cell acute lymphoblastic leukemia: Who? when? why? *biomark Res* (2020) 8(1):66. doi: 10.1186/s40364-020-00247-8

20. Kochenderfer JN, Dudley ME, Feldman SA, Wilson WH, Spaner DE, Maric I, et al. B-cell depletion and remissions of malignancy along with cytokine-associated toxicity in a clinical trial of anti-CD19 chimeric-antigen-receptor-transduced T cells. *Blood* (2012) 119(12):2709–20. doi: 10.1182/blood-2011-10-384388

21. Fried S, Avigdor A, Bielorai B, Meir A, Besser MJ, Schachter J, et al. Early and late hematologic toxicity following CD19 CAR-T cells. *Bone Marrow Transplant* (2019) 54(10):1643–50. doi: 10.1038/s41409-019-0487-3

22. Maude SL, Teachey DT, Porter DL, Grupp SA. CD19-targeted chimeric antigen receptor T-cell therapy for acute lymphoblastic leukemia. *Blood* (2015) 125 (26):4017–23. doi: 10.1182/blood-2014-12-580068

23. Lee DW, Kochenderfer JN, Stetler-Stevenson M, Cui YK, Delbrook C, Feldman SA, et al. T Cells expressing CD19 chimeric antigen receptors for acute lymphoblastic leukaemia in children and young adults: a phase 1 dose-escalation trial. *Lancet* (2015) 385(9967):517–28. doi: 10.1016/S0140-6736(14)61403-3

24. Wang Y, Li H, Song X, Qi K, Cheng H, Cao J, et al. Kinetics of immune reconstitution after anti-CD19 chimeric antigen receptor T cell therapy in relapsed or refractory acute lymphoblastic leukemia patients. *Int J Lab Hematol* (2021) 43 (2):250–8. doi: 10.1111/ijlh.13375

frontiers | Frontiers in Immunology

TYPE Review
PUBLISHED 02 November 2022
DOI 10.3389/fimmu.2022.1049301



OPEN ACCESS

EDITED BY
Alessandro Poggi,
San Martino Hospital (IRCCS), Italy

REVIEWED BY
Stéphane J. C. Mancini,
INSERM UMR1236
Microenvironnement, Différenciation cellulaire, Immunologie et Cancer, France
Dominique Bonnet,
Francis Crick Institute, United Kingdom

*CORRESPONDENCE
Carsten Riether
carsten.riether@insel.ch

SPECIALTY SECTION
This article was submitted to Cancer Immunity and Immunotherapy, a section of the journal Frontiers in Immunology

RECEIVED 20 September 2022
ACCEPTED 20 October 2022
PUBLISHED 02 November 2022

CITATION
Riether C (2022) Regulation of hematopoietic and leukemia stem cells by regulatory T cells.
*Front. Immunol.* 13:1049301.
doi: 10.3389/fimmu.2022.1049301



# Regulation of hematopoietic and leukemia stem cells by regulatory T cells

Carsten Riether [1,2*]

[1]Department of Medical Oncology, Inselspital, Bern University Hospital, University of Bern, Bern, Switzerland, [2]Department for BioMedical Research (DBMR), University of Bern, Bern, Switzerland

Adult bone marrow (BM) hematopoietic stem cells (HSCs) are maintained in a quiescent state and sustain the continuous production of all types of blood cells. HSCs reside in a specialized microenvironment the so-called HSC niche, which equally promotes HSC self-renewal and differentiation to ensure the integrity of the HSC pool throughout life and to replenish hematopoietic cells after acute injury, infection or anemia. The processes of HSC self-renewal and differentiation are tightly controlled and are in great part regulated through cellular interactions with classical (e.g. mesenchymal stromal cells) and non-classical niche cells (e.g. immune cells). In myeloid leukemia, some of these regulatory mechanisms that evolved to maintain HSCs, to protect them from exhaustion and immune destruction and to minimize the risk of malignant transformation are hijacked/disrupted by leukemia stem cells (LSCs), the malignant counterpart of HSCs, to promote disease progression as well as resistance to therapy and immune control. $CD4^+$ regulatory T cells (Tregs) are substantially enriched in the BM compared to other secondary lymphoid organs and are crucially involved in the establishment of an immune privileged niche to maintain HSC quiescence and to protect HSC integrity. In leukemia, Tregs frequencies in the BM even increase. Studies in mice and humans identified the accumulation of Tregs as a major immune-regulatory mechanism. As cure of leukemia implies the elimination of LSCs, the understanding of these immune-regulatory processes may be of particular importance for the development of future treatments of leukemia as targeting major immune escape mechanisms which revolutionized the treatment of solid tumors such as the blockade of the inhibitory checkpoint receptor programmed cell death protein 1 (PD-1) seems less efficacious in the treatment of leukemia. This review will summarize recent findings on the mechanisms by which Tregs regulate stem cells and adaptive immune cells in the BM during homeostasis and in leukemia.

KEYWORDS

**regulatory T cell (Treg), leukemia stem cell (LSC), immune escape, hematopoietic stem cell, hematopoietic stem cell niche**

## Introduction

During the last decade a series of studies have been performed to decipher the role and contribution of non-hematopoietic (osteoblasts, stromal and endothelial cells, pericytes, Schwann cells and sympathetic neurons) as well as mature hematopoietic cells to the hematopoietic stem cell (HSC) niche in the bone marrow (BM). All these different cell types were allocated as components of the HSC niche and even as critical regulators of HSC function. Especially intensive work on cells of non-hematopoietic origin by many different groups unraveled the composition of the HSC niche and the cellular and molecular interactions exchanged between its different stromal and endothelial components and their contribution to HSC function (1). Recent work has highlighted the importance of mature immune cells as constituents of the HSC niche (1). Regulatory T cells (Tregs) have been initially identified as a specialized T cell subpopulation which suppresses immune responses to guarantee immune homeostasis and self-tolerance. Recently, however, Tregs have been shown to also control non-lymphoid processes, insulin resistance in visceral fat, muscle repair and to prevent lung damage (2). In the BM microenvironment Treg frequencies are higher than in other secondary lymphoid organs suggesting a role for Tregs in shaping an immunosuppressive BM microenvironment which may protect HSCs from elimination and damage. However, the current understanding of Tregs in the regulation of HSCs and/or the HSC niche under steady state conditions is still limited. During leukemia development, the immune microenvironment in the BM undergoes massive changes with especially immunosuppressive Tregs infiltrating or accumulating. These Tregs may be able to directly promote leukemogenesis or to protect LSCs from elimination by activated immune cells. However, like for HSCs, the actual interaction of Tregs with LSCs remains in part elusive. Therefore, in this review we discuss recent insights into the communication between Tregs, HSCs and LSCs during health and hematological disease.

## The perivascular HSC niche in the BM

Under homeostatic conditions, the majority of HSCs in the BM are in a quiescent state to prevent HSC exhaustion and to maintain and protect their self-renewal capacity (1). Fundamental HSC characteristics such as self-renewal, differentiation and proliferation are crucially regulated by hematopoietic and stromal components of the HSC niche. Perivascular regions in the BM form distinct niches and have been identified to regulate HSC quiescence and the supply of lineage-committed progenitors (1). Especially NG2-expressing pericytes maintain HSCs in a quiescent state as depletion of NG2-expressing cells resulted in cycling of HSCs, loss of long-term repopulating HSCs and altered HSC localization in the BM. In contrast, cycling HSCs are found near sinusoids and more specifically to sinusoids associated with stem cell factor (SCF) - producing leptin receptor-positive ($LEPR^+$) cells. Depletion of SCF in $LEPR^+$ cells reduced BM HSC numbers (3). Consequently, it is postulated that once entering cell cycle quiescent HSCs translocate from a $NG2^+$ periarteriolar to a $LEPR^+$ perisinusoidal region of the HSC niche. In addition, the low oxygen-permeability of arteriolar blood vessels in the BM promotes HSC quiescence by reducing the accumulation of reactive oxygen species (ROS) in HSCs in contrast to highly oxygen-permeable sinusoids which confer proliferation and differentiation signals to the HSCs (4–6). Furthermore, endothelial cells have been identified together with $LEPR^+$ cells as the main sources of SCF and CXC-chemokine ligand 12 (CXCL-12) required for HSC maintenance in normal young and adult BM (1). Thus, HSCs reside in a hypoxic perivascular niche in which endothelial cells and stromal cells express distinct factors that promote HSC maintenance (1, 3).

## The niche of hematological malignancies

The contribution of the BM microenvironment in the leukemogenesis of leukemias and other hematopoietic neoplasms has been demonstrated in recent years (7). In hematological malignancies and with age, not only hematopoietic cells accumulate genetic alterations but also the HSC niche undergoes an extensive re-organization and thereby contributes to the generation of hematopoietic disorders such as leukemia (8). Nevertheless, despite these findings generated in experimental models, direct evidence that initial lesions in cells of the HSC niche trigger the development of the disease is still lacking for human leukemia.

In contrast, evidence that leukemic cells actively create an aberrant leukemic niche has been extensively generated in parallel to the description of the normal HSC niche. Normal HSCs and LSCs compete for the same region of the endosteal HSC niche (9–12). Through their localization in the normal HSC niche, LSCs co-opt evolutionary conserved signaling cascades of the BM microenvironment to further support the growth of the leukemia (7). In addition, malignant hematopoietic cells interact specifically with stromal and endothelial elements of the HSC niche to induce remodeling. As a consequence, the re-modelled BM microenvironment becomes supportive for AML LSCs and negatively affects healthy hematopoiesis and, specifically, HSCs (8–14). For example, genes in AML MSCs are in general hypomethylated which is accompanied by an altered expression of genes related to inflammation and CXCL-12 signaling (9). Similar results on the provision of pro-inflammatory signals by MSCs to promote leukemogenesis have been described in murine AML and CML models (10). Furthermore, pro-inflammatory

cytokines such as interleukin (IL)-6 and TNF produced by leukemia cells have a central role in the promotion of disease development by promoting differentiation of leukemic progenitors and by simultaneous disruption and alteration of normal HSC function (8, 13, 14). Single cell RNA-sequencing further revealed that MSCs in AML have an impaired potential to differentiate into osteoblasts and to secrete key molecules required for HSCs maintenance such as CXCL-12 and SCF (9). The accumulation of these altered osteoprogenitors/osteoblasts, also characterized by increased production of inflammatory cytokines, modulates the endosteal HSC niche in a way that leukemogenesis is supported while the capacity to support normal hematopoiesis and HSCs is lost (11, 12).

Two recently published studies also highlighted the impact of alterations in the BM vasculature in the endosteal region for the maintenance of LSCs and the loss of HSCs. Increased permeability and reduced perfusion in the endosteal region resulted in hypoxic changes, the overproduction of ROS and nitric oxid, loss of barrier function and cell death. Inhibition of nitric oxid production reduced vascular permeability and preserved normal HSC function (15). Furthermore, enhanced inflammatory signaling in leukemia cells in the endosteal niche was associated with a reduction in vessels and HSCs (13). Importantly, a recent transcriptomic analysis revealed that pathologic crosstalk exists not only between AML and different niche cells but also within niche fractions (15).

The sympathetic nervous system (SNS) also promotes AML development. However, in contrast to normal hematopoiesis (16), nerves fibers get disrupted during AML development resulting in a reduction of HSC-promoting $NG2^+$ niche cells and instruction of $Nestin^+$ stromal cells to generate osteoblasts (17). Furthermore, recent preclinical work indicated a role for the pro-inflammatory cytokine IL-1β in the loss of sympathetic nerve fibers in the BM during MPN development. During early stages of the disease, JAK2V617F-expressing HSCs secrete IL-1β resulting in apoptosis of sympathetic fibers which was further associated with reduced numbers of Nestin-expressing MSCs and concomitant expansion of mutant HSCs (18). Overall, these studies indicate that LSCs, like HSCs, are dependent on signals derived from the HSC niche. Additionally, LSCs actively contribute to the re-organization of the niche from a microenvironment supportive for HSCs into an HSC unfriendly, aberrant leukemic microenvironment.

## Regulation of the HSC niche by immune cells in the BM

Self-renewal and maintenance of HSCs are not exclusively regulated by endothelial and stromal elements of the BM niche. As a primary and secondary lymphoid organ, the BM harbors a variety of different mature and immature cells of hematopoietic origin such as T cells, B cells monocytes/macrophages and neutrophils (7). Apart from developing and mature B cell subsets which occupy specific niches in the BM (19), most other lymphocyte subsets are widely distributed and can in general not be allocated to a specific location in the BM stroma or parenchyma (7). In addition, billions of leukocytes circulate every day through the BM. Recent studies highlighted the substantial contribution of multiple of these immune cell subsets in the regulation of the HSC niche (Table 1). Especially monocytes and macrophages but also different T cell subset have been shown to mediate the mobilization of HSCs indirectly by modulating MSCs (34–36, 39). Monocytes and macrophages comprise around 0.4% of total BM cells and are widely distributed throughout the BM.

## Regulatory T cells in hematopoiesis

The BM microenvironment does not only provide HSCs with key signals for survival, quiescence and self-renewal (1) but it also ensures protection against harmful signals that may drive HSCs differentiation, exhaustion or destruction (7). Tregs is one cellular subset, ideally suited to protect against the negative impact for example of inflammation by shaping an immune-suppressive environment. The BM is considered as a reservoir for Tregs in healthy individuals (40). Under homeostatic conditions, Tregs locate close to sinusoids and close to HSCs located at the endosteal surface in the BM (25) and comprise around 0.5% of all BM mononuclear cells and around one third of all $CD4^+$ T cells in the BM (41). Thereby, Tregs are significantly enriched in frequency in the BM compared to other secondary lymphoid organs such as the spleen or the lymph nodes (40, 42). In contrast to blood and skin, BM Tregs are phenotypically characterized by the expression of CD45RA, C-X-C chemokine receptor type 4 (CXCR4) and the high expression of FOXP3 and CD25 (40, 43). Functionally, BM Tregs have a superior immunosuppressive activity compared to their blood counterparts (40). The BM retains these CXCR4-expressing Tregs through CXCL-12. After adoptive transfer into NSG mice, human Tregs preferentially homed into the BM which harbored elevated levels of CXCL-12. Blockade of the CXCR4/CXCL-12 interaction *via* monoclonal antibody (mAb) abolished the retention of Tregs in the BM but not the spleen (40). Therefore, it is speculated that the BM may represent a niche where naive Tregs accumulate to mature, survive, and/or undergo homeostatic proliferation while maintaining their naive phenotype. Furthermore, BM-resident Tregs may contribute to the formation of the immune-privileged perivascular HSC niche and shield the stem cell compartment from elimination by immune cells, excessive inflammation as well as cell-death.

Total $CD4^+$ T cells (T helper cells and Tregs) secret hematopoietic-related cytokines and are essential for hematopoiesis stimulation during infection and hematologic recovery after BM transplantation [reviewed in (44)]. In addition, early observations that 1) STAT-$4^{-/-}$ mice, which harbor predominately Th2 cells, have

TABLE 1 Immune cell subsets present in the BM stem cell niche and their reported effect on the HSCs and HSC niche function.

| Cell Type | Frequency among total BM cells | Location in BM | Effect on HSC niche and/or HSCs | Effect on LSCs and leukemia niche |
|---|---|---|---|---|
| **Total $CD4^+$ T cells** | ~1% | Widely distributed throughout the BM | Antigen-activated $CD4^+$ T cells modulate basal hematopoiesis (20). T helper cells actively regulate hematopoietic progenitor cell homeostasis (21). The interaction of HSPCs expressing immunogenic antigens with $CD4^+$ T cells results in stem cell differentiation and depletion of immunogenic HSPCs (22). | - |
| **$CD8^+$ T cells** | ~0.5-1% | Widely distributed throughout the BM | -. | $CD8^+$ CTLs are dysfunctional, fail to eliminate CML LSCs *in vivo* and rather promote their expansion (23, 24). |
| **Tregs** | ~0.5% | Widely distributed but closely associated to the endosteum | Protect HSCs from immune destruction (25). Promote HSC maintenance through adenosine generation (26). Modulate lymphopoiesis *via* IL-7 derived ICAM-$1^+$ stromal cells (27). Tregs regulate regulate myelopoiesis (28). Tregs regulate stromal cell function (29). | Protect LSCs from elimination by endogenous $CD8^+$ CTLs and adoptively transferred $CD8^+$ CTLs in CML (30) and AML (31), respectively. Treg depletion in a prophylactic setting (32), and in a minimal residual disease setting (33) promotes anti-leukemic immunity in a murine AML model. |
| **Neutrophils** | ~35% | Widely distributed throughout the BM | Indirect *via* macrophages. Clearance of aged BM neutrophils by macrophages by promotes HSPC mobilization through reduction of CXCL-12 and CAR cells levels (34). | – |
| **Monocytes/ macrophages** | ~0.4% | Widely distributed throughout the BM | Regulate retention of HSCs and HSPCs indirectly by modulating MSCs and CXCL-12 expression in the BM (16, 35, 36). Promote the expansion of myeloid progenitors in response to microbial products (37). | Myeloid cells derived IL-6 and IL-1b modulate the niche in leukemia (18, 38). IL-6 induces myeloid differentiation of MPPs in CML (38). IL-1b induces apoptosis in sympathetic nerve fibers resulting in a loss of MSCs and expansion of HSCs in MPD (18). |

decreased numbers of cycling progenitors (21) and 2) that adoptive transfer of total $CD4^+$ T cells into common gamma chain-deficient mice restored impaired myeloid differentiation indicated that $CD4^+$ T cells regulate HSPC activity and basal hematopoiesis (20). These findings have been recently extended by Hernández-Malmierca and co-workers who demonstrated that the presentation of immunogenic antigens on MHC class II by HSPCs triggers an interaction with $CD4^+$ T cells resulting in stem cell differentiation and depletion of immunogenic HSPCs (22).

Most of the effects observed upon transfer or depletion of total $CD4^+$ T cells may most likely be mediated directly or indirectly by immunomodulatory Tregs. Tregs regulate IL-3 mediated differentiation of myeloid progenitors under homeostatic conditions. Depletion of Tregs *in situ* and co-transplantation of $CD4^+$ $FOXP3^+$ Tregs demonstrated that BM Tregs promote myeloid colony formation *in vitro* and myeloid differentiation of HSCs *in vivo* (28). Importantly, the cognate interaction between Tregs and HSPCs was dependent on MHC class II expression suggesting a role for antigen-specific activation of Tregs in the regulation of HSCs in steady-state. In line with these initial findings, Kim et al. demonstrated that Foxp3 mutant scurfy mice have an enhanced granulopoiesis at the expense of B cell lymphopoiesis. However, this effect of myeloid differentiation was not mediated directly *via* Tregs but indirectly *via* the production of myeloid differentiation-related cytokines such as granulocyte-macrophage colony-stimulating factor (GM-CSF), TNF, and IL-6 by activated effector T cells (45). In addition, it was demonstrated that Tregs regulate the production of IL-7, a fundamental growth factor for lymphopoiesis, by intracellular adhesion molecule 1 (ICAM-1)-expressing perivascular stromal cells in the BM (27). In line with these findings, Camacho et al. recently demonstrated that BM Tregs regulate hematopoiesis indirectly through modulation of stromal cell function *via* secretion of IL-10 (29) (Figure 1 and Tables 1, 2). The role of Tregs in the regulation of stem cells, however, is not a unique feature for the BM and can be further extrapolated to multiple non-lymphoid tissues such as for example the skin, muscle, adipose tissue and brain (46–49). Consequently, accumulating scientific evidence supports the concept that Tregs control stem cells, their proliferation and self-renewal.

In murine BM transplantation models, experimental data demonstrated that Tregs of the host not only suppresses graft-versus host disease but also favors hematopoietic reconstitution and HSC engraftment (50, 51). Similarly, co-transplantation of recipients alloantigen-specific Tregs together with HSC facilitated long-term hematopoietic reconstitution (52). In addition, Tregs activated *ex vivo* with allogeneic APCs also induced long-term tolerance and reconstitution of BM grafts in an antigen-specific manner *in vivo* (53). A potential role for

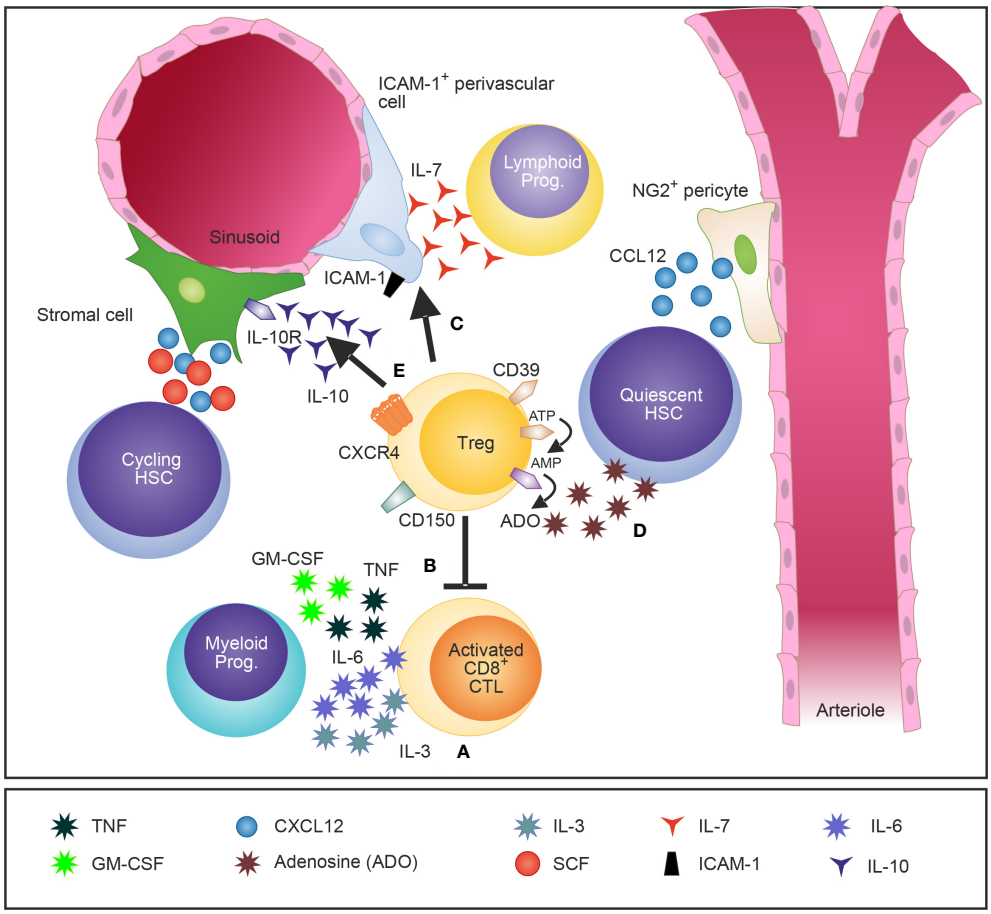


FIGURE 1
A schematic illustration of Tregs in the BM and their attributed effects on the HSCs niche and HSPCs. Tregs in the BM are widely distributed and localize close to the endosteum adjacent to HSCs. Tregs regulate IL-3 mediated differentiation of myeloid progenitors **(A)** (28) and modulate basal hematopoietic output by restricting production of myelopoiesis-promoting cytokine production by activated CD8 T cells in the BM **(B)** (45). Furthermore, Tregs control indirectly lymphopoiesis by mediating the release of the lymphoid cell growth and survival factor IL-7 by ICAM-1$^+$ stromal cells of the HSC niche **(C)** (27). CD150$^+$ Tregs were recently identified as crucial regulators of HSC quiescence and engraftment of HSCs into the BM after allogeneic BM transplantation **(D)** (26). In addition, IL-10 secreting Tregs have been shown to modulate the function of IL-10R-expressing BM stromal cells **(E)** (29).

Tregs in hematopoiesis was further demonstrated in murine allogeneic BM transplantation experiments where depletion of host Tregs resulted in loss of engraftment of stem and progenitor cells to the BM suggesting that Tregs promote hematopoiesis and protect HSCs from elimination (25). In addition, a specific BM Treg subset characterized by the expression the surface markers CD150 and CD39 was recently identified as regulator of HSC quiescence and engraftment of HSCs into the BM after allogeneic BM transplantation. These BM Tregs reside near HSCs in the BM niche and protect HSCs from oxidative stress by secretion of adenosine. In addition, co-transfer of BM Tregs but not splenic Tregs together with allogeneic HSCs prevented the rejection of the graft (26). Mechanistically, long-term hematopoietic reconstitution has been shown to crucially depend on MHC-II signaling in a canine BM transplantation model as delivery of an anti-MHC-II mAb directly after BM transplantation prevented engraftment and hematopoietic reconstitution (54). In contrast, Huss and co-worker demonstrated in various murine allogeneic BM transplantation models that immunological but not hematopoietic recovery is impaired in recipient mice lacking MHC class II expression or treated with an anti-MHC II mAb (55) (Figure 1 and Table 1).

In humans, the role of Tregs in HSC engraftment and long-term reconstitution after BM transplantation is still unclear. While depletion of total T cells from allogeneic BM resulted in rejection of grafts in a majority of the patients, the clinical benefit of Tregs in the graft still has to be demonstrated [reviewed in (50)]. Several clinical studies correlating the number of Tregs in the graft retrospectively with transplantation outcome delivered varying results and could not attribute a fundamental role of

TABLE 2 Treg-mediated immunomodulatory mechanisms in the BM niche at steady state.

| Reference | Target cell | Impact |
|---|---|---|
| Fujisaki (25) | Hematopoietic stem and progenitor cell | Tregs co-localize with HSPCs, generate an immune-privileged niche and support persistence of allogeneic HSCs. |
| Urbieta (28) | Myeloid progenitor cells | Tregs inhibit IL-3/SCF-mediated differentiation of myeloid progenitor through MHC-class II and TGF-β dependent mechanisms. |
| Kim (45) | T cell | Tregs indirectly regulate B cell lymphopoiesis by reducing the production the hematopoietic cytokines GM-CSF, TNF, and IL-6 by effector T cells. |
| Pierini (27) | Perivascular stromal cell | Tregs control normal B-cell lymphopoiesis by regulating the production of IL-7 by ICAM1$^+$ perivascular stromal cells. |
| Camacho (29) | Mesenchymal stromal cell | BM Tregs regulate hematopoiesis indirectly through modulation of MSCs *via* secretion of IL-10. |
| Hirata (26) | Hematopoietic stem cell | Treg-derived adenosine protects HSCs from oxidative stress and maintains their quiescence. In addition, CD150$^+$ Tregs, crucially contribute to the engraftment of HSCs into the BM after allogeneic BM transplantation. |

Tregs to long-term hematopoietic reconstitution. Similarly, conflicting data have been generated on the number of Tregs detected *in vivo* post-transplantation and transplantation outcome. Overall, these data imply a role for Tregs in the regulation of HSC function in mice while the role of Tregs on human hematopoiesis must still be validated.

## The adaptive immune system in leukemia

Experimental and clinical evidence indicates that myeloid leukemias are controlled by cells of the adaptive immune system to a certain extent (56, 57). Leukemic cells in myeloid malignancies are immunogenic, express HLA class I restricted leukemia epitopes and may be recognized by activated cytotoxic CD8$^+$ T cells (CTLs) (7, 56, 57). LSCs and bulk leukemia cells express major histocompatibility and co-stimulatory molecules suggesting that LSCs can be recognized and interact directly with T cells (7, 56).

In addition, immune responses against myeloid leukemias as well as leukemia-antigen specific CD8$^+$ CTLs have been observed in clinical and experimental studies (7, 56). However, activated CD8$^+$ CTLs in myeloid leukemias are dysfunctional and fail to eliminate LSCs *in vivo* (23, 24, 58–60). In CML, T cell exhaustion at diagnosis has been associated with an increased expression of immune inhibitory receptors and a reduced capacity to produce Th1-cytokines compared to patients in remission (59–63). Similar to CML, gene expression profiling of CD8$^+$ CTLs from AML patients at diagnosis indicate that CTLs in intermediate and high risk AML are less functional than in favorable risk AML and exhibit an exhaustion immune signature (24). CD8$^+$ CTL dysfunction was attributed to epigenetic silencing of activating immune checkpoint receptors rather than due to signaling by immune inhibitory immune checkpoint receptors (64). The phenomenon could in part explain the limited efficacy of antibodies that block inhibitory immune check-point inhibitors in AML. Furthermore, instead of promoting elimination, CD8$^+$ CTL-related mechanism may also contribute to the expansion of LSCs and leukemia (23, 24). For example, secretion of the hematopoietic cytokine IL-3 has been shown to expand and maintain leukemia stem and progenitor cells in favorable risk AML patients, while AML cells in more aggressive forms of AML seem to develop largely independent of CD8$^+$ T cell help (24). A systemic impairment/exhaustion of T cells and especially programmed cell death protein 1 (PD-1) and Eomes-expressing memory stem T cells has also been associated with relapse after allogeneic HSCT (65). Furthermore, response to chemotherapy correlated with the immune signatures indicative for the restoration of T cell function (58).

In contrast to CD8$^+$ T cells, the role of CD4$^+$ T cells in the control of leukemia has been studied less intensively (7). Nevertheless, even though less studied, several independent reports demonstrated that myeloid leukemia cells are competent to process and present endogenous immunogenic leukemia peptides in the context of HLA class II resulting in leukemia antigen-specific CD4$^+$ T cell response [reviewed in (7)]. Recently, the HLA class I and class II ligandome was characterized using immunoprecipitation and mass spectrometry in CD34$^+$ stem/progenitor cells from AML and CML patients and CD34$^+$CD38$^-$ healthy controls (66, 67). For AML, the analysis revealed 36 AML-specific leukemia antigens. Importantly, the top-ranked HLA class II leukemia antigens were successfully validated in T cell activation assays *in vitro* (67). A similar analysis for CML identified 44 CML-associated HLA class II antigens (66). A clinical vaccination study which assessed the immunogenicity and anti-tumor activity of a vaccine cocktail comprising 4 b3a2-petides restricted to HLA I and one b3a2-petide restricted to HLA II in b3a2-espressing CML patients with stable measurable residual disease, demonstrated immunological activity of the vaccine as illustrated by CML-peptide specific CD4$^+$ T cells *in vitro* in 13 of 14 evaluable patients (68). Furthermore, vaccination of a 63-year old woman which displayed residual CML cells after

cessation of IFN-α therapy with a immunogenic b2a2 breakpoint derived peptide able to bind several HLA-DR molecules induced a complete molecular response in blood and BM (69). Overall, these data suggest that leukemia-antigen specific $CD4^+$ T cells may potentially also contribute to anti-tumoral immunity in leukemia.

## Immune escape of leukemia and LSCs

In AML, T cells appear to infiltrate the BM microenvironment, but their efficacy to control leukemia and eliminate LSCs is limited. In general, the BM microenvironment in AML may be considered as immune cold (70, 71). Analysis of an 18-gene tumor inflammation signature in solid tumor and AML samples using data from the Cancer Genome Atlas revealed that AML patients have a low expression of this signature which is associated with an immune cold microenvironment (70). Similarly, transcriptomic, and proteomic analysis of AML BM cells demonstrated that 70% of AML patients display an immune-depleted signature (71). Because LSCs reside primarily in the BM, the generation of an immunosuppressive/immune cold environment may be considered as a central mechanism how LSCs escape immune control. However, several different mechanisms may contribute to generation of an immune cold environment and the subsequent immune escape in myeloid leukemia.

### Immune checkpoint ligands/receptors

One mechanism how LSCs can escape immunosurveillance is through the activation of immune checkpoint pathways. Immune checkpoint pathways play a fundamental role in the regulation of immune homeostasis (72). The balance between stimulatory and inhibitory signals determines the amplitude and quality of the antigen-specific T cell responses (72). Immune checkpoint inhibitors targeting the co-inhibitory molecules cytotoxic T-lymphocyte-associated protein 4 (CTLA-4) and PD-1 have been approved for the treatment of various solid tumors and lymphoma (72). Increased expression of the inhibitory ligands for T-cell–regulating checkpoints such as CTLA-4, PD-1, B7-H3 and T cell immunoglobulin and mucin-domain containing-3 (TIM-3) was reported in AML and was associated with T cell exhaustion and poor prognosis (62, 63, 73). This $CD8^+$ T cell exhaustion was in part reversible by blocking the immune checkpoint molecules PD-1, CTLA-4, and TIM-3 (63) or by OX-40 co-stimulation (62). However, in patients, immune checkpoint inhibitors against CTLA-4 and PD-1 seem to be less effective in AML compared to solid tumors (74). One possible explanation for this lack of potency in AML is that BM-infiltrating T cells in AML expressing various inhibitory receptors, such as TIM-3 and lymphocyte-activation gene 3 (LAG-3). Another explanation could be the limited or restricted surface expression of PD-L1 in *de novo* AML (73, 75) and variable kinetic of PD-L1 expression during the progression of the disease. For example, PD-L1 expression increases on AML cells during relapse and could represent an adaptive immune escape mechanism (74). However, it also unclear whether the increased expression of immune inhibitory receptors reflects T cell exhaustion or whether it is indicative for differentiated effector T population. Currently several clinical trials with different antibodies targeting the PD-1/PD-L1 interaction are ongoing in combination with CTLA-4 inhibition, in combination with chemotherapy, or in combination with hypomethylating agents that upregulate the expression of PD-L1 on leukemia cells (76).

### Tregs in myeloid leukemia

Because the efficacy of immune checkpoint inhibitor treatments in myeloid malignancies is limited, other immune-regulatory mechanisms in the BM may be in place. Studies in mice and humans identified the accumulation of Tregs as a potential major immune-regulatory mechanism in myeloid leukemia. Several clinical studies reported increased frequencies of Tregs in blood and/or BM at diagnosis, after allogeneic hematopoietic stem cell transplantation (HSCT) or during induction chemotherapy in myeloid leukemias (77, 78).

#### Tregs in CML

In CML, numbers and frequencies of effector Tregs in peripheral blood and BM are also increased in CML patients at diagnosis and in patients refractory to tyrosine kinase inhibitor (TKI) treatment (59–61). These effector Tregs are characterized by the expression of the immune checkpoints PD-1, TIM-3 and CTLA-4, all markers for an increased suppressive activity (61). Anatomically, Tregs in CML are widely distributed throughout the BM parenchyma in mice and humans. In human CML, the majority of Tregs were localized close to $CD8^+$ CTLs and not close to $CD34^+$ CML stem/progenitor cells (30). Treatment with the TKIs Imatinib, Dasatinib and Nilotinib demonstrated an inhibitory effect of these TKIs on the quantity of Tregs in CML patients. Tregs were especially reduced in patients who achieved a complete cytogenetic response (59, 79). Similarly, Imatinib-treated CML patients in complete molecular remission (CMR) displayed a selective depletion of effector Tregs which was accompanied by an increase in effector/memory $CD8^+$ CTLs in contrast to CMR patients who did not reach a complete molecular remission (80). Furthermore, a successful maintenance of treatment-free-remission (TFR) is associated with reduced numbers of Tregs (81–83). In the frame of the JALSG-STIM213 trial, the frequency

of effector Tregs in the peripheral blood has been identified as potential biomarker for TFR after Imatinib stop (84). Importantly, tyrosine kinase inhibitor (TKI) treatment responses were more potent in patients with less exhausted T cells (60). Because the state of T cell dysfunction at diagnosis is reverted in patients that reach a deep molecular response (60), one may hypothesize that off-target immune-modulatory effects of TKIs trigger already pre-existing anti-tumoral immune responses or interfere with immunosuppressive cells as Tregs. In solid tumors, tyrosine kinase inhibitor (TKI) treatment with Imatinib and Dasatinib has been shown to reduce immunosuppressive immunoindolamine-2, 3-dioxygenase (IDO) expression, a key factor in the generation of Tregs, and to increase the numbers of intratumoral $CD8^+$ CTLs (85, 86). Future therapeutic approaches may therefore aim at an expansion and effector function of CTLs through targeting of Tregs. For example, Tregs expressing the tumor necrosis factor 4 (TNFRSF4, alias OX-40) have recently been identified as the key regulator of immune escape of CML LSCs in mice (30). Stimulation of Tnfrsf4-signaling did not deplete Tregs but reduced the capacity of Tregs to protect LSCs from granzyme-mediated $CD8^+$ CTL- killing in a murine CML model.

## Tregs in AML

Like in CML (30), Tregs in the BM of AML patients are widely distributed throughout the BM parenchyma and are occasionally located close to clusters of $CD8^+$ T cells (Figure 2). Tregs frequencies in blood and BM are significantly elevated in adult and pediatric AML patients compared to Tregs from healthy donors and further increase at relapse (87–89). In general, increased levels of Tregs at diagnosis correlate with poor response to induction chemotherapy and relapse after allogeneic HSCT (78, 90). In contrast to baseline AML biopsies, higher numbers of Tregs early after induction therapy are associated with higher complete remission rates and better overall survival. This discrepancy may be attributed to the different cellular composition of the BM microenvironment early after chemotherapy and at an advanced stage of the disease. Furthermore, a phase IV clinical trial (NCT01347996) which assessed the efficacy of immunotherapy with histamine dihydrochloride (HDC) and low-dose IL-2 in the post-consolidation phase in AML 84 patients in first complete remission demonstrated an association of AML relapse with HDC/IL-2 treatment-induced accumulation of natural Tregs in the blood (91). Therefore, Tregs could either serve as immune-modulators and support hematopoietic recovery or induce immune escape of leukemia by limiting CTL activity. On the other hand, Tregs seem to localize close to HSCs in the niche during homeostasis and may therefore directly facilitate their homing in the BM and emergency hematopoiesis.

In contrast to $CD8^+$ T cells, Tregs from AML patients are not exhausted but rather hyper-functional as illustrated by a higher migratory and immunosuppressive potential than Tregs from blood and BM of healthy volunteers (37). However, even though, the prevalence of Tregs in the BM and blood in AML is identical (92), BM Tregs are more suppressive than Tregs derived from blood of AML patients (77). Phenotypically, BM Tregs of AML patients express the memory marker CD45RO along with CTLA-4 and CD95 and secret low levels of the immunosuppressive cytokines IL-10 and TNF. Furthermore, BM Tregs in AML have

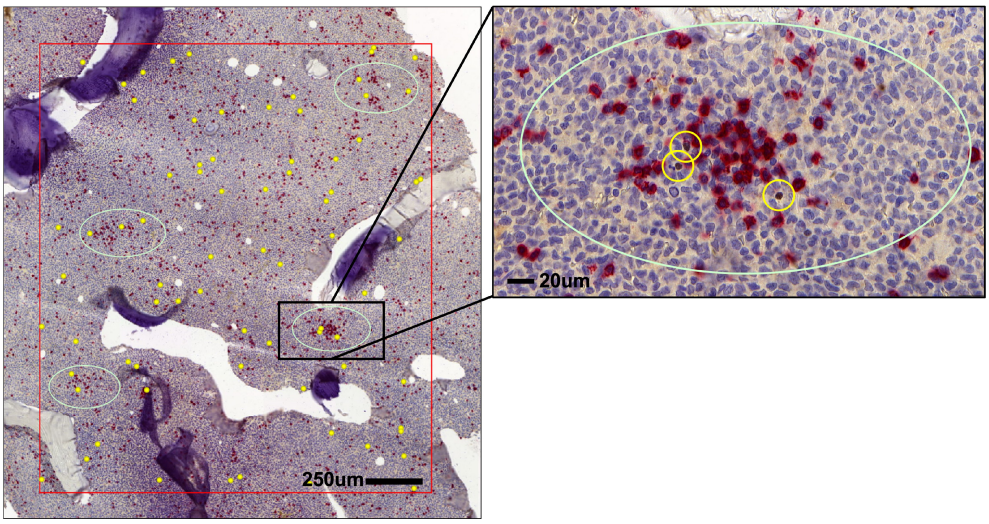


FIGURE 2
Distribution of Tregs and $CD8^+$ T cells in AML bone marrow (BM). Spatial localization of $FOXP3^+$ Tregs (brown, yellow circles) in respect to $CD8^+$ T cells (red) in the BM of AML patients.

a high turnover compared to BM Tregs from healthy donors as indicated by 8-fold higher proliferation and 4-fold higher apoptosis rate (93).

Recently, several mechanisms have been identified that promote the expansion and BM retention of Tregs in AML (37, 94–96). For example, Tregs in blood and BM of patients have been shown to express elevated levels of CXCR4 on the cell surface compared to Tregs derived from healthy donors suggesting that, like in homeostasis, the BM retains CXCR4-expressing Tregs through CXCL-12 in AML (37). Similarly, the frequency of Tregs expressing inducible T-cell co-stimulator (ICOS) has been negatively associated with outcome in AML patients (97). Co-simulation of ICOS signaling through the provision of ICOS-ligand by AML cells expanded Tregs and maintained their suppressive function in a murine C1498 AML model (97) (Figure 3). Another mechanism how Tregs may be expanded and sustained in AML is through IFN-y induced secretion of IDO by mesenchymal stromal cells (94) (MSCs, Figure 3). Blockade of IFN-y production by AML cells lowered IDO1 expression resulting in reduced Treg infiltration and leukemia engraftment. Furthermore, daunorubicin-treated AML cells induce IDO1 secretion in dendritic cells (DCs) resulting in the accumulation of PD-1-expressing Tregs (98). In the BM of newly diagnosed AML patients, high IDO expression in MSCs was associated with elevated levels of Tregs. Furthermore, an IDO1-related immune gene signature has been identified as a negative predictor for overall survival in AML (99). Similarly, MSCs derived from Fanconi anaemia patients with AML secrete high levels of prostaglandins which resulted in Treg induction and subsequent inhibition of $CD8^+$ CTLs (100). Lastly, PD-L1 expression on AML cells have been recently demonstrated to promote the conversion and expansion of PD-$1^+$ Tregs from conventional $CD4^+$ T cells (95).

However, the experimental and clinical evidence that directly links Tregs with T-cell anergy/exhaustion in AML is still limited and mostly restricted to pre-clinical mouse models.

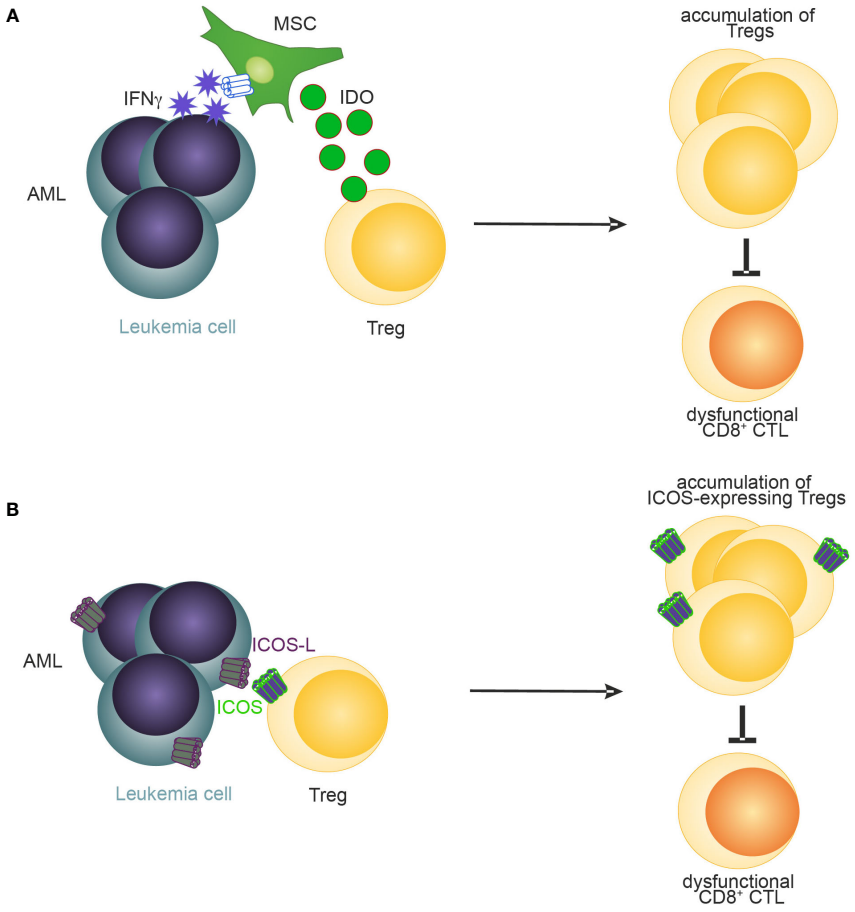


FIGURE 3
A schematic illustration of reported mechanisms leading to accumulation of Tregs in AML. **(A)** MSC-derived IDO (94) and **(B)** ICOS-ICOSL signaling (97) promotes the accumulation of Tregs in AML.

For example, Tregs have been shown to inhibit the function of adoptively transferred AML-specific CTLs. Depletion of Tregs during adoptive transfer of CTLs improved survival of AML mice (31). Similarly, Treg depletion prior to leukemia induction has been shown to trigger an endogenous anti-leukemic CTL response resulting in prolonged survival of MLL-AF9 AML mice (32). Unpublished data from our group and a recent publication by Hasegewa and co-workers support the notion that Tregs in MLL-AF9 mice limit anti-leukemic immunity only in a situation with minimal leukemia load but not in an advanced stage of the disease (33). Similar to human AML (37), BM Tregs in MLL-AF9 mice have shown to express elevated levels of CXCR4 on the cell surface. Blockade of the CCL3/CCR1-CCR5 and CXCL-12/CXCR4 axis prevented the accumulation of Tregs in BM of MLL-AF9 AML mice (32). These data indicate that Tregs create an immunosuppressive microenvironment in the BM thereby reducing CTL function and immunosurveillance of AML cells. In addition, *in vitro* experiments revealed that AML cells themselves secret soluble factors that restrain T cell and NK cell function (101). Of note, Hasegawa et al. using the same AML model and RAG-knockout mice demonstrated that CTLs indeed have the capacity to eradicate leukemia at an early stage of the disease (low leukemia load), whereas antigen-specific CTLs are exhausted in animals with advanced leukemia (33).

However, Tregs in AML may not only hamper anti-leukemic T cell immunity but may also directly affect the survival and function of AML blasts LSCs. It was recently demonstrated that Treg-derived IL-10 promotes stemness of murine and human AML LSCs through activation of PI3K/AKT signaling pathway (96). Similarly, the cytokine IL-35 produced by Tregs promotes the proliferation of AML blasts (102).

Even though leukemia-antigen specificity of $CD4^+$ T cells have been documented in several independent studies (7, 56), whether AML antigen–specific Tregs are part of this $CD4^+$ T cell population is still unclear. In general, the evidence for functional tumor antigen–specific Tregs in cancer is very weak due to the lack of adequate MHC class II tetramers, and antigen-specific Tregs have only been documented in a few solid tumors and in B acute lymphoblastic leukemia (51, 103). Nevertheless, recent findings of a pre-clinical study suggests that antigen stimulation may play an important role in the activation and accumulation of Tregs in CML BM (30).

Overall, these studies imply that LSCs reside in an immune-privileged niche in the BM which harbors multiple immune-regulatory mechanisms. It may be assumed that the accumulation of Tregs in the BM represents one immune-regulatory mechanism in leukemia which limits immunosurveillance of LSCs and thereby contributes to disease progression and LSC maintenance. However, why Tregs accumulate in the BM, how this can be controlled, whether they are leukemia antigen-specific and whether selective targeting of Tregs in myeloid neoplasm (e.g. *via* an agonistic TNFRSF4 antibody) can induce immune control in humans is still unclear.

### Altering the expression of major histocompatibility complex (MHC) molecules

The elimination of cancer/leukemia cells depends on tumor antigen expression on MHC class I and II. In AML, mutations and immune escape mechanisms may result in the downregulation of MHC expression on leukemia cells. However, reduced, or lost MHC expression has been primarily observed on AML cells after allogeneic HSCT. For example, in 17 out of 34 patients, AML cells displayed a reduced expression of MHC class II at relapse after allogeneic HSCT compared to diagnosis. The downregulation of MHC was triggered by epigenetic mechanisms and could be restored by administration of IFN-y (104). Similarly, another study profiling immune signatures in AML cells after allogeneic HSCT identified the downregulation of MHC class II on a transcriptional level as a major immune escape mechanism (105). Furthermore, impaired processing and loading of leukemia-associated antigen on MHC class II has been described as potential immuno-editing process in AML.

## Therapeutic strategies targeting Tregs

Targeting signaling cascades that promote Treg-mediated immunosuppression in myeloid leukemia or Treg-specific surface antigens may be a viable approach to block Treg function or deplete Tregs and induce anti-leukemic immunity.

### CTLA-4

The anti-CTLA-4 mAb ipilimumab has been approved for the treatment of metastatic melanoma. However, despite the increased expression of CTLA-4 on Tregs in the tumor microenvironment (TME) of cancer patients and pre-clinical evidence showing the capacity of ipilimumab to deplete Tregs *via* ADCC-dependent mechanisms, ipilimumab is thought to induce infiltration of intratumoral $CD4^+$ and $CD8^+$ effector T cells without depleting Tregs in the TME in humans (106). In addition, the specificity of CTLA-4 as a Treg restricted target is widely debated because CTLA-4 is widely expressed on activated $CD4^+$ T helper and $CD8^+$ effector T cells and monocyte-derived DCs (72). To ensure a controlled activity of the antibody in the TME and to decouple antitumor efficacy from immunotherapy-related toxicity, a CTLA-4 dual variable domain immunoglobulin (anti-CTLA-4 DVD) was developed where the inner anti-CTLA-4 binding domain is shielded by an outer tumor-targeting domain (106). In the TME, the presence of activated membrane type-serine protease 1 results in cleavage of the outer domain and the liberation of the CTLA-4 binding site. To enhance target specificity, currently bi-specific antibodies targeting CTLA-4

together with other surface receptors with increased expression on Tregs are designed and evaluated. OX-40 is highly expressed on Tregs in AML (60) and CML (30) and is currently studied as a treatment for patients with refractory/relapsed AML as monotherapy or in combination with azacitidine and avelumab (NCT03390296). A human CTLA-4 x OX-40 bispecific antibody (ATOR-1015) which demonstrated efficacy in Treg depletion assays *in vitro* and syngeneic mouse models *in vivo* (106) is currently under evaluation in a first-in-human phase I clinical trial (NCT03782467). Similarly, a humanized CTLA-4 x GITR bispecific antibody (ATOR-1144) was shown to deplete Tregs *in vitro* through ADCC-dependent mechanisms (107).

Clinical trials assessing the potential of targeting CTLA-4 in AML are limited. In a phase 1b study, ipilimumab was tested in 522 patients with hematologic malignancies relapsing after allogeneic HSCT. The complete response rate was 23%. In addition, immune-related adverse events and graft-versus-host disease were reported (108). Ipilimumab is currently evaluated in several clinical phase I trials as a treatment for relapsed/refractory AML patients (NCT03912064, NCT03600155, NCT01822509) and as maintenance therapy for AML and MDS patients alone or in combination the anti-PD-1 antibody Nivolumab and/or azacitidine after allogeneic HSCT (NCT02846376) and for its potential to induce graft-versus-malignancy effects after allogeneic HSCT (NCT00060372).

## CD25

CD25 is highly expressed on activated Tregs in the TME and only marginally on effector T cells (109). Therefore, several therapeutics targeting CD25 have been recently developed and were approved for the prevention of organ transplantation rejection (anti-CD25 mAb Basiliximab) and the treatment of cutaneous T-cell lymphoma (IL-2-diphtheria toxin fusion protein denileukin diftitox). However, clinical studies have demonstrated that denileukin diftitox is ineffective in eliminating Tregs in patients (107). An open-label, multicenter Phase I clinical trial is underway investigating the safety and tolerability of the anti-CD25 depleting antibody RO7296682 in patients with advanced solid tumors (NCT04158583). In addition, the potential of basiliximab conjugated with 1,4,7,10-tetraazacyclododecane tetraacetic acid (DOTA) and radiolabeled with Yttrium-90 given together with fludarabine, melphalan, and total marrow and lymphoid irradiation (TMLI) is evaluated for the treatment of patients with high-risk acute leukemia or myelodysplastic syndrome (NCT05139004). A phase I dose-escalation clinical trial assessed safety and efficacy of Camidanlumab tesirine, an antibody-drug conjugate targeting CD25 in 34 relapsed/refractory AML patients (110). Two patients achieved complete responses with incomplete hematologic recovery. However, the trial was terminated early for reasons other than safety and efficacy.

## FOXP3

FOXP3 serves as a lineage-specific transcription factor of Tregs. As FOXP3 is primarily expressed in the nucleus, FOXP3 has never been considered as a viable target to deplete Tregs in cancer. However, the potential of targeting FOXP3 directly has recently gained considerable interest. A T cell receptor mimic antibody recognizing a FOXP3-derived epitope in the context of HLA-A*02:01 was shown to selectively recognize and eliminate FOXP3-expressing Tregs in a PBMC xenograft model (111). Similar results were obtained when the TCR mimic antibody was engineered in a bispecific T-cell engager. Another strategy currently followed to selectively deplete Tregs in cancer are antisense oligonucleotide against FOXP3. The clinical candidate antisense oligonucleotide AZD8701 demonstrated encouraging efficacy in reducing FOXP3 and Treg immunosuppressive function in primary human Tregs *in vitro* as well as in humanized mouse models *in vivo* (112). The safety and tolerability of AZD8701 is currently evaluated in a phase 1a/b clinical trial with or without Durvalumab in patients with advanced solid tumors (NCT04504669). However, strategies targeting FOXP3 bear the risk for the development of autoimmune disease as FOXP3 expression is most likely not limited to tumor tissues. Clinical trials targeting FOXP3 in myeloid malignancies are pending.

# Concluding remarks

The BM is a hematopoietic organ that harbors in addition to classical niche cells also a variety of different immune cells such as B and T cells. $CD4^+$ T cells including Tregs significantly shape the cytokine milieu in the BM microenvironment and thereby promote key functions of HSC such as quiescence, self-renewal proliferation and differentiation. These mechanisms evolved to guarantee a constant generation of blood cells from all lineages and to prevent damage and exhaustion of the stem cell pool. LSCs co-opt these evolutionary conserved mechanisms of the HSC niche and at the same time re-model the HSC niche to promote leukemogenesis and LSC function and to reduce the HSC reservoir in the BM. In leukemia, Tregs regulate the expansion of LSCs and leukemia progenitors and contribute to immune evasion of leukemia cells by cell-interactions or through secretion of cytokines. Therefore, targeting Tregs seems to be an attractive therapeutic option and warrants further investigation in humans. So far, however, hardly any clinical information on the potential of targeting Tregs in myeloid leukemia is available. Only a limited number of clinical trials currently addresses this possibility mainly by targeting immune-related surface receptors such as CD25, CTLA-4 and TNFRSF4 which are expressed on Tregs. However, whether these approaches will lead to the elimination of LSCs and thereby cure of leukemia is still unknown. Similarly, our knowledge on the emergence of

severe adverse events such as the induction of inflammation or auto-immune disease upon Treg manipulation and their effect on the disease is limited and must be crucially considered prior to initiating and planning clinical trials. Consequently, a better understanding of immune cells including Tregs and their function in the BM microenvironment during disease and homeostasis may contribute to the generation of novel and safe immunotherapeutic strategies aiming at elimination of leukemia at the level of the LSC and the identification of factors and interactions which may translate into the possibility to generate cells of different hematopoietic lineages ex vivo for specific applications, respectively.

## Author contributions

CR conceptualized and wrote the review article.

## Acknowledgments

This work was supported by grants from the Swiss National Science Foundation (310030_179394) and the Stiftung für klinisch-experimentelle Tumorforschung. I thank Adrian F. Ochsenbein for helpful discussions and input during the preparation of the manuscript and Stefan Forster for generating the IHC images. I apologize to the authors whose work was not mentioned due to space limitations.

## Conflict of interest

The author declares that the research was conducted in the absence of any commercial or financial relationships that could be construed as a potential conflict of interest.

## Publisher's note



## References

1. Pinho S, Frenette PS. Haematopoietic stem cell activity and interactions with the niche. *Nat Rev Mol Cell Biol* (2019) 20(5):303–20. doi: 10.1038/s41580-019-0103-9

2. Campbell C, Rudensky A. Roles of regulatory T cells in tissue pathophysiology and metabolism. *Cell Metab* (2020) 31(1):18–25. doi: 10.1016/j.cmet.2019.09.010

3. Asada N, Kunisaki Y, Pierce H, Wang Z, Fernandez NF, Birbrair A, et al. Differential cytokine contributions of perivascular haematopoietic stem cell niches. *Nat Cell Biol* (2017) 19(3):214–23. doi: 10.1038/ncb3475

4. Spencer JA, Ferraro F, Roussakis E, Klein A, Wu J, Runnels JM, et al. Direct measurement of local oxygen concentration in the bone marrow of live animals. *Nature* (2014) 508(7495):269–73. doi: 10.1038/nature13034

5. Simsek T, Kocabas F, Zheng J, Deberardinis RJ, Mahmoud AI, Olson EN, et al. The distinct metabolic profile of hematopoietic stem cells reflects their location in a hypoxic niche. *Cell Stem Cell* (2010) 7(3):380–90. doi: 10.1016/j.stem.2010.07.011

6. Suda T, Takubo K, Semenza GL. Metabolic regulation of hematopoietic stem cells in the hypoxic niche. *Cell Stem Cell* (2011) 9:298–310. doi: 10.1016/j.stem.2011.09.010

7. Riether C, Schurch CM, Ochsenbein AF. Regulation of hematopoietic and leukemic stem cells by the immune system. *Cell Death Differ* (2015) 22(2):187–98. doi: 10.1038/cdd.2014.89

8. Man Y, Yao X, Yang T, Wang Y. Hematopoietic stem cell niche during homeostasis, malignancy, and bone marrow transplantation. *Front Cell Dev Biol* (2021) 9:621214. doi: 10.3389/fcell.2021.621214

9. Baryawno N, Przybylski D, Kowalczyk MS, Kfoury Y, Severe N, Gustafsson K, et al. A cellular taxonomy of the bone marrow stroma in homeostasis and leukemia. *Cell* (2019) 177(7):1915–1932.e16. doi: 10.1016/j.cell.2019.04.040

10. Guarnerio J, Mendez LM, Asada N, Menon AV, Fung J, Berry K, et al. A non-cell-autonomous role for pml in the maintenance of leukemia from the niche. *Nat Commun* (2018) 9(1):66. doi: 10.1038/s41467-017-02427-x

11. Schepers K, Pietras EM, Reynaud D, Flach J, Binnewies M, Garg T, et al. Myeloproliferative neoplasia remodels the endosteal bone marrow niche into a self-reinforcing leukemic niche. *Cell Stem Cell* (2013) 13(3):285–99. doi: 10.1016/j.stem.2013.06.009

12. Frisch BJ, Ashton JM, Xing L, Becker MW, Jordan CT, Calvi LM. Functional inhibition of osteoblastic cells in an *in vivo* mouse model of myeloid leukemia. *Blood* (2012) 119(2):540–50. doi: 10.1182/blood-2011-04-348151

13. Duarte D, Hawkins ED, Akinduro O, Ang H, De Filippo K, Kong IY, et al. Inhibition of endosteal vascular niche remodeling rescues hematopoietic stem cell loss in AML. *Cell Stem Cell* (2018) 22(1):64–77.e6. doi: 10.1016/j.stem.2017.11.006

14. Mead AJ, Neo WH, Barkas N, Matsuoka S, Giustacchini A, Facchini R, et al. Niche-mediated depletion of the normal hematopoietic stem cell reservoir by Flt3-ITD–induced myeloproliferation. *J Exp Med* (2017) 214(7):2005–21. doi: 10.1084/jem.20161418

15. Passaro D, Garcia-Albornoz M, Diana G, Chakravarty P, Ariza-McNaughton L, Batsivari A, et al. Integrated OMICs unveil the bone-marrow microenvironment in human leukemia. *Cell Rep* (2021) 35(6):109119. doi: 10.1016/j.celrep.2021.109119

16. Katayama Y, Battista M, Kao WM, Hidalgo A, Peired AJ, Thomas SA, et al. Signals from the sympathetic nervous system regulate hematopoietic stem cell egress from bone marrow. *Cell* (2006) 124(2):407–21. doi: 10.1016/j.cell.2005.10.041

17. Hanoun M, Zhang D, Mizoguchi T, Pinho S, Pierce H, Kunisaki Y, et al. Acute myelogenous leukemia-induced sympathetic neuropathy promotes malignancy in an altered hematopoietic stem cell niche. *Cell Stem Cell* (2014) 15(3):365–75. doi: 10.1016/j.stem.2014.06.020

18. Arranz L, Sánchez-Aguilera A, Martín-Pérez D, Isern J, Langa X, Tzankov A, et al. Neuropathy of haematopoietic stem cell niche is essential for myeloproliferative neoplasms. *Nature* (2014) 512(1):78–81. doi: 10.1038/nature13383

19. Zehentmeier S, Pereira JP. Cell circuits and niches controlling b cell development. *Immunol Rev* (2019) 289(1):142–57. doi: 10.1111/imr.12749

20. Sharara LI, Andersson A, Guy-Grand D, Fischer A, DiSanto JP. Deregulated TCR alpha beta T cell population provokes extramedullary hematopoiesis in mice deficient in the common gamma chain. *Eur J Immunol* (1997) 27(4):990–8. doi: 10.1002/eji.1830270428/asset/1830270428_ftp.pdf?v=1&t=hygdrznc&s=ba10ebe9016e181ebec8afa71273e494b1105362

21. Broxmeyer HE, Bruns HA, Zhang S, Cooper S, Hangoc G, McKenzie ANJ, et al. Th1 cells regulate hematopoietic progenitor cell homeostasis by production of oncostatin m. *Immunity* (2002) 16(6):815–25. doi: 10.1016/S1074-7613(02)00319-9

22. Hernández-Malmierca P, Vonficht D, Schnell A, Uckelmann HJ, Bollhagen A, Mahmoud MAA, et al. Antigen presentation safeguards the integrity of the hematopoietic stem cell pool. *Cell Stem Cell* (2022) 29(5):760–775.e10. doi: 10.1016/j.stem.2022.04.007

23. Riether C, Gschwend T, Huguenin AL, Schürch CM, Ochsenbein AF. Blocking programmed cell death 1 in combination with adoptive cytotoxic T-cell transfer eradicates chronic myelogenous leukemia stem cells. *Leukemia* (2015) 29:1781–5. doi: 10.1038/leu.2015.26

24. Radpour R, Riether C, Simillion C, Höpner S, Bruggmann R, Ochsenbein AF. CD8 + T cells expand stem and progenitor cells in favorable but not adverse risk acute myeloid leukemia. *Leukemia* (2019) 33:2379–92. doi: 10.1038/s41375-019-0441-9

25. Fujisaki J, Wu J, Carlson AL, Silberstein L, Putheti P, Larocca R, et al. *In vivo* imaging of treg cells providing immune privilege to the haematopoietic stem-cell niche. *Nature* (2011) 474(7350):216–9. doi: 10.1038/nature10160

26. Hirata Y, Furuhashi K, Ishii H, Li HW, Pinho S, Ding L, et al. CD150highBone marrow tregs maintain hematopoietic stem cell quiescence and immune privilege *via* adenosine. *Cell Stem Cell* (2018) 22(3):445–453.e5. doi: 10.1016/j.stem.2018.01.017

27. Pierini A, Nishikii H, Baker J, Kimura T, Kwon H-S, Pan Y, et al. Foxp3+ regulatory T cells maintain the bone marrow microenvironment for b cell lymphopoiesis. *Nat Commun* (2017) 8:15068. doi: 10.1038/ncomms15068

28. Urbieta M, Barao I, Jones M, Jurecic R, Panoskaltsis-Mortari A, Blazar BR, et al. Hematopoietic progenitor cell regulation by CD4+CD25+ T cells. *Blood* (2010) 115(23):4934–43. doi: 10.1182/blood-2009-04-218826

29. Camacho V, Matkins VR, Patel SB, Lever JM, Yang Z, Ying L, et al. Bone marrow tregs mediate stromal cell function and support hematopoiesis *via* IL-10. *JCI Insight* (2020) 5(22):e135681. doi: 10.1172/jci.insight.135681

30. Hinterbrandner M, Rubino V, Stoll C, Forster S, Schnüriger N, Radpour R, et al. Tnfrsf4-expressing regulatory T cells promote immune escape of chronic myeloid leukemia stem cells. *JCI Insight* (2021) 6(23):e151797. doi: 10.1172/jci.insight.151797

31. Zhou Q, Bucher C, Munger ME, Highfill SL, Tolar J, Munn DH, et al. Depletion of endogenous tumor-associated regulatory T cells improves the efficacy of adoptive cytotoxic T-cell immunotherapy in murine acute myeloid leukemia. *Blood* (2009) 114(18):3793–802. doi: 10.1182/blood-2009-03-208181

32. Wang R, Feng W, Wang H, Wang L, Yang X, Yang F, et al. Blocking migration of regulatory T cells to leukemic hematopoietic microenvironment delays disease progression in mouse leukemia model. *Cancer Lett* (2020) 469:151–61. doi: 10.1016/j.canlet.2019.10.032

33. Hasegawa K, Tanaka S, Fujiki F, Morimoto S, Nakajima H, Tatsumi N, et al. An immunocompetent mouse model for MLL/AF9 leukemia reveals the potential of spontaneous cytotoxic T-cell response to an antigen expressed in leukemia cells. *PloS One* (2015) 10(12):e0144594. doi: 10.1371/journal.pone.0144594

34. Casanova-Acebes M, Pitaval C, Weiss LA, Nombela-Arrieta C, Chèvre R, A-González N, et al. XRhythmic modulation of the hematopoietic niche through neutrophil clearance. *Cell* (2013) 153(5):1025–35. doi: 10.1016/j.cell.2013.04.040

35. Chow A, Lucas D, Hidalgo A, Méndez-Ferrer S, Hashimoto D, Scheiermann C, et al. Bone marrow CD169+ macrophages promote the retention of hematopoietic stem and progenitor cells in the mesenchymal stem cell niche. *J Exp Med* (2011) 208(2):261–71. doi: 10.1084/jem.20101688

36. Winkler IG, Sims NA, Pettit AR, Barbier V, Nowlan B, Helwani F, et al. Bone marrow macrophages maintain hematopoietic stem cell (HSC) niches and their depletion mobilizes HSCs. *Blood* (2010) 116(23):4815–28. doi: 10.1182/blood-2009-11-253534

37. Wan Y, Zhang C, Xu Y, Wang M, Rao Q, Xing H, et al. Hyperfunction of CD4 CD25 regulatory T cells in de novo acute myeloid leukemia. *BMC Cancer* (2020) 20(1):472. doi: 10.1186/s12885-020-06961-8

38. Reynaud D, Pietras E, Barry-Holson K, Mir A, Binnewies M, Jeanne M, et al. IL-6 controls leukemic multipotent progenitor cell fate and contributes to chronic myelogenous leukemia development. *Cancer Cell* (2011) 20(5):661–73. doi: 10.1016/j.ccr.2011.10.012

39. Ludin A, Itkin T, Gur-Cohen S, Mildner A, Shezen E, Golan K, et al. Monocytes-macrophages that express α-smooth muscle actin preserve primitive hematopoietic cells in the bone marrow. *Nat Immunol* (2012) 13(11):1072–82. doi: 10.1038/ni.2408

40. Zou L, Barnett B, Safah H, Larussa VF, Evdemon-Hogan M, Mottram P, et al. Bone marrow is a reservoir for CD4+CD25+ regulatory T cells that traffic through CXCL-12/CXCR4 signals. *Cancer Res* (2004) 64(22):8451–5. doi: 10.1158/0008-5472.CAN-04-1987

41. Zhao E, Xu H, Wang L, Kryczek I, Wu K, Hu Y, et al. Bone marrow and the control of immunity. *Cell Mol Immunol* (2012) 9:11–9. doi: 10.1038/cmi.2011.47

42. Price PW, Cerny J. Characterization of CD4+ T cells in mouse bone marrow. i. increased activated/memory phenotype and altered TCR vbeta repertoire. *Eur J Immunol* (1999) 29(3):1051–6. doi: 10.1002/(SICI)1521-4141(199903)29:03<1051::AID-IMMU1051>3.0.CO;2-Y

43. Booth NJ, McQuaid AJ, Sobande T, Kissane S, Agius E, Jackson SE, et al. Different proliferative potential and migratory characteristics of human CD4+ regulatory T cells that express either CD45RA or CD45RO. *J Immunol* (2010) 184(8):4317–26. doi: 10.4049/jimmunol.0903781

44. Camacho V, McClearn V, Patel S, Welner RS. Regulation of normal and leukemic stem cells through cytokine signaling and the microenvironment. *Int J Hematol* (2017) 105:566–77. doi: 10.1007/s12185-017-2184-6

45. Kim S, Park K, Choi J, Jang E, Paik DJ, Seong RH, et al. Foxp3+regulatory T cells ensure b lymphopoiesis by inhibiting the granulopoietic activity of effector T cells in mouse bone marrow. *Eur J Immunol* (2015) 45(1):167–79. doi: 10.1002/eji.201444532

46. Ali N, Zirak B, Rodriguez RS, Pauli ML, Truong H-A, Lai K, et al. Regulatory T cells in skin facilitate epithelial stem cell differentiation. *Cell* (2017) 169(6):1119–1129.e11. doi: 10.1016/j.cell.2017.05.002

47. Mathur AN, Zirak B, Boothby IC, Tan M, Cohen JN, Mauro TM, et al. Treg-cell control of a CXCL5-IL-17 inflammatory axis promotes hair-Follicle-Stem-Cell differentiation during skin-barrier repair. *Immunity* (2019) 50(3):655–667.e4. doi: 10.1016/j.immuni.2019.02.013

48. Liu Z, Hu X, Liang Y, Yu J, Li H, Shokhirev MN, et al. Glucocorticoid signaling and regulatory T cells cooperate to maintain the hair-follicle stem-cell niche. *Nat Immunol* (2022) 23(7):1086–97. doi: 10.1038/s41590-022-01244-9

49. Shao Q, Gu J, Zhou J, Wang Q, Li X, Deng Z, et al. Tissue tregs and maintenance of tissue homeostasis. *Front Cell Dev Biol* (2021) 9:717903. doi: 10.3389/fcell.2021.717903

50. Lussana F, Di Ianni M, Rambaldi A. Tregs: Hype or hope for allogeneic hematopoietic stem cell transplantation? *Bone Marrow Transpl* (2017) 52:1225–32. doi: 10.1038/bmt.2017.30

51. Ahmadzadeh M, Pasetto A, Jia L, Deniger DC, Stevanović S, Robbins PF, et al. Tumor-infiltrating human CD4+ regulatory T cells display a distinct TCR repertoire and exhibit tumor and neoantigen reactivity. *Sci Immunol* (2019) 4(31):eaao4310. doi: 10.1126/sciimmunol.aao4310

52. Trenado A, Charlotte F, Fisson S, Yagello M, Klatzmann D, Salomon BL, et al. Recipient-type specific CD4+CD25+ regulatory T cells favor immune reconstitution and control graft-versus-host disease while maintaining graft-versus-leukemia. *J Clin Invest* (2003) 112(11):1688–96. doi: 10.1172/JCI17702

53. Joffre O, Gorsse N, Romagnoli P, Hudrisier D, Van Meerwijk JPM. Induction of antigen-specific tolerance to bone marrow allografts with CD4+CD25+ T lymphocytes. *Blood* (2004) 103(11):4216–21. doi: 10.1182/blood-2004-01-0005

54. Greinix HT, Ladiges WC, Graham TC, Maslan S, Raff RF, Sandmaier BM, et al. Late failure of autologous marrow grafts in lethally irradiated dogs given anti-class II monoclonal antibody. *Blood* (1991) 78(8):2131–8. doi: 10.1182/blood.V78.8.2131.bloodjournal7882131

55. Huss R, Beckham C, Storb R, Deeg H. Major histocompatibility complex class II expression is required for posttransplant immunological but not hemopoietic reconstitution in mice. *Transplantation* (1994) 58(12):1366–71.

56. Hsieh Y-C, Kirschner K, Copland M. Improving outcomes in chronic myeloid leukemia through harnessing the immunological landscape. *Leukemia* (2021) 35(5):1229–42. doi: 10.1038/s41375-021-01238-w

57. Greiner J, Goetz M, Schuler PJ, Bulach C, Hofmann S, Schrezenmeier H, et al. Enhanced stimulation of antigen-specific immune responses against nucleophosmin 1 mutated acute myeloid leukaemia by an anti-programmed death 1 antibody. *Br J Haematol* (2022) 198(5):866–74. doi: 10.1111/bjh.18326

58. Knaus HA, Berglund S, Hackl H, Blackford AL, Zeidner JF, Montiel-Esparza R, et al. Signatures of CD8+ T cell dysfunction in AML patients and their reversibility with response to chemotherapy. *JCI Insight* (2018) 3(21):323–43. doi: 10.1172/jci.insight.120974

59. Hughes A, Clarson J, Tang C, Vidovic L, White DL, Hughes TP, et al. CML patients with deep molecular responses to TKI have restored immune effectors and decreased PD-1 and immune suppressors. *Blood* (2017) 129(9):1166–76. doi: 10.1182/blood-2016-10-745992

60. Brück O, Blom S, Dufva O, Turkki R, Chheda H, Ribeiro A, et al. Immune cell contexture in the bone marrow tumor microenvironment impacts therapy response in CML. *Leukemia* (2018) 32(7):1643–56. doi: 10.1038/s41375-018-0175-0

61. Harrington P, Dillon R, Radia D, McLornan D, Woodley C, Asirvatham S, et al. Chronic myeloid leukaemia patients at diagnosis and resistant to tyrosine kinase inhibitor therapy display exhausted T-cell phenotype. *Br J Haematol.* (2022). doi: 10.1111/bjh.18302

62. Knaus HA, Berglund S, Hackl H, Blackford AL, Zeidner JF, Montiel-Esparza R, et al. signatures of CD8 + T cell dysfunction in AML patients and their reversibility with response to chemotherapy. *Ref Inf JCI Insight* (2018) 3(21):e120974. doi: 10.1172/jci.insight.120974:e120974

63. Lamble AJ, Kosaka Y, Laderas T, Maffit A, Kaempf A, Brady LK, et al. Reversible suppression of T cell function in the bone marrow microenvironment of acute myeloid leukemia. *Proc Natl Acad Sci U.S.A.* (2020) 117(25):14331–41. doi: 10.1073/pnas.1916206117

64. Radpour R, Stucki M, Riether C, Ochsenbein AF. Epigenetic silencing of immune-checkpoint receptors in bone marrow- infiltrating T cells in acute myeloid leukemia. *Front Oncol* (2021) 11. doi: 10.3389/fonc.2021.663406

65. Noviello M, Manfredi F, Ruggiero E, Perini T, Oliveira G, Cortesi F, et al. Bone marrow central memory and memory stem T-cell exhaustion in AML patients relapsing after HSCT. *Nat Commun* (2019) 10(1):1065. doi: 10.1038/s41467-019-08871-1

66. Bilich T, Nelde A, Kowalewski DJ, Peper J, Schemionek M, Kanz L, et al. Mapping the HLA ligandome landscape of chronic myeloid leukemia identifies novel CD8+ and CD4+ T cell-epitopes for immunotherapeutic approaches. *Blood* (2016) 128(22):4232. doi: 10.1182/blood.V128.22.4232.4232

67. Berlin C, Kowalewski DJ, Schuster H, Mirza N, Walz S, Handel M, et al. Mapping the HLA ligandome landscape of acute myeloid leukemia: a targeted approach toward peptide-based immunotherapy. *Leukemia* (2015) 29:647–59. doi: 10.1038/leu.2014.233

68. Bocchia M, Gentili S, Abruzzese E, Fanelli A, Iuliano F, Tabilio A, et al. Effect of a p210 multipeptide vaccine associated with imatinib or interferon in patients with chronic myeloid leukaemia and persistent residual disease: A multicentre observational trial. *Lancet* (2005) 365(9460):657–62. doi: 10.1016/S0140-6736(05)17945-8

69. Bocchia M, Defina M, Aprile L, Ippoliti M, Crupi R, Rondoni M, et al. Complete molecular response in CML after p210 BCR-ABL1-derived peptide vaccination. *Nat Rev Clin Oncol* (2010) 7:600–3. doi: 10.1038/nrclinonc.2010.141

70. Danaher P, Warren S, Lu R, Samayoa J, Sullivan A, Pekker I, et al. Pan-cancer adaptive immune resistance as defined by the tumor inflammation signature (TIS): results from the cancer genome atlas (TCGA). *J Immunother Cancer* (2018) 6 (1):63. doi: 10.1186/s40425-018-0367-1

71. Davidson-Moncada J, Viboch E, Church S, Warren S, Rutella S. Dissecting the immune landscape of acute myeloid leukemia. *Biomed* (2018) 6(4):110. doi: 10.3390/biomedicines6040110

72. Daver N. Immune checkpoint inhibitors in acute myeloid leukemia. *Best Pract Res Clin Haematol* (2021) 34(1):101247. doi: 10.1016/j.beha.2021.101247

73. Khaldoyanidi S, Nagorsen D, Stein A, Ossenkoppele G, Subklewe M. Immune biology of acute myeloid leukemia: Implications for immunotherapy. *J Clin Oncol* (2021) 39(5):419–32. doi: 10.1200/JCO.20.00475

74. Daver N, Alotaibi AS, Bücklein V, Subklewe M. T-Cell-based immunotherapy of acute myeloid leukemia: current concepts and future developments. *Leuk* (2021) 35(7):1843–63. doi: 10.1038/s41375-021-01253-x

75. Krönig H, Kremmler L, Haller B, Englert C, Peschel C, Andreesen R, et al. Interferon-induced programmed death-ligand 1 (PD-L1/B7-H1) expression increases on human acute myeloid leukemia blast cells during treatment. *Eur J Haematol* (2014) 92(3):195–203. doi: 10.1111/ejh.12228

76. Isidori A, Cerchione C, Daver N, DiNardo C, Garcia-Manero G, Konopleva M, et al. Immunotherapy in acute myeloid leukemia: Where we stand. *Front Oncol* (2021) 11:1558. doi: 10.3389/fonc.2021.656218

77. Shenghui Z, Yixiang H, Jianbo W, Kang Y, Laixi B, Yan Z, et al. Elevated frequencies of CD4+CD25+CD127lo regulatory T cells is associated to poor prognosis in patients with acute myeloid leukemia. *Int J Cancer* (2011) 129 (6):1373–81. doi: 10.1002/ijc.25791

78. Nadal E, Garin M, Kaeda J, Apperley J, Lechler R, Dazzi F. Increased frequencies of CD4(+)CD25(high) t(regs) correlate with disease relapse after allogeneic stem cell transplantation for chronic myeloid leukemia. *Leukemia* (2007) 21(3):472–9. doi: 10.1038/sj.leu.2404522

79. Rojas JM, Wang L, Owen S, Knight K, Watmough SJ, Clark RE. Naturally occurring CD4+ CD25+ FOXP3+ T-regulatory cells are increased in chronic myeloid leukemia patients not in complete cytogenetic remission and can be immunosuppressive. *Exp Hematol* (2010) 38(12):1209–18. doi: 10.1016/j.exphem.2010.09.004

80. Tanaka A, Nishikawa H, Noguchi S, Sugiyama D, Morikawa H, Takeuchi Y, et al. Tyrosine kinase inhibitor imatinib augments tumor immunity by depleting effector regulatory T cells. *J Exp Med* (2020) 217(2):e20191009. doi: 10.1084/jem.20191009

81. Najima Y, Yoshida C, Iriyama N, Fujisawa S, Wakita H, Chiba S, et al. Regulatory T cell inhibition by dasatinib is associated with natural killer cell differentiation and a favorable molecular response–the final results of the d-first study. *Leuk Res* (2018) 66:66–72. doi: 10.1016/j.leukres.2018.01.010

82. Irani YD, Hughes A, Clarson J, Kok CH, Shanmuganathan N, White DL, et al. Successful treatment-free remission in chronic myeloid leukaemia and its association with reduced immune suppressors and increased natural killer cells. *Br J Haematol* (2020) 191(3):433–41. doi: 10.1111/bjh.16718

83. Okada M, Imagawa J, Tanaka H, Nakamae H, Hino M, Murai K, et al. Final 3-year results of the dasatinib discontinuation trial in patients with chronic myeloid leukemia who received dasatinib as a second-line treatment. *Clin Lymphoma Myeloma Leuk* (2018) 18(5):353–360.e1. doi: 10.1016/j.clml.2018.03.004

84. Fujioka Y, Sugiyama D, Matsumura I, Minami Y, Miura M, Atsuta Y, et al. Regulatory T cell as a biomarker of treatment-free remission in patients with chronic myeloid leukemia. *Cancers (Basel)* (2021) 13(23):e5904. doi: 10.3390/cancers13235904

85. Hekim C, Ilander M, Yan J, Michaud E, Smykla R, Vähä-Koskela M, et al. Dasatinib changes immune cell profiles concomitant with reduced tumor growth in several murine solid tumor models. *Cancer Immunol Res* (2017) 5(2):157–69. doi: 10.1158/2326-6066.CIR-16-0061-T

86. Balachandran VP, Cavnar MJ, Zeng S, Bamboat ZM, Ocuin LM, Obaid H, et al. Imatinib potentiates antitumor T cell responses in gastrointestinal stromal tumor through the inhibition of ido. *Nat Med* (2011) 17(9):1094–100. doi: 10.1038/nm.2438

87. Williams P, Basu S, Garcia-Manero G, Christopher, Hourigan S, Oetjen KA, et al. The distribution of T-cell subsets and the expression of immune checkpoint receptors and ligands in patients with newly diagnosed and relapsed acute myeloid leukemia. *Cancer* (2019) 125:1470–81. doi: 10.1002/cncr.31896

88. van Galen P, Hovestadt V, Wadsworth MH, Hughes TK, Griffin GK, Battaglia S, et al. Single-cell RNA-seq reveals AML hierarchies relevant to disease progression and immunity. *Cell* (2019) 176(6):1265–1281.e24. doi: 10.1016/j.cell.2019.01.031

89. Kumar Bansal A, Kumar Sharawat S, Gupta R, Vishnubhatla S, Dhawan D, Bakhshi S. Regulatory T cells in pediatric AML are associated with disease load and their serial assessment suggests role in leukemogenesis. *Am J Blood Res* (2020) 10:90–6.

90. Shenghui Z, Yixiang H, Jianbo W, Kang Y, Laixi B, Yan Z, et al. Elevated frequencies of CD4(+) CD25(+) CD127lo regulatory T cells is associated to poor prognosis in patients with acute myeloid leukemia. *Int J Cancer* (2011) 129 (6):1373–81. doi: 10.1002/ijc.25791

91. Sander FE, Nilsson M, Rydström A, Aurelius J, Riise RE, Movitz C, et al. Role of regulatory T cells in acute myeloid leukemia patients undergoing relapse-preventive immunotherapy. *Cancer Immunol Immunother* (2017) 66(11):1473–84. doi: 10.1007/s00262-017-2040-9

92. Szczepanski MJ, Szajnik M, Czystowska M, Mandapathil M, Strauss L, Welsh A, et al. Increased frequency and suppression by regulatory T cells in patients with acute myelogenous leukemia. *Clin Cancer Res* (2009) 15(10):3325–32. doi: 10.1158/1078-0432.CCR-08-3010

93. Wang X, Zheng J, Liu J, Yao J, He Y, Li X, et al. Increased population of CD4 +CD25highregulatory T cells with their higher apoptotic and proliferating status in peripheral blood of acute myeloid leukemia patients. *Eur J Haematol* (2005) 75 (6):468–76. doi: 10.1111/j.1600-0609.2005.00537.x

94. Corradi G, Bassani B, Simonetti G, Sangaletti S, Vadakekolathu J, Fontana MC, et al. Release of IFNγ by acute myeloid leukemia cells remodels bone marrow immune microenvironment by inducing regulatory T cells. *Clin Cancer Res* (2022) 28(14):3141–55. doi: 10.1158/1078-0432.CCR-21-3594

95. Dong Y, Han Y, Huang Y, Jiang S, Huang Z, Chen R, et al. PD-L1 is expressed and promotes the expansion of regulatory T cells in acute myeloid leukemia. *Front Immunol* (2020) 11:1710. doi: 10.3389/fimmu.2020.01710

96. Xu Y, Mou J, Wang Y, Zhou W, Rao Q, Xing H, et al. Regulatory T cells promote the stemness of leukemia stem cells through IL10 cytokine-related signaling pathway. *Leukemia* (2022) 36(2):403–15. doi: 10.1038/s41375-021-01375-2

97. Han Y, Dong Y, Yang Q, Xu W, Jiang S, Yu Z, et al. Acute myeloid leukemia cells express ICOS ligand to promote the expansion of regulatory T cells. *Front Immunol* (2018) 9:2227. doi: 10.3389/fimmu.2018.02227/full

98. Lecciso M, Ocadlikova D, Sangaletti S, Trabanelli S, De Marchi E, Orioli E, et al. ATP release from chemotherapy-treated dying leukemia cells elicits an immune suppressive effect by increasing regulatory T cells and tolerogenic dendritic cells. *Front Immunol* (2017) 8:22. doi: 10.3389/fimmu.2017.01918

99. Ragaini S, Wagner S, Marconi G, Parisi S, Sartor C, Nanni J, et al. An IDO1 -related immune gene signature predicts overall survival in acute myeloid leukemia. *Blood Adv* (2022) 6(1):87–99. doi: 10.1182/bloodadvances.2021004878

100. Wu L, Amarachintha S, Xu J, Oley F, Du W. Mesenchymal COX2-PG secretome engages NR4A-WNT signalling axis in haematopoietic progenitors to suppress anti-leukaemia immunity. *Br J Haematol* (2018) 183(3):445–56. doi: 10.1111/bjh.15548

101. Orleans-Lindsay JK, Barber LD, Prentice HG, Lowdell MW. Acute myeloid leukaemia cells secrete a soluble factor that inhibits T and NK cell proliferation but not cytolytic function–implications for the adoptive immunotherapy of leukaemia. *Clin Exp Immunol* (2001) 126(3):403–11. doi: 10.1046/j.1365-2249.2001.01692.x

102. Tao Q, Pan Y, Wang Y, Wang H, Xiong S, Li Q, et al. Regulatory T cells-derived IL-35 promotes the growth of adult acute myeloid leukemia blasts. *UICC Int J Cancer IJC* (2015) 137:2384–93. doi: 10.1002/ijc.29563

103. Farrar Pauken A, Williams RT, Jenkins MK, Luke Manlove MS, Berquam-Vrieze KE. Cells by cross-reactive induced regulatory T adaptive immunity to leukemia is inhibited. *J Immunol Ref* (2022) 195:4028–37. doi: 10.4049/jimmunol.1501291

104. Christopher MJ, Petti AA, Rettig MP, Miller CA, Chendamarai E, Duncavage EJ, et al. Immune escape of relapsed AML cells after allogeneic transplantation. *N Engl J Med* (2018) 379(24):2330–41. doi: 10.1056/NEJMoa1808777

105. Toffalori C, Zito L, Gambacorta V, Riba M, Oliveira G, Bucci G, et al. Immune signature drives leukemia escape and relapse after hematopoietic cell transplantation. *Nat Med* (2019) 25(4):603–11. doi: 10.1038/s41591-019-0400-z

106. Sharma A, Subudhi SK, Blando J, Scutti J, Vence L, Wargo J, et al. Anti-CTLA-4 immunotherapy does not deplete FOXP3+ regulatory T cells (Tregs) in human cancers. *Clin Cancer Res* (2019) 25(4):1233–8. doi: 10.1158/1078-0432.CCR-18-0762

107. Attia P, Maker AV, Haworth LR, Rogers-Freezer L, Rosenberg SA. Inability of a fusion protein of IL-2 and diphtheria toxin (Denileukin diftitox, DAB389IL-2, ONTAK) to eliminate regulatory T lymphocytes in patients with melanoma. *J Immunother* (2005) 28(6):582–92. doi: 10.1097/01.cji.0000175468.19742.10

108. Davids MS, Kim HT, Bachireddy P, Costello C, Liguori R, Savell A, et al. Ipilimumab for patients with relapse after allogeneic transplantation. *N Engl J Med* (2016) 375(2):143–53. doi: 10.1056/NEJMoa1601202

109. Arce Vargas F, Furness AJS, Solomon I, Joshi K, Mekkaoui L, Lesko MH, et al. Fc-optimized anti-CD25 depletes tumor-infiltrating regulatory T cells and synergizes with PD-1 blockade to eradicate established tumors. *Immunity* (2017) 46(4):577–86. doi: 10.1016/j.immuni.2017.03.013

110. Goldberg AD, Atallah E, Rizzieri D, Walter RB, Chung K-Y, Spira A, et al. Camidanlumab tesirine, an antibody-drug conjugate, in relapsed/refractory CD25-positive acute myeloid leukemia or acute lymphoblastic leukemia: A phase I study. *Leuk Res* (2020) 95:106385. doi: 10.1016/j.leukres.2020.106385

111. Dao T, Mun SS, Scott AC, Jarvis CA, Korontsvit T, Yang Z, et al. Depleting T regulatory cells by targeting intracellular Foxp3 with a TCR mimic antibody. *Oncoimmunology* (2019) 8(7):e1570778. doi: 10.1080/2162402X.2019.1570778

112. Revenko A, Carnevalli LS, Sinclair C, Johnson B, Peter A, Taylor M, et al. Direct targeting of FOXP3 in tregs with AZD8701, a novel antisense oligonucleotide to relieve immunosuppression in cancer. *J Immunother Cancer* (2022) 10(4):e003892. doi: 10.1136/jitc-2021-003892

frontiers | Frontiers in Immunology

TYPE Review
PUBLISHED 01 December 2022
DOI 10.3389/fimmu.2022.1071188



OPEN ACCESS

EDITED BY
Shenghui Zhang,
First Affiliated Hospital of Wenzhou Medical University, China

REVIEWED BY
Heiko Bruns,
University Hospital Erlangen, Germany
ANM Nazmul Khan,
University at Buffalo, United States

*CORRESPONDENCE
Allyson Guimarães Costa
allyson.gui.costa@gmail.com

†These authors have contributed equally to this work

SPECIALTY SECTION
This article was submitted to Cancer Immunity and Immunotherapy, a section of the journal Frontiers in Immunology

RECEIVED 15 October 2022
ACCEPTED 14 November 2022
PUBLISHED 01 December 2022

CITATION
Magalhães-Gama F, Alves-Hanna FS, Araújo ND, Barros MS, Silva FS, Catão CLS, Moraes JS, Freitas IC, Tarragô AM, Malheiro A, Teixeira-Carvalho A and Costa AG (2022) The Yin-Yang of myeloid cells in the leukemic microenvironment: Immunological role and clinical implications.
*Front. Immunol.* 13:1071188.
doi: 10.3389/fimmu.2022.1071188



# The Yin-Yang of myeloid cells in the leukemic microenvironment: Immunological role and clinical implications

Fábio Magalhães-Gama[1,2,3†], Fabíola Silva Alves-Hanna[1,4†], Nilberto Dias Araújo[1,4], Mateus Souza Barros[1,4], Flavio Souza Silva[1,4], Claudio Lucas Santos Catão[1,5], Júlia Santos Moraes[1], Izabela Cabral Freitas[1], Andréa Monteiro Tarragô[1,4,5], Adriana Malheiro[1,4,5], Andréa Teixeira-Carvalho[1,2,3] and Allyson Guimarães Costa[1,2,4,5,6*]

[1]Diretoria de Ensino e Pesquisa, Fundação Hospitalar de Hematologia e Hemoterapia do Amazonas (HEMOAM), Manaus, Brazil, [2]Programa de Pós-Graduação em Ciências da Saúde, Instituto René Rachou - Fundação Oswaldo Cruz (FIOCRUZ) Minas, Belo Horizonte, Brazil, [3]Grupo Integrado de Pesquisas em Biomarcadores de Diagnóstico e Monitoração, Instituto René Rachou – FIOCRUZ Minas, Belo Horizonte, Brazil, [4]Programa de Pós-Graduação em Imunologia Básica e Aplicada, Instituto de Ciências Biológicas, Universidade Federal do Amazonas (UFAM), Manaus, Brazil, [5]Programa de Pós-Graduação em Ciências Aplicadas à Hematologia, Universidade do Estado do Amazonas (UEA), Manaus, Brazil, [6]Escola de Enfermagem de Manaus, UFAM, Manaus, Brazil

The leukemic microenvironment has a high diversity of immune cells that are phenotypically and functionally distinct. However, our understanding of the biology, immunology, and clinical implications underlying these cells remains poorly investigated. Among the resident immune cells that can infiltrate the leukemic microenvironment are myeloid cells, which correspond to a heterogeneous cell group of the innate immune system. They encompass populations of neutrophils, macrophages, and myeloid-derived suppressor cells (MDSCs). These cells can be abundant in different tissues and, in the leukemic microenvironment, are associated with the clinical outcome of the patient, acting dichotomously to contribute to leukemic progression or stimulate antitumor immune responses. In this review, we detail the current evidence and the many mechanisms that indicate that the activation of different myeloid cell populations may contribute to immunosuppression, survival, or metastatic dissemination, as well as in immunosurveillance and stimulation of specific cytotoxic responses. Furthermore, we broadly discuss the interactions of tumor-associated neutrophils and macrophages (TANs and TAMs, respectively) and MDSCs in the leukemic microenvironment. Finally, we provide new perspectives on the potential of myeloid cell subpopulations as

predictive biomarkers of therapeutical response, as well as potential targets in the chemoimmunotherapy of leukemias due to their dual Yin-Yang roles in leukemia.

KEYWORDS

leukemia, neutrophils, macrophages, myeloid-derived suppressor cells, immune response, tumor microenvironment, immunotherapy

## Introduction

Leukemias correspond to a heterogeneous group of hematological malignancies that are characterized by a blockage in maturation and/or proliferation of hematopoietic cells of the myeloid or lymphoid lineage, which can be divided into acute or chronic forms (1). As a hallmark, acute leukemias have a deep blockage in hematopoietic differentiation, which results in overproduction of leukemic blasts, while chronic leukemias are characterized by the excess production of partially mature differentiated cells (2, 3). Collectively, leukemia affects individuals of all ages; however, in adults, the most common types of leukemia are acute myeloid (AML), chronic myeloid (CML), and chronic lymphocytic leukemia (CLL); while acute lymphoblastic leukemia (ALL) affects mainly children and represents the most frequent pediatric cancer in the world (4–7).

As in other types of cancer, one of the most important mechanisms by which leukemic cells (LCs) promote their development is the generation of an immune microenvironment that inhibits and impairs antitumor responses (8–10). The leukemic microenvironment represents a highly complex cellular compartment that comprises diverse cell populations, which include non-hematopoietic stromal cells, vascular endothelial cells, and innate and adaptive immune cells (11–13). During the process of leukemogenesis, stromal cells within the medullary compartment keep premalignant cells under control; however, as LCs develop, they initiate intense crosstalk with the full range of adjacent cells (11, 14). This dynamic crosstalk between LCs and components of the medullary compartment, in addition to contributing to the increase in the availability of growth and survival factors, also promotes the recruitment and polarization of immune cells into the leukemic niche (10, 11).

Among the immune cells that can infiltrate the leukemic microenvironment are myeloid cell populations, which correspond to a heterogeneous cell group of the innate immune system, including tumor-associated neutrophils (TANs), tumor-associated macrophages (TAMs), and myeloid-derived suppressor cells (MDSCs) (15). These cell populations have received great attention over the last decade because they are recruited to tumor niches on a large scale, and can act as critical components for the suppression of innate and adaptive immune responses, and also in the reduction of efficacy of immunotherapeutic approaches (16, 17). At the same time, due to their high plasticity, the subpopulations of tumor-associated neutrophils and macrophages have been shown to represent important antitumor effector cells, which can eliminate malignant cells and activating other cytotoxic effector cells. This highlights their ability to be reprogrammed into an antitumor phenotype in order to maximize tumoricidal defenses (18–22).

In this context, the advent of a "Yin-Yang" role for these innate immune cell populations in the field of leukemias remains poorly understood, despite their multiple functions and effects in solid tumors being well understood. Thus, in this review, we describe the main aspects related to myeloid cell populations, including their biological characteristics, immunological mechanisms, involvement in tumor-targeted responses, clinical implications, as well as their impact on the leukemic microenvironment. Finally, we provide a new perspective on the importance of investigating the wide diversity of these cell types in hematological malignancies and highlight their potential as prognostic biomarkers and relevant therapeutical targets, which can complement the treatment of patients with leukemia.

## Tumor-associated neutrophils (TANs)

Neutrophils are the most abundant leukocytes in the blood and are considered the first line of defense during inflammatory and infectious processes, in which they release a range of inflammatory mediators (23–25). Besides their classical roles in antimicrobial responses, neutrophils can be found in tumor infiltrates, and are named tumor-associated neutrophils (TANs). They also exhibit great plasticity that allows them to perform diverse and often opposite functions (26–29). TANs can display favorable or harmful responses to the host depending on their polarization, which, in a simplified manner, can be classified into

two distinct phenotypes, N1 (tumor suppressor) and N2 (tumor promoter) (30, 31).

N1 TANs are usually found in the early stages of the tumorigenic process, and act in the recruitment and activation of cytotoxic T cells and T helper (Th) cells (32–35). They emerge mainly from IFN-β–mediated stimuli, and are characterized by the high expression of immuno-activating cytokines and chemokines, such as TNF, IL-12, CCL-3, CXCL-9, and CXCL-10, in addition to the expression of ICAM-1, FAS and low levels of Arginase-1 (26, 36, 37). As for N2 TANs, they appear in later stages, inhibit effector responses and preferentially recruit regulatory T cells (32–35). They differ mainly after stimulation mediated by TGF-β and IL-35 and, unlike N1 TANs, they are characterized by the overexpression of Arginase-1, the presence of protease-enriched granules, such as neutrophil elastase (NE), cathepsin G (CG) and matrix metalloproteinases (MMPs), in addition to the production of a wide range of chemokines that include CCL-2, CCL-5, and CXCL-8 (Figure 1) (26, 34, 36, 38). Notably, TANs are usually distinguished based on their anti- or pro-tumor functions, as mentioned earlier (33). In terms of expression of intracellular and extracellular markers, the literature generally mentions CD11b, HLA-DR$^{lo/int}$, CD15$^{hi}$, CD16$^{hi,}$ and CD66, with varying expression of CD33 and Arginase-1 (16, 36, 39–41). In addition, recent studies have characterized anti- or pro-tumor TAN populations based on the presence and expression of CD54$^{+}$, HLA-DR$^{+}$, CD86$^{+}$ and CD15$^{hi}$; and CD170$^{hi}$ and PD-L1$^{+}$ (42).

Traditionally, neutrophils act as key elements in the immune system, and play a fundamental role in the immune response through a range of mechanisms, which include: phagocytosis and generation of reactive oxygen species (ROS); antibody-dependent cell-mediated cytotoxicity (ADCC); degranulation and release of

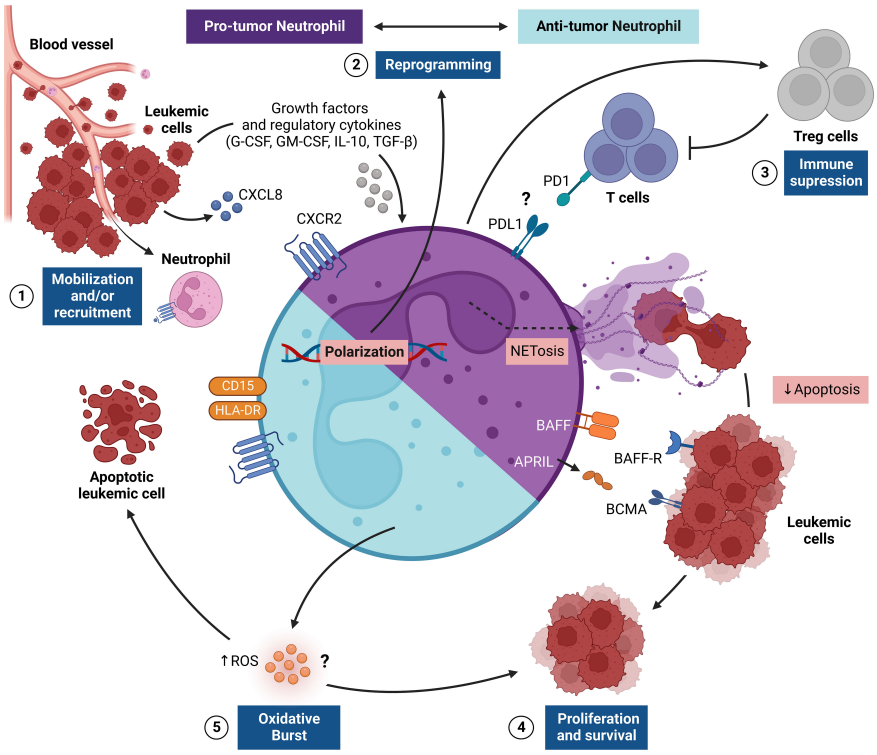


FIGURE 1
Regulation of TAN responses in the leukemic microenvironment. The figure shows the pro-tumor and antitumor activities of tumor-associated neutrophils (TANs), which provide critical signals for leukemic progression. This network of interactions between TANs, leukemic cells (LCs) and other immune cells [e.g., regulatory T cells (Treg)] results in four main events: [1] recruitment and/or mobilization of neutrophils *via* CXCL8/CXCR2 to the leukemic microenvironment, where LCs promote the survival of TANs through the release of G-CSF and GM-CSF; [2] reprogramming of TANs to become pro-tumor (N2) or antitumor (N1) cells through stimulation of the leukemic microenvironment through the cytokines IL-10 and TGF-β; [3] immunosuppression promoted by N2 TANs that can preferentially recruit Treg cells and can suppress T cell effector responses, apparently *via* a PD1-PDL1-mediated pathway; [4] LC proliferation and survival in the leukemic microenvironment regulated by a range of surface molecules (e.g., BAFF and APRIL) expressed by N2 TANs, which also release NETs, which, in turn, delay LC apoptosis; [5] In another scenario, the oxidative burst triggered by N1 TANs can promote the release of reactive oxygen species (ROS) that control proliferation or mediate the killing of LCs. APRIL, A proliferation-inducing ligand; BAFF, B-cell activating factor; G-CSF, granulocyte colony-stimulating-factor; GM-CSF, Human granulocyte-macrophage colony-stimulating factor; NETs, Neutrophil extracellular traps; PD1, Programmed cell death protein 1; PDL1, Programmed cell death-ligand 1; TGF-β, Transforming growth factor-β.

proteases; immune cell modulation; and release of extracellular neutrophil traps (NETs), which consists of modified chromatin decorated with bactericidal proteins from granules and cytoplasm (37, 43–46). However, in the tumor context, the effector function of these cells is usually modified to contribute to cancer cell progression through processes such as extracellular matrix remodeling, angiogenesis and lymphangiogenesis, immunosuppression, and promotion of cancer cell invasion and metastasis (47–52). Given these characteristics, besides the fact that they represent up to 70% of circulating leukocytes and are present in large numbers in the tumor microenvironment (TME), TANs are being increasingly investigated in many types of cancer (53–57).

In the context of hematological malignancies, the role of neutrophils in the TME is poorly studied. In the field of leukemias, the role of TANs has been investigated mainly in CLL, in which it was observed that *in vitro* stimulated neutrophils were more prone to release of NETs, which in turn, have been shown to delay apoptosis and increase the expression of activation markers on LCs (58). This increased susceptibility is driven by the CXCL-8 chemokine, which exhibited significantly elevated levels in the plasma of CLL patients and correlated with the ability to release NETs after neutrophil activation. Of note, plasma from CLL patients has been shown to increase CXCR2 expression in neutrophils, thus allowing CXCL-8-mediated activation; however, the plasma factors responsible for these upregulatory effects remain unknown (58).

Initial observations suggested the possibility that LCs could be driving the maintenance and regulation of TANs to promote leukemic progression. Nonetheless, *via* further investigations, it was observed that LCs promoted TANs survival through release of G-CSF/GM-CSF and induced their reprogramming through IL-10 and TGF-β cytokines in $CD16^{high}$ $CD62L^{dim}$ subsets, which are capable of significantly suppressing the effector functions of T cells, such as proliferation and IFN-γ production (59). Moreover, it has been shown that patients with CLL exhibit increased amounts of circulating immunosuppressive neutrophils ($CD16^{high}$ $CD62L^{dim}$), and that, depending on the disease stage in the intermediate or advanced state, there is a strong trend toward an increase in the frequency of this TANs subset (59). Such observations reinforce the ability of LCs to induce neutrophil reprogramming to the N2 phenotype and suggest their association with a poor prognosis in CLL patients.

CLL is usually accompanied by immunosuppression and susceptibility to infections (60). Studies carried out seeking to compare the characteristics of neutrophils from patients with CLL who had infections with non-infected patients observed a decrease in chemotaxis and oxidative burst in neutrophils in infected patients (60, 61). Similar results were seen in pediatric patients with ALL, in which oxidative burst was shown to be significantly suppressed in these patients at the time of diagnosis and after remission chemotherapy (62). In addition, studies have also shown that neutrophils from CLL patients have impaired bactericidal activity (60, 63). These data are indicative that neutrophils derived from patients with CLL and ALL tend to lose their effector functions while acquiring pro-tumorigenic capabilities, thus polarizing to the N2 phenotype.

Significant differences in phenotypic characteristics of neutrophils were found in another study that evaluated the expression of receptors and adhesion molecules associated with inflammation. An increased frequency of $CD54^{+}$ and $CD64^{+}$ (FcγRI) neutrophils was observed, along with an increase in ROS-generating activity (64). It has been suggested that the activation phenotype of circulating neutrophils could be the result of a systemic inflammatory environment, and is reinforced by high levels of TNF, which would contribute to the survival and proliferation of LCs, while the increase in oxidative potential could be related to chronic activation of the immune system. Interestingly, despite the activation status, neutrophils from CLL patients failed to mount a standard inflammatory response, thus highlighting an unusual activation phenotype with suppressed functional features that possibly comes from stimuli from the leukemic microenvironment (64).

Indeed, stromal cells from the leukemic microenvironment have been shown to interact substantially with neutrophils (65, 66). A study realized in an Eμ-TCL1 CLL murine model indicated that stromal cells from red pulp and the marginal zone of spleens presented LCs infiltrate, overexpressed genes related to neutrophil chemotaxis, including the chemotactic factors S100A8 and S100A9 (MRP8 and MRP14, respectively), the chemokine receptor CXCR2, the pro-inflammatory cytokine IL-1β, and integrin CD11b (Itgam) (65, 66). In addition, neutrophils infiltrated in the leukemic niche were observed to secrete survival cytokines, including APRIL and BAFF, which are important for B cell proliferation. Finally, the neutrophil depletion in Eμ-TCL1 mice, with already developed CLL, demonstrated a reduction in the leukemic burden in spleens, clearly showing that neutrophils support leukemia progression in Eμ-TCL1 mice (65, 66).

Despite all the data presented, little is known about the influence of neutrophils on the development of the antileukemic immune response, especially if we consider the other types of leukemia, which practically remain unexplored. This reinforces the need for investigations into the mechanisms by which neutrophils contribute to disease pathogenesis, besides the impact of their dysfunction on effective immune defense against pathogens and their potential association with the frequent occurrence of severe infections during the period during chemotherapy treatment.

## Tumor-associated macrophages (TAMs)

Macrophages are innate effector cells with high phagocytic power and exhibit high functional plasticity that is context-dependent. In other words, they appear in response to different

stimuli and assume different functional, phenotypic, and morphological identities (67, 68). Overall, macrophages play a crucial role in activating innate and adaptive responses, since they are important components in defense against infections, tissue repair, antigen presentation, and subsequent initiation of T and NK cell responses in different microenvironments (68).. When detecting tissue alterations, non-activated macrophages (Mφ) assume various activation states within a broad phenotypic and functional spectrum, thus characterizing the M1-M2 macrophage polarization system, which indicates whether these innate immune cells are more pro-inflammatory or anti-inflammatory (69).

M1 or 'classically activated' macrophages arise after stimuli mediated by IFN-γ, TNF, GM-CSF, and bacterial LPS. They are capable of producing substantial levels of pro-inflammatory cytokines, such as IL-1β, IL-6, IL-12, IL-23, and TNF (70), and express different intracellular and extracellular markers that allow their distinction, and present cells that are positive for CD68, CD11c, CD14, CD80, CD86, HLA-DR, iNOS and signal transducer and activator of transcription (STAT)-1 (71). On the other hand, M2 or 'alternatively activated' macrophages appear after stimuli mediated by cytokines such as IL-4 and IL-13, and are able to produce anti-inflammatory molecules such as IL-10 and TGF-β (Figure 2) (70). Common intracellular and extracellular markers for M2 macrophages include CD68, CD14, CD163, CD204, CD206, STAT3, STAT6, Arginase-1, VEGF and cMAF (72). It is important to note that the designation M2 covers other macrophage populations (M2a, M2b, M2c, and M2d), whose phenotypic and functional diversity remains poorly understood (72).

The different subsets of macrophages are critically involved in the progression or regression of several diseases, including cancer (73). As the tumors progress, they are accompanied by an extensively dysregulated hematopoiesis, reflecting in a continuous expansion and renewal of myeloid cells in the bone marrow (BM) and in peripheral sites, which travel between different tissues and contribute to immunosuppression or immunosurveillance (74, 75). As highly heterogeneous cells, macrophages are in continuous communication with the periphery beyond the TME. Therefore, the presence of tumor-associated macrophages (TAMs) is now seen as an important signal of the regulation of tumor immunity, since (i) TAMs infiltrate the TME to regulate tumor growth and (ii) the TME shapes the activity and functional use of TAMs to promote cancer cell metastasis and survival (76).

Many signals that shape the M1/M2 polarization vary according to the type, stage, location of the tumor, and result in different highly dynamic TAM phenotypes (77). Each macrophage is not always functionally restricted to a specific role. For example, it is important to note that IL-6 and IL-1β-producing TAMs, possibly M1-like, promote tumor growth through the production of these cytokines, which shows that M1 TAMs are not always able to precisely exert their antitumor functions during cancer progression (78–80). Further strong evidence of this is that, in some tumors, TAMs that exhibit an M2 phenotype ($CD163^+$ $CD206^+$) perform an activity that is equivalent to M1-like TAMs, and initiate antitumor responses (81–83). Therefore, the M1/M2 classification is too simplistic for this highly heterogeneous cell type.

Generally, TAMs have a recognized role in solid tumors, but their involvement in hematologic malignancies, such as leukemia, remains unclear. There is evidence that crosstalk between TAMs and LCs occurs at different sites during leukemia progression (60, 84–90). The fact that these cells are widely distributed in tissues suggests that TAMs travel to leukemic niches and support the proliferation of LCs, which influences the clinical outcome of the disease (90–94). These early insights are supported by several clinical and preclinical findings that have demonstrated that tumor progression affects the biodistribution of TAMs in the BM and at extramedullary sites, in which M1/M2 balance is extensively dysregulated following recruitment and reprogramming of TAMs to a pro-tumor phenotype (M2) (88, 90, 95–99).

Mobilization of TAMs to leukemic niches is supported by chemokines such as CCL2, CCL3, CCL4, and CXCL12, which regulate their biodistribution (100, 101). Among these molecules, CXCL12 promotes the mobilization of CXCR4+ TAMs to the BM microenvironment and supports M2 polarization (87, 102–104). It is important to note that CCL2 also regulates the infiltration of TAMs into the TME, which, in turn, also produces CCL2 and amplifies the mobilization of more CCR2+ macrophages to the tumor niche (104–106). Leukemia patients exhibit elevated levels of CCL2 and CXCL12 in the BM and blood, which can critically influence the activation and recruitment of TAMs (104, 107–111).

Another important point is that extramedullary sites, such as the lymph nodes, the spleen and the liver, also support the growth and metastatic spread of LCs, and macrophages act as essential stromal components in these compartments (112). Therefore, the idea that local macrophage-mediated signaling pathways are decisive elements for tumor progression is well established in the context of leukemia (91, 113, 114). In line with this, several reports have shown that LCs mobilize CCR1+ or CCR4+ TAMs in lymph nodes *via* CCL3 and CCL4 (100, 115), which in turn preserve the survival of LCs through cell-cell interactions (116). Similar events also occur in the spleen and liver of mice, in which a high accumulation of M2 TAMs is regulated by the CCR2-CCL2 axis (95, 117). On the other hand, in some cases, M1 TAMs exhibit a curious predominance in the BM and liver of these mice (118). This is evidenced when spleen-derived macrophages are cultured with LCs and promote greater tumor growth *in vitro* when compared to cultured BM-derived macrophages (99, 119), thus suggesting that different subsets of TAMs may play pleiotropic roles at different sites, since liver TAMs exhibited greater production of inflammatory factors such as CCL5, TNF, and IL-12 than BM and spleen TAMs (120, 121).

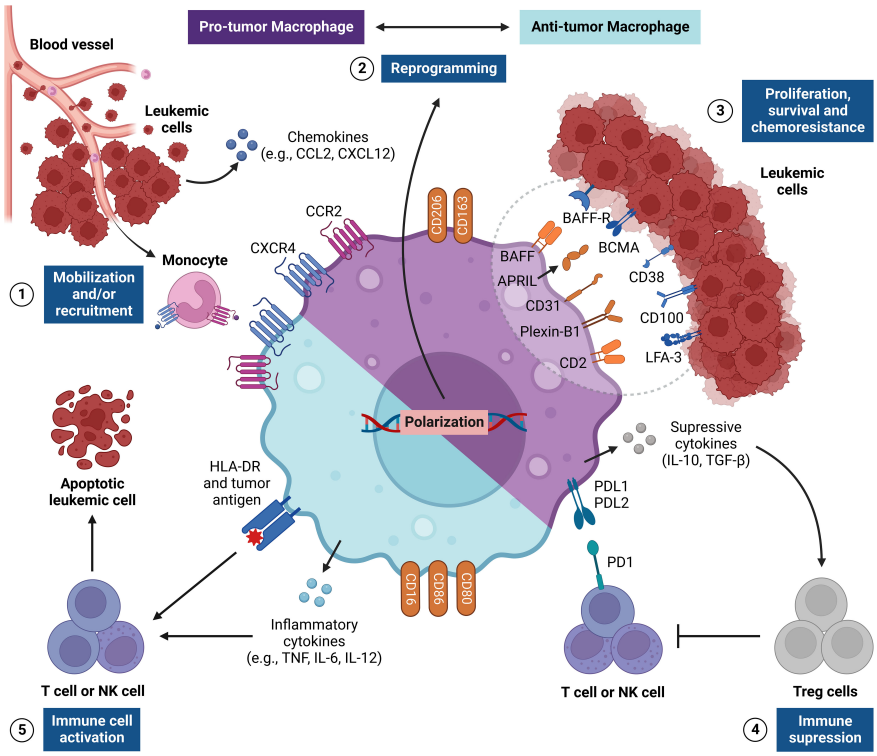


FIGURE 2
Regulation of TAM responses in the leukemic microenvironment. The figure shows the pro-tumor and antitumor activities of tumor-associated macrophages (TAMs), which are critical signs for leukemic progression. This network of interactions between TAMs, LCs and other immune cells [e.g., NK cells and Treg cells] results in five main events: [1] recruitment and/or mobilization of monocytes *via* CXCL8/CXCR2 and CCL2/CCR2 to the leukemic microenvironment, which differentiate into TAMs; [2] reprogramming TAMs to become pro-tumor (M2) or antitumor (M1) cells through many stimuli from the leukemic microenvironment, such as cytokines and cell-cell crosstalk (i.e., context dependent); [3] immune interactions with LCs within the leukemic microenvironment through a wide range of surface molecules that send many signals to stimulate the proliferation, survival and chemoresistance in LCs (e.g., BAFF, APRIL, CD31, Plexin-B1 and CD2); [4] establishment of a strongly tolerogenic environment, such as M2 TAMs, which produce many suppressive cytokines (e.g., IL-10 and TGF-β) and express immune checkpoints (PDL1 and/or PDL2), and which regulate the responses of T NK cells, and stimulate Treg cell activities; [5] establishment of an inflammatory environment, such as M1 TAMs, thus stimulating the cytotoxic activity of T and NK cells by the production of inflammatory cytokines (e.g., TNF and IL-12) and the expression of co-stimulatory molecules (e.g., CD80, CD86 and HLA-DR), which can promote antitumor responses and the death of the tumor. APRIL, A proliferation-inducing ligand; BAFF, B-cell activating factor; BAFF-R, BAFF receptor; BCMA, B-cell maturation antigen; CCR2, C-C motif chemokine receptor 2; CXCR4, C-X-C chemokine receptor 4; HLA-DR, Human leukocyte antigen DR; LFA-3, Lymphocyte function-associated antigen 3; NK, Natural killer; PD1, Programmed cell death protein 1.

By infiltrating different leukemic niches, M2 TAMs produce soluble mediators that support LC expansion and survival (84). When monocytes from healthy donors are cultured with LCs, they differentiate into M2 and increase the resistance of LCs to apoptosis *via* CXCL12 secretion (113). Additionally, some cytokines and chemokines may also participate in this process, since M2 TAMs also secrete IL-8, IL-10, TGF-β, CCL2, CCL4, CXCL13, and other soluble mediators that are capable of inducing tumor growth *in vitro* and *in vivo* (98, 117, 121–125). In turn, LCs can produce substantial levels of IL-4, IL-10, IL-13, NAMPT, Arginase-2, and BMP-4, which regulate the pro-tumor functions of TAMs (84, 122, 123, 126).

An emerging mechanism of cell-cell communication during tumor progression is the release of exosomes, endosomal-derived vesicles, which carry different molecular components (e.g., nucleic acids, proteins, or metabolites) and are present in several biological fluids, being secreted by many cell populations, including immune and cancer cells (127, 128). These extracellular vesicles play an important role in the crosstalk between LCs and TAMs and reprogram these leukocytes into leukemia-supportive effector cells. Previous studies have reported that LC-derived exosomes are able to polarize macrophages to an immunosuppressive phenotype with enriched expression of PD-L1 on the cell surface and overproduction of IL-10 (129, 130). The high expression of PD-L1 by TAMs allows it to suppress the activity of PD1+ T cells and NK cells (11, 117).

Other receptors act to send survival signals to LCs. Studies have shown that CD163 binds to the unknown ligand on LCs, and its expression correlates with an increased leukemia burden

(90, 98). In this sense, it is worth noting that CD163 induces a strong production of IL-10 by macrophages (131), in which this cytokine is a potent stimulator of malignant B cells (132, 133). In addition, M2 TAMs upregulate the expression of BAFF and APRIL, which bind to BAFF-R and BCMA expressed in LCs, respectively (134, 135). These ligands may be related to the resistance of LCs to chemotherapy and apoptosis, as previously reported (134, 136, 137). Finally, the expression of CD31 and plexin-B1 by these cells leads to an increased potential for LC survival (101, 138). This is because LCs express CD38 and CD100, which are receptors for CD31 and plexin-B1, respectively (138, 139). The CD2–LFA-3 axis was also shown to be critical in the crosstalk between M2 TAMs and LCs, as it also acts on the sending of stimulatory signals to LCs (116).

Although the functions of TAMs are often related to leukemic progression, it is still difficult to establish their precise prognostic value in leukemia. While several reports highlight their strong pro-tumor interactions through the production of soluble mediators and surface receptors, some evidence suggests that M1 TAMs can be mobilized to the BM or extramedullary sites (99, 118–121). Whether they are playing a protective role is still an open question, but strong evidence of this is that when M2 TAMs are treated with IFN-γ, they polarize to an M1 profile, inhibit their regulatory activity, and increase HLA-DR expression, CD86, and CD64, and exhibit a high antileukemic response *in vitro* (140). However, the antitumor activity of TAMs in leukemia remains poorly investigated; although, it is evident that M1 TAMs produce inflammatory factors in the TME (120, 121). The fact is that the presence of M2 TAMs is generally associated with an increased leukemic burden and, subsequently, an unfavorable prognosis (90, 118, 141). Therefore, future investigations should focus on the different macrophage subsets and their functional and prognostic relevance in different leukemia subtypes.

## Myeloid-derived suppressor cells (MDSCs)

Myeloid-derived suppressor cells (MDSCs) correspond to a phenotypically heterogeneous cell population that is derived from immature myeloid precursors of the granulocytic or monocytic lineage (16). The ontogeny process of MDSCs involves blocking differentiation in normal hematopoiesis, thus preventing their terminal differentiation, and promoting their expansion. This feature highlights their distinction from terminally differentiated, mature myeloid cells; although their distinction from neutrophils is usually a controversial topic (16, 142). However, studies have shown that these cells can also differentiate from a monocyte-like precursor of granulocytes (143). In humans, there is still a recently discovered subpopulation known as "early MDSCs", which represent less than 5% of the MDSC population; however, little is known about their role (144). In general, as evidenced by their name, pathologically activated MDSCs exhibit strong immunosuppressive capabilities, and act as crucial drivers of an immunosuppressive microenvironment (16).

MDSCs are subdivided into two groups: polymorphonuclear MDSCs (PMN-MDSCs), which are morphologically similar to neutrophils; and monocytic MDSCs (M-MDSCs), which are morphologically similar to monocytes (142, 145). In humans, they are identified from specific cell markers; however, these are far from uniform. PMN-MDSCs are defined as $CD11b^{+}$ $CD14^{-}$ $CD15^{+}/CD66^{+}$ cells (146–148). In turn, M-MDSCs are defined as $CD14^{+}$ $CD15^{-}/CD66^{-}$ $HLA\text{-}DR^{lo/-}$ (144). CD14 is a characteristic surface marker of monocytes, while $HLA\text{-}DR^{lo/-}$ helps distinguish M-MDSCs from mature monocytes and $CD15^{-}$ distinguishes M-MDSCs from PMN-MDSCs (149). As PMN-MDSCs are morphologically and phenotypically like classical neutrophils, the main way to differentiate them is functionally, i.e., based on their ability to suppress other immune cells, since normal neutrophils are not immunosuppressive cells (150–152). On the other hand, there is still an intense debate on the distinction between N2 TANs and PMN-MDSCs, due to shared origin, phenotypic and functional characteristics. However, despite the high similarity between these cell populations, it has recently been shown that lectin-like oxidized LDL receptor-1 (LOX-1), which is highly expressed in human PMN-MDSCs, may represent a specific marker to distinguish these cells from mature neutrophils in peripheral blood and tumor tissues (153).

PMN-MDSCs and M-MDSCs are activated by prolonged stimulation that is mediated by growth factors and pro-inflammatory cytokines (GM-CSF, CSF1, IL-6, and 1L-1β), as seen in conditions such as cancer, chronic infections, and autoimmune diseases (144). The stimuli that lead to their activation occur in two stages, and these are referred to as Phase 1, which is characterized by the expansion of MDSCs, and Phase 2, which is characterized by differentiation into a granulocytic or monocytic lineage (154). The expansion and activation of these cells are both dependent on transcription factors such as STAT1, STAT3, STAT6, and NF-κB, which result in the upregulation of the cytokines IL-10, TGF-β, and, in some conditions, IFN-γ; of immunosuppressive factors such as arginase 1 (ARG1), inducible nitric oxide synthase (iNOS) and reactive oxygen species (ROS); in addition to immunological checkpoint inhibitors such as Programmed death-ligand 1 (PDL1) and V-domain Ig suppressor of T cell activation (VISTA) (Figure 3). Together, these mediators promote anergy of cytotoxic T cells and tumor-specific T helper (Th); expansion of regulatory T cells (Treg); reprogramming of TANs and TAMs in N2 and M2, respectively; and decrease in L-arginine and L-cysteine, which are amino acids necessary for the activation and proliferation of T cells, thus collaborating in the remodeling of an immunosuppressive microenvironment that is susceptible to neoplastic progression (155–162).

In addition, MDSCs may harbor tumor-promoting functions that are independent of immune suppression, such as promoting metastasis and angiogenesis through the production of vascular endothelial growth factor (VEGF), fibroblast growth factor β (FGF-β) and matrix metalloproteinase-9 (MMP9). Furthermore, studies have described that these cells can be mobilized from the

BM through G-CSF, GM-CSF, or hypoxia to metastatic environments, in which pro-inflammatory mediators, such as IL-6, TNF-α, and prostaglandin E2 (PGE2), can increase their immunosuppressive functions (16, 75, 163, 164). Thus, once activated, MDSCs become crucial factors in TME and have a significant role in the development of several solid and hematological neoplasms, in addition to being frequently associated with different stages of cancer (165–169).

In the field of acute leukemias, studies performed in pediatric patients with B-cell ALL showed a significant increase in the frequency of PMN-MDSCs, along with T reg cells in the circulation and BM compartment, which exhibited a positive association with the presence of measurable residual disease (MRD) (170). In addition, it was observed that the number of PMN-MDSCs decreased markedly in patients who went into remission, and was comparable to the control group (171). Similarly, in adult AML patients, MDSCs (CD33+ CD11b + HLA-DRlow/neg) were significantly increased in BM and were associated with extramedullary infiltration and increased serum D-dimer concentration in plasma; however, after induction chemotherapy, there was a decrease in the frequency of these cells (172). In addition, the frequency of M-MDSCs also showed a significant increase, both in circulation and in the percentage of peripheral blood mononuclear cells (PBMCs), which was associated with a low rate of remission, high rate of relapse, and low long-term survival (173).

Regarding chronic leukemias, it was reported that patients with high-risk CML showed an increase in the frequency of PMN-MDSCs, as well as in the expression of Arg-1, which is known to inhibit T cells. In addition, PMN-MDSCs exhibited a positive upregulation for PD-L1, in conjunction with the PD-1 receptor on T cells (174). Studies also observed that the

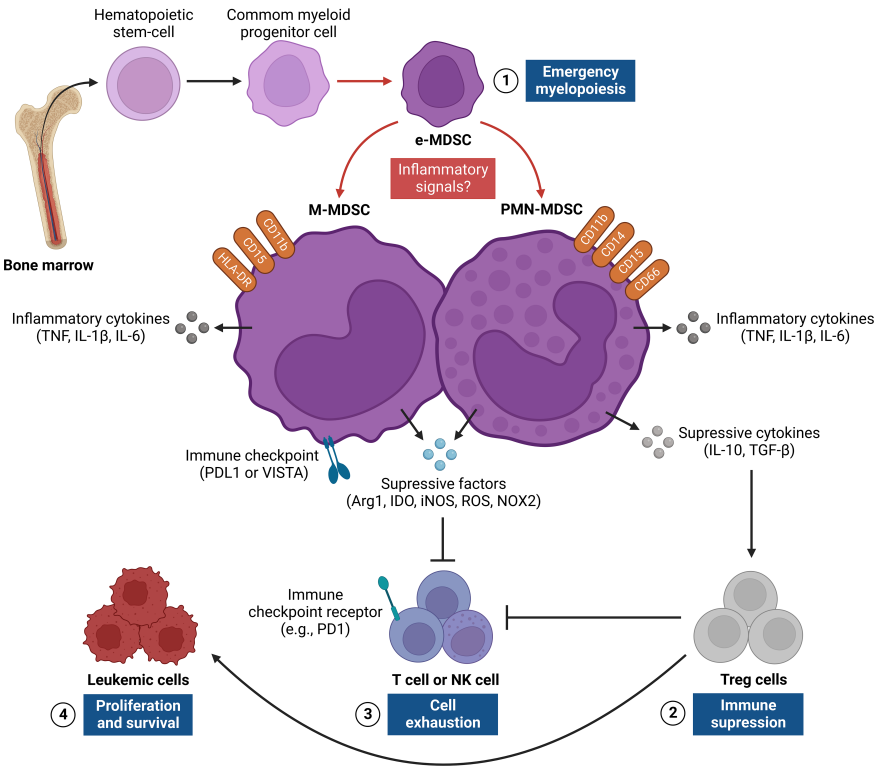


FIGURE 3
Regulation of MDSC responses in the leukemic microenvironment. The figure shows the origin and pro-tumor activities of myeloid-derived suppressor cells (MDSCs), which provide critical signals for leukemic progression. This network of interactions between MDSCs, LCs, and other immune cells [e.g., T cells, NK cells, and Treg cells] results in four main events: [1] emergence of MDSCs in bone marrow from common myeloid progenitor cells that differentiate into PMN-MDSC and M-MDSC after persistent inflammatory signals, thus characterizing a process known as "emergency myelopoiesis"; [2] activation and recruitment of Treg cells through the release of regulatory cytokines (e.g., IL-10, TGF-β), which contribute to immunosuppression of the leukemic microenvironment;[3] exhaustion of T and NK cells from different inflammatory (e.g., IL-6, TNF and IL-1β) and/or anti-inflammatory (e.g., IL-10, TGF-β, Arg1, IDO and iNOS) mediators and surface molecules (PDL1 or VISTA) expressed by MDSCs, which regulate antitumor responses;[4] LC proliferation and survival, which are a consequence of suppression of T cell and NK cell effector responses and activation of Treg cells in the leukemic microenvironment. Arg1, Arginase 1; IDO, Indoleamine; iNOS, nitric oxide synthase; M-MDSC, monocytic-MDSC; NK, Natural killer; PDL1, Programmed death-ligand 1; PMN-MDSC, polymorphic mononuclear-MDSC; TGF-β, Transforming growth factor beta; TNF, Necrosis factor tumoral; Treg, Regulatory T cells; VISTA, V-domain Ig suppressor of T cell activation.

frequency of PMN-MDSCs was elevated at the time of diagnosis, and decreased to normal percentages after imatinib therapy (175). Finally, studies performed on patients with CML and CLL also observed a significant increase in the frequency of M-MDSCs at diagnosis, together with increased expression of IL-10 and TGF-β, which *in vitro* have been shown to induce T cell suppression and activation of Treg cells (174, 176, 177). In general, high frequencies of PMN-MDSCs and M-MDSCs can directly influence the clinical course of acute and chronic leukemias, thus highlighting their role as potential prognostic biomarkers and therapeutic targets in these patients (178–182).

## Concluding remarks and future perspectives

The 'Hallmarks of Cancer' were proposed as a set of functional capabilities acquired by human cells as they progress from normality to neoplastic growth states (183). In the most recent elaboration of this concept, after little more than a decade of incessant research into the immunobiology of cancer, the role of immune cells in the neoplastic progression is well recognized. Today, inflammation and immune evasion are considered hallmarks of cancer progression, highlighting the direct involvement of immune cells, including myeloid lineage cell populations (184). Supporting this fact, TANs, TAMs, and MDSCs represent one of the main immune infiltrates in tumor niches, and are usually associated with suppressive mechanisms that attenuate immune surveillance, cytotoxic response, and, in many cases, the success of T cell-based immunotherapies (16).

Similarly, eosinophils and basophils also infiltrate multiple tumors and are activated to regulate tumor progression, either by directly interacting with cancer cells or indirectly by modulating the TME (185–188). Platelets, small anucleate structures derived from BM megakaryocytes, have also been shown to play a broad role in tumor progression, and favor proliferation from the release of growth factors and drug resistance (189–191). In addition, they act in the formation of secondary niches through a mechanism called "cloaking", in which platelets produce physical protection in cancer cells, thus

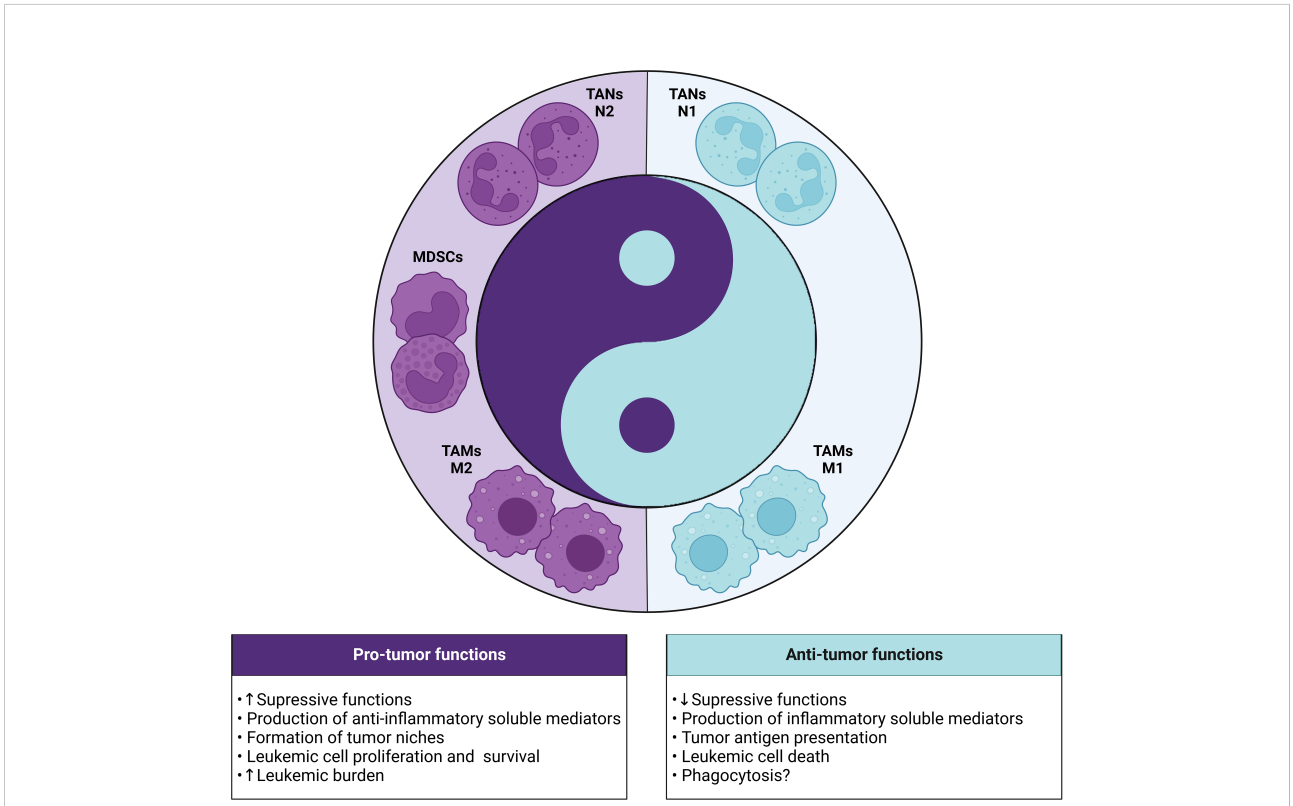


FIGURE 4
Yin-Yang with the dual role (pro and antitumor) of myeloid cells in the leukemic microenvironment. In leukemia, the different subsets of myeloid cells (TANs, TAMs and MDSCs) can exert dichotomous functions dictated by the polarization status of each cell. The pro-tumor phenotype is highlighted by the presence of N2 TANs, M2 TAMs and MDSCs, which show strong immunosuppressive activity through the production of anti-inflammatory mediators and formation of leukemic niches that contribute to the increase in tumor burden. In contrast, the antitumor phenotype involves the presence of N1 TANs and M1 TAMs that can exert protective functions through the release of cytotoxic mediators, tumor antigen presentation, death or phagocytosis of leukemic cells.

TABLE 1 Association of frequency of myeloid cell populations with the clinical implications of leukemia patients.

| Myeloid cells | Leukemia subtype | Clinical implications | References |
|---|---|---|---|
| TANs* | CLL# | Tendency to increase the frequency of circulating immunosuppressive neutrophils ($CD16^{high}CD62L^{dim}$) according to intermediate or advanced stage of the disease. | (59) |
| TAMs | ALL | Increased frequency of M2 TAMs in BM¥ and extramedullary sites as an independent factor for an unfavorable prognosis. | (88, 96, 98) |
| | AML | High infiltration and mobilization of M2 TAMs in BM associated with a worse prognosis. | (88, 92, 95) |
| | CLL | Increased frequency of M2 TAMs in lymph nodes correlated with a high proliferation of LCs. | (90) |
| | CML | High frequency of M2 TAMs in BM during transition from chronic to blast phase correlated with disease progression. | (97,141) |
| MDSCs | ALL | Increased frequency of PMN-MDSCs in BM and blood indicative of positive MRD. | (170) |
| | | Decreased frequency of circulating PMN-MDSCs correlated with a better prognosis. | (171) |
| | AML | High infiltration of MDSCs in the BM associated with positive MRD. | (172) |
| | | High frequency of circulating M-MDSCs correlated with low rate of remission, disease relapse, and poor survival. | (173) |
| | CLL | Increased frequency of MDSCs correlated with greater immunosuppression and increased leukemic burden in untreated patients. | (176, 177) |
| | CML | Frequency of circulating PMN-MDSCs at diagnosis and at the end of treatment correlated with high-risk disease and poor response to chemotherapy. | (174, 175) |

*TANs, tumor-associated neutrophils; TAMs, tumor-associated macrophages; MDSCs, myeloid-derived suppressor cells; #CLL, chronic lymphocytic leukemia; ALL, acute lymphoblastic leukemia; AML, acute myeloid leukemia; CML, chronic myeloid leukemia; ¥BM, bone marrow; LCs, leukemic cells; PMN-MDSCs, polymorphonuclear MDSCs; MRD, Measurable residual disease; M-MDSCs, monocytic myeloid-derived suppressor cells.

assisting in vascular migration and extravasation to the tissues to form metastases (192–194). It is noteworthy that, although promising, these myeloid cell populations and products still present themselves as poorly recognized targets and therefore require further investigation.

In this review, we seek to elucidate the role, mechanisms, and clinical implications of TANs, TAMs, and MDSCs in the leukemic microenvironment (Figure 4), as well as in the prognosis of patients with leukemia (Table 1). Based on the body of evidence, it is possible to suggest that the high frequency of tumor-associated neutrophils and macrophages, leaning towards an anti-inflammatory phenotype (N2 and M2, respectively), along with PMN-MDSCs and M-MDSCs could contribute to the identification of patients that are characterized by high-risk of disease at diagnosis and during treatment. In addition, several studies have highlighted the role of these cell populations as critical determinants of resistance to chemoimmunotherapy and targeted therapy, acting as a "Yin" role (5–10).

On the other hand, we also cannot rule out the potential "Yang" role of myeloid cells in stimulating the immune response. Recent technological advances have helped the generation of genetically modified myeloid cells to enhance their antitumor properties. In summary, through genetic engineering, these cells increase the expression of cell surface receptors and antigens, as well as cytokines capable of modulating TME contributing to a pro-inflammatory environment, thus increasing the activation of cytotoxic immune cells (195). In *in vivo* studies, genetically modified myeloid cells have been shown to be able to migrate to primary tumor niches, which increases antigen presentation and IFN-γ production, promotes T cell activation, and reduces tumor burden (196, 197).

Collectively, these data indicate that the reprogramming or repolarization of myeloid cells presents itself as a promising and effective strategy, which should be explored in the context of immunotherapeutic approaches aimed at leukemias, especially considering the large cellular repertoire of the leukemic microenvironment, in addition to the intense and dynamic crosstalk between LCs and surrounding cells. Finally, it is important to highlight the scarcity of data on the dual role (Yin-Yang) of myeloid cell populations in different types of leukemia, since the characterization of the immune microenvironment of the medullary compartment can indicate relevant therapeutic targets and follow-up biomarkers of patients, in addition to providing promising immunotherapies, which would aid in controlling the disease in the long term and improving quality of life for patients.

## Author contributions

FM-G, FA-H, NA, and AC were responsible for the initial conception, project, and writing of this manuscript. FM-G, FA-H, MB, FS, CC, JM, and IF collected, analyzed, and reviewed the data. MB, FS, and FM-G designed the illustrations. FM-G, NA, FA-H, AT, AM, AT-C, and AC supervised the project development, interpreted the data, and reviewed this manuscript. All authors read, discussed the general outline of the article together and approved the final manuscript.

## Funding

This work was funded by Fundação de Amparo à Pesquisa do Estado do Amazonas (FAPEAM) (Pró-Estado Program [#002/2008, #007/2018 and #005/2019], and POSGRAD Program [#008/2021 and #005/2022]), Conselho Nacional de Desenvolvimento Científico e Tecnológico (CNPq), Coordenação de Aperfeiçoamento de Pessoal de Nível Superior (CAPES) (PROCAD-Amazônia 2018 Program-#88881.200581/2018-01). FM-G, NA, FA-H, MB, and FS have fellowships from FAPEAM, CAPES and CNPq (PhD and MSc students). JM and IF have fellowships from FAPEAM (Scientific Initiation students). AT-C and AM are level 1 and 2 research fellows from CNPq, respectively. AT-C and AC is research fellow from FAPEAM (PECTI-AM program #004/2020 and PRODOC Program #003/2022). The funders had no role in study design and decision to publish, or preparation of the manuscript.

## Acknowledgments

We would like to thank our collaborators at the HEMOAM Foundation, especially the Amazon InterScience and Leukemia Immunology Research Group; the researchers of the Post-graduate Program in Basic and Applied Immunology (UFAM) and of the Post-graduate Program in Hematology Sciences (UEA); as well as our external collaborators from the Integrated Research Group on Biomarkers (FIOCRUZ-Minas) for their critical discussions and insightful and encouraging ideas.

## Conflict of interest

The authors declare that the research was conducted in the absence of any commercial or financial relationships that could be construed as a potential conflict of interest.

## Publisher's note



## References

1. Ehsanpour A, Saki N, Bagheri M, Behzad MM, Abroun S. The expression of microvesicles in leukemia: Prognostic approaches. *Cell J* (2018) 21:115–23. doi: 10.22074/cellj.2019.5847

2. Van Etten RA. Mechanisms of transformation by the BCR-ABL oncogene: New perspectives in the post-imatinib era. *Leuk Res* (2004) 28:21–8. doi: 10.1016/j.leukres.2003.10.005

3. Van Etten RA. Aberrant cytokine signaling in leukemia. *Oncogene* (2007) 26:6738–49. doi: 10.1038/sj.onc.1210758

4. Khwaja A, Bjorkholm M, Gale RE, Levine RL, Jordan CT, Ehninger G, et al. Acute myeloid leukaemia. *Nat Rev Dis Prim* (2016) 2:16010. doi: 10.1038/nrdp.2016.10

5. Houshmand M, Simonetti G, Circosta P, Gaidano V, Cignetti A, Martinelli G, et al. Chronic myeloid leukemia stem cells. *Leukemia* (2019) 33:1543–56. doi: 10.1038/s41375-019-0490-0

6. Bosch F, Dalla-Favera R. Chronic lymphocytic leukaemia: from genetics to treatment. *Nat Rev Clin Oncol* (2019) 16:684–701. doi: 10.1038/s41571-019-0239-8

7. Terwilliger T, Abdul-Hay M. Acute lymphoblastic leukemia: A comprehensive review and 2017 update. *Blood Cancer J* (2017) 7:e577–7. doi: 10.1038/bcj.2017.53

8. Konopleva MY, Jordan CT. Leukemia stem cells and microenvironment: Biology and therapeutic targeting. *J Clin Oncol* (2011) 29:591–9. doi: 10.1200/JCO.2010.31.0904

9. Tabe Y, Konopleva M. Advances in understanding the leukaemia microenvironment. *Br J Haematol* (2014) 164:767–78. doi: 10.1111/bjh.12725

10. Witkowski MT, Kousteni S, Aifantis I. Mapping and targeting of the leukemic microenvironment. *J Exp Med* (2020) 217:e20190589. doi: 10.1084/jem.20190589

11. Höpken UE, Rehm A. Targeting the tumor microenvironment of leukemia and lymphoma. *Trends Cancer* (2019) 5:351–64. doi: 10.1016/j.trecan.2019.05.001

12. Burger JA, Ghia P, Rosenwald A, Caligaris-Cappio F. The microenvironment in mature b-cell malignancies: A target for new treatment strategies. *Blood* (2009) 114:3367–75. doi: 10.1182/blood-2009-06-225326

13. Morrison SJ, Spradling AC. Stem cells and niches: Mechanisms that promote stem cell maintenance throughout life. *Cell* (2008) 132:598–611. doi: 10.1016/j.cell.2008.01.038

14. Awad RM, De Vlaeminck Y, Maebe J, Goyvaerts C, Breckpot K. Turn back the TIMe: Targeting tumor infiltrating myeloid cells to revert cancer progression. *Front Immunol* (2018) 9:1977. doi: 10.3389/fimmu.2018.01977

15. Engblom C, Pfirschke C, Pittet MJ. The role of myeloid cells in cancer therapies. *Nat Rev Cancer* (2016) 16:447–62. doi: 10.1038/nrc.2016.54

16. Haas L, Obenauf AC. Allies or enemies–the multifaceted role of myeloid cells in the tumor microenvironment. *Front Immunol* (2019) 10:2746. doi: 10.3389/fimmu.2019.02746

17. Hinshaw DC, Shevde LA. The tumor microenvironment innately modulates cancer progression. *Cancer Res* (2019) 79:4557–66. doi: 10.1158/0008-5472.CAN-18-3962

18. Brandau S, Dumitru CA, Lang S. Protumor and antitumor functions of neutrophil granulocytes. *Semin Immunopathol* (2013) 35:163–76. doi: 10.1007/s00281-012-0344-6

19. Tamura R, Tanaka T, Yamamoto Y, Akasaki Y, Sasaki H. Dual role of macrophage in tumor immunity. *Immunotherapy* (2018) 10:899–909. doi: 10.2217/imt-2018-0006

20. Jackaman C, Tomay F, Duong L, Abdol Razak NB, Pixley FJ, Metharom P, et al. Aging and cancer: The role of macrophages and neutrophils. *Ageing Res Rev* (2017) 36:105–16. doi: 10.1016/j.arr.2017.03.008

21. Zhang Y, Lee C, Geng S, Li L. Enhanced tumor immune surveillance through neutrophil reprogramming due to tollip deficiency. *JCI Insight* (2019) 4:e122939. doi: 10.1172/jci.insight.122939

22. Kashfi K, Kannikal J, Nath N. Macrophage reprogramming and cancer therapeutics: Role of iNOS-derived NO. *Cells* (2021) 10:3194. doi: 10.3390/cells10113194

23. Borregaard N. Neutrophils, from marrow to microbes. *Immunity* (2010) 33:657–70. doi: 10.1016/j.immuni.2010.11.011

24. Kolaczkowska E, Kubes P. Neutrophil recruitment and function in health and inflammation. *Nat Rev Immunol* (2013) 13:159–75. doi: 10.1038/nri3399

25. Nauseef WM, Borregaard N. Neutrophils at work. *Nat Immunol* (2014) 15:602–11. doi: 10.1038/ni.2921

26. Fridlender ZG, Albelda SM. Tumor-associated neutrophils: Friend or foe? *Carcinogenesis* (2012) 33:949–55. doi: 10.1093/carcin/bgs123

27. Mantovani A, Allavena P, Sica A, Balkwill F. Cancer-related inflammation. *Nature* (2008) 454:436–44. doi: 10.1038/nature07205

28. Shaul ME, Fridlender ZG. Cancer-related circulating and tumor-associated neutrophils – subtypes, sources and function. *FEBS J* (2018) 285:4316–42. doi: 10.1111/febs.14524

29. Shaul ME, Fridlender ZG. The dual role of neutrophils in cancer. *Semin Immunol* (2022), 57:101582. doi: 10.1016/j.smim.2021.101582

30. Coffelt SB, Wellenstein MD, De Visser KE. Neutrophils in cancer: Neutral no more. *Nat Rev Cancer* (2016) 16:431–46. doi: 10.1038/nrc.2016.52

31. Rosales C. Neutrophil: A cell with many roles in inflammation or several cell types? *Front Physiol* (2018) 9:113. doi: 10.3389/fphys.2018.00113

32. Eruslanov EB, Bhojnagarwala PS, Quatromoni JG, Stephen TL, Ranganathan A, Deshpande C, et al. Tumor-associated neutrophils stimulate T cell responses in early-stage human lung cancer. *J Clin Invest* (2014) 124:5466–80. doi: 10.1172/JCI77053

33. Fridlender ZG, Sun J, Kim S, Kapoor V, Cheng G, Ling L, et al. Polarization of tumor-associated neutrophil phenotype by TGF-β: "N1" versus "N2" TAN. *Cancer Cell* (2009) 16:183–94. doi: 10.1016/j.ccr.2009.06.017

34. Mishalian I, Bayuh R, Levy L, Zolotarov L, Michaeli J, Fridlender ZG. Tumor-associated neutrophils (TAN) develop pro-tumorigenic properties during tumor progression. *Cancer Immunol Immunother* (2013) 62:1745–56. doi: 10.1007/s00262-013-1476-9

35. Qian X, Chen H, Wu X, Hu L, Huang Q, Jin Y. Interleukin-17 acts as double-edged sword in anti-tumor immunity and tumorigenesis. *Cytokine* (2017) 89:34–44. doi: 10.1016/j.cyto.2015.09.011

36. Elliott LA, Doherty GA, Sheahan K, Ryan EJ. Human tumor-infiltrating myeloid cells: Phenotypic and functional diversity. *Front Immunol* (2017) 8:86/BIBTEX. doi: 10.3389/FIMMU.2017.00086/BIBTEX

37. Wu S, Awaji S. Tumor-associated neutrophils in cancer: Going pro. *Cancers (Basel)* (2019) 11:564. doi: 10.3390/cancers11040564

38. Zou J-M, Qin J, Li Y-C, Wang Y, Li D, Shu Y, et al. IL-35 induces N2 phenotype of neutrophils to promote tumor growth. *Oncotarget* (2017) 8:33501–14. doi: 10.18632/oncotarget.16819

39. Liu CY, Wang YM, Wang CL, Feng PH, Ko HW, Liu YH, et al. Population alterations of l-arginase- and inducible nitric oxide synthase-expressed CD11b +/CD14-/CD15+/CD33 + myeloid-derived suppressor cells and CD8+ T lymphocytes in patients with advanced-stage non-small cell lung cancer. *J Cancer Res Clin Oncol* (2010) 136:35–45. doi: 10.1007/s00432-009-0634-0

40. Mishalian I, Bayuh R, Eruslanov E, Michaeli J, Levy L, Zolotarov L, et al. Neutrophils recruit regulatory T-cells into tumors *via* secretion of CCL17 - a new mechanism of impaired antitumor immunity. *Int J Cancer* (2014) 135:1178–86. doi: 10.1002/ijc.28770

41. Sconocchia G, Zlobec I, Lugli A, Calabrese D, Iezzi G, Karamitopoulou E, et al. Tumor infiltration by FcIγRIII (CD16)+ myeloid cells is associated with improved survival in patients with colorectal carcinoma. *Int J Cancer* (2011) 128:2663–72. doi: 10.1002/ijc.25609

42. Jaillon S, Ponzetta A, Di Mitri D, Santoni A, Bonecchi R, Mantovani A. Neutrophil diversity and plasticity in tumour progression and therapy. *Nat Rev Cancer* (2020) 20:485–503. doi: 10.1038/s41568-020-0281-y

43. Galdiero MR, Varricchi G, Loffredo S, Mantovani A, Marone G. Roles of neutrophils in cancer growth and progression. *J Leukoc Biol* (2018) 103:457–64. doi: 10.1002/JLB.3MR0717-292R

44. Sionov RV, Fridlender ZG, Granot Z. The multifaceted roles neutrophils play in the tumor microenvironment. *Cancer Microenviron* (2015) 8:125–58. doi: 10.1007/s12307-014-0147-5

45. Thiam HR, Wong SL, Wagner DD, Waterman CM. Cellular mechanisms of NETosis. *Annu Rev Cell Dev Biol* (2020) 36:191–218. doi: 10.1146/annurev-cellbio-020520-111016

46. Vorobjeva NV, Chernyak BV. NETosis: Molecular mechanisms, role in physiology and pathology. *Biochem* (2020) 85:1178–90. doi: 10.1134/S0006297920100065

47. Hanahan D, Folkman J. Patterns and emerging mechanisms of the angiogenic switch during tumorigenesis. *Cell* (1996) 86:353–64. doi: 10.1016/S0092-8674(00)80108-7

48. Lonardi S, Missale F, Calza S, Bugatti M, Vescovi R, Debora B, et al. Tumor-associated neutrophils (TANs) in human carcinoma-draining lymph nodes: A novel TAN compartment. *Clin Transl Immunol* (2021) 10:1–20. doi: 10.1002/cti2.1252

49. López-Otín C, Bond JS. Proteases: Multifunctional enzymes in life and disease. *J Biol Chem* (2008) 283:30433–7. doi: 10.1074/jbc.R800035200

50. Mohamed MM, Sloane BF. Cysteine cathepsins: Multifunctional enzymes in cancer. *Nat Rev Cancer* (2006) 6:764–75. doi: 10.1038/nrc1949

51. Andzinski L, Wu CF, Lienenklaus S, Kröger A, Weiss S, Jablonska J. Delayed apoptosis of tumor associated neutrophils in the absence of endogenous IFN-β. *Int J Cancer* (2015) 136:572–83. doi: 10.1002/ijc.28957

52. Zhang J, Qiao X, Shi H, Han X, Liu W, Tian X, et al. Circulating tumor-associated neutrophils (cTAN) contribute to circulating tumor cell survival by suppressing peripheral leukocyte activation. *Tumor Biol* (2016) 37:5397–404. doi: 10.1007/s13277-015-4349-3

53. Governa V, Trella E, Mele V, Tornillo L, Amicarella F, Cremonesi E, et al. The interplay between neutrophils and CD8+ T cells improves survival in human colorectal cancer. *Clin Cancer Res* (2017) 23:3847–58. doi: 10.1158/1078-0432.CCR-16-2047

54. Hao Y, Hu P, Zhang J. Genomic analysis of the prognostic effect of tumor-associated neutrophil-related genes across 15 solid cancer types: an immune perspective. *Ann Transl Med* (2020) 8:1507–7. doi: 10.21037/atm-20-6629

55. Jensen HK, Donskov F, Marcussen N, Nordsmark M, Lundbeck F, Von Der Maase H. Presence of intratumoral neutrophils is an independent prognostic factor in localized renal cell carcinoma. *J Clin Oncol* (2009) 27:4709–17. doi: 10.1200/JCO.2008.18.9498

56. Lecot P, Sarabi M, Pereira Abrantes M, Mussard J, Koenderman L, Caux C, et al. Neutrophil heterogeneity in cancer: From biology to therapies. *Front Immunol* (2019) 10:2155. doi: 10.3389/fimmu.2019.02155

57. Reid MD, Basturk O, Thirabanjasak D, Hruban RH, Klimstra DS, Bagci P, et al. Tumor-infiltrating neutrophils in pancreatic neoplasia. *Mod Pathol* (2011) 24:1612–9. doi: 10.1038/modpathol.2011.113

58. Podaza E, Sabbione F, Risnik D, Borge M, Almejún MB, Colado A, et al. Neutrophils from chronic lymphocytic leukemia patients exhibit an increased capacity to release extracellular traps (NETs). *Cancer Immunol Immunother* (2017) 66:77–89. doi: 10.1007/s00262-016-1921-7

59. Podaza E, Risnik D, Colado A, Elías E, Belén M, Grecco HF, et al. As células de leucemia linfocítica crônica aumentam a sobrevivência dos neutrófilos e promovem sua diferenciação no subconjunto imunossupressor CD16 CD62L. *Int J Cancer* (2018) 144(5):1128–34. doi: 10.1002/ijc.31762

60. Hanna BS, Öztürk S, Seiffert M. Beyond bystanders: Myeloid cells in chronic lymphocytic leukemia. *Mol Immunol* (2019) 110:77–87. doi: 10.1016/j.molimm.2017.11.014

61. Itala M, Vainio ORK. Functional abnorma lities in granulocytes predict susceptibility to b acterial in chronic lymphocy tic le ukaernia. *Eur J Haematol* (1996) 57:46–53. doi: 10.1111/j.1600-0609.1996.tb00489.x

62. Tanaka F, Goto H, Yokosuka T, Yanagimachi M, Kajiwara R, Naruto T, et al. Suppressed neutrophil function in children with acute lymphoblastic leukemia. *Int J Hematol* (2009) 90:311–7. doi: 10.1007/s12185-009-0412-4

63. Kontoyiannis DP, Georgiadou SP, Wierda WG, Wright S, Albert ND, Ferrajoli A, et al. Impaired bactericidal but not fungicidal activity of polymorphonuclear neutrophils in patients with chronic lymphocytic leukemia. *Leuk Lymphoma* (2013) 54:1730–3. doi: 10.3109/10428194.2012.750723

64. Manukyan G, Papajik T, Gajdos P, Mikulkova Z, Urbanova R, Gabcova G, et al. Neutrophils in chronic lymphocytic leukemia are permanently activated and have functional defects. *Oncotarget* (2017) 8:84889–901. doi: 10.18632/oncotarget.20031

65. Gätjen M, Brand F, Grau M, Gerlach K, Kettritz R, Westermann J, et al. Splenic marginal zone granulocytes acquire an accentuated neutrophil b cellhelper phenotype in chronic lymphocytic leukemia. *Cancer Res* (2016) 76:5253–65. doi: 10.1158/0008-5472.CAN-15-3486

66. Wachowska M, Wojciechowska A, Muchowicz A. The role of neutrophils in the pathogenesis of chronic lymphocytic leukemia. (2022) 23(1):365. doi: 10.3390/ijms23010365

67. Lavin Y, Mortha A, Rahman A, Merad M. Regulation of macrophage development and function in peripheral tissues. *Nat Rev Immunol* (2015) 15:731–44. doi: 10.1038/nri3920

68. Hirayama D, Iida T, Nakase H. The phagocytic function of macrophage-enforcing innate immunity and tissue homeostasis. *Int J Mol Sci* (2018) 1998. doi: 10.3390/ijms19010092

69. Mosser DM, Edwards JP. Exploring the full spectrum of macrophage activation. *Nat Rev Immunol* (2008) 8:958–69. doi: 10.1038/nri2448

70. Duque GA, Descoteaux A. Macrophage cytokines: Involvement in immunity and infectious diseases. *Front Immunol* (2014) 5:491. doi: 10.3389/fimmu.2014.00491

71. Jayasingam SD, Citartan M, Thang TH, Mat Zin AA, Ang KC, Ch'ng ES. Evaluating the polarization of tumor-associated macrophages into M1 and M2

phenotypes in human cancer tissue: Technicalities and challenges in routine clinical practice. *Front Oncol* (2020) 9:1512. doi: 10.3389/fonc.2019.01512

72. Roszer T. Understanding the mysterious M2 macrophage through activation markers and effector mechanisms. *Mediators Inflammation* (2015) 2015:816460. doi: 10.1155/2015/816460

73. Gentles AJ, Newman AM, Liu CL, Bratman SV, Feng W, Kim D, et al. The prognostic landscape of genes and infiltrating immune cells across human cancers. *Nat Med* (2015) 21:938–45. doi: 10.1038/nm.3909

74. Hiam-Galvez KJ, Allen BM, Spitzer MH. Systemic immunity in cancer. *Nat Rev Cancer* (2021), 21:1–15. doi: 10.1038/s41568-021-00347-z

75. Gabrilovich DI, Ostrand-Rosenberg S, Bronte V. Coordinated regulation of myeloid cells by tumours. *Nat Rev Immunol* (2012) 12:253–68. doi: 10.1038/nri3175

76. DeNardo DG, Ruffell B. Macrophages as regulators of tumour immunity and immunotherapy. *Nat Rev Immunol* (2019) 19:369–82. doi: 10.1038/s41577-019-0127-6

77. Mantovani A, Allavena P, Marchesi F, Garlanda C. Macrophages as tools and targets in cancer therapy. *Nat Rev Drug Discovery* (2022) 21:799–820. doi: 10.1038/s41573-022-00520-5

78. Bardi GT, Smith MA, Hood JL. Melanoma exosomes promote mixed M1 and M2 macrophage polarization. *Cytokine* (2018) 105:63–72. doi: 10.1016/j.cyto.2018.02.002

79. Wan S, Zhao E, Kryczek I, Vatan L, Sadovskaya A, Ludema G, et al. Tumor-associated macrophages produce interleukin 6 and signal *via* STAT3 to promote expansion of human hepatocellular carcinoma stem cells. *Gastroenterology* (2014) 147:1393–404. doi: 10.1053/j.gastro.2014.08.039

80. Radharani NNV, Yadav AS, Nimma R, Kumar TVS, Bulbule A, Chanukuppa V, et al. Tumor-associated macrophage derived IL-6 enriches cancer stem cell population and promotes breast tumor progression *via* stat-3 pathway. *Cancer Cell Int* (2022) 22:122. doi: 10.1186/s12935-022-02527-9

81. Wu K, Lin K, Li X, Yuan X, Xu P, Ni P, et al. Redefining tumor-associated macrophage subpopulations and functions in the tumor microenvironment. *Front Immunol* (2020) 11:1731. doi: 10.3389/fimmu.2020.01731

82. Chong BF, Tseng L, Hosler GA, Teske NM, Zhang S, Karp DR, et al. Mohan c. a subset of CD163+ macrophages displays mixed polarizations in discoid lupus skin. *Arthritis Res Ther* (2015) 17:324. doi: 10.1186/s13075-015-0839-3

83. Yang M, McKay D, Pollard JW, Lewis CE. Diverse functions of macrophages in different tumor microenvironments. *Cancer Res* (2018) 78:5492–503. doi: 10.1158/0008-5472.CAN-18-1367

84. Wang L, Zheng G. Macrophages in leukemia microenvironment. *Blood Sci* (2019) 1:29–33. doi: 10.1097/BS9.0000000000000014

85. Petty AJ, Yang Y. Tumor-associated macrophages in hematologic malignancies: New insights and targeted therapies. *Cells* (2019) 8:1526. doi: 10.3390/cells8121526

86. Li Y, You MJ, Yang Y, Hu D, Tian C. The role of tumor-associated macrophages in leukemia. *Acta Haematol* (2020) 143:112–7. doi: 10.1159/000500315

87. Cencini E, Fabbri A, Sicuranza A, Gozzetti A, Bocchia M. The role of tumor-associated macrophages in hematologic malignancies. *Cancers (Basel)* (2021) 13:3597. doi: 10.3390/cancers13143597

88. Song JX, Wen Y, Li RW, Dong T, Tang YF, Zhang JJ, et al. Phenotypic characterization of macrophages in the BMB sample of human acute leukemia. *Ann Hematol* (2020) 99:539–47. doi: 10.1007/s00277-020-03912-y

89. Fiorcari S, Maffei R, Atene CG, Potenza L, Luppi M, Marasca R. Nurse-like cells and chronic lymphocytic leukemia b cells: A mutualistic crosstalk inside tissue microenvironments. *Cells* (2021) 10:1–12. doi: 10.3390/cells10020217

90. Boissard F, Laurent C, Ramsay AG, Quillet-Mary A, Fournié JJ, Poupot M, et al. Nurse-like cells impact on disease progression in chronic lymphocytic leukemia. *Blood Cancer J* (2016) 6:e381. doi: 10.1038/bcj.2015.108

91. Miari KE, Guzman ML, Wheadon H, Williams MTS. Macrophages in acute myeloid leukaemia: Significant players in therapy resistance and patient outcomes. *Front Cell Dev Biol* (2021) 9:692800. doi: 10.3389/fcell.2021.692800

92. Xu ZJ, Gu Y, Wang CZ, Jin Y, Wen XM, Ma JC, et al. The M2 macrophage marker CD206: A novel prognostic indicator for acute myeloid leukemia. *Oncoimmunology* (2020) 9:e1683347. doi: 10.1080/2162402X.2019.1683347

93. Guo R, Lü M, Cao F, Wu G, Gao F, Pang H, et al. Single-cell map of diverse immune phenotypes in the acute myeloid leukemia microenvironment. *biomark Res* (2021) 9:1–16. doi: 10.1186/s40364-021-00265-0

94. Zhou X, Xu N, Sun X, Lin T, Fan Z, Cao R, et al. Tumor-associated macrophages maybe associated with acute myeloid leukemia survival and prognosis. *Blood* (2017) 130:5090–0. doi: 10.1182/blood.V130.Suppl_1.5090.5090

95. Al-Matary YS, Botezatu L, Opalka B, Hönes JM, Lams RF, Thivakaran A, et al. Acute myeloid leukemia cells polarize macrophages towards a leukemia supporting state in a growth factor independence 1 dependent manner. *Haematologica* (2016) 101:1216–27. doi: 10.3324/haematol.2016.143180

96. Hohtari H, Brück O, Blom S, Turkki R, Sinisalo M, Kovanen PE, et al. Immune cell constitution in bone marrow microenvironment predicts outcome in adult ALL. *Leukemia* (2019) 33:1570–82. doi: 10.1038/s41375-018-0360-1

97. Song JX, Dian ZJ, Wen Y, Mei F, Li RW, Sa YL. Assessment of the number and phenotype of macrophages in the human BMB samples of CML. *BioMed Res Int* (2016) 2016:8086398. doi: 10.1155/2016/8086398

98. Komohara Y, Niino D, Saito Y, Ohnishi K, Horlad H, Ohshima K, et al. Clinical significance of CD163+ tumor-associated macrophages in patients with adult T-cell leukemia/lymphoma. *Cancer Sci* (2013) 104:945–51. doi: 10.1111/cas.12167

99. Chen S-Y, Yang X, Feng W-L, Liao J-F, Wang L-N, Feng L, et al. Organ-specific microenvironment modifies diverse functional and phenotypic characteristics of leukemia-associated macrophages in mouse T cell acute lymphoblastic leukemia. *J Immunol* (2015) 194:2919–29. doi: 10.4049/jimmunol.1400451

100. Burger JA, Quiroga MP, Hartmann E, Bürkle A, Wierda WG, Keating MJ, et al. High-level expression of the T-cell chemokines CCL3 and CCL4 by chronic lymphocytic leukemia b cells in nurselike cell cocultures and after BCR stimulation. *Blood* (2009) 113:3050–8. doi: 10.1182/blood-2008-07-170415

101. Zucchetto A, Benedetti D, Tripodo C, Bomben R, Bo MD, Marconi D, et al. CD38/CD31, the CCL3 and CCL4 chemokines, and cd49d/vascular cell adhesion molecule-1 are interchained bysequential events sustaining chronic lymphocytic leukemia cell survival. *Cancer Res* (2009) 69:4001–9. doi: 10.1158/0008-5472.CAN-08-4173

102. Beider K, Bitner H, Leiba M, Gutwein O, Koren-Michowitz M, Ostrovsky O, et al. Multiple myeloma cells recruit tumor-supportive macrophages through the CXCR4/CXCL12 axis and promote their polarization toward the M2 phenotype. *Oncotarget* (2014) 5:11283–96. doi: 10.18632/oncotarget.2207

103. Tian Y, Matsui S, Touma M, Wu Q, Sugimoto K. MicroRNA-342 inhibits tumor growth *via* targeting chemokine CXCL12 involved in macrophages recruitment/activation. *Genes to Cells* (2018) 23:1009–22. doi: 10.1111/gtc.12650

104. Dander E, Fallati A, Gulić T, Pagni F, Gaspari S, Silvestri D, et al. Monocyte–macrophage polarization and recruitment pathways in the tumour microenvironment of b-cell acute lymphoblastic leukaemia. *Br J Haematol* (2021) 193:1157–71. doi: 10.1111/bjh.17330

105. Gandhi V, Balakrishnan K. CCL2 in chronic lymphocytic leukemia: A macro in microenvironment? *Leuk Lymphoma* (2012) 53:1849–50. doi: 10.3109/10428194.2012.688966

106. Schulz A, Toedt G, Zenz T, Stilgenbauer S, Lichter P, Seiffert M. Inflammatory cytokines and signaling pathways are associated with survival of primary chronic lymphocytic leukemia cells *in vitro*: A dominant role of CCL2. *Haematologica* (2011) 96:408–16. doi: 10.3324/haematol.2010.031377

107. Magalhães-Gama F, Kerr MWA, de Araújo ND, Ibiapina HNS, Neves JCF, Hanna FSA, et al. Imbalance of chemokines and cytokines in the bone marrow microenvironment of children with b-cell acute lymphoblastic leukemia. *J Oncol* (2021) 2021:1–9. doi: 10.1155/2021/5530650

108. De Vasconcellos JF, Laranjeira ABA, Zanchin NIT, Otubo R, Vaz TH, Cardoso AA, et al. Increased CCL2 and IL-8 in the bone marrow microenvironment in acute lymphoblastic leukemia. *Pediatr Blood Cancer* (2011) 56:568–77. doi: 10.1002/PBC.22941

109. Rigo A, Gottardi M, Zamò A, Mauri P, Bonifacio M, Krampera M, et al. Macrophages may promote cancer growth *via* a GM-CSF/HB-EGF paracrine loop that is enhanced by CXCL12. *Mol Cancer* (2010) 9:1–13. doi: 10.1186/1476-4598-9-273

110. Sánchez-Martín L, Estecha A, Samaniego R, Sánchez-Ramón S, Vega MÁ, Sánchez-Mateos P. The chemokine CXCL12 regulates monocyte-macrophage differentiation and RUNX3 expression. *Blood* (2011) 117:88–97. doi: 10.1182/blood-2009-12-258186

111. Kerr MWA, Magalhães-Gama F, Ibiapina HNS, Hanna FSA, Xabregas LA, Alves EB, et al. Bone marrow soluble immunological mediators as clinical prognosis biomarkers in b-cell acute lymphoblastic leukemia patients undergoing induction therapy. *Front Oncol* (2021) 11:696032. doi: 10.3389/fonc.2021.696032

112. Whiteley AE, Price TT, Cantelli G, Sipkins DA. Leukaemia: A model metastatic disease. *Nat Rev Cancer* (2021) 21:461–75. doi: 10.1038/s41568-021-00355-z

113. Burger JA, Tsukada N, Burger M, Zvaifler NJ, Dell'Aquila M, Kipps TJ. Blood-derived nurse-like cells protect chronic lymphocytic leukemia b cells from spontaneous apoptosis through stromal cell-derived factor-1. *Blood* (2000) 96:2655–63. doi: 10.1182/blood.v96.8.2655

114. Tsukada N, Burger JA, Zvaifler NJ, Kipps TJ. Distinctive features of "nurselike" cells that differentiate in the context of chronic lymphocytic leukemia. *Blood* (2002) 99:1030–7. doi: 10.1182/blood.V99.3.1030

115. Zucchetto A, Tripodo C, Benedetti D, Deaglio S, Gaidano G, Del Poeta G, et al. Monocytes/macrophages but not T lymphocytes are the major targets of the CCL3/CCL4 chemokines produced by CD38+CD49d+ chronic lymphocytic leukaemia cells: Correspondence. *Br J Haematol* (2010) 150:111–2. doi: 10.1111/j.1365-2141.2010.08152.x

116. Boissard F, Tosolini M, Ligat L, Quillet-Mary A, Lopez F, Fournié J-J, et al. Nurse-like cells promote CLL survival through LFA-3/CD2 interactions. *Oncotarget* (2017) 8:52225–36. doi: 10.18632/oncotarget.13660

117. Hanna BS, McClanahan F, Yazdanparast H, Zaborsky N, Kalter V, Rößner PM, et al. Depletion of CLL-associated patrolling monocytes and macrophages controls disease development and repairs immune dysfunction in vivo. *Leukemia* (2016) 30:570–9. doi: 10.1038/leu.2015.305

118. Yang X, Feng W, Wang R, Yang F, Wang L, Chen S, et al. Repolarizing heterogeneous leukemia-associated macrophages with more M1 characteristics eliminates their pro-leukemic effects. *Oncoimmunology* (2018) 7:e1412910. doi: 10.1080/2162402X.2017.1412910

119. Amrein MA, Bührer ED, Forster S, Isringhausen S, Schürch CM, Bhate SS, et al. Splenic CD24low red pulp macrophages provide an alternate niche for chronic myeloid leukemia stem cells. *Blood* (2019) 134:1634–4. doi: 10.1182/blood-2019-126593

120. Yang X, Feng W, Wang R, Yang F, Wang L, Chen S, et al. Hepatic leukemia-associated macrophages exhibit a pro-inflammatory phenotype in Notch1-induced acute T cell leukemia. *Immunobiology* (2018) 223:73–80. doi: 10.1016/j.imbio.2017.10.009

121. Yang F, Feng W, Wang H, Wang L, Liu X, Wang R, et al. Monocyte-derived leukemia-associated macrophages facilitate extramedullary distribution of t-cell acute lymphoblastic leukemia cells. *Cancer Res* (2020) 80:3677–91. doi: 10.1158/0008-5472.CAN-20-0034

122. Audrito V, Serra S, Brusa D, Mazzola F, Arruga F, Vaisitti T, et al. Extracellular nicotinamide phosphoribosyltransferase (NAMPT) promotes M2 macrophage polarization in chronic lymphocytic leukemia. *Blood* (2015) 125:111–23. doi: 10.1182/blood-2014-07-589069

123. Valencia J M, Fernández-Sevilla L, Fraile-Ramos A, Sacedón R, Jiménez E, Vicente A, et al. Acute lymphoblastic leukaemia cells impair dendritic cell and macrophage differentiation: Role of BMP4. *Cells* (2019) 8:722. doi: 10.3390/cells8070722

124. Chen S, Yang X, Feng W, Yang F, Wang R, Chen C, et al. Characterization of peritoneal leukemia-associated macrophages in Notch1-induced mouse T cell acute lymphoblastic leukemia. *Mol Immunol* (2017) 81:35–41. doi: 10.1016/j.molimm.2016.11.014

125. Bürkle A, Niedermeier M, Schmitt-Gräff A, Wierda WG, Keating MJ, Burger JA. Overexpression of the CXCR5 chemokine receptor, and its ligand, CXCL13 in b-cell chronic lymphocytic leukemia. *Blood* (2007) 110:3316–25. doi: 10.1182/blood-2007-05-089409

126. Dilillo DJ, Weinberg JB, Yoshizaki A, Horikawa M, Bryant JM, Iwata Y, et al. Chronic lymphocytic leukemia and regulatory b cells share IL-10 competence and immunosuppressive function. *Leukemia* (2013) 27:170–82. doi: 10.1038/leu.2012.165

127. Dai J, Su Y, Zhong S, Cong L, Liu B, Yang J, et al. Exosomes: Key players in cancer and potential therapeutic strategy. *Signal Transduct Target Ther* (2020) 5:145. doi: 10.1038/s41392-020-00261-0

128. van Niel G, D'Angelo G, Raposo G. Shedding light on the cell biology of extracellular vesicles. *Nat Rev Mol Cell Biol* (2018) 19:213–28. doi: 10.1038/nrm.2017.125

129. Jafarzadeh N, Safari Z, Pornour M, Amirizadeh N, Forouzandeh MM, Sadeghizadeh M. Alteration of cellular and immune-related properties of bone marrow mesenchymal stem cells and macrophages by K562 chronic myeloid leukemia cell derived exosomes. *J Cell Physiol* (2019) 234:3697–710. doi: 10.1002/jcp.27142

130. Haderk F, Schulz R, Iskar M, Cid LL, Worst T, Willmund KV, et al. Tumor-derived exosomes modulate PD-L1 expression in monocytes. *Sci Immunol* (2017) 2:eaah5509. doi: 10.1126/sciimmunol.aah5509

131. Philippidis P, Mason JC, Evans BJ, Nadra I, Taylor KM, Haskard DO, et al. Hemoglobin scavenger receptor CD163 mediates interleukin-10 release and heme oxygenase-1 synthesis: Antiinflammatory monocyte-macrophage responses *In vitro*, in resolving skin blisters *In vivo*, and after cardiopulmonary bypass surgery. *Circ Res* (2004) 94:119–26. doi: 10.1161/01.RES.0000109414.78907.F9

132. Alhakeem SS, McKenna MK, Gachuki BW, Rangnekar VR, Byrd JC, Muthusamy N, et al. The role of IL-10 in b-cell chronic lymphocytic leukemia cell survival. *J Immunol* (2016) 196:211. doi: 10.4049/jimmunol.196.Supp.211.17

133. Fitch B, Hermiston ML, Wiemels JL, Kogan SC. Mechanism of IL-10 protective effect in development of childhood b cell acute lymphoblastic leukemia. *Blood* (2016) 128:4075–5. doi: 10.1182/blood.v128.22.4075.4075

134. Nishio M, Endo T, Tsukada N, Ohata J, Kitada S, Reed JC, et al. Nurselike cells express BAFF and APRIL, which can promote survival of chronic lymphocytic leukemia cells *via* a paracrine pathway distinct from that of SDF-1α. *Blood* (2005) 106:1012–20. doi: 10.1182/blood-2004-03-0889

135. Craxton A, Magaletti D, Ryan EJ, Clark EA. Macrophage- and dendritic cell-dependent regulation of human b-cell proliferation requires the TNF family ligand BAFF. *Blood* (2003) 101:4464–71. doi: 10.1182/blood-2002-10-3123

136. McWilliams EM, Lucas CR, Chen T, Harrington BK, Wasmuth R, Campbell A, et al. Anti–BAFF-R antibody VAY-736 demonstrates promising preclinical activity in CLL and enhances effectiveness of ibrutinib. *Blood Adv* (2019) 3:447–60. doi: 10.1182/bloodadvances.2018025684

137. Bolkun L, Grubczak K, Schneider G, Zembko P, Radzikowska U, Singh P, et al. Involvement of BAFF and APRIL in resistance to apoptosis of acute myeloid leukemia. *J Cancer* (2016) 7:1979–83. doi: 10.7150/jca.15966

138. Deaglio S, Vaisitti T, Bergui L, Bonello L, Horenstein AL, Tamagnone L, et al. CD38 and CD100 lead a network of surface receptors relaying positive signals for b-CLL growth and survival. *Blood* (2005) 105:3042–50. doi: 10.1182/blood-2004-10-3873

139. Deaglio S, Aydin S, Grand MM, Vaisitti T, Bergui L, D'Arena G, et al. CD38/CD31 interactions activate genetic pathways leading to proliferation and migration in chronic lymphocytic leukemia cells. *Mol Med* (2010) 16:87–91. doi: 10.2119/molmed.2009.00146

140. Gautam S, Fatehchand K, Elavazhagan S, Reader BF, Ren L, Mo X, et al. Reprogramming nurse-like cells with interferon γ to interrupt chronic lymphocytic leukemia cell survival. *J Biol Chem* (2016) 291:14356–62. doi: 10.1074/jbc.M116.723551

141. Brück O, Blom S, Dufva O, Turkki R, Chheda H, Ribeiro A, et al. Immune cell contexture in the bone marrow tumor microenvironment impacts therapy response in CML. *Leukemia* (2018) 32:1643–56. doi: 10.1038/s41375-018-0175-0

142. Movahedi K, Guilliams M, Van den Bossche J, Van den Bergh R, Gysemans C, Beschin A, et al. Identification of discrete tumor-induced myeloid-derived suppressor cell subpopulations with distinct T cell–suppressive activity. *Blood* (2008) 111:4233–44. doi: 10.1182/blood-2007-07-099226

143. Mastio J, Condamine T, Dominguez G, Kossenkov AV, Donthireddy L, Veglia F, et al. Identification of monocyte-like precursors of granulocytes in cancer as a mechanism for accumulation of PMN-MDSCs. *J Exp Med* (2019) 216:2150–69. doi: 10.1084/jem.20181952

144. Veglia F, Sanseviero E, Gabrilovich DI. Myeloid-derived suppressor cells in the era of increasing myeloid cell diversity. *Nat Rev Immunol* (2021) 21:485–98. doi: 10.1038/s41577-020-00490-y

145. Bronte V, Brandau S, Chen S-H, Colombo MP, Frey AB, Greten TF, et al. Recommendations for myeloid-derived suppressor cell nomenclature and characterization standards. *Nat Commun* (2016) 7:12150. doi: 10.1038/ncomms12150

146. Kim HR, Park SM, Seo SU, Jung I, Yoon HI, Gabrilovich DI, et al. The ratio of peripheral regulatory T cells to lox-1 1 polymorphonuclear myeloid-derived suppressor cells predicts the early response to anti–PD-1 therapy in patients with non–small cell lung cancer. *Am J Respir Crit Care Med* (2019) 199:243–6. doi: 10.1164/rccm.201808-1502LE

147. Kumar V, Donthireddy L, Marvel D, Condamine T, Wang F, Lavilla-Alonso S, et al. Cancer-associated fibroblasts neutralize the anti-tumor effect of CSF1 receptor blockade by inducing PMN-MDSC infiltration of tumors. *Cancer Cell* (2017) 32:654–668.e5. doi: 10.1016/j.ccell.2017.10.005

148. Si Y, Merz SF, Jansen P, Wang B, Bruderek K, Altenhoff P, et al. Multidimensional imaging provides evidence for down-regulation of T cell effector function by MDSC in human cancer tissue. *Sci Immunol* (2019) 4:eaaw9159. doi: 10.1126/SCIIMMUNOL.AAW9159

149. Mengos AE, Gastineau DA, Gustafson MP. The CD14+HLA-DrlO/NEG monocyte: An immunosuppressive phenotype that restrains responses to cancer immunotherapy. *Front Immunol* (2019) 10:1147. doi: 10.3389/fimmu.2019.01147

150. Lv M, Wang K, Huang XJ. Myeloid-derived suppressor cells in hematological malignancies: Friends or foes. *J Hematol Oncol* (2019) 12:1–12. doi: 10.1186/s13045-019-0797-3

151. De Lerma Barbaro A, Palano MT, Cucchiara M, Gallazzi M, Mortara L, Bruno A. Metabolic rewiring in the tumor microenvironment to support immunotherapy: A focus on neutrophils, polymorphonuclear myeloid-derived suppressor cells and natural killer cells. *Vaccines* (2021) 9:1178. doi: 10.3390/vaccines9101178

152. Zhou J, Nefedova Y, Lei A, Gabrilovich D. Neutrophils and PMN-MDSC: Their biological role and interaction with stromal cells. *Semin Immunol* (2018) 35:19–28. doi: 10.1016/j.smim.2017.12.004

153. Condamine T, Gabrilovich DI, Dominguez GA, Youn J-I, Kossenkov AV, Mony S, et al. Lectin-type oxidized LDL receptor-1 distinguishes population of human polymorphonuclear myeloid-derived suppressor cells in cancer patients. *Science Immunology* (2016), 1:1–32. doi: 10.1126/sciimmunol.aaf8943.Lectin-type

154. Condamine T, Mastio J, Gabrilovich DI. Transcriptional regulation of myeloid-derived suppressor cells. *J Leukoc Biol* (2015) 98:913–22. doi: 10.1189/jlb.4ri0515-204r

155. Ostrand-Rosenberg S, Beury DW, Parker KH, Horn LA. Survival of the fittest: how myeloid-derived suppressor cells survive in the inhospitable tumor microenvironment. *Cancer Immunol Immunother* (2020) 69:215–21. doi: 10.1007/s00262-019-02388-8

156. Wang W, Xia X, Mao L, Wang S. The CCAAT/Enhancer-binding protein family: Its roles in MDSC expansion and function. *Front Immunol* (2019) 10:1804. doi: 10.3389/fimmu.2019.01804

157. Huang B, Pan P-Y, Li Q, Sato AI, Levy DE, Bromberg J, et al. Gr-1 + CD115 + immature myeloid suppressor cells mediate the development of tumor-induced T regulatory cells and T-cell anergy in tumor-bearing host. *Cancer Res* (2006) 66:1123–31. doi: 10.1158/0008-5472.CAN-05-1299

158. Ostrand-Rosenberg S, Sinha P, Beury DW, Clements VK. Cross-talk between myeloid-derived suppressor cells (MDSC), macrophages, and dendritic cells enhances tumor-induced immune suppression. *Semin Cancer Biol* (2012) 22:275–81. doi: 10.1016/j.semcancer.2012.01.011

159. Sinha P, Clements VK, Bunt SK, Albelda SM, Ostrand-Rosenberg S. Cross-talk between myeloid-derived suppressor cells and macrophages subverts tumor immunity toward a type 2 response. *J Immunol* (2007) 179:977–83. doi: 10.4049/jimmunol.179.2.977

160. Filipazzi P, Huber V, Rivoltini L. Phenotype, function and clinical implications of myeloid-derived suppressor cells in cancer patients. *Cancer Immunol Immunother* (2012) 61:255–63. doi: 10.1007/s00262-011-1161-9

161. Wang J-C, Sun L. PD-1/PD-L1, MDSC pathways, and checkpoint inhibitor therapy in ph(-) myeloproliferative neoplasm: A review. *Int J Mol Sci* (2022) 23:5837. doi: 10.3390/ijms23105837

162. Wang L, Jia B, Claxton DF, Ehmann WC, Rybka WB, Mineishi S, et al. VISTA is highly expressed on MDSCs and mediates an inhibition of T cell response in patients with AML. *Oncoimmunology* (2018) 7:e1469594. doi: 10.1080/2162402X.2018.1469594

163. Hanahan D, Coussens LM. Accessories to the crime: Functions of cells recruited to the tumor microenvironment. *Cancer Cell* (2012) 21:309–22. doi: 10.1016/j.ccr.2012.02.022

164. Kiss M, Van Gassen S, Movahedi K, Saeys Y, Laoui D. Myeloid cell heterogeneity in cancer: not a single cell alike. *Cell Immunol* (2018) 330:188–201. doi: 10.1016/j.cellimm.2018.02.008

165. Umansky V, Sevko A, Gebhardt C, Utikal J. Myeloid-derived suppressor cells in malignant melanoma. *JDDG - J Ger Soc Dermatol* (2014) 12:1021–7. doi: 10.1111/ddg.12411

166. Li W, Wu K, Zhao E, Shi L, Li R, Zhang P, et al. HMGB1 recruits myeloid derived suppressor cells to promote peritoneal dissemination of colon cancer after resection. *Biochem Biophys Res Commun* (2013) 436:156–61. doi: 10.1016/j.bbrc.2013.04.109

167. Youn JI, Gabrilovich DI. The biology of myeloid-derived suppressor cells: The blessing and the curse of morphological and functional heterogeneity. *Eur J Immunol* (2010) 40:2969–75. doi: 10.1002/eji.201040895

168. Ma P, Beatty PL, McKolanis J, Brand R, Schoen RE, Finn OJ. Circulating myeloid derived suppressor cells (MDSC) that accumulate in premalignancy share phenotypic and functional characteristics with MDSC in cancer. *Front Immunol* (2019) 10:1401. doi: 10.3389/fimmu.2019.01401

169. Bizymi N, Bjelica S, Kittang AO, Mojsilovic S, Velegraki M, Pontikoglou C, et al. Myeloid-derived suppressor cells in hematologic diseases: Promising biomarkers and treatment targets. *HemaSphere* (2019) 3:e168. doi: 10.1097/HS9.0000000000000168

170. Salem ML, El-Shanshory MR, Abdou SH, Attia MS, Sobhy SM, Zidan MF, et al. Chemotherapy alters the increased numbers of myeloid-derived suppressor and regulatory T cells in children with acute lymphoblastic leukemia. *Immunopharmacol Immunotoxicol* (2018) 40:158–67. doi: 10.1080/08923973.2018.1424897

171. Liu Y, Chen Y, He Y, Wang J, Yang J, Zhong S, et al. Expansion and activation of granulocytic, myeloid-derived suppressor cells in childhood precursor b cell acute lymphoblastic leukemia. *J Leukoc Biol* (2017) 102:449–58. doi: 10.1189/jlb.5MA1116-453RR

172. Sun H, Li Y, Zhang ZF, Ju Y, Li L, Zhang BC, et al. Increase in myeloid-derived suppressor cells (MDSCs) associated with minimal residual disease (MRD) detection in adult acute myeloid leukemia. *Int J Hematol* (2015) 102:579–86. doi: 10.1007/s12185-015-1865-2

173. Wang H, Tao Q, Wang Z, Zhang Q, Xiao H, Zhou M, et al. Circulating monocytic myeloid-derived suppressor cells are elevated and associated with poor prognosis in acute myeloid leukemia. *J Immunol Res* (2020) 2020:7363084. doi: 10.1155/2020/7363084

174. Christiansson L, Söderlund S, Svensson E, Mustjoki S, Bengtsson M, Simonsson B, et al. Increased level of myeloid-derived suppressor cells, programmed death receptor ligand 1/Programmed death receptor 1, and soluble CD25 in sokal high risk chronic myeloid leukemia. *PloS One* (2013) 8:1–12. doi: 10.1371/journal.pone.0055818

175. Giallongo C, Parrinello N, Tibullo D, La Cava P, Romano A, Chiarenza A, et al. Myeloid derived suppressor cells (MDSCs) are increased and exert immunosuppressive activity together with polymorphonuclear leukocytes (PMNs) in chronic myeloid leukemia patients. *PloS One* (2014) 9:e101848. doi: 10.1371/journal.pone.0101848

176. Jitschin R, Braun M, Büttner M, Dettmer-Wilde K, Bricks J, Berger J, et al. CLL-cells induce IDOhi CD14+HLA-DRlo myeloid-derived suppressor cells that inhibit T-cell responses and promote TRegs. *Blood* (2014) 124:750–60. doi: 10.1182/blood-2013-12-546416

177. Kowalska W, Agnieszka B-J. Monocytic MDSC as a source of immunosuppressive cytokines in chronic lymphocytic leukemia (CLL) microenvironment. *Folia Histochem Cytobiol* (2020) 58:25–36. doi: 10.5603/FHC.a2020.0006

178. Xu H, Liu J, Shen N, Zhao Z, Cui J, Zhou S, et al. The interaction of tumor cells and myeloid-derived suppressor cells in chronic myelogenous leukemia. *Leuk Lymphoma* (2020) 61:128–37. doi: 10.1080/10428194.2019.1658098

179. Ahn A, Park CJ, Kim MS, Cho YU, Jang S, Bae MH, et al. Granulocytic and monocytic myeloid-derived suppressor cells are functionally and prognostically different in patients with chronic myeloid leukemia. *Ann Lab Med* (2021) 41:479–84. doi: 10.3343/ALM.2021.41.5.479

180. Zahran AM, Moeen SM, Thabet AF, Rayan A, Abdel-Rahim MH, Mohamed WMY, et al. Monocytic myeloid-derived suppressor cells in chronic lymphocytic leukemia patients: A single center experience. *Leuk Lymphoma* (2020) 61:1645–52. doi: 10.1080/10428194.2020.1728747

181. Zarobkiewicz M, Kowalska W, Chocholska S, Tomczak W, Szymańska A, Morawska I, et al. High m-MDSC percentage as a negative prognostic factor in chronic lymphocytic leukaemia. *Cancers (Basel)* (2020) 12:1–20. doi: 10.3390/cancers12092614

182. Ferrer G, Jung B, Chiu PY, Aslam R, Palacios F, Mazzarello AN, et al. Myeloid-derived suppressor cell subtypes differentially influence T-cell function, T-helper subset differentiation, and clinical course in CLL. *Leukemia* (2021) 35:3163–75. doi: 10.1038/s41375-021-01249-7

183. Hanahan D. Hallmarks of cancer: New dimensions. *Cancer Discovery* (2022) 12:31–46. doi: 10.1158/2159-8290.CD-21-1059

184. Hanahan D, Weinberg RA. Hallmarks of cancer: The next generation. *Cell* (2011) 144:646–74. doi: 10.1016/j.cell.2011.02.013

185. Grisaru-Tal S, Itan M, Klion AD, Munitz A. A new dawn for eosinophils in the tumour microenvironment. *Nat Rev Cancer* (2020) 20:594–607. doi: 10.1038/s41568-020-0283-9

186. Grisaru-Tal S, Rothenberg ME, Munitz A. Eosinophil–lymphocyte interactions in the tumor microenvironment and cancer immunotherapy. *Nat Immunol* (2022) 23:1309–16. doi: 10.1038/s41590-022-01291-2

187. Zhang J, Yin H, Chen Q, Zhao G, Lou W, Wu W, et al. Basophils as a potential therapeutic target in cancer. *J Zhejiang Univ B* (2021) 22:971–84. doi: 10.1631/jzus.B2100110

188. Khan ANH, Emmons TR, Wong JT, Alqassim E, Singel KL, Mark J, et al. Quantification of early-stage myeloid-derived suppressor cells in cancer requires excluding basophils. *Cancer Immunol Res* (2020) 8:819–28. doi: 10.1158/2326-6066.CIR-19-0556

189. Goubran HA, Stakiw J, Radosevic M, Burnouf T. Platelets effects on tumor growth. *Semin Oncol* (2014) 41:359–69. doi: 10.1053/j.seminoncol.2014.04.006

190. Yan M, Jurasz P. The role of platelets in the tumor microenvironment: From solid tumors to leukemia. *Biochim Biophys Acta - Mol Cell Res* (2016) 1863:392–400. doi: 10.1016/j.bbamcr.2015.07.008

191. Zhang L, Liu J, Qin X, Liu W. Platelet–acute leukemia interactions. *Clin Chim Acta* (2022) 536:29–38. doi: 10.1016/j.cca.2022.09.015

192. Schmied L, Höglund P, Meinke S. Platelet-mediated protection of cancer cells from immune surveillance – possible implications for cancer immunotherapy. *Front Immunol* (2021) 12:640578. doi: 10.3389/fimmu.2021.640578

193. Nieswandt B, Hafner M, Echtenacher B, Männel DN. Lysis of tumor cells by natural killer cells in mice is impeded by platelets. *Cancer Res* (1999) 59:1295–300.

194. Betz SA, Foucar K, Head DR, Chen IM, Willman CL. False-positive flow cytometric platelet glycoprotein IIb/IIIa expression in myeloid leukemias secondary to platelet adherence to blasts. *Blood* (1992) 79:2399–403. doi: 10.1182/blood.V79.9.2399.2399

195. Goswami S, Anandhan S, Raychaudhuri D, Sharma P. Myeloid cell-targeted therapies for solid tumours. *Nat Rev Immunol* (2022) 11. doi: 10.1038/s41577-022-00737-w

196. Kaczanowska S, Beury DW, Gopalan V, Tycko AK, Qin H, Clements ME, et al. Genetically engineered myeloid cells rebalance the core immune suppression program in metastasis. *Cell* (2021) 184:2033–2052.e21. doi: 10.1016/j.cell.2021.02.048

197. Brempelis KJ, Cowan CM, Kreuser SA, Labadie KP, Prieskorn BM, Lieberman NAP, et al. Genetically engineered macrophages persist in solid tumors and locally deliver therapeutic proteins to activate immune responses. *J Immunother Cancer* (2020) 8:e001356. doi: 10.1136/jitc-2020-001356

# Frontiers in Immunology

**Explores novel approaches and diagnoses to treat immune disorders.**

The official journal of the International Union of Immunological Societies (IUIS) and the most cited in its field, leading the way for research across basic, translational and clinical immunology.

## Discover the latest Research Topics

See more →


**Frontiers**

Avenue du Tribunal-Fédéral 34
1005 Lausanne, Switzerland
frontiersin.org

**Contact us**

+41 (0)21 510 17 00
frontiersin.org/about/contact